THE THUNDERSTORM

UNIVERSITY
OF FLORIDA
LIBRARIES

[illegible] p. 133

UNITED STATES DEPARTMENT OF COMMERCE. Charles Sawyer, *Secretary*
WEATHER BUREAU, F. W. Reichelderfer, *Chief*

THE THUNDERSTORM

REPORT OF THE THUNDERSTORM PROJECT

(A joint project of four U. S. Government Agencies: Air Force, Navy, National Advisory Committee for Aeronautics, and Weather Bureau)

HORACE R. BYERS, *Director*

ROSCOE R. BRAHAM, Jr., *Senior Analyst*

WASHINGTON, D. C.
JUNE 1949

ENGINEERING
SCIENCES
LIBRARY

Approved for publication by the Director of the Budget, April 26, 1949

For sale by the Superintendent of Documents, U. S. Government Printing Office, Washington 25, D. C. - - - - - - - Price $2.25 (buckram)

Published Contributions of the Thunderstorm Project

No. 1 "The 'Bright Line' in Radar Cloud Echoes and Its Probable Explanation," H. R. Byers and R. D. Coons, *Journal of Meteorology*, vol. 4, No. 3, June 1947, pp. 75–81.

No. 2 "Guided Propagation of Radar in Thunderstorm Conditions," R. D. Coons, *Bulletin of the American Meteorological Society*, vol. 28, No. 7, September 1947, pp. 324–329.

No. 3 "The Use of Radar in Determining the Amount of Rain Falling over a Small Area," H. R. Byers and Collaborators, *Transactions of the American Geophysical Union*, vol. 29, No. 2, April 1948, pp. 187–196.

No. 4 "A Report on Thunderstom Conditions Affecting Flight Operations," U. S. Weather Bureau *Technical Paper No. 7*, Washington, D. C., April 1948.

No. 5 "Inflow Patterns of Thunderstorms as Shown by Winds Aloft," H. R. Byers and E. C. Hull, *Bulletin of the American Meteorological Society*, vol. 30, No. 3, March 1949, pp. 90–96.

No. 6 "Thunderstorm Structure and Circulation," H. R. Byers and R. R. Braham, Jr., *Journal of Meteorology*, vol. 5, No. 3, June 1948, pp. 71–86.

No. 7 "Causes of Thunderstorms of the Florida Peninsula," H. R. Byers and H. R. Rodebush, *Journal of Meteorology*, vol. 5, No. 6, December 1948, pp. 275–280.

No. 8 "Measurements of Rain Temperature," H. R. Byers, H. Moses, and P. J. Harney, *Journal of Meteorology*, vol. 6, No. 1, pp. 51–55.

No. 9 "Some Effects of Vertical Wind Shear on Thunderstorm Structure," H. R. Byers and L. J. Battan, *Bulletin of the American Meteorological Society*, vol. 30, No. 5, May 1949, pp. 168–175.

Reports to Chief, U. S. Weather Bureau:

No. 1 "Operation and Activity of the Thunderstorm Project to September 20, 1946," Chicago, Ill., November 1946.

No. 2 "Summary of Pilot Reports, The Thunderstorm Project Phase I," Chicago, Ill., March 1947.

No. 3 "Operation and Activity of the Thunderstorm Project," April 1–October 1, 1947, Chicago, Ill., November 1947.

Miscellaneous:

"Station Handbook of the Thunderstorm Project, Wilmington, Ohio," U. S. Weather Bureau, Washington, D. C., November 1947.

"The Thunderstorm Project: Operational Report on Phase I," Fred D. White, *Bulletin of the American Meteorological Society*, vol. 27, No. 9, November 1946, pp. 549–550.

"The Thunderstorm Project: Operational Report on Phase II," Fred D. White, *Bulletin of the American Meteorological Society*, vol. 29, No. 4, April 1948, pp. 192–194.

"Further Studies of Thunderstorm Conditions Affecting Flight Operations: Turbulence," R. R. Braham and Capt. F. W. Pope, Air Weather Service *Technical Report 105–39*, Washington, D. C., March 1949.

Reports Issued by the National Advisory Committee for Aeronautics

"Preliminary Analysis of N.A.C.A. Measurements of Atmospheric Turbulence within a Thunderstorm—U. S. Weather Bureau Thunderstorm Project", Harold B. Tolefson, *N.A.C.A. Technical Note No. 1233*, March 1947.

"Evaluation of Gust and Draft Velocities from Flights of P-61c Airplanes within Thunderstorms", *N.A.C.A. Research Memoranda*, 1946–1948.

"A Statistical Analysis of Gust-Velocity Measurements as Affected by Pilots and Airplanes", H. Press, *N.A.C.A. Technical Note No. 1645*, June 1948.

"An Analysis of the Relation between Horizontal Temperature Variations and Maximum Effective Gust Velocities in Thunderstorms", H. Press and J. K. Thompson, *N.A.C.A. Technical Note No. 1917*, July 1949.

"An Evaluation of the Use of Ground Radar for Avoiding Severe Turbulence Associated with Thunderstorms", J. K. Thompson and V. W. Lipscomb, *N.A.C.A. Technical Note No. 1960*, October 1949.

"An Application of the Statistical Theory of Extreme Values to Gust-Load Problems", H. Press, *N.A.C.A. Technical Note No. 1926*, November 1949.

PREFACE

This publication is to be considered as the final report of the present phase of the Thunderstorm Project. All of the research possibilities suggested by the data obtained on the Project have not been explored. Only the more obvious results are presented herewith, but it is expected that some of the participants in the analysis and other meteorologists will use the abundant material to glean additional knowledge of thunderstorms.

Four U. S. Government agencies — Air Force, Navy, National Advisory Committee for Aeronautics, and Weather Bureau — through their cooperation and support made major contributions to the success of this Project. In a project as large as this, it is difficult to single out the individuals who contributed most to its results. In the final analysis work and writing of the report, the senior analyst, Roscoe R. Braham, Jr., and the three analysis section heads, Louis J. Battan, Harry L. Hamilton, Jr. and Harry Moses have performed the bulk of the scientific work. Analysts who served under their guidance in the final stages of the report were: Bernice Ackerman, Herbert S. Appleman, Robert F. Bowes, Charles M. Caswell, Patrick J. Harney, William A. Hass, Edwin C. Hull, William A. Jenner, Mrs. Myrtle M. Johnson, Ellis D. Pike, and Mary Ellen Thomas. They were assisted by a subprofessional team consisting of George W. Polensky, John J. Ciezarek, Franklin A. Hill, and Mrs. Margie E. Metivier. An Air Weather Service group consisting of Capt. Fred W. Pope, M/Sgt. Collon A. Norcross, T/Sgt. William M. Metivier, and Corp. Robert W. Fett took a prominent part in the analysis work, particularly with reference to aviation aspects.

In listing the principal contributors to the results of the Project, it is necessary to go back to those who had the most important part in designing and operating the system of investigation. In determining the general method of approach to the problem, the Project had the counsel of a group of experts appointed by the Chief of the Weather Bureau to serve as a Thunderstorm Advisory Committee. This committee was composed of the following: Mr. Alan C. Bemis, Dr. J. Bjerknes, Dr. C. E. Buell, Mr. C. H. Colvin, Dr. Ross Gunn, Mr. H. T. Harrison, Col. B. G. Holzman, Dr. H. G. Houghton, Mr. D. M. Little, Comdr. R. H. Maynard, Mr. A. F. Merewether, Mr. Dan O'Keefe, Dr. F. W. Reichelderfer, Mr. R. V. Rhode, Dr. C–G. Rossby, Dr. C. F. Sarle, Dr. Harry Wexler, Dr. E. J. Workman. Mr. Ferguson Hall of the University of Chicago served as Field Research Coordinator during the Florida season, succeeded by Fred D. White in the preparation and carrying out of the Ohio observations. Mr. White also held the post of senior analyst for a considerable period of time. During both operation periods Lawrence M. Dye acted as official in charge of administrative and organizational matters of the Project. Mr. C. O. Schick, Executive Officer, handled the administrative reins in Washington, helped in organizing reports of the Project, and supervised their distribution.

The following analysts participated in the evaluation and interpretation of the data at various times: William C. Anderson, Milo J. Andre, James F. Appleby, Werner A. Baum, Ralph A. Berry, John D. Bledsoe, Richard D. Coons, Joyce Corn, Harold W. Dubach, Paul G. Goldberg, Dean A. Jones, Charles K. Nevins, Chester W. Newton, Mrs. Harriet R. Newton, David T. Prophet, Marvin R. Rogers, and James K. Thompson. They were assisted by Jack H. Cheney, John J. Condon, Ralph L. Cutshall, Mrs. Elizabeth H. Celis, Stanley R. Hulsizer, Howard B. Jones, Dorothy I. Krikstanas,

Opal I. Langley, Billy V. Matthews, Robert C. Muffly, John A. Neumann, Lewis W. Porter, Margaret W. Rice, Frank L. Sivard, Margaret V. Supplee, Eugene J. Wenglowski, and Mary Louise White.

In the editing and preparation of the manuscript, unusual, unrewarded efforts were put forth by the editorial assistant, Miss Jean McLain and by the Project secretary, Miss Phyllis Borrelli.

While no individual mention is given to those who took part only in the observation program, it should be pointed out that it was only through their devotion to duty that the Project succeeded. Finally, a great debt of gratitude is due the pilots and crew members who almost daily subjected themselves to unusual flying risks in order to obtain the airplane data which formed the backbone of the studies.

HORACE R. BYERS,
Director, Thunderstorm Project.

DEPARTMENT OF METEOROLOGY
THE UNIVERSITY OF CHICAGO
CHICAGO, ILL.,
May 1949.

TABLE OF CONTENTS

	Page
PREFACE	iii
LIST OF TABLES	vi
INTRODUCTION	
History of the Thunderstorm Project	3
Design of the Observational System	4
Areas of Operations	6
Character of Data Obtained	13
PART ONE. DESCRIPTION OF THE THUNDERSTORM	
Chapter	
I. Thunderstorm Structure and Circulation	17
1. Convection and the Thunderstorm Cell	17
2. Stages of Development of the Thunderstorm Cell	19
3. Temperature Within the Thunderstorm	27
4. Horizontal Inflow and Entraining	31
II. Turbulence and Hydrometeors Within the Thunderstorm	39
1. Thunderstorm Turbulence	39
2. Hydrometeors Within the Thunderstorm	46
III. Thunderstorm Weather Near the Surface	50
1. Thunderstorm Rainfall	50
2. Wind Field Beneath the Thunderstorm	52
3. Temperature Field Beneath the Thunderstorm	60
4. Pressure Field Beneath the Thunderstorm	66
5. Humidity Field Beneath the Thunderstorm	72
6. Development of New Thunderstorm Cells	77
IV. Electric Fields Inside the Thunderstorm	80
V. The Thunderstorm as Disclosed by Radar	90
1. Use of Radar for Cloud Detection	90
2. Vertical Growth and Extent of Thunderstorms	92
3. Horizontal Extent of Thunderstorms	97
VI. Effect of Environment Wind Field on Existing Thunderstorms	101
1. Causes and Effects of Vertical Shear of Thunderstorms	101
2. Movement of Thunderstorms	108
VII. Preferred Areas of Thunderstorm Development	115
1. Topographical Effects	115
2. Geographical Effects	119
VIII. Squall Lines	122
PART TWO. FLIGHT OPERATIONS IN THUNDERSTORM CONDITIONS	
IX. The Thunderstorm as It Affects Airplanes in Flight	133
X. The Thunderstorm as It Affects Ground Operations	141
PART THREE. EXAMPLES	
Introduction	149
July 9, 1946	151
August 6, 1947	175
August 13, 1947	181
August 14, 1947	199
August 17, 1947	235
Squall-line Examples	245
REFERENCES	255
APPENDIX	
1. Surface Instruments	261
2. Upper-air Equipment	267
3. Radar Equipment	270
4. Airplane Instruments	272
5. Photography	279
INDEX	285

LIST OF TABLES

Page

Introduction:

1. Total thunderstorm days in period from 1904 to 1943, inclusive, at selected cities in the United States. (Source: U. S. Weather Bureau, Hydrometeorological Report No. 5.) 8
2. Tabulation of number of flights made and approximate total time of data record obtained at each flight altitude 13
3. Distribution of heights of records obtained from upper-air soundings 13
4. Summary of amount and type of photographically-recorded data obtained from airplane flights, surface observations, and radar equipment 14

Chapter I:

5. Drafts used in temperature study, classified according to type and stage of cell development and source of data.. 29
6. Deviations (° C.) of the maximum (updraft) or minimum (downdraft) draft temperatures from the mean clear-air temperatures for thunderstorms in various stages of development 30

Chapter II:

7. Frequency distribution of updraft speeds measured at various flight altitudes (in thousands of feet) for two seasons of project operation 40
8. Frequency distribution of updraft widths measured at various flight altitudes during two seasons of Project operation 41
9. Frequency distribution of all vertical rates of growth of radar clouds (based on RHI-radar data for Ohio thunderstorms) 41
10. Frequency distribution of downdraft speeds measured at various flight altitudes (in thousands of feet) for two seasons of Project operation 42
11. Frequency distribution of downdraft widths measured at various flight altitudes during two seasons of Project operation 42
12. Frequency distribution of maximum effective gust velocity per 10-second interval of traverse at various altitudes (based upon P-61C flights through Ohio thunderstorms, 1947) 45
13. Frequency distribution of maximum effective gust velocity per 3,000-foot interval of traverse at various altitudes (based upon P-61C flights through Florida thunderstorms, 1946) 45
14. Frequency (N) and percentage distributions of various rain intensities at a given altitude
    (a) Based upon 1946 data from Florida thunderstorms 47
    (b) Based upon 1947 data from Ohio thunderstorms 47
15. Frequency (N) and percentage distributions of various snow intensities at a given altitude
    (a) Based upon 1946 data from Florida thunderstorms 47
    (b) Based upon 1947 data from Ohio thunderstorms 48
16. Frequency (N) and percentage distributions of various hail intensities at a given altitude
    (a) Based upon 1946 data from Florida thunderstorms 48
    (b) Based upon 1947 data from Ohio thunderstorms 48
17. Average speeds for drafts measured at various flight levels during 1947 and the speeds of drafts associated with reports of hail 48
18. Frequency (N) and percentage distributions of various icing intensities at a given altitude
    (a) Based upon 1946 data from Florida thunderstorms 49
    (b) Based upon 1947 data from Ohio thunderstorms 49

Chapter III:

19. Wind and temperature data obtained from soundings made before and after the passage of the cold-air discontinuity over the Ohio surface network stations on June 29, 1947..... 56
20. Mean speeds of the movement of the first-gust line and the component of the first gust normal to the line (for 11 Ohio thunderstorms) 59
21. Mean speeds of the first-gust line, temperature-break line, and the leading edge of the rain area; and the time difference between the occurrence of the first gust and temperature break, and between the first gust and first rain. (Averages computed from all stations for nine Ohio thunderstorms during 1947.) 65
22. Average rainfall rates for designated 5-minute intervals associated with the period of occurrence of a pressure nose. 71
23. Frequency distribution of rainfall rates occurring during the 5-minute interval in which the humidity dip began... 75
24. Frequency distribution of temperature changes which occurred during the time of humidity falls associated with the relative-humidity dip 75
25. Frequency distribution of decrease in mixing ratio associated with the relative-humidity dip 76
26. Number of new echoes which formed per 1,000 sq. mi. per 5 min. in designated areas around parent cells 78

Chapter IV:

27. Relationship of thunderstorm drafts to the electric field (based upon measurements made during airplane flights through thunderstorms in Ohio) 83
28. Frequency distribution of maximum effective gust velocity per 10-second interval of traverse for five low-level flights (based on observations made in Ohio thunderstorms) 84
29. Frequency distribution of electrical potential gradients encountered in five low-level flights (based on observations made in Ohio thunderstorms) 84
30. Frequency distribution of 10-second intervals of flight in positive and negative electric fields, and the mean maximum value of the field in each interval, for several weather conditions and altitudes of flight 86

Page

Chapter V:

31. Comparison of mean and maximum ascent rates of the radar cloud tops between 20,000 and 25,000 ft. with the updrafts measured within the thunderstorm at the 20,000- and 25,000-foot levels by airplanes equipped by the N. A. C. A. 93
32. Summary of characteristics of successive turrets of 32 multi-turreted thunderstorms studied. Data based on observations of Ohio thunderstorms with the AN/TPS–10 radar set 94
33. Frequency distribution of types of turret echoes, classified according to the quarter of the period of vertical growth in which maximum ascensional rate occurred 95
34. Frequency distribution, by types of storm, of the maximum vertical heights of thunderclouds detected by AN/TPS–10 radar 96
35. Frequency distribution of maximum heights reached by the thundercloud echoes from air-mass thunderstorms on particular days 96
36. Ratios of horizontal cross-sectional area covered by radar clouds at any level to that covered at 10,000 ft. (based upon analysis of Ohio thunderstorms detected by the AN/TPS–10 radar set) 99
37. Vertical distribution of the percentage coverage by radar clouds, with assumed coverages for 10,000 ft. 100
38. Vertical distribution of percentage coverage of radar and visual clouds under average and maximum conditions of radar cloud coverage 100

Chapter VI:

39. Summary of characteristics of PPI radar echoes used in study of cloud movement 109
40. Summary of characterstics of radar clouds from available RHI data 109
41. Tabulation of correlation coefficients relating radar cloud movement and various wind parameters 111

Chapter VII:

42. Frequency distribution of the ratio of the number of new echoes per square mile of water to the number per square mile of land for Florida data 116
43. Frequency distribution of the ratio of the number of new echoes per square mile of water to the number per square mile of land with data corrected for the translation of the clouds before detection by the radar set 116

Chapter VIII:

44. Surface weather associated with the passage of 27 squall lines over the Ohio surface network 123
45. Lengths and widths of 11 squall lines observed on the 200-mile radar 'scope during Ohio operations 125

Chapter IX:

46. Percentage of thunderstorm drafts encountered by Project P–61C airplanes which caused altitude displacements of more than 500 ft. (based on N. A. C. A. evaluated records for planes flying various altitudes of traverse during both seasons of Project operation) 137

Chapter X:

47. Frequency distribution of altimeter readings lower than true altitude values due to error resulting from pressure rises (based on surface pressure measurements made beneath Ohio and Florida thunderstorms) 143
48. Frequency distribution of altimeter readings higher than true altitude values due to error resulting from pressure falls (based on surface pressure measurements made beneath Ohio and Florida thunderstorms) 143

Appendix:

49. Listing of camera equipment utilized during the Florida and Ohio Project operations 279

THE THUNDERSTORM

INTRODUCTION

History of the Thunderstorm Project

During World War II, development and research projects were carried out which were aimed at solving problems of bad-weather flying. Fog and low visibility received attention through the development of fog-dissipation systems, or, more particularly, through the perfection of blind-landing methods. Ice formation on aircraft was the subject of intensive investigation, with the result that engineering devices for combating this hazard were greatly improved. A study of precipitation static in all its aspects led to improved methods for alleviating it.

Still uninvestigated at the close of the war was a weather hazard that had caused many serious accidents to commercial and military aircraft, namely, the thunderstorm. The severe turbulence occurring inside most thunderstorms was counted as one of the worst hazards of flying. No longer could the old admonition to stay out of thunderstorms be strictly followed by commercial or military pilots, whose flights could not be restricted to fair weather. In the interests of safety, therefore, information was needed concerning the internal structure and behavior of the thunderstorm. Attempts to obtain such information had been made by the National Advisory Committee for Aeronautics before the war. From a series of flights into cumulonimbus clouds made by an XC–35 airplane, data had been collected which gave some indication of the character of the turbulence in the clouds, but a detailed description of the thunderstorm in all its phases was needed.

Prior to the close of the war, these needs had stimulated the preparation of thunderstorm research proposals. In 1943, Dr. C. E. Buell, Chief Meteorologist of American Airlines, in a letter to the Civil Aeronautics Board, outlined such a project; the Air Transport Association vigorously supported his proposals. Weather Bureau staff members, especially Messrs. A. K. Showalter, L. P. Harrison and H. L. Thompson, studied the program carefully and made specific suggestions on the subject. In January and March 1944, under the Chairmanship of Mr. D. M. Little of the Weather Bureau, a committee of experts from the air lines, Air Force, Navy, Civil Aeronautics Board, University of Chicago, Massachusetts Institute of Technology, Carnegie Institution of Washington, and Weather Bureau met for preliminary planning. Working committees were formed to study the theoretical and laboratory phases, and to formulate a preliminary design of the investigation including a description of suitable field instruments. The Weather Bureau issued a progress report in June 1944 and the main committee subsequently approved a preliminary design of the experiment prepared by Dr. H. R. Byers, University of Chicago, and Mr. L. P. Harrison, Weather Bureau. Early in 1945 the final decision to launch a major project was made and the Weather Bureau by common consent assumed responsibility for organizing the project.

Congress appropriated the necessary funds to the Weather Bureau for making a beginning in the fiscal year starting in July 1945. By August 2, 1945, the Director had been appointed and had reported for duty. Two weeks later the war ended, a circumstance most fortunate for the development of what was by this time officially designated as the Thunderstorm Project. It made possible the release for peacetime use of equipment, airplanes, and personnel to perform thunderstorm investigations on a much more complete scale than up to this time had been considered possible.

To take advantage of this situation and to foster a concerted effort on the part of all agencies able to contribute to the research, the plans for the Project were referred to the Subcommittee on Aviation Meteorology of the Air Coordinating Committee. This subcommittee appointed a working group consisting of Col. B. G. Holzman of the Army Air Forces; Comdr. R. H. Maynard of the Aerology Section, Office of Chief of Naval Operations; and Dr. H. R. Byers, the Project Director, to draw up plans for a coordinated project. At meetings of this working group at Asheville, N. C., and Orlando, Fla., in October 1945, final plans were drawn up and military directives were drafted. Assisting in these deliberations were Dr. (then Maj.) Harry Wexler and Maj. J. O. Fletcher of the Air Forces.

The next step was arranging with the National Advisory Committee for Aeronautics for its Aircraft Loads Division, under Mr. R. V. Rhode and Mr. Philip Donely, to participate in the airplane measurements of turbulence. The formalities of this cooperation were accomplished by Dr. F. W. Reichelderfer, Chief of the U. S. Weather Bureau, through the then director of aeronautical research of the N. A. C. A., Dr. G. W. Lewis.

Meanwhile, the Project Director had arrived at a detailed plan of research operations in consultation

with his colleagues at the University of Chicago, especially Dr. Michael Ference, Jr., Dr. John C. Bellamy, and Mr. Ferguson Hall. Assisting in formulating the general approach to the problem was a group of experts appointed by the Chief of the Weather Bureau to serve as a Thunderstorm Advisory Committee. This committee, the members of which are listed on page v, met to offer suggestions and to give advice periodically throughout the active life of the Project.

At first, plans were made to carry out the observational program in the Middle West where it would be possible to obtain information on different kinds of thunderstorms, both frontal and nonfrontal. After a review of facilities of the Army Air Forces, it was decided instead to divide the operations into two observational phases, one in Florida and the other in a middle-latitude, continental location. Selection of the Orlando, Fla., area for 1946 summer operations was based largely on the existence of exactly the type of Air Forces' facilities and organization that were needed. There was no hesitation in accepting this location, however, because it is in the region of maximum thunderstorm occurrence in North America.

Similar facilities and organization were available by the summer of 1947 in the All-Weather Flying Division of the Air Materiel Command, operating at the Clinton County Air Force Base, Wilmington, Ohio. So, after the 1946 season, the Project was transferred from the jurisdiction of the Proving Ground Command, which handled the Air Force matters at Pinecastle (near Orlando), Fla., to the Air Materiel Command. Twenty-two railroad freight cars transported the equipment, except self-mobile trucks and jeeps, from Florida to Ohio in the winter of 1946–47. Here as in Florida the area selected for operations represented very flat terrain, which was advantageous, since the Project was not prepared to deal with complications produced by mountains or ranges of hills.

In the following pages the system of observations and other details of the field operations in Florida and Ohio are set forth.

Design of Observational System

The observational program was designed as a result of conferences of the Project Director with the Thunderstorm Advisory Committee and with colleagues at the University of Chicago and elsewhere. A review of current ideas concerning thunderstorms indicated that the following elements in thunderstorms were either considered as their main characteristics or as important in reflecting the character and intensity of the thunderstorm processes.

1. Vertical motions (updrafts and downdrafts), considered to be the lifeblood of the thunderstorm, although little was known of the downdraft.
2. Horizontal motions (inflow, outflow, vorticity), recognized as necessary compensations resulting from the vertical motions.
3. Horizontal and vertical temperature gradients, recognized as the determining factors for convective motions.
4. Electrical fields, apparently indicative of thunderstorm intensity.
5. Rainfall distribution and intensity, indicative of the nature and intensity of the thunderstorm.
6. Temperature changes at the ground, indicative of intensity and of the nature of the thermodynamic processes.
7. Pressure changes at the ground, indicative of vertical accelerations.
8. Surface wind fluctuations, indicative of thunderstorm intensity and suggestive of the nature of thunderstorm circulation, related to (2) above.
9. General turbulence or gustiness encountered by an airplane, used as the basic measure of thunderstorm intensity.

Accordingly, plans were made to measure all of these factors and to make a few additional easily obtained observations in and around individual thunderstorms. A review of existing techniques as well as those under development resulted in the decision to obtain measurements of the above-listed characteristics in the following manner:

1. *Vertical motions.*—Photographically recording airspeed and altimeter instruments designed by the N. A. C. A. for use in airplanes were available and could provide a measure of updrafts and downdrafts. For flights at constant power settings the altitude changes induced by the pilot could be inferred from the airspeed trace, and further checks could be obtained through use of control-position recorders and radio altimeters. It was also decided to continue the development of balloon-borne vertical airspeed indicators, being carried on at the University of Chicago, since some aeronautical experts had advised that the airplane might be unsuitable as a probe for thunderstorms because of the great dangers involved in making the flights. The airplanes proved highly satisfactory for this purpose, however, and the balloon-borne in-

strument development encountered technical difficulties retarding its ultimate use so that very little was done with it; hence, the airplane data provided the principal information concerning vertical motions.

2. *Horizontal motions.*—Carefully tracked balloons, released simultaneously from a number of stations within and around each thunderstorm, were decided upon as the best means of obtaining a measure of the disturbance in the horizontal wind flow caused by the thunderstorm. For this purpose two systems were available: the radio-direction finding equipment for use with radiosondes (rawinsondes) and a radar-tracking system for target-equipped balloons (rawins). Since technicians had disagreed concerning the relative merits of each type, it was decided to use some of each. Six SCR–658 rawinsonde stations were agreed upon for the surface network and four, later five, rawin stations. In view of doubts concerning the possibility of tracking the radar balloons inside thunderstorms, it was decided to place radar-wind-finding stations on the outer periphery of the network. This proved to be a wise decision, since for thunderstorms over the network the radar balloons were mostly outside the region of strong radar cloud echo.
3. *Horizontal and vertical temperature gradients.*—Vertical temperature gradients could be measured by the conventional radiosondes, and in a close network, with simultaneous releases some ideas of the horizontal gradients could also be obtained in this way. However, for precise determination of temperature contrasts in all parts of the thunderstorm, it was decided to equip the airplanes with sensitive, recording, temperature instruments which were in the process of development. This development was completed in time for use in most of the Florida flights, but it was not until the 1947 season in Ohio that a suitable housing for the sensing element was obtained.
4. *Electric field.*—Airborne electric field meters developed by the Naval Research Laboratory were selected and ordered for installation on the airplanes, but they were not delivered in time for use in the Florida observations. Attempts to obtain equipment for ground recordings of the electric field fell short of expectations, but fairly complete work on this particular aspect of thunderstorms was and still is being carried on elsewhere.
5, 6, 7, 8. *Surface rainfall, temperature, pressure and wind.*—In order to obtain a continuous record of these elements, a surface micronetwork of 55 stations was planned. In Florida these were set up with a spacing of 1 mi. between stations, and in Ohio the same number of stations was spread out with a 2-mile separation. These stations were to be equipped with the following instruments, attended by observers who serviced them and changed the record sheets daily:
   (a) Weighing rain gage, with sensitivity increased by enlarging the mouth to 2½ times the usual size and using a 6-hour clock drum.
   (b) Hygrothermograph contained in a Cotton-Region-type shelter, placed on a 12-hour drum gear.
   (c) A sensitive barograph operating on a 12-hour drum.
   (d) Gust-recording anemometer and wind vane, magneto- and battery-operated respectively, each operating a recording milliameter. Owing to late delivery of this equipment, double-register recordings for conventional cup anemometers and vanes had to be used during most of the Florida season.
9. *Gust measurements.*—The well-developed technique of the N.A.C.A. was adopted, using, in addition to the airspeed-altimeter recorder mentioned above, a photographically recording accelerometer.

The problem of tying all of these data together to obtain a unified picture of each thunderstorm required exact radar tracking or radio-direction finding in connection with planes and instruments. To have the radar link connect all of the measurements required that the location of the thunderclouds be precisely determined by means of the echoes reflected from them and photographed; and that the airplanes in flight be located in time and space with respect to the thunderstorm. The latter was accomplished by fitting the airplanes with beacons which registered on the radar 'scope. In addition, of course, special means of time synchronization were necessary.

Successful completion of such a plan of operations required the full cooperation, with the U. S. Weather Bureau, of the U. S. Air Force, U. S. Navy, the National Advisory Committee for Aeronautics, and other agencies.

Selection and instrumentation of an airplane.—Selection of the airplane to be used to fly the thunderstorms was a result of consideration of both safety

factors and instrument needs. There were a number of requisite qualities. As for size, the result of a conference with the responsible Air Force officers was the decision that the airplane to be used must carry not more than a bare minimum of personnel; it must thus be fairly small but, on the other hand, there had to be room for the various instruments and the radar if it was not already installed. Insofar as was possible, it was planned to install self-recording instruments or photographic equipment for the instrument readings. For maximum safety, the selected plane had to be relatively slow but structurally sound in case of high speeds. It had to be stressed sufficiently and be stable enough to successfully navigate the storms selected for study. It was necessary also that it have a high service ceiling, to make the study of storms at high altitudes possible; and a high rate of climb so that it might reach the flight altitude rapidly. Its range and available flight time had to be great enough to allow completion of a mission with sufficient fuel remaining to take the pilot and crew to another field in the event of closed weather conditions at the home field. In addition, high wing loading was desirable; and finally, the planes should be easy to procure and have a low maintenance rate.

The P–61C, or Black Widow, manufactured by the Northrup Aircraft Co., had these desirable qualities. Since the Air Force had previously used some of these planes in weather reconnaissance squadrons, which were disbanded following the war, some were available. The Air Force provided ten P–61C's, a number sufficient to insure that five would be available for each flight. It was planned that five planes, flying at 5,000, 10,000, 15,000, 20,000, and 25,000 ft. (m.s.l.), respectively, would be used in each flight.

Although considerable doubt was expressed in many quarters concerning the desirability, from the safety viewpoint, of making experimental flights into thunderstorms, it was decided to inquire among highly competent instrument pilots of the Air Force for volunteers for this work. The response was extremely gratifying and brought to the Project experienced crews, most of whom had served as instrument flight instructors. Since it was decided to make use of the SCR–720 radar installed in the P–61C's, each crew was to consist of a pilot and a radar officer. Following the great success of these flights in the Florida season, it was decided to add a weather observer to the crew for the Ohio flights. The details of the airplane instrumentation are described in the appendix (4).

The possibility of using sailplanes for the measurement of up- and downdrafts which occur in thunderstorms appeared to be very promising. A group from the Soaring Society of America volunteered to make sailplane flights into thunderstorms for the Project. These aircraft were equipped with a somewhat reduced number of instruments similar to those used on the airplanes. Although some sensational thunderstorm flights were made in the Florida season, the airplanes proved to be so useful and practical that for the Ohio season the sailplane part of the program did not appear to be necessary and was therefore eliminated.

For the Ohio operations an AT–6 was instrumental for obtaining measurements inside growing cumulus clouds.

Areas of Operations

PHASE I — ORLANDO, FLA.

The field measurements and observations for the first phase of the Thunderstorm Project were carried out near the center of the Florida peninsula, in the vicinity of Orlando (fig. 1). This location was selected because of the very adequate Army and Navy facilities in the area, combined with the circumstance of North America's highest frequency of thunderstorm occurrence. Since use of a fixed network requires high thunderstorm frequency if measurement of very many storms is desired, this latter point is important.

Climatology of the Florida area.—Interpolation based upon 40 years of record from nearby first-order Weather Bureau stations gives the number of about 80 days with thunderstorms, per year, for a station in the vicinity of Orlando, Fla. Actual records may prove this figure to be higher. These thunderstorms have a more pronounced maximum during the summer months (table 1), as well as in midafternoon (fig. 2) than at most locations in the United States. Relatively few of them can be classified as night storms. Frontal activity is rare in the summer months, with tropical maritime air covering the peninsula most of the time. Byers and Rodebush [**21**] have shown that the thunderstorms are associated with horizontal convergence resulting from sea breezes entering the peninsula from both sides and only rarely are associated with fronts or large-scale disturbances.

FIGURE 1.—Map of Florida showing Orlando and the area of operations for the summer of 1946. The location of the control radar set is indicated.

One objection to the Florida area from the standpoint of storm study is that very few hailstorms occur, at least at the surface. However, the advantage of storm frequency in the area exceeds this disadvantage.

Physiography of the Florida area.—Thunderstorm Project operations in Florida were conducted near the border of the Florida Lake Region (sometimes called Upland of Central Florida) and the broad, flat, sandy Sea Terrace of the East Coast. The topography of the lake regions has been largely determined by solution of the Ocala (Eocene) limestone and the somewhat less soluble. overlying Hawthorne (Miocene) limestone layers. The result is a terrain that is gently rolling, with many small ridges reaching approximately 100 ft. above sea level. The surface of this region is covered with sand or a very sandy soil. The main control radar was situated on one of these low sand-covered hills.

Most of the surface network was in the district more properly called the Sea Terrace of the East Coast, which at this point extends approximately 60

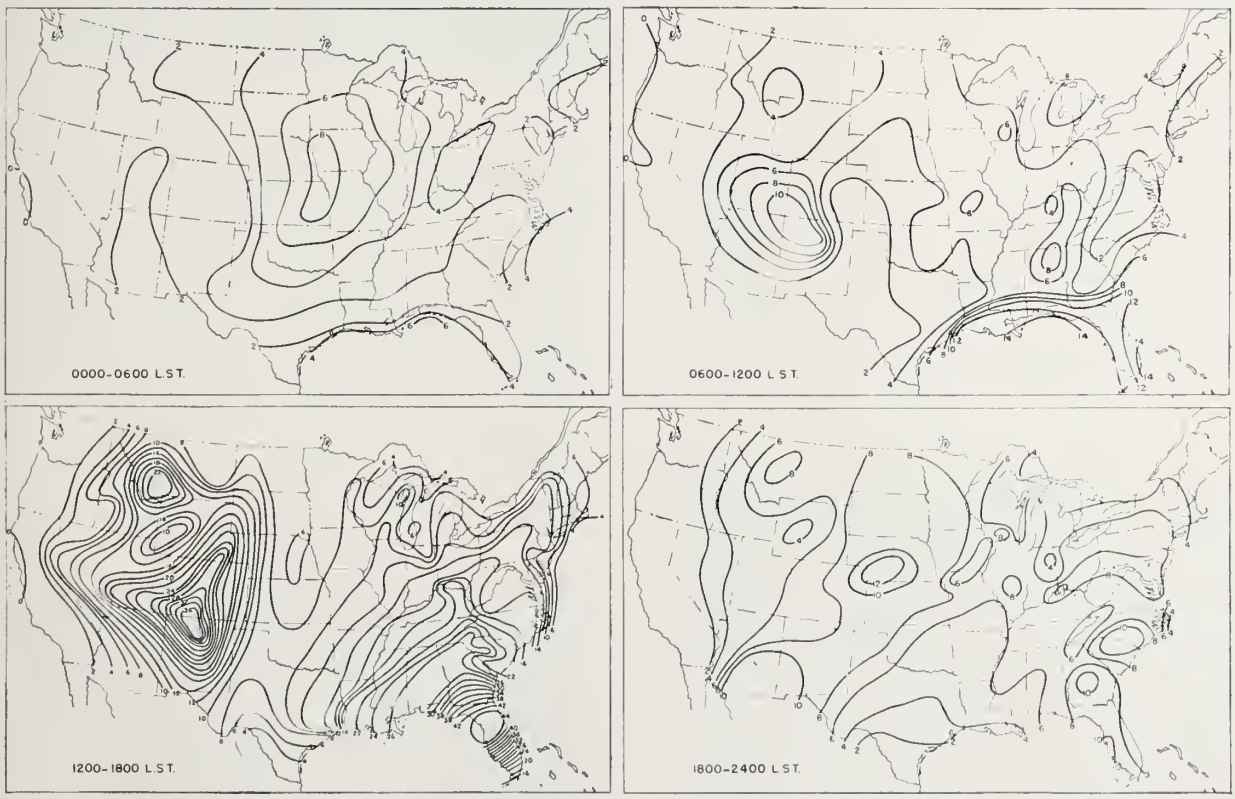

FIGURE 2.—Charts showing the average number of thunderstorms reported during the four quarters of the day for June, July, and August. Isopleths have been geometrically smoothed and, while not representative of local frequency differences, are fairly reliable for large-scale differences in frequency. Data used are 20-year averages (1906—1925) from 192 reporting stations. (Charts taken from U.S. Weather Bureau Hydrometeorological Report No. 5 [55].)

841051—50——2

TABLE 1.—*Total thunderstorm days in period from 1904 to 1943, inclusive, at selected cities in the United States (Source: U. S. Weather Bureau, Hydrometeorological Report No. 5)*

Station	January	February	March	April	May	June	July	August	September	October	November	December	Annual average
Amarillo, Tex.	7	9	34	111	260	273	291	283	158	98	17	2	39
Atlanta, Ga.	32	64	150	169	260	435	534	426	186	36	26	30	59
Boise, Idaho	4	7	30	51	121	115	129	103	69	23	9	4	17
Boston, Mass.	4	4	31	42	112	153	200	165	79	19	5	7	21
Cheyenne, Wyo.	0	0	6	100	288	457	548	468	188	38	0	0	52
Chicago, Ill.	14	21	89	133	223	306	288	273	184	75	37	3	41
Cincinnati, Ohio	24	31	128	161	284	368	431	313	200	72	27	18	51
Cleveland, Ohio	9	22	73	114	201	263	314	225	163	81	27	7	37
Columbus, Ohio	17	28	112	146	250	378	389	276	164	57	32	10	46
Duluth, Minn.	2	3	13	50	146	260	274	232	133	45	11	0	29
El Paso, Tex.	9	14	27	48	112	197	370	375	151	88	18	11	35
Hatteras, N. C.	32	48	96	125	188	250	316	264	147	49	40	31	40
Havre, Mont.	0	0	5	24	111	295	282	213	73	6	0	0	25
Jacksonville, Fla.	41	75	122	164	315	556	752	637	336	86	21	33	78
Key West, Fla.	45	59	77	121	204	376	510	510	478	178	40	49	67
Little Rock, Ark.	68	87	192	278	285	372	368	324	184	99	83	60	60
Los Angeles, Calif.	22	26	43	29	16	10	6	16	19	21	8	20	6
New Orleans, La.	79	97	154	194	265	457	627	603	316	94	48	73	75
New York, N. Y.	12	17	39	89	188	268	332	216	117	47	22	9	35
Omaha, Nebr.	4	9	54	138	279	386	343	346	234	101	26	4	48
San Antonio, Tex.	32	53	117	201	279	175	222	159	176	92	49	32	40
San Diego, Calif.	18	11	14	8	6	11	19	24	10	15	12	14	4
San Francisco, Calif.	10	19	7	9	3	3	1	6	5	7	5	9	2
Santa Fe, N. Mex.[1]	5	11	40	91	261	366	724	625	285	97	16	1	66
Sault Ste. Marie, Mich.	1	2	26	55	101	166	180	168	142	73	18	1	23
Seattle, Wash.	3	4	14	17	31	45	28	31	34	24	12	7	6
Tampa, Fla.	43	60	104	138	319	652	870	799	517	123	22	29	92
Washington, D. C.	7	24	53	105	207	300	346	253	138	39	17	10	37

[1] 38 years of record.

FIGURE 3.—Florida surface network station 18. Note the pine forest in the background.

FIGURE 4.—Florida surface network station 10. The grassy meadow was formed by the receding water of Lake Tohopekaliga.

FIGURE 5.—Florida surface network station 36. The low brush is typical of many of the station locations.

to 70 mi. inland. This terrace is very flat, sandy, and, in this region, characterized by numerous swamps and small lakes. The natural vegetation in the network area was characteristically a light stand of pine with a sparse undergrowth of low shrubs and brush. In the swamp areas cypress groves were common. Much of the western and central parts of the network have been cleared of their pine forests and are now used for grazing purposes. The photographs of figure 3, station 18; figure 4, station 10; and figure 5, station 36, illustrate the type of terrain and vegetation characteristic of the surface network area[1].

Physical layout of the operations area.—The surface network for the Florida operations was approximately rectangular, with the long axis lying east-west. There were 55 surface stations spaced in a grid fashion with a separation of 1 mile, insofar as the terrain, vegetation, and roads would permit. Each station was equipped with instruments for measuring the surface wind, temperature, rainfall, relative humidity, and pressure. The surface stations were numbered 1 through 55 (shown in fig. 6). At six of the regular surface stations (9, 20, 26, 40, 51, 54) was located SCR-658 rawinsonde equipment. Surrounding the network were four auxiliary stations having the 584 radar which provided wind measurements. The stations were serviced daily by motorized observers who were based at station 26, in St. Cloud. Figure 7 shows the general view of station 26.

The airplanes were based at Pinecastle Army Air Base, approximately 13 mi. north of St. Cloud and 9 mi. southeast of Orlando. The main control radar was located at Orlo Vista, about 25 mi. northwest of St. Cloud. Located at this site were the large search radar used to track the airplanes and to spot and identify the thunderstorms, and the range-height radar used to secure records of the vertical dimensions of the thunderstorm.

The focal point of the Florida operations was the Project headquarters at Orlando Army Air Base. Here the directing personnel and administrative offices were located, as well as the supply center, instrument-repair center, records checking unit, records file, and temporary living quarters for many of the Project personnel. Army activities at Orlando Army Air Base, required to keep the Project operating, necessitated that Project headquarters be there.

Banana River Naval Base is situated approximately 42 mi. east of St. Cloud. Active liaison between the Project and the Banana River Base was required during the summer operations.

PHASE II—WILMINGTON, OHIO

The second phase of observations and measurements was conducted in a middle-latitude continental region during the summer of 1947. Again it was the location of Army facilities that was the deciding factor in choosing Wilmington, Ohio, as the precise operations area (fig. 8). At Clinton County Air Force Base in Wilmington is the All-Weather Flying Division, Air Materiel Command, an organization and facility well suited for this type of project. The Base is also close to the large Air Force supply installation at Wright Field, Dayton, Ohio. In moving the observations area from Florida it was realized that fewer storms would occur in Ohio and consequently it would be harder to secure representative data. On the other hand, squall-line and cold-frontal storms do not occur in Florida, making it imperative that further research be conducted in a more northerly latitude.

Climatology of the Ohio area.—With the 40 years (1904 to 1943) of record from first-order station data, interpolation gives an average of about 50 days with thunderstorms per year in the vicinity of Wilmington, Ohio (table 1). Contrasted with the storms of the

[1] There is available, on loan to anyone making use of the Project measurements for further research, a photographic record of the exposure of each surface station.

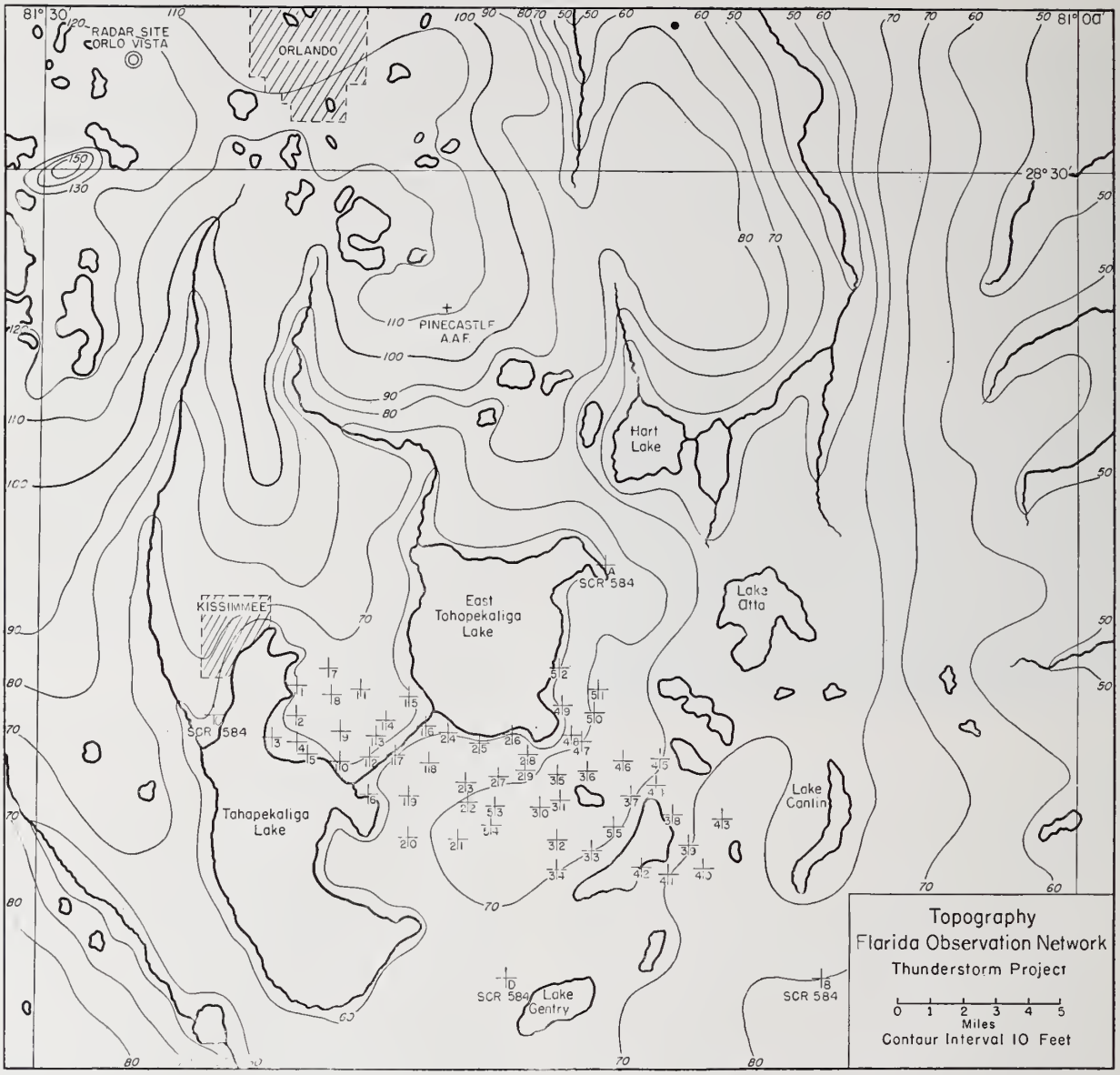

FIGURE 6.—Topographic map of the Orlando-Kissimmee, Fla., area showing the locations of the surface network and outlying stations. Contour lines, lakes, and water courses are shown.

Florida area, those in Ohio are more scattered through the day (fig. 2) and through the year, but there are definite summer and late-afternoon maxima. Ohio is east of the belt of true "night" thunderstorms; most of the night storms in Ohio are associated with frontal activity.

Hail is observed at the surface in approximately 5 percent of the Ohio thunderstorms. It is thus evident that the Project measurements are not representative of the region of hail maximum for the United States, located farther west in the Great Plains.

Physiography of the Ohio area.—The terrain of the Ohio surface network area results from the fact that once it was near the southern limit of the Great Wisconsin Ice Sheet, which dumped enormous quantities of till material on a surface eroded into the roughly north-south striking Devonian and Mississippi sediments flanking the east side of the Cincinnati Arch. The northern end of the network was established on the so-called "Till Plain." Here only occasional low ridges of morainic origin interrupt the otherwise nearly flat surface. The main control radar was sit-

FIGURE 7.— A view of station 26 of the Florida surface network showing supply and office buildings. This station was used as the headquarters for the field staff.

FIGURE 8.—Map of Ohio showing Wilmington and the area of operations for the summer of 1947.

uated on one of the higher moraine ridges just southeast of Jamestown. In the southeastern part of the network the glacial material is much thinner, with the result that streams flow in preglacial valleys and the topography has a rolling to locally hilly nature.

Throughout the area drainage is not a problem, and much of the land is tilled. In the hilly southeastern part of the network, woodlands of deciduous trees are standing, while the remainder is largely cleared. Figure 9, a photograph taken near station 42, and figure 10 (station E) illustrate the type of terrain and vegetation in the Ohio surface network. Between some of the stations in the southern sector, the terrain is

FIGURE 9.—A scene near station 42 of the Ohio surface network showing the nature of the terrain and vegetation.

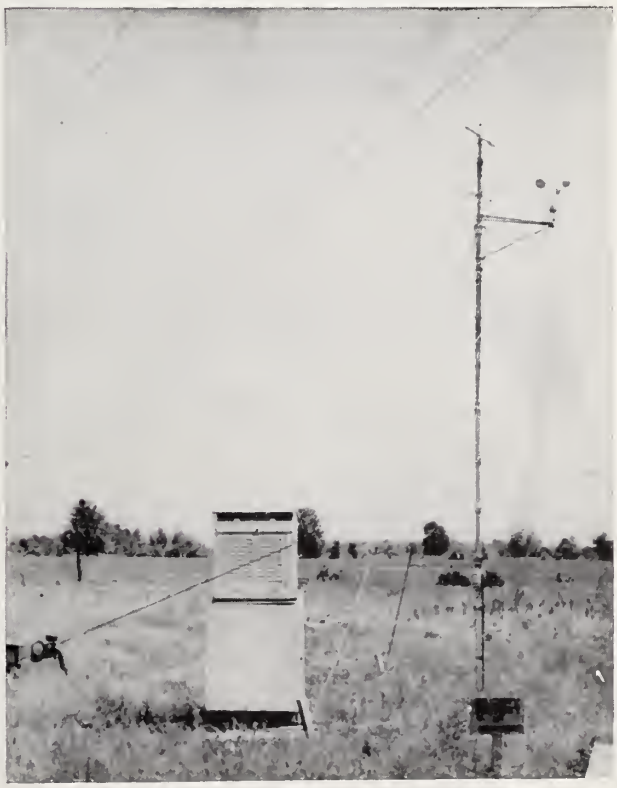

FIGURE 10.—Ohio surface network station E. This flat pasture area is typical of many of the station locations. The guy wires in the foreground support a radio antenna.

FIGURE 11.—Topographic map of the Wilmington, Ohio, area showing the locations of the surface network and outlying stations. Contour lines and water courses taken from U. S. Geological Survey Map of Ohio, edition of 1917, reprinted 1941.

more broken than indicated in these photographs. Station sites were selected to minimize any effect of terrain.

Physical layout of the operations area.—The surface network in Ohio extended as a large rectangle with the long axis north-south, (fig. 11). There was a 2-mile separation between surface stations instead of 1 mile as was used in Florida. This increase in spacing between stations was decided upon in order to make the available stations cover a larger area, and from indications from the Florida data that a wider spacing might not be detrimental. The instrumentation was essentially the same as was used in the Florida operations, and the numbering system was similar. Stations 7, 19, 39, 47, C, and E were equipped with SCR–658 rawinsonde equipment in addition to regular surface instruments. The 584-radar stations were located at the corners of the network in a fashion similar to that of Florida.

The airplanes were based at Clinton County Air Force Base, approximately 4 mi. north of the northern edge of the network, where the administrative offices, supply center, and other Project functions were established.

There was considerable delay in preparing the main-control radar for operation, so early operations were conducted, using for control a partially satisfactory radar already installed at Clinton County Air Force Base. On July 11, 1947, control was moved to the main-control installation on a slight hill southeast of Jamestown (approximately 17 mi. north of Clinton County Air Force Base). Also located there was the range-height radar for studying the vertical dimensions of the thunderstorm.

Character of Data Obtained

The surface network in Florida operated from May 1, 1946, through September 20, 1946. During this time there were 179 periods in 111 days when rain was recorded at 10 or more of the surface network stations. From these cases of rain, 91 were selected for study because they were identified as due to convection and data on them were sufficiently detailed to warrant their analysis. During the Ohio observations program the surface network was operated from May 17, 1947, through September 22, 1947. Of the thunderstorms which passed over the surface network during this time, 88 were selected for study.

During both seasons of observations the airplane flights through thunderstorms were made at altitude separations of 5,000 ft., with the lowest level of flight at 6,000 ft. (m.s.l.) in Florida, and at 5,000 ft. (m.s.l.) in Ohio. Insofar as was possible, five airplanes were used on a mission, each flying at a particular altitude level and making as many traverses through the thunderstorm as was possible. The number of traverses depended primarily upon the availability

TABLE 2.—*Tabulation of number of flights made and approximate total time of data record obtained at each flight altitude*

Flight altitude (ft. m.s.l.)	Number of days flown	Number of traverses	Total record time (min.)
FLORIDA			
26,000	23	81	311
21,000	33	115	461
16,000	34	128	490
11,000	34	131	576
6,000	23	96	446
OHIO			
25,000	22	111	245
20,000	30	164	388
15,000	31	208	533
10,000	34	217	521
5,000	21	112	247

TABLE 3.—*Distribution of heights of records obtained from upper-air soundings*

Altitude interval (ft.)	Number of releases reaching given altitudes	
	Rawinsonde (SCR–658)	Rawin (SCR–584)
FLORIDA		
0–9,999	55	15
10,000–19,999	39	37
20,000–29,999	48	35
30,000–39,999	46	63
40,000–49,999	88	103
>50,000	153	36
Total number of releases.	429	289
OHIO		
0–9,999	14	9
10,000–19,999	41	33
20,000–29,999	40	41
30,000–39,999	54	64
40,000–49,999	[1] 294	40
>50,000		27
Total number of releases.	443	214

[1] Evaluation of the rawinsonde soundings taken during the Ohio operations was not carried above the 40,000-foot level due to lack of personnel. In no case, however, was the tracking of the instrument discontinued before losing the signal due to interference, weak signal, etc.

TABLE 4.—*Summary of amount and type of photographically recorded data obtained from airplane flights, surface observations, and radar equipment*

Source and description of photographs	Exposure interval	Size of film	Amount of film
FLORIDA OPERATIONS			
CONTROL RADAR			
PPI 'scope indicating thunderstorm echoes	10 sec. during airplane operations... 2½ min. when planes were not in air.	35 mm.	1,100 ft.
PPI 'scope indicating plane positions	10 sec.	35 mm.	900 ft.
RHI 'scope indicating thunderstorm height	Variable	35 mm.	700 ft.
AIRPLANES IN FLIGHT			
Instrument panel	(5⅓ frames per sec.)	16 mm.	3,800 ft.
SCR–718 radio altimeter	½ sec.	16 mm.	4,500 ft.
SCR–720 airborne radar	4 sec.	16 mm.	1,350 ft.
Cloud pictures (taken by flight crews)		5 x 5 in.	300 pictures.
SAILPLANES IN FLIGHT			
Instrument panel	½ sec.	16 mm.	3,700 ft.
GROUND NETWORK STATIONS			
Cloud pictures (time-lapse)	10 sec.	16 mm.	2,800 ft.
Cloud pictures (still photographs)		5 x 5 in.	700 pictures.
OHIO OPERATIONS			
CONTROL RADAR			
PPI 'scope indicating thunderstorm echoes	2 min. (about)	35 mm.	4,400 ft.
PPI 'scope indicating plane positions	10 sec.	35 mm.	1,300 ft.
RHI 'scope indicating thunderstorm height	[1]2 sec.	35 mm.	11,100 ft.
AIRPLANES IN FLIGHT			
Instrument panel	¼ to ⅛ sec.	35 mm.	83,500 ft.
Radio altimeter and airborne radar	2½ sec.	35 mm.	18,000 ft.
AT–6 FLIGHT IN CUMULUS CLOUDS			
Instrument panel	¼ sec.	35 mm.	1,250 ft.
GROUND NETWORK STATIONS			
Cloud pictures (time-lapse)	6 sec.	35 mm.	1,100 ft.
Cloud pictures (still photographs)		5 x 5 in.	2100 pictures

[1] The RHI was operated on a "sector-scan" basis. The time between successive 'scope pictures during an azimuth sweep was 2 sec. There was an elapsed time of 1 to 3 min. between successive azimuth sweeps.

of film in the data-recording cameras. All but two of the flights were made into daytime storms. The first mission of the Florida operations was on June 27, 1946; the last, on September 18, 1946. The first mission of the Ohio operations was on May 13, 1947; the last, on September 15, 1947. During these indicated intervals, 38 days' flights, or missions, were flown in both Florida and Ohio. Table 2 shows the number of flights and traverses at each particular level of flight for which data were obtained.

A total of 824 rawinsonde and 503 rawin soundings also was made during the two seasons of operations. These observations were divided between periods of prior to, during, and after thunderstorm development[2]. Table 3 shows the height distribution of the records obtained and evaluated for the total number of balloon releases made.

Data from instruments located inside the airplanes, from the radar equipment, and from certain surface installations were photographically recorded by cameras described in the appendix (5). Table 4 summarizes the types of data obtained and indicates the total amount of photographic film obtained for each as well as the interval which elapsed between successive exposures of the film.

[2] See appendix (2).

PART ONE. DESCRIPTION OF THE THUNDERSTORM

CHAPTER I. THUNDERSTORM STRUCTURE AND CIRCULATION

1. Convection and the Thunderstorm Cell

The thunderstorm represents a violent and spectacular form of atmospheric convection. In its method of development it appears to be a cumulus cloud gone wild. Lightning and thunder, usually gusty surface winds, heavy rain, and occasionally hail, accompany it[3]. These phenomena are indicative of violent motions and complex physical processes going on within the cloud.

Nature of convection.—In principle, convective overturning in the atmosphere is similar to that occurring in a layer of fluid made thermally unstable by the addition or subtraction of energy from a localized area. Extension of laboratory results to the atmosphere in order to explain convective clouds and thunderstorms has been attempted at various times since the now classical paper (1901) by Henri Bénard [**7**] called attention to the cellular nature of convection patterns within an unstable layer of liquid. The basic principle of the convection patterns noted by Bénard can be observed in an easily reproduced demonstration. If a thin layer of metallic paint, having as its vehicle a volatile liquid, such as benzine, is placed in an open dish or tray, it will develop a definite and regular pattern of convective motion as evaporation cools the liquid from the top surface[4]. This patterned convection appears in the form of prismatic polygonal cells, usually roughly hexagonal in shape, when a steady state is obtained. The diameter of the cells is approximately three times their depth, so that if the depth of the liquid varies, cells of various diameters are present. The motion within these cells, made visible by the suspended metallic particles, is upward in the center, radially outward at the top, and downward around the periphery, with the maximum downward motion taking place along the vertical lines forming the common boundary of three, adjacent, hexagonal prisms. A vertical cross section through the center of one of these cells would show a streamline pattern as given in figure 12.

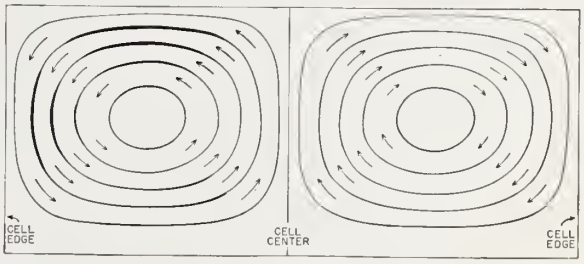

FIGURE 12.—A vertical cross section through the center of a convection cell. Solid curves represent streamlines and arrows show the direction of motion.

If horizontal motion is superimposed upon the circulation pattern produced by convection in the fluid under discussion, the hexagonal cells are replaced by pairs of horizontal rolls, or vortices, rotating in opposite directions. A cross section perpendicular to the direction of flow would show a streamline pattern similar to the one given in figure 12, with the upward motion occurring between the two adjacent rolls.

Brunt [**13**], Phillips and Walker [**40**], Mal [**36**], Chandra [**22**], Graham [**25**], and others proceeded from the observations of liquids to the observations of gases, wherein similar convective circulation patterns were noted. However, one important difference observed between circulation patterns of liquids and of gases is a reversal in the direction of motion in a gas, the cell having a downward movement in the center and an upward movement around the periphery[5].

It is of fundamental importance to recognize in these laboratory demonstrations that there is a net transport of fluid upward in some regions and a net transport downward in other regions and that the

[3] For reporting purposes, the thunderstorm has been defined as "thunder and lightning observed at station, i.e., with not more than 10 sec. difference of time between sight and sound."—English text of resolutions adopted at International Meteorological Committee meeting, 1937, Salzburg.

[4] This effect, first recorded by Weber [**59**] in 1885 may also be produced by uniform heating of the bottom of the layer. A review of mathematical treatments by Rayleigh, Jeffreys, and others, has been published by Stommel [**53**].

[5] In layer clouds, configurations have often been observed which have been interpreted as showing that either type of motion may exist in the atmosphere [**13**].

regions of net upward and downward flow are joined by radial flow from the top of the updraft and the base of the downdraft. It may be said that these conditions are typical of convective circulations established in any fluid layer.

Convection in the atmosphere.—As the atmosphere becomes unstable, regardless of cause, it too undergoes convective overturning. It is reasonable to assume that, under the proper conditions, the convection cells of this overturning would form a regular pattern. However, because of a different set of boundary conditions, the nonuniform character of the atmosphere, and the release of energy through the phase change of water at the condensation and freezing levels, the steady-state convection cells produced in the laboratory are rarely, if ever, duplicated in atmospheric layers as deep as those involved in the development of cumuliform clouds. Instead, in the areas which would correspond to the rising core of the cell produced in the laboratory, cumulus and cumulonimbus clouds are set off. As a result, the atmosphere is in such a disturbed state that the identity of the original convection cell is largely obscured.

Among the observed differences between convection patterns in the atmosphere and those produced in the laboratory is the spacing of the areas of net upward and downward flow. Instead of the regular pattern (fig. 13) of the laboratory, the convection pattern of the atmosphere may resemble that of figure 14(a) during random air-mass convection conditions, and that of figure 14(b) during squall-line conditions. In the latter two examples, the upflow areas are not of equal size, and it is impossible to designate downflow areas as accompanying specific areas of upflow. It is possible that the downflow does not extend throughout the entire region between upflow areas.

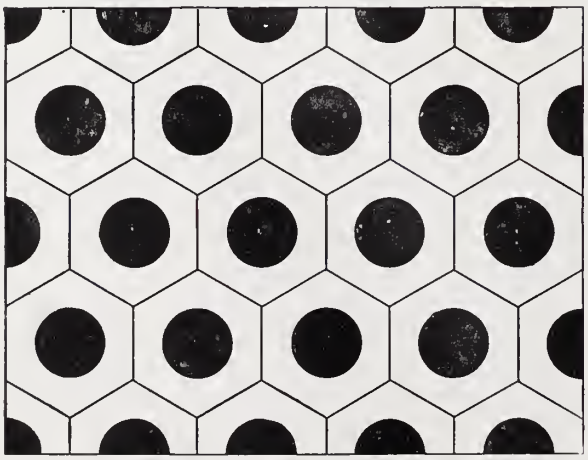

FIGURE 13.—Schematic diagram of cells in a fluid undergoing regular convection. Each hexagon represents a convection cell in which the white area indicates net downward motion and the black area indicates net upward motion.

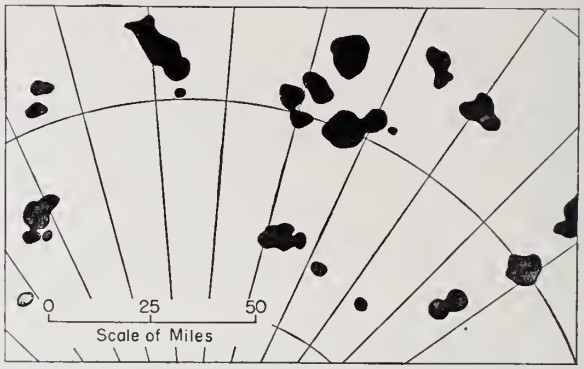

FIGURE 14(a).—Schematic representation of actual radar echoes on a day of random air-mass thunderstorms. The black areas (storm echoes) are regions of net upward motion and the white area is a region of net downward motion. The radial lines and the arcs indicate the azimuths and ranges from the radar site.

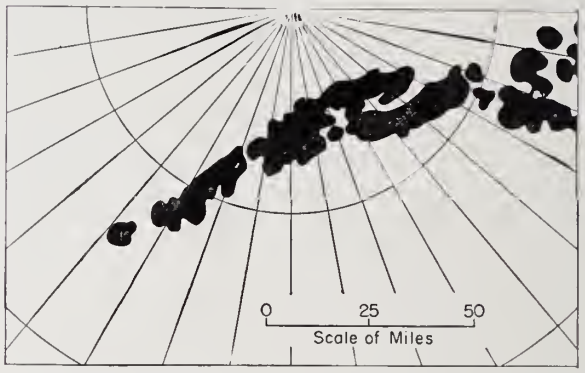

FIGURE 14(b).—Schematic representation of actual radar echoes on a day of squall-line thunderstorms. The black areas (storm echoes) are regions of net upward motion and the white area is a region of net downward motion. The radial lines and the arcs indicate the azimuths and ranges from the radar site.

It has been fairly well established, however, that the downflow spreads over an area many times larger than the areas of upflow. Since continuity must prevail over long periods of time, mean upward speeds are much greater than mean downward speeds. Actually, the compensating downward motion is very slow. It will be designated in this discussion as the "return settling," in order to distinguish it from the strong downdraft which develops within the thunderstorm itself.

In contrast to the active cumulus development in the regions of vigorous or sustained updrafts, the areas of return settling are cloudless or have only low clouds and growth-arrested cumuli. Therefore, the interest of the meteorologist has concentrated on the cumulus congestus and cumulonimbus clouds present in the areas of net upward flow.

Once these clouds have formed, the energy released through the phase changes of the water within them exceeds the energy of the simple "Bénard Cell"-type convective motion. As a result, in the region of *net* upward flow, updrafts become localized into areas of relatively small cross section where some perturba-

ation proves especially favorable for their initiation. This release of energy accounts for a very important thermodynamic difference between the convective currents of the cumulonimbus and the circulations produced in the laboratory. Since, in the cloud, this energy is released continuously as the air rises, the specific momentum of the air is continually increased. In the laboratory models thus far produced, this has not been true. However, as air rises in updrafts, there is an outflow at the top and downward motion in the surrounding environment much the same as in a laboratory demonstration.

The thunderstorm cell.—Under favorable conditions, each of the individual updraft areas forming as described above develops into a unit of convective circulation characteristic of a thunderstorm. Many of these units are initially detectable as separate echoes appearing on a radar 'scope. Also, if interpreted in terms of like stage of development, observed conditions—of both surface weather elements and of drafts, turbulence, and weather conditions encountered in flying through these convection units—are found to repeat themselves. This leads to the fundamental concept that in the thunderstorm there are convection units having similar properties and characteristics and which are therefore capable of analysis as a class of convection phenomena. These units, or subdivisions, are called thunderstorm cells and are defined as regions of localization of convective activity within the thunderstorm. Just as in the laboratory experiments with fluids, where it is found that the cellular circulation frequently does not extend throughout the medium, portions of the thunderstorm cloud often cannot be identified as separate cells, nor can they be considered as parts of other, well-defined cells. Occasionally such cloud is stratiform in character, and when sufficient observations are available to so identify it, its elimination from consideration in a study of the active circulation units of the thunderstorm follows as a matter of course.

Use of the term cell, as applied to these convection units, is not new; many previous investigations have indicated that there are subdivisions within a thunderstorm. However, there has been some confusion concerning the use of the term, since the identifying features of the units depended upon the nature of the particular investigation. Workman, Holzer, and Pelsor [**63**], for example, in studying the electrical effects of the thunderstorm reported that ". . . examination of the . . . (data) . . . lead(s) to the following interpretations. In any extensive and well-developed storm, several strong updrafts may exist. These regions have a certain dynamical stability, may exist for periods in excess of half an hour, and tend to move with the body of the storm." From a study of thunderstorm rainfall, Brancato [**9**] concluded that thunderstorms occur in groups or families. The detailed and more comprehensive observations made by the Thunderstorm Project have permitted the identification and study of the individual cells.

2. Stages of Development of the Thunderstorm Cell

The life cycle of the thunderstorm cell is divided naturally into three stages depending upon the direction and magnitude of the predominating vertical flow. They are:

1. Cumulus stage—characterized by updraft throughout the cell.
2. Mature stage—characterized by the presence of both updrafts and downdrafts at least in the lower half of the cell.
3. Dissipating stage—characterized by weak downdrafts prevailing throughout the cell.

Within the bulging cumulus, during the first stage of the cell's development, is an updraft that extends throughout most of the cloud. The presence of this updraft is reflected at the ground level below by a region of slightly lower surface pressure and gently converging surface winds. As the updraft causes the cloud to extend in height, air flows in through the sides of the cloud ("entraining") and mixes with the updraft, in response to pressure differences and various drag forces. With continued upward motion, a large amount of free water is liberated which in time exceeds the amount that can be supported by the updraft, and the water starts to fall. Because of viscous drag, aided by decreased thermal stability brought about by the entrainment of environment air, this falling water soon initiates a vigorous downdraft in part of the region which previously contained an updraft. This is the start of the mature stage of development. The air of the downdraft reaches the ground as a cold core in the rain area and spreads over the surface, causing an abrupt change in the wind pattern and a sharp drop in temperature. In this area of the cold outflow, there is a rise in surface pressure and divergence of surface winds.

The downdraft develops at the expense of the updraft, and soon after the maximum downdraft speed is reached, the updraft is completely cut off from its source region and the cell enters the dissipating stage. With the dissipation of the updraft and the subsequent removal of the source of rainfall, the downdraft weakens and finally dies out completely. The

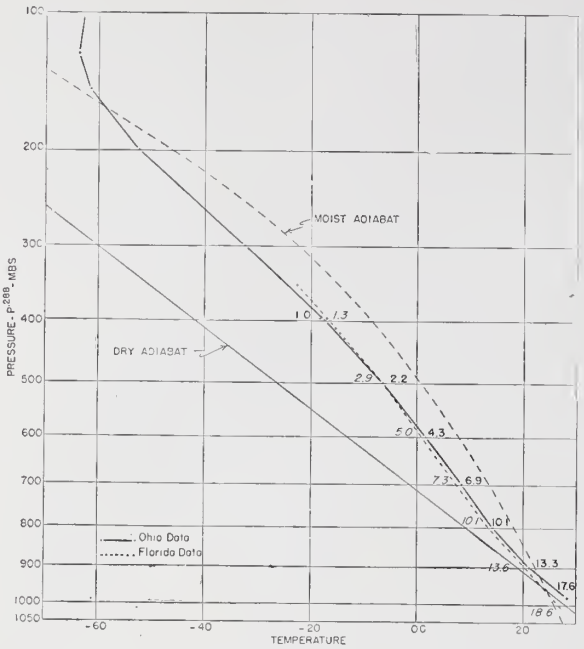

FIGURE 15.—Pseudo-adiabatic diagram showing the average lapse rate of temperature and moisture content (gm/kg) in Florida and Ohio during convective conditions. These curves are based on averages of observations made on 39 days of thunderstorms in Florida (1946) and on 30 days of thunderstorms in Ohio (1947).

surface pressure, surface wind, and other elements then return to normal.

This life cycle for the cell has been found to exist in the storms observed in both Florida and Ohio. Most of these storms, whether of the frontal, squall-line, or air-mass type, occurred in maritime tropical air. Temperature and moisture distribution with height in this type of air mass, over both Florida and Ohio, are shown in figure 15. These curves represent an average of the conditions on approximately 30 thunderstorm days in each area.

THE CUMULUS STAGE

In its initial stage every thunderstorm is, of course, a cumulus cloud, although only an extremely small number of cumuli actually continue their growth through the necessary stages to attain thunderstorm proportions. On any particular day the number of thunderstorms that occur is determined in general by the instability of the atmosphere. Whether or not an individual cloud proceeds through the entire cycle of development depends upon peculiarities of its immediate environment.

As a cumulus cloud, a cell first produces no radar echo[6] although to the naked eye it appears as a swelling cumulus and seems to be growing in vertical extent at a rapid rate. The first radar echo, denoting the presence of numerous, sizable water drops, is obtained from the cloud after its top extends above the freezing level[7]. During the period of development, several small cumuli may unite to form a single cell which, at the time of initial detection by the radar, may be as small as ¾ to 1 mi. in horizontal diameter, with a top extending only 2,000 or 3,000 ft. above the freezing level. While still in this initial stage of development, the cloud may grow until its visible top extends to a height where the temperature is —30° C. or lower.

Structure.—The predominant feature of the cumulus stage of the thunderstorm cell is the updraft. Measurements made in cells in this stage show that throughout the entire cell, from the lowest to the highest levels flown, 5,000 to 26,000 ft., respectively, the area is characterized by updraft. This upward motion may vary in both horizontal and vertical magnitude, as well as with time. Maximum speed in this stage occurs at the higher altitudes late in the period. Speeds as great as 50 ft/sec are not unusual.

That the updraft extends from the ground level is demonstrated by the occurrence of horizontal convergence in the surface wind field. Figure 16(a) shows this convergence as it was observed prior to the development of cumulus clouds over the surface network in Florida on July 22, 1946. In figures 16(b) and 16(c), showing conditions respectively 30 min. and 1 hr. later than those of figure 16(a), it can be seen that the centers of convergence persisted after the initial cumuli appeared at 0915 E.S.T. Such convergent flow at the surface of the earth necessitates an upward motion in the lower levels of the atmosphere, which is associated with the developing cumuli.

Figure 17 shows a vertical cross section through a thunderstorm cell in the cumulus stage of development. For simplicity, the updraft in this figure is depicted as having a symmetrical velocity profile at each level, although in actuality this symmetry probably would not be realized. Mass continuity within the cell is maintained by horizontal inflow through the sides of the cloud. The inflow process is called "entraining,"[8] or "entrainment," and is the result of pressure differences as well as the drag and exchange of momentum between the moving air of the draft and adjacent, relatively still air. Entraining brings about a mixing of air from the environment with air of the cloud column and is of great importance to the consideration of the thermodynamic and hydrodynamic mechanisms involved in the thunderstorm.

Temperature.—During this early period of the thunderstorm's existence, the air temperature within

[6] Statements regarding the radar echo refer to those detected by equipment used on the Thunderstorm Project. Radar sets having different characteristics could be used to obtain data that would not agree with all of the radar-detectable features of thunderstorms described in this report. See appendix (3) for description of the radar installation and operating technique.

[7] See ch. V, sec. 2.

[8] See section on Entraining.

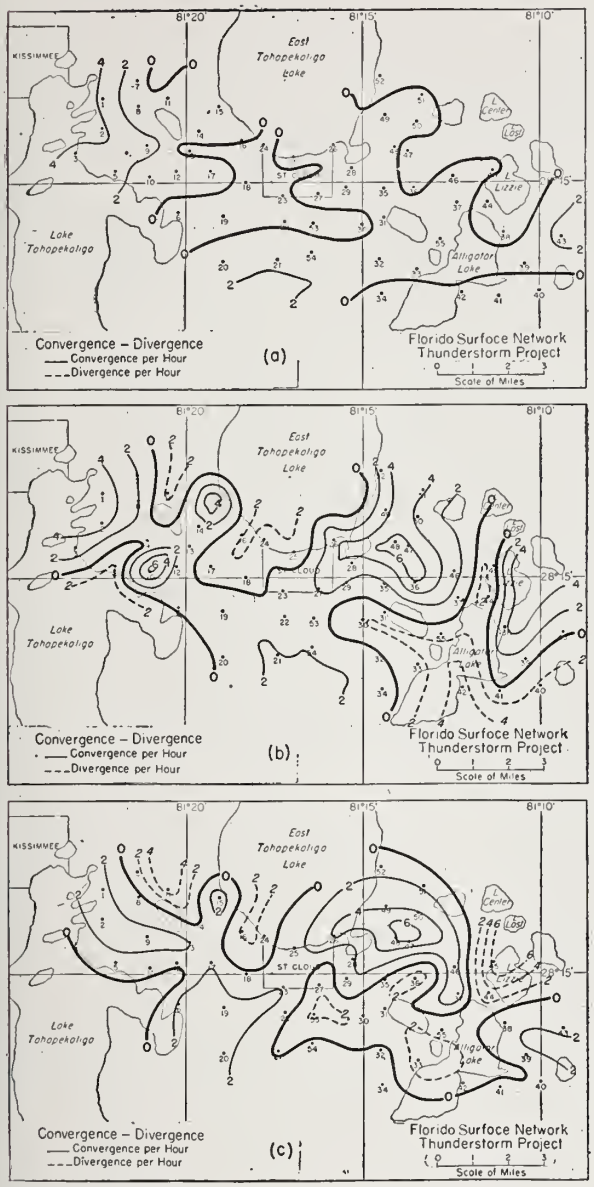

FIGURE 16.—Charts showing horizontal convergence in the surface wind field over the Florida observation network on July 22, 1946. Convergence values were computed from the winds observed at network stations.
(a) Pre-convective conditions at 0845 E.S.T.
(b) Conditions at the time of formation of first cumulus, 0915 E.S.T.
(c) Conditions at 0945 E.S.T. showing the persistence of the centers of convergence.

the cloud area forming the cell is everywhere higher than the environment air temperature. The variations of the heights of selected isotherms are shown on the cross section through the thunderstorm cell in figure 17. The greatest differences between the in-cloud and the environment temperatures are found in areas of greatest updraft speeds, at the upper levels.

The magnitude of these positive temperature anomalies in the updraft area increases with time, reaching a maximum at the end of the cumulus stage of development. At this time, a region of negative temperature anomalies (cloud colder than the environment) appears in the lower levels, somewhat removed from the region of maximum temperatures within the cell.

Precipitation.—Observations made by flight crews show that the quantity of visible water and size of water particles in the cloud during the cumulus stage is small at first but continually increases with time. The greatest concentrations of hydrometeors—liquid, solid, or both—occur at the freezing level and above. While these hydrometeors are reported as rain or snow, they are occurring in an updraft, so their rate of fall relative to the earth is slight or even negative. In an updraft the hydrometeors may occur as liquid water, or rain, several thousand feet above the zero isotherm. Still higher may be found a gradual transition from rain, to snow and rain mixed, to wet snow, and finally to dry snow. The transition zone in which the water passes from a liquid to a solid state varies in depth, depending upon the speed of the updraft. This may be attributed to the likelihood that the water being carried upward does not change temperature as rapidly as does ascending air, and that, accordingly, the drops continue to be warmer than the air surrounding them.

Duration.—During the cumulus stage of development, the thunderstorm cell, which has an initial diameter of perhaps 1 to 2 mi., grows until its major axis is perhaps as great as 6 mi. in length. It is difficult to establish a definite time duration for this stage, since it actually begins with the initial appearance of the cumulus cloud that is going to become the thunderstorm cell. If the duration is reckoned from the time of the initial detection of the radar echo, which is soon after the visible cloud top extends above the freezing level, it may be said that a cell usually remains in the building stage between 10 and 15 min. During this time, the visible cloud grows until its top reaches 25,000 or 30,000 ft., although, as has been mentioned earlier, these dimensions would vary in air masses having properties different from those of the storms studied by the Project.

THE MATURE STAGE

With the continued updraft during the cumulus stage, more and more vapor condenses, and the drops and ice crystals within the cloud become more numerous and increase in size. When the size, and consequently the mass, of individual drops or ice particles increases to such an extent that they can no longer be supported by the existing updraft, they begin to fall, relative to the earth.

The initial occurrence of rain at the earth's surface has been chosen as the identifying feature by which the transition from the cumulus to the mature stage of development can be recognized, because simultane-

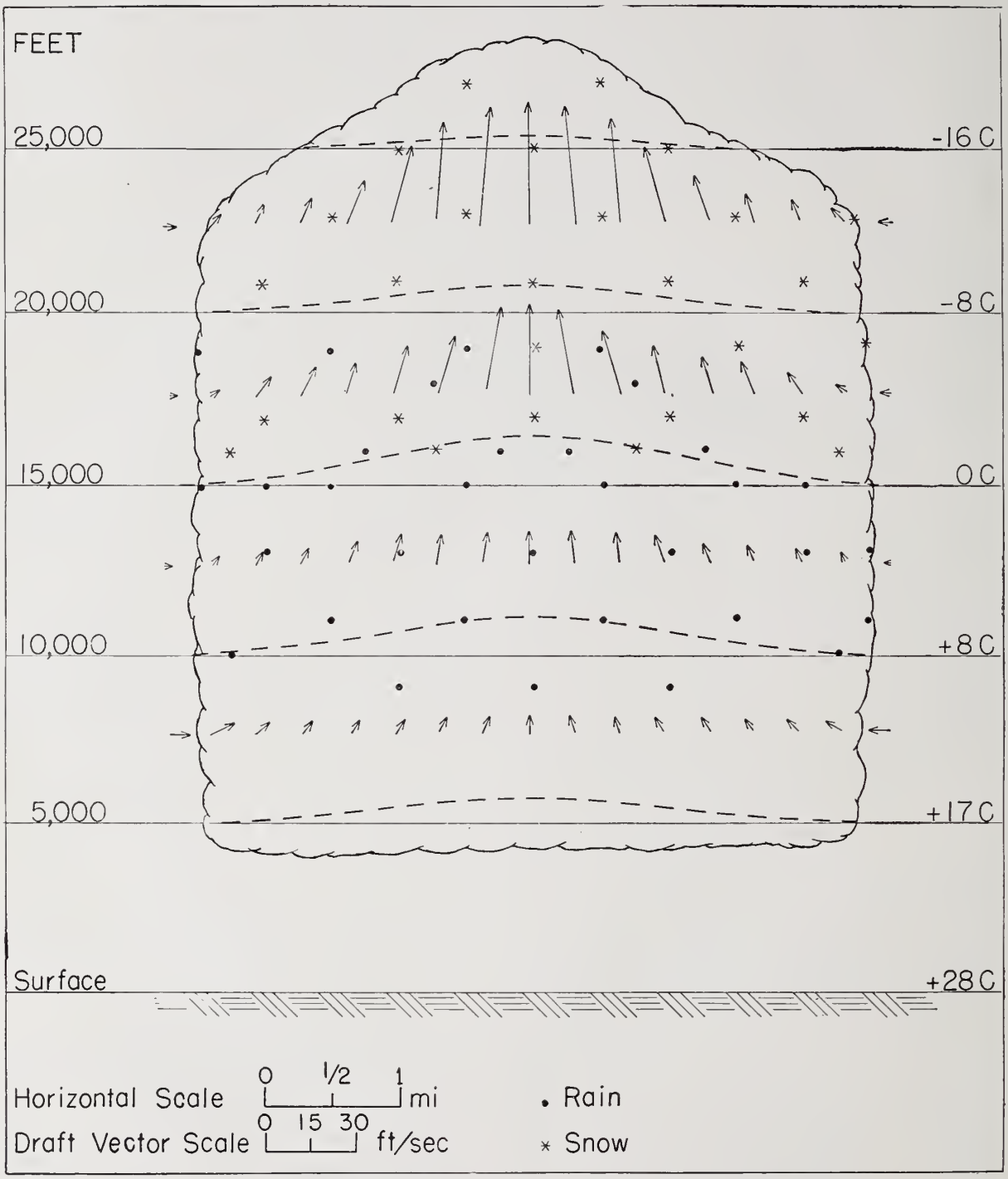

FIGURE 17.—An idealized cross section through a thunderstorm cell in the cumulus stage of development. The velocity, temperature and hydrometeor distributions have been represented here in a symmetrical manner although such fields would not be expected in actuality. These data are based upon observations and show conditions that might be expected within a thunderstorm cell in the cumulus stage. It should not be construed that this figure places limits upon the magnitudes or regions of occurrence of the phenomena represented. It is probable, for instance, that liquid water frequently is present at levels considerably higher than that at which rain is shown in this figure.

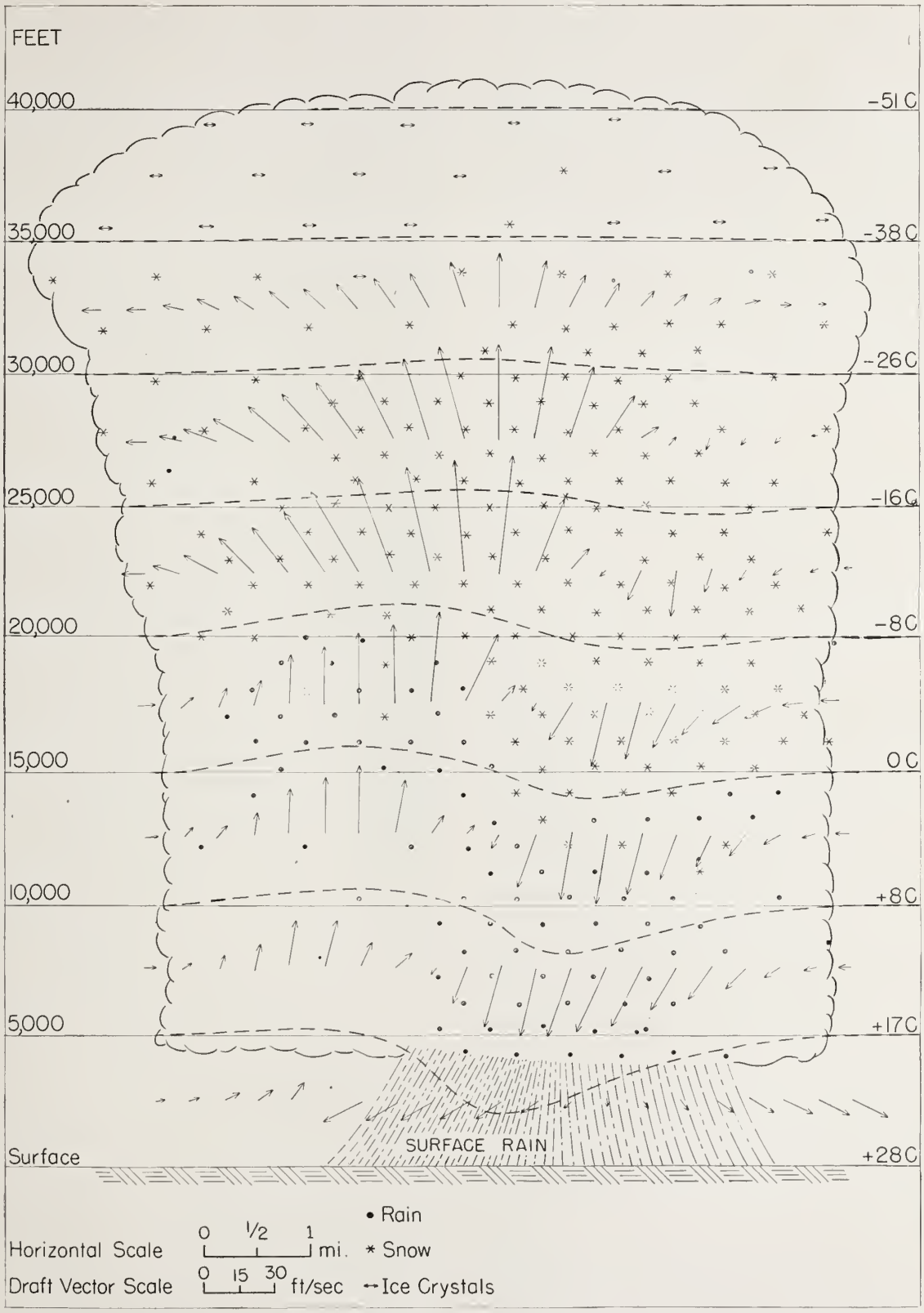

FIGURE 18.—Conditions that might be expected in a thunderstorm cell at approximately the middle of the mature stage. This figure is based upon observed data but has been presented in an idealized manner for simplicity. The caution regarding the interpretation of the material presented in figure 17 applies equally to this cross section.

841051—50——3

ously with this event certain significant changes take place in the circulation pattern within the cell.

Structure.—In a portion of that area where measurements by airplanes had shown the primary movement of the air to be upward (in the early stage), a downdraft now is found. This downdraft is adjacent to the continuing portion of the updraft and has its greatest horizontal extent in the lower levels of the cell. The processes involved in its formation include the drag on the ascending air by the precipitation, which is falling relative to the air itself[9]. This is one of the reasons for the coincidence of rain at surface levels with the initial appearance of the downdraft aloft. The downdraft, which at first is found only in the middle and lower levels of the cell, gradually increases in horizontal and vertical extent.

Figure 18 shows a vertical cross section through an average thunderstorm cell at a time approximating the middle of its mature stage. The draft vectors are schematic only, since, as was mentioned earlier, draft areas do not exist as zones of uniform flow but have local maxima and minima. In general, the updraft still increases in speed with altitude through the lower 25,000 ft., where measurements have been made. The strongest updrafts in thunderstorm cells occur early in the mature stage when the speeds may locally exceed 100 ft/sec. The downdraft speed is more nearly constant with altitude, although a minimum below 5,000 ft. is necessitated by the boundary afforded by the earth's surface. Above this region of deceleration, downdraft speeds of 40 ft/sec are not uncommon.

The moving air of the downdraft does not come to rest at the surface of the earth, but changes its direction of motion as would any jet stream striking a plate. Thus, the vertical motion is transformed into horizontal motion and produces one of the most characteristic of the meteorological phenomena observed at the surface in conjunction with thunderstorms—the gusty surface current that flows outward from the area of rainfall. The outflow is represented by strong horizontal divergence in the wind field at the surface, and a wind squall produces a marked discontinuity at the advancing edge of the outflowing current (fig. 19). Accompanying the wind change is a sharp drop in surface temperature and a surface pressure rise, characteristic of thunderstorms, which occur under the area of the downdraft. As the cold air spreads out horizontally, a pressure rise is observed over the entire outflow area.

Temperature.—The region of negative temperature anomalies that appears toward the end of the cumulus stage of the cell grows larger and becomes more intense during the mature stage. This cold portion of the cloud is found to be coincident with the area of downdraft, with the maximum negative anomalies occurring in the lower levels. The updraft is still warmer than the clear air surrounding the cloud and, of course, has considerably higher temperatures than the downdraft at corresponding altitudes. The warmest regions at each level are found in the area of maximum updraft speed, and the coldest areas occur where the downdraft is strongest.

Precipitation.—During the mature stage of the cell, rain is found in the lower levels, snow and rain mixed in the middle levels, and usually only snow at the highest level flown by Project airplanes. It is during the mature stage that hail occurs, although this hydrometeor is not found in every storm. Above 26,000 ft., of course, no direct observations have been made of hydrometeors, but from radar echoes returned from cells in the mature stage of development, it is concluded that the size of individual particles and their number are probably large to heights as great as 60,000 ft. in some cases. With extraordinarily strong updrafts (up to 100 ft/sec), it is possible that the liquid water may be carried to very high sections of the cloud before it can cool sufficiently to freeze. Only one case of heavy rain was reported at the 26,000-foot flight level during the two seasons of Project operation, and it was associated with a strong updraft (53 ft/sec).

At the surface, the area of heaviest rain is coincident with the area of maximum divergence in the surface winds. Since the rain is always falling, with respect to the air of the downdraft, the maximum rain occurs somewhat earlier than the maximum divergence.

Turbulence.—Although the turbulence might be classified as "heavy" by an experienced pilot flying in

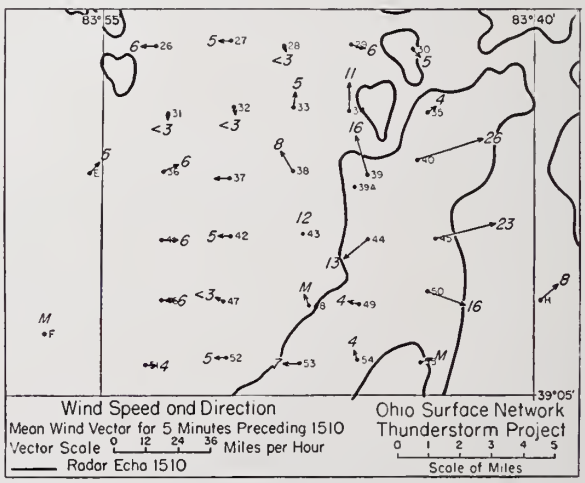

FIGURE 19.—A section of the plotted surface wind chart for the Ohio observation network for 1510 E.S.T., August 14, 1947. Note the marked outflow from the area beneath the radar echo from the thunderstorm and the opposing winds at the stations in the two rows on the western side of the network.

[9] Brooks [10] was one of the first to suggest that the falling raindrops initiate a downdraft in the cloud.

both cumulus and mature stages of a cell, it is during the mature stage that it reaches a maximum. It is strongest in the regions of the maximum updraft and downdraft speeds, but definite zones of decreased turbulence, lasting for one or more 10-second or 3,000-foot interval, exist between adjacent cells. Although least severe in the lowest altitudes, even there the turbulence at some points is usually great enough to be classified as "heavy."

Duration.—As the rainfall continues throughout the mature stage of the cell, the downdraft area increases in size until, in the lower levels, it extends over the entire storm cell. This is considered to be the end of the mature stage, which usually lasts for a period of 15 to 30 min. During this stage the cell reaches its greatest height, which is normally about 40,000 ft., although an occasional cell extends higher than 60,000 ft. and many complete the life cycle without extending higher than 30,000 ft.

THE DISSIPATING STAGE

Structure.—The downdraft, through the spread of its momentum and creation of new areas of descending air by the precipitation falling from the remaining updraft, spreads rapidly over the entire area of the cell at successively higher and higher altitudes. During the dissipating stage of the cell's history, this process continues until the entire vertical and horizontal extent of the cell contains only downdraft or air with little or no vertical motion. As the downdraft expands laterally, the corresponding decrease in the volume of ascending air causes the total amount of liquid water being released within the cell to become progressively smaller. This reduces the mass of water available to accelerate the descending air.

Turbulence, too, becomes less severe with the reduction of vertical velocities in the drafts, although its intensity at some points is usually great enough to warrant a classification of "heavy" while the cell is in the early part of the dissipating stage. The minimum of turbulence marking the zone between cells is less pronounced during this stage, but it still exists.

Temperature.—As would be expected, the area of maximum temperature associated with the updraft area, still present at the beginning of the dissipating stage, does not persist. The spread of the downdraft quickly causes the entire cell to cool to a temperature below that of the environment. This, however, is a transitory condition; with decreasing downdraft speeds, the temperature within the cell rises to a value approximately equal to that of the environment at corresponding levels. The temperature distribution within the cell during the period when the downdraft is still well-defined is shown on the cross section in figure 20.

Precipitation.—As would be necessary, the liquid water encountered during this stage of the cell's development is less than when the cell is in the mature stage, and it continues to decrease with time. Correspondingly, the precipitation at the surface diminishes until finally the last residual drops have fallen. This may be as long as 20 min. after the cessation of significant vertical motion in the cell.

With the abatement of rainfall and the decrease in the downdraft speed, the velocity divergence at the ground level likewise diminishes, until, at the end of the dissipating stage, no distortion of the surface wind field attributable to the storm is apparent. The pressure at the surface, which rose during the mature stage, now falls, rapidly at first and then more gradually. A value corresponding to that in the areas not affected by the storm is assumed by the end of the dissipating stage.

Duration.—The assignment of a definite time duration to the dissipating stage is difficult, since the thunderstorm frequently degenerates into layers of stratified cloud from which light, intermittent precipitation may fall for a considerable length of time. In general, however, the period from the beginning of this stage until the time when vertical motion within the cloud becomes insignificant is approximately 30 min.

EFFECTS OF ADJACENT CELLS

The preceding discussion of the stages through which the thunderstorm cell passes in its life cycle presents a somewhat idealized situation, in which a unicellular storm develops and goes through a life cycle without additional cells developing in the adjacent area. While this frequently happens, it is seldom that such a cell attains a vertical development comparable to that of a cell in close proximity to other cells. It follows that the weather phenomena—such as rainfall, draft speeds, and high surface winds—associated with a cell of this type are considerably less intense than similar manifestations of a cell that is one of a group. Studies of the PPI echoes[10] from isolated-cell thunderstorms show that they have a very short life, producing an echo for an average of only 20 min. Since the presence of an echo can be taken as an indication of the presence of large hydrometeors either precipitating or being suspended in a rising flow of air, the short duration of an echo is ample evidence that the total rainfall per unit area of such storm would be small when compared to that of a multicellular storm with a total echo duration approximately three times as long.

From data collected by radar it has been found that, as a multicellular storm develops, each successive cell attains a greater height than did previous ones. This

[10] Echoes presented on the plan-position-indicating 'scope of the radar.

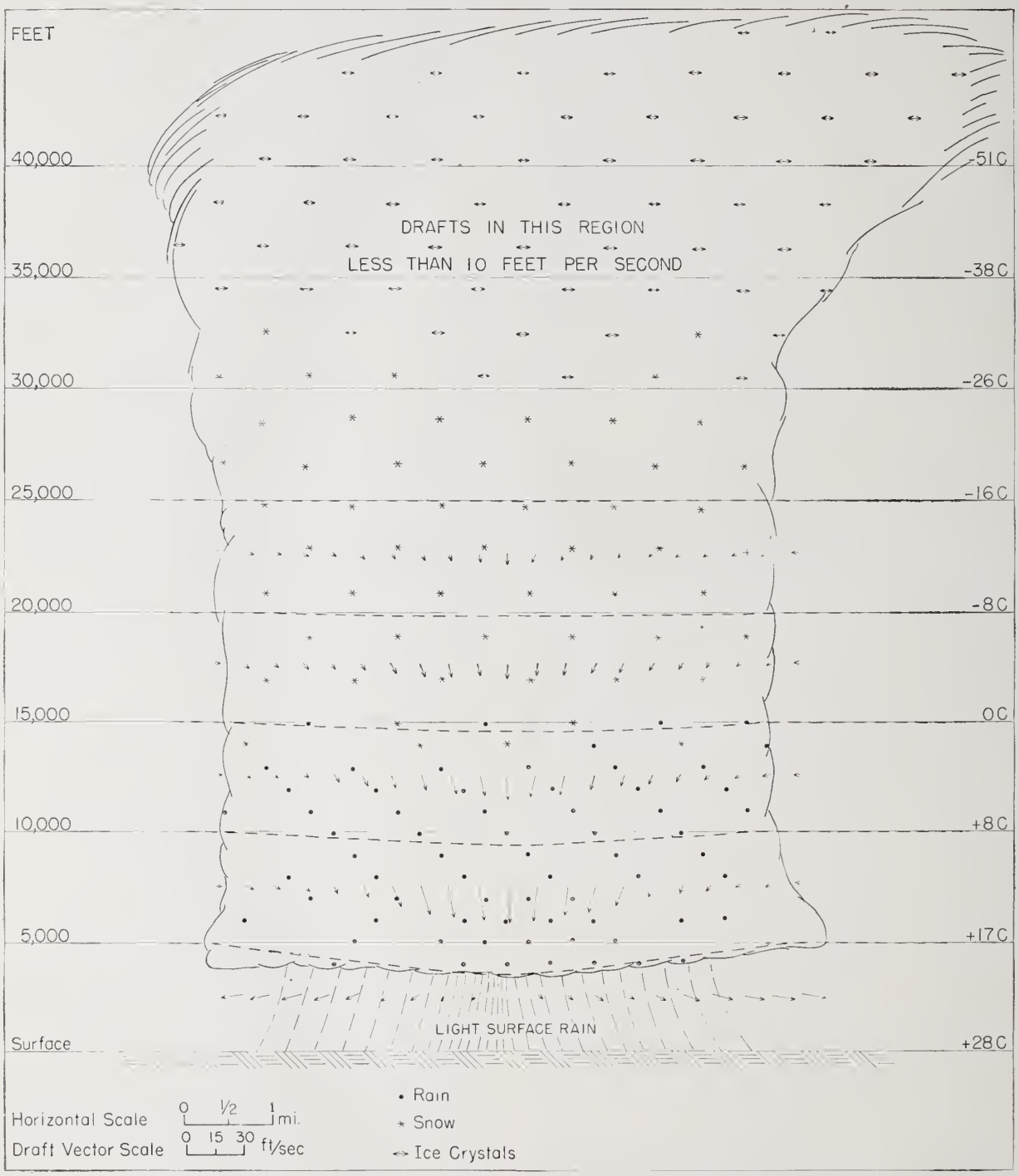

FIGURE 20.—An idealized cross section through a thunderstorm cell in its dissipating stage of development. As in the figures representing the earlier stages of development, the data shown here are based upon many actual observations, but are not intended to suggest that somewhat different conditions might not be found in a study of individual cells.

occurs because lateral mixing across the boundary of cells which develop later would involve the saturated air from the earlier cells rather than the relatively dry air of the environment which completely surrounded the initial cell.

EFFECTS OF SHEAR

Where there is a marked increase with height in the horizontal wind speed, the mature stage of the cell may be prolonged. The increasing speed of wind with height produces considerable tilt to the updraft of the cell and, in fact to the visible cloud itself. Thus, the falling precipitation passes through only a small section of the rising air; it falls thereafter through the relatively still air adjacent to the updraft, perhaps outside the cell boundary. In that case, since the drag effects of the falling water are not imposed upon the rising currents within the thunderstorm cell, the updraft can continue until its source of energy is exhausted. The cell may then dissipate without undergoing a period when the principal vertical motion is downward, as is characteristic of the normal dissipating stage. Precipitation falling from the tilted cloud may produce a downdraft area outside the visible cloud, but the downdraft is necessarily discontinuous in nature, since the descending, unsaturated air can only fall a short distance before coming into density equilibrium with its environment. Such a condition accounts for the occasional reports of downdrafts outside the cloud and for the precipitation that is frequently reported in the clear air adjacent to a thunderstorm but under its tilting wall or canopy.

ARRESTED DEVELOPMENT OF CUMULI

It is well known that the growth of most cumulus clouds is arrested before they can reach thunderstorm proportions. These clouds, therefore, do not go through the stages of development which have been outlined on the preceding pages. It was one of the aims of the Thunderstorm Project to study cumulus clouds of this type in order to determine, if possible, the reason for their failing to continue in development. In this phase of the investigation use was made of sailplanes and an AT–6 airplane which were equipped to measure vertical motion and temperature.

Some of the clouds studied were bulging cumuli (with tops at 10,000 to 12,000 ft.) which showed very little sign of continuing development. Weak upward and downward motions were found inside them, generally of speeds less than 1 m/sec. The measured temperatures indicated that the clouds were in approximately density equilibrium with the environment. On the other hand, flights made into cumuli of similar size which continued to develop into thunderstorms showed updrafts significantly stronger than 1 m/sec and temperatures higher than the environment air.

It may be concluded either that in the former clouds the updraft was cut off for some reason, or that such a psuedo-dormant period is common to most cumulus clouds and that those which develop into thunderstorms undergo a change in which there is a strengthening of the updraft. The former explanation seems more plausible for reasons to be covered later. When some of the cumuli have obtained considerable vertical extent, the return settling in their environment tends to inhibit further development of neighboring clouds. Once a cloud has developed to thunderstorm proportions the cold-air outflow from cells in the mature stage may add the necessary impetus to cause cumuli in the immediate vicinity to continue development.

3. Temperatures within the Thunderstorm

Elementary physical reasoning and experiment indicate that when convection occurs in a medium, the colder portions of the medium descend while the warmer masses ascend. It follows that in the convective system of a thunderstorm the updraft should be warmer than its environment and the downdraft colder. The vertical motions may be regarded in terms of buoyancy forces, in which the upward acceleration on any volume having a virtual temperature T', in an environment which at the same height has a virtual temperature T, is given by

$$a = g\frac{T' - T}{T},$$

where g is the acceleration due to gravity. Frictional drag and mixing with the environment modify the upward acceleration but do not nullify its dependence on temperature difference.

Temperature differences existing among updrafts, downdrafts, and environment air are therefore the critical factors determining the convective processes. Heretofore, little information has been available on the temperature distribution in thunderstorms, not because of the lack of attention given to this important matter, but because of the difficulties encountered in obtaining measurements that could be considered reliable. Such measurements as have been obtained are inconclusive; in some cases they can be interpreted to mean, paradoxically, that the rising air of the convective cloud column is colder than its environment.

Measuring in-cloud temperatures.—Most of the attempts to measure in-cloud temperatures have in-

volved the use of airplanes or gliders as vehicles for carrying the measuring element[11]. With them it is possible to make numerous measurements at the same level and in the same parts of the cloud. Many such measurements are required if the temperature field is to be delineated. Having the measuring element mounted on a glider or airplane has two main disadvantages, however:

(1) With the airplane or glider it is difficult to reach altitudes high enough to sample the entire vertical extent of the cumulonimbus cloud. Many of these clouds reach peak heights in excess of 40,000 ft., whereas temperature measurements above 15,000 ft. usually have not been feasible in past investigations. It is now known that at these relatively low altitudes the cumulonimbus, for a major portion of its life, is predominantly under the influence of the cold downdraft, and measurements at lower levels are biased by this. To obtain temperature measurements representative of the updraft, it is necessary to sample the storm cells during the building stage, or if during a later stage, above 20,000 or 25,000 ft., where the influence of the downdraft is much less.

(2) The high speed of the airplane introduces difficulties in instrumentation and in the reduction of the data for analysis purposes. In general, the airplane is in the updraft or downdraft less than 30 sec., and the instruments for measuring the temperature must have a very small time lag if correct data are to be obtained. Fortunately, such thermometers are available, so this difficulty is not of great importance. However, the speed of the airplane is responsible for another and by far more serious obstacle in the determination of exact temperatures. In the area of stagnation pressure at the leading edges of the surfaces of both airplane and measuring element, the air temperature increases because of the compression. For measurements in dry air, or when the thermometer is effectively shielded from liquid water, this is not serious, because the amount of the temperature rise due to the compression can easily be calculated for various airspeeds, once the coefficient of dynamic heating[12] has been experimentally determined. On the other hand, if the temperature-measuring element is not effectively shielded from the liquid water in the atmosphere, it is difficult to find out what temperature the element is actually measuring. The surface of the element may become completely wetted so that it indicates the wet-bulb temperature of the air; however, if the element is only partially wetted, the indicated temperature lies somewhere between the wet- and dry-bulb temperatures of the air. These conditions would occur if the temperature of the water striking the measuring element were the same as, or somewhat higher than, the temperature of the air. If the water temperature is lower than that of the air, the element tends to measure the temperature of the water. In addition to this lack of knowledge of the nature of the temperature being indicated by the thermometer, the problem of whether to apply a dynamic-heating correction based upon a dry-adiabatic rate or one based upon a moist-adiabatic rate must be resolved. If the element is completely wetted, but not flooded, the moist rate applies; and some rate between the wet and the dry can be used if the wetting is only partial.

These disadvantages and difficulties arising in the use of the airplane as a platform from which to measure temperature within a thunderstorm are outweighed by the fact that repeated measurements at the same level and in the same portion of the cloud are possible. In addition, the space available in an airplane makes possible constant monitoring of the recording device, thus permitting the separation of irregularities due to extraneous effects. Furthermore, with the airplane it is possible to obtain data that can be used in relating temperatures to other meteorological quantities.

Method used by the Thunderstorm Project.—The Thunderstorm Project equipment for measuring temperatures from airplanes consisted of a small ceramic resistor (thermistor) connected through a suitable amplifier to a meter on a panel, on which were also located airspeed, altitude, and other indicators. These dials were photographed by a motion-picture camera. The ceramic resistor was mounted in a housing especially designed with a view to prevention of wetting.

In order to put the temperature data obtained into a more usable form, variations due to altitude changes during a flight were eliminated by reducing the readings to the intended level of flight in each case. Such reductions should be made using a lapse rate corresponding to that of the air in which the temperature measurements are made. However, the actual lapse rate is not usually known for either the cloud or the environment air. In addition, such lapse rates are not constant with time because under thunderstorm conditions the thermodynamic structure of the atmosphere is constantly undergoing readjustment. For convenience, therefore, the convention was established of using the dry-adiabatic lapse rate for altitude adjustments of temperature measurements made outside the cloud, and the moist-adiabatic lapse rate for measure-

[11] Attempts at using balloons for carrying the measuring element (radiosonde) have not proven satisfactory for measuring temperatures inside the thunderstorm. Some of the reasons are that it is not possible to know accurately the times when the balloons are in the cloud, and even when this is known, the element is subjected to wetting and icing, etc., which cause spurious indications that cannot be easily identified in the data. Furthermore, use of a balloon allows only one measurement for each level penetrated.

[12] The coefficient of dynamic heating varies with the installation, but it has been determined that a coefficient of approximately 0.8 is suitable for most methods of mounting the thermometers. This means that the actual rise of temperature is approximately 0.8 of that to be expected from computations based upon the increase in pressure at the point of stagnation.

ments made inside the cloud. This procedure introduces errors in the resultant computed temperature for the reference level, but these errors must be small. In Project flights the mean deviation from the reference altitude prior to entry into the cloud was only 13 ft., while within the cloud, 88 percent of the temperature measurements were made within 600 ft. of the reference altitude. Even if the lapse rate within the cloud had been the dry-, instead of the assumed moist-adiabatic, this would have resulted in an error of only 0.9° C. in the temperatures expressed. However, it is very improbable that the lapse rate within the cloud is greatly different from the moist-adiabatic; accordingly, it is estimated that the errors in computed temperatures due to altitude corrections were less than ± 0.25° C.

In order to obtain the relationship between the temperature within the cloud and the environment air temperature, as well as the change in this relationship with altitude and time, the difference between the temperature within the cloud and a mean environment temperature was found. Environment temperature was determined from the temperature records obtained from the airplanes rather than from radiosondes.

The temperature field within the cell.—The thunderstorm is, as previously described, a group of drafts separated into units designated as cells. The vertical motion within a single cell varies in speed and changes in sense from updraft to downdraft as the cell passes through its life cycle. Temperature, as was pointed out, is a determining factor in maintaining the motion.

The Thunderstorm Project analyzed four of the missions flown, in an attempt to relate temperature fields with identifiable up- and downdrafts. The flights provided data for 101 traverses through 26 thunderstorm cells in the mature stage of development; 8 traverses through 6 cells in the building stage; and 13 traverses through 8 cells in the dissipating stage.

Drafts were identified from a photographic record of altitude and air speed (furnished and analyzed by N. A. C. A.), from which the displacement in altitude of an airplane encountering a draft was used to compute draft velocities[13]. In order to obtain a maximum amount of data from these few missions, the photopanel records were re-examined for drafts rejected for computation by the N. A. C. A. (cases in which it was believed that extraneous influences on the plane accounted for altitude displacements). Rough calculations made from these records made possible additional identifications of drafts and computation of velocities—computed only when the indicated altitude changes coincided with (a) quasi-constant airspeed; (b) increasing airspeed and increasing altitude, indicating ascent with the nose down; or (c) decreasing airspeed and decreasing altitude, indicating descent with climb attitude. At best, only an estimate of average draft velocities was obtained in this manner. Table 5 shows the classification, according to type and stage of cell development, of the 58 drafts studied in the temperature analysis and indicates the source of the data obtained.

[13] See footnote 29, p. 40.

TABLE 5.—*Drafts used in temperature study, classified according to type and stage of cell development and source of data*

Stage of cell and type of draft		Source of data		Total
		N. A. C.A.	Photopanel	
BUILDING	Updraft	3	3	6
MATURE	Updraft	26	10	36
	Downdraft	5	10	15
DISSIPATING	Downdraft	1	.....	1
Total		35	23	58

Table 6 gives the maximum deviations from the mean clear-air temperature observed for these drafts in the various stages of cell development. The mature stage is divided into two periods because of the change in the temperature anomalies found in the updrafts in the latter portion of this stage. Six drafts measured during mature stages could not be definitely identified as to whether occurring in the early or late portion of this stage.

During the building and the first portion of the mature stages[14], the updraft is associated with temperatures that are warmer than those of the environment. Accompanying the marked change in vertical motion within the cell as it enters the mature stage is a change in the temperature field. The updraft continues warmer than the environment; however, in the region of the downdraft, negative temperature anomalies are found in the middle and lower levels of the cell. These relatively low temperatures are in an increasingly larger region of the cell as the horizontal and vertical extent of the downdraft increases. Slight negative anomalies are occasionally found in the updraft during the late mature stage. Their existence suggests that during this stage the updraft is residual in nature, perhaps continuing only because of momentum acquired earlier in its history, or because of pressure differences produced by the current of air above that is still rising under the influence of buoyancy forces. With the decreasing downdraft speed as the cell enters the dissipating stage, negative temperature anomalies begin to decrease, until, with the cessation of the vertical motion within the cell, the tem-

[14] It is pointed out that the division of the mature stage into an early and a late period was based upon structural analysis of the cells made prior to the study of the temperatures.

TABLE 6.—*Deviations (° C.) of the maximum (updraft) or minimum (downdraft) draft temperatures from the mean clear-air temperatures for thunderstorms in various stages of development*

Altitude of measurement (ft.)	Building stage		Mature stage						Dissipating stage	
			Early period		Late period		Unknown			
	Updraft	Downdraft	Updraft	Downdraft	Updraft	Downdraft	Updraft	Downdraft	Updraft	Downdraft
6,000	+0.9	.....	.....	−0.8	−1.3	−1.1	.....	−0.8	.....	.....
	.....	.....	.....	.....	− .3	−3.5	.....	.....	.....	.....
	.....	.....	.....	.....	.....	−3.8	.....	.....	.....	.....
	.....	.....	.....	.....	.....	−2.3	.....	.....	.....	.....
10,000	.....	.....	+0.9	− .8	− .4	− .6	.....	− .3	.....	−1.4
	.....	.....	+ .6	.....	− .1	−1.6	.....	.....	.....	.....
	.....	.....	+1.7	.....	+ .1	.....	.....	.....	.....	.....
	.....	.....	+ .1	.....	+ .5	.....	.....	.....	.....	.....
	.....	.....	.....	.....	− .1	.....	.....	.....	.....	.....
	.....	.....	.....	.....	− .2	.....	.....	.....	.....	.....
	.....	.....	.....	.....	− .1	.....	.....	.....	.....	.....
	.....	.....	.....	.....	+ .1	.....	.....	.....	.....	.....
	.....	.....	.....	.....	− .1	.....	.....	.....	.....	.....
	.....	.....	.....	.....	− .3	.....	.....	.....	.....	.....
	.....	.....	.....	.....	− .3	.....	.....	.....	.....	.....
15,000	+3.6	.....	+ .3	.....	−1.3	.....	.....	−1.1	.....	.....
	.....	.....	.....	.....	− .7	.....	.....	−1.5	.....	.....
	.....	.....	.....	.....	+ .6	.....	.....	.....	.....	.....
	.....	.....	.....	.....	−1.7	.....	.....	.....	.....	.....
	.....	.....	.....	.....	− .3	.....	.....	.....	.....	.....
20,000	+2.1	.....	+1.4	.....	+ .7	−1.0	− .4	.....	.....	.....
	+1.0	.....	+1.5	.....	+1.0	− .2	.....	.....	.....	.....
	+1.1	.....	+2.3	.....	+ .4	.....	.....	.....	.....	.....
	+2.0	.....	+2.4	.....	.....	.....	.....	.....	.....	.....
	.....	.....	+1.0	.....	.....	.....	.....	.....	.....	.....
	.....	.....	+ .3	.....	.....	.....	.....	.....	.....	.....
25,000	.....	.....	.....	.....	− .3	.....	.....	− .6	.....	.....
	.....	.....	.....	.....	− .3	.....	.....	.....	.....	.....
	.....	.....	.....	.....	+ .6	.....	.....	.....	.....	.....

peratures there have assumed values that place the air of the cell in density equilibrium with environment air.

The highest temperatures at any level within the cell are reached in the updraft, prior to the appearance of the downdraft at that level. Maximum negative temperature anomalies are found in the region of the downdraft, which, from its earliest appearance, is colder than surrounding air. This fact suggests that most investigators, who in the past have reported cold thunderstorms, have obtained their temperature measurements in storm cells in a mature or dissipating stage of development and perhaps predominately in the lower levels. This possibility was pointed out by Wenzel [**60**] and Veryard [**57**] but largely ignored by others.

Figure 21 is a vertical cross section illustrating the temperature change with time within a cell at any given level. Vectors representing draft velocities are also shown to demonstrate the association of the temperature deviations with the drafts. As in past examples, a symmetric draft and smooth temperature

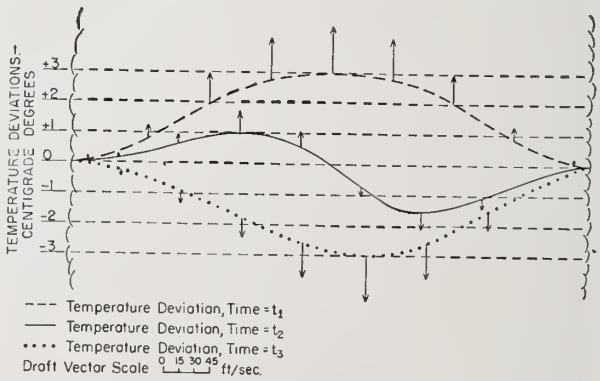

FIGURE 21.—A chart showing the variation of temperature with time within a thunderstorm cell at any given level. The curves represent the differences in temperature between the air within the cell and the clear-air environment of the cell. The deviations are given in centigrade degrees with the positive values indicating that the temperature within the cell is higher than the outside temperature. The stage of development represented by each of the lines shown would be dependent upon the assumed altitude. Thus, while lines t_1 and t_3 would always represent the conditions in the cumulus and the dissipating stages, respectively, line t_2 represents conditions that occur later in time at successively higher levels. However, these same changes of temperature distribution would occur at every level during the history of the thunderstorm cell.

gradients are assumed for purposes of simplicity. The curves shown in this figure, each representing a different time, may also be considered to represent different altitudes at the same time during the mature stage of a thunderstorm cell. Then curve t_3 represents the lowest level, where the downdraft predominates; t_2 is an intermediate level, where both updraft and downdraft are present; and t_1 is the highest level, where only the updraft is present. Thus it can be seen that temperature distribution varies with time and with altitude and constantly changes throughout the life history of the thunderstorm cell.

In addition to a qualitative association of high temperatures within the cloud with regions of updraft and low temperatures with downdrafts, there is evidence that a quantitative relationship exists between temperature anomalies and draft velocities. Figure 22 is a scatter diagram of draft velocities plotted against maximum or minimum deviations from the environment temperature measured within each draft area. The coefficient of correlation for this grouping is .744. This diagram shows that the higher-speed drafts are associated with the greater anomalies; downdrafts and negative anomalies are associated, and updrafts and positive anomalies or small negative anomalies are related.

If the mean temperature deviations within the draft area are considered instead of the maxima or minima, the relationship is as given in figure 23. As would be expected from the nature of the distribution of the points, the correlation coefficient for these variables is considerably lower, being only .635.

The regression lines for both of these scatter diagrams cross the axes to the right and below the origin, suggesting that updrafts slightly colder than their environment can exist, and that the measurements previously discussed have not been due purely to chance.

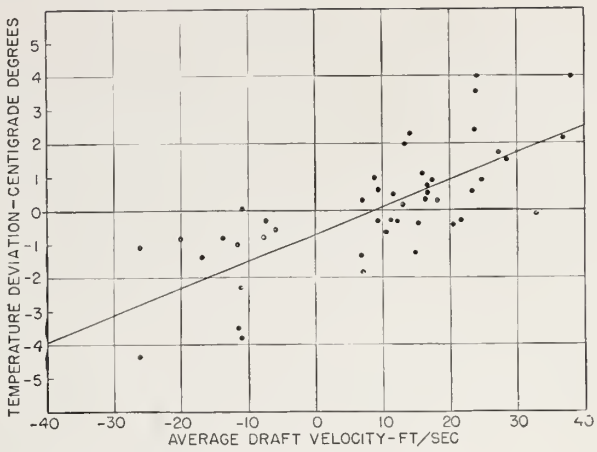

FIGURE 22.—A scatter diagram showing the *maximum* positive temperature deviations within updrafts and the *maximum* negative temperature deviations within downdrafts related to the average draft velocities. The oblique line is the linear regression curve for this distribution. The correlation coefficient for this distribution is .74.

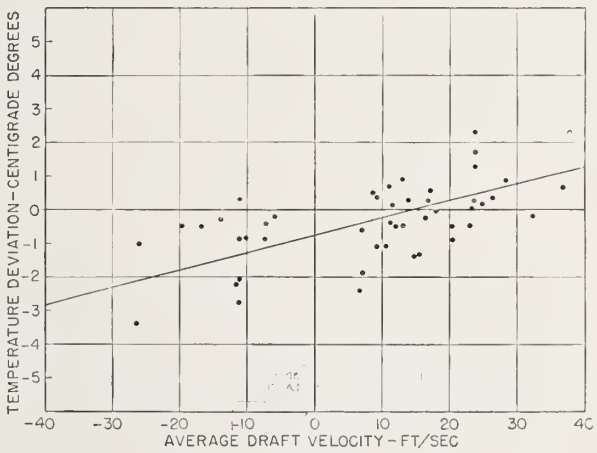

FIGURE 23.—A scatter diagram showing the mean temperature deviations within updrafts and downdrafts related to average draft velocities. The sloping line through the scattered points is the linear regression curve. The correlation coefficient for this distribution is .63.

4. Horizontal Inflow and Entraining

The importance of horizontal inflow through the sides of the cloud as a factor in the formation, growth, and dissipation of the thunderstorm has only recently been realized. Since the first use of thermodynamics in studying the nature of vertical motions in the atmosphere, the updraft inside the cumulus cloud was visualized as a moist-adiabatic ascent through an environment either unaffected by the process or warmed and dried by the resulting countercurrent[15]. Friction between the rising air and the environment was neglected, and motions were considered to be such that pressure equilibrium would be maintained between the rising air and its environment.

In the last few years, however, evidence has been assembled which shows conclusively that these simple theories do not adequately describe or account for the vertical motions in cumulus clouds. More recently it has been shown that the air inside a cumulus cloud must be a mixture of air that has risen from lower levels with air from the environment that has been pulled in through the sides of the cloud. As a result, the meteorologist borrowed from the hydrodynamicist the concept of a fluid jet stream which mixes with its environment, believing that a similar mixing of updraft and environment occurs in a cumulus cloud. The following discussion of this mixing or entraining presents the description of the process in the light of recent observations made by the Thunderstorm Project.

[15] According to the parcel method of stability analysis, the environment is unaffected by the process, whereas the slice method takes into consideration the resulting vertical motion of the environment.

ENTRAINING

Entraining, as the term is presently used in meteorology, is the process whereby a moving stream pulls in, because of pressure forces, or captures and drags along because of viscous forces, part of the environment air. As a result the stream then reflects a mixture of the properties of the original stream and the environment. The entraining in a cumulus updraft may be described as a process in which a parcel of air rises and mixes with some of the environment, with the mixture then attaining moisture and temperature equilibrium. As a result of entraining, the updraft is cooled, both by mixing with a cooler environment and by the consequent loss of heat required to evaporate water and bring the entrained environmental air to saturation. The liquid-water content of the updraft is consequently reduced in these mixing and evaporation processes. As can be seen in figure 24, where the process is diagramatically illustrated on a thermodynamic chart (T vs $ln\ P$), the positive area (work done by buoyancy forces on a parcel) is considerably reduced in comparison with that resulting from a moist-adiabatic ascent without entraining, and the amount of liquid water in the updraft is also materially reduced.

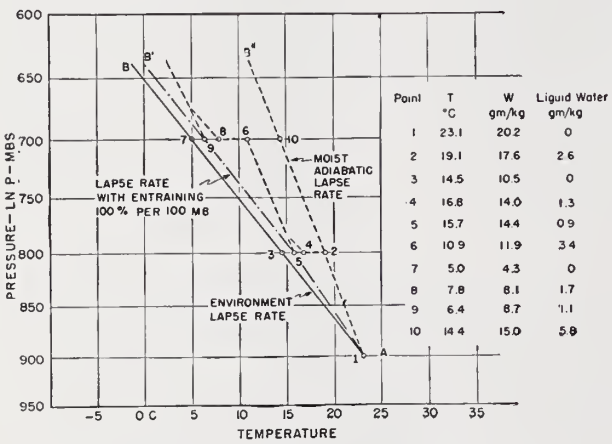

FIGURE 24.—A graphical illustration of the entrainment process.

Proof of entraining in cumulus clouds.—One of the first published reports on entraining in cumulus clouds was that of Stommel [**54**][16], who concluded that some such process must occur to account for lapse rates which were observed to be less than moist-adiabatic in trade-wind cumuli. This conclusion is undoubtedly correct, though it is difficult to verify because, at the present time, measurements of temperature inside cumulus clouds are subject to considerable error (as explained in the previous section).

[16] Schmidt [**49**], in a paper published in 1947, considered some of the effects of entraining in cumulus clouds. Normand [**39**] invokes the necessity of entraining at high levels to account for the low surface temperatures observed in the cold outflow.

More tangible proof of the existence of entraining resulted from computations of horizontal divergence, based on data obtained from balloon runs made during the field operations of the Thunderstorm Project (as reported in an earlier paper by Byers and Hull [**19**]). Observations consisted of rawin and rawinsonde runs made by as many as 10 stations within an area of 160 sq. mi. in an attempt to determine the horizontal displacements of the several balloons as they were released into the thunderstorm cloud or the area nearby. The data show wind direction and speed for each 1,000-foot level, as well as the location of the balloon at the time it reached that level. These data were coordinated with the photographic records obtained from the PPI 'scope of the large control radar, which showed the outline and location of the storm echo for the times of the balloon observations.

For inflow measurements, cases were selected from these data in which several balloons were located on two or more sides of the storm radar echo. Situations were chosen in which the thunderstorm was isolated, in order that effects noted could be ascribed to a single cloud and results could be easily interpreted. When winds were plotted relative to the cloud echo, it was immediately evident that the normal, smooth pattern of the wind field is destroyed in the vicinity of the storm. Winds at a distance continue on a consistent and orderly course, whereas winds near the storm have markedly different directions and speeds.

The amount of the deviation from the normal wind field could be used to compute the convergence or divergence present in the wind field ascribed to the cloud.

Computations were made by a graphical method using the nomogram designed by Bellamy [**6**]. When applied in suitable situations, this method determined the horizontal velocity divergence over the area of a triangle formed by three balloon positions. When the number of balloons permitted, several triangles were formed and computed separately. Each was then considered a separate measurement of the divergence.

Seventeen cases satisfying the conditions of an isolated storm and the presence of several balloons, well distributed around the cloud, and passing through the altitude levels at nearly the same time, were selected for computations of divergence using this graphical technique. Ten of the seventeen cases were storms which had rain and in which a downdraft developed. Each of them showed divergence in the lowest few thousand feet, convergence above this, and divergence again above 20,000 to 25,000 ft. There was notable consistency among similarly-situated triangles of the same storm, and also from storm to storm. Divergence at the base of the storm usually extended to 3,000 ft. and sometimes to 5,000 ft. The

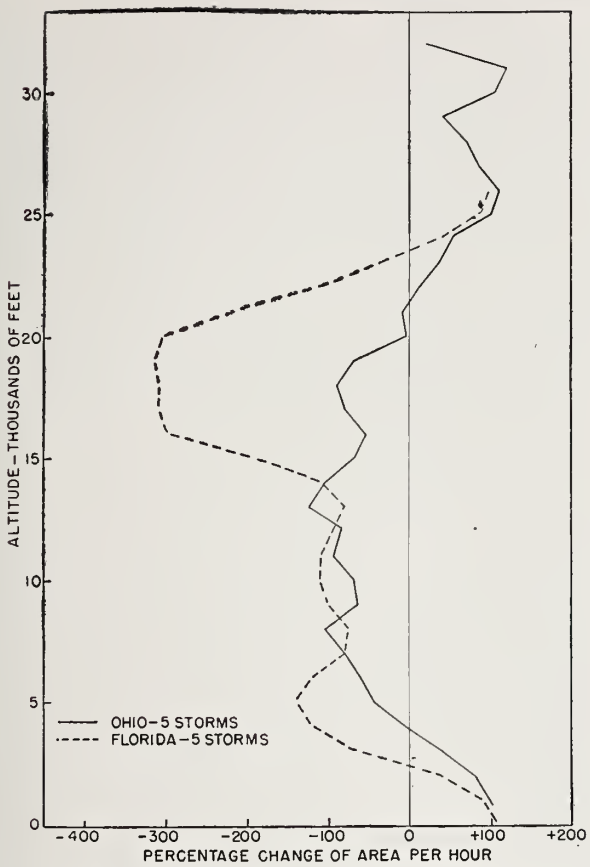

FIGURE 25.—A graph showing the change with height of the divergence about thunderstorms from which rain was falling. These curves represent averages based upon five thunderstorms in Florida and five thunderstorms in Ohio. The divergence is expressed as the percentage change in area per hour, with a positive value representing divergence. Computations were based upon the horizontal displacements of several balloons passing through given levels at approximately the same time.

FIGURE 26.—A graph showing the change with height of the divergence about growing cumuli from which heavy rain had not begun to fall. These curves represent averages based upon three sets of observations in Florida and four sets of observations in Ohio. The divergence has been calculated from the horizontal displacements of several balloons passing through given levels at approximately the same time and is expressed as a percentage change in area per hour; a positive value represents divergence.

convergence overlying the divergence in the surface layers continued as high as 20,000 ft. in most of the 10 cases. In none did the convergence extend above 25,000 ft. A generalized pattern for this type of storm is shown in figure 25. The divergence from the surface up to 3,000 to 5,000 ft. is evidently caused by the outward-flowing cold air of the downdraft. The convergence above is a measure of the horizontal inflow into the sides of the cloud.

The remaining seven sets of balloon ascents were made around growing cumuli before heavy rain had begun at the surface. They gave values of convergence-divergence aloft which are less consistent among themselves; but they differed markedly from the other ten cases in that they did not show the divergence in the lower levels; instead, they showed convergence at all levels, including the surface. The convergence at the surface continued during most of the periods of ascent. The mean curve of the divergence with height drawn for these seven storms (fig. 26) is similar, above 4,000 ft., to the mean curve drawn for the other ten, but the degree of convergence is not as great. These seven cases are considered as typical of cells in the cumulus or growing stage.

All of these computations show clearly that the cloud region up to a level of about 25,000 ft., is one of convergence, that there is a lateral flow of air across the boundary of the cloud. It also seems reasonable to conclude that the outflow above 25,000 ft. is general in all thunderstorms. Unfortunately, however, in this method of computing convergence it is hard to sort out time and altitude variations of inflow, because the balloons continually rise and computations can only apply to a particular level for a particular time.

Cause of entraining.—In the case of a mechanically-driven jet stream, environment is entrained frictionally and distributed through the jet by eddy diffusion and turbulent mixing. Through assumptions of conservation of momentum, hydrodynamicists have had considerable success in studying such cases. These studies are, in general, extensions of the theory of

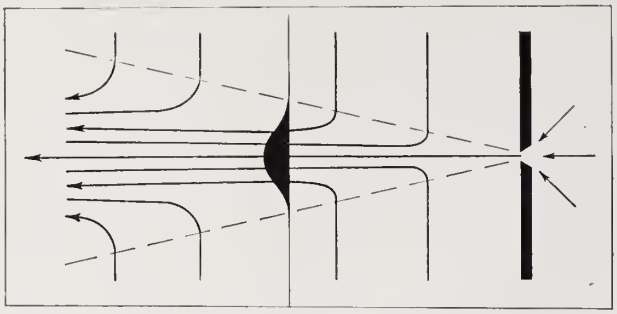

FIGURE 27.—Streamlines of the flow associated with a mechanically-driven jet stream. Note the inflow normal to the axis of the jet and the expansion of the cross-sectional area downstream from the source. The heavily shaded area midway downstream represents a velocity profile.

turbulence and have led to the concept of an apparent shearing stress[17] and the general conclusion that, under these conditions, the jet gradually expands in horizontal area downstream from the source. In addition to the motion of the jet there is established an inflow normal to the axis of the jet (shown in fig. 27). The apparent shearing stress is also present in the case of a moving stream of air in the atmosphere, and it contributes to the inflow around such clouds as were measured by the balloons. In addition to such "frictional" entraining there are, in the thunderstorm, accelerating vertical currents of air that pull in air from the environment by pressure readjustments. These accelerations are brought about by the continual change of potential energy into kinetic energy (releases of heat of condensation for instance), which means that the momentum of the updraft is not conserved.

It is difficult, therefore, to apply conclusions of previous investigators to the problems of entraining in updrafts of thunderstorms. For this reason, as well as for the lack of adequate measurements of the inflow, most of the work done to date in meteorology has dealt with the consequences of entraining rather than the causes thereof.

Region affected by inflow.—The distance from the cloud to which measurable inflow extends is not accurately known. The upper-air measurements made by the Project indicate that the inflow field occasionally extends as far as 5 mi. from the edge of the cloud[18]. Within this distance there are very noticeable deviations in the winds, which are indicative of the horizontal inflow.

The present data are too crude to allow determination of the symmetry or magnitude of the inflow field around the cloud. It seems reasonable, however, that if the predominant cause of the inflow is pressure readjustment and not frictional drag, the inflow will predominate on the side of the cell containing the updraft. One cause of apparent inflow is that, under certain conditions the cumulus cloud moves slower than its environment[19]. When this occurs, the air in the vicinity of the cloud may actually blow around the cloud in the higher levels. As a result, a balloon on the upwind side may appear to be pulled toward the cloud in response to a horizontal inflow, whereas actually there may not be inflow at all. This points out the necessity of considering such factors as the relative motion of the clouds and the environment in computing horizontal inflow. Such refinement is not possible with the present data.

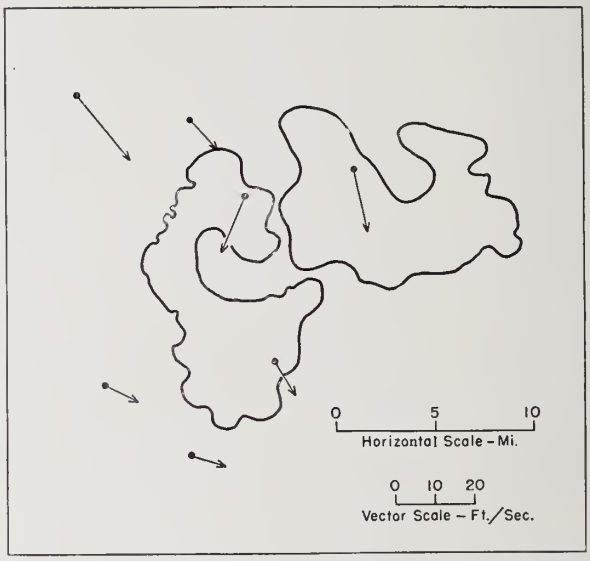

FIGURE 28.—The wind field at the 10,000-foot level about a thunderstorm on August 7, 1947. The wind vectors have been plotted from approximately simultaneous measurements made by rawin and rawinsonde equipment. The radar echo from the PPI 'scope of the control radar has been used to indicate the location of the thunderstorm.

Figure 28 illustrates the non-uniformity of the wind field in the vicinity of the thunderstorm. The variations in the wind, as measured at different points, appear to be due to horizontal inflow. The use of perturbation vectors[20] as an analysis technique for the study of the horizontal inflow has been suggested, but reliable measurements of the environment wind field are usually not available.

Magnitude of entraining.—Although presentation of horizontal inflow in terms of the inflow vector probably would be the most easily understood method, such measurements are not available and, as a result, inflow must be discussed in terms of the mixing that occurs. Inflow rates or entraining rates are usually expressed in terms of the amount of air brought in

[17] Shearing stress resulting from the turbulent motions rather than the viscosity of the fluid.

[18] In this analysis the edge of the cloud was assumed to be defined by the edge of the PPI radar echo.

[19] See ch. VI, sec. 2.

[20] Vector differences between the unaffected wind of the environment and the wind in the vicinity of the cloud.

through the sides as compared with the amount of air moving vertically in the air stream. A useful dimension of entraining rates was proposed by the Project in an earlier paper—the percentage increase in mass of the rising stream per unit change of pressure. In thermodynamical equations it is sometimes more convenient to express entraining as the percentage increase in mass of the rising stream per unit change in altitude.

Various sets of data reported in recent papers have indicated that there is considerable range in the rate of entraining into the cumulus cloud. Winds aloft measurements made by the Project indicate that the cumulus cloud which develops into a thunderstorm entrains environmental air at a rate of approximately 100 percent per 500 mb[21]. On the other hand, Stommel computed the entraining rate in trade-wind cumuli [**54**], and he reported that the mass flux doubles as the cloud air rises from approximately 940 mb. to 840 mb. This indicates an entraining rate considerably greater than that computed from the winds aloft measurements. As will be pointed out in a later paragraph, considerations of the effect of entraining leads one to believe that active cumulus clouds which develop into thunderstorms entrain at the rate of approximately 100 percent per 400 mb. This rate is considerably less than that calculated by Stommel, but it must be remembered that the methods by which the rates were determined are entirely different.

Entraining and the updraft.—Environment air entrained in a thunderstorm updraft causes changes in the lapse rate of the updraft that are thought to be requisite for the formation of the downdraft and, with it, the cold surface outflow so characteristic of the thunderstorm. If complete mixing be assumed, the effects of entraining can easily be determined by the graphical technique first described by Austin [**4**]. In this technique the process is broken down into three steps:

1. The air in the updraft rises moist-adiabatically for a unit distance from Z to $Z + \Delta Z$.
2. At the new level, $Z + \Delta Z$, it is mixed with a portion of the environment, but evaporation and saturation of the drier environment air is not allowed to occur.
3. The mixture comes to temperature and moisture equilibrium through evaporation of enough of the liquid water to saturate the mixture.

A T vs $ln\ P$ chart may be used as a working base for the representation of these three steps. Consider an example in which the lapse rate of temperature in the atmosphere is represented by the line AB of figure 21. (In this case, the instability of the atmosphere is somewhat exaggerated in order to make representation of the process easier.) Point 1 is the condensation level for the parcel of air under consideration. Application of the conventional parcel method gives line AB″ as the lapse rate of temperature of the ascending air. The effect of entrainment in reducing the temperature of the updraft from the temperature which results from application of the parcel method can be determined by considering, in order, each of the three above steps.

A saturated parcel of air from point 1 (temperature: 23.1° C.; mixing ratio: 20.2 gm/kg) is lifted moist-adiabatically a unit distance (in this example 100 mb.) to point 2, where it has a temperature of 19.1° C. and is still saturated, with a mixing ratio of 17.6 gm/kg. The liquid-water content of this parcel, assuming that no water falls out, is 2.6 gm/kg (20.2 — 17.6) which results from the condensation accompanying the ascent.

After reaching point 2, the air is allowed to mix with air of the environment, which at this level, point 3, has a temperature of 14.5° C. and a mixing ratio of 10.5 gm/kg. The amount of air entrained and mixed with the unit mass of updraft determines the entraining rate. For the purpose of this illustration it is assumed that the updraft mixes with an equal amount of environment air in every 100 mb. of ascent (entraining rate: 100 percent per 100 mb.).

As a result of the mixing, we now may consider that there are 2 kg. of air containing 28.1 gm. (17.6 + 10.5) of water vapor, or 14 gm/kg, and the 2.6 gm. of liquid water is now shared by the 2 kg. of air to make 1.3 gm/kg. The temperature of the mixture will be the arithmetical mean of the temperatures of the two masses, or $\frac{19.1 + 14.5}{2} = 16.8°$ C.

These values are indicated by point 4 of the diagram.

This mixture is then allowed to come to moisture and temperature equilibrium through evaporation of enough of the liquid water to preserve saturation. The evaporation will cool the mixture to its wet-bulb temperature. This temperature is found by taking the air dry-adiabatically to its condensation level and returning it moist-adiabatically to its actual pressure. This produces the condition represented by point 5, namely, a temperature of 15.7° C., mixing ratio of 14.4 gm/kg. The liquid water used is given by the amount of water required to saturate the mixture and is the increase of water

[21] Doubling of the mass for a rise of 500 mb.

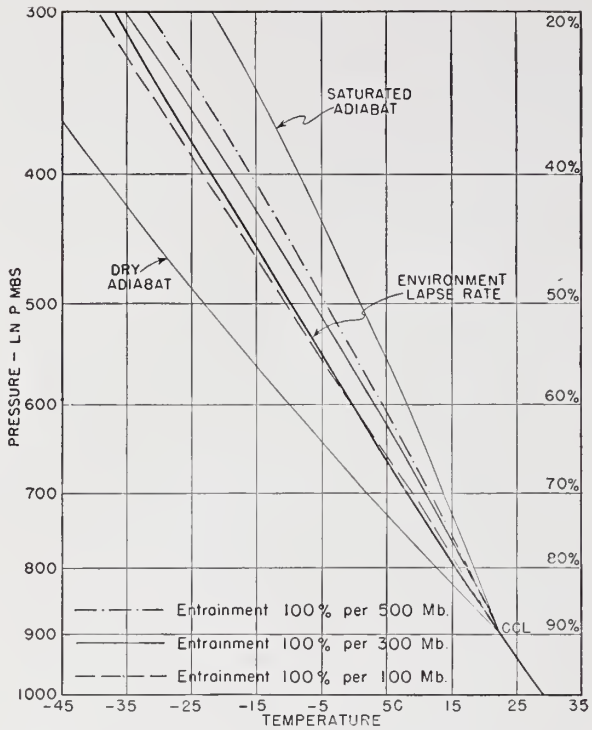

FIGURE 29.—A thermodynamic diagram showing computed lapse rates in updrafts, under specified rates of entraining. The environment lapse rate is halfway between the moist- and the dry-adiabatic curves that pass through the convective condensation level (900 mb). The relative humidity of the environment is plotted for each 100-millibar level.

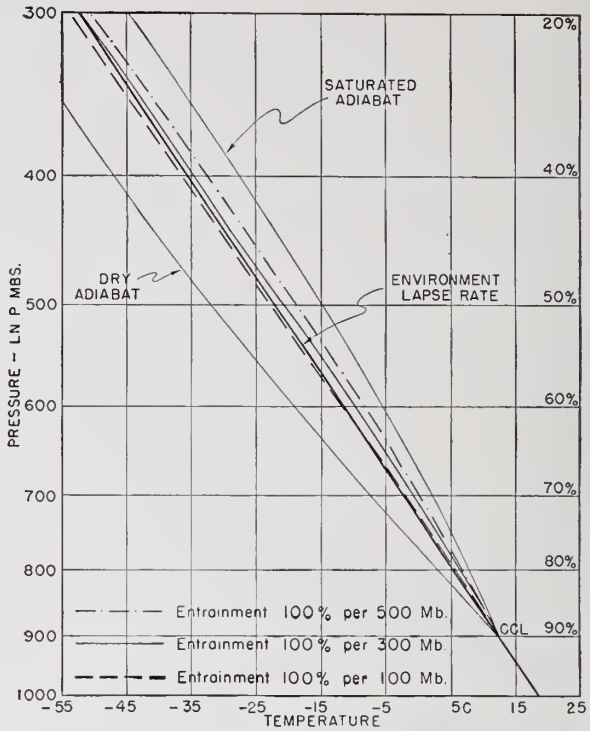

FIGURE 30.—A thermodynamic diagram showing computed lapse rates in updrafts under specified rates of entraining. The environment lapse rate is halfway between the moist- and the dry-adiabatic curves that pass through the convective condensation level (900 mb). The relative humidity of the environment is plotted for each 100-millibar level. Note the difference between the "positive areas" in this figure and in figure 29. The only initial condition that has changed is the specified temperature at the surface.

vapor represented by 0.4 gm/kg (14.4 — 14.0). This leaves 0.9 gm/kg (1.3 — 0.4) as the amount of liquid water in the updraft as a result of ascent with entrainment at the assumed rate.

As the air continues to ascend to lower pressure and entrains more environment air, the process is allowed to repeat, and at the 700-millibar level (point 9) air in the updraft has a temperature 6.4° C. and a liquid-water content of 1.1 gm/kg.

It is thus seen that when entraining takes place the properties of the updraft are considerably different than would be expected from the conventional parcel considerations. In general, it may be said that an updraft undergoing entraining has less liquid water content and a lapse rate steeper than the moist-adiabatic. It must be carefully pointed out here that this is not necessarily an unstable situation. The lapse rate that results from entraining should be considered as one of neutral stability for the *particular process*. It represents a lapse rate that is the result of a *process in action*, and as long as the process continues, the lapse rate in the rising air will be preserved. If entraining suddenly were to stop, the air, being warmer than its environment, would rise, the temperature would decrease at the moist-adiabatic rate, and the entraining lapse rate would be destroyed.

The degree to which the updraft lapse rate is made steeper than the moist-adiabatic depends on the temperature lapse rate and moisture content of the environmental atmosphere, as well as on the rate of entraining. The drier the environment or the more rapid the entraining, the steeper will be the resulting temperature lapse rate in the updraft. By assuming high rates of entraining, it is possible to theorize an updraft colder than the environment. This would mean that convection is forced rather than free. That such a situation is a possibility has been proposed by Barrett and Riehl [**5**]. However, as is shown in another part of this report, temperatures measured from the Project airplanes show that convection of the type studied by the Project is essentially free convection, with updrafts warmer than the environment and downdrafts colder than the environment.

These conditions of free convection thus place rather severe limitations on the rates of entraining that can exist. Using the technique outlined above, a series of charts was constructed, showing the difference in temperature between updraft and environ-

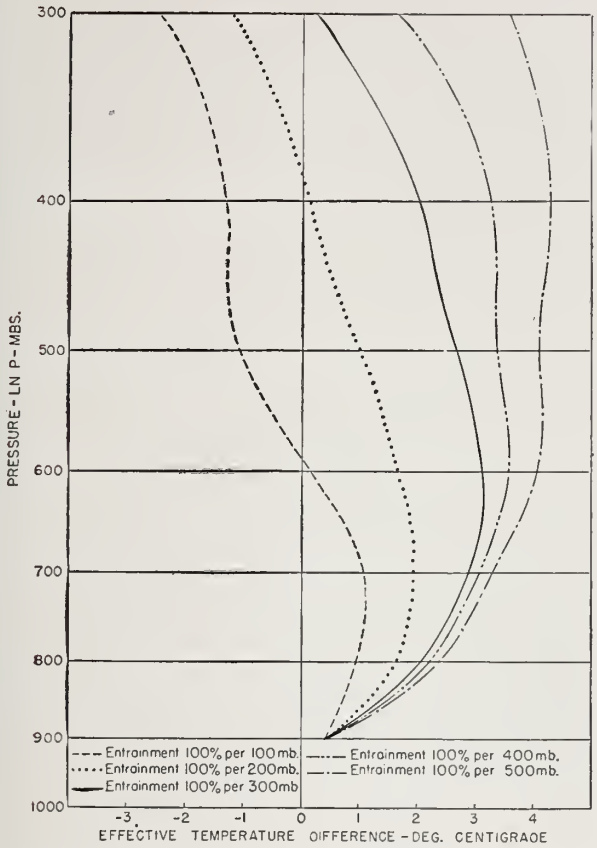

FIGURE 31.—A chart showing the change with height of the computed effective temperature difference between the air of the updraft and the air of the environment under specified rates of entrainment. These curves represent effective temperature differences for the lapse rates shown in figure 29.

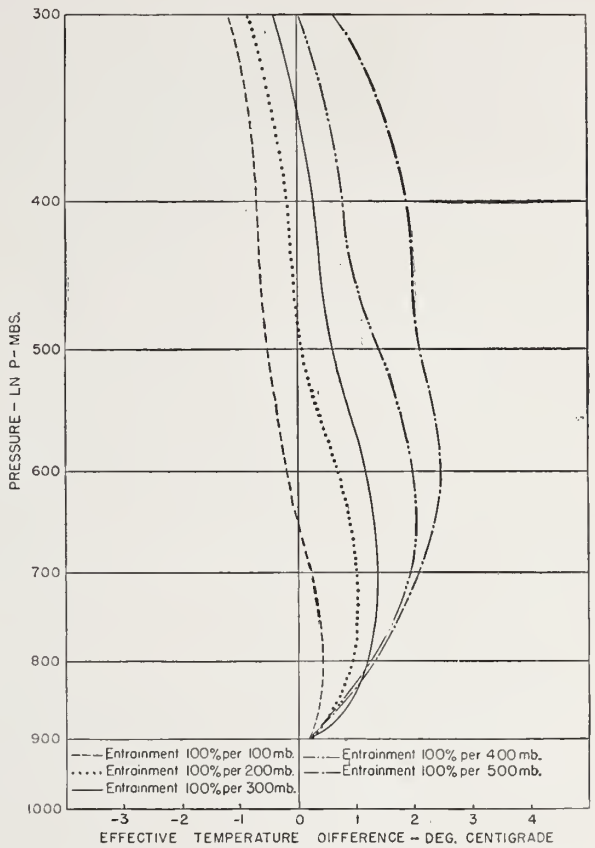

FIGURE 32.—A chart showing the change with height of the computed effective temperature difference between the air of the updraft and the air of the environment under specified rates of entrainment. These curves represent effective temperature differences for the lapse rates shown in figure 30.

ment for a group of different environments and different entraining rates (figs. 29 through 32). For each environment is shown the effective temperature difference[22] between the updraft and the environment that would result from each of several rates of entraining.

As can be seen from these examples, entraining rates greater than 100 percent per 200 mb. are unfavorable for the growth of cumulus clouds to heights great enough to produce the thunderstorm in maritime tropical air[23]. These charts are based upon the assumption that the mixing of environmental air with the rising air is complete. Actually, it is known that the mixing is not complete. As is shown in the section of this report on temperatures inside the thunderstorm, the updraft has a core that may be several degrees warmer than its edges, indicating that the mixing is not complete.

[22] The effective temperature difference is the temperature difference between the air of the updraft and its environment, reduced by the amount which is required to produce a buoyancy force equivalent to the drag force exerted by the contained water. It is therefore the temperature difference available for overcoming other retarding forces and for accelerating the air.

[23] In other types of air masses even lesser rates of entraining would be unfavorable for thunderstorms.

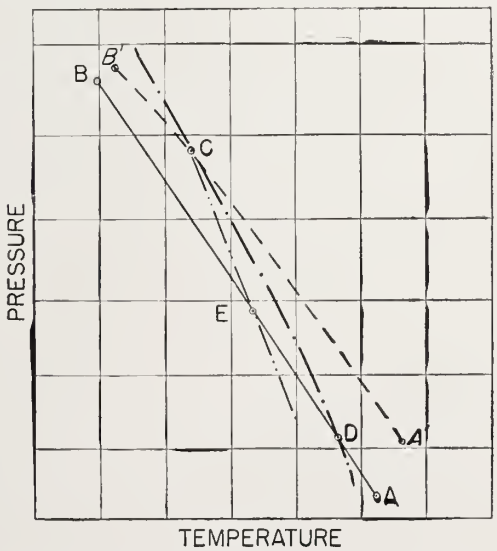

FIGURE 33.—A graphical representation of the formation of the downdraft within a thunderstorm. The coordinates of the diagram are temperature (increasing to the right) and natural logarithm of pressure (increasing downward). The environment lapse rate is represented by line AB and the lapse rate within the cloud is represented by the line A'B'. Curve CD is a moist adiabat and line CE represents a lapse rate under assumed conditions of entraining in the downdraft.

Entraining and the downdraft.—The formation of the downdraft in the thunderstorm depends upon the existence of lapse rates in the updraft which, by entraining, have been made steeper than moist-adiabatic. The lapse rate in a typical, well-developed, bulging cumulus cloud is represented by line A′B′ in figure 33, and the lapse rate of the environment by line AB. If a saturated parcel of air is displaced downward from point C, it warms at the moist-adiabatic rate CD, if no environment air is entrained. If environment air is entrained, the parcel warms at some other rate, such as CE. Should the parcel then rise from some point along CD or CE, it would follow the moist adiabat or an entraining adiabat, depending on whether or not there is continuing entraining. If, however, the parcel is originally displaced downward beyond point D or E, it will continue to sink to higher pressures. The presence of large amounts of liquid water in the thunderstorm provides the means whereby a parcel in a thunderstorm can be forced below point D or point E, from where it continues as the thunderstorm downdraft.

With sufficient water available to maintain saturation, the parcel continues to the ground, reaching the surface with a temperature several degrees lower than the surface-level environment wet-bulb temperature.

Effect of entraining on adjacent cells.—Entrainment by new cells can result in an arrested life cycle of cells which existed previously, particularly if the updraft of the newer cell or cells is considerably stronger than the updraft in the earlier ones. For example, consider a cell that begins with a normal cumulus stage of development. Before the process of droplet accumulation and coalescence produces hydrometeors that would fall from it as precipitation, a newly formed, adjacent cell exerts its influence. The entraining into the updraft of the new cell and the convergence of winds into the area beneath it cause a depletion of the saturated air from the upper portion of the older cell and a reduction of the actual volume of air being carried aloft into it. As a result of this cutting off of the updraft, the original cell may rapidly dissipate without going through the mature stage of development; this means, of course, that only slight, if any, rain would fall to the surface. A cell undergoing such a modified life cycle would be characterized by the usual area of updraft in its initial stage, but a rapid transition from updraft to downdraft would follow. In the absence of precipitation, the downdraft, in all probability, would be the result of descent of air that had "overshot" its level of density equilibrium with its environment.

CHAPTER II. TURBULENCE AND HYDROMETEORS WITHIN THE THUNDERSTORM

1. Thunderstorm Turbulence

The term "turbulence" as applied to thunderstorms usually connotes a sequence of irregular vertical or horizontal motions of the air within the storm area. For an understanding of the thunderstorm, it is useful to separate these motions into the two classes, *drafts* and *gusts*, defined as follows:

Draft—A sustained, nonhorizontal, current or stream of air in a thunderstorm. Drafts are continuous over regions as large as a thunderstorm cell, and vertical components are greater than approximately 1 m/sec.

Gust—An irregular, local, transitory variation in a velocity field. These irregular variations are usually considered to be a number of small eddies superimposed on the general air flow[24]. They may be found both inside and outside the main drafts.

Of these two basically different classes of motion, drafts are by far the more important as far as thunderstorms are concerned, since they make possible the principal energy releases of strong convection.

DRAFTS

During the period of activity, virtually the entire region occupied by the thunderstorm cell is composed of drafts. As has been pointed out in earlier sections, direction of the draft is largely dependent upon the stage of development of the cell. In early stages of development, motion is predominantly upward; and throughout later stages, predominantly downward, particularly where rain develops. Thunderstorm drafts are horizontally continuous for areas as large as 25,000 ft. in diameter (in extreme cases), extend vertically from near the cloud base to heights of 30,000 to 60,000 ft., and may last as long as 15 to 30 min.[25]

Causes of the updraft.—The primary cause of the updraft is the buoyancy force arising from lower density of the updraft as compared with the air of the environment. This lower density is brought about primarily by the temperature, which is higher than that of the environment, although the reduction in density due to presence of a greater amount of water vapor in the updraft is not to be ignored.

The temperature difference between updraft and environment is not as great as would be expected from considerations of the parcel method of stability analysis—a fact that has been recognized for many years. Effects of entraining and mixing of environment air with the updraft are responsible for this smaller difference. The difference is largest at higher levels and early in the stage of cell development. As the cell advances to late maturity, lower regions of the updraft are very little, if any, warmer than the environment. The motion by this time may be due to the dissipation of momentum acquired earlier in the life of the updraft.

An application of the simple buoyancy equation shows that measured temperature differences are considerably more than are required to account for the observed accelerations of the air, and it must be concluded that part of the temperature difference provides the force necessary to overcome various frictional losses. Actually a temperature difference of 0.4° C. would bring about, in the absence of friction, an acceleration of the updraft from 0 ft/sec to 30 ft/sec in a distance of 10,000 ft., an acceleration greater than is commonly observed in the thunderstorm. Even with a zero temperature difference, the density difference brought about by greater water vapor content of the updraft, relative to its environment, could produce, in the absence of friction, accelerations of similar magnitude. It is easily seen, therefore, that most of the buoyancy force is used to perform work against various frictional forces.

There are two main frictional forces: First, there is the body and form drag of the current rising in the environment air; secondly, there is the drag of water droplets imbedded within the draft itself. It is dif-

[24] Adapted from *Weather Glossary*, U. S. Weather Bureau, Washington, D. C., 1946.

[25] It is thus seen that thunderstorm drafts are restricted to smaller areas than the currents produced by orographic barriers.

841051—50——4

ficult to determine with any satisfactory degree of accuracy the magnitude of the body and form drag[26], but it is obvious that the drag of the droplets, which are falling at terminal speeds, is equal to the total weight of the droplets. One gram of liquid water per cubic meter of air at the 400-millibar level produces drag on an updraft or downdraft equivalent to the decrease in buoyancy force brought about by a temperature reduction of approximately 0.5° C. At 900 mb. the effect of the drag of one gram of water per cubic meter of air is equivalent to a temperature reduction of approximately 0.25° C. It is thus apparent that drag due to the contained liquid water can constitute a large part of the total drag on an updraft. Water contents as high as 6.5 gm/m^3 at approximately 700 mb. pressure in the free atmosphere have been reported by Cunningham and Miller [**23**]. This means that if such amounts of water are found in an updraft at 400 mb., the temperature of the updraft must be at least 3 centigrade degrees warmer than the environment in order for the air to rise[27].

It is interesting to speculate that the coalescence of droplets into drops is important in the life cycle of a thunderstorm; it is thus possible for the liquid water to fall out of an updraft and keep the drag due to the contained liquid water at a minimum, with the result that the updraft might be able to accelerate to thunderstorm proportions.

Dimensions of the updraft.—Studies of structure of the thunderstorm cell indicate that during the cumulus stage of development the entire cell may be an updraft area, and during this stage, updrafts may have horizontal extents as great as 20,000 ft. The cell itself may expand in horizontal extent in later stages of development, and it is conceivable that the updrafts may also, on occasion, expand to a horizontal size as large as 40,000 ft. In general, however, it is unlikely that the updraft is, at any stage of development, more than 25,000 ft. across.

In the cumulus stage the updraft extends from the cloud base to the cloud top, in many cells a height greater than 25,000 ft. During the mature stage the updraft disappears from the lowest levels of the cloud, although it continues in the upper levels. From indications of the height-finding radar[28], it seems likely that in some cells in the mature stage of development, the updraft may extend from 20,000 to 60,000 ft. For altitudes below 25,000 ft., the best information regarding the dimensions of the updraft

[26] For a discussion of body and form drag of cumulus clouds in an environment, see Schmidt [**19**].

[27] An assumption is made that the drops are small enough that their effect extends throughout the air in question. If, however, the liquid water present is aggregated into a few very large drops, the effect would be to have spheres of air under the influence of the drop being dragged downward through the air that is rising.

[28] AN/TPS–10—generally referred to as an RHI (range-height-indicating radar). For details of this equipment, see appendix (3).

TABLE 7.—*Frequency distribution of updraft speeds measured at various flight altitudes (in thousands of feet) for two seasons of Project operation*

Draft speed (ft/sec)	Florida					Ohio				
	Flight altitude (m.s.l.)					Flight altitude (m.s.l.)				
	6	11	16	21	26	5	10	15	20	25
0– 9.9...	8	5	11	9	6	2	14	9	9	2
10–19.9...	17	35	37	38	22	9	45	40	21	13
20–29.9...	11	32	26	30	27	1	24	25	17	16
30–39.9...	2	6	22	14	11	—	22	22	7	12
40–49.9...	—	2	4	9	4	—	3	5	3	4
50–59.9...	—	5	1	3	2	—	—	3	4	3
60–69.9...	—	—	—	—	1	—	—	1	—	2
70–79.9...	—	1	[1]1	1	—	—	—	—	—	—
80–89.9...	—	1	—	—	—	—	—	—	—	1
90–99.9...	—	—	[1]1	—	—	—	—	—	—	—

[1] Subject to question.

is obtained from data taken from flights of the P-61 airplanes[29].

From the records of two seasons of thunderstorm flying in Florida (1946) and Ohio (1947), during which 1,363 penetrations were made through 76 or more storms, it was possible to evaluate 747 updrafts. Their speeds and extents are given in tables 7 and 8. From the tables it appears that maximum speeds were observed in middle and upper levels of flight in both Florida and Ohio. There was little variation in the minimum speeds of the updraft encountered at the several altitudes. The maximum updraft speed encountered was 84 ft/sec (11,000-foot level, August 22, 1946, in Florida)[30]. The widest updraft was

[29] The characteristic response of an airplane encountering a draft is a systematic displacement in altitude. It is this displacement that enables one to compute draft size and speed. On the Thunderstorm Project, data for evaluating drafts from the responses of the P–61 were obtained from an airspeed-altitude recorder used in conjunction with a synchronous timer (1-second interval) and a control-position recorder (see appendix (4) for description of instruments and installation). These instruments, designed, furnished, and serviced by the N. A. C. A. recorded their measurements photographically.

The average rate at which the airplane was displaced in altitude due to the draft was considered to be the velocity of the draft experienced. However, changes in the attitude of the airplane, induced by gusts as well as by control movement, can also produce changes in altitude, so it was necessary to limit draft evaluations to those cases in which airspeed remained relatively constant during the altitude change. These conditions indicate that the airplane was in level flight even though being displaced in altitude. In order to obtain the maximum amount of usable data from the drafts encountered, the Project pilots were instructed to fly through the thunderstorms using an absolute minimum of control, consistent with safety, and to maintain a constant power setting. In spite of these precautions, many draft velocities could not be evaluated because of excessive variations in airspeed associated with them. This resulted in many instances of an airplane's passing through an area in which a draft was known to furnished, and serviced by the N. A. C. A., recorded their measurements of drafts were made) but whose velocity could not be calculated.

In the structural analysis of thunderstorms, many changes in altitude were used as qualitative indications of drafts, even though variations in the airspeed of the airplane during the altitude change made it impossible to compute an actual value for the speed of the draft. The validity of such a procedure is recognized when it is realized that an increase in airspeed accompanying a gain of altitude, under conditions of constant power, means that the airplane is diving relative to the ascending air of the draft. This makes it impossible to evaluate correctly the speed of the draft but in no manner negates the existence of the updraft. Similar reasoning applies to losses in altitude when the airspeed of the airplane is decreasing. Even by using this technique to obtain the maximum possible number of spatial locations of drafts, analysis of the storms shows that less than 70 percent of the total possible indications of drafts were detected.

[30] Higher updraft speeds, as shown in the tables, were computed but are regarded as unreliable.

TABLE 8.—*Frequency distribution of updraft widths measured at various flight altitudes during two seasons of Project operation*

[Width and height values expressed in units of thousands of feet]

Draft width	Florida					Ohio				
	Flight altitude (m.s.l.)					Flight altitude (m.s.l.)				
	6	11	16	21	26	5	10	15	20	25
0– 0.9...	0	0	1	0	0	0	0	0	0	0
1– 1.9...	0	4	4	1	0	1	4	4	1	2
2– 2.9...	2	6	9	6	7	2	8	8	3	6
3– 3.9...	6	9	9	16	6	0	13	11	8	5
4– 4.9...	5	7	15	11	14	1	16	8	5	6
5– 5.9...	5	11	5	15	6	0	11	16	5	10
6– 6.9...	5	9	10	10	6	1	9	15	7	6
7– 7.9...	0	5	11	6	4	1	12	9	5	1
8– 8.9...	1	7	8	6	5	1	6	7	5	3
9– 9.9...	2	4	7	7	3	0	7	7	2	5
10–10.9...	4	4	3	1	3	1	7	4	0	2
11–11.9...	1	5	3	4	2	1	4	5	4	1
12–12.9...	3	6	2	7	4	0	4	1	5	2
13–13.9...	1	2	2	4	1	1	1	5	0	2
14–14.9...	1	0	1	1	3	1	1	0	3	0
>15 ...	2	8	13	9	12	1	5	5	8	2

37,716 ft. (26,000-foot level, on July 22, 1946, in Florida); the most frequent width of updraft encountered was about 5,000 ft. The relatively few updrafts encountered at lower levels of flight express the condition that during some stages of a cell's development, little or no updraft is present in the lower 10.000 to 15.000 ft.

For altitudes above 25,000 ft., information regarding draft speeds was obtained from the RHI radar. From motion picture records of the 'scope of the RHI radar, rates of growth of tops of thunderstorms were calculated. Inasmuch as this rate of growth corresponds closely to the updraft speed within the thunderstorm (see p. 92), one can obtain estimates of draft velocities at altitudes considerably greater than those flown by the Project aircraft. Table 9 shows a frequency distribution of such data by altitude interval. It is immediately apparent that maximum rates of growth, and consequently maximum updraft speeds, are present at altitudes below 35,000 ft., although updrafts in excess of 30 ft/sec are probable at altitudes greater than 50,000 ft. in thunderstorms extending above that level.

Causes of the downdraft.—The processes contributing to formation and maintenance of the thunderstorm downdraft appear to be more complicated than those producing the updraft. In general, it is possible to determine the probable relative importance of contributing factors and fit together a sequence of events which could lead to the formation of vigorous downdrafts. Unfortunately, present data do not permit the conclusion that the series of events outlined below represents the only way in which downdrafts may be formed, although it must be admitted that the proposed process fits observed data in a satisfactory manner.

The key to development of thunderstorm downdrafts is entraining within the updraft during the cumulus stage of development. As a consequence of entrainment, the lapse rate within the updraft becomes approximately that of the environment. The result is that any air forced downward by the drag of liquid water within the updraft will undergo a temperature change at the moist-adiabatic rate and very quickly become more dense than the air of the environment. From this point the air would continue to descend because of its density as well as the drag force of the drops; and, as long as sufficient water remains to keep the descending air saturated, it will reach the surface colder than the environment surface air[31]. Rain falling from the updraft supplies the necessary water. It is thus seen that the thunderstorm downdraft develops in the very region where updrafts have existed and that its development is dependent upon the drag force of the contained liquid water drops.

[31] For thermodynamic details of the manner in which the downdraft is initiated, see ch. I, sec. 4.

TABLE 9.—*Frequency distribution of all vertical rates of growth of radar clouds (based on RHI-radar data for Ohio thunderstorms)*

Rates of growth (ft/sec)	Height (thousands of feet)							
	15–19.9	20–24.9	25–29.9	30–34.9	35–39.9	40–44.9	45–49.9	50–54.9
0.1– 9.9	30	71	64	53	24	18	12	—
10.0–19.9	36	92	92	77	47	18	9	—
20.0–29.9	30	82	95	66	38	12	13	4
30.0–39.9	9	15	36	36	24	22	8	—
40.0–49.9	2	6	10	17	17	13	7	1
50.0–59.9	1	4	6	7	7	4	1	—
60.0–69.9	—	1	1	—	—	—	—	—
70.0–79.9	—	—	—	—	—	—	—	—
80.0–89.9	1	2	1	1	—	—	—	—
Total	109	273	305	257	157	87	50	5
Mean rate of growth	18	18	21	22	24	26	23	29

Inasmuch as the drops are always falling relative to the air, it would be expected that the strongest downdraft would follow the heaviest rain at the surface, and, indeed, such a sequence invariably occurs.

It is also possible that the thunderstorm downdraft represents a moist-adiabatic descent of air which has overshot the equilibrium and, through continued entrainment, has become considerably colder than the environment at a high level in the atmosphere. In which case, it is easily seen that a downdraft could result if this air, which is colder than the environment, spilled over the edges of the updraft and descended moist-adiabatically. However, the liquid water content in the updraft at this altitude would probably not be sufficient to allow the air to descend more than a few thousand feet before it again would reach density equilibrium with the environment and would spread out horizontally.

Analysis of radar echoes from thunderstorms[32] suggests that downdrafts, having mean speeds of approximately 12 ft/sec, do exist above 25,000 ft. The formation of these drafts can be attributed to the process of overshooting, although the possibility that they too result from drag produced by excessive amounts of water present in the ascending column cannot be ignored.

Dimensions of the downdraft.—Thunderstorm downdrafts are slower and have smaller horizontal and vertical extents than updrafts. From an analysis of the draft structure of the cell, it might be expected that the maximum extent of the downdraft would occur late in the mature stage and in the dissipating stage. During these later periods, however, the speed of the downdraft is considerably less than is found earlier in the mature stage. From the airplane data, using the technique outlined on page 40, it was possible to evaluate 339 downdrafts. Their speeds and extents are given in tables 10 and 11. It is evident that the maximum downdraft speeds were obtained in the middle and upper levels of flight in both Florida and Ohio. There is little variation in the mean speed of the downdrafts encountered at the various flight altitudes, but, in general, the mean downdraft speed is less than the mean updraft speed. The maximum downdraft evaluated was 79 ft/sec (25,000-foot level, on August 5, 1947, in Ohio). The widest downdraft was 23,132 ft. across (25,000-foot level, on September 10, 1947, in Ohio); the most frequent width of downdraft encountered was about 4,000 ft. The fact that relatively few measurements of downdrafts were made at the lowest level of flight is partially due to the fewer number of flights at this level, and also to the fact that pilots flying at the 5,000- or 6,000-foot level hesitated to allow their airplanes to be displaced in altitude for great distances, particularly by downdrafts.

TABLE 10.—*Frequency distribution of downdraft speeds measured at various flight altitudes (in thousands of feet) for two seasons of Project operation*

Draft speed (ft/sec)	Florida					Ohio				
	Flight altitude (m.s.l.)					Flight altitude (m.s.l.)				
	6	11	16	21	26	5	10	15	20	25
0– 9.9...	4	6	4	7	4	6	13	9	5	2
10–19.9...	11	20	28	17	17	5	15	20	11	8
20–29.9...	5	10	12	7	10	1	16	7	9	5
30–39.9...	1	5	6	1	3	—	4	4	1	3
40–49.9...	—	—	2	1	3	—	1	2	—	2
50–59.9...	—	—	—	—	1	—	—	1	—	1
60–69.9...	[1]1	—	—	—	—	—	—	—	—	—
70–79.9...	—	—	—	—	—	—	—	—	—	1
80–89.9...	—	—	[1]1	—	—	—	—	—	—	—
90–99.9...	—	—	—	—	—	—	—	—	—	—

[1] Subject to question.

TABLE 11.—*Frequency distribution of downdraft widths measured at various flight altitudes during two seasons of Project operation*

[Width and height values expressed in units of thousands of feet]

Draft width	Florida					Ohio				
	Flight altitude (m.s.l.)					Flight altitude (m.s.l.)				
	6	11	16	21	26	5	10	15	20	25
0– 0.9...	0	0	0	0	0	0	0	0	0	0
1– 1.9...	0	1	1	0	0	0	3	3	0	0
2– 2.9...	1	5	7	1	2	0	8	7	2	3
3– 3.9...	3	7	9	6	3	1	6	11	5	4
4– 4.9...	3	5	12	2	3	1	8	2	2	2
5– 5.9...	3	6	7	4	4	0	5	1	3	4
6– 6.9...	3	7	5	3	5	0	5	7	3	3
7– 7.9...	0	5	2	5	1	1	1	0	1	1
8– 8.9...	1	2	3	4	3	1	1	2	2	0
9– 9.9...	1	0	2	5	4	0	3	2	1	1
10–10.9...	0	1	1	0	1	3	1	3	2	1
11–11.9...	3	1	2	1	2	1	0	2	1	0
12–12.9...	1	0	0	0	0	1	1	0	2	0
13–13.9...	2	0	1	0	2	0	1	2	0	0
14–14.9...	1	0	0	1	2	1	4	0	1	0
>15 ...	0	1	1	1	6	2	2	1	1	3

The downdraft continues below the base of the cloud until it reaches very close to the earth's surface and spreads out as a layer of cold air. There is relatively little information on the speed and size of the downdraft beneath the cloud base, although Project measurements made on one flight below the cloud base indicate that significant downdraft speeds may exist at levels as low as 300 to 400 ft. above the terrain. Obviously the speed of the draft at these low levels is dependent upon several things, including: (1) the speed and horizontal extent of the down-

[32] See ch. V, sec. 2.

draft at some higher level, and (2) the length of time that the downdraft had been striking the ground—which largely determines the level at which the downdraft begins to spread out in response to the barrier imposed by the earth's surface.

GUSTS

Superimposed on the large-scale continuous flow of the drafts are many irregular, local, transitory variations which are known as gusts. There is no reason to believe that these gusts are fundamentally different from the variations in the surface airflow which have been studied for many years by meteorologists [**15**].

Causes of thunderstorm gusts.—Gusts within thunderstorms lend themselves to a fairly simple explanation, but it must be recognized that gusts are frequently encountered in nonconvective clouds and occasionally in the clear air. Under these conditions they usually do not have the speeds found in gusts associated with thunderstorm drafts [**30**]. These smaller gusts are in many cases due to the shear between two horizontal layers of air of different velocities, or they are caused by orographic effects such as forced lifting or the rise of small parcels of air from a heated surface.

Gusts within a thunderstorm are believed to result from shear zones associated with the thunderstorm drafts. The turbulent flow follows recognized principles of hydrodynamics; the gusts may be considered as small eddies or whirling bits of air driven by and superimposed upon the thunderstorm drafts. Once such an eddy has been created it can travel laterally a considerable distance from the shear zone before its energy is dissipated through friction and its motion ceases. Observations made within the thunderstorm show the association of gusts with the drafts which provide the driving mechanism of the gust. There were, however, many instances of fairly large gusts being encountered by Project airplanes without the occurrence of an accompanying response which is characteristic of a draft. It is concluded that in such cases the gusts encountered had become separated from the draft, which was off the course of the airplane and not encountered on the traverse.

That the gusts are a product of the draft is indicated in figure 34, which relates the velocity of the maximum gust within a draft to the mean speed of that draft. As would be expected, there is considerable scatter of the data, brought about by the fact that on many traverses the airplanes missed the center of the draft area but encountered gusts resulting from shear zones associated with the draft. The linear correlation coefficient of 0.42 may be considered highly significant for the large number of cases plotted.

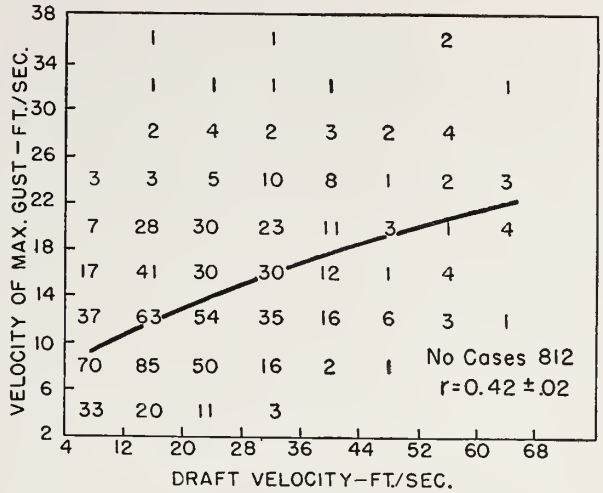

FIGURE 34.—A scatter diagram relating the speed of the maximum gust encountered within a region of a draft to the average speed of the draft. The figures indicate the number of observations for which the speeds fell within the particular range of values. The curve is the regression function of mean maximum gust velocity on draft velocity. The correlation coefficient for this distribution is 0.42±0.02.

Description and magnitude of thunderstorm gusts.—The vortices or eddies characterizing thunderstorm gusts vary in size from those only inches (or even centimeters) in diameter, which would usually be called micro-turbulence, to whirling masses of air several hundred feet in diameter. Superimposed upon the larger gusts are many smaller variations of the velocity field, which would in turn be termed "gusts," according to the broadest definition.

The only information on thunderstorm gusts available to date comes from measurements of the response of airplanes flown through convective clouds and subjected to these gusts. The characteristic response of an airplane intercepting a series of gusts is a series of sharp accelerations without a systematic change in altitude, although the acceleration may be accompanied by pitch, yaw, or roll deflections. These accelerations are caused by the abrupt changes in the velocity field encountered by the airplane. Obviously, in any area of turbulence in the atmosphere there exists an entire spectrum of gusts if classification is made by gust dimension or gust velocity. From this spectrum each airplane, because of its span, chord length, and wing loading, has a band to which it responds most actively. Airplanes of different characteristics passing through the same area of turbulence conceivably could react to entirely different gust bands. In actuality, however, most airplanes of conventional design respond to approximately the same band of gustiness expressed in terms of the dimensions of the airplane; consequently, the results observed in one airplane may be used in conjunction with measurements from other airplanes.

The Gust Loads Section of the National Advisory

Committee for Aeronautics has conducted extensive investigations of this type of atmospheric turbulence, using an airplane as the vehicle for carrying measuring instruments. In their work they used the term "gust" to mean the discontinuities in the velocity field which cause sharp accelerations of the airplane and which can be studied through the magnitude and frequency of these accelerations. Such a definition includes only those abrupt changes in the velocity field and vortices which are large enough to cause a measurable airplane response. It is this somewhat restricted definition that is used through this report when referring to the term "gust," inasmuch as it was from the accelerations experienced by Project airplanes that computations were made of thunderstorm gustiness.

In speaking of the strength of thunderstorm gusts, it is common practice to make use of the concept of an "effective gust velocity" [**44**]. This term represents the velocity of a "sharp-edged gust" that would have produced a normal acceleration equal to that experienced by the airplane. Use of this concept allows the computation of a value for the gust velocity even though the airplane was not in straight and level flight immediately prior to experiencing the recorded acceleration. It is important to remember, however, that the gust velocities thus computed are not the same as the actual speed or changes in speed of the wind in the gust, such as would be measured by an anemometer mounted within the cloud. Among other things the effective gust velocity is somewhat dependent upon the gust shape, gradient distance, airplane used to obtain the measurement, and the manner in which the airplane is flown. On the other hand, it has been the experience of aeronautical engineers that the concept of "effective gust velocity" is a very useful one, since the variations imposed by these factors are of second order.

To permit the recording of the normal acceleration imposed on the airplane, the P–61C's used by the Project were equipped with the following instruments[33]:

1. N. A. C. A. air-damped recording accelerometer
2. N. A. C. A. control-position recorder
3. N. A. C. A. synchronous timer (1-second interval)

Although a gust may have speeds in several directions, for simplicity of evaluation only the vertical component of the acceleration produced by the gust was considered. Studies by the N. A. C. A. have shown that vertical and horizontal gust components have practically the same intensity, under the same meteorological conditions, and that the use of the single measurement of vertical component is reasonable and adequate for statistical analysis.

The control-position recorder was used to permit the separation of accelerations induced by control-surface deflections from those caused by gusts. The synchronous timer recorded time ticks at 1-second intervals on the records of the other instruments which were made on photographic film.

To obtain the effective gust velocity, U_e, data from these instruments were evaluated by means of the following formula:

$$U_e = \frac{2\ \Delta n\ W}{\rho_0\ V_e\ a\ SK},$$

where U_e = effective gust velocity, ft/sec;
Δn = acceleration increment, g units;
W = weight of airplane at the time the acceleration increment was experienced, pounds;
ρ_0 = air density at sea level, slugs per cubic foot;
a = slope of lift coefficient curve corrected for Mach number effect, per radian;
V_e = equivalent airspeed of the airplane, ft/sec $= V\left(\frac{\rho}{\rho_0}\right)^{1/2}$;
V = true airspeed, ft/sec;
ρ = density of ambient air, slugs per cubic foot;
S = wing area, square feet;
K = relative alleviation factor (1.19 for wing loading of 45.7 lb./sq. ft.).

Because of the large number of gusts encountered by the Project airplanes, evaluation was made of only the maximum upward and the maximum downward gust velocities in a given interval (3.000 ft. in Florida, 1946; 10 sec. in Ohio, 1947). In addition, the total number of gusts occurring within the interval was also tabulated. Evaluation and analysis of all gust velocities indicated for a limited number of records shows that the use of maximum upward and downward values together with the number of gusts occurring gives a reasonable description of the field of gustiness within the interval.

Tables 12 and 13 show the frequency of occurrence of gusts of certain velocities at the various levels of flight during the two seasons of operations. These data are simply a statistical summary of all available measurements and do not take into account the stage of development of the cells in which the turbulence was encountered. For each interval the effective velocity of the maximum gust encountered, regardless of whether it produced an upward (positive) or downward (negative) acceleration, was determined and used for the preparation of these tables. As would be expected, at all levels of flight gusts of low effective velocities occur more frequently than do those

[33] See appendix (4) for description of the instruments and their installation.

TABLE 12.—*Frequency distribution of maximum effective gust velocity per 10-second interval of traverse at various altitudes (based upon P-61C flights through Ohio thunderstorms, 1947)*

Maximum effective gust velocity (ft/sec)	Flight altitude (ft., m.s.l.)					
	5,000	10,000	15,000	20,000	25,000	Total
0– 3.9	736	1,053	1,219	812	622	4,442
4– 7.9	470	798	850	527	285	2,930
8–11.9	231	474	527	345	200	1,777
12–15.9	88	234	226	168	92	809
16–19.9	22	88	95	63	38	306
20–23.9	7	37	36	24	14	118
24–27.9	5	5	12	6	12	40
28–31.9	0	5	6	2	2	15
32–35.9	0	2	2	2	1	7
36–39.9	0	0	2	1	0	3
40–43.9	0	0	1	0	0	1
Total	1,559	2,695	2,976	1,949	1,266	10,446
Total miles flown	791.8	1,350.8	1,579.5	1,178.6	776.6	5,677.2
Mean of maximum gust velocities above 4 ft/sec	8.6	9.5	9.5	9.6	9.9	9.4

TABLE 13.—*Frequency distribution of maximum effective gust velocity per 3,000-foot interval of traverse at various altitudes (based upon P-61C flights through Florida thunderstorms, 1946)*

Maximum effective gust velocity (ft/sec)	Flight altitude (ft., m.s.l.)					
	6,000	11,000	16,000	21,000	26,000	Total
0– 3.9	586	937	1,099	981	774	4,377
4– 7.9	605	1,017	1,050	840	611	4,123
8–11.9	372	538	498	414	266	2,088
12–15.9	131	217	221	165	114	848
16–19.9	42	86	104	55	39	326
20–23.9	14	26	39	24	7	110
24–27.9	6	8	6	7	3	30
28–31.9	0	2	6	5	3	16
32–35.9	0	1	1	1	0	3
36–39.9	0	0	1	0	0	1
40–43.9	0	0	0	0	0	0
Total	1,756	2,832	3,025	2,492	1,817	11,922
Total miles flown	978.7	1,557.3	1,689.3	1,401.1	1,006.9	6,633.3
Mean of maximum gust velocities above 4 ft/sec	8.9	8.9	9.1	8.8	8.6	8.9

of high velocity. Also, the mean of these maximum effective gust velocities is approximately the same for each level of flight for the two seasons. There is a relationship between the magnitude of the maximum effective gust velocity and the number of gusts per 3,000-foot interval of flight, as is shown in figure 35.

The sizes of gusts that caused a measurable response in the P-61's can also be determined from Project records. Computation technique allows calculation of the "gust gradient distance," which is defined as the horizontal distance along the flight path from the edge of the gust to the point at which the gust reaches its maximum speed. Figure 36 illustrates the frequency distribution of the gradient distances of 1,810 gusts chosen at random from the Florida and Ohio records. If it be assumed that a gust is sym-

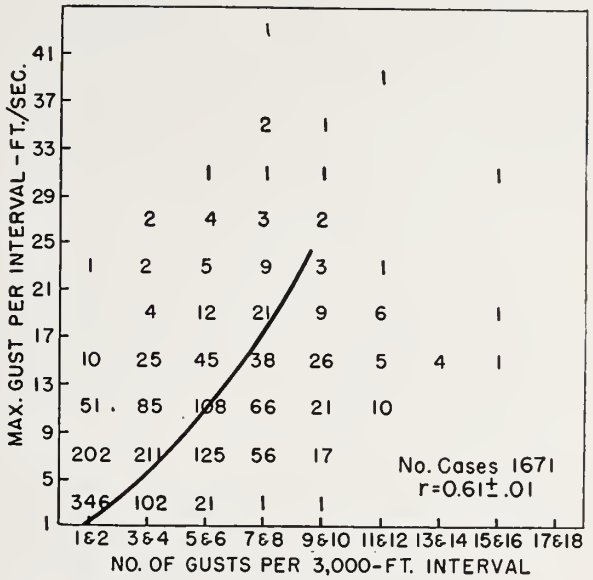

FIGURE 35.—A scatter diagram relating the speed of the maximum gust encountered within a given interval (3,000 ft.) and the number of gusts occurring within that interval. The figures indicate the number of observations for which the speed and the number of gusts fell within the particular range of values. The curve is the regression function of mean gust frequency on gust velocity. The correlation coefficient for this distribution is 0.61±0.01.

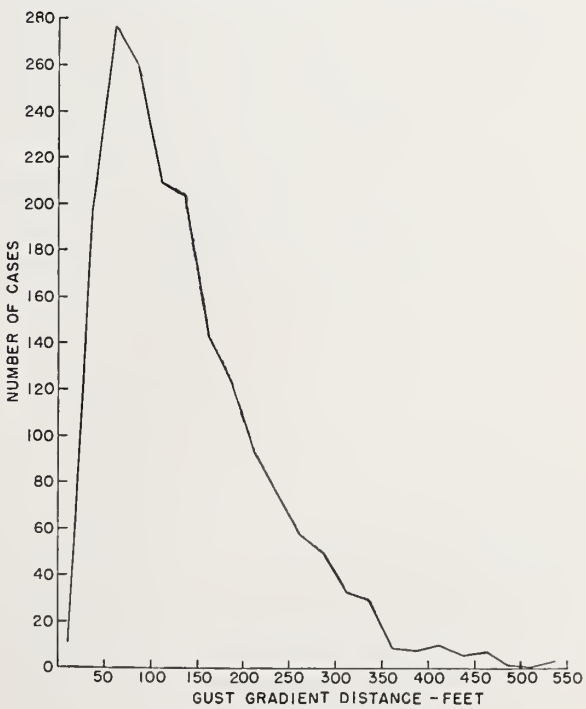

FIGURE 36.—A frequency diagram of the gradient distances of 1,800 gusts chosen at random from the records of the Florida and Ohio flights.

metrical and that the gust gradient distance is about one-half the size of the gust, it is evident that most of the gusts measured by the Project ranged in size from 25 ft. to 800 ft. The most frequent size of gust encountered was about 150 ft. in diameter.

The significance of conclusions drawn from these data depends to a large extent upon the degree to which the measurements may have been affected by characteristics of the airplanes and the manner in which they were flown. It is believed that the major airplane characteristics are allowed for by use of the sharp-edged gust formula, in which the airplane speed, altitude, weight, and airfoil properties are important. As for the other factor, it has frequently been assumed that the characteristics of pilot technique do not bias the observations. To test the validity of such an assumption, Press [41], of N. A. C. A., made a statistical study of the data from the Florida flights of the Thunderstorm Project. In order to carry out this study, it was necessary to assume that:

1. The flight assignments of airplanes and pilots are random and independent.
2. The effects of extraneous factors such as altitude, storm intensity, and stage of storm development are random.
3. The size of the sample is sufficiently large so that the effects of extraneous factors are largely averaged out.

From the results of this study Press concluded that the characteristics of pilot technique appear to influence gust measurements. Although it is recognized that the data used were insufficient to yield definite conclusions, they do indicate that with the same intensity of gustiness and the same type planes, the effective gust velocities encountered by one pilot may be greater than those encountered by another even though both pilots are instructed to use the minimum amount of control consistent with safety.

Since it seems likely that the initial conditions he assumes were not completely fulfilled, great confidence should not be placed in the absolute value of his numerical results. On the other hand, the range of the number of traverses required for a pilot to encounter a gust having an effective gust velocity equal to or greater than 25 ft/sec was from 22 to 26 (for the three pilots who flew 50 or more thunderstorm traverses during the Florida operations). The range was even wider in the case of pilots who flew fewer than 50 traverses. Restricting consideration to those pilots who flew 50 or more traverses should tend to equalize variations brought about by extraneous factors such as storm intensity and flight altitude, and variations resulting from differences in control technique should be more evident.

The interpretation of the interrelation of gusts and drafts as the constituent parts of thunderstorm turbulence stems from a realization that the gusts, or the sharp accelerations and attitude deflections caused by the gusts, determine the intensity of "turbulence" for the average flight crew member. Studies have been made relating gust speeds and gust frequencies encountered by Project airplanes with the turbulence intensity reported by the highly experienced personnel who made up the Project flight crews. It was found that the intensity of turbulence reported by these crews was almost entirely determined by the gusts encountered by the airplanes and not, as one might at first suspect, by the displacements in altitude which the airplanes experienced as a result of thunderstorm drafts. In particular, these investigations show that if the most intense gust in a group of several contiguous gusts exceeds about 15 ft/sec while at the same time the frequency of the gusts is greater than 8 per 3,000-foot interval of flight, Project flight crews classified the turbulence as "heavy." When the region under consideration is extended to the length of one complete traverse through a thunderstorm, it is found that heavy turbulence was reported for even smaller values of gust velocities and gust frequencies[34].

[34] Complete details of the investigation relating pilot reports of the intensities of the turbulence to measured gust parameters is contained in Pt. Two, ch. IX.

2. Hydrometeors within the Thunderstorm

The character and intensity of the hydrometeors associated with the thunderstorm at the surface can be easily observed. Within the thundercloud itself, identification and determination of the intensity of these elements is considerably more difficult. No instrument suitable for measuring all hydrometeors in the cloud, whether liquid or solid, has been devised, and visual observation is difficult in aircraft, owing to the high speed of travel.

During the operations of the Thunderstorm Project, all observations of hydrometeors within the storms traversed were made visually by the flight crews. Of course, such observations were subjective in nature. As the personnel became accustomed to the conditions within thunderstorms, their opinions as to the severity of the weather encountered were probably modified, and it is therefore likely that intensities of the elements, as reported, decreased as the experience of the observers increased. Since assigned flight altitudes were rotated among the various flight crews, the preponderance of a single man's judgments with respect to data for any one level was avoided. Obser-

TABLE 14 (a).—*Frequency* (N) *and percentage distributions of various rain intensities at a given altitude (based upon* 1946 *data from Florida thunderstorms)*

Rain intensity	Flight altitude (ft. m.s.l.)									
	6,000		11,000		16,000		21,000		26,000	
	N	%	N	%	N	%	N	%	N	%
Light	29	30	35	27	33	26	3	3	0	0
Moderate	22	23	32	24	14	11	5	4	0	0
Heavy	41	43	16	35	24	19	2	2	0	0
Unclassified	4	4	13	10	21	16	10	8	1	1
No rain	0	0	5	4	36	28	95	83	80	99
Total	96	100	131	100	128	100	115	100	81	100

TABLE 14 (b).—*Frequency* (N) *and percentage distributions of various rain intensities at a given altitude (based upon* 1947 *data from Ohio thunderstorms)*

Rain intensity	Flight altitude (ft. m.s.l.)									
	5,000		10,000		15,000		20,000		25,000	
	N	%	N	%	N	%	N	%	N	%
Light	23	20	45	21	38	18	7	4	0	0
Moderate	23	20	63	29	37	18	3	2	0	0
Heavy	47	42	82	38	22	11	10	6	1	1
Rain and snow	0	0	4	2	55	26	4	2	1	1
Unclassified	5	5	12	5	10	5	6	4	4	3
No rain	14	13	11	5	46	22	134	82	105	95
Total	112	100	217	100	208	100	164	100	111	100

vations in Ohio were more complete than those in Florida, since for this second season of flights a special weather observer was added to each flight crew. For these reasons, data for the two seasons are not strictly comparable, and, accordingly, a separate tabulation has been made for each season.

PRECIPITATION

The form of the precipitation which occurs at various levels during the three stages of the thunderstorm cell has been discussed earlier in this chapter. Further discussion of these weather phenomena is of interest, since it is possible to point out the most frequently observed intensities of precipitation at each level of observation, when the entire storm, rather than the individual cell, is considered.

Before discussing the observations, it is necessary to consider the perceptions that indicate "precipitation" to a man traveling at high speed through a cloud. If he notes that the airplane is getting wet, especially on the windshield, he will report rain. This water may be falling to the ground, or it may be suspended in, or ascending with, the rising currents of the cloud. Whatever its movement relative to the earth's surface, this water will be classified as precipitation by the observer. Small hail may be differentiated from rain only by the sound it produces on striking the windshield or canopy. Snowflakes and large hail would, in most cases, be easily identified. Graupel probably cannot be distinguished from small hail or snow forms. Snow crystals, snow pellets, soft hail, ice needles, and other special forms of hydrometeors are practically unidentifiable at high speeds.

The tables presented in the following paragraphs represent a compilation of the greatest intensity of given forms of precipitation observed on each thunderstorm penetration.

Rain.—Liquid water was encountered within the thunderstorms at all levels at which observations were made, although, as shown in tables 14(a) and 14(b), it was encountered most frequently and in greatest intensity at the lower levels. In fact, from the freezing level downward, rain was observed on almost every penetration of a thunderstorm. The fact that a "no-rain" report was more frequent for the lower levels in Ohio than for those in Florida is attributable, at least in part, to the fact that in Ohio a greater percentage of observations was made in cells in a very early stage of development.

The single observation of heavy rain at 25,000 ft. was made during a traverse through an updraft with a speed of 52 ft/sec.

Snow.—As shown in tables 15(a) and 15(b), the maximum frequency of moderate and heavy snow occurred at the two upper levels of flight in Florida and Ohio. As might be expected, almost every occurrence of mixed rain and snow in Ohio occurred at 15,000 ft., the approximate altitude of the freezing level[35]; the reporting of this phenomenon was not provided for during Florida operations. There was little difference in the storms in Ohio and Florida as far as snow was concerned, except at the 10,000- and 11,000-foot levels. The occurrence of snow at 10,000 ft. in Ohio was a result of the occasional lowering of the freezing level in that area during the operating season.

[35] See fig. 15, p. 20 for the mean temperature values obtained for radiosonde ascents.

TABLE 15 (a).—*Frequency* (N) *and percentage distributions of various snow intensities at a given altitude (based upon* 1946 *data from Florida thunderstorms)*

Snow intensity	Flight altitude (ft. m.s.l.)									
	6,000		11,000		16,000		21,000		26,000	
	N	%	N	%	N	%	N	%	N	%
Light	0	0	0	0	42	33	41	36	29	36
Moderate	0	0	0	0	23	18	28	24	11	13
Heavy	0	0	0	0	10	8	25	22	15	19
Unclassified	1	1	0	0	12	9	9	8	18	22
No snow	95	99	131	100	41	32	12	10	8	10
Total	96	100	131	100	128	100	115	100	81	100

TABLE 15 (b).—*Frequency* (N) *and percentage distributions of various snow intensities at a given altitude (based upon* 1947 *data from Ohio thunderstorms)*

Snow intensity	Flight altitude (ft. m.s.l.)									
	5,000		10,000		15,000		20,000		25,000	
	N	%	N	%	N	%	N	%	N	%
Light	0	0	13	6	50	24	58	35	45	40
Moderate	0	0	5	2	33	16	41	25	24	22
Heavy	0	0	0	0	13	6	37	23	24	22
Rain and snow	0	0	4	2	55	27	4	2	1	1
Unclassified	2	2	11	5	13	6	5	3	7	6
No snow	110	98	184	85	44	21	19	12	10	9
Total	112	100	217	100	208	100	164	100	111	100

Hail.—Relatively few instances of hail were noted in either Florida or Ohio thunderstorms. As shown in tables 16(a) and 16(b), hail was observed most frequently at the middle levels flown. It was seldom present at more than one or two levels in the same storm, and when it was present, it was found on 25 percent or less of the traverses through the storm at the level of its occurrence[36].

[36] It should be borne in mind that the regions of operations of the Thunderstorm Project were considerably removed from the region of maximum occurrence of hail at the surface [55].

TABLE 16 (a).—*Frequency* (N) *and percentage distributions of various hail intensities at a given altitude (based upon* 1946 *data from Florida thunderstorms)*

Hail intensity	Flight altitude (ft. m.s.l.)									
	6,000		11,000		16,000		21,000		26,000	
	N	%	N	%	N	%	N	%	N	%
Light	0	0	1	1	4	3	1	1	2	3
Moderate	0	0	1	1	6	4	3	3	0	0
Heavy	0	0	1	1	3	3	0	0	0	0
No hail	96	100	128	97	115	90	111	96	79	97
Total	96	100	131	100	128	100	115	100	81	100

TABLE 16 (b).—*Frequency* (N) *and percentage distributions of various hail intensities at a given altitude (based upon* 1947 *data from Ohio thunderstorms)*

Hail intensity	Flight altitude (ft. m.s.l.)									
	5,000		10,000		15,000		20,000		25,000	
	N	%	N	%	N	%	N	%	N	%
Light	1	1	9	4	0	0	5	3	2	2
Moderate	0	0	2	1	2	1	3	2	0	0
Heavy	0	0	5	2	4	2	0	0	0	0
Unclassified	1	1	10	5	4	2	2	1	1	1
No hail	110	98	191	88	198	95	154	94	108	97
Total	112	100	217	100	208	100	164	100	111	100

Hail appears to be associated with particular cells within the storm, rather than with the storm as a whole. The presence of both updrafts and downdrafts in the regions where hail occurs, and the fact that in those storms for which sufficient data were available for cell analysis hail was observed during the mature stage, suggest that it is during this stage that most, if not all, of the hail occurs.

Although the number of cases available for study is small, there is evidence to suggest that the cells in which hail occurs have within them updrafts of greater than average speeds. Studies of the rates of vertical growth of the radar echoes from four cells in which hail was observed showed that in every case the draft speed within the cell must have exceeded 50 ft/sec. These four cells were portions of storms that occurred on three different days. On these same three days, three cells in which it is fairly certain that hail did not occur showed rates of growth of less than 40 ft/sec. Table 17 shows the speeds of drafts measured by the airplane instruments in the regions in which hail was reported, as well as the average draft speed for each particular level. As is evident from the table, draft speeds associated with observations of hail are greater than the average in almost every case. At the 25,000-foot level there were no reports of hail that could be located accurately enough to permit relating them to a particular draft.

TABLE 17.—*Average speeds for drafts measured at various flight levels during* 1947 *and the speeds of drafts associated with reports of hail*

Flight altitude (ft.)	Average updraft speed (ft/sec)	Speed of drafts associated with reports of hail		Reports of hail in areas where draft speeds could not be computed (No. of reports)
		Updrafts (ft/sec)	Downdrafts (ft/sec)	
5,000	14	.....	26.7	2
10,000	21	31.2	27.2	14
		30.0	10.8	
		10.0	28.0	
		36.7	17.6	
			29.4	
15,000	24	36.2	20.8	12
		32.7		
		16.9		
		39.4		
		56.4		
		31.9		
		17.4		
20,000	23	7.4	.....	3
		17.9		
		32.5		
		40.3		
		37.7		

ICING

In those storms observed by the Thunderstorm Project, conditions producing icing were experienced on approximately one-half of all the penetrations at the two upper levels of flight, as is shown in tables 18(a) and 18 (b). The observations of the occurrence of icing on the airplanes in Florida did not include a classification of the type of ice. In Ohio, however, where ice was classified according to type as well as intensity, it was found that the majority of cases were called rime icing. Heavy icing was encountered very infrequently, and on no occasion during the two seasons of operations did ice accumulate to such an extent as to make impossible safe flight in the P-61C airplanes. In almost every instance, the airplanes were in the clear air between traverses for a period sufficiently long to allow the ice to evaporate. The fact that only small amounts of ice were accumulated is consistent with the short period of time during which the airplanes were subjected to icing conditions on each traverse. In this regard it should be pointed out that on July 22, 1946, a project sailplane, spiraling upward within an updraft region in a thunderstorm, iced so heavily that the pilot lost the use of the elevator control surfaces. In this instance, the sailplane had been in the cloud above the freezing level about 12 min. before the ice accretion reached such proportions.

TABLE 18 (a).—*Frequency* (N) *and percentage distributions of various icing intensities at a given altitude (based upon* 1946 *data from Florida thunderstorms)*

Icing intensity	Flight altitude (ft. m.s.l.)									
	6,000		11,000		16,000		21,000		26,000	
	N	%	N	%	N	%	N	%	N	%
Light	0	0	5	4	34	27	42	36	22	27
Moderate	0	0	0	0	1	1	26	23	5	6
Heavy	0	0	0	0	1	1	8	7	5	6
No icing	96	100	126	96	92	71	39	34	49	61
Total	96	100	131	100	128	100	115	100	81	100

TABLE 18 (b).—*Frequency* (N) *and percentage distributions of various icing intensities at a given altitude (based upon* 1947 *data from Ohio thunderstorms)*

Icing intensity	Flight altitude (ft. m.s.l.)									
	5,000		10,000		15,000		20,000		25,000	
	N	%	N	%	N	%	N	%	N	%
Rime—light	0	0	5	2	35	17	38	23	23	21
Rime—moderate	0	0	0	0	1	1	14	8	8	7
Rime—heavy	0	0	0	0	0	0	3	2	5	5
Rime and clear	0	0	0	0	3	1	10	6	1	1
Clear	0	0	1	1	2	1	5	3	2	2
Unclassified	0	0	6	3	18	8	24	15	15	13
No icing	112	100	205	94	149	72	70	43	57	51
Total	112	100	217	100	208	100	164	100	111	100

CHAPTER III. THUNDERSTORM WEATHER NEAR THE SURFACE

1. Thunderstorm Rainfall

The water droplets formed in the ascending current of a cumulus cloud usually are so small that they are carried upward with essentially the speed of the updraft. In the cumulus stage, continued ascent with condensation in most cases produces more and more droplets rather than promoting the growth of existing ones. Then something happens that makes droplets grow to the size of raindrops. In the clouds studied by the Thunderstorm Project, this event always seemed to be associated with the penetration of the cloud to heights at which ice crystals could form and play the role ascribed to them by the Bergeron theory of precipitation. According to the international cloud classification, the cloud at this stage is a cumulonimbus.

If the updraft is of appreciable speed, coalescence of large drops may take place while they are still being carried upward. In any case, the amount of water soon exceeds that which can be supported by the updraft. The water particles then begin to descend, slowly at first, then more rapidly as they drag the air with them, and finally they reach the ground as rain. This marks the beginning of the mature stage in the thunderstorm life cycle (ch. I, sec. 2).

In the following paragraphs, distribution of the rainfall over the surface, its duration and general character, and its relationship to the observed radar echo are discussed.

Rainfall pattern.—In the thunderstorms studied by the Project, it was found that the rainfall pattern under a thunderstorm follows closely the arrangement of the cells in the storm and reflects, to a considerable extent, their various stages of development. A single, isolated thunderstorm cell is comparatively rare in the regions studied, and when it does occur, it is generally weak and not representative of the average thunderstorm. Usually a thunderstorm consists of a group of three or more cells adjacent to each other, each manifesting itself in the rainfall pattern.

The first rain reaching the ground is limited in area to a few square miles. Later, as the cell develops, the rain area expands along with the increase in horizontal extent of the downdraft with which the rain is associated. Since the cold air of the downdraft spreads out radially after reaching the surface, while the rain falls to the ground, an ever-expanding outer area of cold air without rain develops. In the dissipating stage of the cell, the rain area contracts while the cold air continues to spread. As would be expected, under a moving cell the area of rain advances over the surface approximately at the speed of movement of the cell itself. Minor variations may result from shifts of the rain area within the cell and from lateral spreading as raindrops are carried outward by a strong and deep divergent airflow. Because of the latter effect, the rain may spread out asymmetrically with respect to the cell. It is also characteristic that the progression of the rain area is more rapid at the leading edge of the cell than at the lateral or trailing edges.

The sharpness of the rain-area boundary varies with the age of the cell. Early in the mature stage, the horizontal gradient of the rate of rainfall is usually steep; values of 0.60 in/5 min/mi have been observed. As the cell ages, this rainfall intensity gradient decreases, and by the time the cell reaches the dissipating stage, gradients are weak.

Duration of rainfall period.—The duration of moderate or heavy rain from a single cell of a storm may vary from a few minutes in the case of weak, short-lived cells to almost an hour in the case of large, active ones. It is in the latter, of course, that strong updrafts persist for considerable periods, providing a long-continuing source of rain. However, the duration of the rain period observed at a surface station depends upon a number of factors and is therefore more variable than that of a single cell. First, the number, size, and longevity of the cells in a storm passing over a surface station determine the duration of rainfall from that storm. Second, the duration of rain varies with the position of the station with respect to each passing cell; stations to the rear or on the lat-

eral edges of a cell receive smaller rainfall amounts and have shorter periods of rainfall than stations in the path of the center of the cell. Third, the rate of storm movement determines how long a station in its path will be under its influence. An analysis of 16 Florida storms, made without an attempt to separate any of the above factors, shows that the average time duration of rainfall at a station was 27 min.; for Ohio, a similar analysis of 11 storms yielded an average duration of 24 min. The difference between these two is statistically insignificant.

Rainfall rates.—There is considerable variation in the rainfall rates which occur over the area influenced by thunderstorms. Maximum rates occur at the location of a cell core within 2 or 3 min. after the first measurable rain from the cell reaches the ground, and the rain usually remains very heavy for a period of 5 to 15 min. Thereafter the rainfall rate decreases, but much more slowly than it increased. Lesser rates occur around the edges of a cell. With the 2-mile spacing used in the Ohio network, the heaviest rain from a single cell was usually recorded by only two or three stations, although others may have recorded heavy rainfall according to the Weather Bureau criteria[37].

A study was made of the variation with time of the rainfall rates observed at each of the surface stations within the rain areas of 18 thunderstorms observed in Florida and Ohio. Data were taken from rainfall tabulation sheets on which were entered the rainfall amounts accumulated in successive 5-minute intervals of the rain period — intervals beginning and ending at an integral number of 5 min. past the hour. For example, accumulated rain amounts for periods such as 1305–1310, 1310–1315, 1315–1320, etc. were used. These accumulated amounts were then used to obtain values representing the ratio of each 5-minute rainfall rate to the average rainfall rate observed at the station for the particular rainfall period. This quantity was termed the "rainfall-rate ratio." Such ratios were computed for each period of rainfall recorded at each station. Then, by means of relating corresponding time intervals (e.g., first, second, and third, etc. 5-minute interval in which rain occurred) in the rainfall periods for all stations recording rain from a particular storm, average ratios were obtained for *each storm*. From the same group of individual station averages, average ratios were also computed for *all storms* studied. In the graph of figure 37, the latter ratios are shown plotted against elapsed time from the beginning of measurable rain.

Results of this study show that the rainfall rate at a station reaches its maximum within the first 10 to 15 min. of the rain period. Inasmuch as the majority of the storms upon which the study was based moved relatively slowly, it may also be said that these results indicate that the major portion of the rainfall occurs in the early part of the rain period. For any one storm, the passage of several cells over a given station may cause a great variation in the rainfall rates observed at the station. The rainfall-rate ratio chart for storm 48 of July 17, 1946 (fig. 38), shows such variations in a striking fashion.

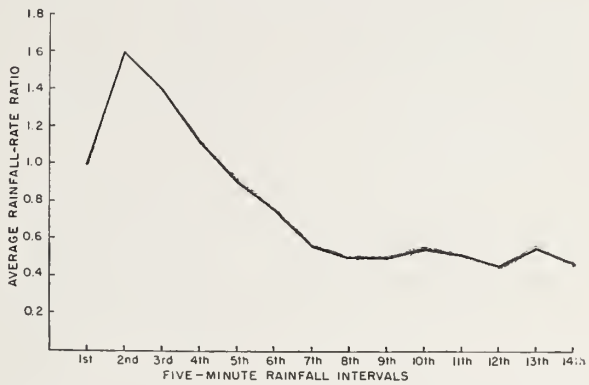

FIGURE 37.—A graph showing the ratios of rates of rainfall during 5-minute intervals to the average rate of rainfall over the entire rain period. Values shown are averages computed from a study of 18 storms in Florida and Ohio.

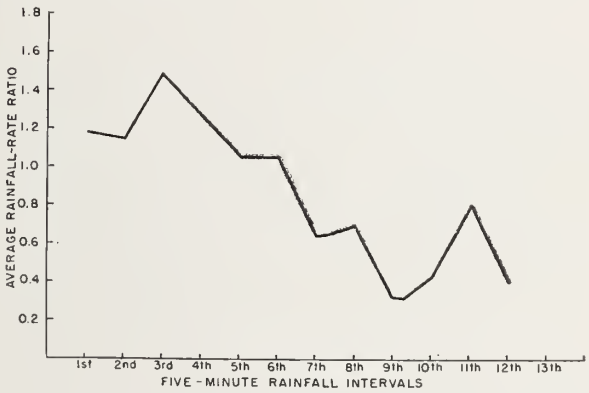

FIGURE 38.—A graph showing the ratios of rates of rainfall during 5-minute intervals to the average rate of rainfall over the entire rain period. Values shown are averages computed from observations over the entire network during the storm of July 17, 1946. The plateaus and secondary maxima in this curve reflect rainfall from new cells.

The use in this study of recorded rain data tabulated for 5-minute intervals had one disadvantage. Since the rain may not have fallen during the entire 5 min. of the first and last 5-minute intervals, the values of the rainfall-rate ratios are too low for these intervals. In spite of the shortcoming, the time distribution of the rainfall rate is, for the most part, representative.

Radar-rainfall relationships.—It is well known that liquid water in the atmosphere will reflect a portion of the radiant energy from a radar set. If this reflected energy is suitably detected, it indicates the location and, roughly, the concentration of the liquid water

[37] According to Circular N, rainfall rates greater than 0.30 in/hr are defined as heavy in intensity.

particles. Since large concentrations of liquid water occur within thunderstorms, it has been proposed that radar can be used not only for detecting the thunderstorm's position but also for estimating the amount of rain falling from it. From data obtained in the Florida operations it was shown that there is a high degree of correspondence between the PPI radar echo of the type of 10-centimeter control radar set used and the associated rainfall pattern as determined from observations made at the surface network stations [**18**]. The empirical relationship between the area of rain (A_{rain}) and area of radar echo (A_{echo}) in square miles obtained by using this particular radar set in Florida was

$$A_{echo} = 3.15 \text{ sq. mi.} + 1.01\ A_{rain},$$

representing the average relationship for many observations. The same regression equation would not be expected to hold for other radar sets. However, there is reason to believe that further developments will make possible quantitative determination of the amount of rain falling from thunderstorms solely from indications of a radar set. Notable advances along these lines have, in fact, already been reported by Atlas [**3**], and Langille, Gunn, and Palmer [**33**].

In a consideration of the correspondence of radar echoes to rainfall observed on the ground, several points should be noted. Since it takes time for the raindrops formed in the region of coalescence in the clouds to reach the ground, the radar echo appears on the 'scope several minutes before the beginning of the rainfall. In addition, in the case of small echoes which remain on the 'scope for only a few minutes, frequently no rain is observed at the surface. This may be due to complete evaporation of the raindrops before they reach the ground. Also, in the final stages of the thunderstorm, after the PPI echo disappears, areas of light rain may persist for a time longer than that necessary for the raindrops to fall from the levels of coalescence. This may be explained by the fact that the water concentration in the region where the drops are formed is below the minimum detectable at that range for the particular radar used.

2. Wind Field beneath the Thunderstorm

In the surface winds under a thunderstorm are reflected much of the complex structure and many of the processes of the individual thunderstorm cells. When a cell is in the early building stage and only an updraft is present, there is a gentle inward turning of the surface wind, forming a weak horizontal-convergence area under the updraft. Except for changes in the electric field, this change in wind is the first surface manifestation of the developing thunderstorm[38]. As the storm cell grows and a downdraft develops, the surface winds take on an entirely different character, becoming strong and gusty as they flow outward from the downdraft region.

Technique of calculating divergence.—In the analysis of surface data from thunderstorms the convergence or divergence of the measured surface wind has proved to be a valuable tool for determining vertical motions in the lowest layers of the atmosphere. This follows from a consideration of the continuity principle, resulting in the following expression for the divergence of the velocity:

$$Div\ C = \frac{\partial u}{\partial x} + \frac{\partial v}{\partial y} + \frac{\partial w}{\partial z}$$

where u, v, and w are the velocity components respectively in the x (eastward), y (northward) and z (upward) directions. In cases where the fluid is not compressed, the total divergence, $Div\ C$, must equal zero; therefore

$$Div_2\ C = \frac{\partial u}{\partial x} + \frac{\partial v}{\partial y} = -\frac{\partial w}{\partial z}$$

where $Div_2\ C$ is the horizontal velocity divergence. If $Div_2\ C$ is positive, w must decrease with height. Since w must be zero at the earth's surface, positive divergence is associated with downward motion of the air ($w < 0$). Conversely, negative horizontal velocity divergence (convergence) is associated with the upward motion of the air[39]. In practice, it is customary to represent $Div_2\ C$ by $\frac{\Delta u}{\Delta x} + \frac{\Delta v}{\Delta y}$, which in the absence of discontinuities, is not significantly different from $\frac{\partial u}{\partial x} + \frac{\partial v}{\partial y}$. In the analysis of Project surface data the terms $\frac{\Delta u}{\Delta x}$ and $\frac{\Delta v}{\Delta y}$ were determined from the 5-minute averages of winds measured by the surface stations of the network.

In calculating the divergence from the Florida measurements, isopleths of u and v were drawn. From these, the magnitudes of $\frac{\Delta u}{\Delta x}$ and $\frac{\Delta v}{\Delta y}$ were deter-

[38] Strictly speaking, this is true only of thunderstorms which are, at least in part, set off in response to low-level conditions and whose bases are only a few thousand feet above the ground.

[39] For complete development of the divergence equation, the reader is referred to any of the standard texts on dynamic meteorology.

mined. Generally, Δx and Δy were taken as 1 mi. Florida measurements were obtained from the double-register type of wind equipment which measured the direction to only eight points of the compass; wind speed was measured by the length of time it took a nautical mile of wind to pass the station.

In Ohio, gust-recording wind equipment was available and provided continuous and nearly-instantaneous values of the wind. Divergence calculations in this area were made by means of a slightly different technique. The stations in the network were arranged in rather uniform rows and columns. Therefore it was possible to prepare tables of u and v for the complete range of wind speeds and directions from which, by means of double interpolation, the divergence values were computed. The divergence value based upon the winds at the stations forming the four vertices of a square was plotted at the middle of the square[40].

Inflow field.—Characteristic patterns in the wind velocity-divergence field are associated with the various stages of the thunderstorm life cycle. During the early cumulus stage, even 20 to 30 min. before the radar echo appears, the surface winds turn toward the areas of convection, where relatively weak convergence develops. In general, the speed of the wind during the period of inflow is light, 4 to 8 mi/hr. The inflow field, which frequently extends over a radius of 6 to 8 mi., is best observed during the development of an isolated thunderstorm cell or the first cell of a group. When there are numerous cells in the vicinity, the outflow of one may so completely dominate the surface wind flow that it is impossible to detect the inflow field of another. The magnitude of the convergence found in the inflow fields ranged up to about 4 hr^{-1}.

The "calm before the storm" often mentioned in literature may be explained as the establishment of inflow components counter to the prevailing wind direction. A complete blocking of the winds may thus occur, resulting in calm conditions prior to the development of the more violent, mature stage of a thunderstorm.

Outflow field.—When the cold downdraft of a cell reaches the surface layers of the atmosphere, it spreads out in a fashion similar to that of a fluid jet striking a flat plate. As a result, there is an immediate reversal from the inflow which was present during the cumulus stage of the cloud development. The outward-flowing cold air underruns the warmer air and a discontinuity in the wind and temperature fields is established. This discontinuity, or actually this discontinuity zone, moves outward with the spreading cold air from the downdraft. Strong divergence in the surface

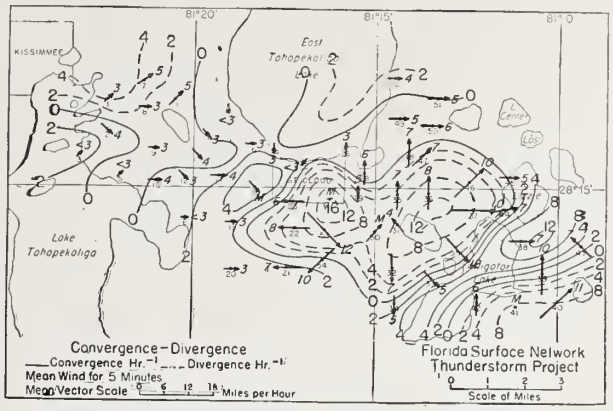

FIGURE 39.—An illustration of the outflow resulting when the air of the downdraft spreads over the surface. Downdrafts from two cells were centered over the network and it is apparent that a third was located south or southeast of stations 40 and 41. Note the radial nature of the outflow from the divergence centers of 12 hr^{-1} and 16 hr^{-1}. The convergence center of 12 hr^{-1} results from the confluence of two outflows and should not be compared with convergence centers resulting from inflow into a region of convective activity. Convergence resulting from opposing outflows sometimes attains values as high as 20 hr^{-1}.

winds develops as the downdraft spreads out over the surface, and it is the strongest observed during the thunderstorm. Values as high as 29.0 hr^{-1} have been computed from Project data.

In relatively slow-moving storms, the outflow is almost radial (fig. 39), and as it continues, an area of light winds develops immediately beneath the center of the downdraft area. In most instances, however, the outflow field is asymmetrical, with wind speeds on the downstream side substantially higher than those on the upstream side (Example, Aug. 13, 1947, 1610 E.S.T.). This is due to the reinforcement, or cancellation as the case may be, of the radial outflow by the prevailing air movement in the lower layers. As is shown in chapter VI, section 2, radar echoes representing storm cells move with the mean wind between the gradient level and the 20,000-foot level. As relatively high horizontal momentum, characteristic of the upper layers, is transported downward, surface outflow wind speeds in the direction of the cloud movement are reinforced while those in the opposite direction are retarded.

As a result, it is not infrequently observed with moving storms that almost all of the cold downdraft air spreads out in the direction toward which the cell is moving; consequently, the wind discontinuity at the trailing edge of the storm area is ill-defined, whereas at the leading edge the discontinuity may assume the appearance of a micro-cold front. In such cases the winds on the lateral edges usually have a component in the direction of the cloud movement but have speeds smaller than those near the leading edge.

The outflow air of the thunderstorm downdraft forms a dome-shaped mass of cold air extending from

[40] It was necessary to determine correction values for each square, since the stations were not quite equally spaced in rows and columns. These corrections were applied to the computed divergence values.

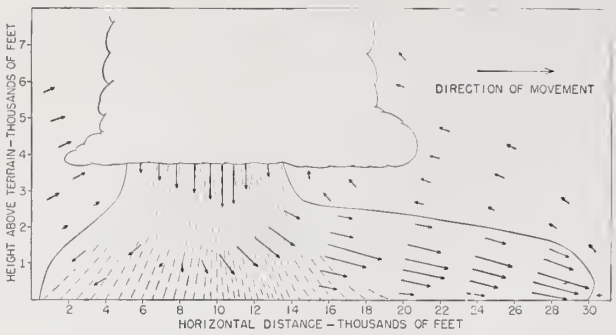

FIGURE 40.—A schematic vertical cross section through the dome of cold air beneath a thunderstorm cell in the mature stage. The arrows represent wind vectors and the dashed lines indicate rainfall.

the surface to several thousand feet. This mass of cold air has been termed the cold dome. A vertical cross section through a cold dome is illustrated schematically in figure 40. In this drawing the thunderstorm cell is considered to be in the mature stage and is moving from left to right. Note that the cold air has spread out considerably farther on the downwind side of the cell than on the upwind side.

After the outflow has been spreading 15 to 20 min., the discontinuity zone will have traveled about 5 or 6 mi. from the cell center. The surface winds near the discontinuity surface are still strong and gusty, but farther behind, inside the cold-air dome, the surface wind speeds have decreased so that the strongest winds are no longer underneath the cell itself. This increase in the wind speed (illustrated in fig. 40) as one approaches the discontinuity zone from the cold-air side results from a continued settling of the outflow air.

Depth of the layer of cold outflow air.—At the present time there are insufficient measurements to provide an adequate picture of the geometrical configuration of the cold-air dome bounded by the discontinuity surface, although isolated soundings made through this cold air provide data concerning its vertical extent at a particular point and time. Since, for any given cell, the height of the cold dome is a function of space and time, isolated measurements are insufficient to determine its structure and temporal variations. However, the few available direct and indirect measurements yielding information on this are summarized below:

1. Data for three thunderstorms obtained by wind- and temperature-measuring equipment located on a tower operated by the Daniel Guggenheim Airship Institute, Akron, Ohio, provide a detailed picture of the wind field from the surface to 350 ft. The data indicate that the discontinuity surface extends at least to that height. Although the data were admittedly sparse, the traces shown in figure 121, p. 142, indicate that there is a marked velocity gradient between 40 ft. and 350 ft., with the wind speeds at the upper level substantially greater than those at the lower level.
2. Data, taken from the Eiffel Tower and presented by Koschmeider [**32**], show that the cold air extends to at least 1,000 ft. From these data, however, it cannot be determined to what extent the cold air runs out ahead of the air in the lower layers which is retarded by surface friction.
3. Radiosonde observations taken over the surface network shortly before and after the arrival of a thunderstorm showed cooling which sometimes extended up to 10,000 ft. The cooling was most marked in the lower layers, where the outflow air — potentially the coldest air in the thunderstorm — spreads out over the surface. Soundings taken through the cold dome usually showed an inversion or region of stable lapse rate below the 5,000-foot level. The top of the stable layer or the inversion may be considered the top of the cold dome, although this upper boundary is not always a well-defined discontinuity, particularly during the later stages of the outflow. Figure 41 illustrates this cooling as shown by soundings made both before and after the passage of the wind discontinuity zone at a station.
4. Divergence computations made from wind measurements taken in the vicinity of cells in the mature stage of development[41] show that the outflow (divergence) changes to inflow (convergence) at an average height of 2,500

[41] These computations are treated in greater detail in ch. I, sec. 4.

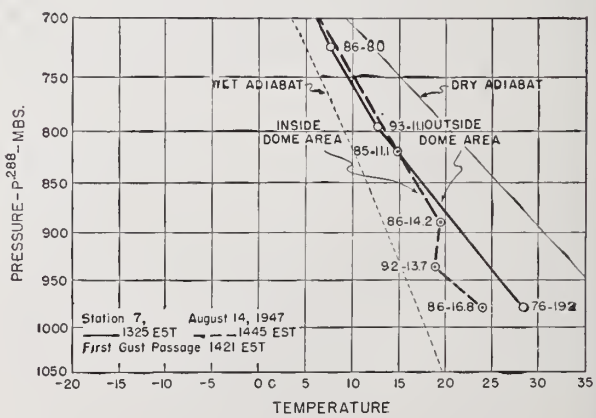

FIGURE 41.—A pseudo-adiabatic chart showing the temperature lapse rates outside and inside the cold dome of air associated with the outflow from a thunderstorm on August 14, 1947. Relative humidity, in percent, and mixing ratio, in gm/kg, for the dashed curve are shown on the left and for the full curve on the right.

ft. Individual measurements varied from 1,000 to 5,000 ft.

5. Additional information on the depth of the cold air in the lower layers is contained in data obtained during the storm of June 29, 1947. On this day, winds-aloft measurements and temperature soundings were made before and after the passage of the cold-air discontinuity surface, associated with a line of thunderstorms oriented in a northeast-southwest direction, which passed over the network. It should be pointed out that, being associated with a line of thunderstorms, this was a complex situation and the cold-air dome studied might not be similar in every respect to the domes produced by downdrafts in isolated storms. Isochrones of the first-gust line associated with this storm are shown in figure 42.

The height of the cold-air dome at any point was considered as the level at which the difference in the temperature measured on the earlier and later soundings was less than 4°C. An examination of those data presented in table 19 indicates that the top of the cold dome was not a sharply defined discontinuity with respect to wind flow or temperature. The temperature and wind differences between the two masses of air were at a maximum in the lower layers and decreased to relatively small quantities with height.

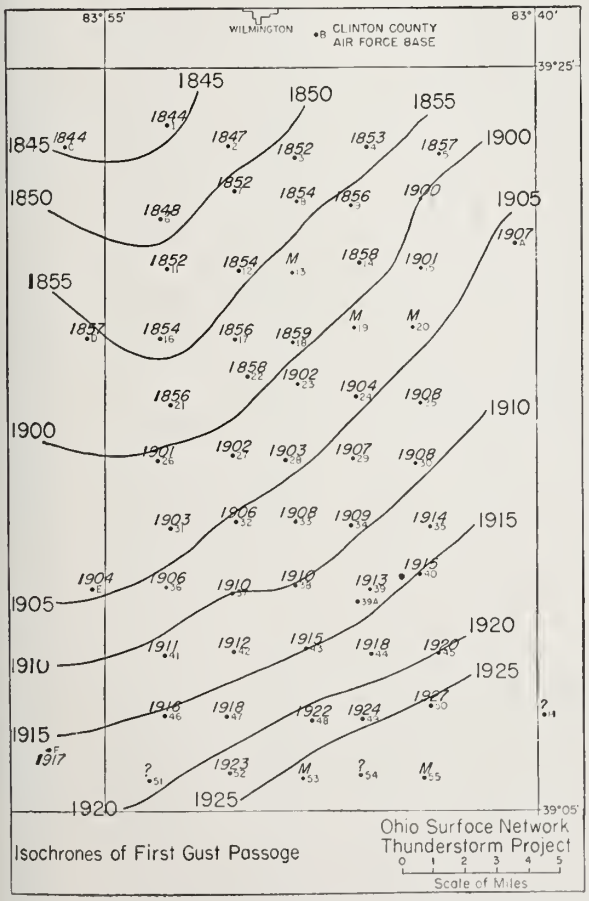

FIGURE 42.—A chart showing the isochrones of the passage of the first-gust line (surface wind discontinuity) over the Ohio network on June 29, 1947.

It may be seen from the data of table 19 that the northern stations, which were well back of the first-gust line at 1930 E.S.T., the time of the second sounding, showed that the velocity discontinuity between the warmer and colder air had a height of 6,000 to 8,000 ft. (The velocity discontinuity was considered to exist only if the wind direction difference exceeded 25°.) The southern stations, which were much closer to the surface first-gust line, showed the top of the discontinuity zone between 4,000 to 6,000 ft. In this case the height of the velocity discontinuity boundary appeared to increase with the distance from the first-gust line.

The height of the temperature discontinuity was generally several thousand feet less than that of the wind discontinuity. This indicates that there was a mixing zone of at least several thousand feet above the top of the cold dome as defined above.

The discontinuity zone.—The discontinuity zone, which everywhere marks the limit of the cold downdraft air, is one of the most interesting of all surface weather features associated with the thunderstorm passage. With the passage of this zone at a station directly underneath the center of a cell in the early mature stage, there is a sharp increase in the wind speed and a marked reduction in temperature. The sharp increase in wind speed has been termed the "first gust," since it often appears as a first major gust of a period of high, gusty winds. After the cold air spreads outward, the wind speeds near the boundary of this air decrease. The rate of decrease depends upon the following factors:

1. Surface friction.
2. Stability of the air being underrun.
3. The downward transport of horizontal momentum.
4. The speed of movement of the cloud itself.
5. The amount of air involved in the downdraft.

Frequently a new thunderstorm cell develops on the downwind side of an existing cell, and the cold air of the downdraft falls into a region where the surface air has already been displaced by the cold air from the previous cell. In cases of this kind the new source of cold air reinforces the original outflow, with the result that an otherwise unexpected increase in wind speeds occurs.

TABLE 19.—*Wind and temperature data obtained from soundings made before and after the passage of the cold-air discontinuity over the Ohio surface network stations on June 29, 1947*

Altitude of measurement (ft.)	Wind						Temperature (° C.)		
	Before passage		After passage		Algebraic difference				
	Direction (deg.)	Speed (mi/hr)	Direction (deg.)	Speed (mi/hr)	Direction (deg.)	Speed (mi/hr)	Before passage	After passage	Algebraic difference
STATION "C" [Passage of discontinuity surface: 1844 E.S.T. Soundings taken at 1757 E.S.T. and 1926 E.S.T.]									
Surface	[1]230	[1]5	[1]350	[1]8	[1]120	[1]3			
2,000	229	18	325	27	96	9			
4,000	226	20	290	25	64	5			
6,000	236	22	262	22	26	0			
8,000	253	18	254	24	1	6			
10,000	254	21	257	29	3	8			
12,000	255	28	261	30	6	2			
14,000	254	32	271	32	17	0			
16,000	265	31							
18,000	268	24							
20,000	271	20							
STATION NO. 7 [Passage of discontinuity surface: 1852 E.S.T. Soundings taken at 1755 E.S.T. and 1925 E.S.T.]									
Surface	210	10	345	8	135	−2	30.0	22.0	−8.0
2,000	218	18	338	22	120	4	27.5	19.1	−8.4
4,000	224	21	306	29	82	8	22.4	19.5	−2.9
6,000	234	20	272	19	38	−1	17.4	15.7	−1.7
8,000	255	21	259	25	4	4	12.4	11.7	−0.7
10,000	257	19	261	25	4	6	9.6	7.5	−2.1
12,000	257	26	262	31	5	5	5.3	4.0	−1.3
14,000	262	28	271	30	9	2	0.7	1.9	1.2
16,000	269	28	271	23	2	−5	−3.2	−0.7	2.5
18,000	261	21	269	24	8	3	−3.4	−4.6	−1.2
20,000	277	21	260	33	−17	12	−6.1	−8.0	−1.9
STATION "D" [Passage of discontinuity surface: 1857 E.S.T. Soundings taken at 1755 E.S.T. and 1925 E.S.T.]									
Surface							30.0	22.8	−7.2
2,000							27.1	22.9	−4.2
4,000							21.5	20.2	−1.3
6,000							16.8	17.1	0.3
8,000							13.7	13.2	−0.5
10,000							9.9	8.4	−1.5
12,000							5.9	6.1	0.2
14,000							2.1	2.9	0.8
16,000							−1.5	−0.3	1.2
18,000							−5.3	−3.7	1.6
20,000							−6.3	−7.1	−0.8
STATION NO. 19 [Passage of discontinuity surface: [2]1901 E.S.T. Soundings taken at 1755 E.S.T. and 1930 E.S.T.]									
Surface	210	10	360	12	150	2	29.5	21.6	−7.9
2,000	228	15	326	17	98	2	27.1	19.1	−8.0
4,000	227	21	291	23	64	2	22.3	16.8	−5.5
6,000	241	21	279	22	38	1	17.6	12.8	−4.8
8,000	258	16	268	26	10	10	13.3	9.9	−3.4
10,000	267	15	276	13	9	−2	9.4	7.1	−2.3
12,000	265	23	276	22	11	−1	5.3	3.9	−1.4
14,000	274	25	275	26	1	1	1.0	0.7	−0.3
16,000	265	25	274	24	9	−1	−3.3	−2.2	1.1
18,000	261	16	277	24	16	8	−5.4	−5.0	0.4
20,000	282	18	254	24	−28	6	−5.8	−10.0	−4.2
STATION "E" [Passage of discontinuity surface: 1904 E.S.T. Soundings taken at 1755 E.S.T. and 1925 E.S.T.]									
Surface	225	8	360	9	135	1	30.3	21.6	−8.7
2,000	233	14	321	29	88	15	27.3	20.1	−7.2
4,000	233	20	280	20	47	0	21.8	19.1	−2.7
6,000	241	22	248	15	7	−7	17.1	14.7	−2.4
8,000	264	20	267	30	3	10	13.5	10.4	−3.1
10,000	264	15	256	22	−8	7	9.7	8.7	−1.0
12,000	260	27	259	26	−1	−1	5.8	4.7	−1.1
14,000	260	28	253	27	−7	−1	2.2	1.3	−0.9
16,000	270	29	265	28	−5	−1	−1.6	−0.4	1.2
18,000	258	23	259	22	1	−1	−3.8	−3.8	0
20,000	273	14	250	21	−23	7	−5.9	−8.5	−2.6

[1] Estimated.

[2] Estimated from first-gust isochrone chart.

TABLE 19.—*Wind and temperature data obtained from soundings made before and after the passage of the cold-air discontinuity over the Ohio surface network stations on June 29, 1947—Continued*

Altitude of measurement (ft.)	Wind						Temperature (° C.)		
	Before passage		After passage		Algebraic difference		Before passage	After passage	Algebraic difference
	Direction (deg.)	Speed (mi/hr)	Direction (deg.)	Speed (mi/hr)	Direction (deg.)	Speed (mi/hr)			
STATION "A" [Passage of discontinuity surface: 1907 E.S.T. Soundings taken at 1755 E.S.T. and 1930 E.S.T.]									
Surface	190	5	360	25	170	20	...	...	...
2,000	215	11	354	30	139	19	...	...	...
4,000	225	18	300	28	75	10	...	...	...
6,000	235	21	263	26	28	5	...	...	...
8,000	258	16	258	22	0	6	...	...	...
10,000	265	17	251	23	−14	6	...	...	...
12,000	267	22	264	24	−3	2	...	...	...
14,000	267	29	272	24	5	−5	...	...	...
16,000	271	30	...	...	...	...	...	...	...
18,000	262	19	...	...	...	...	...	...	...
20,000	275	22	...	...	...	...	...	...	...
STATION "F" [Passage of discontinuity surface: 1917 E.S.T. Soundings taken at 1800 E.S.T. and 1925 E.S.T.]									
Surface	225	3	360	20	135	17	...	...	...
2,000	233	12	340	21	107	9	...	...	...
4,000	233	20	285	17	52	−3	...	...	...
6,000	241	23	254	19	13	−4	...	...	...
8,000	244	24	256	24	12	0	...	...	...
10,000	242	25	258	27	16	2	...	...	...
12,000	234	19	255	24	21	5	...	...	...
14,000	262	20	266	25	4	5	...	...	...
16,000	268	28	265	17	−3	−11	...	...	...
18,000	266	22	275	30	9	8	...	...	...
20,000	288	22	...	...	...	...	...	...	...
STATION NO. 47 [Passage of discontinuity surface: 1918 E.S.T. Soundings taken at 1800 E.S.T. and 1928 E.S.T.]									
Surface	240	8	340	4	100	−4	30.5	24.0	−6.5
2,000	231	16	323	16	92	0	29.2	22.3	−6.9
4,000	234	17	294	12	60	−5	24.0	19.3	−4.7
6,000	245	22	308	22	63	0	18.9	17.1	−1.8
8,000	264	16	304	29	40	13	14.4	14.6	0.2
10,000	278	14	...	...	...	...	11.3	...	...
12,000	275	19	...	...	...	...	7.7	...	...
14,000	274	25	...	...	...	...	3.5	...	...
16,000	265	28	...	...	...	...	−0.1	...	...
18,000	253	23	...	...	...	...	−2.8	...	...
20,000	261	17	...	...	...	...	−5.2	...	...
STATION "H" [Passage of discontinuity surface: [3]1930 E.S.T. Soundings taken at 1755 E.S.T. and 1915 E.S.T.]									
Surface	240	5	250	3	10	−2	...	...	...
2,000	232	15	246	15	14	0	...	...	...
4,000	235	19	263	16	28	−3	...	...	...
6,000	246	18	286	18	40	0	...	...	...
8,000	271	17	295	15	24	−2	...	...	...
10,000	293	11	295	14	2	3	...	...	...
12,000	271	19	286	16	15	−3	...	...	...
14,000	266	24	282	19	16	−5	...	...	...
16,000	269	31	270	22	1	−9	...	...	...
18,000	263	21	276	24	13	3	...	...	...
20,000	266	21	...	...	...	...	...	...	...

[3] Estimated from isochrones of temperature break.

Speed of movement of the discontinuity zone.—Not only the wind speed but also the rate of progression of the discontinuity zone itself is affected by the factors mentioned above. A study was made of its speed of movement by plotting the time of arrival of the first gust at each of the surface stations and drawing isochrones, as shown in figure 43. Such an analysis for 20 Florida storms indicated an average speed of movement of 18.2 mi/hr. A similar analysis for 11 Ohio storms showed an average speed of movement of 16.7 mi/hr. Because of the asymmetry in the outflow field, the rate of progression of the discontinuity zone varies with respect to its distance and direction from the cell, but the storm average represents, in general, the speed of the discontinuity zone at its leading edge.

Curiously enough, it is found that at least during some stages of the storm the discontinuity zone at the ground moves faster than the normal component of the winds immediately behind it. This conclusion results from the analysis made by means of the following technique:

1. In a chart such as shown in figure 44, the areas of the surface network over which the wind-speed discontinuity progressed steadily were delineated. An attempt was made to choose areas in which there were no effects due to new cell development. In each of these areas, three or four measurements of the speed of the surface discontinuity were made.
2. The wind component normal to the first-gust line was determined. For this purpose the maximum velocity associated with the first gust was used. All such wind components in the areas marked off (fig. 44) were averaged to give the average wind speed normal to and behind the first-gust line.

The results of the analysis, presented in table 20, indicate that the discontinuity zone, or first-gust line, frequently moves faster than the winds associated with it. This may be explained by the fact that there is rapid flow of colder air toward the ground along the

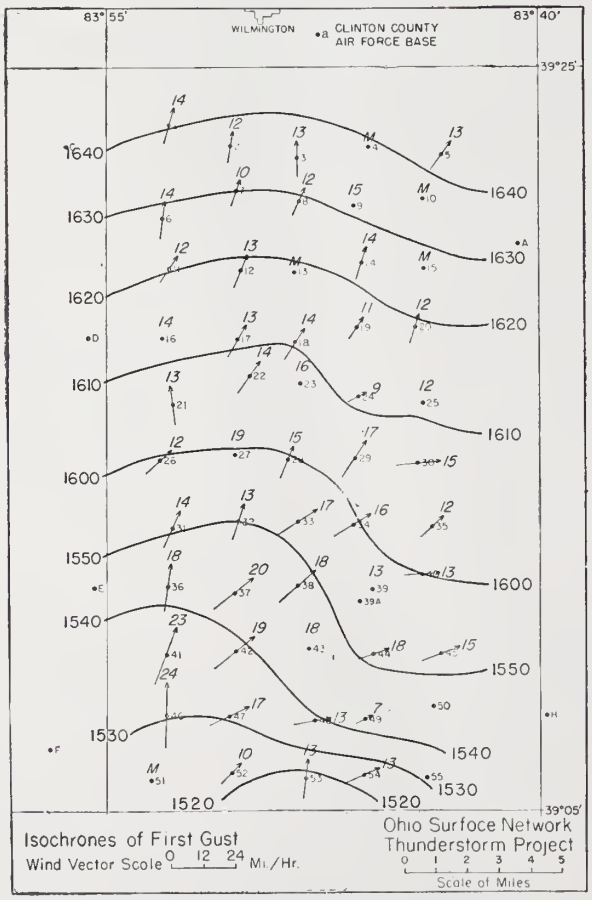

FIGURE 43.—A chart showing the isochrones of the occurrence of the first gust at the surface network stations during thunderstorms on August 13, 1947. The vectors and speeds plotted at each station show the velocity of the maximum wind associated with the first gust.

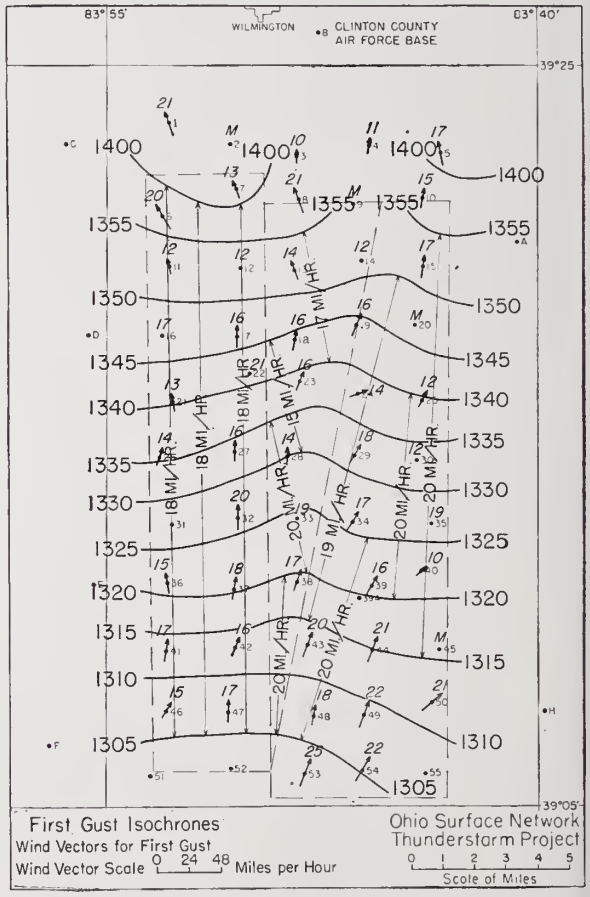

FIGURE 44.—A work chart used for comparing the speed of the first-gust line with that of the normal component of the maximum wind velocity associated with the first gust. The double-headed arrows between isochrones represent the distances over which the first-gust-line speed measurements were made. The speed values are indicated near the centers of the double-headed arrows. The vectors and speeds plotted at each station show the velocity of the maximum wind associated with the first gust. This wind discontinuity occurred with a thunderstorm on September 12, 1947.

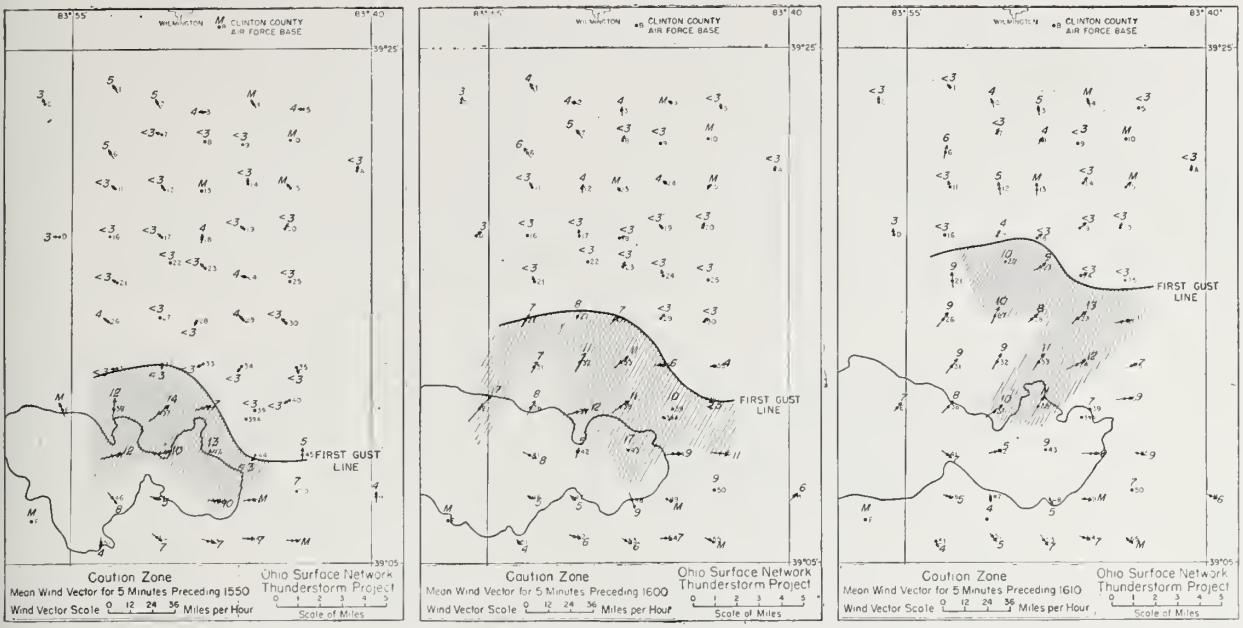

FIGURE 45.—A series of charts showing the progression of the caution zone (shaded area) across the surface network during a 20-minute interval. The irregular full lines are the outlines of the PPI radar echoes from the storm that produced the outflow. The numbers at the arrowheads represent 5-minute mean wind speeds. This outflow area was associated with a thunderstorm on August 13, 1947, over the Ohio network.

boundary zone. Thus, part of the progression of the discontinuity zone is due to downward-transported thrusts and part due to the horizontal wind. As may be expected, in areas of downward-flowing air, divergence develops behind the first-gust line and convergence ahead of it.

TABLE 20.—*Mean speeds of the movement of the first-gust line and of the component of the first gust normal to the line (for 11 Ohio thunderstorms)*

Storm No.	Date (1947)	Mean speed of first-gust line (mi/hr)	Mean first-gust velocity component (mi/hr)
151	Aug. 6	16.1	12.1
152	Aug. 6	23.6	11.1
158	Aug. 13	15.1	12.6
160	Aug. 14	13.9	14.7
163	Aug. 16	18.9	18.6
166	Aug. 17	12.8	11.3
167	Aug. 20	12.0	11.9
173	Aug. 25	19.2	19.8
182	Sept. 9	15.9	15.0
186	Sept. 12	18.4	15.2
187	Sept. 12	18.3	11.1

The caution zone.—In a previous publication [**56**] the caution period was defined as a period, following the first gust, during which the mean wind speed during any consecutive 5-minute interval is greater than 10 mi/hr. In the series of maps shown in figure 45, the caution-period area is indicated by hatching. Such an area has been termed the "caution zone." This zone spreads out radially from the center of surface activity but is frequently markedly suppressed at the trailing side of the cloud and reinforced at the leading edge. As the storm ages, the winds near the center decrease, so that the caution zone becomes a band of high wind speeds. This band increases in width as it moves outward from the position of a radar echo until a maximum width is attained; then it starts to shrink. In the later period of the storm, the caution zone may be seen as a relatively narrow band of higher wind speeds 10 to 12 mi. away from its point of origin at the surface. This band of higher wind speeds surrounding the slower-moving cold air in the general area where the storm developed, indicates that one or both of the following occurs:

1. Cold air glides downward within the upper regions of the cold dome in the manner indicated by the arrows of figure 40.
2. The entire cold-air pool flattens out.

It has been possible to observe only a few cases in which the caution zone spread outward, leaving the relatively immobile pool of cold air behind. This phenomenon was infrequently noted, since it may be seen only when a small group of storms present at one edge of the network is unaffected by other storms nearby. It is reasonable to assume that, with a larger surface network, separations of the caution zone from the storm would be observed often.

In a study of 20 Ohio storms, it was found that the caution period persisted at a station for an average of 17 min. after the occurrence of the first gust; however, in individual cases, the high, gusty winds remained for 2 or 3 min. or continued for as long as 90 min.

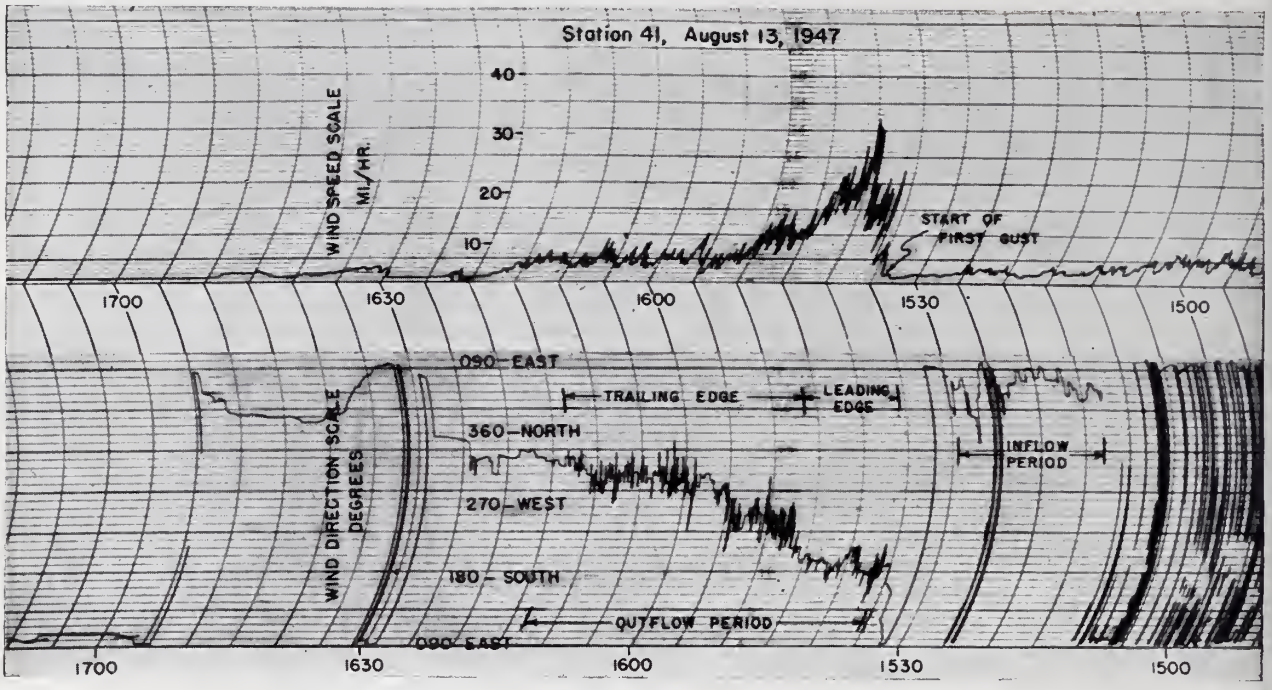

FIGURE 46.—Records of the wind direction and speed at station 41 of the Ohio surface network during a thunderstorm period on August 13, 1947. Time progresses from right to left. (See EXAMPLES, p. 181.)

Surface wind direction.—During the passage of a thunderstorm the surface winds at any given station may change in direction by as much as 180°, and direction changes may occur several times. This apparent inconsistency of the surface winds at a station in the path of a thunderstorm is resolved when the inflow, outflow, and movement components associated with each thunderstorm cell are considered. An example of direction changes at one station is shown in figure 46. This example shows how the wind changes from east to northeast due to the inflow effect and then changes to south due to the outflow. Because of the movement of the thunderstorm and its associated outflow field, the station is eventually in the trailing portion of the outflow area, which results in the wind's veering to northwest. Following the thunderstorm passage, the prevailing wind direction of east is resumed.

In the central region of surface activity, the change from the previously prevailing wind direction to the direction of the cold outflow takes place almost instantaneously. The amount of direction change, of course, depends on the position of the observation point with respect to the cloud cell and the previously prevailing wind direction. As may therefore be expected, direction changes of 180° are not rare. The sharpness of the change underneath the cell may be contrasted with the gradual character of the change some distance away.

At a distance of 5 or 6 mi. from the center of activity, the wind direction changes to that of the cold-air outflow as much as 5 or 10 min. before the arrival of the cold air. Although this early direction change may be used as a warning of the arrival of the caution zone, its usefulness is limited since it is pronounced only at distances from the cell core where the wind speeds are no longer great. Thus, when there are several cells with independent cold-air outflows, this precursory indication of the arrival of the first gust may become obliterated.

3. Temperature Field beneath the Thunderstorm

Although, as evidenced by the inflow, there are measurable changes in the wind field under a cell in the cumulus stage, no effect on the surface air temperature can be detected prior to or during the cumulus stage. At the time of formation of summer afternoon thunderstorms, particularly in the eastern United States, the temperature at the surface has reached its maximum value, usually above 85° F. Of course, the combined effects of differences in station elevation, exposure, and instrumental error result in a temperature field showing variations of a few degrees from one point to another over the surface network.

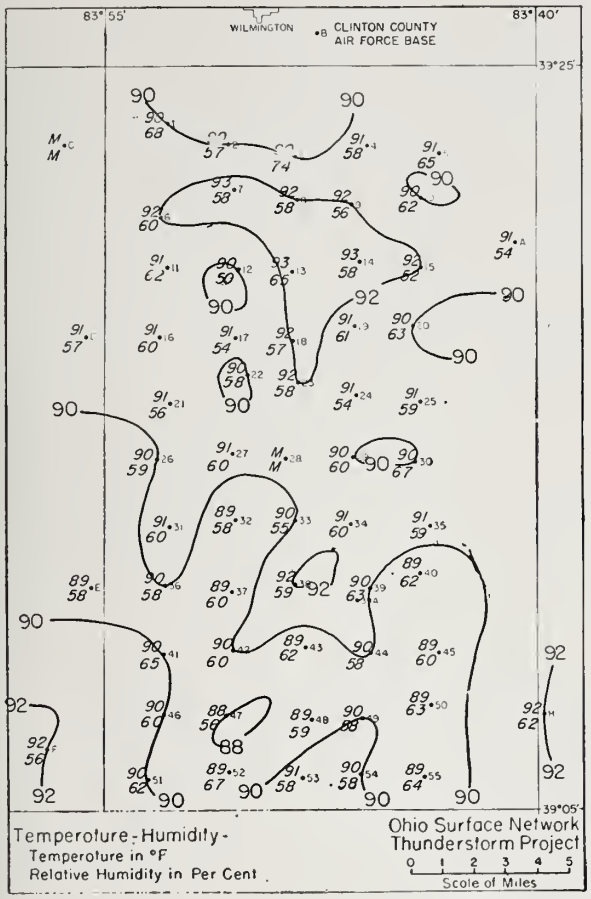

FIGURE 47.—A chart of the surface network showing the temperature field 45 minutes before the detection of the first storm-cloud radar echo on August 25, 1947. The figures plotted at each station are the temperature, in degrees Fahrenheit (above) and the relative humidity, in percent (below).

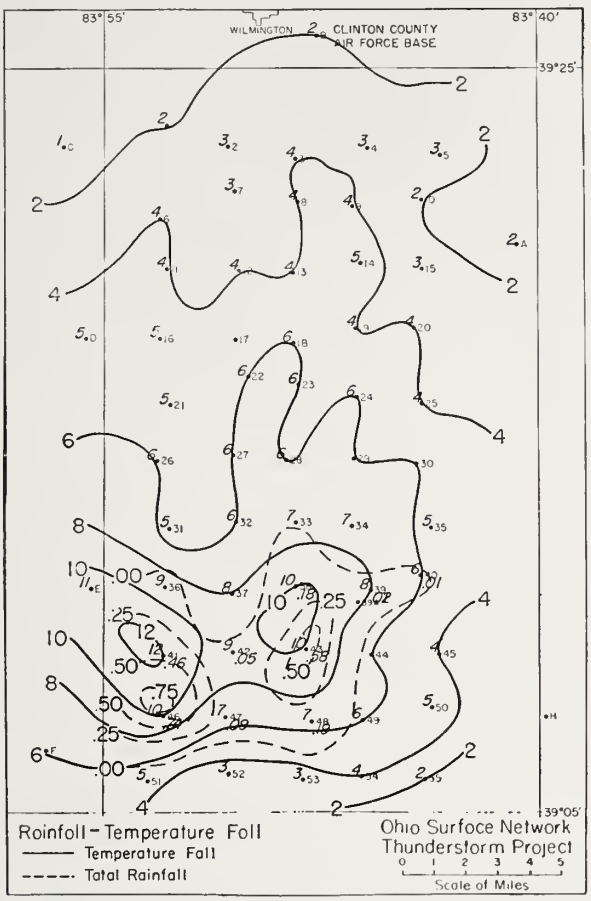

FIGURE 48.—A chart of the surface network showing isohyets of total rainfall from the storm of August 13, 1947, and lines of equal fall in temperature during the 30-minute period following the arrival of the cold outflow air from the storm. Rainfall amounts are expressed in inches, and temperature falls are given in Fahrenheit degrees. Note the displacement of the areas of maximum rate of cooling from the areas of maximum total rainfall.

This may be seen from the example shown in figure 47, representing a temperature field 45 min. before a storm cloud echo appeared on the radar 'scope.

Temperature field in the outflow.—Pronounced changes in the temperature field first occur when the cold mass of air of the thunderstorm downdraft reaches the earth's surface and spreads out. As a result, there are noticeable temperature drops in a considerable area influenced by the storm. The area affected by the cooling is, in fact, many times greater than that over which rain occurs (fig. 48). Cooling may be detected as much as 15 to 20 mi. downstream along the path of the storm's movement, although over a much smaller distance behind the storm due to the characteristic asymmetrical outflow of the downdraft. The rapidity of the cooling and the amount follow a general pattern with respect to the location of individual cells of the storm. Near the center of the cell, cooling is rapid, and the temperature reaches a minimum within 10 to 15 min. after the beginning of the drop. Farther from the cell the temperature drop is much slower and lasts longer. The amount of the temperature drop observed in any given storm varies inversely with the horizontal distance of the observation point from a cell core. Apparently, mixing of the colder air with warmer air which it displaces, and the effects of warming by the heated earth's surface are the chief factors preventing larger temperature falls in areas away from the cell center. In the 20 cases studied areas of maximum cooling were found to coincide with areas of maximum rainfall in 12 of the storms. In the remaining 8, the areas of maximum cooling were displaced slightly toward the downwind side of the areas of maximum rainfall (as shown in fig. 48).

If the cold-air outflow causing these temperature patterns comes from a cell of a moving storm, it spreads out asymmetrically with respect to the cell. The resulting temperature pattern is also asymmetrical. An example is shown in the graphs of figure 49, which is the presentation of the thermograph traces

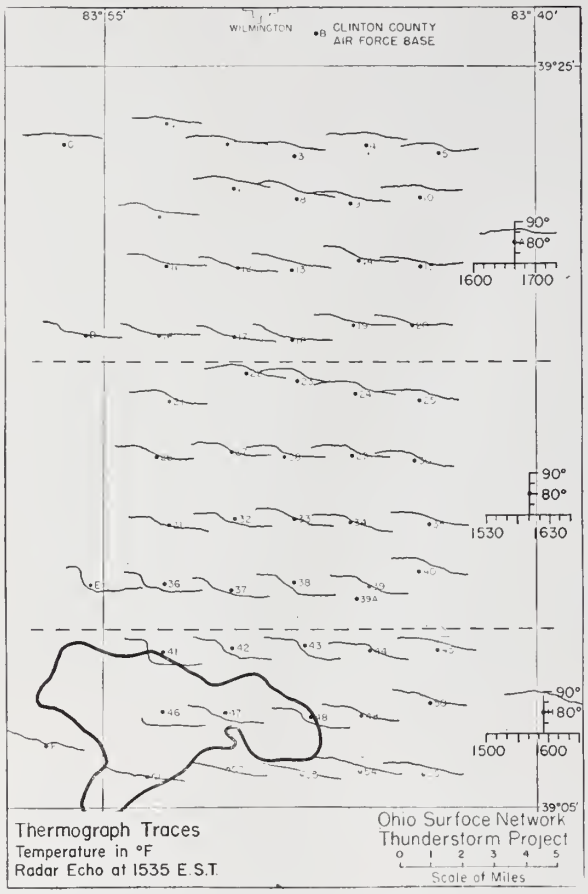

FIGURE 49.—A chart of the surface network showing reproductions of thermograph traces from each of the stations. Each trace shows the period of cooling following the arrival of the cold outflow air at the station. The stations have been divided into three groups for timing purposes and the plotting model for each section of the network is shown along the right-hand edge of the chart. Traces shown are for August 13, 1947.

for the storm of August 13, 1947. The traces of this storm, typical of 30 from Florida and Ohio which were analyzed, show the asymmetrical cooling pattern and the decreased rate of cooling with distance from the cell core. Also, they show that the temperature discontinuity is sharp and well-defined under the cell core but farther away is less pronounced. This discontinuity, marked by the point on the thermograph trace (point A of fig. 50) at which the temperature falls sharply, has been termed the "temperature break."

From the Project data it appears that the arrival of the cold air of the downdraft, as indicated by the temperature break, is preceded by the beginning of rainfall from the storm cell, which is not surprising since the water droplets in the cell fall with respect to the air in the downdraft and thus would be expected to reach the surface first. Surface data for the passage of 17 cells in the Ohio storms show that in 8 cases rain reached the surface before the time of the temperature break; in two, the downdraft and the rain first appeared together; and in the remaining seven studied, the temperature break occurred first. For the cases in which the rainfall reached the earth's surface at the same time or after the cold air, the apparent sequence of events can be ascribed to the limitations of observational equipment. In the first place, the rain gages used were insensitive to rainfall amounts of less than 0.01 in.; for this reason the very light rain which precedes the heavy downpour may not have been detected. Secondly, because of the coarseness of the 2-mile spacing of network stations, it is not unreasonable to assume that the initial rainfall, which usually occurred between stations, was not recorded. In such cases the temperature drop would be recorded first because of the spreading action of the downdraft. In the light of these limitations, the conclusion that some rain reached the earth's surface before the beginning of the cold-air outflow is a reasonable one.

In the early mature stage of a cell, the area of maximum rainfall rate and the area of minimum temperature are nearly coincident. In addition, it is in this area that the temperature falls most rapidly and the lowest temperatures associated with the storm are attained. This indicates that the coldest air must descend early in the life of the downdraft. Later, as the cell moves, the rainfall area moves with it, but the area of minimum temperature remains relatively stationary.

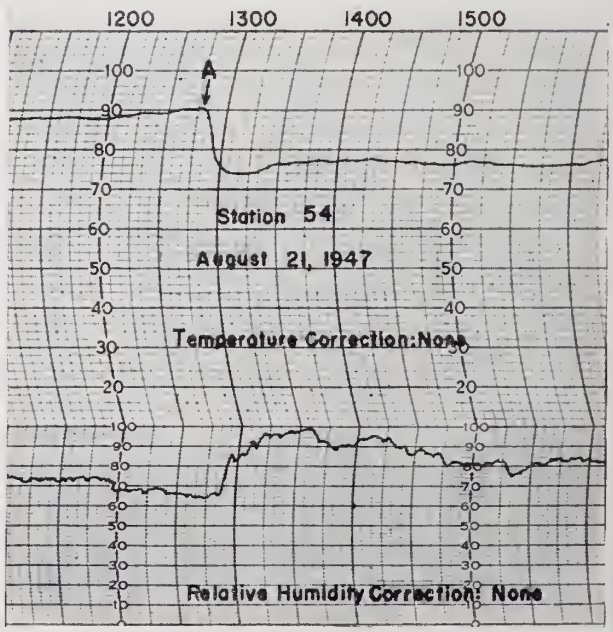

FIGURE 50.—The hygrothermograph trace from station 54 of the Ohio network on August 21, 1947, illustrating the "temperature break" (point A).

After the passage of the thunderstorm, the general area of lower temperature at a station is maintained for several hours, since the temperature of the air later passing over the moist, cool earth's surface is lowered. An example of this may be seen in figure 51, where the cold-air minima in the vicinity of stations 10, 23, 31, and 42 persisted for as much as 1 hr. after the rain stopped. High surface winds tend to minimize this effect.

Surface temperature field variations.—The variations which occur in the surface temperature field during the life of an afternoon thunderstorm are represented by the schematic diagrams of figure 52. In the first few minutes during which the cold air reaches the ground, the surface temperature falls rapidly (fig. 52 (b)). Since the downdraft with which this temperature drop is associated is only a few miles in diameter, the area over which this rapid fall occurs is relatively small. As a result, strong horizontal temperature gradients are created; gradients exceeding 20° F. per mile have been observed. However, as the storm ages, the cold air spreads out and the magnitude of the horizontal temperature gradient decreases.

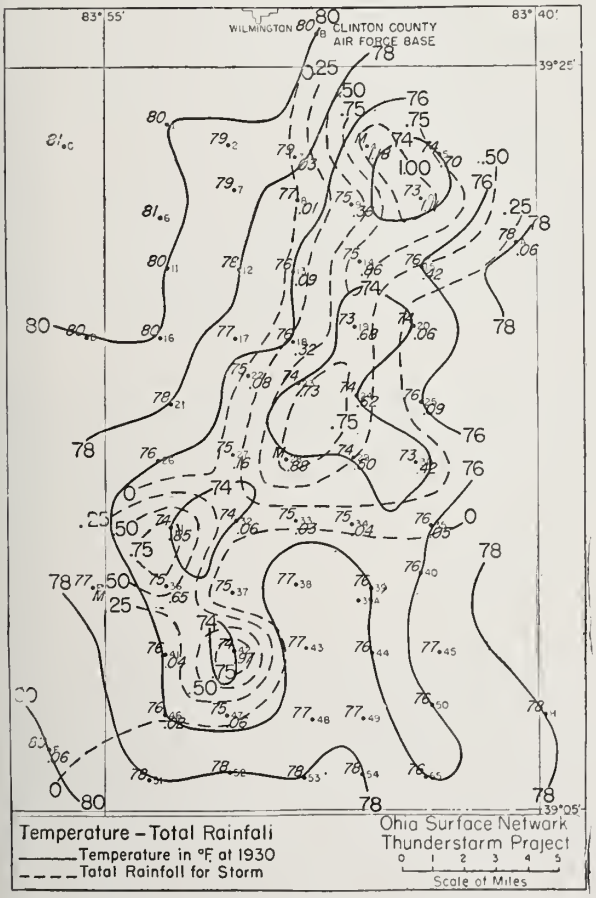

FIGURE 51.—A chart of the surface network showing the persistence of areas of low temperature one hour after the last rainfall was recorded on August 20, 1947. The isohyets show the total rainfall from the storm, in inches, The isotherms are in degrees Fahrenheit.

After the cold air has been spreading out for about 20 min. the isotherms appear as shown in figure 52 (c). By this time the temperature gradient near the center of the storm has decreased but it is still strong along the edge of the outflow. The asymmetry of the temperature pattern is again evident from the diagram.

One hour after the beginning of the outflow the cell has dissipated and the rain has stopped. The area of temperature minimum has remained in the general location where the cold downdraft made its first appearance at the surface (fig. 52 (d)). The temperature gradient is less pronounced, as might be expected.

The foregoing represents the effect of the outflow from a single cell. Since single, isolated cells are rarities, the picture represented here is usually modified by the presence of other cells. It, however, does indicate the contribution of the individual cell to the total picture.

Movement of the cold-air boundary.—There are several ways in which the movement of the boundary between the cold air and the warmer air can be traced in its progression across the surface network. One method is to draw isochrones representing the observed times of occurrence of the temperature break. An example of this technique is shown in figure 53, in which the movement of a temperature discontinuity is illustrated. In this example, the cold air overspreading the network prior to 1528 E.S.T. was due solely to the outflow from a storm located about 4 mi. south of the surface network. After this time the northward moving cold air was augmented by a downdraft which developed in the storm over station 46. It is to be noted that there was an increase in the rate of progression of the temperature discontinuity with the addition of the cold air from the latter storm. In spite of minor irregularities in its rate of advance, the cold air boundary progressed across the network at a rather uniform rate, except for a slight decrease in speed as its distance from the storm increased.

In table 21 are tabulated the average rates of movement of the temperature break for 9 Ohio storms. The average for all was 15.7 mi/hr. It must be emphasized that the rate of progression of the discontinuity boundary depends upon the position of the measurement point with respect to the cell. In the trailing edge of the cell, the rate of progression of the temperature break may be very slow, especially in rapidly-moving storms; whereas its speed at the leading edge

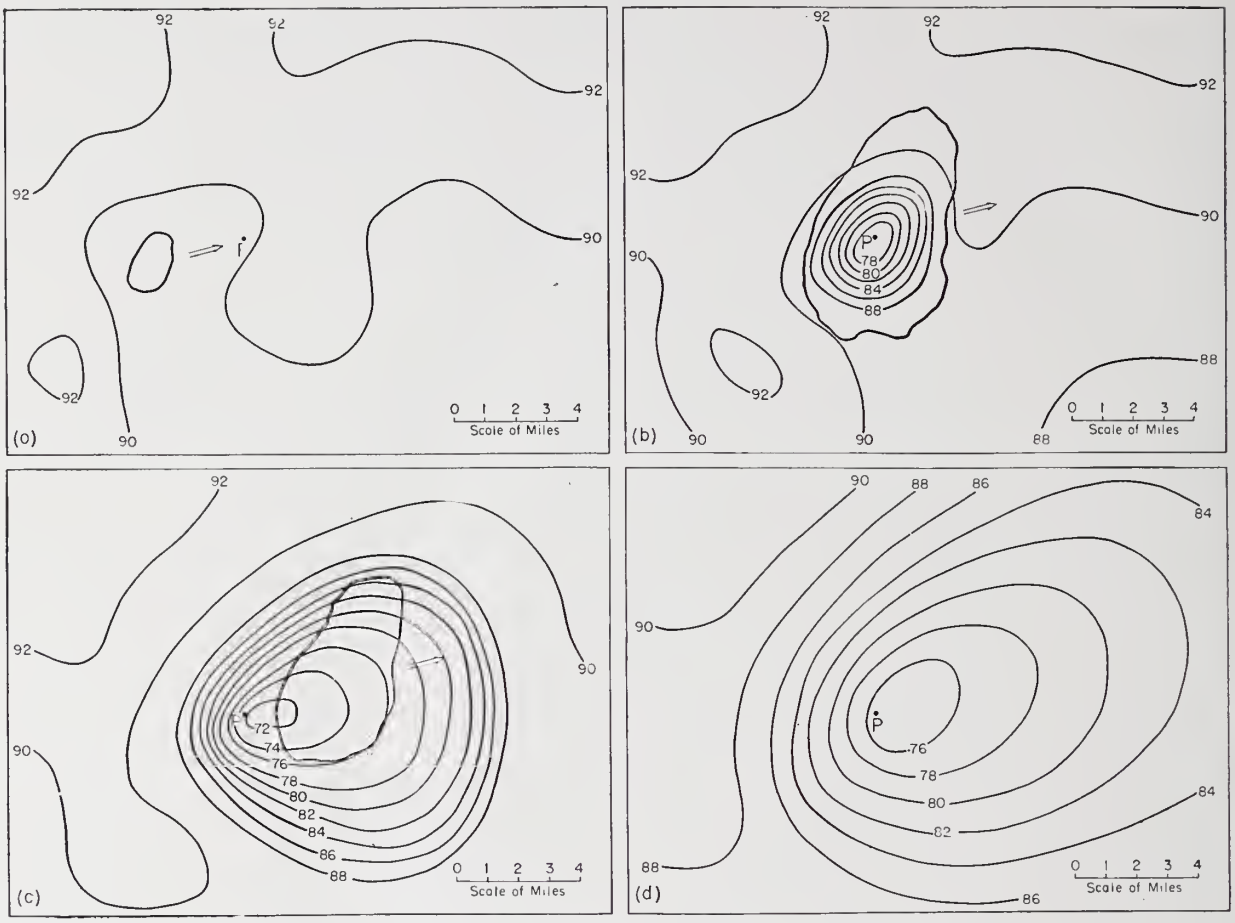

FIGURE 52.—Schematic diagram showing the temperature field variations associated with a summer, early-afternoon, single-cell thunderstorm. The storm cloud radar echo is outlined in the heavy full line. The thinner full lines are isotherms labeled in degrees Fahrenheit. Point P represents the surface station at which the first rain was recorded. The arrow shows the direction of movement of the radar echo. Its speed was 10 mi/hr.
(a) Temperature field during the cumulus stage.
(b) Temperature field 20 min. later, during the beginning of the mature stage.
(c) Temperature field 40 min. after (a), during the early dissipating stage.
(d) Temperature field 1 hr. and 20 min. after (a). This is approximately 30 min. after the last rain had fallen in the area.

is comparatively rapid. The significance of average speeds of progression of the discontinuity zone, as indicated by the temperature break or the first gust, must be interpreted in this light. Averages given in table 21 represent averages taken in the direction of the leading edge of the progressing cold air.

Wind, temperature, and rain interrelationships.—As the discontinuity surface between the warm and cold air passes a station, wind velocity changes markedly and temperature starts to fall. Because there is a zone of mixing along this discontinuity surface, the transition from warm to cold air takes several minutes. Therefore, the temperature break may lag behind the first gust. In a study of 9 Ohio storms, the time lag was found to be less than 2 min. The first gust may thus be considered as heralding the arrival of the colder air. Figure 54 shows corresponding first-gust and temperature-break lines within a fraction of a mile of each other, remaining close together throughout their progression across the surface network. This relationship was observed without exception in the storms studied.

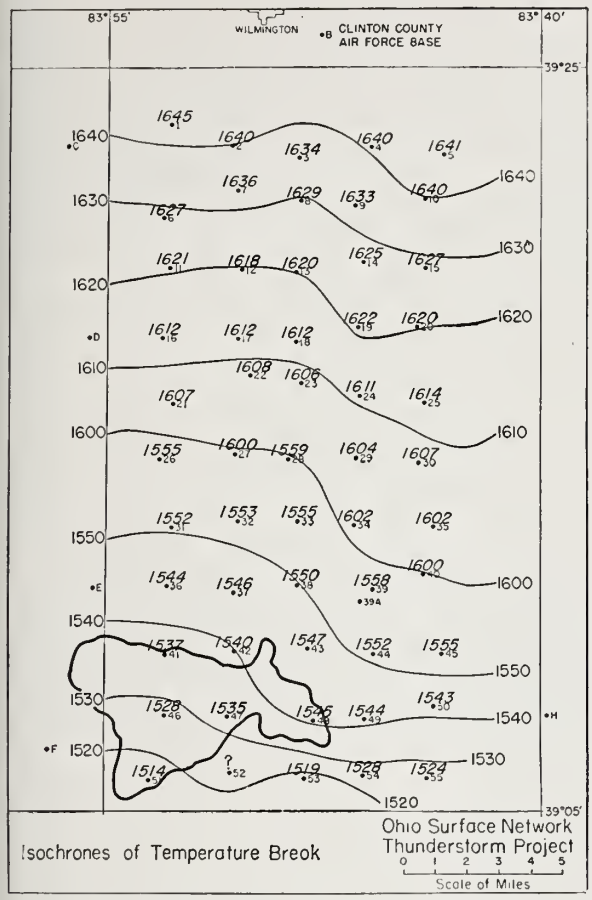

FIGURE 53.—A chart showing the isochrones of the temperature break for August 13, 1947. The time of occurrence of the temperature break is plotted for each network station. The area enclosed by the heavy full line represents the PPI radar echo.

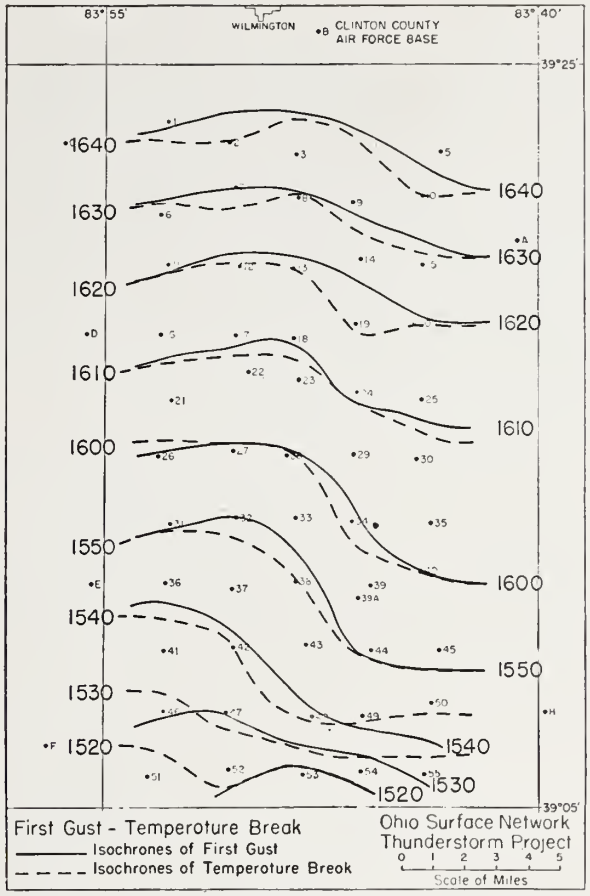

FIGURE 54.—A chart showing the relative positions of corresponding first-gust and temperature-break isochrones over the surface network during thunderstorm activity on August 13, 1947. Each isochrone represents the position of the first-gust line or the temperature-break line at the time indicated.

TABLE 21.—*Mean speeds of the first-gust line, temperature-break line, and the leading edge of the rain area; and the time difference between the occurrence of the first gust and temperature break, and between the first gust and the first rain. (Averages computed from all stations for nine Ohio thunderstorms during* 1947.)

Storm No.	Date (1947)	Mean speed (mi/hr)			Mean time difference (min.) between—	
		First-gust line	Temperature-break line	First rain	First gust and temperature break	First gust and first rain
151....	Aug. 6	16.1	17.3	10.6	+2.37	+26.6
158....	Aug. 13	15.1	15.3	7.8	+1.09	+14.5
160....	Aug. 14	13.9	13.8	11.3	+0.73	+ 3.4
163....	Aug. 16	18.9	20.8	19.5	+2.33	+ 1.8
166....	Aug. 17	12.8	11.9	9.8	+2.12	+ 8.9
167....	Aug. 20	12.0	11.5	8.2	+0.89	+22.6
173....	Aug. 25	19.2	19.2	17.8	+2.23	+20.2
182....	Sept. 9	15.9	13.9	12.0	+1.49	+13.9
186....	Sept. 12	18.4	17.9	18.8	+2.62	+ 5.4
Mean	.....	15.8	15.7	13.2	.....	.....

Near the center of the cell in the early mature stage of the thunderstorm, where the total rainfall, the rate of rainfall, and the temperature drop have their maximum values, the wind speeds associated with the first gust are greatest. Away from this area the wind speed decreases; however, the first gust may be traced as far as 20 mi. from the point of its first appearance at the surface. It was impossible to determine from Project observations if this distance was the maximum over which the progression of the first gust is perceptible, since the discontinuity could not be followed beyond the boundaries of the comparatively small observation network.

The rate of spread of rainfall is a function of the movement of the thunderstorm cell. In fast-moving cells, it spreads rapidly. The rate of spread of rain is considerably smaller than the rate of cold air outflow. As may be seen from table 21, the average rate of spread of rainfall was 13.2 mi/hr, whereas the

average rate of progression of the cold-air discontinuity surface was about 15.7 mi/hr. At the cell core the first appearance of rainfall, temperature break, and first gust occur within a few minutes of each other. At stations farther away, the first gust arrives before the rainfall. The time difference between the appearance of the first gust and the rainfall, or the temperature break and the rainfall is then a measure of both the distance from the cell core and the age of the storm cell. At stations 5 to 10 mi. away from the cell, the first gust and temperature break may be experienced without rainfall.

As is commonly known, and as can be easily seen from the Examples, (Pt. Three of this report) an area of heavy rain at the surface coincides with an area of strong divergence in the surface winds. The magnitude of maximum divergence is related to the maximum rate of rainfall (fig. 55) although the maximum divergence may lag behind the maximum rate of rainfall by approximately 5 min.

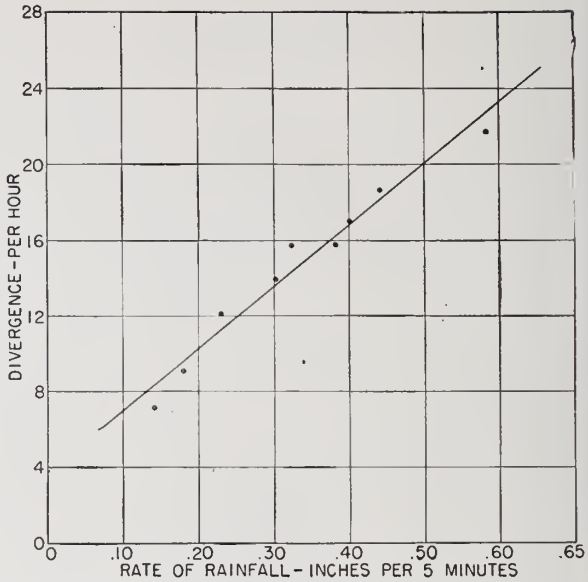

FIGURE 55.—A scatter diagram showing the relationship between the maximum rate of rainfall during a given 5-minute interval and the maximum value of horizontal divergence associated with the area of rainfall. The line through the scatter of points is the linear regression line for the distribution. The correlation coefficient is .98. This relationship is based upon the study of nine rain centers associated with Ohio thunderstorms. A similar study of nine rain centers associated with Florida storms gives a correlation coefficient of .91.

4. Pressure Field beneath the Thunderstorm

Many of the physical processes which take place in the air during a thunderstorm, such as vertical accelerations, condensation, and divergence are reflected in the surface pressure variations. Since some of these processes may simultaneously exert opposing influences on the pressure, only small net changes may result. The problem of determining the effect of any single process is exceedingly difficult. However, from a knowledge of the variations of such quantities as the liquid water concentration, draft magnitudes, or amount of cold air over an area, it is possible to explain some of the characteristic features of a thunderstorm pressure trace. In the following paragraphs such explanations are attempted.

Processes causing pressure changes.—The atmospheric pressure, defined as the force exerted by the atmosphere per unit area, varies at the surface of the earth in accordance with two factors: (1) the mass of the overlying atmosphere; and (2) vertical component of acceleration. In static equilibrium, the changes in pressure at any point are determined by changes in the mass of the overlying atmospheric column, since the acceleration of gravity may be considered as constant; indeed, the pressure itself is given by the weight of the column. During strong convection, the vertical acceleration of moving air particles becomes appreciable and must be considered along with the acceleration due to gravity. In general, however, it is believed that pressure variations at the ground due to changes in mass of the overlying column are more important than those due to changes in vertical accelerations.

Mass variations are treated in meteorological textbooks in accordance with the tendency equation of J. Bjerknes or variations of it. For conditions at the surface of the earth, the relationship shows that two processes produce pressure changes: (1) the addition to or removal from the column of mass by advection, that is the bringing in of colder heavier air or warmer lighter air; (2) the addition or removal of mass by horizontal mass convergence or divergence. In a thunderstorm, Project data and other evidence indicate that an additional mass effect may be contributed by the convergence and condensation of water vapor. The liquid water drops in the column, which have been supplied by the influx of water vapor, themselves add appreciably to its weight.

General nature of thunderstorm pressure changes.—Air rising from the earth's heated surface in the embryonic stage of a developing cumulus represents

part of a convective circulation in which small, barely detectable, horizontal pressure gradients are established. The idealized convective circulation, which this closely represents, consists of inflowing air at the surface which feeds into the ascending current. At some higher altitude the upward motion ends and the air, rather than accumulating there, flows outward and is thought to return again to the surface. It is probable that at first the upward acceleration in the updraft contributes to a reduction of pressure at the ground and may, in fact, produce an initial pressure fall.

As the convection current forms a heavy cumulus cloud, there is, added to the horizontal divergence aloft, a lateral expansion of the air due to the release of latent heat of condensation. This may act to reduce the surface pressure further, thus intensifying the low-level convergence.

During the cumulus stage of cell development, the barograph trace usually shows a leveling off, after the early pressure fall, suggesting a steady-state convection system in which the mass convergence in the low levels is completely balanced by the mass divergence aloft, and the vertical velocities are either steady and unaccelerated or are instantaneously compensated by mass-flow effects. If, however, the horizontal mass-divergence aloft is greater than the mass convergence at the ground, the pressure may continue to fall. This may happen, since the inflow must overcome surface friction, but an approximate balance is soon established. Wind patterns in the vicinity of thunderstorms, discussed in section 2, showed velocity convergence in the developing stages, with divergence above 20,000 ft., suggesting a mass balance. In the later stages of development, the addition of appreciable weights of liquid water may help to maintain this balance and prevent further pressure falls at the ground. In well-developed cumulonimbi extending to about 35,000 ft., in which an average liquid-water concentration of 1 gm/m^3 is assumed, the net increase of surface pressure due to the accumulation of liquid water may amount to as much as 1 mb. Liquid-water concentrations as high as 10 gm/m^3 for layers of limited thickness have been reported [**33**][42].

As the cell passes into the mature stage of development, a cold downdraft develops, with the result that the mean density of the column in which the downdraft occurs, and in which water is being evaporated, becomes greater than that of the environment. Inasmuch as this process may result in a lowering of the mean temperature of the lower 5,000 ft. of the air column by as much as 5 centigrade degrees, this could result in an increase in mass of the column, which, if uncompensated, could produce a surface pressure increase of 3 mb. under average conditions. However, compensations do occur, and the actual surface pressure rise due to this effect alone is probably less than 1 mb.

A further pressure increase results from the impact of the downdraft on the surface. Since the lapse rate in the lower few thousand feet of the environment is almost dry-adiabatic, whereas the lapse rate of the downdraft may be almost moist-adiabatic, the temperature difference between the downdraft and the environment increases with nearness to the ground. As a result, the air must continue to accelerate as it moves downward and it hits the ground with relatively high speed, to produce an impact pressure. The downward acceleration itself must also have an effect in increasing the pressure.

The outflow air in spreading from underneath the thunderstorm cell displaces warmer and less dense air. Because of the density increase in the lower layers, the surface pressure rises. This is an advective pressure change, as described at the beginning of this section. It follows that the surface pressure should go up when the discontinuity (marking the cold-air boundary) passes a station, an effect which was observed in Project studies.

To compensate for the divergence in the lower air layers, which is associated with the outflow, convergence aloft must occur to maintain mass balance. The presence of convergence in the levels above 5,000 ft. was observed in the study of wind patterns surrounding cumulonimbus clouds (ch. I., sec. 4). Because of the surface friction suddenly encountered by the outflowing downdraft air, the net inflow aloft may for a time even exceed the outflow near the surface, disturbing the balance. This would add to the surface pressure increase. The convergence measurements aloft were inadequate, however, for determining the extent or duration of this lack of compensation.

Surface pressure during the cumulus stage.—Early in the cumulus stage of a thunderstorm, a fall in surface pressure almost invariably occurs in the area beneath a cell. This fall is observed before the radar echo forms, and it is recorded over an area several times the maximum horizontal extent of the echo. When the radar echo appears, the pressure trace levels off in the region directly underneath it, but continues to fall and frequently at a more rapid rate in the surrounding areas. The pressure drops in the cumulus stage are usually small in magnitude—less than 0.02 in. below the diurnal trend—and take place over a period of 5 to 15 min. Following the fall, the pressure trace levels off and may remain steady for as long as 30 min. before starting its rise.

The pressure falls appear to be caused by the combined effects of vertically accelerated air motions,

[42] These values were computed from radar indications. Actual measurements of liquid-water concentrations as high as 6.5 gm/m^3 have been made [23].

the expansion of the air due to the release of latent heat, and the failure of the convergence near the surface to fully compensate the expansion or divergence aloft.

Although surface pressure decreases may first appear in the area under the region where the echo is in the process of forming, they are not the largest associated with the cell, because the pressure stops falling in the area directly underneath the echo shortly after it forms. Underneath the radar echo, the pressure becomes steady or even rises because of the high concentration of liquid water. In the area surrounding this water core the effects of accelerating upward motions and divergence aloft continue to reduce the surface pressure. Consequently, the pressure may continue to fall in surrounding areas, with the result that the most pronounced pressure drops may be found there. The Example of August 13, 1947, 1520–1550 E.S.T., (Pt. Three) is an illustration of this.

After the downdraft develops, large amounts of air are cooled by evaporation of rain. This cooling, together with the copious quantities of rain present, causes the surface pressure directly under the radar echo to rise even before the rain reaches the surface. Since the end of the cumulus stage and the beginning of the mature stage has been defined as the time when rain reaches the ground under the cell, the pressure has completed its fall and is already rising at the time of transition. Farther away, the pressures are still low and falling at this time.

Surface pressure during the mature stage.—As indicated in a previous section, the cold downdraft follows the rain by a few minutes. It is reasonable to expect that the displacement of the warmer air by this cold outflowing air would result in a rise in surface pressure. This was confirmed by a study of 206 pressure records of stations in the Project surface network for which first-gust and temperature-break data were available; it was found that in 182 of the traces there was a pressure rise associated with the arrival of the cold-air dome. The rate and total amount of pressure rise is a function of the slope of the cold air associated with the discontinuity zone and of the mean temperature difference between the displaced warm and the cold air which takes its place, the depth of the cold air, and the speed with which the system travels. It is therefore to be expected that the most marked pressure changes attributable to these causes are found near the cell and decrease with distance from it.

The pressure trace at a station relatively near the cell, but outside the area underneath the cell echo, may be seen in figure 56. Since the pressure rise is believed to be due to a large extent to the cold-air dome and the appearance of the general pressure increase is also dome-shaped, as delineated by points A, B, and C of this figure, this part of the trace has been termed the "pressure dome." A trace of a pressure dome (ABC) at a station under the radar echo and not far from a point under the cell center is shown in figure 57.

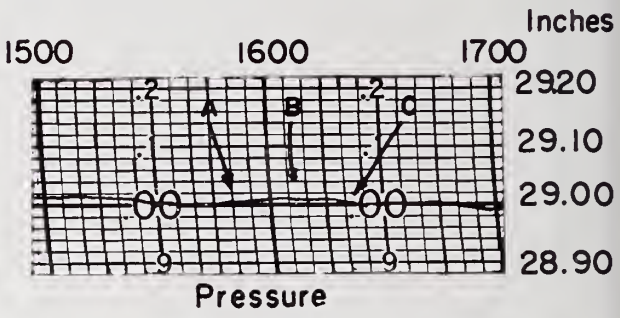

FIGURE 56.—A portion of the microbarograph record for August 13, 1947, from station 26 of the Ohio surface network. Points A, B, and C delineate the pressure dome. Station 26 was near the cell but not in the area beneath the radar echo from the storm during the period when the dome was recorded. The pressure values on the right of the figure are given only to show the scale and should not be considered as indicating actual pressure.

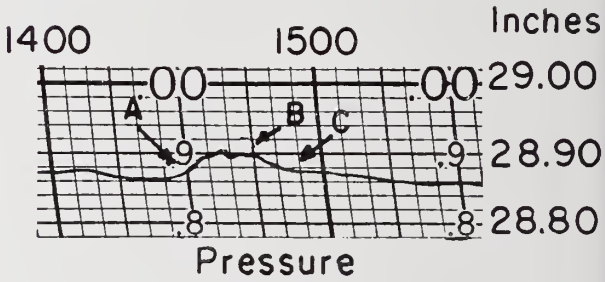

FIGURE 57.—A portion of the microbarograph record for August 14, 1947, from station 3 of the Ohio surface network. Points A, B, and C delineate the pressure dome. Station 3 was located beneath the radar echo from the storm during the period when the dome was recorded. The pressure values on the right of the figure are given only to show the scale and should not be considered as indicating actual pressure.

The pressure dome is seen to occur in most storms in which the cold-air outflow is pronounced. An examination of 206 pressure traces recorded for 8 storms which passed over the surface network showed that the beginning of the pressure rise occurs, on the average, at about the same time as the first gust. The areal extent of the pressure dome is similar to that covered by the cold air. As a result of this colder air, the pressure at a station remains high for a period of from one-half hour to several hours, depending on the amount of cold air involved. Near the center of a cell the amplitude of the rise is usually a few hundredths of an inch.

In addition to the static effect of the weight of the cold air on the pressure rise characteristic of this period, it must be remembered that appreciable accelerating, descending motions occur within the cold dome, which, no doubt, also contribute to the pressure rise.

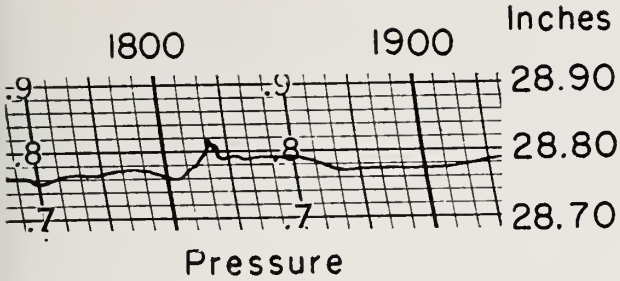

FIGURE 58.—A portion of the microbarograph record for July 14, 1947, from station 53 of the Ohio surface network. This trace shows, an excellent example of a pressure nose superimposed upon the pressure dome. The station was beneath the radar echo from the storm, in an area of heavy rainfall during the period when the nose was recorded. The pressure values on the right of the figure are given only to show the scale and should not be considered as indicating actual pressure.

The pressure nose.—The pressure traces at stations near the center of a cell often showed an additional hump superimposed on the pressure dome associated with the mature stage of cell development (fig. 58). This hump has been termed the "pressure nose." In uncomplicated cases it initiates the pressure dome.

The distinction between the pressure nose and the pressure dome can only be made with difficulty on the conventional barograph traces, as the time scales are much more compressed than on the traces of the Project barographs. The drums on the former usually make one revolution in 3, 4, or 7 days as compared with one revolution in 12 hr. made by the latter. No distinction has been made in the literature between these two features of the thunderstorm barograph trace, but the pressure rise associated with thunderstorms has been loosely referred to as the pressure nose, hump, jump, or thunderstorm high.

For the sake of objectivity in studying the pressure nose appearing on Project traces, only those which fulfilled the following conditions were considered:

1. A rate of pressure rise of 0.02 in/5 min or more.
2. A total rise equal to or greater than 0.02 in.
3. A pressure fall of at least 0.01 in. within the 10 min. following the maximum pressure associated with the pressure rise.

A pressure nose meeting these requirements was observed during 8 of 43 storms in the Florida data and 17 of 44 storms in Ohio. These data are not strictly comparable, however, since the Ohio network was several times the size of the Florida network and the stations had twice the separation.

Results of the study show that in nonfrontal thunderstorms the area over which the pressure nose appears is relatively small and its duration is short. The fact that at any given time it was usually detected by one station per cell in Ohio indicates that the maximum diameter of the area in which it occurs is usually less than 5 mi. It is thus apparent that the pressure nose is caused by a transitory process which exists for only a brief period. By the time the air in which the processes are taking place moves a mile or two away, these processes have become sufficiently attenuated to result in only insignificant pressure rises superimposed on the pressure dome at that location.

As will be shown in the succeeding paragraphs, the pressure nose occurs at approximately the same time as the commencement of the mature stage. Each of the pressure-increasing processes may contribute to the pressure rises associated with the pressure nose. However, at this time the weight of the liquid water and the lack of balance between convergence and divergence are at a maximum. When the downdraft becomes established, it reverses at least part of the vertical circulation pattern and reduces or perhaps even changes the sign of the divergence above 20,000 ft. Should this happen before the divergence in the surface layers becomes well established, the net increase in convergence could result in a substantial surface pressure rise. For example, convergence of a magnitude of 1 hr^{-1} per second (a very conservative value for thunderstorm convergence) at 20,000 ft. within a layer only 1,000 ft. thick would result in the surface pressure increasing at a rate exceeding 0.01 in/min, provided no compensation occurred.

Pressure changes related to drafts.—A number of meteorologists, notably Levine [**35**], Buell [**14**], Mal and Rao [**37**], and Schaffer [**48**] have written on surface pressure changes resulting from vertical motions during thunderstorms. It was hoped that the draft measurements over the surface network would yield useful information and provide a check on the relationships between surface pressures and vertical velocities proposed by the above writers. Unfortunately, it was found that insufficient data were available for this purpose. Other Project analysis shows that the downdraft at lower levels is under an updraft at a higher level. When this occurs, there is the tendency for the pressure effects to compensate one another. Generally speaking, draft measurements were not made in the same vertical plane, so that the actual distribution of vertical velocity with height is not well defined. Since the surface pressure changes are the resultant of many processes occurring simultaneously, and since so few draft measurements were available over the surface network, no direct conclusions could be drawn concerning the effect of drafts on the surface pressure.

Surface pressure during the dissipating stage.—During the dissipating stage, when weak downdrafts are prevalent at all levels, the surface pressure is higher than would be expected from the general pres-

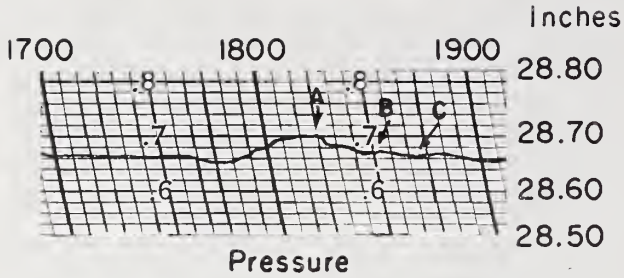

FIGURE 59.—A portion of the microbarograph record for July 14, 1947, for station 9 of the Ohio surface network. The section of the trace labeled A, B, and C represents the return of the pressure to a normal value during the dissipating stage of a thunderstorm. The pressure values on the right of the figure are given only to show the scale and should not be considered as representing the actual pressure.

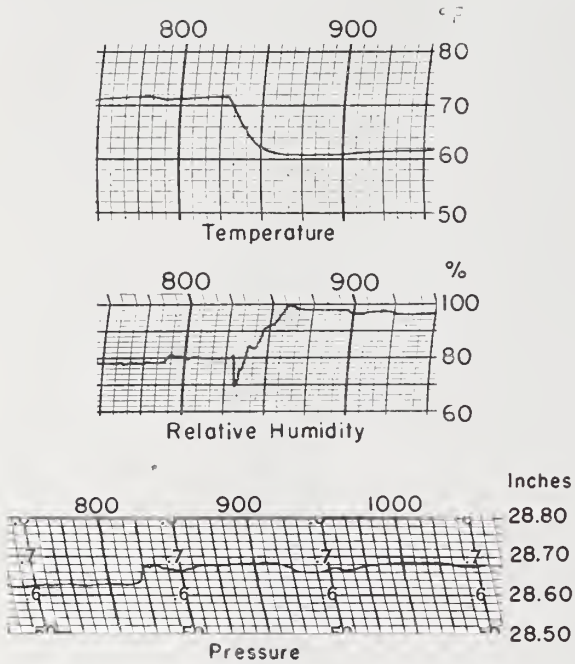

FIGURE 60.—Portions of microbarograph, hygrograph, and thermograph records from station 46 of the Ohio network on May 29, 1947. The sharp discontinuity on these traces occurred at the time of the passage of a squall line. Note the relative humidity dip at this time.

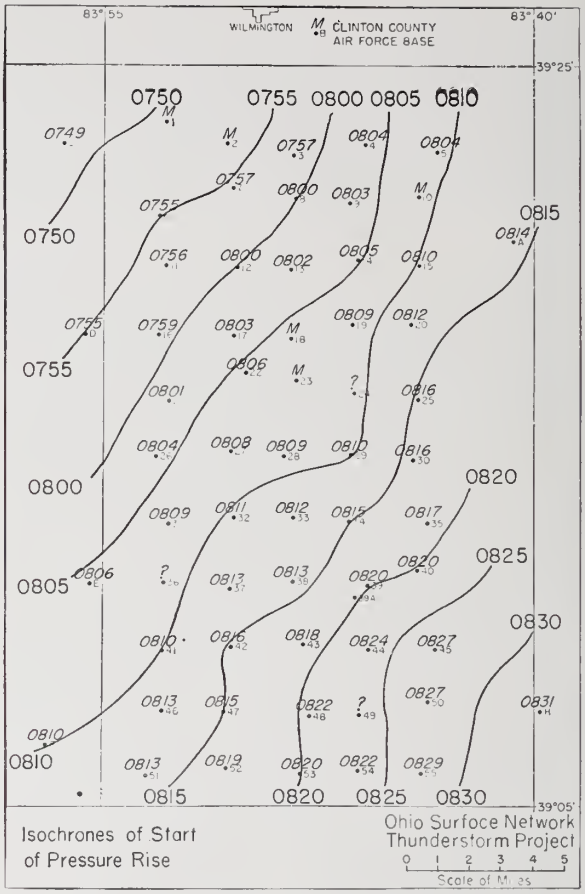

FIGURE 61.—A chart showing isochrones of the beginning of the pressure rise at the stations of the Ohio surface network on May 29, 1947. The numbers plotted at each station give the time of the beginning of the pressure rise (Eastern Standard Time) to the nearest minute. This pressure discontinuity was associated with the passage of a squall line.

sure trend controlled by large-scale atmospheric processes. In this stage the two factors which are probably most responsible for this higher pressure are the greater static weight of air in the lower layers made denser by evaporation cooling, and the divergence in the cold dome incompletely balancing the convergence aloft. In figure 59 the trace ABC, representing the end of a pressure dome, is typical of pressure variation recorded in the dissipating stage.

Other typical traces.—In nonfrontal thunderstorms the characteristic pressure trace shows a return to the pressure trend prevailing before the passage of the storm. In contrast to this, when a thunderstorm associated with a cold front or a fast-moving squall line passes a station, the pressure may rise sharply and remain high for some time (fig. 60) due to the continuous advection of cold air from behind the front.

Isochrones of the beginning of such a pressure rise show the progression of the pressure discontinuity (fig. 61) across the surface network. It is evident from this figure that the progression of the pressure discontinuity is similar to that of the first gust and the temperature break and occurs at approximately the same time.

Another feature sometimes seen on a barograph trace is the small but sharp fall in pressure immediately preceding the pressure nose, as shown on the trace in figure 58. It usually occurs in severe storms. An explanation of the mechanism which causes this pressure dip is not attempted here.

Relationship between radar cloud heights and pressure.—A study was made of eight relatively isolated radar echoes, selected so that the surface phenomena associated with each of them were clearly related to the echo in question and relatively uninfluenced by

the presence of other echoes nearby. The height-time curve of the top of one such echo is shown in figure 62. On the same chart is also plotted a pressure-time curve for the station directly underneath the echo. The following features, evident from this graph, are characteristic of the other situations used in this study:

1. The pressure begins to fall a few minutes prior to the first appearance of the PPI radar echo.
2. The radar echo begins to grow upward rapidly while the pressure is low at the surface. It is not until the top of the radar echo is fairly near the maximum height that the maximum rate of pressure rise occurs.
3. The maximum gust at station 46 was 23 mi/hr. As in all other cases observed in this study, the maximum gust occurred while the pressure was rising, i.e., before the maximum pressure was reached. The maximum gust usually occurred within a few minutes of the peak echo heights.

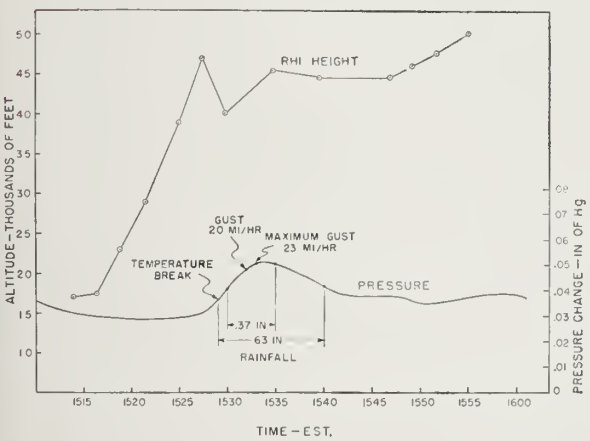

FIGURE 62.—A chart showing the variation with time of the height of an RHI radar echo and of the surface pressure beneath the echo. Significant variations in the wind, temperature, and rainfall have been indicated along the pressure trace. The maximum rainfall rate, .37 in/5 min., occurred between 1530 and 1535 E.S.T. During the period of heavy rainfall, .63 in. accumulated. These surface measurements were made at station 46 of the Ohio surface network on August 13, 1947.

Pressure-rainfall studies.—Since the weight of the liquid water can cause appreciable pressure changes at the surface, it appeared desirable to investigate further the nature of the relationship between pressure and rainfall. If uncompensated by divergence or outflow, each new gram of water suspended in an air column of 1 sq. cm. in cross-sectional area could cause a surface pressure rise of nearly 1 mb. under the column. Such concentrations are reasonable in view of the quantitative measurements mentioned above.

One pressure-rainfall investigation was designed to find the relation between the beginning of rainfall and the beginning of the pressure nose. To insure that both were associated with the same cell, only those cases were included in which the rainfall began within 10 min. of the start of the pressure rise. Of the 37 cases used in this study, the beginning of rain preceded the pressure rise in 19 instances, followed it in 16, and occurred simultaneously with it in 2. The rain began before the initiation of the pressure rise by an average of 0.4 min.; the standard deviation of the difference in times of occurrence was 5.0 min.

In another study, the variation of the rate of rainfall with the occurrence of the pressure nose was investigated. The data of rainfall accumulations for each of two 5-minute periods, preceding and following the start of the pressure rise, were compiled. A similar compilation was made with respect to the time of maximum pressure. For the 37 cases, the time interval between the start of the pressure rise and the pressure maximum averaged 4.8 min. The results of this study are presented in table 22. It may be concluded from an analysis of the results that very heavy rain usually occurs after the start of the pressure rise associated with a pressure nose. Very heavy rain is also recorded in the 5-minute intervals preceding and following the peak pressure but the intensity decreases thereafter.

TABLE 22.—*Average rainfall rates for designated 5-minute intervals associated with the period of occurrence of a pressure nose*

Time of—	Average rainfall rate—			
	10–5 min. before	5–0 min. before	0–5 min. after	5–10 min. after
Beginning of pressure rise	0.02	0.05	0.17	0.15
Peak pressure	.05	.17	.18	.09

In the thunderstorm it has been found that if one of the surface elements such as rainfall or wind is intense, the other elements are also severe. From this it would be expected that when the pressure nose has a large amplitude, the intensity of the other elements would be high. Andre and Bleeker[43] of the University of Chicago, in a study of maximum pressure variations during thunderstorms, have found that, in general, the greater amounts and rates of rain are associated with large pressure variations.

[43] "Convective Phenomena in the Atmosphere," unpublished manuscript, University of Chicago.

5. Humidity Field beneath the Thunderstorm

Because of the lack of adequate measurements, little has been written about the changes in surface relative humidity during thunderstorms. Although hair hygrometers used by the Thunderstorm Project have serious shortcomings, measurements made under humid, warm, summer conditions were sufficiently good to depict faithfully the humidity field and its changes during the thunderstorm's life cycle.

The whole problem of moisture redistribution in the atmosphere as a result of the thunderstorm is one of considerable interest. First, the thunderstorm processes bring about a net transport of moisture from lower to upper levels of the atmosphere; second, in the levels below 20,000 ft. there is a net horizontal water vapor flux into the thunderstorm. With respect to the moisture in the environment, the thunderstorm may be regarded as a moisture sink, since a substantial portion of its moisture condenses and drops out. Because the rain which falls to the ground from the storm is taken from the atmosphere, there must be a net desiccation of the entire air volume affected.

It is interesting to observe, however, that soundings made in the air where a thunderstorm has recently occurred show an increase in the water vapor content at all levels for which measurement is possible with present-day radiosonde equipment. This net moisture increase in the thunderstorm area must, of course, take place at the expense of the moisture in the surrounding space.

A study of the variations in the surface humidity distribution yields interesting information concerning some of the thermodynamic processes operating at upper levels. It is especially profitable to study the humidity variations in conjunction with the behavior of the other meteorological elements such as rainfall, temperature, and wind.

Humidity field prior to onset of the thunderstorm.—Prior to afternoon thunderstorms in spring and summer maritime tropical air, the surface relative humidity ranges from 50 to 70 percent. It decreases to these values from the near-saturation conditions which prevail in the early morning hours. In spite of this drop, there is an increase in the mixing ratio of 3 or 4 gm/kg over the same period. The relative humidity decreases because of the heating of the air in the surface layers, but the mixing ratio increases primarily because of the increased evapotranspiration from the sun-heated surface. Some of the mixing-ratio rise can also be attributed to mixing of the lower air with the air above the nocturnal inversion, where in the early morning the mixing ratio is frequently higher than it is near the surface.

Prior to nocturnal thunderstorms occurring after 10 o'clock in the evening, the surface relative humidity will again be near 100 percent, due to surface radiation cooling. The cool, nearly saturated air in the lower layers, is thermodynamically similar to that in the storm downdraft which later reaches the surface. Therefore, there is little difference in the surface air before and after a nocturnal thunderstorm. A similar condition exists during the day after the first of a series of thunderstorms. The surface air is cooled and moistened by the first thunderstorm, and in succeeding thunderstorms there is little difference between the air of the downdraft and that already found near the surface.

Humidity field in the outflow air.—The relative humidity, of course, rises with the onset of rain. However, an examination of the relative humidity traces for various stations indicates that there are wide variations in the humidity patterns, depending on whether the station is located beneath the center of a storm cell, a little to one side, or some distance away. The features of typical traces for each of these locations are discussed below.

Near the cell center the rain is recorded at stations either simultaneously with, before, or after the cold downdraft. When the rain appears before the cold air, the relative humidity begins to rise quite rapidly at first (as shown in fig. 63). However, it fails to rise to a saturation value immediately; it may even begin to fall for a time, while the rain continues. In such cases the mixing ratio often rises at first, but it also falls later as both temperature and relative humidity become lower. Mixing-ratio minima may occur, surprisingly enough, during the heavy rainfall when the temperature is near its minimum, provided the relative humidity also has decreased. Usually the mixing ratio drops from about 20 gm/kg to about 16 or 17 gm/kg; on occasion it may drop as low as 11 gm/kg in the heavy rain.

In areas away from the center of maximum cell activity, where the rainfall is less and the temperature falls more slowly, the temperature break and first gust occur some time before the rain begins. In such locations the relative humidity shows a rise to near-saturation values before the advent of rain, as is shown in figure 64. A substantial portion of this rise is due to the horizontal advection of moister air from the cold-air outflow.

The cold air of the downdraft, of course, overspreads a much larger area than does the rain. In the regions reached by the cold air, but not by the rain, the relative humidity rises appreciably, as seen in the example of figure 65, although the rise is usu-

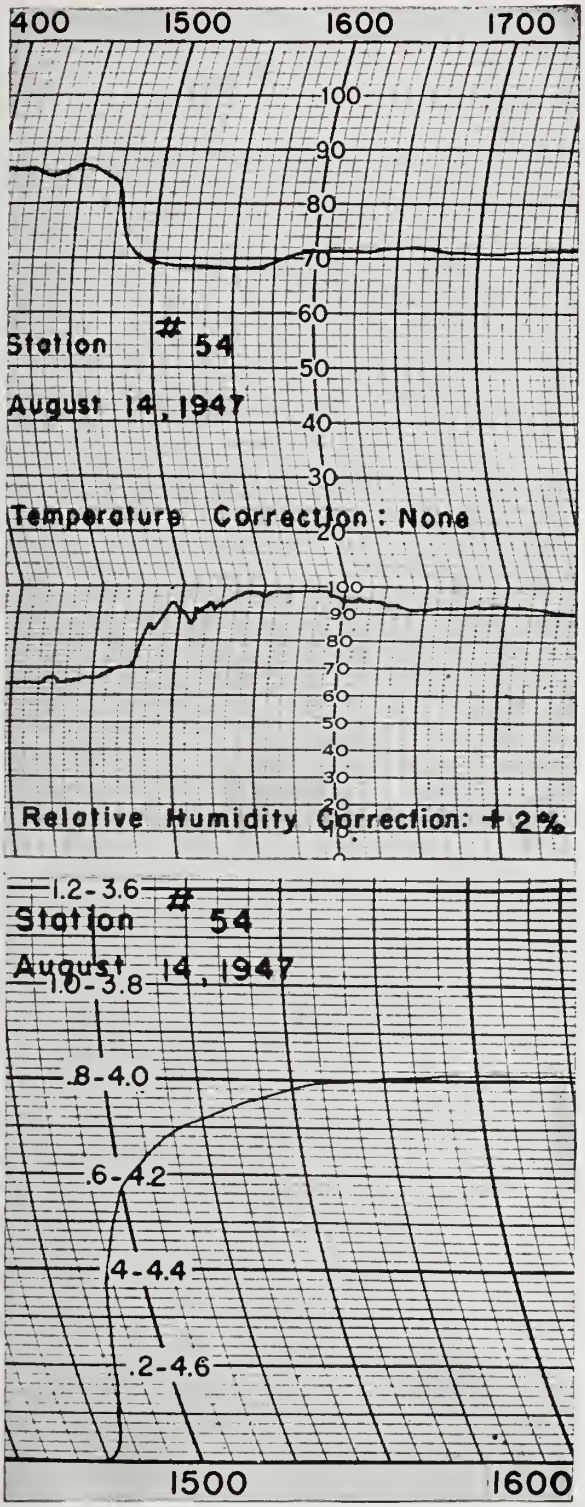

FIGURE 63.—Sections of records from station 54 of the Ohio surface network on August 14, 1947. These traces show the sharp temperature fall, the increase in humidity, and the heavy rainfall associated with a thunderstorm downdraft. The temperature is given in degrees Fahrenheit, the relative humidity in percent, and the rainfall in inches (read from the figure on the left for the first traverse of the scale). Note that the time scale for the rain-gage chart does not correspond to the other time scale.

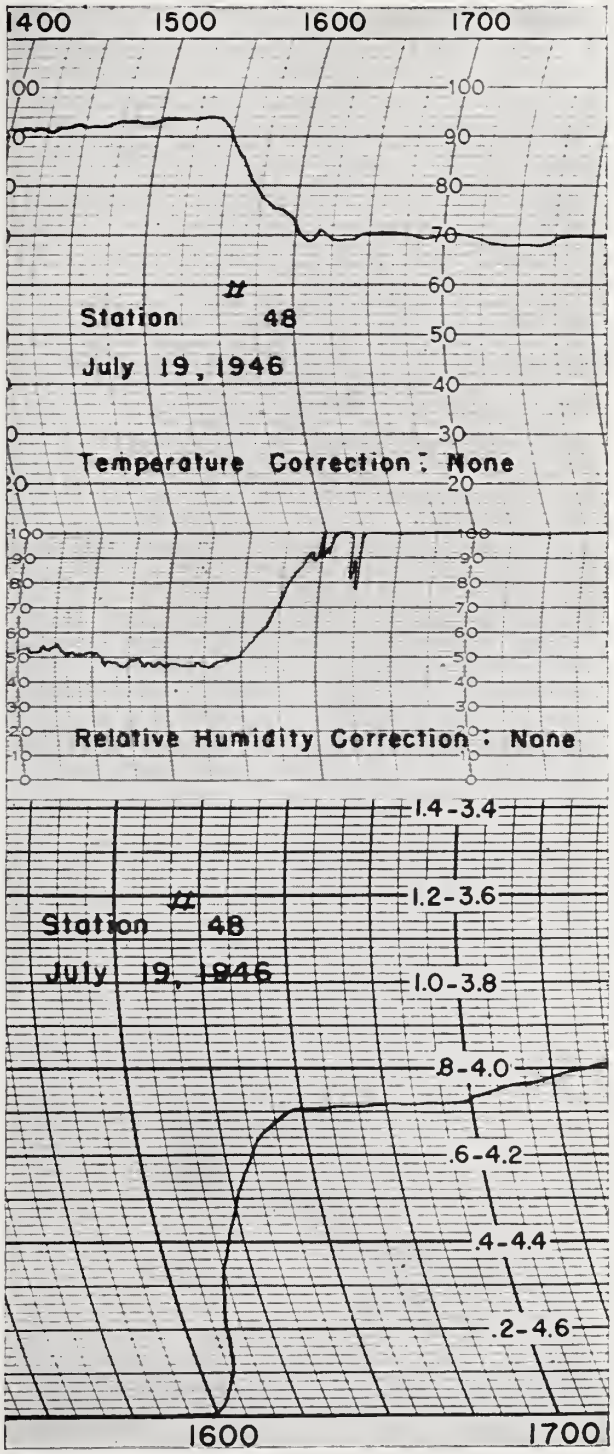

FIGURE 64.—Section of the records from station 48 of the Florida surface network on July 19, 1946. These traces show the temperature fall, the increase in humidity occurring with the passage of the first-gust line, but preceding the beginning of rainfall at the station. The temperature is given in degrees Fahrenheit, the relative humidity in percent, and the rainfall in inches (read from the figure on the left for the first traverse of the scale). Note that the time scale for the rain gauge chart does not correspond to the other time scale.

ally quite slow, and the humidity does not reach saturation. The mixing ratio frequently rises also but only slightly.

After the rain stops, the higher relative humidities persist at a station for several hours just as the lower temperatures do. This is reasonable, since the ground is wet and water is evaporating continuously into the air above. The temperature and relative humidity recovery is such that the mixing ratio returns to or even exceeds its value prior to the thunderstorm.

Relative humidity dip.—As illustrated previously (fig. 63), the surface relative humidity may fail to reach 100 percent even during rain at the station. As was stated, in some instances it may even drop during the rain, from near 100 percent to values as low as 60 or 70 percent, and return to its previous value in a few minutes. Such a fluctuation has been termed the "relative-humidity dip" (fig. 66). For the sake of objectivity in studying this phenomenon, it was defined as a drop of 8 percent or more in the recorded relative humidity value followed by a return to the previous value within 10 min. This definition eliminates from consideration many smaller fluctuations, as well as the frequently observed large decreases

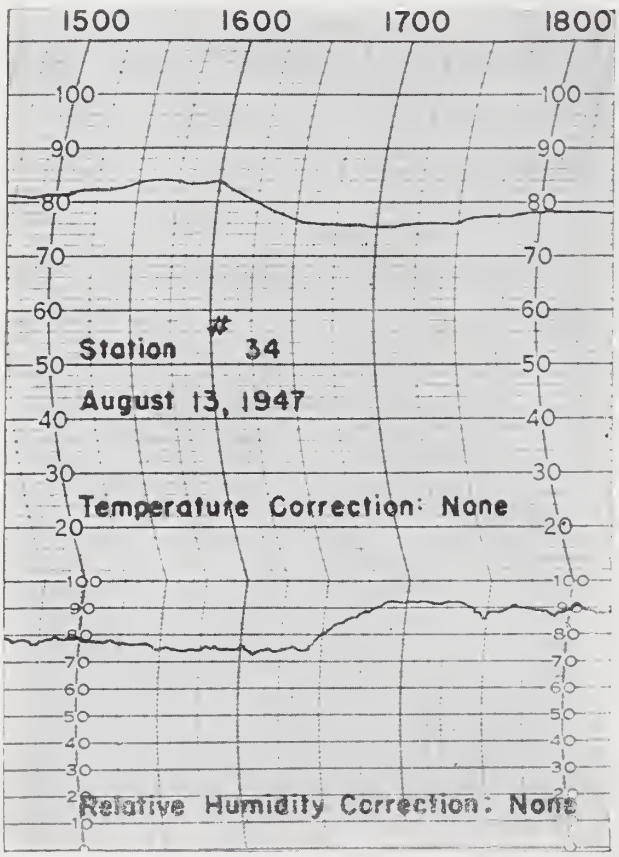

FIGURE 65.—Section from the hygrothermograph record from station 34 of the Ohio surface network on August 13, 1947. No rain fell at this station during the period covered by these charts but the passage of a first-gust line did occur. Note that the air at this station did not become saturated and that the temperature fall was not as rapid as those shown in figures 63 and 64. The temperature is given in degrees Fahrenheit and the relative humidity in percent.

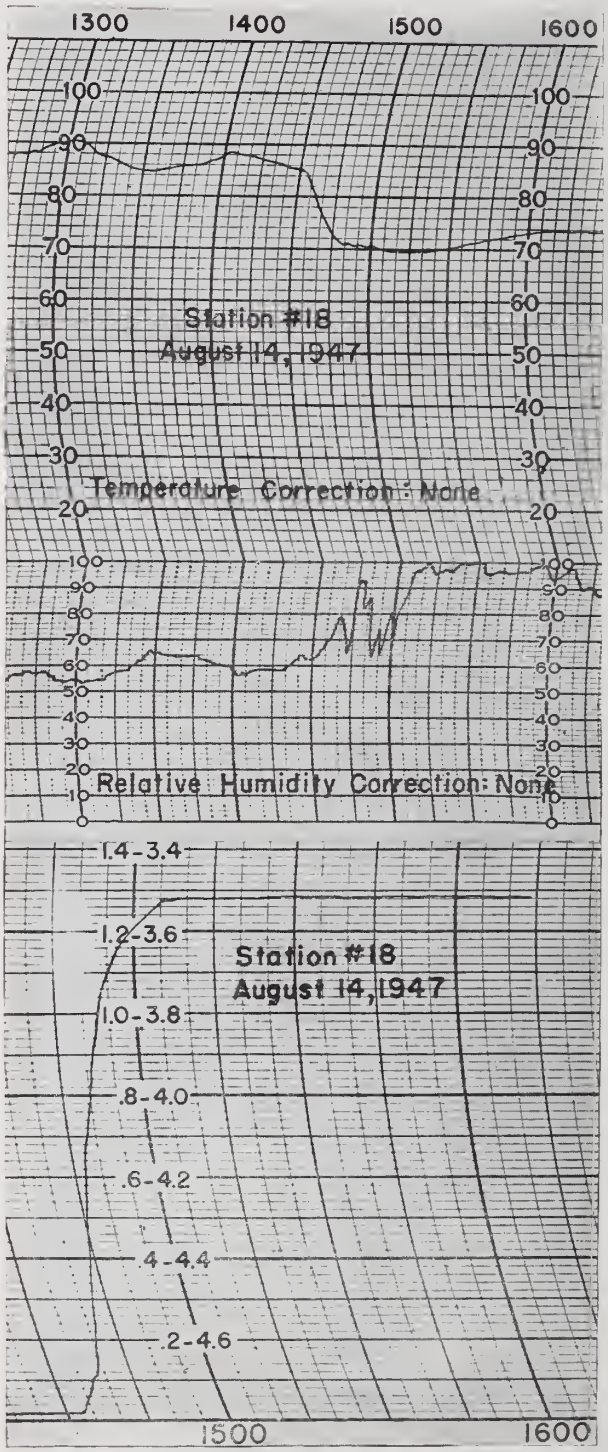

FIGURE 66.—Sections of the records from station 18 of the Ohio surface network on August 14, 1947. Note the decrease in the relative humidity at approximately 1450 E.S.T., while rain was still falling at the station.

(20 percent or greater) which take place over an interval of ½ hr. or more.

In the study, the time and location of the occurrence of this dip were compared with the locations of PPI radar echoes and changes in weather elements observed at the surface. The following paragraphs summarize the relationships which available data show.

Humidity dip and radar echo.—Of 69 station traces showing relative humidity dips, it was found that on 53 of them the dip began at a time when the station was under a PPI echo; in the remaining 16, the stations were within 2 mi. of the echo edge. Sometimes the dips occurred near the center of the echo, where rainfall, wind, and other surface elements were most intense. A large percentage, however, appeared to occur a few miles away from the center areas, pointing to a greater tendency for their development near the periphery of the echo. Because of the size of the photographed echoes and the coarseness of the station network, it is at present impossible to establish this definitely.

Humidity dip and rain.—It is paradoxical that the relative humidity should fall sharply while rain is occurring at a very heavy rate, but this has been frequently found in both the Florida and Ohio data (table 23). Of 79 cases[44] of recorded humidity dips, 57 occurred during the rain period; all but 3 of the remaining number were associated with a rain area. All of the cases occurred during the influence of the cold-air outflow and its associated downward motions.

TABLE 23.—*Frequency distribution of rainfall rates occurring during the 5-minute interval in which the humidity dip began*

Rainfall accumulation (hundredths of an inch)	Number of cases[1]
0– 2.9	37
3– 5.9	9
6– 8.9	3
9–11.9	4
12–14.9	2
15–19.9	4
20–24.9	6
25–29.9	5
30–34.9	2
35–39.9	2
40–44.9	4

[1] A humidity dip used in the other studies is not included because of failure of the rain gages.

A tabulation was made of the rainfall rates before, during, and after the start of the relative-humidity dip. The 5-minute rain accumulations for the numbered twelfths of the clock hour were used for that purpose. The rainfall rate during the start of the humidity dip was, therefore, the accumulation for the 5-minute interval in which the humidity started to fall. From these data, it is seen that the rainfall rate for the 5-minute interval following that of the humidity dip decreased in 38 of the cases and increased in 21; in the remainder there was either no change or rain did not occur. In 33 cases the rain during the 5-minute interval prior to the dip was greater than that of the interval in which the dip occurred. The opposite was true in 20 cases, and in the remaining number there either was no rainfall or no change in rainfall rate.

Humidity dip and divergence.—It was found that the humidity fluctuations occur almost exclusively in areas of divergence. This is not surprising, since, as was shown in preceding paragraphs, the majority of the dips occur during rainfall and underneath the radar echo. Of 41 relative-humidity dips for which divergence calculations were available, 35 occurred in divergent areas, 2 in areas of zero divergence, and the remaining 4 in areas of slight convergence. However, there is evidence that divergence may actually have been present in the latter areas, although it was not indicated on the records due to the coarseness of the station spacing. In view of the above analysis we may conclude that downward motion is almost always present when the humidity dip occurs.

Humidity dip and surface temperature.—Since the relative-humidity dip occurs in the cold-air outflow, it follows the temperature break. In the majority of cases studied the temperature was already falling at the time the relative humidity began to fall. Table 24 gives the frequency distribution of temperature changes that occurred during the periods of the falling relative humidity associated with humidity dips.

TABLE 24.—*Frequency distribution of temperature changes which occurred during the time of humidity falls associated with the relative humidity dip*

Temperature changes (° F)	Number of cases
Rising:	
0–0.9	17
1–1.9	4
Falling:	
0–0.9	24
1–1.9	18
2–2.9	10
3–3.9	3
≧ 4	3

From the records of stations located under the center of a cell in the early mature stage, it is frequently found that the relative-humidity dip occurs after the temperature has reached its lowest point. In such cases a temperature rise of 2° or 3° F. is seen to accompany the relative-humidity dip (see fig. 67). Because of the lag of the Bourdon thermal element the

[44] Ten cases for which no radar data were available were added to the 69 used in the previous study.

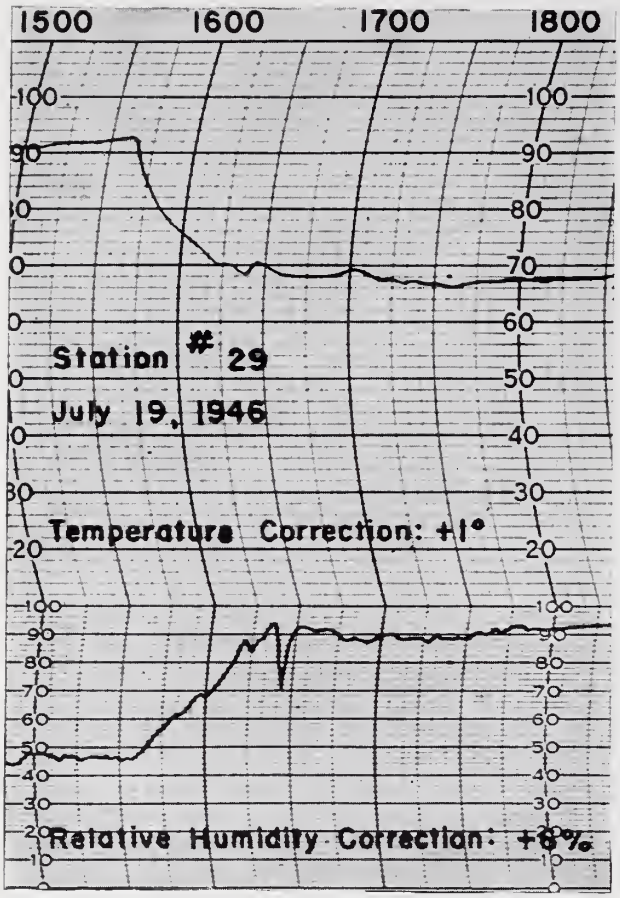

FIGURE 67.—A section of the hygrothermograph record from station 29 of the Florida surface network on July 19, 1946. Note the peak in the temperature during the period of the relative humidity dip.

actual rise may be larger than that indicated on the trace.

If it is assumed that the relative-humidity dip is caused by a desiccation of the downdraft (discussed in a later paragraph), then this rise in temperature may be explained by the fact that the down-rushing air, having attained sufficient vertical momentum in its nearly dry-adiabatic descent, will overshoot its equilibrium position. It will, therefore, continue downward in spite of having become 2° or 3° F. warmer than the ambient air. Additional temperature measurements in lower layers of the atmosphere during thunderstorms are needed to substantiate this reasoning.

Since the temperature is usually falling at the time of the relative-humidity dip, the mixing ratio must necessarily fall also — considering that pressure changes are quite small. Based on the cases used in this study, a frequency distribution was tabulated to show the amount of decrease in mixing ratio associated with the relative-humidity dip (table 25). The average drop was 3.3 gm/kg and the fall ranged from 1 gm/kg to 8.0 gm/kg. In many instances horizontal advection could not possibly account for the degree of mixing-ratio decrease; this forces the conclusion that the relative-humidity dip resulted from a relatively dry downdraft.

TABLE 25.—*Frequency distribution of decrease in mixing ratio associated with the relative-humidity dip*

Mixing ratio decrease (gm/kg)	Number of cases
0–0.9	0
1–1.9	12
2–2.9	25
3–3.9	26
4–4.9	7
5–5.9	6
6–6.9	1
7–7.9	1
8–8.9	1

Humidity dip and wind.—There appears to be no direct relationship between the wind speed or direction and the occurrence of the relative-humidity dip. Wind speeds ranging from less than 3 to 21 mi/hr were recorded at the time of the dip. However, the dips almost always occurred within the caution period and generally in a zone of decreasing wind speed. Winds from all directions were recorded at the times of the dip.

Humidity and pressure.—A study was made of the relationship between the relative-humidity dip and the pressure nose. To increase the likelihood that the two phenomena were associated with the same cell, only those cases were used in which the phenomena had occurred within 15 min. of each other.

Of the 79 relative-humidity dips discussed earlier, pressure noses were recorded with only 7. On the other hand, of the 58 pressure noses used in this study, 19 exhibited relative-humidity dips. Seven of these occurred before the start of the pressure rise, four between the start of the pressure rise and the pressure maximum, one at the time of the maximum, and seven following it. From this, it follows that for the average thunderstorm the pressure nose and humidity dip are not directly related, although they may both occur within a few minutes at a station.

As indicated earlier, the dip usually occurs within the rain area and underneath the radar echo. Since this is where the pressure dome is also present, it may be said that in most instances the dip occurs under the pressure dome.

Areal extent of the humidity dip.—In some cases the relative-humidity dip, as a discontinuity, can be traced from station to station much the same as the temperature break; however, the dip is quickly dissipated so that the same one is identifiable at only a few stations. The area covered by the relative-humid-

ity dip is smaller than that over which rainfall occurs but larger than the area covered by the pressure nose.

The unsaturated downdraft.—The failure of surface air to become saturated during the heavy rain, together with the frequently observed relative-humidity dip, suggest that the downward-flowing air becomes unsaturated as it descends, even in the presence of large concentrations of liquid water. Two processes which may account for this seemingly anomalous condition have been suggested by Project analysts. Unfortunately the data do not permit a definite conclusion as to which, if either, of the processes brings about the observed conditions.

The first suggested process is that the downdraft air is desiccated by the cold precipitation particles. If the precipitation particles, such as rain or hail, are sufficiently colder than the ambient air, the water-vapor pressure near the surface of these particles will be lower than that of the surroundings, thus resulting in a water-vapor flux directed toward the particles. These will grow at the expense of the water vapor in the ambient air and thereby reduce its relative humidity.

The accompanying chart (fig. 68) shows the conditions of ambient air temperature and relative humidity under which the rain droplets will evaporate or grow. No vapor pressure correction was made for the effects due to droplet curvature or the presence of solutes. For example, if the air temperature is 75° F. and the relative humidity 90 percent, such as at point A, a drop will grow if its temperature is below 71.9° F., and it will evaporate if its temperature is higher than this value.

In measurements made by the Project of the average rain temperature 3 ft. above the ground, it was found that in afternoon thunderstorms the raindrop temperature in the first few minutes of the rain period is several degrees lower than that of the ambient air. This of course would be sufficient to keep the relative humidity from reaching 100 percent.

Temperatures of the various raindrops at any given height below the freezing level, at a particular time, probably have a range of several degrees. This follows from considering the fact that the diameters of

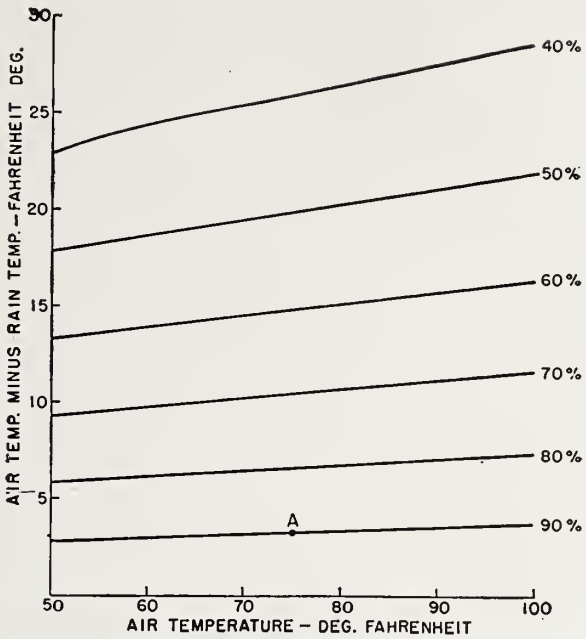

FIGURE 68.—A chart showing conditions of ambient air temperature and relative humidity under which raindrops will evaporate or grow. When the air temperature is 75°F. and the relative humidity is 90 percent, the conditions are represented by point A. Reading from the ordinate, an air-minus-rain temperature difference of 3.1 Fahrenheit degrees is obtained. If rain, falling through the specified air has a temperature below 71.9°F., the drops will grow, if the temperature is above this value, the drops will evaporate.

drops in thunderstorms vary from a few microns to 5 mm., thus resulting in different terminal fall velocities. At any instant, therefore, some drops are evaporating, while others are growing. The resultant relative humidity at that height is therefore determined by the net evaporation or condensation. It is evident that a sufficient number of colder water drops can prevent the air of the downdraft from remaining at saturation.

The second process suggested to explain the lack of saturation is that the downdraft is unable to remain saturated because the rate of evaporation of the water drops is too slow to provide for the increase in the saturation mixing ratio as the air descends to lower levels. In that case the air of the thunderstorm downdraft would be heated at a rate between that of the moist- and the dry-adiabatic and would reach the ground in an unsaturated state.

6. Development of New Thunderstorm Cells

In the discussion of the life cycle of the thunderstorm on pp. 19 to 27, it was brought out that new cells have a tendency to form adjacent to those which have already developed. By viewing the course of events over a large area by means of radar echoes, it can be seen that new developments taking place are clustered around the initial cells, with independent growths appearing less frequently. The following processes would favor such a grouping:

1. Cold-front action of the outflowing cold air in underrunning and lifting the neighboring warmer air.
2. Nourishment of new cloud developments with saturated air entrained from the parent cell. It is to be noted that the higher the relative humidity in the entrained air, the less the temperature will be reduced by the mixing in the cloud.

3. Addition of moisture to the neighboring air by light precipitation falling from an overhanging cloud canopy which has grown out of the parent cell.
4. Spontaneous production of updrafts in the area of cell clusters, due in some cases to thermal or orographic processes, but, in a homogenous, level region, apparently caused by local areas of surface convergence or upper-level divergence.

From a study of numerous cases of new-cell development, the action of the cold outflowing air appears, unmistakably, as causing or contributing to the new growth. In some cases, however, the time interval between the beginning of the outflow and the appearance of the new cell on the radar 'scope is too short to permit explanation of the new development as a result of the underrunning cold air. There are cases in which one or a cluster of new cells come into existence, as indicated by the radar echoes, almost simultaneously with the initial or mother cell, which suggests that a preferred region of updrafts favors the development (fourth factor in the above list).

The extent to which the processes of (2) and (3) contribute to new development may only be surmised. It should be pointed out, however, that they, like (1), would require that considerable time should lapse between the appearance of the first radar echo and the dependent ones. When the time lapse is very short, some cause such as described in process (4) must be involved[45].

In order to demonstrate the tendency for new cells to develop adjacent to old ones rather than at distant points, a statistical study was made of the relative positions of the initial and new cells.

TREATMENT OF DATA

Radar observations made on eight days — three in Ohio and five in Florida — were included in this study. The data were treated as follows:

1. Outlines of echoes from the off-center PPI 'scopes of the control radar sets were copied on a base map of the area for a series of consecutive 5-minute intervals. These were considered as the initial echoes for each interval. Only echoes larger than 3 sq. mi. were treated in this way.
2. A band 3 mi. in width and another 9 mi. in width were delineated about each echo.
3. The direction of echo movement was determined. The echo and the area within the 3-mile band were divided into four equal sectors, as shown in figure 69, by drawing two perpendicular lines intersecting at the geometric center of the echo and making a 45-degree angle with the direction of movement. These lines were terminated at the outer boundary of the 3-mile band. This divided the echo and the adjacent 3-mile band into a leading sector, a trailing sector, and right and left lateral sectors.
4. The areas of each of the four sectors, the 9-mile band, the 3-mile band, overlapping areas of the 3-mile bands, the radar echo, and the area outside the 9-mile band were measured, and the number of new echoes which had developed in each of them during each consecutive 5-minute interval was counted and tabulated.

RESULTS OF THE ANALYSIS

A total of 426 new echoes were found to have developed in the period under consideration. In table 26 the results of the counting and tabulation are summarized and presented as probabilities of new echo development for each of the areas. The average picture is presented in figure 69, in which the numbers indicate the relative probability of new echo development in the various area divisions, with the development outside the 9-mile band considered as unity. The area division formed by the intersection of 3-mile

[45] It is estimated that a minimum of 25 min. would be required from the first appearance of a parent echo to that of a dependent echo.

TABLE 26.—*Number of new echoes which formed per 1,000 sq. mi. per 5 min. in designated areas around parent cells*

Place of formation	Florida storms (1946)					Ohio storms (1947)			Average (or relative probability)
	Jul. 9	Jul. 19	Jul. 23	Aug. 14	Aug. 26	Aug. 14	Aug. 25	Sept. 12	
Leading sector	6	2	2	10	19	9	4	2	7
Trailing sector	4	6	4	4	7	2	6	2	4
Right lateral sector	6	7	0	12	24	3	1	1	7
Left lateral sector	6	2	10	7	6	5	5	4	5
3-mile band (minus area of overlap).	5	5	4	8	16	2	4	2	6
Dual overlap sector	12	12	2	9	16	13	14	0	11
Area between 3- and 9-mile boundaries.	1	2	1	3	6	1	4	1	2
Area outside 9-mile boundary	0.2	0.9	2	1	2	1	1	1	1

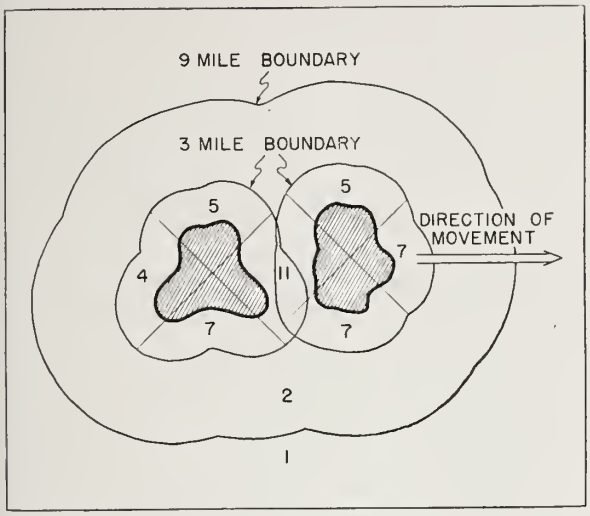

FIGURE 69.—A chart showing the relative probability of the formation of new thunderstorm cells in the vicinity of parent cells. The hatched areas represent the PPI radar echoes from the parent cells and the irregular closed curves represent the limits of the 3-and 9-mile zones surrounding the echoes. The numbers indicate the relative probability of new echo (cell) formation in the zones and quadrants with the probability outside the 9-mile zone being considered as unity. The number 11 in the area of overlap of the 3-mile zones represents the probability in that region. For the trailing quadrant of the leading echo and for the leading quadrant of the trailing echo, the probabilities would be four and seven respectively.

bands from two echoes has been termed "dual overlap" area; areas which contained the overlap of bands from three, four, etc., echoes were termed "triple, quadruple, etc. overlap" areas, respectively.

Based on these data the following conclusions may be drawn:

1. The most probable area for new echo development is within a zone where the 3-mile bands overlap. The probability that new echoes will form there is 11 times greater than that they will form outside the 9-mile band. This is not surprising, since, as shown in another section of this report, the area between the echoes is one where marked surface convergence occurs, especially if the cold air outflow from both echoes affects the same area. The air between the echoes then is forced aloft.
2. The probability of new echo development is higher in the leading and lateral sectors than at the trailing edge. This is not surprising since the outflow is more pronounced in the former sectors. In the trailing sector the cold-air outflow is markedly reduced by the prevailing winds and the movement of the cloud itself. The fact that the most frequent development of new echoes occurs where the outflow is greatest tends to support the hypothesis that the cold air of the downdraft underruns the convectively unstable air ahead of it, triggering new cell development.
3. The difference in the average relative probabilities between the right and left sectors, 5 and 7, cannot be considered significant. In individual storms one side may show markedly higher probabilities than the other.

The 3- and 9-mile bands of the study were arbitrarily chosen. Bands of other widths may yield significantly higher probabilities of new echo development. However, these results point out that new echoes form near those already present.

These results have implications in connection with concepts of regions of compensating sinking of air around thunderstorms (Schmidt [**49**]). The tendency for development of updrafts in the immediate neighborhood of existing cells indicates that the compensating downward motions must take place at some distance away from the cell, apparently 10 mi. or more, rather than adjacent to it as some writers have assumed.

APPLICATION OF RESULTS

The results of this study may be applied to planning of flights in the neighborhood of thunderstorms. It is shown elsewhere in this report, that in the building stage of the thunderstorm, strong updrafts may be present. It is also shown that there is a direct relationship between the magnitude of the gustiness and the strength of the drafts, i.e., the more intense the draft, the greater the gustiness. From this it is apparent that the chances of encountering severe turbulence would be reduced if areas having a high probability of new echo development were avoided. Since the probability of new cell formation is high near the leading edge of a radar echo and between neighboring echoes less than 6 mi. apart, flight hazards due to turbulence may be reduced by staying out of those areas. Should it become necessary that a line of thunderstorms be traversed, it is advisable that, if possible, the pilot choose his course near the trailing edge of the radar echo at a point where there is no other echo close by.

CHAPTER IV. ELECTRIC FIELDS INSIDE THE THUNDERSTORM

It has long been known that thunderstorms produce radical changes in the fair-weather electrical potential gradient in the atmosphere. The fair-weather gradient in the lower layers is directed downward, i.e., the earth has a negative charge with respect to the atmosphere. This potential gradient usually has a magnitude of about 100 v/m. With the development of thunderstorm cumulonimbus clouds a striking change in the electrical field occurs. Repeated observations by many investigators have shown that centers of charge concentration are distributed in such a manner as to make the upper portion of the cloud positive and the lower portion negative, figure 70. The negative cloud base induces a positive charge on the ground, reversing in sign the fair-weather field in the low levels. Measurements show that the center of the positive-charge concentration in the cloud is located a few thousand feet above the negative-charge center, the mean position of the latter being slightly above the freezing level. Simpson and Scrase [**52**] also found smaller centers of positive charge in the lower part of the cloud.

One of the highest measured potential gradients ever reported was 3,400 v/cm [**27**]. This measurement was made by an Army-Navy Precipitation Static Project airplane at 12,900 ft. just before it was struck by lightning. This value is small in view of the measured dielectric strength of the air for which the breakdown potential is variously judged to be between 10,000 and 30,000 v/cm. When the actual break-down potential is reached, lightning discharges occur. The thunder is the noise produced by these discharges. Some of the lightning discharges are confined to the cloud only, presumably concentrated in the region of strong gradient between the charge centers, and some discharges occur between the cloud and the ground.

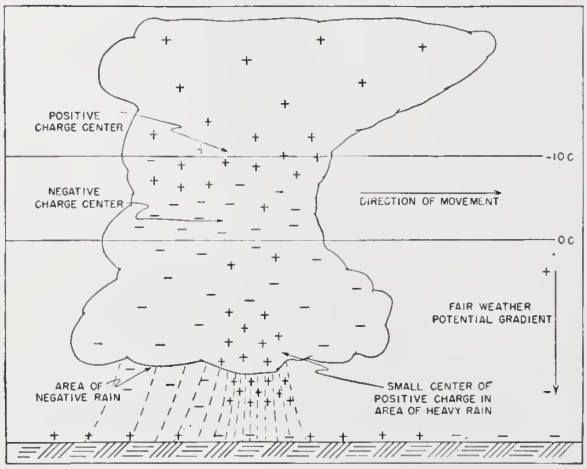

FIGURE 70.—A schematic diagram showing the charge distribution of a thunderstorm cell.

The relative locations of the positive- and negative-charge centers within the cloud have been demonstrated by results of soundings made with balloon-borne equipment [**51**], by data from aircraft measurements [**26**], and by observations made at surface stations of a network [**63**].

With data obtained by means of the latter two techniques, it has been shown that these electric charges were arranged in a cellular configuration. From measurements of the potential gradient at the surface, Workman, Holzer, and Pelsor [**63**] found that there were several centers of positive and negative charge concentrations in a single thunderstorm. They also found that in the later stages of cloud development the positive centers appeared to descend and move to one side of the negative centers, although at no time did they drop below the level of the negative centers. These centers appeared to be grouped into couplets of one positive and one negative charge as is shown in figure 71. This horizontal cross section shows that dimensions of each couplet of charges were approximately 4.5 mi. by 3 mi. It is probable that the couplets indicated by these electrical measurements are the same as, or closely related to, the convection cells delineated by the arrangement of the drafts within the thunderstorm.

Electric field measurement from airplanes.—One of the basic aims of the Project was to further the knowledge concerning thunderstorm electric fields and for this purpose the Project P–61C airplanes were equipped with electric field meters in addition to the instruments for measuring the air motions[46]. Two meters were installed on each airplane, from which it

[46] For a more detailed description of the instruments, see appendix (4).

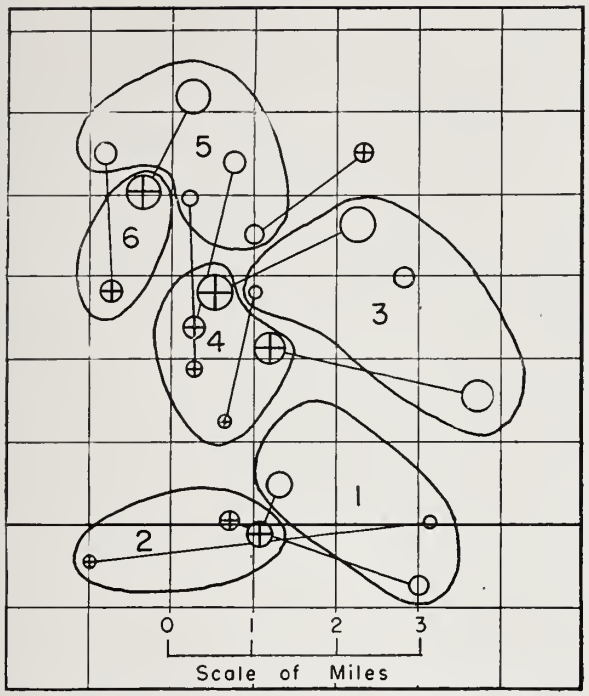

FIGURE 71.—A diagram showing the charge centers within a thunderstorm. Note the grouping of the centers into couplets composed of one positive ⊕ and one negative O charge. (Based on data presented by Workman, Holzer, and Pelsor.)

was possible to determine only the vertical component of the electric field. The meter readings indicated by these instruments reflected: (1) the external, or "exogenous," field created by the existence of charge centers within the thundercloud; and (2) the "autogenous" charge, or charge collected on the skin of the airplane by frictional contact with ice crystals or dry snow. To determine the strength of the electric field developed by the external charge in flights above the freezing level, two or more electric field meters were necessary; of the two used, one was located on the top and the other on the belly of the airplane fuselage.

The instruments were connected in such a manner that, neglecting local distortion, the top meter indicated the difference between, and the bottom meter the sum of, the exogenous and autogenous components. Since the airplane skin is an equipotential surface, the exogenous field is distorted and correction factors had to be applied to the upper and lower meter readings. These factors were unequal because the airplane is geometrically asymmetrical.

Unfortunately the Project experienced considerable difficulty with the meter located on the top of the fuselage of each airplane. Consequently, of all the measurements taken, only those from flights below the freezing level could be used in the analysis; this is due to the fact that at these levels the autogenous charging is negligible. In these cases the lower meter indicated the exogenous field multiplied by a correction factor (K) which remained constant.

Relation of electric field to cell structure.—The formation, growth, and dissipation of thunderstorm cells have been discussed in the preceding chapters of this report. The following discussion presents the relationship of the electric field to the cell structure of the thunderstorm, as indicated by the limited data available. This can best be done by means of an example. Of the five Ohio flights for which usable electric field data were available, the one which best shows this relationship is that of mission 19 on August 7, 1947. It was made through a fairly isolated storm, located over the surface network, in which no lightning was observed.

On five successive traverses through the same part of a cell, one plane flew at altitudes ranging from 2,000 to 4,000 ft., m. s. l. The data obtained on these traverses are plotted on figure 72. Information concerning the path of the airplane through the cell was obtained from photographs of the 'scopes of the PPI and beacon radar sets. The drafts encountered by the airplane, computed from records of the plane's altitude (in conjunction with records of airspeed), are plotted relative to the position in the echo at which they were encountered. Electric field measurements, evaluated in the manner previously described, are plotted relative to the point of measurement. The intensity of the rainfall from this storm cell was measured by means of surface rain gages. The quantity accumulated in each 5-minute interval during the rain period was calculated for each station, and the station showing the maximum value for each interval was considered as the rainfall center. It is possible, of course, that the absolute center of rainfall during any of these intervals was located between stations, since the stations of the observational network were approximately 2 mi. apart.

The only draft encountered by the plane was a downdraft in the northern portion of the cell. It was present on four of the five traverses. The measured draft values are plotted in figure 72 at their positions relative to the radar echo.

Analysis consisted of a superposition of these flight data from the five traverses, from which it was possible to determine the change of the electrical field pattern with time, and a correlation of the build-up and dissipation of the electrical field with the height of the radar echo, the intensity of surface rain, and the measured drafts.

The cell was in the mature stage during the first two traverses, reaching its peak height at the time of the second traverse, and then began to dissipate. Rain fell for 30 min. prior to the first traverse. A downdraft was encountered on the first and second trav-

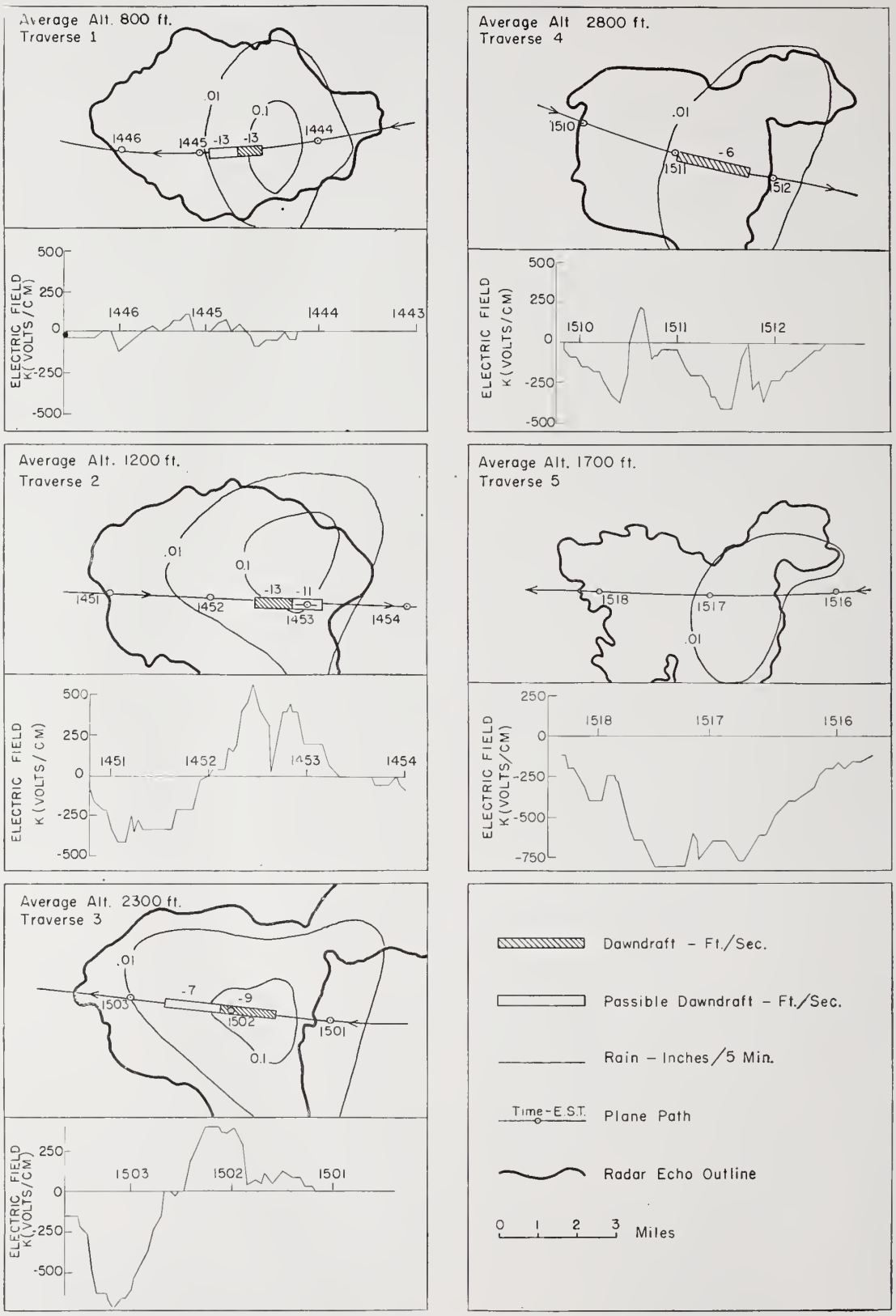

FIGURE 72.—A series of charts showing five low-level traverses through a thunderstorm cell. The location of the cell is indicated by the radar echo. For each traverse of the cell, the electric field measurements, the draft measurements, and the 5-minute isohyets are presented. This flight was made over the Ohio surface network on August 7, 1947.

erses, and rainfall increased during the second traverse at which time the radar showed the peak height. During the remaining traverses the height of the echo and intensity of the surface rainfall decreased, and the downdraft became much weaker; for the time of the last traverse it could not be evaluated from the records.

On traverse 1, the electrical potential gradient was fairly weak, with the trace indicating alternately positive (directed-earthward) and negative gradients. There was no particularly pronounced field associated with the downdraft. On traverse 2, the gradient reached the greatest positive value (+560 v/cm) measured during the entire mission; this occurred in the rain and downdraft area, at the time when both rain and downdraft intensities reached their peak values. The southern (left side of cells shown in fig. 72) portion of the cell (believed to contain an updraft) showed a negative gradient (—400v/cm). On traverse 3, the peak positive gradient (+400v/cm) again occurred in the rain and downdraft area, although the values were weaker; and the gradient in the southern part of the cell reached strong negative values. By the time of traverse 4, the cell had fairly well dissipated. The rainfall and downdraft intensities were much weaker. The electric field measurements showed only a very small, weak area of positive gradient, in the middle of the cell, surrounded by an area of negative gradient. The positive potential gradient had completely disappeared by the time of traverse 5 and strong negative gradients were observed throughout the traverse.

Thus, the changes in the electric field in the cell followed a definite pattern. The first traverse showed an almost neutral field. However, only 8 min. later, with increased cell height and rainfall, the positive field became strong in the rain area and the negative field strong outside the rain area, although the negative field did not reach its peak until 32 min. later. Then, with dissipation of the cell and decreased rain intensity, the positive field vanished and was replaced by a negative one.

The finding of the positive charge in the rain core in traverses 2 and 3 appears to bear out the findings of Simpson and his co-workers, namely, that a positively-charged region may occur near the base of the thundercloud. The more commonly observed charge distribution in a thunderstorm, with the cloud base negative with respect to the ground, was found under the updraft in the southern end of the cell, and in the rain area after the time of maximum rain. Measurements by a number of investigators have shown that raindrops falling to the ground usually carry a net positive charge. Simpson [50], extending theories of Lenard [34] and Elster and Geitel [24], ascribes the positive charge to an effect of breaking drops. The data of this Project flight showing a positive potential gradient in the rain core are presented, with no intention of supporting or proposing an explanation of the physical processes involved.

Electric fields and thunderstorm drafts.—The relationship of the electric field to the drafts within the storm of August 7, 1947, was discussed in the previous paragraphs. In addition to the drafts of that storm, drafts measured for two other missions were studied for the purpose of determining the magnitude and sign of the vertical potential gradient within them. It was recognized that a comparison of the magnitude of the electrical potential gradient within the draft with that of its environment would also yield valuable information; however, with the data available it was difficult to identify the location of the edge of the draft, and such a study was not attempted.

The results of the study of the vertical component of the electric field in relation to seven drafts—evaluated by the N. A. C. A. from the records of these three flights, including the one of August 7, 1947 — are shown in table 27.

TABLE 27.—*Relationship of thunderstorm drafts to the electric field (based on measurements made during airplane flights through thunderstorms in Ohio)*

Date (1947)	Mission No.	Traverse	Altitude (ft., m.s.l.)	Type of draft	Mean electric field (v/cm)
June 7	7	2	10,000	Updraft	−260
				Downdraft	−290
				Downdraft	−200
Aug. 7	19	2	2,000–4,000	Downdraft	+290
		3	2,000–4,000	Downdraft	+160
		4	2,000–4,000	Downdraft	−230
Aug. 21	30	1	10,000	Downdraft	−260

As can be seen from this table, both positive and negative gradients are found inside drafts at the lower levels in the thunderstorm. It is interesting to note that all of the measurements at 10,000 ft. show negative fields, which means that the negative-charge center is above that level. The two cases of positive gradients found in the 2,000 to 4,000-foot layer may be explained as previously stated, by the fact that positive charge centers may exist near the base of the cloud in the rain area.

Electric fields and turbulence.—In this study, the turbulence parameter considered was the absolute value of the maximum effective gust velocity per 10-second interval of traverse. The electric field data were obtained from the readings of the lower meter on five low-level missions and the measurements obtained were divided into the same 10-second intervals used to obtain the turbulence values. The mean values

of the electric field were thus determined for 364 such intervals available for study. From these data the frequency distribution of electric-field and turbulence measurements were tabulated (tables 28 and 29).

TABLE 28.—*Frequency distribution of maximum effective gust velocity per 10-second interval of traverse for five low-level flights (based on observations made in Ohio thunderstorms)*

Maximum effective gust velocity (ft/sec)	Number of 10-second intervals
0– 2	163
2– 4	37
4– 6	57
6– 8	38
8–10	18
10–12	19
12–14	14
14–16	8
16–18	5
18–20	2
20–22	2
22–24	0
24–26	0
26–28	1

TABLE 29.—*Frequency distribution of electrical potential gradients encountered during five low-level flights (based on observations made in Ohio thunderstorms)*

Electrical potential gradient (100 v/cm)	Number of 10-second intervals
0– 1	88
1– 2	102
2– 3	55
3– 4	40
4– 5	30
5– 6	15
6– 7	8
7– 8	5
8– 9	6
9–10	8
10–11	0
11–12	3
12–13	2
13–14	1
14–15	0
15–16	1

These mean electric-field values and turbulence measurements were also used to plot scatter diagrams representing the turbulence-electric field relationships for each flight and for all flights combined. The latter diagram is shown in figure 73. The scatter diagram shows no correlation between the values of turbulence and electric field strength. This conclusion is substantiated by application of the Chi-square test to the data for the class intervals shown in tables 28 and 29. A consolidation was made of the end rows and columns because of the small number of intervals in which the higher values of field strength and turbulence occurred. The final value of Chi-square was 23.93 with 24 degrees of freedom, giving a value of probability, P, of approximately 0.45. With this value of P there is no reason to believe that the occurrence of particular electric field values with certain gust values was due to anything but chance. The results of this study appear to question a widely held belief that an airplane electric field meter can be used as a turbulence sensing element in thunderstorms.

These results were not unexpected, inasmuch as it is not the gusts — local, irregular or transitory variations in the velocity field — which produce electrical charge separation. It is more reasonable to expect that only large-scale vertical motions, such as drafts, are effective in this process. Furthermore, it is also likely that other processes, not directly associated with gusts and drafts are very important in producing the electric field. Many of the existing theories of charge generation in a thunderstorm invoke processes involving particles of condensation and precipitation, particularly effects produced by falling raindrops or frozen hydrometeors. Thus, turbulence would appear to represent only part of the mechanism.

Electric fields and rain areas.—A study was made of the relationship between the intensity of the electric field in thunderstorms as measured by the airplane and the presence of hydrometeors. As the presence of hydrometeors was recorded by manually controlled indicator lights on the instrument panel of the plane (appendix (4)), continuous photographs of the indicator lights and the electric field meter made the study possible. No indication as to the intensities of the precipitation was available.

As in the preceding study, the data used were obtained from five low-level flights. The graphs of the electric field measurements were divided into 10-second intervals, and the maximum value of the field was determined for each interval. The electrical field measurements per 10-second interval were then grouped into four classifications, depending upon whether they were made: (1) in the clear air near the cloud; (2) in cloud but not in rain; (3) in cloud and rain; and (4) in rain but not in cloud.

Although the data presented in table 30, are too few to permit correlation of altitude and the field intensity for the various categories mentioned above, certain relationships are indicated between the measured field intensity and its position with respect to the cloud. The weakest fields were encountered when the airplane was in the clear. However, even when the airplane was neither in cloud nor in rain, it might still have been below the cloud and consequently under the direct influence of the lower charge center in the cloud. Therefore, the strength of the field measured in the clear air at the lower levels is undoubted-

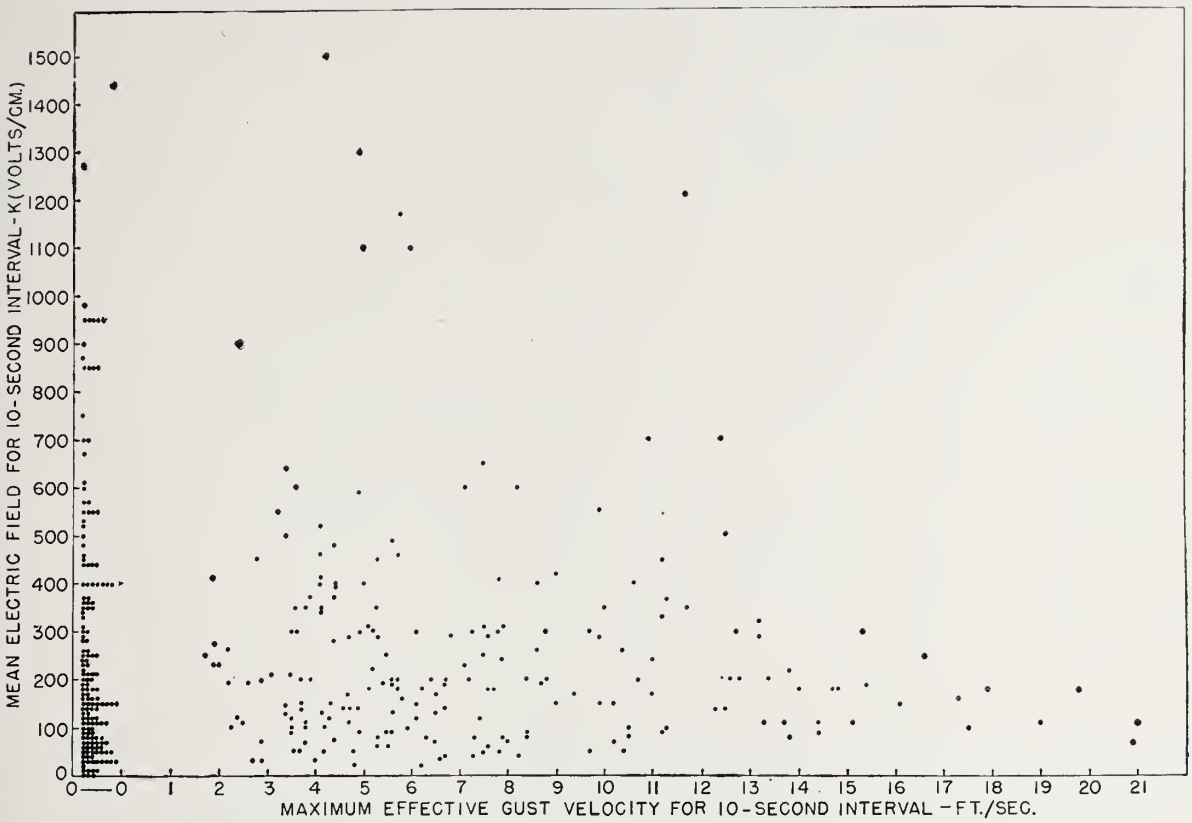

FIGURE 73.—A scatter diagram relating the electric field to the effective gust velocities. This chart is based upon 364 measurements of the electric field and the maximum effective gust velocity during corresponding 10-second intervals. Five low-level traverses through Ohio thunderstorms were studied.

ly greater than would have been the case had the measurements all been made at the side of the cloud.

The recorded field intensities increased when the airplane was in the cloud (except for the 6,000-foot level), and increased still more when the airplane entered the rain area in the cloud. Thus, it appears as if the pattern of the electric field associated with a thunderstorm is weakest outside the cloud and reaches its maximum intensity in the rain area in the cloud.

It should also be noted that the preponderance of negative fields at the 10,000-foot level means that the negative-charge center is above that level. The increased frequency of intervals of positively directed fields at the low levels is indicative of the fact that the base of the cloud may sometimes contain a positive charge, although at the lower levels, also, negatively directed fields are preponderant.

Electrical field measurements at the surface.—As has been pointed out earlier in the chapter, measurements of electric field from surface equipment can be used to obtain information concerning thunderstorm electric fields and, as a consequence, information concerning the lightning frequency inside the thunderstorm. To complete this important part of the Thunderstorm Project instrumentation program, there were installed in the surface network three point collectors (described in appendix (1)) for the purpose of obtaining such measurements.

A point collector is essentially a needle mounted several feet in the air and grounded to the earth's surface. When the earth's surface becomes positively charged in response to a negative-charge center in a thunderstorm overhead, the point collector attracts negative ions and the field in its immediate vicinity is thus intensified. When the potential gradient thus created exceeds a critical value, a sudden surge or "corona discharge" of positive ions from the collector to the atmosphere occurs. After this discharge has taken place, a positive space charge surrounds the collector tip weakening the gradient and causing the corona discharge to cease. The entire process is then repeated. The frequency of repetition of these corona discharges depends, among other things, on the shape and size of the collector tip and the strength of the electric field. The frequency was normally quite high in the vicinity of thunderstorms with the type of point collectors used by the Thunderstorm Project—a matter of thousands of cycles per second. Since the recorders used were incapable of recording individual variations of such high frequency, the resulting

TABLE 30.—*Frequency distribution of 10-second intervals of flight in positive and negative electric fields, and the mean maximum value of the field in each interval, for several weather conditions and altitudes of flight*

Category of measurement and flight altitude (ft., m.s.l.)	Total number of intervals	Positive intervals		Negative intervals		Intervals both positive and negative		
		Number	Mean maximum gradient	Number	Mean maximum gradient	Number	Mean positive maximum gradient	Mean negative maximum gradient
			v/cm		*v/cm*		*v/cm*	*v/cm*
In clear air:								
2,000 to 4,000	13	1	100	9	330	3	63	172
6,000	37	2	116	28	361	7	53	41
10,000	127	12	102	103	141	12	100	80
In cloud, not in rain:								
2,000 to 4,000	31	3	177	23	471	5	131	147
6,000	45	7	155	29	362	9	131	95
10,000	126	8	73	101	365	11	138	155
In cloud and rain:								
2,000 to 4,000	31	10	335	18	539	3	119	87
6,000	21	5	173	14	588	5	180	110
10,000	122	11	233	93	401	18	131	230
Outside cloud, in rain:								
2,000 to 4,000	33	7	179	19	497	7	81	162

record represents the mean value of the corona current.

Unfortunately, the use of the corona current as a measure of the electric field is limited by the fact that a critical value of field intensity must be attained before a corona discharge takes place, and also by the fact that the relationship between the field intensity and the magnitude of the corona current is not linear. These shortcomings are readily seen from the calibration curve shown in figure 74. The collector points were calibrated by means of artificially created electric fields.

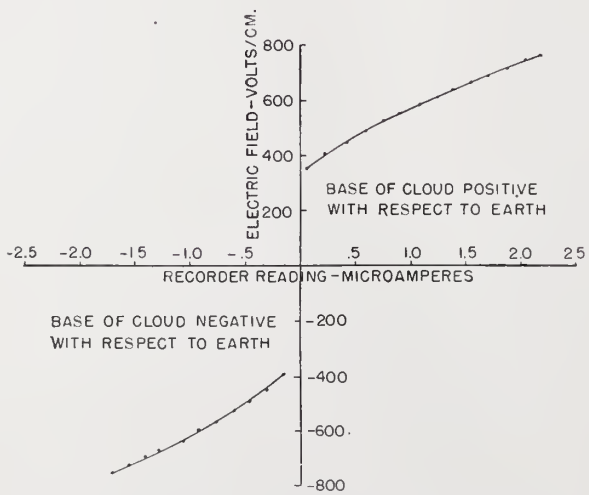

FIGURE 74.—The calibration curve for a point-collector type electric-field intensity indicator. The curve shows the relationship between the electric-field intensity and the magnitude of the corona current.

In addition to the corona current, current flows from ground to the needle point in response to lightning discharges which produce changes in the electric field affecting the collector. The effect of such discharges may be readily distinguished from the corona current by the magnitude and rapidity of the variations in the meter reading. When the current flow is due to a change in the electric field, the charges may never leave the antenna but remain bound at the tip by induction. The current continues until equilibrium is reached. If the charge in the cloud base weakens, a proportionate number of charges will leave the antenna tip and return to ground, causing a deflection which is opposite in sign to that which results from corona flow. Thus the sharp deflections caused by the rapid changes in the electric field, as a result of lightning discharges, may have the same or opposite signs as those caused by corona current and sometimes occur when the corona current is undetectable. Although the magnitude of these deflections does not accurately represent the changes in the field intensity, their recurrence frequency is believed to be a measure of the frequency of lightning occurrence.

Lightning frequency, cell height, and surface rain intensity.—It is a well-known fact that lightning is never found in small cumulus clouds, but that as the cloud grows into the cumulonimbus stage, lightning begins; as the intensity of the storm increases, so does the frequency of lightning. Inasmuch as the previous analysis indicated that charge generation and charge

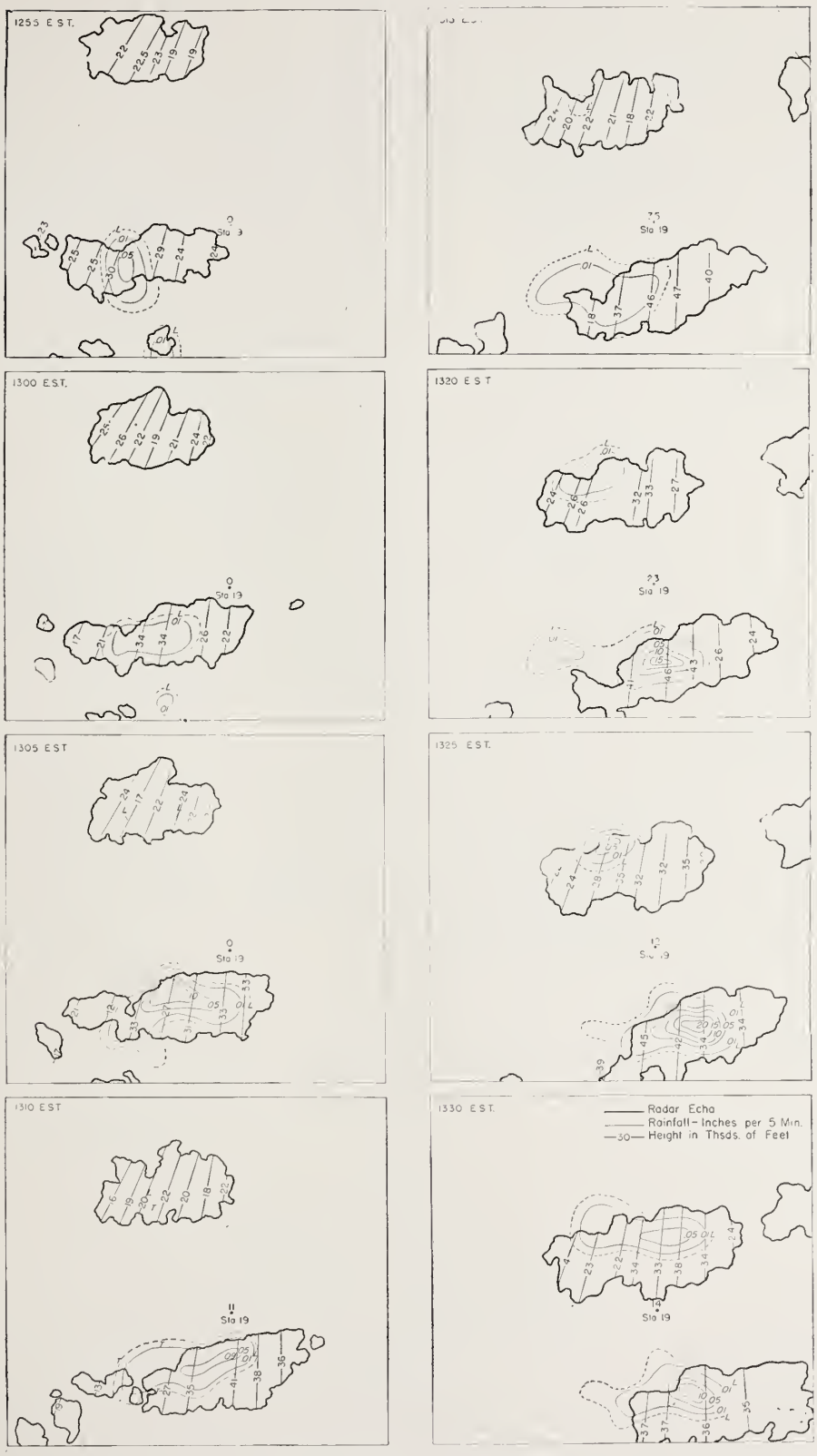

FIGURE 75.—The thunderstorms of August 21, 1947—1255 through 1330 E.S.T. The legend for 1330 E.S.T., applies to all times. The heights of the tops of the sections through the echoes were obtained from the RHI radar. The number of lightning discharges recorded at station 19 during the 5-minute interval preceding the map time is plotted.

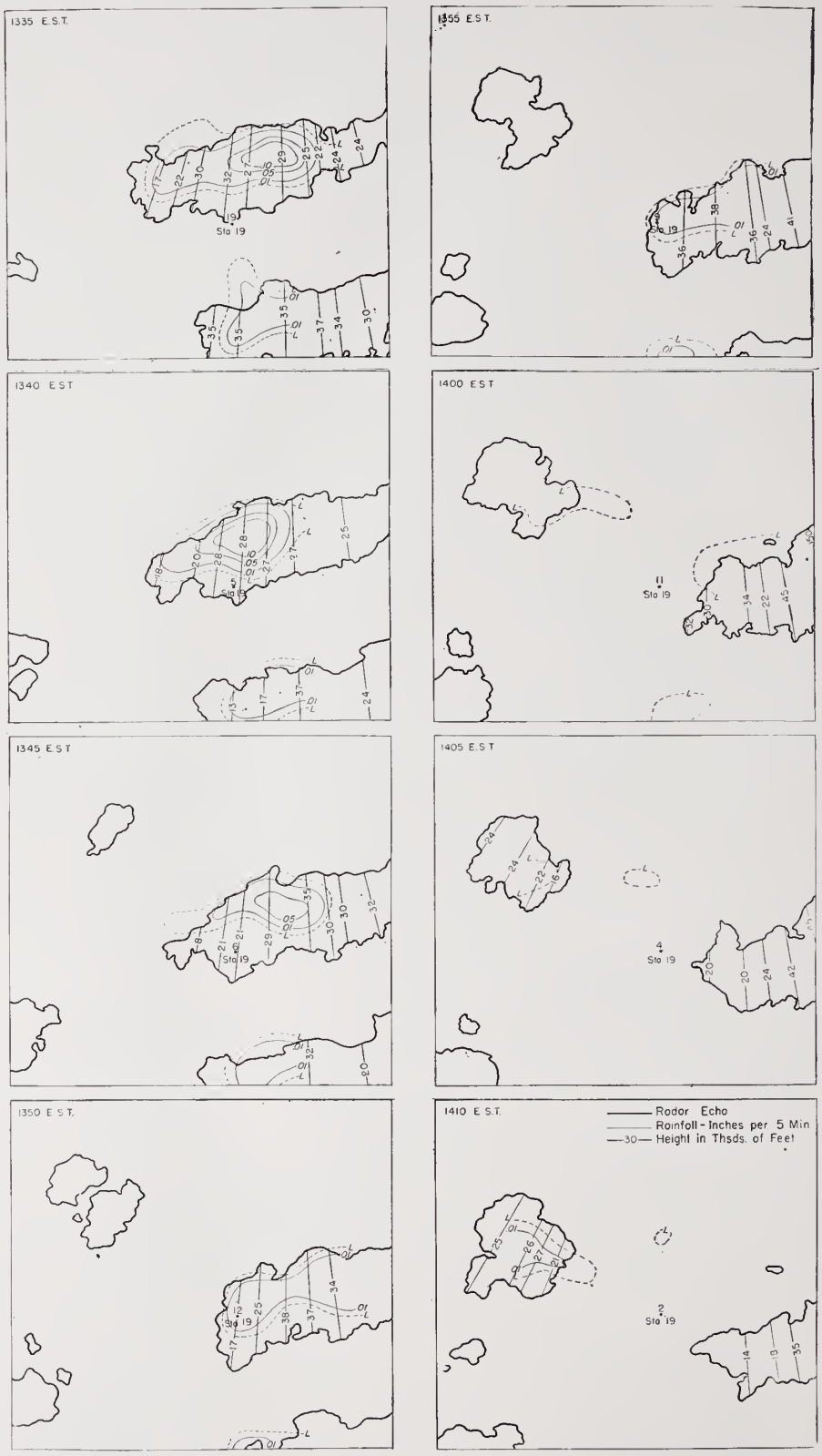

FIGURE 76.—The thunderstorms of August 21, 1947—1335 through 1410 E.S.T. The legend for 1410 E.S.T., applies to all times. The heights of the tops of the sections through the echoes were obtained from the RHI radar. The number of lightning discharges recorded at station 19 during the 5-minute interval preceding the map time is plotted.

separation were a function of the individual cell, it was hoped that the relationship between cell height and lightning frequency could be obtained from the Project data. Unfortunately, cells which reach heights great enough to contain lightning usually occur in groups, making it impossible—at least with the equipment used by the Project—to determine which of the lightning discharges were produced by a particular cell.

It is therefore desirable to present the complete data on cell heights and lightning frequency for a typical situation to illustrate the general nature of the relationships observed. The case of August 21, 1947, was selected for this purpose and the following data are presented in figures 75 and 76:

1. PPI echoes of the thunderstorms, as determined by the control radar located at Jamestown, Ohio.
2. Thunderstorm heights, as determined from data of the RHI radar (AN/TPS–10), also located at Jamestown, Ohio.
3. Lightning frequency, as indicated by the electrostatic-field recorder located at station 19.
4. Five-minute rainfall amounts recorded at stations of the surface network.

There are several points of interest which are evident on these charts:

1. In the case of the southern cell, the cloud top exceeded a height of 29,000 ft., where the environment temperature was —21° C., before lightning was recorded at the surface. It was observed in other examples that temperatures of this magnitude are required before initiation of lightning.
2. The maximum cell height (consequently the minimum temperature at the cloud top) and the maximum lightning frequency occurred together.
3. As the height of the thunderstorm decreased, the frequency of lightning also decreased.
4. It appears that a greater cell height (or lower temperature of the cloud top) was necessary to initiate lightning than is required to maintain it once it has been initiated.
5. The maximum frequency of lightning preceded the time of the maximum 5-minute rainfall.

Examination of figures 75 and 76 shows that two storms west of station 19 moved to the east, causing the recorded electrical activity. The radar indicated that the maximum height of both storms exceeded 40,000 ft. By 1244 E.S.T., the southern most storm was within 4 mi. of station 19 and had reached a height of about 29,000 ft., where the temperature was —21° C., but no lightning had yet been recorded at the surface. The first lightning occurred between 1305 and 1310 E.S.T. when the thunderstorm top was at approximately 41,000 ft. As the storm reached greater heights, lightning became more frequent, with the maximum frequency and the maximum storm height occurring at approximately the same time. By 1314 E.S.T. the northernmost storm had moved sufficiently close to station 19 to make impossible the determination of which storm caused the recorded lightning. However, by 1330 E.S.T. the southern storm was sufficiently far to the southeast of the station to make it appear likely that the remainder of that recorded lightning was due to the northern storm.

CHAPTER V. THE THUNDERSTORM AS DISCLOSED BY RADAR

1. Use of Radar for Cloud Detection

Thunderstorms frequently extend to such great heights that a complete description from airplane data is practically impossible. In previous chapters a discussion is given of the structural features of the thunderstorm as indicated by measurements made at levels up to only 25,000 ft. This restriction was dictated by the lack of observational flights above that altitude. However, as has been shown in the Introduction, a large number of photographs of thunderstorm echoes on radar 'scopes of different types were collected. From these it was possible to obtain information on rates of growth of and horizontal and vertical extent of thunderstorms.

Radar is a useful meteorological instrument because of its ability to detect and depict on a cathode-ray tube a picture of that part of a cloud within which there is a large quantity of water either in the liquid or frozen state. Several recent publications have given detailed discussions of this use of radar [**61**]. It is considered sufficient here to state that the intensity of the radar echo from a cloud depends, among other factors, upon the mass of free water per unit volume of the cloud. Although the amount of data on frozen hydrometeors is scanty, indications are that the relationship is valid for the solid as well as the liquid state [**47**]. From these considerations it would be expected that during the developing stage of the thunderstorm—when strong updrafts are lifting, or suspending, large quantities of water and ice—there is closer agreement between the visual cloud and radar cloud[47] than during the dissipating stage—when the large hydrometeors have fallen out of the cloud, leaving only the smaller particles which return a small fraction of the incident energy.

A limited amount of data is available which demonstrates the relationship between the tops of the radar cloud and the visual thundercloud when the AN/TPS–10 height-finding radar[48] is utilized for the observations. An example of thunderstorms, as detected and presented on the 'scope of this radar, is shown in figure 77. On five occasions, airplanes of the Thunderstorm Project were flown through or near the tops of clouds which were being observed by this radar set. The mean difference in height of the visual and radar cloud top measurements was less than 500 ft., with the latter having the lower value.

Other evidence of the correspondence of radar clouds to visual clouds is reported by Reynolds and Workman [**43**]. In their report it is shown that at the time of maximum radar cloud height the tops of the echoes were lower than the visual cloud tops by an average of 2,400 ft. (7 cases considered). At the time of initial detection, however, agreement was much poorer, improving as the cloud grew upward. In general, altitude changes of the tops of the radar cloud were accompanied by similarly-directed altitude changes of the visual cloud. The type of radar (AN/APQ–13) used by Reynolds and Workman was different from the one used in the Project study; the characteristics of the two pieces of equipment are such that comparable or, more probably, better agreement of radar and visual cloud tops can be expected with the AN/TPS–10.

Throughout this study the effects of rain and range attenuation on the radar response were neglected, although in some cases their magnitudes could have been considerable. The lack of power measurements and records of the settings of the radar controls precluded the determination of accurate corrections. However, for certain purposes, measurements of thunderstorms beyond 40 mi. were excluded from the data, since they are considered as probably too much affected by attenuation to be trustworthy.

Levels of first formation of radar cloud.—In chapter I it is pointed out that a thunderstorm usually consists of several cells, each of which goes through a certain life cycle of development and dissipation. It is emphasized that the cells often do not become clearly delineated until precipitation begins and that the falling rain influences the history of the cell. In view of these facts, information dealing with the

[47] The terms radar cloud, radar thunderstorm, thunderstorm echo, and cloud echo are to be interpreted as the radar echo from the cloud or thunderstorm, and in most cases may be considered synonymous.

[48] See page 271 for technical details of this radar set which was used during 1947 in Ohio.

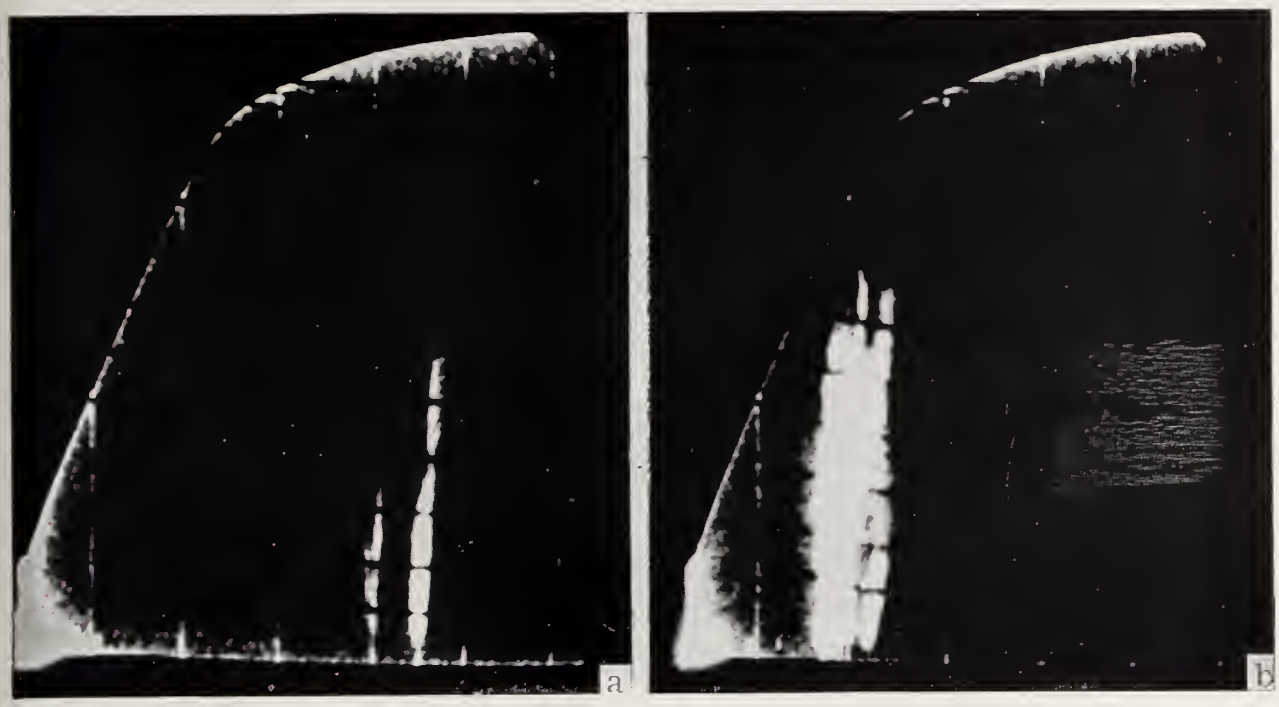

FIGURE 77.—Photographs of the RHI 'scope of the AN/TPS-10 radar set. Vertical lines indicate slant range from the radar site and the curved, roughly horizontal lines indicate height (5,000-foot intervals) above ground; (a) is an example of the type called "single-turret" echoes, while (b) represents a "multi-turret" echo.

process of drop coalescence becomes important for an understanding of cell behavior.

Since the fraction of the transmitted energy which is returned to the radar receiver from a cloud is a function of the drop diameter, it seems reasonable to conclude that when a cloud, which has been in existence for a period of time of the order of 10 min. without giving a detectable radar return, suddenly produces an echo, there has been rapid droplet growth and an increase of the water concentration. In accordance with the Bergeron theory for the formation of precipitation, it would be expected that rapid coalescence does not occur until the cumuliform cloud penetrates the freezing level, and, as a consequence, that the first radar echo from a cloud should appear just above this level.

The radar data of the Project were examined to determine whether or not this theory was substantiated. From the photographic records of the RHI 'scope it was possible to obtain data on the altitude of first formation of 66 radar echoes from convective clouds. Figure 78 presents the frequency distribution of the differences between altitudes of the tops of initial echoes and the concurrent heights of the freezing levels. To obtain a measurement of the latter during stable atmospheric conditions, the 0300 G. C. T. sounding from Huntington, W. Va., or Nashville, Tenn., was used. This was done because other Project measurements showed that a sounding made during thunderstorm conditions is often unrepresentative of the atmosphere at the time of first cloud formation[49].

[49] On August 14, 1947, for example, 15 radiosonde instruments were released in three groups at intervals of 1 hr. The range of measurements of the freezing level over the 2-hour period was more than 3,000 ft. To check the permissibility of using the 0300 G. C. T. soundings, a comparison was made of the height of the zero-degree isotherm as measured by Huntington or Nashville, and the mean of all the height measurements made by the network radiosonde stations on the same day. Of the seven cases examined, it was found that the two values had a mean difference of 520 ft., and a maximum difference of 1,490 ft., with the network stations having the higher values in every case. These results were a partial justification for the use of the Huntington or Nashville sounding; they further indicate that the values of freezing-level height thus obtained may have been slightly low.

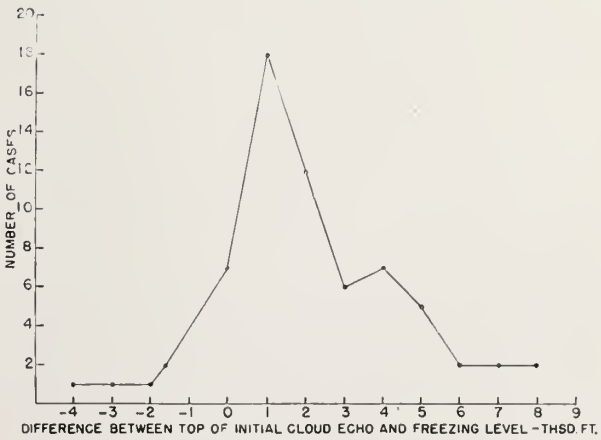

FIGURE 78.—A frequency distribution of the differences between the tops of initial radar echoes and heights of the freezing level at the time of measurements. The radar echo tops were measured on the RHI 'scope of the AN/TPS-10 radar set and the heights of the freezing levels were obtained from radiosonde ascents.

It can be seen that the distribution of figure 78 has a pronounced mode at +1,000 ft. The mean of this distribution is +2,200 ft. These indicate that the top of the initial radar echo usually appeared slightly above the freezing level. Several factors which influence these data and dictate this qualitative conclusion are the following:

1. There is some uncertainty about the technique used for obtaining the height of the freezing level.

2. Since the radar cross sections are from 3° to 4° apart in azimuth, it is possible that one showing a new echo was not through the highest part of the cloud, and, consequently, measurements of the top of the first echo used are too low. Many of the low observations of first echo tops are probably explainable in this way.

3. The time between successive vertical scans on the same cloud was from 1 to 3 min. In this time the cloud could have grown a substantial amount, with the result that the level of first detection was several thousand feet above the freezing level. This probably explains many of the values on the high end of the distribution.

In 10 cases studied by the New Mexico School of Mines group [**43**], tops of initial echoes were located on the average of about 5,000 ft. above the freezing level. The discrepancies in the results of the two studies are apparently the result of differences in detection capabilities of the radar sets utilized for the observations. It is also possible that there are geographical differences.

2. Vertical Growth and Extent of Thunderstorms

The thunderstorm model proposed in chapter I shows that each thunderstorm cell goes through three stages: the cumulus stage, during which the vertical motion is entirely upward; the mature stage, during which part of the updraft changes to downdraft; and the dissipating stage, during which almost all of the motion is downward. Special features of the thunderstorm, which were treated lightly in chapter I because of the paucity of good visual observations and the limitations of draft measurements, were the behavior of the top of the convective cloud cell, its duration, and description of the horizontal variations of the updrafts. Radar, however, made it possible to investigate these points in greater detail.

Before discussing the results of the analysis, it is well to consider the significance of the ascent of the radar cloud top. There may be a vertical growth of the convective echo by either of the following processes:

1. The upward transport of the detectable hydrometeors by an updraft.
2. The increase and growth of the hydrometeors at progressively higher levels to the number and size that make detection by the radar set possible.

Lack of reliable visual observations of the tops of the clouds used in this analysis precluded disassociation of the two processes or even calculation of orders of magnitude. Observations of radar and visual cloud tops by Reynolds and Workman [**43**] showed that as the thundercloud developed, the difference in elevation between the two tops became smaller. In three of their cases for which necessary data were available, the average rate of growth of the radar cloud top relative to the visual cloud top—from the level of first detection to the maximum height—was about 2.5 ft/sec in two cases, and 5.5 ft/sec in the other. These facts would indicate that the second process listed above is significant and that the ascent rate of the radar cloud top may be somewhat higher than that of the visual cloud, at least in the middle and lower altitudes where there is sufficient water present to permit the rapid growth of the energy-scattering particles. At the very high levels, where most of the hydrometeors are in frozen form, the ascent of the top of the radar cloud resulting from the transport by the updraft of scattering media from the lower levels probably greatly exceeds the other factor.

Evidence which supports this belief, namely, that the rates of growth of the radar cloud are related to the vertical motion within the cloud, is supplied by Thunderstorm Project data. Airplane measurements of updrafts were made at the 20,000- and 25,000-foot levels in one or more storms on several of the days for which data on the vertical velocities of the radar cloud tops were available between these two altitudes. Although the measured updraft values are not strictly comparable to the vertical rates of growth, since the latter apply only to the top of the radar cloud, whereas the measured updraft values are not necessarily those which existed at the cloud top, some kind of relationship is still to be expected. In table 31 the maximum and mean values of the measured updrafts on particular days are compared to the mean and maximum values of the vertical rates of radar cloud growth between the 20,000- and 25,000-foot levels on the same days. For each echo, the growth rate was

determined by dividing the observed change of altitude by the time between successive observations. It can be seen that with the exception of September 10, there was good agreement. In order to make the mean values of the cloud-top ascent rate more comparable to those of the measured updrafts, only those values greater than 10 ft/sec were included in the calculations, since many updrafts below this magnitude were not evaluated.

TABLE 31.—*Comparison of mean and maximum ascent rates of the radar cloud tops between 20,000 and 25,000 ft. with the updrafts measured within the thunderstorm at the 20,000- and 25,000-foot levels by airplanes equipped by the N. A. C. A.*

Date	Max. rate of growth (ft/sec)	Max. updraft (ft/sec)	Mean rate of growth (ft/sec)	Mean updraft (ft/sec)	Mean rate of growth +3 ft/sec	Difference (ft/sec)
Aug. 13	31.5	[1]10.3	23.4	27.1	26.4	−0.7
Aug. 15	26.7	26.7	17.2	21.3	20.2	−1.1
Aug. 17	27.8	33.8	19.2	22.0	22.2	+0.2
Aug. 20	45.1	44.7	21.8	27.7	24.8	−2.9
Aug. 21	58.4	53.8	22.7	28.9	25.7	−3.2
Sept. 10	26.2	61.6	15.5	32.0	18.5	−13.5

[1] Includes only one traverse at 20,000 ft. and none at 25,000 ft.

In most cases the updraft velocities exceeded the vertical velocities of the radar cloud top. This may be surprising when the maximum values are considered, since the sample of radar cloud-top velocities was much larger than that of the draft velocities. However, there have been no corrections applied for the terminal velocities of the water and ice particles relative to the air. When a correction is made, the agreement is improved; in the last two columns of table 31, mean values of the radar cloud growth rate with 3 ft/sec added are given, as well as the difference of these data from the updraft data. This is a conservative correction in view of the fact that it implies that only small water droplets and possibly heavy snow particles are present at these levels.

From these results, it appears feasible to use the data on the vertical velocities of the radar cloud top as an indication of the orders of magnitude of the vertical updraft velocities at the higher altitudes. It must be realized, however, that strictly speaking the growth measurements apply only to conditions at the top of the radar cloud as it passes through any particular level, and that the discrepancies between the vertical rate of growth of the radar echo and the vertical velocity of the air at the top of the cloud decrease with altitude as the water droplets are converted to snow particles.

Growth of thunderstorms.—In studying the growth of the radar thunderstorms, graphs were drawn with the maximum height of the cloud echo at any time plotted against time. It was noted that in most cases

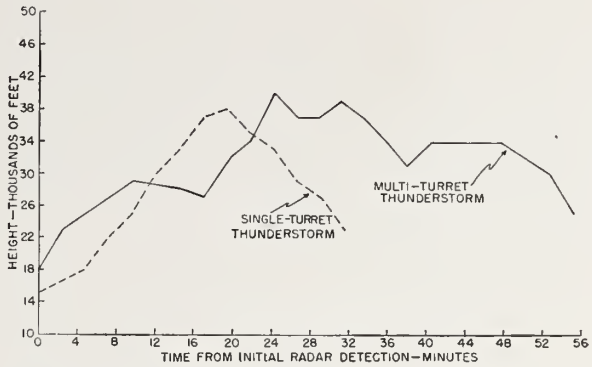

FIGURE 79.—A growth graph in which the height of the top of the storm radar echo is plotted against time reckoned from the detection of the initial echo. Two separate echoes are considered here. The multi-turretted echo showed several height maxima while the single-turretted echo showed a relatively smooth rate of growth and dissipation. This graph is based upon measurements made of Ohio thunderstorms with the AN/TPS-10 radar set.

the thunderstorm top ascended in a series of "steps." Between the "steps" was a short period during which the top of the echo remained essentially at the same altitude or subsided as much as several thousand feet. Figure 79 presents an example of a growth graph which illustrates this type of behavior.

Since most of the echoes studied by the Project were those of thunderstorms consisting of several cells, the "steps" were usually interpreted as manifestations of the growth of additional cells in close proximity to an already existing one. In some cases observations indicated that within the updraft region of a single thunderstorm cell there is more than one locality of maximum updraft magnitude; that these regions are displaced from one another in time or space, or both; and that they result in the development of individual cloud columns. This suggests, of course, that the common picture of the horizontally-symmetrical updraft with its maximum speeed at the center is not always correct. These regions within an updraft may be considered as subdivisions, or "sub-cells," within the cell; probably, relative to the rest of the draft, they have much the same characteristics that an individual updraft has to its environment.

One theory for such a process of growth proposes that the single updraft within a cell is pulsating. Although there were some cases in the Project studies which might be explained by assuming the existence of a single, symmetrical, pulsating updraft, in most of them each of the maxima of radar cloud height occurred at different positions relative to the center of the cloud. In this regard, it is also significant to note that several simple, single-celled radar thunderstorms whose complete history could be followed did not exhibit large variations in the ascent and descent rates.

A second explanation is proposed by Schmidt [49] for the development of a new cloud tower in close

proximity to an already existing one. In a theoretical treatment of the growth of a cumulus cloud he takes into account form and friction drag and shows that as a result of friction drag and horizontal diffusion of vertical momentum there is ascending air outside of the actual cloud; he proposes that if this air has realized its conditional instability, another cloud tower may develop.

Whether the rising air is of a new cell or sub-cell when it has risen above the top of the already existing cloud, there may be an extension of the cloud to higher levels. Each of the resulting vertical protuberances of the tops of the radar storm is given the name "turret" in the discussion which follows. Without other types of data, most of which are unavailable because of present-day deficiencies in instrumentation, it is impossible to determine the exact nature of the vertical stream of air which produces most turrets.

Project observations indicated that thunderclouds which grew to the highest levels usually exhibited several turrets during their history. Figure 80 presents a scatter diagram of the maximum height attained by a thunderstorm plotted against the number of maxima in rate of growth observed during its existence. Only those radar clouds which were initially detected at a level near the freezing level and which reached a single maximum altitude over 30,000 ft. were considered. Those maxima which occurred after the one which resulted in the cloud's reaching its greatest altitude were also included in counting the total number. For the 32 cases of simple, multi-turreted thunderstorms studied, the correlation coefficient was .67 ± .10, which shows that a relationship exists between the number of turrets in the cloud and the maximum height of its top.

Other features characteristic of the successive turrets are shown in table 32, which summarizes the results of the analysis:

1. Although in all cases every turret did not grow to higher levels than the preceding one, when mean values of the differences in absolute maximum altitude of consecutive turrets were calculated, it was found that the second was about 5,000 ft. higher than the first. Also, the third was higher than the second but by a significantly smaller amount. The single case of a fourth step does not permit any generalization.
2. The mean time between successive turrets was 17.8 min.

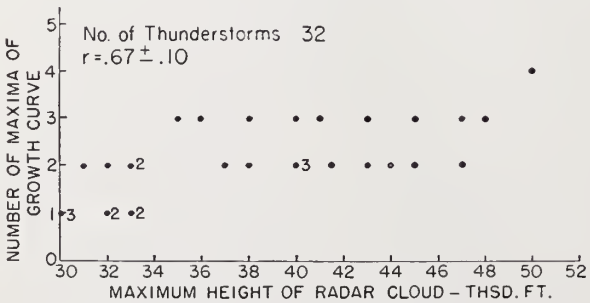

FIGURE 80.—A scatter diagram showing the relationship between the number of maxima of the growth curve for a particular echo and the maximum height attained by that echo. The figures beside several of the points indicate the number of coincident observations represented by the particular point. The data were obtained from observations of Ohio thunderstorms with the AN/TPS-10 radar set.

TABLE 32.—*Summary of characteristics of successive turrets of 32 multi-turreted thunderstorms studied. Data based on observations of Ohio thunderstorms with the AN/TPS-10 radar set*

Sequence number of turret	Number of cases	Mean height above preceding maximum (ft.)	Mean time since preceding maximum (min.)
1	32	[1]15,900	[1]17.5
2	24	5,200	17.4
3	10	400	18.9
4	1	7,000	17.1

[1] Height and time of maximum of growth curve measured from level and time of initial detection of radar cloud.

Use of the concept of entraining of environmental air into the updraft of a thunderstorm (discussed in ch. I), with the assumption that each turret may be ascribed either to a new cell or sub-cell, makes possible an explanation for this extension of the second turret to higher levels than the first. The convergence into the updraft of the first column of relatively dry air and the subsequent reduction of the virtual temperature difference between environmental air and updraft air as water drops are evaporated into the mixture results in a decrease of the upward accelerating force. However, when there is a cloud in close proximity to the updraft, the air being entrained is more moist than air from a cloud-free environment. As a consequence, the amount of evaporation required to preserve saturation is less, resulting in the removal of a smaller amount of heat and thereby causing less deceleration. Thus, the second turret of the thunderstorm, which entrains the pre-moistened air, has a higher vertical velocity and may grow to higher levels than the first, which was produced by a convective current entraining drier air. If it is further accepted that a greater fraction of the air which converges into subsequent turrets is closer to saturation, it follows readily that they may then reach higher altitudes than either of the first two. In this reasoning, it is assumed, of course, that all factors other than entraining which affect the strength of the updraft are constant.

Growth of the convective cloud turret.—In the preceding paragraphs it was shown that the radar thunderstorm top progresses upward in steps as new cloud turrets outgrow those which have reached their

maximum heights. A discussion will now be given of the growth of the individual cloud turret as recorded by the radar set. Only the first of the turrets of a complex thunderstorm are discussed, since the others were usually not evident until their tops ascended above previously existing ones. The main criteria for the selection of cases for study were, first, that radar observations extended over the period from the time when the cloud first became detectable as a result of droplet growth to the time when vertical cloud growth ceased; and second, that the growth graph appeared to give a reasonably reliable picture of the vertical growth of the cloud. From the available data it was possible to select 35 echoes which satisfied these requirements.

A review of the vertical distribution of ascensional rates revealed that maximum values in all cases did not occur during the same relative part of the "growth period" (period during which the top of the radar cloud was ascending). In order to study this feature, the growth period was divided into four equal parts. The radar cloud turrets were then classified by type according to the quarter of the period during which the maximum cloud-top vertical velocity was measured (table 33). In seven cases the same maximum vertical rate of growth occurred in two quarters, and they were not included in the tabulation. It is to be noted that there was not a preponderance of cases of any one type.

TABLE 33.—*Frequency distribution of types of turret echoes, classified according to the quarter of the period of vertical growth in which maximum ascensional rate occurred*

Type	Quarter of the period	Number of cases
I	First	9
II	Second	6
III	Third	8
IV	Fourth	5

For each type a composite growth curve was drawn. The mean length of time of the quarters and the mean rate of vertical growth during each quarter were determined, and they were used to plot a graph of height against time. To show the rate of descent immediately following the time of maximum vertical extent, the rate of change of altitude of the top was calculated for an arbitrarily selected fifth time interval, equal in duration to the previous quarters. The curves for each type of turret are presented in figure 81. The fifth curve in the figure is a composite drawn for the clouds in all type classifications plus the seven additional ones which had equal maximum rates of growth in two quarters.

It can be seen from the curves that the mean length of the growth period was about 16 min. The mean

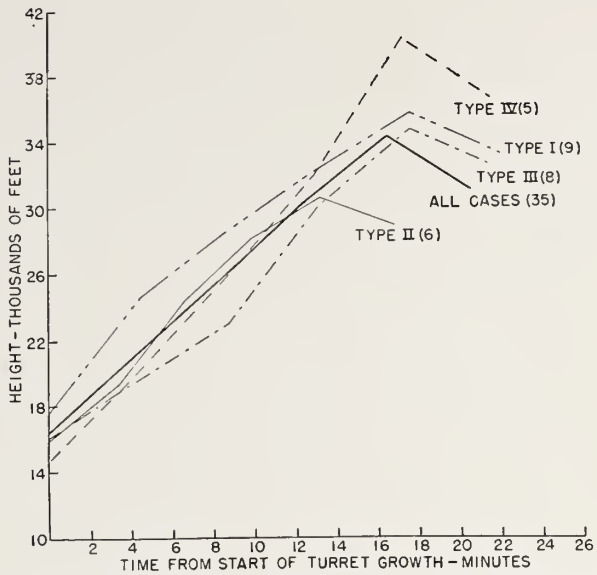

FIGURE 81.—Growth curves for groups of single turrets. The mean height for all turrets of each type has been plotted against time. Time is reckoned from the start of the turret growth. The group classification and the number of cases studied are indicated for each curve.

time from the start of growth to the end of the subsidence interval was about 20 min. This period closely approximates the "cell" duration of about 20 min. reported by others [**43**]. The shortness of the mean duration of the growth period of Type II cases probably results from a poor sample of cases.

Other features of figure 81 which are worthy of note are the following:

1. Although there is considerable variation from one quarter to another for the different types, the slope of the height against time curve which was obtained by using all the radar cases is almost constant (about 18 ft/sec).
2. The radar cloud top usually did not remain at the maximum height it attained but rather started subsiding at a mean rate of about 12 ft/sec. In view of the fact that at these high levels most of the hydrometeors were probably in the frozen form, having a low terminal velocity, the descent of the echo top may be ascribed to a downdraft which carried the hydrometeors downward. It is concluded that during the dissipating stage of the thunderstorm downdrafts may exist even at the very highest levels.

Although in most cases the descent of the radar cloud top was soon followed by another growth, eight single-turret, convective clouds were observed which, after reaching their maximum heights, subsided more or less regularly until the echoes completely dissipated. A height-time curve showing the growth of this type of radar cloud is presented in figure 79. It

TABLE 34.—*Frequency distribution, by types of storm, of the maximum vertical heights of thunderclouds detected by AN/TPS-10 radar*

[All heights expressed in thousands of feet above the surface]

Type of storm	Heights of radar clouds							Number of days	Number of storms	Mean heights
	25–29.9	30–34.9	35–39.9	40–44.9	45–49.9	50–54.9	55–59.9			
Air-mass	22	27	20	17	15	11	2	6	114	37
Squall-line	16	7	15	13	11	8	0	5	70	38
Frontal	3	3	2	0	7	0	0	2	15	38
Total	41	37	37	30	33	19	2	13	199	37

was found that for these eight cases the mean rate of growth from the level of first detection (average, about 16,000 ft.) to the maximum height (average, about 31,500 ft.) was 16.7 ft/sec, while the mean rate of descent was 16.5 ft/sec. The mean duration of these radar clouds was approximately 26.5 min.

Heights of thunderclouds.—In order to permit a significant statistical treatment of the maximum heights attained by thundercloud tops, a large number were observed by means of the radar set, and a frequency distribution was made for the absolute maximum heights reached (table 34). Each case could not be verified as a thunderstorm—as defined by the International Meteorological Organization (see footnote[3], p. 17)—because there were no observers in the vicinity. However, since the airplane crews reported that when a cloud was a thundercloud it usually extended to the highest flight level (26,000 ft.), it was arbitrarily decided for this study to consider only the convective-type echoes which grew to at least 25,000 ft. In the tabulation each case represents a thundercloud which may have consisted of many cells. If two or more echoes merged and continued to build to higher levels, they were regarded as one thundercloud.

The 199 thunderstorms included in the tabulation were classified by type, i.e., squall-line, frontal, and air-mass, according to the following definitions:

Squall-line thunderstorms—Those which were associated with prefrontal squall lines. This does not mean that all the storms were part of a particular line but rather that they occurred on days when the preponderance of thunderstorms in the area were associated with prefrontal squall lines.

Frontal thunderstorms—Those which developed over or along a frontal surface, presumably as a result of lifting of moist, unstable air over the frontal surface.

Air-mass thunderstorms—Those which developed in areas where there were apparently no frontal or prefrontal influences, although in some cases they may have developed into a line of thunderstorms. In the discussion to follow, this type will be called "air-mass thunderstorms" although it is realized that storms have been included in this category which may not have been purely air-mass (heat) thunderstorms according to the common classifications. Some classifications include all nonfrontal thunderstorms in the "air-mass" category, but here a distinction is made between prefrontal squall lines and the other types.

From the table, it can be seen that over 60 percent of the thunderstorms extended above 35,000 ft. The mean of the sample was between 37,000 and 38,000 ft., with the mean value of squall-line storms slightly higher than those of air-mass storms. The absolute maximum height was that of an air-mass thunderstorm whose top was measured at 56,000 ft. It is to be borne in mind that these data give the radar-measured tops and that the actual cloud probably extended somewhat higher in all cases.

Table 35 presents a frequency distribution of the maximum heights reached by radar thunderclouds on several days of air-mass storms. The data indicate variations in the distributions from one air-mass day to another, i.e., on some days a high proportion of the storms grew to very high levels, while on other days most of the storms were restricted to relatively lower levels[50]. As shown in chapter VI, strong vertical wind shear is a factor which has a tendency to limit the heights to which the thunderclouds develop.

[50] It was noted from a study of the noise level on the RHI 'scope that on August 16, and September 10, the gain setting was lower than usual. This was undoubtedly a factor in restricting the maximum extent of the radar echoes; however, it is felt that it does not entirely account for the difference in the distribution for those days.

TABLE 35.—*Frequency distribution of maximum heights reached by the thundercloud echoes from air-mass thunderstorms on particular days*

[All heights expressed in thousands of feet above the surface]

Date	Maximum heights							Number of storms	Mean height
	25–29.9	30–34.9	35–39.9	40–44.9	45–49.9	50–54.9	55–59.9		
Aug. 13	—	—	2	1	4	2	—	9	45
Aug. 16	8	4	3	2	—	—	—	17	31
Aug. 20	5	5	1	3	—	1	1	16	35
Aug. 21	14	18	9	8	10	6	1	66	37
Sept. 10	3	3	7	3	1	—	—	17	35

3. Horizontal Extent of Thunderstorms

Another feature essential to a complete description of the thunderstorm is its actual configuration as an object in space. The deficiency of information of this nature in the past has resulted from the difficulty of making measurements of clouds which often extend over 40,000 ft. With the radar set AN/TPS–10, however, it was possible to collect data on radar clouds which can be utilized to obtain a general qualitative idea of not only the vertical extent of the cloud but the variation with height of the horizontal cross-sectional area of the cloud.

In the preceding section it was stated that the top of the radar thundercloud on the 'scope of the AN/TPS–10 bears a reasonably close relationship to the top of the visual cloud during the development of the thunderstorm because of the transport of echo-producing hydrometeors to the higher levels by the updrafts. When comparing the *sides* of the visual and radar cloud, a similar agreement is not necessarily to be expected. In order to calculate the differences, knowledge is required of the horizontal distribution of water content within the thundercloud and the capabilities of the radar equipment being used for the observations.

A limited amount of information is available which may be used to obtain an order of magnitude of the differences in diameter of the visual and radar clouds. The length of time Project airplanes were within visible clouds while making essentially straight-line traverses was compared with the length of time that the airplane was within the PPI echo as shown on the long-range control radar set. In the mean, the time within the visual cloud was greater at all altitudes. The best agreement was found at the 10,000-foot level, where the mean visual cloud diameter was about 19 percent greater than the mean radar echo diameter. As is pointed out later, the 10,000-foot level is the one at which the radar echo has its greatest horizontal extent. It should be noted, however, that the characteristics of the control radar set used are such that a comparison of this type is not strictly valid[51].

The fraction of the actual cloud which was detected by the radar equipment was not constant with altitude due to the variations of the reflectivity of the hydrometeors in different types and different parts of clouds. Visual observations of thunderstorms generally indicate that there is a maximum of horizontal cloud extent at the lower levels in the developing stages. Around the base of the thunderstorm are usually found "outriders"—smaller cumulus, stratocumulus, and stratus clouds. Often the quantity of free water in these is insufficient to produce a detectable echo. In the later stages of the thunderstorm, when the anvil forms, the cirrus-type clouds which form the anvil have small free-water concentrations within them and are usually not detected by the AN/TPS-10 radar set. The relatively low reflectivity of ice particles in the anvil top also tends to prevent detection. On some occasions, however, when the equipment was operating under the most favorable conditions, the anvil cloud showed up as a very weak echo. Figure 82 presents an exceptional vertical cross section through a radar cloud, showing both an anvil top and a stratified deck of clouds at lower altitude.

Horizontal cross-sectional area of thunderstorms.—The data obtained by the AN/TPS–10 equipment were used to draw horizontal cross sections for every 5,000-foot interval through convective radar clouds for times about 10 min. apart during 6 days in August for which suitable data were available. In the analysis, an attempt was made to obtain data from thunderstorms which were single-celled or at least consisted of a small number of cells, since large agglomerations of convective clouds prohibit the determinations of horizontal cross-sectional areas which can be meaningfully compared to one another. In some instances, one of the cells of a two-celled thunderstorm extended substantially higher than the other, but the storm was considered as one case. This practice tended to make the mean cloud cross section largest in horizontal extent at the lower levels. Fortunately, the number of such cases was relatively small.

As a first step in the analysis, the clouds were classified into groups, depending on the altitude of the tops of their echoes at the time of observation. Each group included all the radar clouds which fell

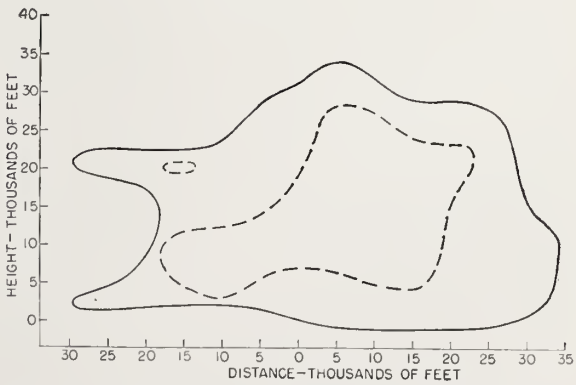

FIGURE 82.—A vertical cross section through a radar thunderstorm. Note the shelf and the anvil. This profile was obtained from successive RHI observations made at 3-degree intervals of azimuth. The dashed lines enclose areas of the radar cloud where its width, perpendicular to this cross section, was more than three miles. This thunderstorm occurred near Wilmington, Ohio, on August 20, 1947.

[51] The very wide vertical-beam width of this set results in a PPI echo which more closely approximates a projection of the entire radar cloud on a conical surface rather than a horizontal slice through it.

within a 5,000-foot class interval having altitudes divisible by 5,000 ft. as the upper and lower limits; for example, an echo which extended to 37,000 ft. was in the 35,000- to 40,000-foot interval. Mean values of the horizontal cross-sectional areas at particular altitudes were then calculated and plotted against altitude. The resulting curves are presented in figure 83.

FIGURE 83.—A graph showing the horizontal cross-sectional areas, at given heights, of radar thunderstorms. Each curve represents the mean values for a group of storms, classified according to the maximum height attained by the echo. The figures at the base of each curve give the number of cases included in the group.

These graphs must not be interpreted in an exact numerical sense because of the nature of the data used to obtain them. The radar set did not have a constant cloud detection sensitivity from one day to the next, or even during one day's operation. In the absence of power measurements interpretation of echoes required some subjectivity. Also, the isolation of particular thunderstorm echoes on the RHI 'scope photographs was made more difficult, at times, by the effect of light diffusion from the very bright echoes. In some cases this factor became so pronounced that there appeared to be a shelf of weak stratified clouds extending out from the radar cloud. Sometimes a shelf of clouds actually did exist, but the character of the echo usually permitted proper identification. In most instances during the analysis the stratified clouds were not considered when calculating mean values of cross-sectional areas. These stratified layers of weak echo were often difficult to delineate; however, they were a characteristic of a particular thunderstorm or groups of thunderstorms rather than a common feature of every one.

Despite these difficulties, it is evident that the areas stand essentially in the proper relationships. It can be seen from figure 83 that the radar thunderstorm usually decreases in horizontal extent with altitude above 10,000 ft. The decrease of cross-sectional area from 10,000 to 5,000 ft. is of doubtful significance, since in some cases the radar-detected cloud base was probably above this lower altitude. Since the radar does not differentiate between cloud and precipitation, a continuous echo extends throughout the cloud and down to the surface when the rain is falling at a sufficiently high rate. Under these conditions the *base* of the cloud cannot be determined from the radar. Beneath the base of the cloud, the rain core would be expected to have a somewhat smaller diameter than just above it, since there is some evaporation into the clear air at the edges of the rain area.

A point to bear in mind when interpreting the maximum at 10,000 ft., is that when a mass of water in the frozen state melts, its reflectivity increases[52]. Since the height of the zero-degree isotherm during the days used in the study was about 15,500 ft., it appears that the increase of horizontal extent of the radar cloud at 10,000 ft. may have been partly a result of the increase of reflectivity of the falling hydrometeors. The trends of the curves are such that a continual increase of horizontal cloud extent is to be expected down to the lowest layers of the thunderstorms. As has already been mentioned, visual observations show this general type of thundercloud geometry before the marked cirrus blow-off occurs.

Another interesting indication of figure 83 is that the height to which the radar thundercloud extends is related to its horizontal extent—the higher the cloud, the greater its horizontal extent.

The second step in the analysis was the drawing of generalized vertical cross sections through the radar thunderstorms. To permit this, all horizontal slices were assumed to be circular and diameters for each 5,000-foot level were determined. Again data on all clouds in a particular altitude group were used to draw a mean vertical profile for thunderclouds of that extent. The height of the mean cloud for each group was obtained by averaging the altitudes of the tops of all the radar clouds in the group. The resulting vertical cross sections of the average thunderstorms are presented in figure 84.

One feature which is immediately evident is that the radar thunderclouds have comparable vertical and horizontal dimensions. Although individual cloud turrets protruding upward from the cloud may resemble a narrow cylinder, in the mean configuration of the entire radar thunderstorm, the resulting profile loses the appearance of a tall, narrow column.

It can also be seen from the profiles that the diameter of the radar thundercloud decreases relatively little with height up to levels about 10,000 ft. from the top. In terms of importance to pilots this means that even when an airplane is at an altitude as high as 35,000 ft., it may encounter thunderstorms having diameters greater than 6 mi.

[52] This phenomenon is described in some detail by Ryde [47].

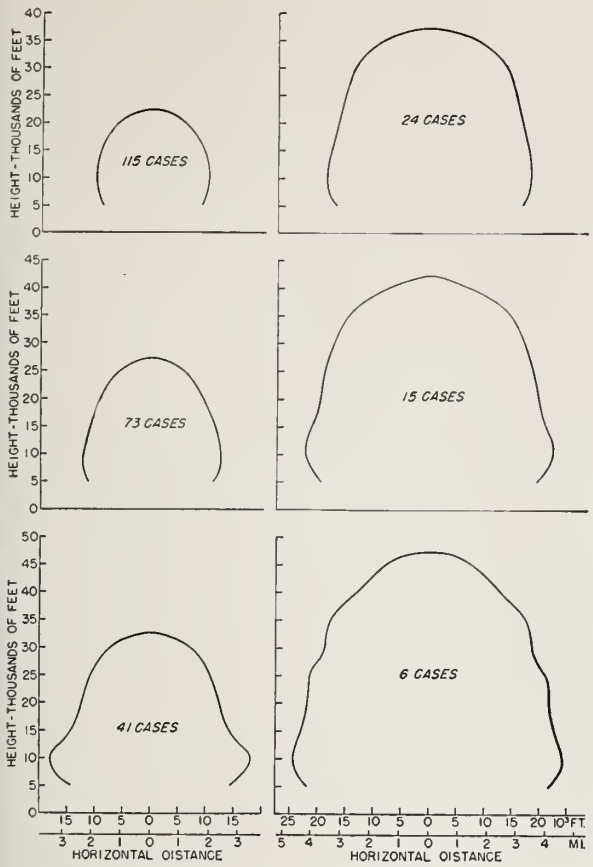

FIGURE 84.—Profiles of vertical cross sections through radar thunderstorms. Each section of this figure represents the mean profile for a group of storms having tops extending to the 5,000-foot interval indicated. The number of cases studied in each group is shown. These data are based on studies of echoes from Ohio thunderstorms detected by the AN/TPS-10 radar set.

In an effort to obtain representative measurements of the relative amount of convective cloud cover at various heights, the Project made a special study based upon the data from the RHI radar. In the extracting of radar cloud data from photographic records the only factor influencing selection of the thunderstorms for inclusion in the study was that reasonably reliable measurements of cross-sectional area be available at all the levels. Radar echoes which extended above 20,000 ft. and were not produced by stratified types of clouds or thunderstorms in an advanced stage of dissipation were included. It seems reasonable to assume that the size distribution of thunderstorms, as shown by the number of cases observed in each class interval of altitude (fig. 84), approximates the distribution under average thunderstorm conditions over any particular area in Ohio. Of course, in some situations at a particular time, the size distribution could be somewhat different. For example, in the vicinity of a squall line the number of thunderstorms extending to the highest levels might be a greater fraction of the total number of storms than under the assumed mean conditions.

Radar cloud coverage.—As air traffic at the higher altitudes increases, information dealing with the cloud coverage at these levels becomes of greater importance. These data on radar clouds, though inexact, permit calculation of orders of magnitude of radar cloud coverage at different levels. As has been shown, visual clouds have greater extents, but since the radar echo delineates that part of the cloud wherein the higher concentrations of water or ice within the cumulonimbus are located, the radar data supply important information. As is shown in chapter IX, heaviest turbulence is encountered in regions of heaviest rainfall. Also, a statistical verification of the coexistence of radar echoes and heaviest turbulence has been given by Press and Binckley [**42**], based on data obtained at altitudes below 30,000 ft.

For each of the radar clouds used in the study, the ratio of its horizontal cross-sectional area at each 5,000-foot level to that at 10,000 ft. was determined, and average values of the ratios for all thunderstorms which occurred in each height group were calculated (table 36). The 10,000-foot level was selected as the standard because the radar clouds usually had their maximum horizontal extent there. The table also shows a mean value for the ratio of coverage at any altitude level to that at 10,000 ft., obtained by weighting the individual average ratios of any height group according to the number of thunderstorms which were observed in that group. An interesting point to be noted is that there is little change in the latter ratios between levels of 20,000 and 30,000 ft. Above and below these altitudes there is a general decrease with increasing altitude. (The ratio at the 5,000-foot level is smaller than at 10,000 ft. for reasons presented in a previous paragraph.

TABLE 36.—*Ratios of horizontal cross-sectional area covered by radar clouds at any level to that covered at* 10,000 *ft. (based upon analysis of Ohio thunderstorms detected by the AN/TPS-10 radar set)*

[All height values expressed in thousands of feet above the surface]

Altitude	Height limits of thunderstorm groups							Mean ratio
	20–24.9	25–29.9	30–34.9	35–39.9	40–44.9	45–49.9	50–54.9	
5	.78	.82	.85	.86	.75	.80	1.12	.76
10	*1.00*	*1.00*	*1.00*	*1.00*	*1.00*	*1.00*	*1.00*	*1.00*
15	.86	.83	.87	.96	.91	.89	1.30	.87
20	.37	.56	.66	.82	.78	.81	.91	.54
25	—	.22	.51	.73	.73	.77	.77	.44
30	—	—	.23	.58	.59	.59	.94	.18
35	—	—	—	.19	.15	.54	.84	.27
40	—	—	—	—	.11	.29	.41	.17
45	—	—	—	—	—	.10	.15	.10
50	—	—	—	—	—	—	.02	.05
Number of cases	115	73	41	24	15	6	1	

By making use of the mean ratios given in table 36, the percentage of a particular area covered by thunderstorm echoes at any level can be determined, given the percentage coverage at 10,000 ft. over the same area. Table 37 gives calculated coverages of radar clouds at each 5,000-foot level for assumed percentage coverages at 10,000 ft.

TABLE 37.—*Vertical distribution of the percentage coverage by radar clouds, with assumed coverages for 10,000 ft.*

Altitude	Percentage coverage									
5,000	8	15	23	30	38	46	53	61	68	76
10,000	*10*	*20*	*30*	*40*	*50*	*60*	*70*	*80*	*90*	*100*
15,000	9	17	26	35	44	52	61	70	78	87
20,000	5	11	16	22	27	32	38	43	47	54
25,000	4	9	13	18	22	26	31	35	40	44
30,000	5	10	14	19	24	29	34	38	43	48
35,000	3	5	8	11	14	16	19	22	24	27
40,000	2	3	5	7	8	10	12	14	15	17
45,000	1	2	3	4	5	6	7	8	9	10
50,000	0	1	2	2	2	3	4	4	4	5

A study by one of the Project analysts has indicated that if the area between the ranges of 20 and 50 mi. (over 55,000 sq mi.) was considered, the area on the PPI 'scope covered by echoes averaged about 10 percent and had a maximum of about 40 percent[53]. The vertical distribution of the percentage coverage of radar clouds, assuming that these mean and maximum values of coverage apply to the 10,000-foot level, are reproduced in table 38. Also shown are values of visual cloud coverages for corresponding levels, calculated by using the findings from airplane flights that the difference of the average diameters of the visual and radar clouds at 10,000 ft. was 19 percent. The 19-percent difference was used under the assumptions that (a) this value is valid for radar data of the AN/TPS–10 equipment; (b) that the clouds had circular cross sections; and (c) that this percentage difference is constant with height.

These data on visual cloud coverage are subject to serious question because the assumptions made are not strictly valid. The use of the same factor of conversion of radar to visual cloud coverage at all levels introduces the greatest errors. However, the lack of suitable measurements of visual and radar clouds at the higher levels prevents computation of more correct values. In this regard, it is also to be recalled that thunderstorms showing signs of stratification were usually neglected. These are the cases for which the difference between visual and radar cloud would be greatest. It is felt that the results presented in table 38 may be used in a qualitative sense to obtain a general idea of the coverage during thunderstorm conditions when most of the thunderclouds are in the earlier stages.

The "maximum" coverage of 40 percent of about 55,000 sq. mi. for radar clouds is not to be taken as the absolute maximum to be expected. The cases used to obtain it did not include cases of widespread thunderstorm activity under severe squall-line conditions. It is probable that in this type of situation the percentage coverage of radar clouds may be higher than 80 percent at 10,000 ft. and may be correspondingly large at the higher levels.

[53] The values came from a total of 35 observations made on 4 days.

TABLE 38.—*Vertical distribution of percentage coverage of radar and visual clouds under average and maximum conditions of radar cloud coverage*

Conditions of cloudiness	Altitude (thousands of feet)									
	5	10	15	20	25	30	35	40	45	50
Average:										
Echoes	8	10	9	5	4	5	3	2	1	0
Clouds	11	14	12	8	6	7	4	2	1	1
Maximum:										
Echoes	30	40	35	22	18	19	11	7	4	2
Clouds	43	57	49	31	25	27	15	10	6	3

CHAPTER VI. EFFECT OF ENVIRONMENT WIND FIELD ON EXISTING THUNDERSTORMS

1. Causes and Effects of Vertical Shear of Thunderstorms

The cumulonimbus cloud is made up of relatively small particles having little mass, except when hail is present, and subject to displacements by the wind stream within which they are imbedded. When the horizontal flow of air within the cloud increases with height, the cloud tilts in the direction of the wind-shear vector, except when the cloud is growing irregularly. This effect has long been recognized by meteorologists as one of the factors which, when strongly pronounced, inhibits the development of cumulus clouds into thunderstorms. Even when the magnitude of the wind shear is not sufficient to prevent the formation of a thundercloud, it has considerable influence on the shape and on the life history of the cloud.

In order to determine the vertical shear of any cloud, it is necessary to know the vertical distribution of the wind *within* the cloud, which is not always the same as that in the environment. The main reason for the discrepancy is that there is a vertical transport of horizontal momentum between the upper and lower levels in the cloud.

The shearing of many types of clouds, particularly the cumuliform ones, frequently has heen observed visually, but measurements of magnitude have heen difficult to obtain, and it appears that no precise data on the subject have been published. By the use of radar, however, it was possible to collect data which permit the necessary calculations.

Radar cloud data used in this study were obtained from photographic records of the range-height-indicator (RHI) 'scope of the radar set AN/TPS–10[54]. As with other studies using this type of data, effects of rain and range attenuation were considered only in a qualitative fashion. This usually consisted of selecting thunderstorms which were not at extreme ranges, and those in which there were no intervening echoes or the character of the intervening echoes indicated small rain attenuation. Although in some cases attenuation may have been of a significant magnitude, the unavailability of power measurements and records of settings of the radar controls precluded the determination of accurate correction for it.

Qualitative demonstration of radar cloud shear.—When the wind shear has a strong component along the azimuth direction of an RHI cross section through a thunderstorm, the effects of the shear become evident from a single vertical sweep of the radar. Figures 85 (a) and (b) are typical examples of such observations. These vertical cross sections were along azimuths of 219° and 353°, respectively, and were obtained within 9 min. of each other. No concurrent upper-wind data were available in the immediate vicinities of the thunderstorms; however, the winds from Huntington, W. Va.[55], which was in the same, broad current, indicated that between the levels of 10,000 ft. and 25,000 ft. the vertical wind shear was toward 170° at 15 mi/hr.

Although the Huntington release was made 6 to 7 hours after the radar observations, synoptic upper-air charts indicated that the situation was such as to permit the use of this wind for a qualitative comparison. When the component of the shear along the respective azimuths was calculated, it was seen that the bending of the radar thunderstorm was in the proper direction.

The progressive displacement of the upper part of a thundercloud relative to the lower is illustrated by the series of radar cross sections presented in figure 86. The observations were along an azimuth of about 180° through a thunderstorm which occurred on August 17, 1947. The vertical wind shear between 15,000 ft. and 40,000 ft., at approximately the same time, had a component of 21 mi/hr toward 180° and was strongest between 30,000 ft. and 35,000 ft. Another interesting feature to be noted is that as the

[54] With the 'scope calibration used during Ohio operations, it was usually possible to detect vertical shear of clouds as slight as 0.5 mi. in 40,000 ft. of altitude.

[55] Approximately 110 mi. southeast of the radar site.

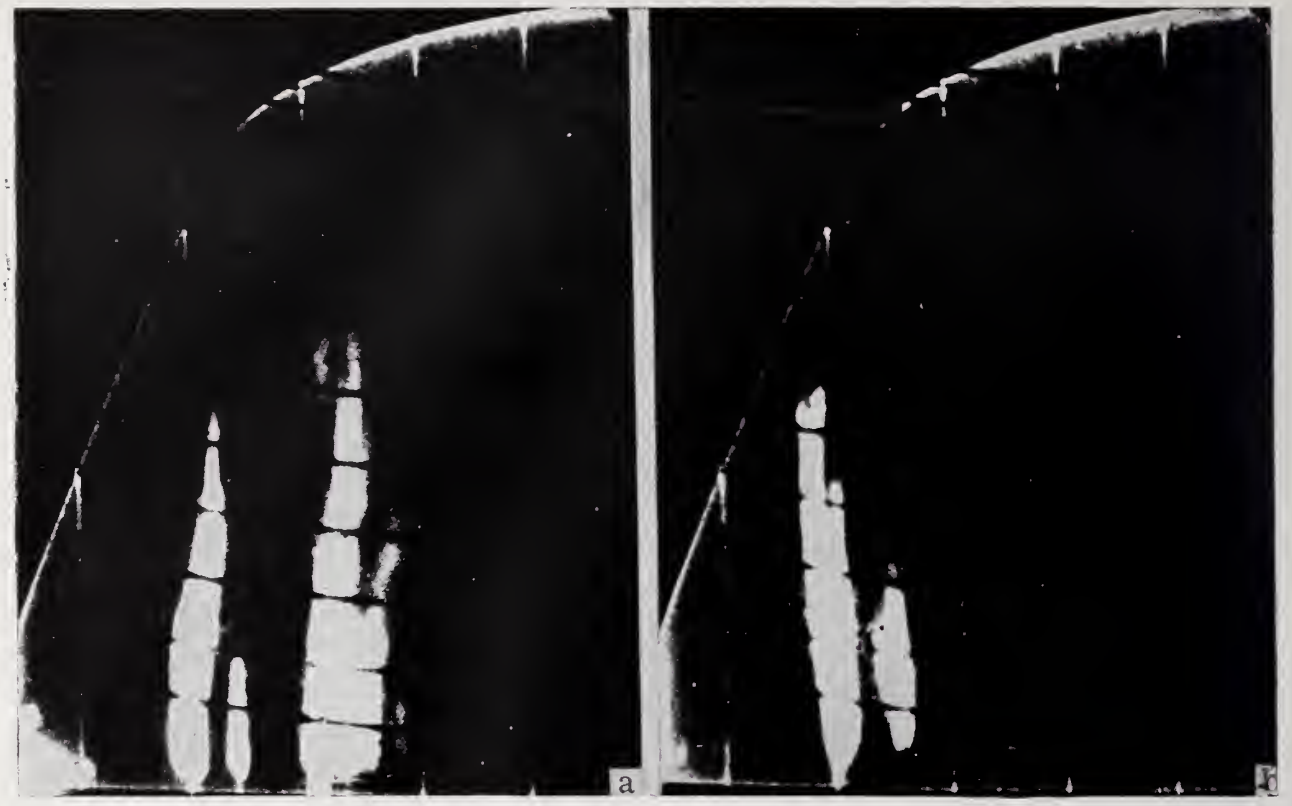

FIGURE 85.—Photographs of radar thunderstorms as depicted by the RHI echoes. (a) shows radar thunderstorms along an azimuth of 219°; (b) shows radar thunderstorms along an azimuth of 353°. These photographs were taken within nine minutes of each other on September 10, 1947. In each photograph, the radar site is at the left. Note that the echoes to the southwest (a) tilted away from the radar site and the echoes to the northwest (b) tilted toward the radar site.

top of the radar cloud was carried downstream by the strong upper wind, another radar cloud turret grew vertically from the lower section of the original cloud. The part of the radar echo which was carried downstream can be seen to dissipate rapidly.

The effects of wind shear can also be seen on the PPI 'scope of the 10-centimeter control-radar set. This equipment has a wide vertical beam which, at a range of about 25 mi., extends higher than most thunderstorms. Figure 87 is a sample of photographs of its 'scope taken on August 14, 1947, a day on which there was relatively strong wind shear toward the southwest between the levels of 10,000 ft. and 35,000 ft., the latter being still below the maximum heights to which some fully developed thunderstorms extended. The upper part of the storm subjected to this displacement force was carried toward the southwest. Since the displaced portion of the cloud intercepted only a fraction of the radar beam, and since the larger hydrometeors were falling out of this part of the cloud and probably evaporating, it would be expected that the southwestern edge of the echo would be less intense than the rest of the echo. The photographs, in fact, indicate this distribution of intensity. The crew of an airplane which flew through one of these storms observed a shelf on the southwestern side of the cloud. On one traverse, the airplane flying at 15,000 ft. reported light snow falling from this deck of clouds extending out from the storm. The not infrequent reports of rain, snow, and hail outside a thundercloud can probably be explained by consideration of similar wind-shear action.

Measurements of vertical cloud shear.—In order to find the relationship between wind shear of the environment and shear of the radar cloud, the vector difference between wind velocities at two selected altitudes was compared with the rate of horizontal displacement of the radar cloud at the upper altitude relative to the lower. The technique used for calculating such rates of displacement was the following (see fig. 88):

1. A radar cloud was chosen which extended to a height of about 30,000 to 35,000 ft., had well-defined outlines, and, if possible, was of strong intensity.

2. At time t_1 the horizontal distances R_{h1} and R_{h2} from the radar site to the axis of the selected cross section at altitudes h_1 and h_2, respectively, were measured, and the difference, R_a, between R_{h2} and R_{h1} was determined.

3. At time t_2 the horizontal distance to the axis of

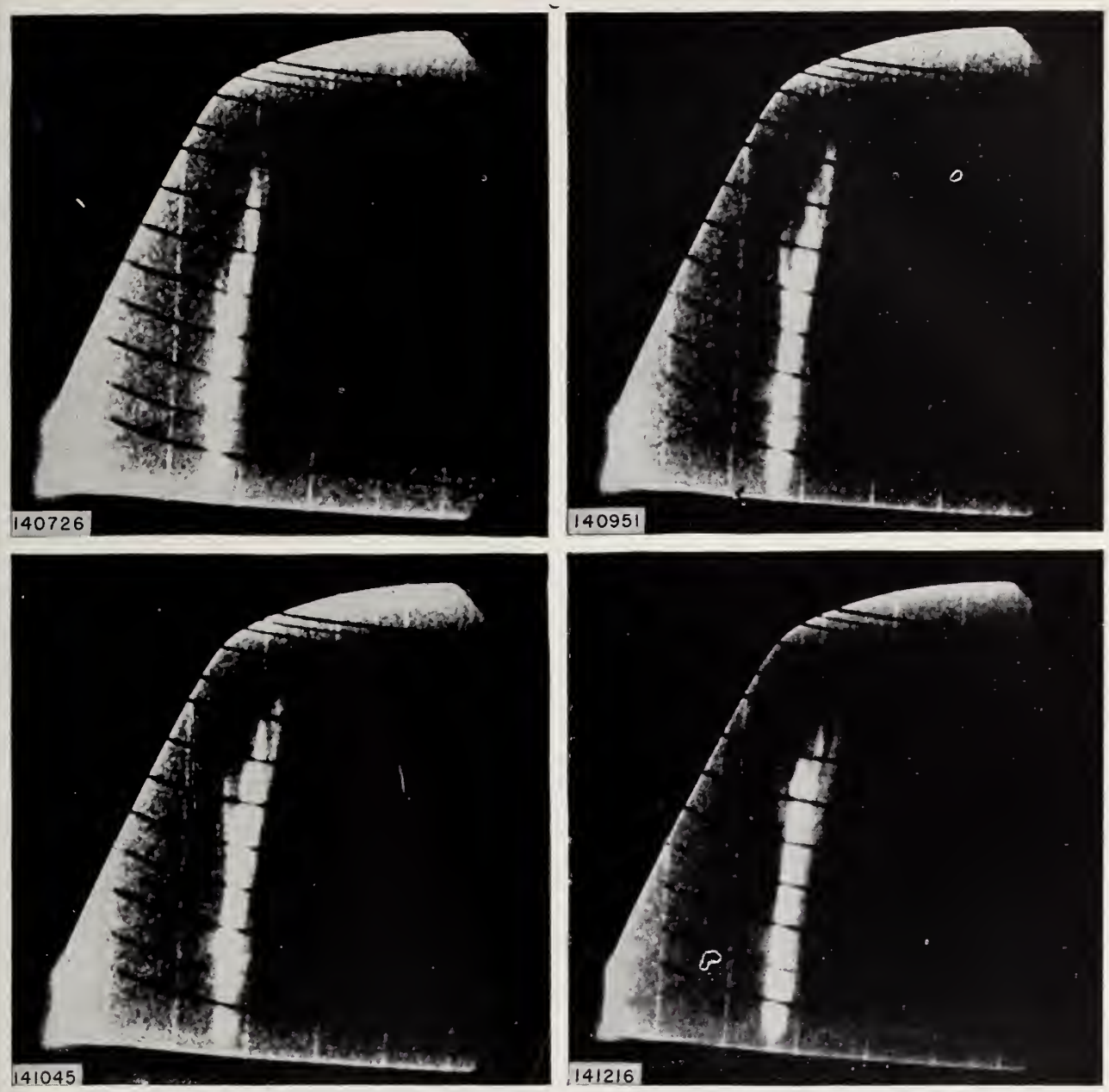

FIGURE 86.—Photographs of a radar thunderstorm as depicted by the RHI echo. The number on each photograph gives Eastern Standard Time in hours, minutes, and seconds. Note the displacement and dissipation of the original turret and its replacement by a second turret during this short time period. The radar was directed along the same azimuth for each photograph. This storm occurred in the vicinity of Wilmington, Ohio, on August 17, 1947.

the same vertical cross section of the cloud at altitudes h_1 and h_2 were measured and R_b was determined.

4. The magnitude of the rate of displacement of the cloud at altitude h_2 relative to h_1 along the selected azimuth V_c, was then calculated[56] by using:

$$V_c = \frac{R_b - R_a}{t_2 - t_1}.$$

[56] Strictly speaking, the radar cloud shear is given by $\frac{V_c}{h_2 - h_1}$; however, in this chapter the vector difference of the velocity at two altitudes is referred to as the "shear between the two levels." This practice is not uncommon among meteorologists.

During the early stages of the thunderstorm, when the RHI echo has a relatively small diameter (1 to 2 mi.) and is intense and sharply defined, the measurements of horizontal distance are very reliable. In the later stages, after the echo has begun to spread out and to become weak and diffuse in character, there is difficulty in accurately determining its outlines, and measurements are regarded as uncertain. Another factor which contributes to uncertainty in some cases results from the fact that the echoes constantly change in size and shape due to phenomena other than wind

FIGURE 87.—A photograph of the off-center PPI 'scope showing a thunderstorm radar echo. Note the weak intensity of the echo at the southern extremity of the large storm. Such diffuse echo offers evidence that the upper portion of the storm has been displaced southward.

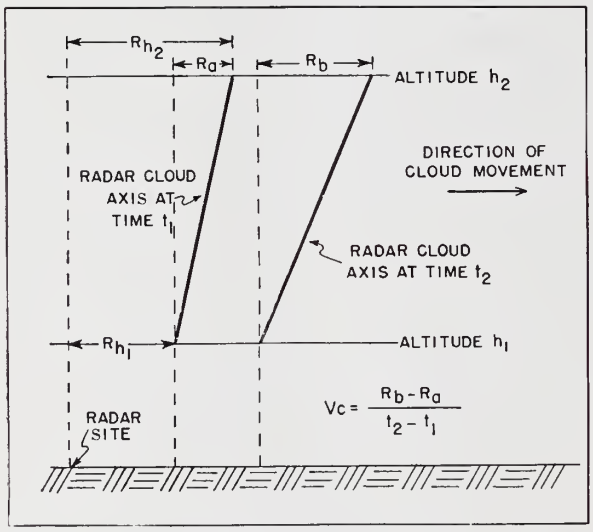

FIGURE 88.—A diagram showing the measurements made in order to determine the effective shear between two levels within the radar cloud.

shear. This is significant when the shear effect is small relative to the other distortions. Another difficulty is introduced because successive vertical cross sections through the same thunderstorm cannot always be selected through exactly the same part of the thunderstorm, owing to the radar's scanning of slices only about every 3° or 4° of turning.

The vector difference of the environment wind velocities between altitudes h_1 and h_2 was computed from hodographs drawn for the measurements of the upper wind stations of the Thunderstorm Project, taken at approximately the same time as the radar cloud observations (within 1 hr. in all cases except

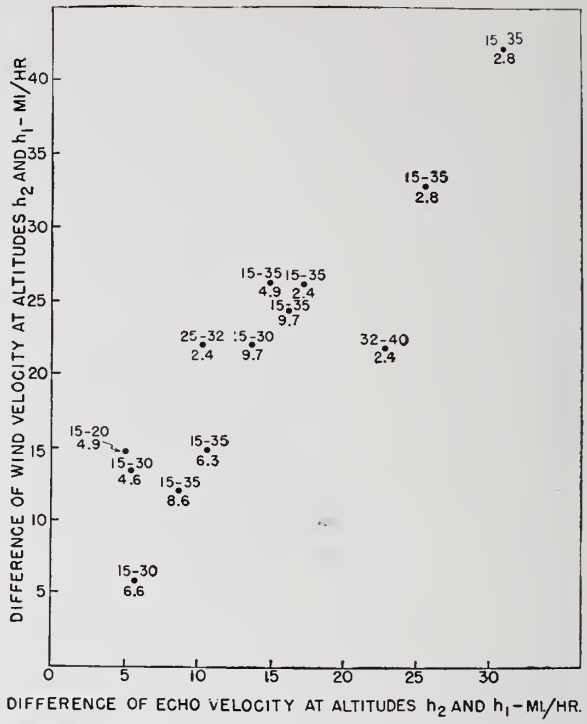

FIGURE 89.—A scatter diagram of the vector difference of radar cloud velocities at altitudes h_2 and h_1, along a particular azimuth, plotted against the component of the vector difference of average wind velocities at the same altitudes and along the same azimuth. The numbers above the plotted points give the altitudes between which vector differences were measured. The numbers below the points give the time, in minutes, between the successive radar observations used.

one, in which the time difference was about 2 hr.)[57]. If a thunderstorm, as indicated by the PPI 'scope of the control radar, was located over or close to a station making a balloon release, the wind record from that station was not used, since it has been found that the circulation set up by a storm results in distortion of the normal wind field in its vicinity. The magnitude of the component of this environment vector difference for the two selected altitudes, in the same direction as the radar cross section, was calculated from each wind record, and a mean value was determined[58]. The average was used because in most cases each wind record yielded different results, and it was felt that the average would be more representative than any single value.

Figure 89 presents a scatter diagram of the calculated radar cloud velocity at altitude h_2 relative to h_1 along a particular azimuth, plotted against the component along the same azimuth of the vector difference of the environment wind velocities at h_2 and h_1. The data were obtained by using 12 storms and selecting two levels between which reasonably reliable shear measurements could be made. For those cases

[57] All storms studied were located within 30 mi. of the center of the wind network, with one exception which was about 70 mi. away.

[58] It is to be recognized that the radar cross section was usually not in the direction of maximum velocity of the top of the radar cloud relative to the lower.

in which the rate of change of echo geometry and intensity were not too great, it was possible to use relatively long time intervals. In the figure, numbers plotted above the dots give the altitudes between which the measurements were made; those below the dots give the time, in minutes, between the two observations used in the computation. The distribution of the points indicates that a definite relationship exists between the two variables. It is also evident that in almost every case the vertical wind shear of the environment exceeds the shear of the radar cloud and would, therefore, exceed the vertical wind shear within the thundercloud itself. Each of several factors which serve to bring about this situation is discussed individually in the following paragraphs.

There is a tendency for development of the cloud on the upwind side of the shear vector, since the air of the updraft tends to rise vertically as the upper part of the cloud is sheared downstream. The characteristics of the radar observations do not permit a definite statement as to the magnitude of this effect on the radar-cloud shear measurements.

Effects of entraining and momentum transfer.—One of the important factors which determines the vertical wind shear within the thunderstorm is the transport of horizontal momentum by the updrafts and downdrafts. The concept of the vertical transfer of momentum in a turbulent layer is familiar to meteorologists. The treatment of the problem is usually applied to the lower levels of the atmosphere in considering the mixing by small eddies. It is evident, however, that the drafts within the thunderstorm are parts of very large eddies, whereby horizontal momentum as well as other conservative properties of the air may be transported from one level to another at a rapid rate[59]. This discussion of the effects of drafts may be regarded as one in which the thunderstorm circulation is considered as a single large eddy which can be studied individually.

In studying the resultant horizontal momentum of a huge parcel of air within the thundercloud, it is necessary to know the horizontal momenta of the incremental parts which form the parcel. Since there is entraining into the thundercloud up to high levels, the resulting momentum of the parcel will depend upon the altitude distribution of entraining and the wind shear of the environment which is entrained. In a recent paper, Malkus [38] treated the effects of this phenomenon on trade-wind cumuli and concluded that this rising jet of air inside the cloud has a vertical shear subtantially lower than that of the environment.

The following mathematical treatment of the effects of entraining on the in-cloud wind shear deals only with the thunderstorm cell in the cumulus stage, which is characterized by vertical motions directed only upward. A similar approach may be used to study the transfer of momentum in the late stage of the cell when the vertical motions are almost entirely downward. During the period of the storm history when there are both updrafts and downdrafts of comparable extent within the cell (mature stage), the problem becomes considerably more complex.

Transfer of momentum by the updraft.—Considering the effects of entraining alone, the horizontal velocity of the updraft portion of the cloud mass at any level is governed by the law of the conservation of momentum

$$\sigma\left[m_0 + \int_0^z dm\right] = m_0 c_0 + \int_0^z c_z\, dm, \qquad (1)$$

where σ is the velocity of the cloud at height z, m_0 is the original mass starting at the base of the cloud (taken as $z = 0$), c_0 is the initial velocity at the base of the draft, and c_z is the velocity of the entrained element dm, that is, the velocity of the environment at height z. This equation states that the horizontal momentum of the cloud layer at altitude z is equal to the sum of the horizontal momenta of the parcels which are a part of the cloud layer. Equation (1) may be written

$$\sigma = \frac{m_0 c_0 + \int_0^z c_z\, dm}{m_0 + \int_0^z dm}. \qquad (2)$$

For the sake of simplicity, it is assumed that the percentage of mass entrained is constant with height

$$\frac{1}{m}\frac{dm}{dz} = K_0. \qquad (3)$$

Then the total mass at any height, and the increment of mass entrained are

$$m_z = m_0\, e^{K_0 z}, \qquad (4)$$

and

$$dm = K_0\, m_0\, e^{K_0 z}\, dz. \qquad (5)$$

Assuming the wind to be constant in direction and linearly increasing in speed with height,

$$c_z = c_0 + K_1 z. \qquad (6)$$

Substituting these assumptions in (2) and solving,

$$\sigma = c_z + \frac{K_1}{K_0}(e^{-K_0 z} - 1),$$

$$= c_0 + K_1\left[z - \frac{1}{K_0}(1 - e^{-K_0 z})\right], \qquad (7)$$

[59] Humphreys [31] considered the consequences of such momentum transport on the pressure change under a thunderstorm.

which defines the velocity of the cloud mass at any level. The rate of wind shear within the clouds is then

$$\frac{d\sigma}{dz} = K_1 \left(1 - e^{-K_0 z}\right). \tag{8}$$

From this expression it is seen that, if only the effects of entrainment are considered, the vertical shear within the updraft is zero at the base and approaches that of the environment with increasing height.

If a ratio of final to original mass is assumed, K_0 may be computed from (4), and upon substitution of this into (7) the profile of the horizontal velocity of the updraft may be calculated. Sample velocity curves (solid lines) for various rates of entrainment and an assumed value of K_1 are shown in figure 90. The entrainment observed in updrafts is of the order of 100 percent in 400 mb. to 100 percent in 200 mb. This would result in a total mass entrainment of 2.9 to 8.0, respectively, as the air rises from 900 to 300 mb. It is assumed, of course, that the inflow extends to the 300-millibar level and that $\frac{1}{m}\frac{dm}{dp}$ equals a constant. With the assumption that the cloud consists of several layers within which the value of K_0 is constant, the velocity shear between the top and bottom of each layer was computed, and the dashed curves of figure 90 were obtained. It is evident from the families of curves that the vertical distribution of entrainment has an important effect on the horizontal velocity distribution within the cloud. It is also to be noted that the values of cloud shear which would be indicated by these curves are generally smaller than the measured values shown in figure 89.

From qualitative considerations, it would be expected that in a downdraft starting at the top of the cloud, the velocity curve would be similar to the dotted curve of figure 90. It appears reasonable to expect that the entrainment into the downdraft would be smaller than into the updraft, because the lateral pressure differences which produce inflow into the latter may not even exist[60]. This means that the descending parcel of air would undergo relatively little mixing with air having a different momentum and that, when the downdraft extends through most of the thundercloud, the vertical shear of the horizontal wind within it would be small.

Effects of drag and friction forces upon the cloud.—In figure 89 it was shown that the observed ratio of radar cloud shear to environment wind shear in mature thunderstorms generally ranged from 50 to 75 percent, the higher values being observed with high values of environment shear. In view of the excess of observed over computed shear, it is evident

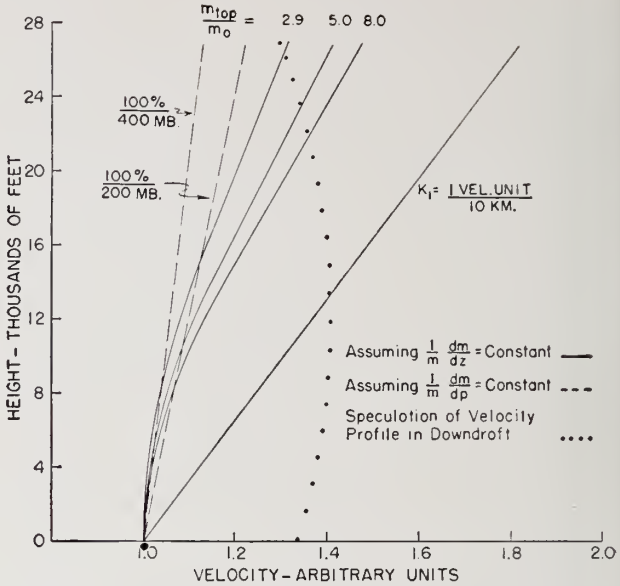

FIGURE 90.—Curves representing the change in horizontal velocity of an updraft under assumed conditions of entrainment and a constant change in wind speed with height in the environment. The dashed lines indicate the resultant vertical velocity gradient when the mass entrained per uniform increment of pressure is constant; the solid curves indicate the resultant vertical velocity gradient when the mass entrained per uniform increment of height is constant. The sloping straight line represents the assumed environment wind speed, and the dotted curve shows an assumed vertical gradient of horizontal velocity in a downdraft.

that factors other than entrainment are important in contributing to the shear of the cloud. Among these are the drag and friction forces which act between the cloud air and its environment and tend to cause the velocity of the convective cloud to approach the velocity of its environment.

When a thundercloud is imbedded in faster-moving air, some of this environment air will flow around or over the cloud or flow vertically along its sides and exert acceleration forces on the cloud mass. It has also been suggested by Malkus [**38**] that some of the air flows through the cloud by a process of entrainment on the upwind side and detrainment on the downwind side. It is impossible at this time to assay the extent to which each of these processes takes place, but the fact that the radar clouds accelerate horizontally with height at a greater rate than would be expected considering only the effects of entrainment and the transfer of momentum by the draft is evidence that the drag and friction forces of the environment are important.

A mathematical treatment of the problem of the effects of form and friction drag of the environment on the cloud would be very complex and is not attempted here[61]. Several qualitative conclusions can be drawn, however, by considering the thundercloud as a rigid vertical cylinder of infinite length imbedded in a fluid flowing at a constant velocity (sev-

[60] See ch. I, sec. 4.

[61] Schmidt [49] has given a theoretical treatment of the drag and friction forces on the growth of cumuli.

eral diameters upstream) perpendicular to its axis. If the cylinder has a lower velocity of movement than the environment, there would be a transfer of momentum to it by both viscous forces, as the air flows around it, and by impact forces, as the air strikes it on the upwind side. The transfer of momentum would accelerate the cylinder in the direction of the fluid flow, and the difference of the velocities of the environment and the cylinder would decrease. The rate of acceleration would depend upon the velocity difference, and thus, as this difference becomes smaller, acceleration decreases. The velocity differences would approach zero only when the time of interaction approaches a relatively high value.

When the radar cloud is considered, the problem becomes more involved because of the vertical cloud motions, the lack of rigidity of the clouds, and the unsteadiness of the circulation. It may not, however, be unreasonable to assume that the cloud would behave as a rigid cylinder. This leads to the conclusion that the effects of the drag and friction forces would make the cloud velocity approach that of the environment. Also, the smaller the cloud, the sooner would the velocity difference between cloud and environment approach zero if there were no vertical motion. Since the velocity difference decreases with time, the difference is also a function of the vertical velocity of the draft, because the greater the updraft speed, the smaller will be the time during which the cloud mass is subjected to the external forces at any particular level.

Other factors affecting the cloud shear.—Other factors which would have to be considered in a rigorous treatment of the problem of the velocity of the thundercloud relative to the environment are the following:

1. The effects of the unbalance of the coriolis and pressure forces which result from differences in the horizontal velocity inside and outside the cloud, and which may cause the wind direction inside the cloud to veer or back, depending on whether the speed is larger or smaller than that of the environment.
2. The effects of lateral pressure differences between environment and cloud, produced by such conditions as temperature and vertical acceleration differentials.

The unsteadiness and non-uniformity of the air flow, which is one of the characteristic features of all thunderstorms, prevent the evaluation of the magnitudes of these effects at this time.

Wind shear and the thunderstorm's vertical extent.—It has been suggested that when strong wind shear exists no thunderstorm can develop [**10**]. Although the shear undoubtedly acts to prevent the development of the thundercloud, its effect depends upon whether it overbalances the factors which favor the creation of the thunderstorm. Also, the maximum vertical extent of the convective cloud is dependent upon the excess of creating forces over the destroying forces, one of which is the wind shear. The two most important factors to be considered when determining the possibilities of convection suppression by wind shear appear to be the following:

1. The horizontal cross-sectional area of the updraft.
2. The speed of the updraft.

It can be readily seen that the kinetic energy of the thunderstorm is a function of these parameters. If they are small (low value of kinetic energy) while the wind shear is large, the tops of the clouds may be blown off as soon as they start to penetrate the zone of strong shear. This phenomenon is often observed during the early part of the convection period, when the cumulus clouds are small and have relatively weak updrafts within them. However, when the updraft has a large cross-sectional area and a high velocity (large value of kinetic energy), it can cause the cloud to extend a considerable distance into the shear zone before its upper part is displaced relative to the lower to such an extent that it is cut off from its source of energy, the updraft, and begins to dissipate. It is concluded that the critical value of vertical wind shear necessary for the prevention of thunderstorms is dependent upon the available energy or "punch" of the convective cloud. It has been assumed in this discussion that no strong inversions, dry layers, or other convection-suppressing conditions are present to prevent the growth of the thunderstorms. When such conditions are present, the maximum height attained by the clouds is largely determined by factors other than wind shear.

To show the effects of environment wind shear on the maximum heights attained by the radar thunderstorms, scatter diagrams of the two variables were drawn. Figure 91 (a) shows the environment wind shear on 11 days, between the levels of 5,000 ft. and 30,000 ft., plotted against the maximum height attained by any radar thunderstorm during the same day. Figure 91 (b) presents the wind shear plotted against the *mean* of the maximum heights reached by the echoes on the same day. The wind shear values were obtained by taking the vector average of the wind shear between 5,000 ft. and 30,000 ft., using the wind record of the Project network stations which made simultaneous releases, and then taking an arithmetic mean of the several vector averages available during the thunderstorm period. These levels were selected so that the lowest was above the mean

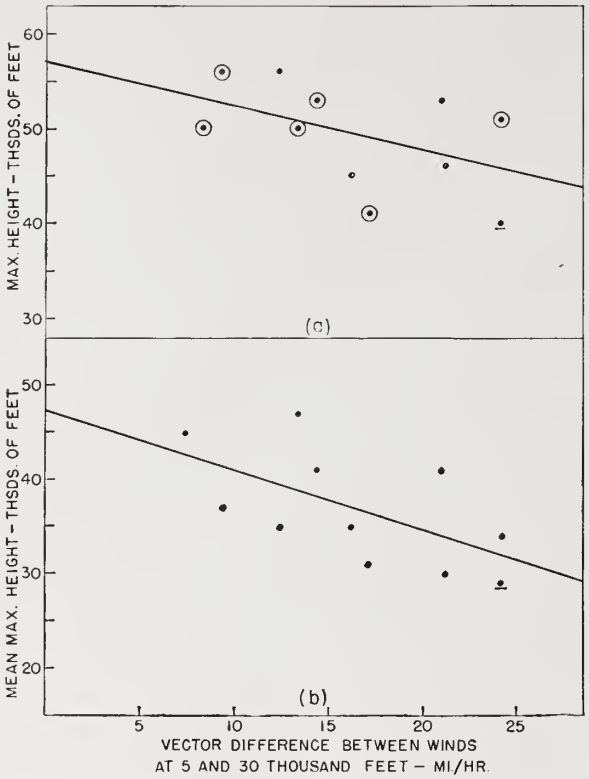

FIGURE 91.—Scatter diagrams showing the relationship between the wind shear with height and the height attained by radar thunderstorms. (a) relates the wind shear to the maximum height reached by any storm on the particular day and (b) relates the wind shear to the mean of the maximum heights attained by all of the storms on a particular day. These data are based on 11 days of observations of Ohio thunderstorms with the AN/TPS-10 radar set. The encircled points represent observations of thunderstorms whose tops extended above the calibrated portion of the RHI 'scope; 1,000 feet was added to the maximum measurable height of these storms, although most appeared to extend considerably higher than the heights obtained in this manner. The height value for the observation represented by the underlined point is subject to question.

cloud base and the upper was below the maximum heights attained. The figures indicate that even with an average wind shear in excess of 20 mi/hr between 5,000 ft. and 30,000 ft., thunderstorms did occur. They also show a tendency for the strong wind shear to restrict the maximum height reached by thunderstorms. The scattering may be attributed to several causes:

1. The length of time of the radar observations and the area of radar coverage were not the same in all cases. For this reason the mean heights are probably more significant.
2. The number of wind observations was not the same on every day considered.
3. On some days, the vertical wind shear between intermediate levels was of the same order of magnitude but different in direction than that between the altitudes of 5,000 ft. and 30,000 ft.
4. Other meteorological factors influencing convection were not the same every day.

No records of the operating sensitivity of the radar equipment are available, but examination of the 'scopes indicated differences in gain control settings from one day to the next. This factor affected the observations of maximum vertical extent of the radar thunderstorms. However, it does not appear to be the factor controlling the distribution.

2. Movement of Thunderstorms

In short-term forecasting and in air navigation the movement of individual thunderstorms or cumulonimbus clouds frequently has to be determined. Rules for predicting these motions are difficult to establish because thunderstorms are too small to be studied in detail from the data of the usual synoptic networks and too large for precise visual examination. The obvious solution to this problem, as recognized by H. Brooks [**11**] and others, comes from a study of a great many cloud echoes detected on long-range radar equipment. The photographically-recorded data from the PPI radar equipment used in the two summers of operation of the Thunderstorm Project provide a much more complete source of information on this subject than has existed before.

Definition.—The problem is confused by a loose terminology. For example, the "movement" of a thunderstorm may be considered as consisting of its propagation or growth around the edges due to the formation of new cells as well as its general movement with the wind currents. Thus, the result obtained for the motion of the edge of a thunderstorm may be appreciably different from that for the center. Again, what is termed a thunderstorm from synoptic chart analysis may actually be a series of thunderstorms. A squall line consisting of thunderstorms has its most apparent motion normal to itself, as is the case in an advancing cold front, yet the individual thunderstorm elements may also have a considerable component of motion along the line. In discussing movement it is thus necessary to specify whether the displacement of the line or the movement of the elements of the line is intended. Faulty conclusions have been reached from failure to appreciate fully these differences [**16**].

In studying Thunderstorm Project data, a method was devised whereby the translational component of the cloud motion could be separated from the growth

or dissipative component. Tracings on map grids were made from projections of photographs of the radar 'scopes taken 2 to 5 min. apart. On each selected echo, at the initial time of measurement, the point representing the geometric center of the echo was determined. This point was then identified and its displacement measured on succeeding tracings. Identification was made by overlaying the tracing of one photograph on that of the previous one so that the corners, indentations, protuberances, etc. of the echoes matched. From the changes in the plotted position of the initially-selected point the echo movement was determined. In some cases, owing to the development of new cells or the dissipation of old ones, this point was not very near the geometric center of the echo for the last few measurements, but with tracing its location every 2 to 5 min. in the described manner there was no mistaking its identity.

A test was conducted to see whether or not the degree of subjectivity in this method was high enough to cause appreciable error. Two analysts independently calculated the movement of 50 echoes in this way; their results showed agreement to within 10° and 2 mi/hr in over 90 percent of the cases.

In order to avoid measurement complications which might result from a confused state of the clouds, only those cases in which echoes were clear-cut, relatively small, and fairly isolated were used. As proved by the independent observations of Reynolds and Workman [43] and those made in connection with the many hundreds of radar-monitored flights of the Project, echoes of the type studied here represent cumulonimbus or thunderclouds, the visual extent of which is only slighty greater than the size of the radar echo. Therefore, these measurements truly characterize the thunderstorm movements.

Character of data analyzed.—The characteristics of the radar echoes used in the study of movement are summarized in table 39. To bring out more clearly the effect of winds on the translational component of the radar cloud motion, the echo data are divided into two groups. In group I are those cases for which the mean environment wind speed from the surface to 20,000 ft. was less than 10 mi/hr; and in group II those for which the mean wind speed from the surface to 20,000 ft. equalled or exceeded 10 mi/hr. The 120 PPI echoes listed in the table were observed for an average period of 26.3 min. each. The greater portion of them were increasing in size: 47 percent were growing throughout the entire period of observation; 14 percent grew to a maximum and then decreased; and only 36 percent were decreasing throughout the measurement period. The character of the remaining 3 percent was indeterminate.

In order to compare the speed and direction of the radar cloud movement with the winds of the air layer in which it was imbedded, the cloud heights were determined from RHI radar measurements (table 40). Unfortunately RHI data were not avail-

TABLE 39.—*Summary of characteristics of PPI radar echoes used in study of cloud movement*

Data	Group classification of echoes	Number observed	Mean speed	Mean area— At beginning of measurement	Mean area— At time of maximum size	Mean area— At end of measurement	Duration of measurement
			mi/hr	*sq. mi.*	*sq. mi.*	*sq. mi.*	*min.*
Florida	I	13	6.8	9.2	21.3	20.2	28.5
	II	34	11.8	8.5	21.1	18.6	29.1
	Both	47	10.4	8.7	21.2	19.1	29.1
Ohio	I	32	5.5	8.4	12.4	8.3	23.2
	II	41	20.3	11.8	23.0	16.1	25.4
	Both	73	13.8	10.3	18.4	12.7	24.4
All data		120	12.4	9.7	19.5	15.2	26.3

TABLE 40.—*Summary of characteristics of radar clouds from available RHI data*

Data	Group classification of echoes	Number observed	Mean speed	Mean echo area— At beginning of measurement	Mean echo area— At end of measurement	Mean echo area— At time of maximum size	Mean echo height— At beginning of measurement	Mean echo height— At end of measurement	Mean echo height— At time of maximum height	Duration of measurement
			mi/hr	*sq. mi.*	*sq. mi.*	*sq. mi.*	*ft.*	*ft.*	*ft.*	*min.*
Florida	I	1	9.0	5.0	25.0	25.0	29,700	36,700	39,000	30.0
	II	4	9.2	5.5	22.0	25.0	32,000	34,800	39,200	28.8
	Both	5	9.2	5.4	22.6	25.0	31,300	39,100	35,100	29.0
Ohio	I	26	5.3	9.6	9.2	14.1	20,400	18,800	23,100	24.0
	II	13	19.5	12.5	19.7	21.8	17,300	19,400	20,600	21.2
	Both	39	10.1	10.7	12.6	17.7	19,300	19,000	22,400	24.1
All data		44	10.4	10.0	13.8	18.5	20,700	20,800	21,300	21.6

able for all of the storms studied; there were only five measurements from the Florida RHI photographs, as indicated in the table. Photographs of the RHI 'scope were taken at 4-degree intervals of azimuth. To obtain a value for the height of the radar cloud at a given time, the mean of the echo heights for each 4° of azimuth was calculated. This mean height was used to compute the average heights in table 40. Obviously, its use resulted in smaller heights in the tabulation than would have been the case had only the peaks of the radar clouds been used, since the mean includes the "shoulders" of the cloud as well as the peak. This type of mean height, however, was considered the most significant for wind movement correlations.

Upper-air winds used in the study were obtained from the SCR-658 rawinsonde and SCR–584 rawin observations of the Project network. Observations of winds not influenced by local thunderstorm wind components were used for comparison with the measured direction and speed of the echoes. Generally, at least four separate wind measurements were available for obtaining the wind velocity of the undisturbed field, and as a rule there was little variation among the simultaneous observations.

Correspondence of movement to winds at a particular level.—In previous studies, others have concluded that thunderstorms or radar cloud movement is best represented by the winds at a particular level. For example, H. Brooks [**11**] states that small radar echoes move with the winds at the 5,000-foot level and that larger ones move with the winds of the 11,000-foot level. Brancato [**9**] writes that cumulonimbus clouds move with the winds at the 6,000-foot level. Some other meteorologists believe that thunderstorms move with the winds at the freezing level.

The relationship between the movement of the radar clouds and wind at particular levels for group II data is shown in figure 92. These curves indicate that the zone of correspondence between air and cloud movement lies in the lower layers. It must be pointed out, however, that the curves represent average conditions since storms in all stages of development were included in the study. Correlation coefficients relating echo and wind speeds measured in Ohio were greater than those for Florida because of the greater range of cloud speed measurements in the former location, but an examination of the original data relating wind and echo speeds indicates about the same degree of dispersion about the regression line for both sets of data.

Similar calculations were made for the group I data, but conclusions concerning zones of correspondence between cloud and air motion are difficult to draw. There are large variations in the correlation co-

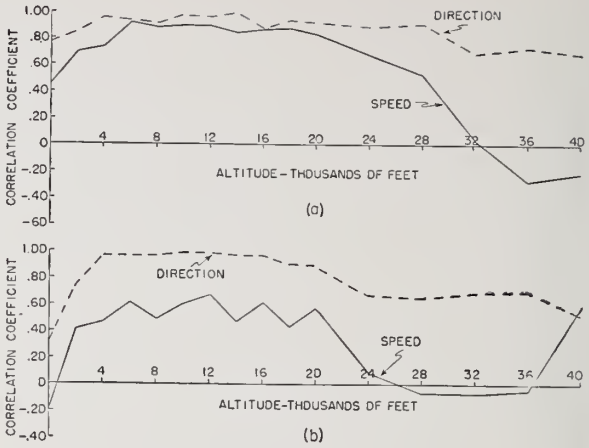

FIGURE 92.—Graphs showing the variation with altitude of the correlation coefficients relating the speed and direction of the radar-cloud movement to the observed wind at the various levels. Only cases where the mean environment-wind field (from the surface to 20,000 ft.) was greater than 10 mi/hr (group II data) were used.
(a) Based on measurements of 34 Florida storms.
(b) Based on measurements of 41 Ohio storms.

efficients from one level to the next because of the greater variability of both direction and speed of air currents when the speeds are low. However, of the 47 echoes in group I, only two showed a translational speed exceeding 10 mi/hr., and in each case this speed was 11 mi/hr.

To supplement the correlation analysis for the group II data, charts showing the mean differences in the speed and direction of clouds and air were constructed. The following notation was utilized:

Θ_c = Direction of the radar cloud movement in degrees
Θ_w = Direction of the wind in degrees
U_c = Speed of the radar cloud in mi/hr
U_w = Speed of the wind in mi/hr
N = Number of cases

The quantities $\frac{\Sigma(\Theta_c - \Theta_w)}{N}$ and $\frac{\Sigma(U_c - U_w)}{N}$, representing the average deviations of the wind direction and speed from that of the radar cloud movement, were determined for each level and plotted as shown in figures 93 (a) and 93 (b). Two features apparent from these charts are worth noting:

1. The average speed of movement of the clouds is less than the average of the wind speeds at all levels above the friction layer for the Ohio data.
2. The average of the wind directions from the gradient level (2,000 ft. in Florida; 4,000 ft. in Ohio) to 20,000 ft. gives the average direction of cloud movement for both sets of data. (Note that in figure 93 (a) area ABC is approximately equal to area CDE, and in figure 93 (b) area GHJ approximately equals area JKL.)

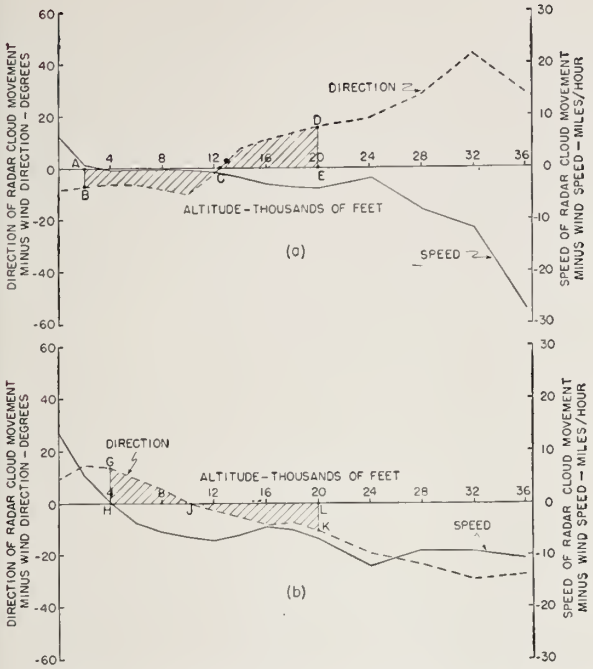

FIGURE 93.—Graphs showing the variation with altitude of the average difference between the speed of the radar-cloud movement and the wind speed at the various altitudes; and the variation with altitude of the average differences between the direction of the radar-cloud movement and the wind directions at the various altitudes. Only cases where the mean environment wind was greater than 10 mi/hr (group II data) were used.
(a) Based on measurements of 34 Florida storms.
(b) Based on measurements of 41 Ohio storms.

The quantities $\frac{\Sigma|\Theta_c - \Theta_w|}{N}$ and $\frac{\Sigma|U_c - U_w|}{N}$, representing the average absolute difference between the cloud and air movement were also determined for each altitude and graphed as shown in figures 94 (a) and 94 (b). These charts point out that the absolute differences in speed and direction were relatively small up to about 20,000 ft.

Similar analyses were made for group I data. The means of the differences in speed were small, as was to be expected, since with low wind speeds the clouds move slowly; the means of the differences in direction were large because of the greater variability in direction of lighter winds.

Correspondence of movement to the mean wind from gradient level to 20,000 ft.—The fact that the average of all the wind directions—measured at 2,000-foot intervals from the gradient level to the 20,000-foot level—equalled the average of the cloud movement directions for both the Ohio and Florida group II data suggested correlating the vector average of the wind velocity from the gradient to the 20,000-foot levels with the speed of radar cloud movement. High correlation coefficients were obtained, as is indicated by table 41 and figures 95 and 96.

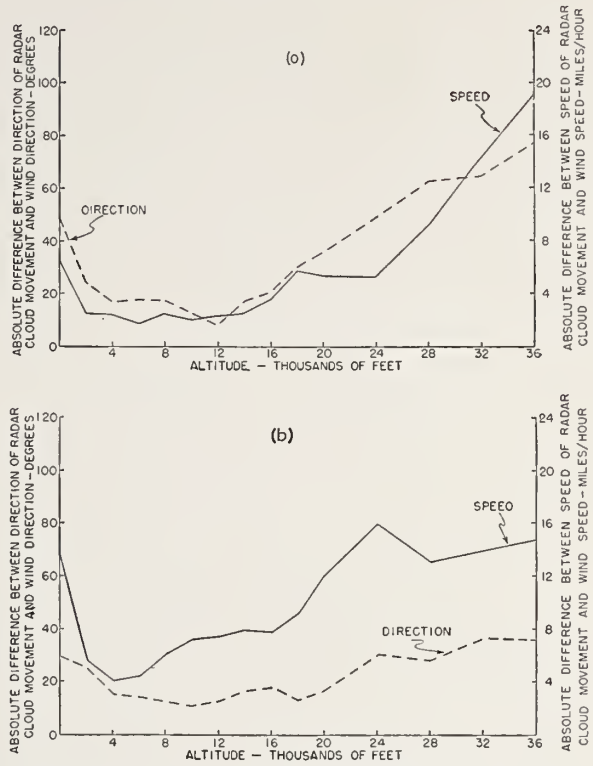

FIGURE 94.—Graphs showing the variation with altitude of the average *absolute* difference between the speed of the radar-cloud movement and the wind speed at the various altitudes; and the variation with altitude of the average *absolute* difference between the direction of the radar-cloud movement and the wind direction at the various altitudes. Only cases where the mean environment wind was greater than 10 mi/hr (group II data) were used.
(a) Based on measurements of 34 Florida storms.
(b) Based on measurements of 41 Ohio storms.

TABLE 41.—*Tabulation of correlation coefficients relating radar cloud movement and various wind parameters*

Wind parameter	Florida		Ohio	
	Group I	Group II	Group I	Group II
Mean of cloud layer:				
Speed	—	—	.81	.96
Direction	—	—	.97	.88
Mean: gradient level—20,000 ft.:				
Speed	.65	.75	.93	.93
Direction	.96	.99	.95	.97
Wind at level of best agreement:				
Speed	.63	.67	.78	.91
Level (ft.)	12,000	12,000	6,000	6,000
Direction	.94	.99	.94	.98
Level (ft.)	12,000	10,000 12,000	6,000	11,000

In spite of the relatively high correlation coefficient, it is evident from figure 96 (b) that a straight line does not best represent the relationship between the cloud speed and this vector mean wind speed. From

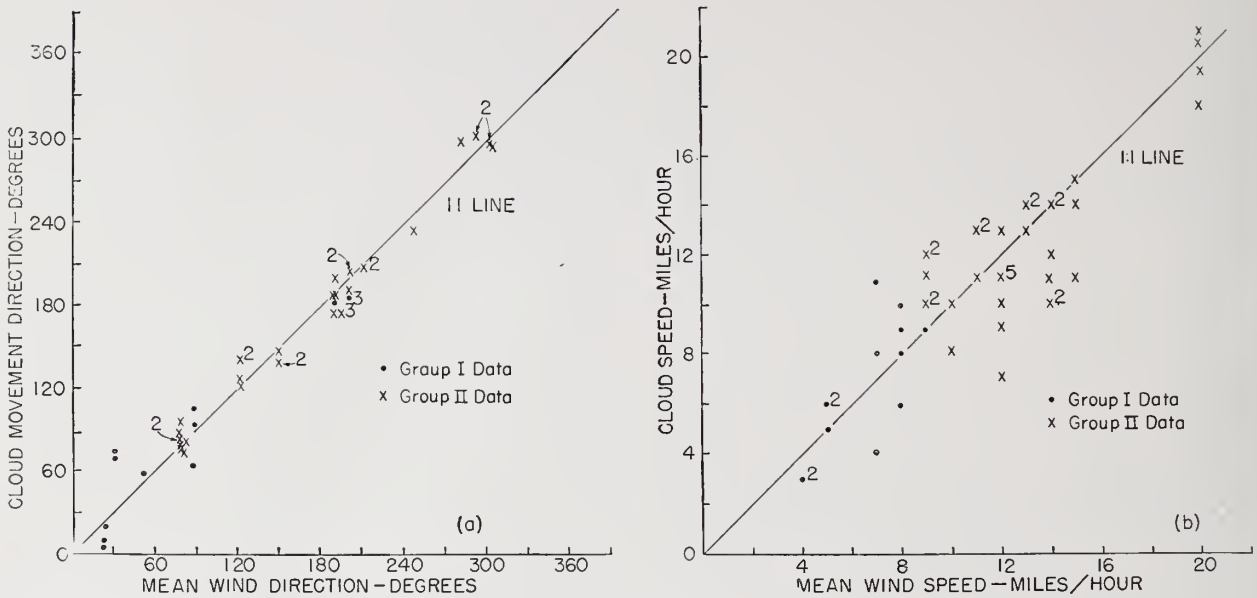

FIGURE 95.—Scatter diagrams relating the radar-cloud movement to the mean wind velocity in the layer from the gradient to the 20,000-foot level. The numerals beside the plotted points represent the number of coincident values. Based on measurements of Florida storms.
(a) Radar-cloud movement direction *vs* mean wind direction.
(b) Radar-cloud movement speed *vs* mean wind speed.

this diagram it is evident that the clouds move more slowly than this mean wind, and that the higher the mean wind, the greater the discrepancy. If U_c equals the cloud speed and U_w, the vector mean wind speed, then $U_w = 1.9 + 0.65\ U_c + .020\ U_c^2$ describes the relationship between these two variables better than a straight line.

Correlation coefficients were also computed to relate this vector mean wind with the movement of 15 of the tallest clouds in the Ohio sample of RHI photographs. The mean maximum height of these clouds ranges from 25,000 ft. to 39,000 ft. The correlation coefficient found in relating speeds was .99, and in relating directions was .94, suggesting that this mean wind vector is useful for indicating the movement of tall cumulonimbi as well as those reaching only 20,000 ft.

Correspondence of movement to mean wind of the cloud layer.—Humphreys [**31**] has suggested that the vector mean wind of the layer in which the cloud is imbedded corresponds closely to the speed and direction of the cloud movement. This is true for many

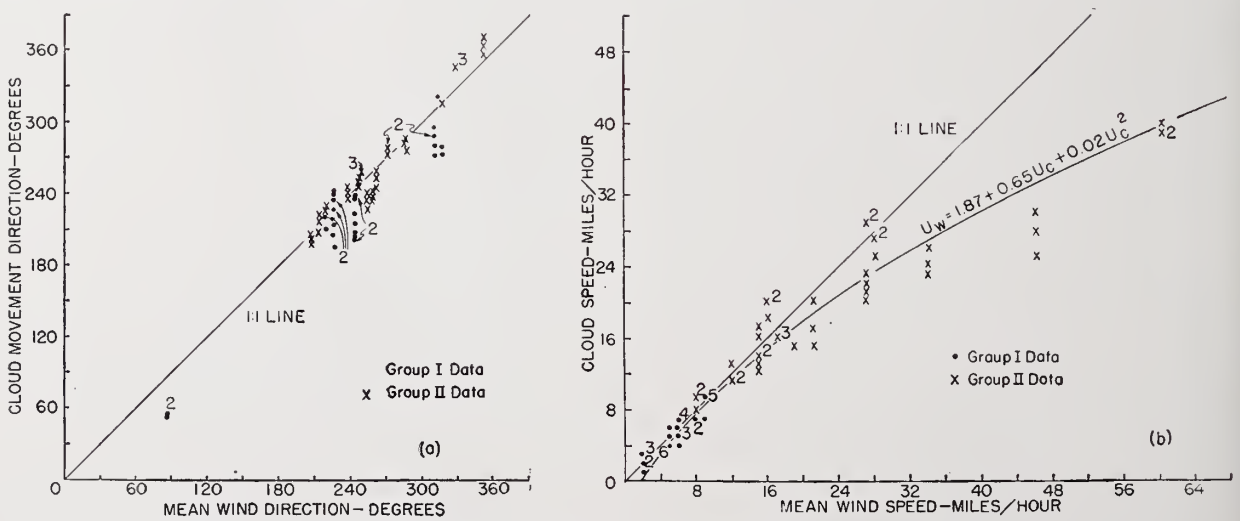

FIGURE 96.—Scatter diagrams relating the radar-cloud movement to the mean wind velocity in the layer from the gradient to the 20,000-foot level. The numerals beside the plotted points represent the number of coincident values. Based on measurements of Ohio storms.
(a) Radar-cloud movement direction *vs* mean wind direction.
(b) Radar-cloud movement speed *vs* mean wind speed. The curved line represents a curvilinear regression line for this distribution of points.

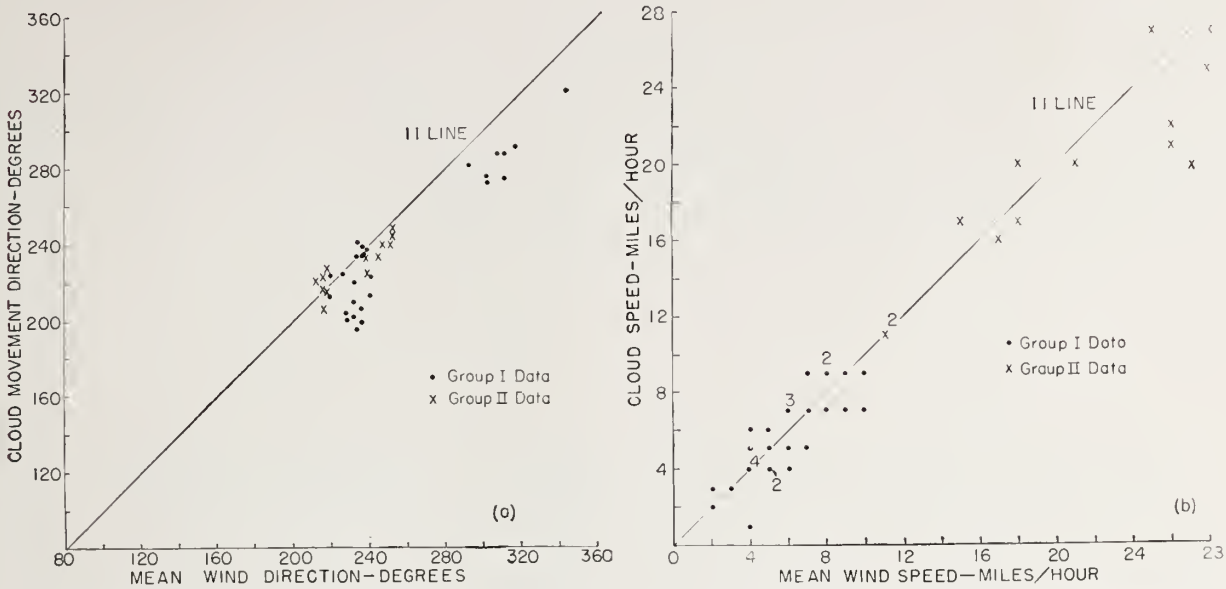

FIGURE 97.—Scatter diagrams relating the radar-cloud movement to the mean wind velocity in the layer in which the cloud is imbedded. The numerals beside the plotted points represent the number of coincident values. Based upon measurements of Ohio storms.
(a) Radar-cloud movement direction *vs* mean wind direction.
(b) Radar-cloud movement speed *vs* mean wind speed.

cases, but under some conditions marked deviations may occur. The motion of the cloud within any layer is a function of the vertical drafts which have prevailed in it. In the later stages of the thunderstorm life, when downdrafts predominate, the winds of the upper levels may be more influential than those of the lower levels. In view of this, deviations of the cloud motion from that of the mean wind in the layer where the cloud exists are to be expected. Greatest deviations were observed in this study in cases when the radar cloud extended from a few thousand feet above the ground to over 30.000 ft., and the air flow in the upper 15,000 ft. was opposite to that in the lower 15,000 ft.; however, only a few such cases were available for study.

As seen from the scatter diagrams shown in figures 97 (a) and 97 (b), and from table 41, the relationship between the cloud movement and the vector mean wind of the cloud layer is good for the Ohio data. Since RHI photographs were necessary to determine the vertical extent of the cloud, the data presented are limited to those days in which RHI pictures were available. Unfortunately an insufficient amount of data was at hand from Florida to make a similar analysis.

Exceptional movements.—The path of movement of the radar cloud frequently curves to the right or left, resulting in a change in direction amounting to as much as 30° in a period of 10 min. Such curvature may be explained by the effects of vertical transport of horizontal momentum by the strong vertical air currents found in thunderstorms. During the building stage of a thunderstorm cell, when updrafts are present, the transport of horizontal momentum upward causes the motion of the cloud to be influenced by the winds of the lower layers. During the mature and dissipating stages of the thunderstorm, the downdrafts initiated by the falling rain transport horizontal momentum downward, causing the cloud particles in the lower layers to be influenced by the winds of the upper levels. Whether or not curvature occurs during the life cycle of a thunderstorm depends on the amount of vertical transport of momentum, which in turn is a function of the amount of shear present and the magnitude of the wind speeds in the stratum considered.

An illustration of echo path curvature may be seen in figure 98. The areas shown in the figure are cross sections of a radar cloud obtained by fitting together the vertical slices of the radar cloud from the photographs of the RHI 'scope taken at every 4° of azimuth. The movement of the cloud at a given level was observed by overlaying upon one another several successive cross sections representing the cloud at regular time intervals. It is evident from the figure that from 1435 to 1437 E.S.T. the cloud moved toward the northeast and veered thereafter toward the southeast. Consideration of the draft structure and the winds aloft provides a reasonable explanation for the change in the motion of this cloud.

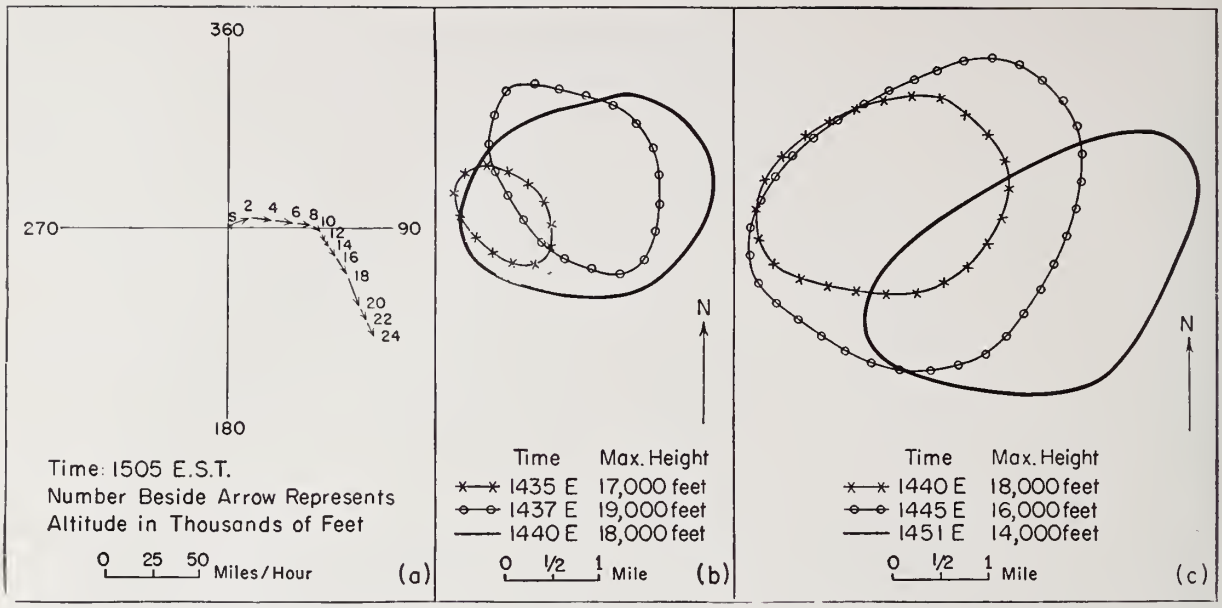

FIGURE 98.—Charts showing the variation of the wind velocity with height and the change in cloud-echo movement due to the vertical transfer of horizontal momentum by the updraft and the downdraft.

(a) Wind speed and direction at each 2,000-foot level. Wind vectors are means of seven observations taken over the Ohio network. No balloon approached nearer than four miles to the radar echo.

(b) and (c) Outlines of the cross section of the radar cloud at the 5,000-foot level for successive times. The maximum height given is for the top of the echo. Note that the movement was toward the northeast during the first time interval, during which the echo was increasing in height. As the echo decreased in height, the echo movement became more southeasterly.

CHAPTER VII. PREFERRED AREAS OF THUNDERSTORM DEVELOPMENT

1. Topographical Effects

The important influence of terrestrial features on the distribution of convective clouds has long been recognized. Most striking is the effect of hills and mountains on the formation of clouds. Air blowing up the slopes receives a forced impetus upward which is conducive to the formation of clouds of marked vertical development, i.e., cumulus or cumulonimbus. An equal, if not greater effect, especially in summer and with very light winds, is that due to the higher temperature of the air on the elevated terrain compared with that in the free air at the same height, because of the absorption of the sun's radiation by the mountain in contrast to an almost complete lack of absorption in the atmosphere. The heated air rises to form convective clouds.

Temperature contrasts between water bodies and the adjacent land also determine preferred areas for cumulus and cumulonimbus development. Some of these effects are so pronounced as to appear in climatological data. For example, with prevailing westerly winds, the precipitation on the east side of Lake Michigan is greater in winter than on the west side; but in summer the situation is reversed, with the greater amount of precipitation on the west side. In winter the lake, which never freezes over, is a heat source, while in summer, since the water is cold relative to the land, convection diminishes eastward across the lake. This chapter discusses some of the effects of the much smaller lakes and swamps in Florida on convective activity.

Another role in convective activity has been ascribed by von Ficker [**58**] to small bodies of water and also to swamps, woods, and other areas kept cool by evaporation. He suggests that cool air drifting outward from these areas pushes the surrounding warm air upward enough to start it into convective motions of a scale sufficiently large to produce thunderstorms. He visualizes this action at so-called "thunderstorm hearth" areas as the principal way in which non-frontal thunderstorms are first formed over flat, continental terrain, and cites the Spreewald near Berlin as an example of a hearth region.

With the use of radar, it becomes possible to study individually and statistically the formation of convective systems in relation to terrain features. Florida is a region of innumerable small lakes, so an excellent opportunity was afforded for examining the effects of small bodies of water on the frequency of radar cloud echoes. In Ohio, the region of hills and ravines formed by stream dissections to the southeast and to the west of the network were also scanned by radar for possible "preferred" areas of echo formation.

Effects of Florida lakes.—From the 1946 data in Florida, a study was carried out to determine whether or not the difference between the frequency of convective cloud formation over the lakes and over the land is sufficiently great to be observed statistically. On the 16 days considered, 1,067 echoes were observed to develop on an off-center PPI 'scope of the control radar with the diameter set at about 40 mi. The procedure followed in analyzing the data was to note the azimuth and the range to a new echo appearing on the radar 'scope, and then to use these coordinates to plot the echo position on a map of Florida. Since the land area was about 10 times the lake area, data for each day were expressed as a density, i.e., the number of echoes per square mile. Table 42 presents a frequency distribution of the ratio of the number of echoes per square mile of water to the number of echoes per square mile of land. The mean value of the ratio for the echoes of all 16 days is also included.

On 68 percent of the days, as the table shows, the echo density over the land was greater than over the water. The mean ratio of the densities, using all of the data, indicates only a slight tendency for more development over land. Two major reasons may be offered to explain why this ratio is not smaller:

TABLE 42.—*Frequency distribution of the ratio of the number of new echoes per square mile of water to the number per square mile of land for Florida data*

Ratio	Number of days	Percent of days
0.2–0.39	2	12.5
0.4–0.59	4	25.0
0.6–0.79	2	12.5
0.8–0.99	3	18.9
1.0–1.19	1	6.2
1.2–1.39	2	12.5
1.4–1.59		
1.6–1.79	1	6.2
1.8–1.99		
2.0–2.19		
2.2–2.39	1	6.2
Total	16	

Mean ratio: 0.88

TABLE 43.—*Frequency distribution of the ratio of the number of new echoes per square mile of water to the number per square mile of land with data corrected for the translation of the clouds before detection by the radar set*

Ratio	2-mile displacement	10-minute displacement
0.2–0.39	1	2
0.4–0.59	3	1
0.6–0.79	6	4
0.8–0.99	2	4
1.0–1.19	1	2
1.2–1.39	2	2
1.4–1.59	—	—
1.6–1.79	—	—
1.8–1.99	1	1
Total	16	16
Mean ratio	0.75	0.85

(1) the many swamps in this part of Florida were considered as part of the land, and (2) no account was taken of the fact that the actual cumulus cloud may have been formed several miles upwind and carried by the air while developing from the convective condensation level to the height at which it was first detected.

An effort was made to overcome the effect of the second factor on the ratio values obtained by moving all new echoes upwind a certain distance for plotting purposes. When a displacement of 1 mi. was used, the fraction of the echoes which developed over the lakes became higher; however, when it is considered that in Florida the convective condensation level is at about 3,000 ft. while the average level of the cloud tops at initial detection was probably about 15,000 ft., it can be seen that to assume a displacement of 1 mi. presupposes a horizontal wind velocity of only 5 mi/hr if the rate of growth of the cloud is taken as 1,000 ft/min. If the winds at 10,000 ft. are to be used as indicative of cloud velocity, the value of 5 mi/hr appears to be too low.

Other values of cloud displacements, that of 2 mi. and another given by multiplying the wind velocity at 10,000 ft. by a time period of 10 min., were then used. The ratio distribution resulting from the use of each is given in table 43. It can be seen that the ratio of density of new echoes over water to their density over land becomes smaller but still is not as definitely indicative as would be expected. The effects of swamp areas, however, still were not considered.

Another factor, which is pertinent but which could not be taken into account, is the effect that outflowing cold air from under a large thunderstorm has in influencing the development of cumulus clouds (see ch. III). The pseudo-cold front which is established could have assisted the formation of cumuli over the water, as well as over the land, and thus may have resulted in an increase of the relative number of new echoes over the lakes and swamps. During three of the days considered, weak fronts were located over the area of observation. Although on one of these days the ratio of the density of new echoes over water to that over the land exceeded a value of one, on the other two days it was significantly less than one.

Swamp areas and new developments.—In order to take the swamp areas into account in a qualitative fashion, the new echoes were plotted (position uncorrected for cloud movement) on a map showing the swamps as indicated by a topographic map of this region. The area covered by the radar 'scope was divided into squares of equal area, each one being 2.8 sq. mi. The number of new echoes which developed in each square was determined and isolines were drawn. When an echo formed on a line between two squares, each of them was allotted one-half of the echo. Figure 99 presents a map of the area under consideration showing the lakes and swamps and the isolines of 4 echoes per 2.8 sq. mi. for the 16 days. All areas within the isoline have been shaded. Although there are some exceptions, the figure shows a definite tendency for the preponderance of new echoes to be over the dry land.

Diurnal variation of convective echo development in Florida.—From the radar data on 17 days[62] it was possible to study the time distribution of the rate of formation of radar clouds during the convection period. The mean duration of the radar observations was about 4.4 hr. per day, with most of the records covering the hours between 1300 and 1700 E.S.T. A graph (fig. 100) was drawn to show the number of initial convective echoes per hour of observation for the period between 1100 and 1800 E.S.T. The smaller

[62] One additional day on which the 'scope was centered differently from its setting in the 16 days used in previous analysis was included here.

FIGURE 99.—A section of a map of Florida showing the region covered by the off-center PPI 'scope. The stippled areas are those enclosed by the isolines representing the occurrence of four newly-developed echoes per 2.8 sq. mi. per 16 days. The areas delineated by the horizontal hatching are swamps and marshes. Note that for the most part the new-echo development was over dry land.

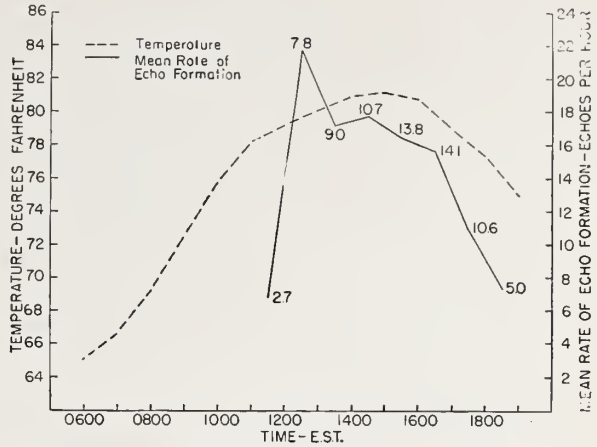

FIGURE 100.—A graph showing the mean rate of echo formation per hourly interval during the period of radar observation. This graph is based on observations made over a 17-day period. The numbers along the curve indicate the total number of hours of record for each hourly interval. The temperature curve is based upon a mean of hourly values recorded at five stations of the surface network during the 17 days and is considered as representative for the area shown in figure 99.

sample of observations during the early and late parts of the convection period resulted in mean values having less significance than those during the afternoon. The total hours of record for each hourly interval are indicated on the curve.

Also shown in figure 100 is a graph of the diurnal variation of temperature over the area under consideration. The values used to plot the graph were obtained by selecting 5 stations of the surface network and tabulating their recorded temperatures for every hour on the 17 days for which data on new echo development were available. Mean values of the temperature at each hour were calculated and assumed to be representative of conditions over the area shown in figure 99. Although the temperature varies smoothly with time and has a rather flat maximum at about 1500 E.S.T. the rate of formation of the convective echoes rises sharply to a maximum at about noon and remains high until about 1700 E.S.T., after which time a sharp decrease occurs. Although the actual shape of both graphs may be subject to some question because of the limited number of observations, the general trends are reasonable. It is evident, as would be expected, that the maxima of both temperature and rate of cloud development occur over the same period of the day, roughly from 1230 to 1630 E.S.T. In the next section of this paper it will be shown that temperature plays an important indirect part in the development of afternoon thunderstorms over the Florida peninsula.

Orography and the formation of convective clouds.—Orographic features such as hills and mountains may contribute to the development of cumulus clouds for one or more of the following reasons: (1) They form obstructions to the horizontal wind and force the air to rise vertically on their windward sides, thus encouraging the realization of the instability of a convectively unstable air mass. (2) The roughness of the terrain results in a series of vertical perturbations, some of which may trigger the formation of a cumulus cloud in a conditionally unstable air mass. (3) The hills and mountains act as high-level heat sources due to the differential heating of their tops and of the free air at the same altitudes.

The integrated effects of these causes can be studied by using the data on radar cloud formation which was collected in southern Ohio during 1947. The topography in this area is discussed in some detail in the Introduction of this report. Generally, the terrain is rough in the vicinity of the principal streams, where elevation differences may be as much as several hundred feet. The time and location of the initial appearance of 584 radar clouds on 21 days were obtained from the plan-position indicators of the control radar sets. The position of each new echo was plotted on a map of the area covered by the radar 'scope (about 40 mi. in diameter), showing contours of elevation at an interval of 100 ft. The area was divided into squares having an area of 4 sq. mi., and the number of new echoes which appeared within each was counted and plotted at the centers. A smooth pattern of isolines of new convective echoes was then drawn, as shown in figure 101.

In the interpretation of the isoline patterns of new echoes, the previously discussed complicating factors should be borne in mind. As has been shown in

FIGURE 101.—A section of a topographic map of Ohio showing the region covered by the off-center PPI 'scope. The isolines enclose areas over which more than 3 or more than 5, newly-developed echoes per 4 sq. mi. appeared during the 21 days of observation. The contour lines are drawn for intervals of 100 ft.

chapter III, there is a strong tendency for more convective echoes to develop in the immediate vicinity of an already existing thunderstorm than in isolated locations. In view of the relatively small sample of cases available, it might be supposed that the final distribution of echoes was influenced by a few, large, slow-moving thunderstorms. It seems, however, that this influence was not the dominating one in determining the final pattern. Daily echo distributions were plotted for a number of days to further investigate this factor. It was noted from them that there was a tendency for certain areas to show a larger number of echoes from day to day than others, indicating the existence of some stationary mechanism contributing to the formation of convective clouds within these areas.

Another factor to be recognized in the interpretation of the isoline patterns is that although the wind direction was most frequently westerly, wind velocities differed from one day to the next. As a result, a marked preponderance of new echoes on a particular side of a ridge is not to be expected. Another reason for the lack of echo concentration on one side of a ridge is that a cloud could have moved several miles

from the time of formation to the time of first radar detection. Some of the cumulus clouds may have started to form on the windward sides of ridges and were not detected until they had moved a few miles leeward.

It can also be seen from figure 101 that, as was expected, the most frequent development of radar clouds occurred over the more rugged terrain in the eastern and northwestern sections of the area being observed. New radar clouds were initially detected over almost all parts of the area; however, the distribution is sparser and more random over the flatter parts than over those with more pronounced orographical features.

2. Geographical Effects[63]

It has been shown in the preceding section that topographical features play an important part in determining the distribution of cumulonimbus clouds over a relatively small area. It remains to be demonstrated why thunderstorms develop more frequently over one particular geographical region, such as the Florida peninsula, in preference to another. Recent investigations have provided increasing evidence of the importance of dynamically-induced, as contrasted with purely thermally-induced, horizontal convergence in strong convection over a large area. Over the Florida peninsula, a more or less permanent zone of horizontal convergence could be present as a result of (1) a permanent or diurnal trough of low pressure, properly placed with respect to the peninsula, at some level of the atmosphere; or (2) a permanent or diurnal disturbance in the low-level wind field caused by the physical presence of the peninsula.

Riehl [**46**] ascribes the Florida thunderstorm maximum to the first of these causes and shows that the mean trough at 700 mb. in summer extends across the northern portion of Florida into the Gulf. Actually, the mean position was obtained for a trough that wanders widely across the Gulf and adjacent Atlantic and sometimes disappears and reappears. Since the frequency of thunderstorms is much greater on the peninsula than in other areas where the trough's influence is felt, there must be another contributing factor.

Sea-breeze effects.—The second type of convergence effect to be looked for is that brought about by the geographical situation of the peninsula in relation to the air flow. It was decided to test the hypothesis that the afternoon sea breeze moving into the peninsula from all sides would produce low-level convergence almost daily. Such a two-sided sea breeze is, of course, peculiar to this type of land mass and would be expected to have its maximum effect at a season and time of day corresponding closely with the Florida thunderstorm maximum (see fig. 2).

Despite occasional variation, the sea breeze usually begins 2 or 3 hr. after sunrise. Although it does not reach full strength until the time of maximum heating in the afternoon, the general convergence of air in the lower levels over Florida begins almost immediately, since the sea breeze is acting inward on both sides of the peninsula at the same time. It is reasonable to expect that the convergence would continue and increase in strength until the sea breeze reaches maximum intensity shortly after the time of the maximum temperature; that at night it would cease as the air currents develop land-breeze components. Such convergence could maintain the intensity of the thunderstorm activity which exists in Florida, particularly when the gradient winds are light and no other source of convergence is present.

Measurement of convergence.—In order to determine the nature of the diurnal variation of convergence due to the sea breeze, the amount of convergence or divergence in the lowest 5,000 ft. of the atmosphere was computed for the entire summer of 1946 (May 1 to September 15) by using the regular synoptic wind measurements made four times each day. The values for convergence were obtained by utilizing the method developed by Bellamy [**6**]. In general, this method gives the change in area of a triangle due to the effects of the wind at the vertices. The assumptions involved make this method more accurate if a small triangle is used for the calculations; however, results of this computation were satisfactory despite the large area of the triangle used as a base. Jacksonville, Miami, and Tampa, Fla., were selected as the vertices, since the area enclosed by this triangle includes all of the central portion of the peninsula; further, these three stations are strongly affected by the sea breezes, and it was believed that their wind data would be representative of the coastal sea-breeze distribution. The values of divergence obtained from the computation are expressed as percentage change of area per hour.

The calculated values of divergence, obtained by this triangle method, were averaged for each time of day at each 1,000-foot level, and the average amounts of convergence for each level were graphically plotted against time of day. These averages were obtained for each month and for the entire summer (fig. 102). It is pointed out that the times of maximum and minimum values as indicated by the curves in the figure are not

[63] The information contained in this section was extracted from contribution No. 7 of the Thunderstorm Project: *Causes of Thunderstorms of the Florida Peninsula*, by H. R. Byers and Harriet R. Rodebush.

841051—50——9

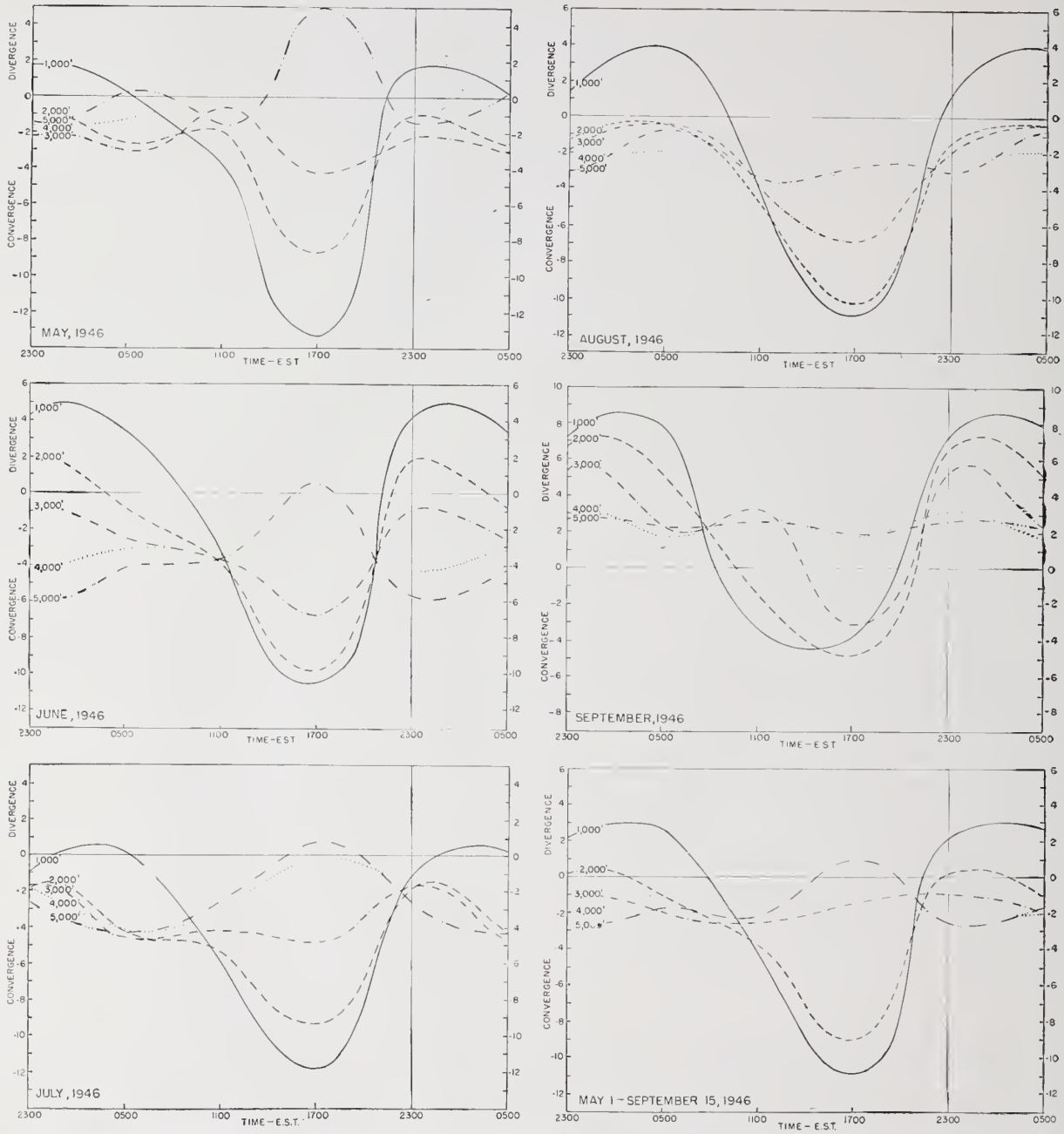

FIGURE 102.—Charts showing the diurnal variation of convergence and divergence in the lowest 5,000 ft. of the atmosphere for selected months in the year 1946, and for the period from May 1 to September 15, 1946. The divergence and convergence are expressed in percentage change in area per hour. These data were obtained from winds aloft observations from Jacksonville, Miami, and Tampa, Fla.

exact, since the 6-hourly wind values had to be interpolated over a 24-hour period. However, the general trends and amounts are sufficiently accurate for the purposes of the investigation.

The most striking and significant feature of the graphs is the appearance of a strong maximum value of convergence in the lower 2,000 ft. of the atmosphere around 1700 E.S.T., on the monthly as well as the summer average graphs. On the summer mean graph, the maximum appears at 1,000 ft. and is of the value of 11 percent per hour. On the monthly graphs the 3,000-foot level also shows a maximum value sufficiently great to indicate that the sea breeze causes enough convergence at the proper time of day to support thunderstorm convection.

From the curves it may be seen that the maximum convergence is built up slowly during the day, reaching its peak soon after the time of maximum

temperature, and then decreases rapidly until by midnight (shown on all the monthly averages except July) divergence appears at 1,000 ft., indicating the beginning of the shallow land breezes. The divergence reaches a maximum sometime during the night, although the exact time is impossible to determine from these data. Soon after sunrise, however, the trend starts toward the convergence maximum again. The shallow nature of the land breeze is illustrated here, except on the curve for September. Apparently the 1,000-foot level is the only one affected by the divergence caused by the land breeze, except in the case of September when the land breeze appears to extend to 3,000 ft. Since the data for September cover only 15 days, however, it is inadvisable to draw definite conclusions from them.

On all of the curves, except that for August, slight divergence shows up at the 5,000-foot level at the time of maximum convergence in the lower levels. This may represent the beginning of the outflow above the sea breeze. On the mean summer graph (fig. 102, lower right), the 5,000-foot level shows maximum divergence above the convergence maximum in the lower levels, while both the 3,000- and 4,000-foot levels are more or less constant, showing a slight convergence at all times. This follows the pattern that would be expected for convergence and divergence caused by the sea breeze. The reversal of sign in the upper levels shows the beginning of the return flow and the general tendency toward establishment of mass compensation. From these results, it seems that the average effective depth of the sea breeze is between 3,000 and 4,000 ft.

The fact that the convergence decreases upward at the time of its maximum also nullifies any hypothesis that part of the convergence so indicated may be a result rather than a cause of the thunderstorm activity over Florida. As shown in chapter I, the convergence associated with individual thunderstorms usually is found to extend from near the surface to heights as great as 20,000 to 25,000 ft.

There were, as mentioned, some exceptions to the general trends shown by the graphs. September shows a smaller amount of convergence than the other months, perhaps due to the fact that insolation is less in this month. As a matter of fact, convergence appears only in the lower 3,000 ft. of the atmosphere and during the middle of the day. The rest of the time, divergence appears at all levels. Conversely, July shows an extreme amount of convergence at all times at all low levels. Although these deviations may be due to other factors than the different amounts of heat received during these two months, it is impossible to go into many details of this sort when the data have been collected for only one summer.

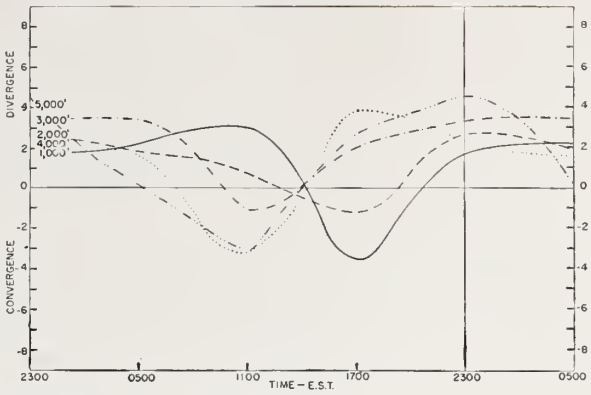

FIGURE 103.—A chart showing the diurnal variation of convergence and divergence in the lowest 5,000 ft. of the atmosphere for June 1946, over the triangular area between Tallahassee and Pensacola, Fla., and Montgomery, Ala. The divergence and convergence are expressed in percentage change in area per hour. Note that the pronounced maximum apparent in the data for the Florida peninsula is not present here.

In general, it may be said that the average depth of the convergence caused by the sea breeze was found to be about 3,800 ft. The divergence caused by the land breeze was very small compared to the magnitude of the sea breeze effect and occupied only the lower 1,500 ft. of the atmosphere.

Comparison with north Gulf Coast.—In order to investigate how much was contributed to the amount of convergence by the fact that the sea breeze is doubly effective in the Florida peninsula, a similar analysis of convergence was carried out for a triangle with the vertices at Tallahassee, Fla., Montgomery, Ala., and Pensacola, Fla., for the month of June 1946. This triangle is affected by the sea breeze only along its southern side. As indicated by figure 103 which shows the results of the calculations, no strong maximum of convergence appears. The sea breeze apparently causes a slight maximum in the lower 2,000 ft. of the atmosphere around 1700 E.S.T., of the order of 3.5 percent per hour. However, convergence of equal strength appears at 1100 E.S.T. in the upper levels. Too many factors are involved to make any statements as to the cause of the pattern shown in figure 103, but the patterns serve as illustrations of the fact that the dynamic effects of the sea breeze over the Florida peninsula are peculiar to that area and a result of its peninsular shape.

In summary, it may be said that the large-scale convection pattern in Florida is governed by thermally induced convergence, and that the smaller scale distribution of cumuliform clouds depends to a large degree on local variations of temperature. In other geographical regions dynamic effects produced by the thermal, orographical, or general circulation characteristics of the region are probably of major importance in determining the frequency and distribution of thunderstorms.

CHAPTER VIII. SQUALL LINES

The squall line is usually defined as a line of high winds, other than along a strong surface cold front, resulting from atmospheric instability. These winds are usually of short duration and are sometimes accompanied by thunder, lightning, and precipitation. Squall lines are characteristically several hundred miles in length and are most clearly defined when associated with a cyclonic pressure system having a strong surface cold front with which the squall lines are usually indirectly associated.

Although phenomena such as upper fronts and pressure waves may cause lines of high winds (as reported by Tepper[64] and Brunk [**12**]), the most frequent cause is a line of thunderstorms, and it is the latter phenomenon which is referred to as a squall line in this report[65].

A similar definition has been used by other investigators [**28**] who have studied the squall line from its appearance on the large-scale weather map.

Recognizing the need for a more detailed description of the squall line than is possible from a study of the surface map alone, Project personnel undertook a study based upon measurements obtained from a long-range radar in Ohio. With these data it was possible to partially overcome the limitations of the map data imposed by the coarse station spacing of the regular reporting network. The Project study was largely restricted to the period from May 17, 1947, through September 21, 1947, in order to make use of data from the micronetwork and the long-range control radar. During this 127-day period, there were 56 thunderstorm days on which extensive radar data were obtained from Project operations. On 32 of these days lines of thunderstorms were observed. The lines on 6 days occurred along surface fronts, on 19 days were ahead of surface cold fronts, and on the remaining 7 days apparently had no connection with the surface fronts. It is to be noted that, compared with the number of lines of convective storms which occurred ahead of the surface front, relatively few occurred along the front. Even more surprising, however, is the number of lines which apparently were not associated with surface fronts.

Although differences in the appearance of the three types of lines are usually evident on the radar 'scope, it is not likely, in most cases, that a pilot encountering these lines would be able to distinguish between them. Furthermore, at the surface, the sequences of weather variations accompanying a squall line are usually not sufficiently distinctive to enable one to separate the three types of lines.

To obtain more detailed information about these variations, a study was made of the surface weather which accompanied the passage of 27 lines over the Project micronetwork. It was evident early in the study that the sequence of weather events accompanying some lines is similar to that which occurs when a large air-mass thunderstorm passes over a station. It is not infrequent, however, particularly with a squall line preceding a surface cold front, that the variations of surface weather elements are typical of those accompanying the passage of a well-defined surface cold front. Table 44 summarizes the observed weather conditions that accompanied the passage of these 27 squall lines. Taken as a whole, all the lines showed typical air-mass thunderstorm surface weather variations.

From the table it can also be seen that 17 of the 27 lines observed caused surface wind gusts as great as 25 mi/hr in excess of the wind speeds prevailing prior to the squall-line passage. It must be recognized, however, that of the data presented in this table, the gusts with the highest speeds were associated with those lines which preceded active cold fronts; furthermore, gust speeds higher than any in this table are frequently reported, particularly in connection with squall lines occurring in the early spring.

AIR-MASS SQUALL LINES

As was pointed out, seven of the squall lines observed apparently were not associated with surface fronts. Of these, three were associated with some type of large-scale cyclonic disturbance, two were on the west side of a warm anticyclone, and the other two were in rather flat, uniform pressure fields. Most of these lines, regardless of whether they were associated with cyclones or anticyclones, frequently behaved in a manner which suggested that they resulted from some type of relatively large-scale atmospheric

[64] "A Proposed Mechanism of Squall Lines," paper read at American Meteorological Society Meetings, April 1949, Washington, D. C.

[65] Most meteorologists and aviators refer to a squall line aa a line of thunderstorms.

TABLE 41.—*Surface weather associated with the passage of 27 squall lines over the Ohio surface network*

Date	Approximate interval during which line was over network	Surface synoptic classification of line	Distance ahead of cold front, when pre-cold-frontal	Nature of associated pressure trace following initial pressure rise	Maximum associated surface gust	Deviation of maximum gust from prevailing surface wind	Maximum station rainfall	
							Amount	Duration
1947	*E.S.T.*		*mi.*		*mi/hr*	*mi/hr*	*in.*	*min.*
May 25	1200–1330	Pre-cold-frontal	15	Remains high	35	30	0.16	8
29	0800–0900	Pre-cold-frontal	75	[1]Remains high	41	33	.48	30
June 2	0100–0115	Pre-cold-frontal	310	Returns to normal	35	26	.14	20
7	1100–1215	Air-mass	—	....do	39	23	.56	11
11	1330–1445	Pre-cold-frontal	45	....do	33	23	.91	19
13	1845–2015	Pre-cold-frontal	120	....do	42	35	1.28	28
27	1915–2030	Air-mass	—	....do	40	37	.68	20
29	1800–2030	Pre-cold-frontal	50	[1]Remains high	37	27	.40	10
July 10	1345–1500	Air-mass	—	Returns to normal	21	14	.46	15
13	1700–2100	Pre-cold-frontal	145	....do	52	43	.28	155
14	1700–1900	....do	70	....do	45	40	1.60	45
15	1230–1500	Air-mass	—	....do	20	14	.13	6
16	1430–1500	....do	—	....do	19	14	.39	15
18	1800–1900	Pre-cold-frontal	90	....do	25	15	.15	7
31	1000–1445	....do	50	....do	24	13	.06	3
Aug. 5	1010–1215	Stationary frontal	—	....do	48	45	.37	15
6	1545–1730	....do	—	....do	49	45	.36	11
7	1130–1600	Pre-cold-frontal	130	....do	63	60	2.13	33
14	1300–1600	....do	155	....do	45	42	.98	15
17	1300–1415	Air-mass	—	....do	22	19	.30	9
Sept. 4	1500–1630	Pre-cold-frontal	470	....do	21	20	.04	15
5	1100–1200	....do	170	....do	22	16	.30	42
9	1530–1730	Stationary-frontal	—	....do	45	43	1.18	30
10	1600–1800	Air-mass	—	....do[1]	37	32	.56	40
11	1330–1430	Pre-cold-frontal	480	....do	26	21	.12	3
12	1415–1500	....do	320	....do[1]	31	29	.50	70
13	0200–0500	....do	210	....do	49	35	.10	7

[1] Very abrupt pressure rise associated with the passage of the squall line over all stations of the network.

disturbance. Lines of this type are called air-mass squall lines.

Figures 105 and 107 illustrate the general appearance of air-mass squall lines as presented on the 'scope of the long-range control radar[66]. Shown in figures 104 and 106 are sections of the surface weather chart for the approximate time of the photographs. The line shown in figure 107, which may be considered as typical of most of the air-mass lines observed, has a length of approximately 125 mi. and the echoes along the line are separated by distances up to 15 mi. in some areas. In contrast, however, the line shown in figure 105 appears as large and continuous as many pre-cold-frontal squall lines. Most of the air-mass lines observed in this study were short (75 to 100 mi. in length), tended to be parallel to the winds below the 10,000-foot level, and in general were less well defined than the typical pre-cold-frontal line.

[66] In interpreting these figures, the limitations of the radar equipment should be kept in mind; the total length of the squall line and the density of echoes along the line are dependent upon the range and the amount of rain attenuation of the radar signal.

PRE-COLD-FRONTAL SQUALL LINES

The squall line exhibits the greatest length and causes the maximum gusts at the surface when it is followed by a well-defined surface cold front. For this reason, special attention was given the pre-cold-frontal squall line. In this study, use was made of the long-range radar and the surface micronetwork.

Of the 56 days on which squall lines were observed and for which adequate radar data were available,

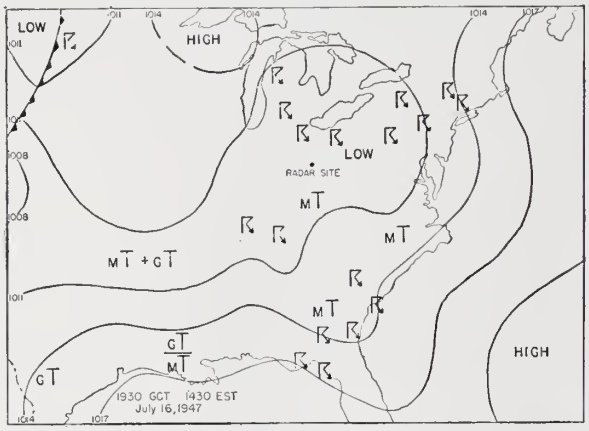

Figure 104.—A surface synoptic chart for 1430 E.S.T., July 16, 1947. (Based on the hourly sequence from regularly reporting stations.)

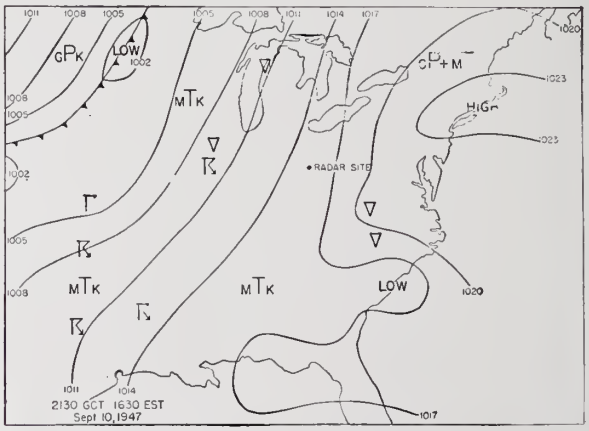

Figure 106.—A surface synoptic chart for 1630 E.S.T., September 10, 1947. (Based on the three-hourly sequence from regularly reporting stations.)

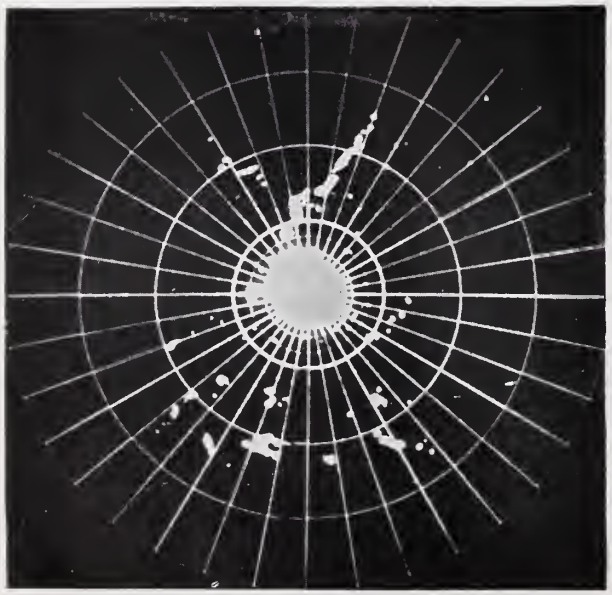

Figure 105.—A photograph of the 200-mile-range PPI 'scope showing a line of thunderstorms at 1456 E.S.T., July 16, 1947.

Figure 107.—A photograph of the 200-mile-range PPI 'scope showing a line of thunderstorms at 1600 E.S.T., September 10, 1947. The one visible range circle indicates a distance of 50 mi. from the radar site.

20 days had squall lines preceding a well-defined, regularly moving cold front within 500 mi. of Wilmington, Ohio.

Examination of the data for these 20 days made it evident that in the area of convective activity ahead of the cold front there occasionally were several roughly parallel lines of thunderstorms rather than a single well-defined squall line. The area within which these individual lines occur is termed the "squall-line zone." It is to be recognized that from the ordinary synoptic weather reports, it is usually impossible to distinguish individual lines occurring within a zone of activity, and as a consequence, the radar 'scopes indicated the existence of several lines when only one was shown on the regular synoptic chart.

Since the data for some of the 20 days were discontinuous or too short to allow a reliable determination of the properties of the squall lines, 12 cases of well-defined, regularly moving cold fronts preceded by the squall-line activity were selected for study. In 8 of these cases the radar echoes were on a 200-mile-range 'scope, and the remainder were obtained from a 'scope with a 50-mile radius. In the 12 cases, it was possible to distinguish a total of a least 37 individual line formations, of which 17 persisted for a sufficient length of time to permit measurement of their dimensions and velocities of movement. An example of such a squall line is shown in figure 108.

Dimensions of the pre-cold-frontal squall line.—Using only the data from the 200-mile range radar 'scope, it was possible to determine measurements of the length and width of 11 lines. These do not include lines which extended beyond the edge of the 'scope and for which no measurements of length could be made. Because the lines were observed to grow and dissipate, dimension measurements were determined for every 10-minute interval during the life of the line, or the period of available data. The measurements were of the following nature:

1. Total length—length of line including all radar echoes which appeared to be part of the line.
2. Solid length—length of that part of the line in which the separations between echoes were less than 10 mi.
3. Maximum width—maximum width measured normal to the axis of the line of that part of the line in which the separations between echoes were less than 10 mi.

From the 10-minute measurements, mean values of the dimensions for each line were determined. These means are presented in table 45. It is important to realize that these dimension values have not been corrected for attenuation effects and consequently are smaller than the actual dimensions of the line.

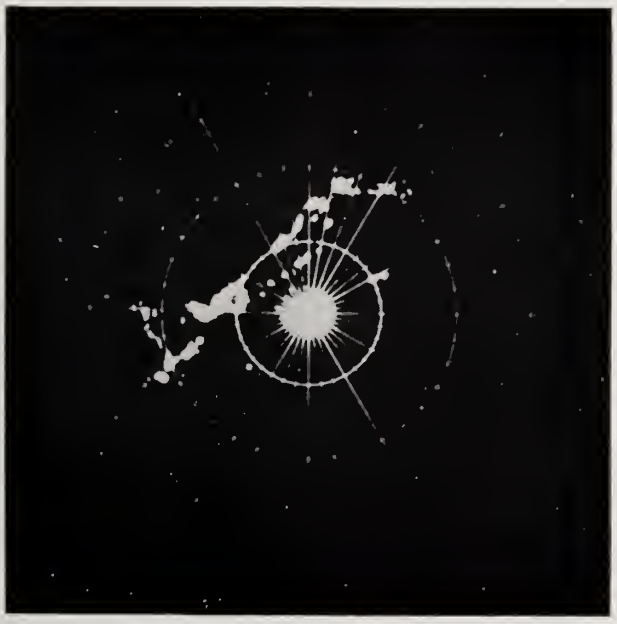

FIGURE 108.—A photograph of the 200-mile-range PPI 'scope showing the squall line at 1230 E.S.T., August 25, 1947.

TABLE 45.—*Lengths and widths of 11 squall lines observed on the 200-mile radar 'scope during Ohio operations*

Date	Mean total length (mi.)	Mean solid length (mi.)	Mean maximum width (mi.)
1947			
July 11	204	83	25
July 11	175	64	47
July 11	139	43	27
July 18	157	80	30
Aug. 14	227	151	44
Aug. 14	64	48	17
Sept. 5	162	129	38
Sept. 5	157	118	35
Sept. 12–13	108	89	35
Sept. 12–13	210	175	—
Sept. 12–13	186	125	63
Mean	163	103	36

Orientation of pre-cold-frontal squall lines.—It has been pointed out by several investigators that pre-cold-frontal squall lines are parallel to the related cold front. The data obtained by the Thunderstorm Project shows, in general, that this is true, although individual lines show considerable variation in this respect. Figure 109 is a scatter diagram of the mean hourly line orientation plotted against the corres-

ponding mean frontal orientation[67]. It can be seen that the line orientation has a tendency to be clockwise from that of the front, although squall-line orientation ranged from +60 deg. (clockwise) to −25 deg. (counterclockwise) from that of the front, and the average was +13 deg. The orientation of the squall line tends to be counterclockwise from the orientation of the overlying 700-mb contour lines (fig. 110).

[67] In this study, the segment of the front which was used in the frontal orientations was determined by projecting the ends of the squall line back to the front along lines perpendicular to the front. The points of intersection of the perpendiculars and the front were connected with a straight line which was then considered to represent the orientation of the front. The orientation of the squall line was considered to be the orientation of the major axis of the line which, in most cases, could be determined with little difficulty.

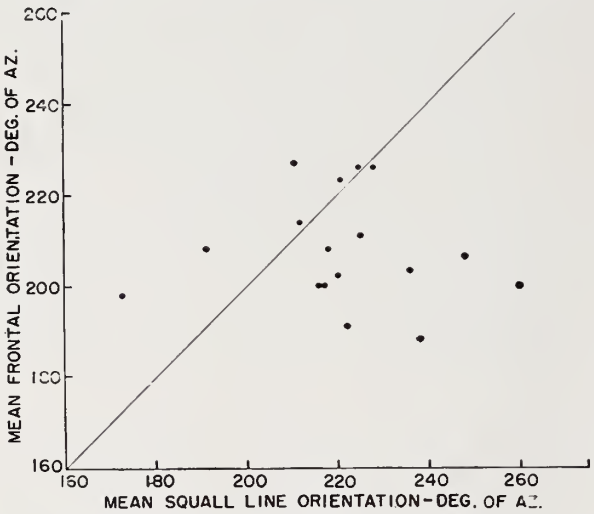

FIGURE 109.—A scatter diagram relating the orientation of the squall line to the orientation of the associated cold front. (Based on means of hourly observations.) The correlation coefficient for this distribution is −.69.

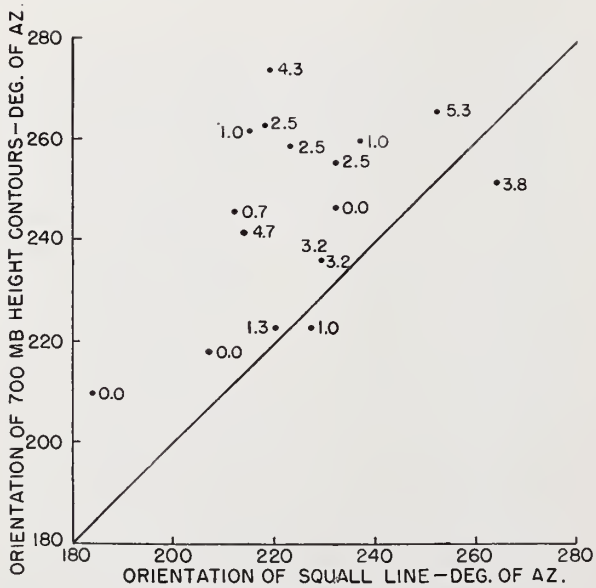

FIGURE 110.—A scatter diagram showing the relationship between the orientations of squall lines (from radar observations) and of contour lines of the height of the 700-millibar surface. The difference between the time of the radar observation and the 700-mb. chart is shown in hours beside each point. The correlation coefficient for this distribution is .49.

Movement of the pre-cold-frontal squall line.—The movement of the squall line, as distinguished from the movement of the individual storms along the line, must be considered as the displacement of the line in the direction normal to itself. The speed of the pre-cold-frontal squall lines compared with frontal speed in the cases studied by the Project is shown in figure 111. The scatter of points in this figure indicates that there is little relationship between these two variables. These results are not in strict agreement with those of Harrison and Orendorf [**28**], who found that, in the mean, the speed of movement of the front was less than that of the squall line; however, since the phenomena considered in the two studies are not strictly identical, discrepancies in the results are to be expected.

The effects of attenuation on the radar signal produced errors in the determination of speed which could not be corrected and were consequently neglected. In most cases, however, it appeared that those errors were relatively small. The effects of propagation[68] were often significant and, in two instances, resulted in negative relative velocities, i.e., the line became closer to the front. It is to be noted that the contribution of propagation to the apparent movement of the line becomes large when the actual transport of convective clouds by the airflow is small.

Normal life span of a pre-cold-frontal squall line.—The pre-cold-frontal squall line, as detected on the

[68] The term "propagation" is used to designate either the growth or the dissipation of the radar echo.

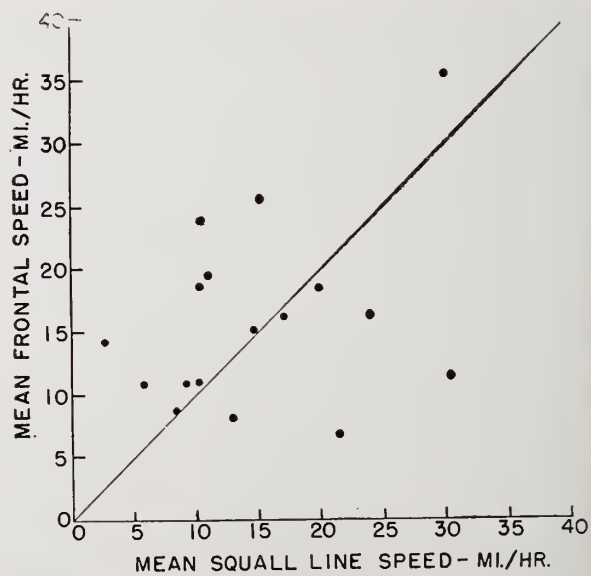

FIGURE 111.—A scatter diagram relating the speed of movement of the squall line to the speed of movement of the front. Based on means of speeds determined from hourly displacements. The correlation coefficient for this distribution is .58.

ordinary synoptic weather map, is frequently observed to last for periods as long as 24 hr., during which it may travel several hundred miles. When viewed on the radar, it was found that there is usually a zone of convective activity comprising several lines and, although the zone may persist for a considerable period of time, the lines within it are constantly undergoing change—new lines forming and older ones dissipating. In an exceptionally long period of continuous radar measurements, one line remained identifiable for a period of 11 hr. This line was very intense and had a maximum solid length of more than 250 mi. at the time of maximum intensity. Shorter lines were frequently observed to have durations of less than 2 hr.

The squall-line element.—The components of the squall line are, of course, the individual echoes indicative of convective clouds which have a sufficiently high water content to return a detectable fraction of the incident radar energy (echo). The term "element" has been applied to any individual echo or group of echoes which is identifiable from one radar observation to the next. The elements in a line ranged from a single isolated echo from 1 to 2 mi. in diameter to a large aggregate of storms appearing on the 'scope as a single, more or less homogeneous echo having a maximum dimension of over 30 mi. The number of separate elements in a line varied, from 4 or 5 small echoes in the early stages to as many as 40 or 50 at the time of maximum echo intensity.

For the most part, elements were found to form and dissipate on a given squall line, suggesting the existence of a preferred line formation. However, there were some exceptions in cases of isolated storms which moved or developed toward a line and became part of it. On two occasions a new line was formed by the splitting of an intense line. In a few cases, two adjacent lines having different orientations tended to merge, showing an apparent "transfer" of echoes from one line to the other.

The direction and speed of movement of the elements of a line were determined by matching the outlines of a particular echo appearing on consecutive 10-minute tracings of the radar echoes presented on the 'scope, and by carrying forward a point representing the position of the center of the element at the time of the first observation. Such a technique was adopted to eliminate, at least in part, the effects of propagation on the measurements of element movement.

For each line, four or five elements spaced along it were selected and their velocities were determined in this manner. The vector mean of the element velocities for each line was then calculated and its direction was plotted against the line orientation in figure 112. A significant feature of element movement relative to the line is that every element considered moved toward a direction which was clockwise from the long axis of the squall line, although never as much as 90°. For practical purposes, this means that a pilot of an airplane flying toward an *approaching* pre-cold-frontal squall line may expect the individual storms in the line to have a component of movement along the line and slightly toward the right.

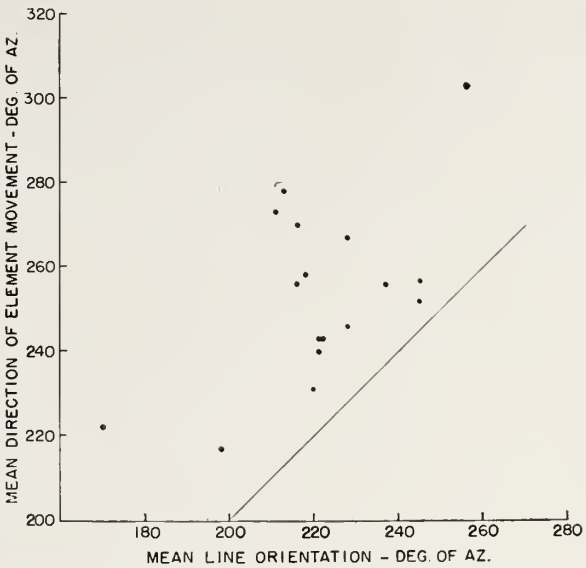

FIGURE 112.—A scatter diagram relating the direction of movement of an element of a squall line to the orientation of the line. Based on a mean of hourly observations of the line orientation and on a mean of the movement of all discrete elements during the period of observation. The correlation coefficient for this distribution is .58.

It was also found that all the elements in the line did not have the same velocity. This was to be expected, especially when the line axis made a large angle with the direction of air flow and when opposite ends of the line were in different wind fields. Variations of the element velocities for any one line were as great as 27° and 14 mi/hr, and averaged 12 deg. and 5.6 mi/hr. One result of these conditions is an increase or decrease of the line length when the components of the element velocities along the line differ. The differences of element velocity also resulted in the rotation of the axis of the squall line.

The squall-line zone.—In an earlier paragraph it was stated that on some occasions the convective activity observed was in the form of several lines of echoes which were roughly parallel. These observations led to the concept of the pre-cold-frontal "squall-line zone" as an area within which the convective echoes were likely to develop, essentially in the form of individual lines[69]. Not all of the pre-cold-frontal convection, however, was in the form of a zone with several lines. In some instances, the echoes

[69] See Pt. Three for a series of examples showing a pre-cold-frontal squall-line zone.

were in the form of one line or a large amorphous mass. Of seven cases of cold fronts within the range of the 200-mile radar set, three had definite squall zones and two had a distribution of echoes which suggested that a zone probably existed. Generally, the individual lines are most clearly delineated during the night or early hours of the day. At the time of maximum diurnal heating the increase in the size and number of convective clouds within the zone made it difficult to identify the individual line formations.

Accurate determination from the radar of the characteristics of the squall zone was precluded by such factors as attenuation and the fact that on some occasions part of the zone extended off the 'scope. Nevertheless, the measurements were made with the understanding that the results would indicate orders of magnitude. The maximum zone widths thus determined for five cases ranged from 110 to 250 mi. and averaged 200 mi. When mean widths for each situation were determined, they were found to range from 80 to 210 mi. and averaged 150 mi.

In most cases the ends of the squall zone extended off the edge of the 'scope, and, as a result, no significant statements of length measurements can be made. Harrison and Orendorf found an average "squall-line" length of 324 mi., with values ranging from 175 to 500 mi. Since the squall line indicated by the surface chart probably closely approximates the squall zone considered here, it is to be expected that the 200-mile-range radar set is often incapable of detecting the entire zone.

If all the squall lines which formed in a particular zone, regardless of the time of formation, are considered, the most frequent number of identifiable lines was three per zone. The maximum number of lines seen at any particular time within a squall zone was five. Measurements of the distance between adjacent lines ranged from 10 to as much as 185 mi.[70]. The areas between lines were frequently intervals of relative inactivity showing nothing but small, isolated echoes in the well-defined situations. This condition was most pronounced in the case of night-time squall lines. With strong heating and related convective activity, the echo coverage often increased to such an extent that the separate squall lines became obscured.

The squall lines within a particular zone usually tended to be parallel, although in some instances relatively large differences in orientation occurred. From maximum variations determined at half-hour intervals for 5 squall zones, it was found that 50 of the 63 determinations yielded maximum angular differences less than 30°, and the mean variation in orientation at any given time was 17°.

[70] The method used for determining this space between two lines having slightly different orientations was to rotate each line around the midpoint of the axis of the line until it was parallel to a line bisecting the angle between the lines.

When making comparison of some of the features of the squall zone and the associated cold front, the long axis down the middle of the zone was considered as the zone. Although such factors as poor definition of the zone boundaries and the attenuation make the location of this axis questionable, it was usable for obtaining orders of magnitude of the separation of front and zone. The mean of such separations obtained from hourly determinations ranged from 115 to 265 mi. and averaged 170 mi. for the five zones observed. The absolute minimum and maximum of the sample considered were 80 and 325 mi., respectively. Generally, there was an area of relative inactivity between the cold front and the trailing edge of the zone; however, on at least one occasion the convective activity extended back to the front itself. These measurements are in general agreement with the findings of Harrison and Orendorf.

The poor definition of the zone in most cases prohibited a meaningful quantitative treatment of such features of the zone as orientation and movement. It must suffice to state that the orientation of the zone showed a tendency to be slightly clockwise from the front and that the movement of the squall zone and front were, in general, in the same direction.

Small-Scale Features of the Squall Line

Since the diameters of individual thunderstorms which form a squall line are much smaller than the spacing between the regular stations of the weather-reporting network, the small-scale features of the squall line normally cannot be studied. However, from the data obtained from the Project micronetwork of recording stations in Ohio, it was possible to make a detailed analysis of a small section along several squall lines.

It has been noted from a study of surface maps such as those given in Part Three of this report that the variations of the surface weather elements with the passage of some squall lines, particularly those which occur in the midsummer, are similar to the variations which occur when a large air-mass thunderstorm passes over a station. The similarity in behavior may be seen by a comparison of the maps of storms observed on August 13, 1947, with those of August 14, 1947 (see maps included in Part Three of this report). The storms on the latter date formed part of a pre-cold-frontal squall line; those of August 13, 1947, occurred on a day when the thunderstorms were not primarily in the form of lines. It is to be noted that on both days, after the thunderstorm had passed over a certain point, the conditions slowly returned to those which prevailed before the arrival of the storms.

The essentially similar surface meteorological conditions and the tendency for them to be more severe with the passage of the squall line than with an air-mass thunderstorm are to be expected in view of the known structure of thunderstorms. The squall line, of course, consists of a number of thunderstorms, each of which contains one or more cells which follows the life cycle presented in chapters I, II, and III. It is shown in chapter III that when rain begins there is outflow of cold air from under the thunderstorm cell which produces a sharp increase of wind velocity, a rise of pressure, and a decrease of temperature as the line of discontinuity (the first-gust line) between the cold air from aloft and the warm surface air passes over a station. The pressure beneath the individual cell rises sharply at the center of the heavy rain and falls as the rain decreases. However, even after the rain has stopped, the pressure over an area as large as four to five times the area of the thunderstorm is above normal, presumably because of the overlying cold-air dome (see ch. III, sec. 4).

Along the squall line there may be many linearly aligned cells which are in a late stage of development and whose downdrafts transport large quantities of cold air from higher levels to the surface. Since the flow from adjacent cells would tend to prevent outflow in the direction parallel to the line, there would be a reinforcement of the cold-air outflow on the leading boundary and an increase of the intensity of the discontinuity. However, as has been shown in chapter III, near the rear boundary of the line, the squall winds oppose the general circulation and, as a result, the surface discontinuity usually is not very pronounced. The large quantity of cold air brought down from higher levels produces a large cold-air dome having an elongated axis parallel to the squall line. The hydrostatic effect of the cold air creates a high pressure ridge roughly parallel to the squall line and just upwind from the line of discontinuity of temperature and wind. The ridge would have a maximum under each of the individual cells (see ch. III, sec. 4). Some of the characteristics of this high-pressure region have been discussed by Williams **[62]**. It is pointed out that the cold air associated with some squall lines (especially those which produce a "cold-front-type pressure trace," table 44) covers too large an area and appears to be too deep to have resulted from the thunderstorm downdraft. In many such instances, the measurements made at the surface and by the radiosondes indicate that a large-scale air-mass discontinuity is involved.

Since there are many sources of cold air in the squall line, each one of them having a somewhat different "capacity," the boundaries of the cold dome are often characterized by undulations. If, for example, a north-south-oriented squall line moving eastward contains a thunderstorm cell with a strong, sustained downdraft located just south of a cell having a weak, short-lived one, the surface of discontinuity moves toward the east and has a wave-like perturbation superimposed on it. Figure 113 presents a schematic drawing of a segment of an idealized squall line which shows these conditions.

Figure 114 presents three surface synoptic charts showing the variations of the surface conditions as a squall line passed over the Ohio network. The following characteristics are to be noted:

1. The marked discontinuities of wind and temperature at the forward edge of the cold air.
2. Perturbations on the surface line of discontinuity.
3. Ridge of pressure behind the line of discontinuity.

These features were also found by Williams **[62]** who has referred to the perturbations as "micro-waves" and the areas of low pressure around the waves as "micro-lows."

A study of the pressure and wind distributions around these micro-lows leads to the suggestion that they may supply the triggering action for tornadoes

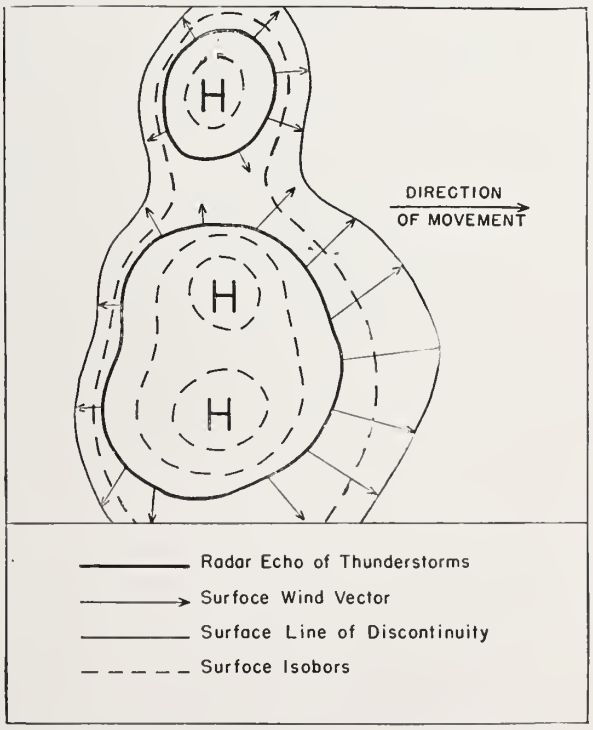

FIGURE 113.—A schematic drawing of a segment of a squall line showing the undulating nature of the boundary surface of the cold-air dome beneath the cells forming the line.

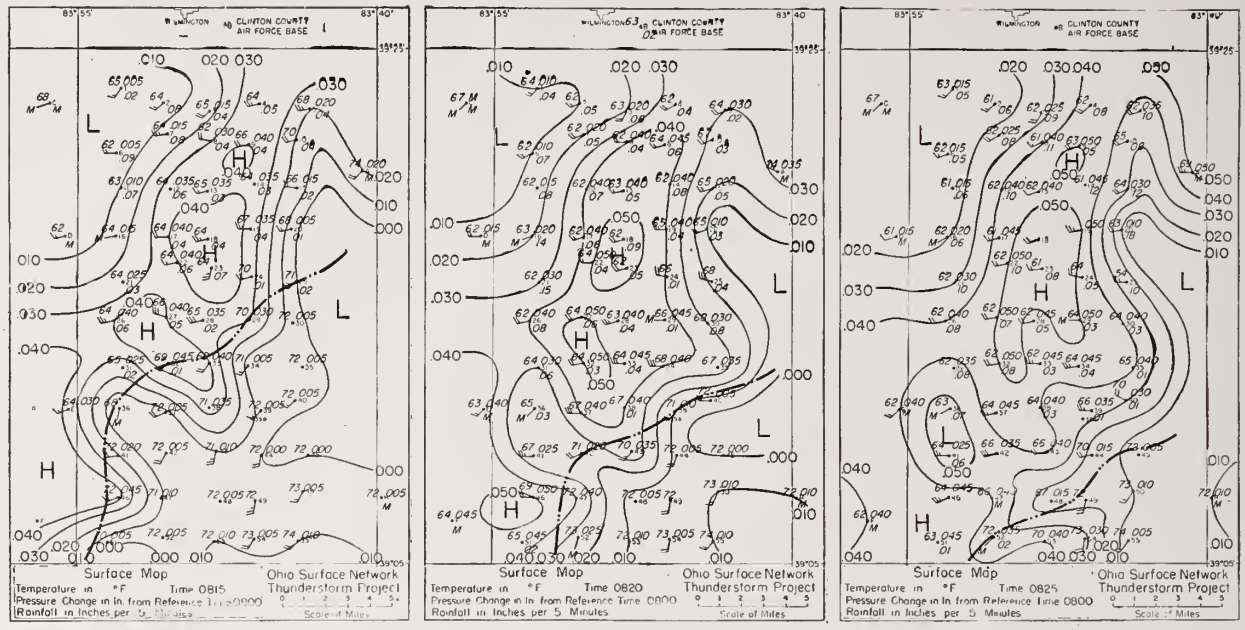

FIGURE 114.—Synoptic charts for the Ohio surface network at 5-minute intervals beginning at 0815 E.S.T., May 29, 1947. Each full wind barb represents two points on the Beaufort scale. The heavy, dotted and dashed line represents the wind-shift line.

which are known to form most frequently along squall lines. The values of convergence in the vicinity of these micro-lows could probably exceed 20 hr^{-1} and must produce extremely strong vertical motions which would lower the pressure at the center of the low. Pressure gradients as high as 2 mb/mi have been observed. Large values of convergence and vertical stretching of the column of air would result in an increase of the cyclonic vorticity initiated by the cyclonic wind shear. The maps of figure 114 and those shown by Williams indicate strong cyclonic circulation around the micro-low. It appears that under the proper conditions, a tornado could eventually form. Williams reports that the damage produced by the squall winds was greatest along the path of the micro-low, which lends support to the belief that the micro-low is the source of a phenomenon having extremely high wind velocities. A detailed investigation of this speculation concerning the possible source of tornadoes is greatly to be desired.

The first-gust line preceding a line of thunderstorms may extend for many tens of miles without breaks. It forms the "pseudo-cold front" which has been mentioned by Harrison and Orendorf and others as one of the most important factors for propagation of the thunderstorm line in a direction roughly normal to itself. The strong convergence at the first-gust line and the lifting induced by the cold dome serve to cause a realization of the latent instability of the lifted air and the formation of convective clouds and thunderstorms. It appears possible that the outrunning cold air, which is restricted to the lowest 5,000 ft. and has a considerably higher velocity than the parent thunderstorm, could result in the formation, not only of isolated thunderstorms, but also of another line of thunderstorms upwind from the initial one.

PART TWO. FLIGHT OPERATIONS IN THUNDERSTORM CONDITIONS

CHAPTER IX. THE THUNDERSTORM AS IT AFFECTS AIRPLANES IN FLIGHT

From studies reported in chapter I, it is now known that the thunderstorm consists of a group of cells in which are concentrated the gustiness, drafts, hail, and other weather elements that make flights through the storm hazardous. The intensity of the disturbed conditions experienced on thunderstorm flights depends largely upon a cell's stage of development and the location of the airplane flying within it. At the present time, a practical way is not available for a pilot approaching a thunderstorm to determine, or be informed of, the number and location of the cells in it and their varying stages of development. In view of these conditions, about the only solution of the problem of thunderstorm flying is the selection of a flight altitude and piloting technique that will give a flight the greatest chance for success.

From its two seasons of observations and studies of thunderstorms in Florida and Ohio, the Thunderstorm Project has been able to outline the major structural features of the thunderstorm (chs. I, II, and III of this report). In addition, the details of the weather elements such as gustiness and precipitation have been measured and tabulated (chs. II and IV of this report). It is the purpose of the following discussion to interpret these meteorological observations in terms of the requirements of aviation.

In this chapter the term "airplanes in flight" is used in a somewhat restricted sense to refer to airplanes in normal cruising flight and not in the process of take-off and landing. In many respects, take-offs and landings may be considered as ground maneuvers. The thunderstorm as it affects these maneuvers is treated in the next chapter.

Size and distribution of thunderstorms.—Data of the Project show that a thunderstorm consists of one or more thunderstorm cells and covers an area ranging from approximately 20 sq. mi. to more than 200 sq. mi. The largest storms contain many cells. In many cases, the tops of well-developed cells extend into the stratosphere, although it was found that the average cell in Ohio does not exceed 40,000 ft. in height. Storms may occur individually or in groups and masses that at times present an almost solid wall of convective clouds.

However, it is well known that most of the low scud and "shelf clouds" which form a part of the cloud mass in the region of a thunderstorm do not extend to very high altitudes. In addition, measurements by the Project show that during *average* airmass thunderstorm conditions, less than 10 percent of the sky is filled with convective clouds at 20,000 ft.; and at 30,000 ft., the cloud cover is less than 8 percent. During periods of *maximum* coverage, such as along strong squall lines, the coverage at 20,000 ft. may be as much as 30 percent, decreasing to 27 percent at 30,000 ft. (A more complete discussion of the altitude distribution of convective clouds is presented in ch. V, sec. 3.) Thus, even with conditions of maximum coverage, it should be possible to plan a flight above 20,000 ft. that would avoid the clouds associated with convective cell cores and, consequently, the most hazardous conditions. This can be done with the help of radar.

Thunderstorm cell structure.—Studies showed that precipitation, gustiness, drafts, hail, and lightning activity are largely features of the individual cell, and that between cells there is a distinct minimum of these hazardous elements. Since the highest concentration of liquid water is within the cell, radar can be utilized to indicate cell location. Thus, there is reason to believe that further development of radar equipment will enable the pilot to make use of it for selecting a flight path through the cloudy air between the cells of a storm, where hazardous conditions will be at a minimum[71].

Thunderstorm turbulence.—Since the hazardous features of thunderstorm flight are associated with the individual cells, it is important for an understanding of the storm as it affects flight operations to be aware of the nature of these features and their variation with stages of cell development. One of these is turbulence. As was pointed out in earlier chapters, the feature of the thunderstorm that flight crews denote as turbulence is actually a combination of gustiness and the effects of drafts. The drafts cause systematic

[71] Many gusts travel considerable distances from the draft areas where they are produced. Therefore, the region between cells is not always devoid of gusts. Project measurements show, however, that there is a distinct minimum of gusts in these areas.

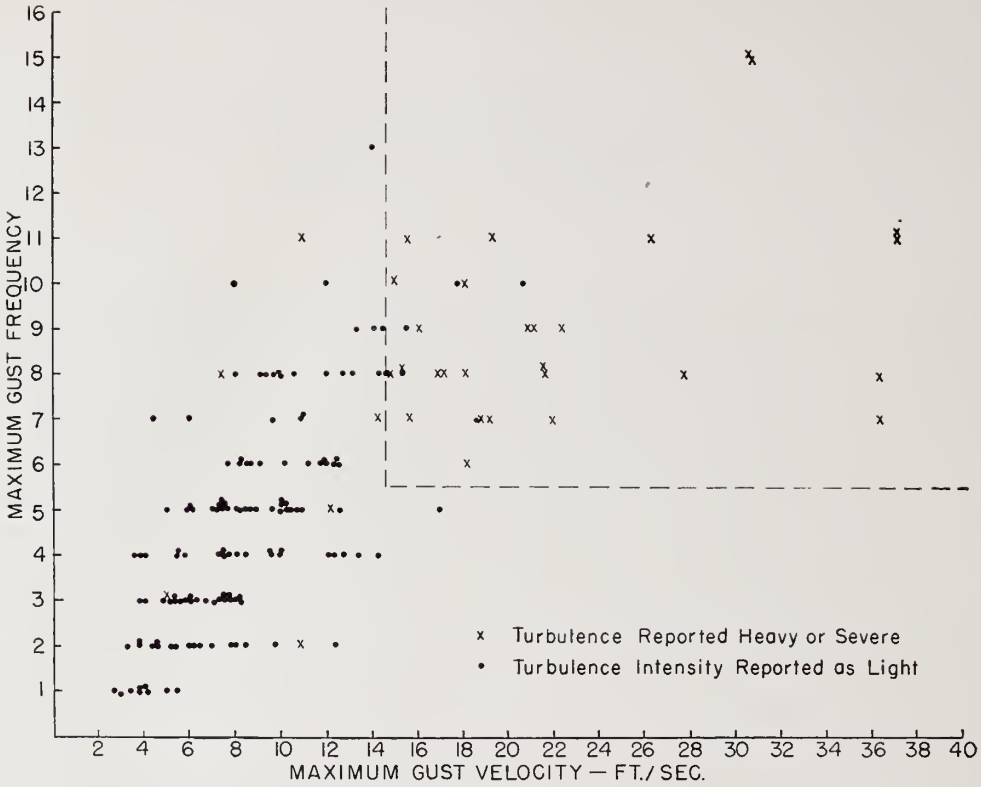

FIGURE 115.—A scatter diagram showing the relative importance of the maximum gust velocity and the number of gusts, within a 3,000-foot interval of flight, in determining the subjective turbulence report during that interval of flight. The area to the right and above the dashed lines encloses that portion of the chart considered representative of heavy turbulence. This diagram is based upon reports of turbulence encountered in Ohio thunderstorms.

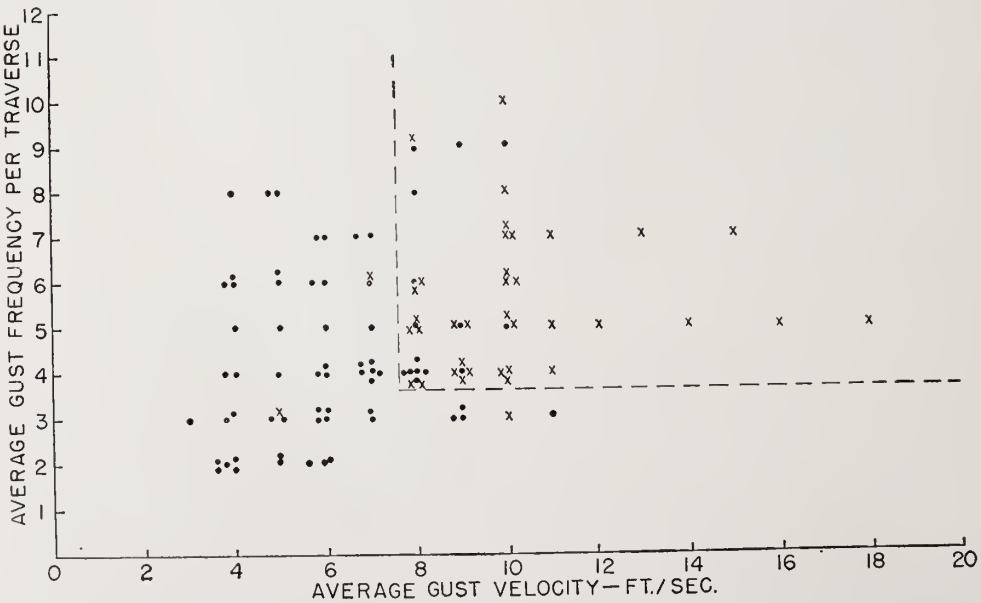

FIGURE 116.—A scatter diagram showing the relative importance of the average gust velocity and the average gust frequency, along an entire traverse, in determining the subjective turbulence report for that traverse as a unit. The area to the right and above the dashed lines encloses that portion of the chart wherein most reports of heavy turbulence would fall. This diagram is based upon reports of turbulence encountered on traverses through Florida thunderstorms.

changes in the altitude of a plane, whereas the gusts cause pitching, rolling, and yawing, and accelerations of the plane without a systematic change in altitude. The following paragraphs describe the contributions of both gusts and drafts to the intensity of the turbulence reported.

In describing turbulence as it may affect flight operations, it is necessary to have some method of denoting the varying degrees which may be encountered. Several turbulence scales have been proposed, but they have not come into general use, mainly because setting up of the standards for them requires information which cannot be obtained by a pilot flying through a storm, or which may be overlooked or intentionally ignored by him in the general state of uneasiness caused by the turbulence itself. Many meteorologists use the classification of light, moderate, and heavy for turbulence without having a clear realization of what constitutes turbulence of various intensities. Most flight crews, too, use these subdivisions, but to them turbulence intensity has some subjective meaning in terms of the airplane response or the degree to which it hinders them in carrying out their duties within the airplane.

From examination and analysis of in-flight and post-flight reports of the Project crews, an attempt was made to arrive at an objective evaluation of the relative importance of various turbulence parameters in determining the intensities of turbulence which were reported. Such a study was deemed desirable inasmuch as it might provide some more objective definition of turbulence intensity, and it appeared worthwhile in view of the fact that the Project pilots had similar levels of flight experience as military instrument pilots. For the purpose of the evaluation, it was assumed that the individual subjective estimates of turbulence intensity made by each pilot were based upon reasonably similar conditions of drafts and gusts.

Through comparison of pilot reports of turbulence intensity during the flights with the measurements of effective gust velocities and gust frequencies the planes encountered, it was found that if the largest gust in a group of several contiguous gusts exceeded about 14 ft/sec, and at the same time the gust frequency was greater than 6 per 3,000 ft. of traverse, the Project flight crews most frequently reported turbulence as "heavy." When the region under consideration was extended to the length of one complete pass through the thunderstorm, it was found that heavy turbulence usually was reported for the traverse as a whole if the mean maximum effective gust velocity per 3,000 ft. of traverse exceeded 8 ft/sec and the frequency exceeded 4 per 3,000 ft. of traverse. Figures 115 and 116 show the relative importance, according to the reports, of other combinations of gust velocities and gust frequencies in producing sensations of various turbulence intensities.

Although the edges of some drafts were sharp enough to have been classified as gusts, investigation revealed that the altitude displacements of the plane which were caused by the drafts were of secondary importance in the pilots' determination of the turbulence intensity. However, it must be remembered that these pilots made a business of flying thunderstorms and were aware of the likelihood of experiencing marked altitude changes as a result of the drafts. Further, most drafts are large enough so that, when intercepted by a plane flying at a speed as low as 180 mi/hr (approximately the speed used by the P–61 pilots), their effects extend over long periods of time and the element of surprise is reduced. On the other hand, if the thunderstorm were flown at a speed significantly greater than that used by the P–61's, more pronounced effects on the airplane would result. Likewise, if the pilot were unaware of the likelihood of encountering drafts, the resulting altitude displacements might cause him to become alarmed and to magnify the effects produced by the draft alone.

Whether or not the turbulence scale found to apply to Project flights would also apply to other airplanes and other flight crews is uncertain. Different airplanes cannot be expected to respond with the same degree of roll or pitch for the same general conditions of gustiness, and it is believed that the angular motions of the airplane (rolling and pitching) must have entered into the classification of the turbulence intensities reported. They are undoubtedly related to the general intensity of the gusts which were reported, although they are not necessarily related to the effective gust velocities measured by the airplane. However, data gathered from the P–61 flights indicated that the reports of turbulence intensity were largely based on accelerations or "bumps" or "jolts" experienced and not on the degree of roll and pitch of the plane.

Turbulence and airspeed.—The use of the effective gust velocity as a measure of the strength of a gust has the advantage that it is a "conservative" property and not dependent upon the airplane affected by the gust. In applying it to a turbulence scale, however, it is important to realize that the acceleration increment produced by a particular gust will not be the same for all airplanes. Actually, it is a function of the airplane's characteristics and the speed at which the plane intercepts the gust. Doubling the airspeed will normally double the acceleration increment[72].

[72] Effective gust velocities are computed from the sharp-edged gust formula, in which the acceleration caused by the gust is directly proportional to the airspeed (ch. II, sec. 1).

Since studies made by the Project indicated that the accelerations induced by the gusts were more important than the rolling and pitching effects in the pilots' determinations of turbulence intensity, it follows that the degree of turbulence found in a thunderstorm is also directly proportional to the airspeed. It was seen that a 15-ft/sec gust was classified as heavy turbulence. Such a gust produced an acceleration of approximately 0.6 that of gravity in the P–61 flying at 180 mi/hr. For the same airplane flying at 300 mi/hr, an equivalent acceleration would result from a gust of 9 ft/sec. By the same standards of turbulence intensity, this gust of 9 ft/sec would be called "heavy" turbulence, although when encountered at a speed of 180 mi/hr it probably would have been called "moderate."

In addition to increasing the severity of turbulence, high airspeeds increase the airframe stress induced by the gusts. In a study made by the N. A. C. A. [**45**] of the experience of three domestic airlines (for a total of 26,834 mi. of flight), it was found that although all three used DC–3 airplanes and flew comparable continental routes, the operational life[73] of the planes on one line was about 10 times longer than that of the other two. It is believed that the difference was due to the fact that the indicated airspeed used in turbulence flying was about 30 mi/hr less in the case of the airline whose planes had the longest operational life. It was concluded that "operating speed in regions of turbulence is of primary importance in the determination of the operational life of airplanes." It is easy to see, therefore, that in order to reduce the stress on the airplane, it is desirable to fly thunderstorms at an airspeed somewhat below normal cruising speed.

Pilot augmentation of gust loads.—Although very few quantitative data on the subject are available, it has been speculated from time to time that the manner in which an airplane is controlled may influence the intensity of the turbulence encountered and the strength of the loads on the airplane induced by the gusts. That this may be true, even though a pilot is attempting to maintain essentially a level flight attitude at a constant airspeed, was pointed out in an earlier paragraph (p. 46). The nature of the minor variations in control technique which causes different pilots in the same region of gustiness to experience different intensities of turbulence and different gust loads is unknown at the present time.

The combination of the effects of the gusts and its augmentation by the pilot is known as the "gust load." American commercial airplanes are designed for a gust load equivalent to that which would be produced by a gust having an effective gust velocity of 30 ft/sec at an airspeed equal to the maximum for level flight. It was seen in a preceding paragraph that gusts of a magnitude much less than this would be classified as heavy by the Project flight crews.

Altitude distribution of turbulence.—Thunderstorm Project measurements showed that there is a distinct minimum of high-velocity gusts near the base of the storm [**8**]; the maximum number of these were found at altitudes greater than 10,000 ft. above the terrain. These facts are brought out in figures 117 and 118, which show the number of miles it was necessary for the planes to fly in thunderstorms[74] for them to encounter gusts greater than a given speed. Although the data include measurements up to only 26,000 ft. (m.s.l.), there is considerable evidence that there are many strong gusts at even higher altitudes in the storms. From the RHI radar 'scope it was possible to obtain rates of growth of the cloud top, which, at certain stages of development, is thought to ascend at the rate of the updraft within the cloud. These measurements indicate that strong drafts exist at altitudes considerably greater than the highest level of

[73] Flight time, in hours, required for an airplane to exceed the limit load factor.

[74] The data from Florida also include a few miles of flight in the immediate vicinity (1 or 2 mi.) of thunderstorms.

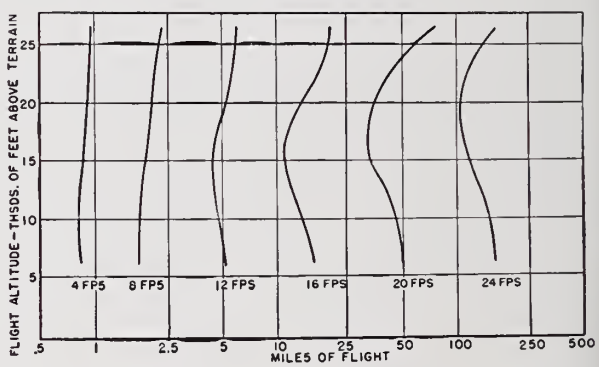

FIGURE 117.—A chart showing the miles of flight necessary in thunderstorms to encounter a maximum gust greater than indicated. These curves are based upon data gathered on flights through Florida thunderstorms.

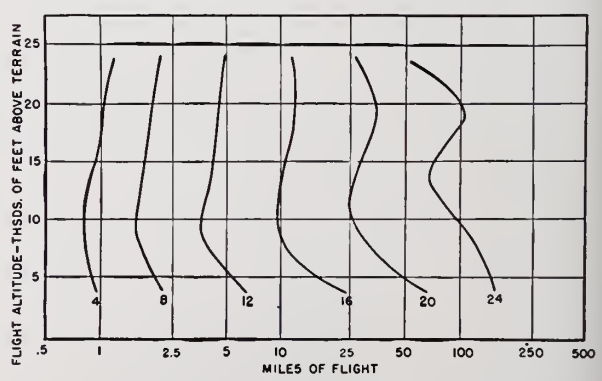

FIGURE 118.—A chart showing the miles of flight necessary in thunderstorms to encounter a maximum gust greater than indicated. These curves are based upon data gathered on flights through Ohio thunderstorms.

flight on the Thunderstorm Project. Since it has been shown that there is a relation between the speed of the draft and the speeds of the gusts encountered (fig. 34), it might be assumed, lacking more conclusive data, that the mean gust velocities increase with height in a thunderstorm cell up to an altitude of 5,000 ft. to 10,000 ft. below the top of the cloud. This would be true, at least, for the cumulus and mature stages of development.

Because gust speeds are indicative of turbulence intensities, it must be concluded that, on the average, the least severe turbulence will be encountered by planes flying the lower levels of a thunderstorm, particularly near or below the cloud base. Although the Project investigations were restricted to Florida and Ohio, it is believed that there is sufficient reasonableness in the data obtained to allow an extension of this conclusion to storms of other regions and other seasons. It is important to point out, however, that even though the turbulence at these low levels is at a minimum, it is frequently strong enough to be classified as "heavy to severe."

Drafts within the cloud.—As has been stated, drafts are of secondary importance in the determination of turbulence intensity; however, they are of considerable importance because of the altitude displacements which may result when an airplane flies through them. This displacement depends upon the draft width and speed, and upon the forward speed of the airplane. For an airplane flying at 180 mi/hr, the displacement is not likely to exceed 2,000 ft., although in exceptionally severe storms, such as those flown by the Project on August 22, 1946, and August 5, 1947, upward displacements as great as 5,000 ft. may occur. Project experience indicated, however, that displacements of this extreme magnitude are rare: only 2 percent of all updrafts encountered caused displacements greater than 3,000 ft.; and the maximum downward displacement was about 1,400 ft. In general, the drafts encountered by Project airplanes were such as to indicate that the altitude displacement an airplane is likely to experience increases with height.

Approximately half of all drafts encountered caused displacement greater than 500 ft. Thus, if a pilot attempts to stay within the airspace assigned for his flight, he will find it necessary to apply corrective action to reduce this altitude change in approximately half of all drafts encountered (table 46). It is unfortunate that such action is necessary in view of the fact that the resulting maneuver loads add to the gust loads applied to the airframe. Furthermore, the attitude of the plane resulting from attempting to combat the effects of the draft may lead to an inadvertent stall, or to a dive which may result in an increase in airspeed. For these reasons, many of the pilots of the Thunderstorm Project considered the drafts in thunderstorms potentially more hazardous than the gusts.

Downdrafts below the cloud base.—A very important part of the thunderstorm is the cold downdraft that is found in the area of heavy rain. This downdraft continues below the base of the cloud and may, under certain circumstances, constitute a definite aeronautical hazard. As it approaches the ground it spreads out, as would a jet of water directed toward a flat plate, and forms a layer of relatively cold air over the surface. This layer is approximately 3,000 ft. thick during the time when the downdraft of the storm is well developed (see p. 54). Figure 40 (p. 54) indicates the general motions of the air in the cold dome of a typical thunderstorm. In the immediate area of rain, the downdraft possesses considerable downward momentum and may approach much closer to the ground than might be expected from considering the depth of the cold air layer that it forms. Measurement by the Project indicated that significant downdrafts may exist at altitudes less than 1,000 ft. above the ground.

The only place where the downdraft beneath the cloud base is likely to have a speed great enough to be hazardous to airplanes is in the rain core. On August 7, 1947, a Project airplane flying below the base of a thunderstorm found a downdraft of approximately 14 ft/sec on two traverses less than 1,500 ft. above the ground. From surface measurements made at the same time, it was found that the rain averaged approximately 0.1 in/5 min, reaching 0.3 in/5 min as a point maximum. It might be expected that when a repetition of these surface rainfall values occurs, in other thunderstorms, they might be associated with similar significant downdrafts in levels between the cloud and the ground. Studies of the data measured by the surface network of the Project indicate that approximately one-half of all thunderstorms in

TABLE 46.—*Percentage of thunderstorm drafts encountered by Project P-61C airplanes, which caused altitude displacements of more than 500 ft. (based on N. A. C. A-evaluated records for planes flying various altitudes of traverse during both seasons of Project operation)*

Flight altitude (ft., m.s.l.)	Florida, 1946		Ohio, 1947	
	Updrafts	Downdrafts	Updrafts	Downdrafts
	Percent	*Percent*	*Percent*	*Percent*
5,000 or 6,000	28	27	30	58
10,000 or 11,000	48	7	33	18
15,000 or 16,000	45	23	50	18
20,000 or 21,000	42	34	57	34
25,000 or 26,000	61	53	53	40
Mean	45	29	45	32

Florida and one-fourth of all storms in Ohio have surface rain intensities of this magnitude and, therefore, in all probability, would have significant downdrafts in the area of heaviest rain beneath the cloud base.

The distance that an airplane will be carried downward in flying through the downdraft area beneath a storm depends upon the extent and speed of the draft and the forward speed of the plane. From measurements of draft extent (p. 42), and from considerations based upon the sizes of cells, it is not considered likely that an airplane will encounter a downdraft extending more than 3 mi. In such a draft, having a speed of 20 ft/sec (almost twice that measured on August 7, 1947), an airplane flying at 180 mi/hr would be displaced downward about 1,200 ft., provided that no corrective action were taken by the pilot in the 60 sec. that it would take the plane to traverse the draft. Although more than one draft may be encountered beneath a storm if the plane enters the rain areas from two separate cells, studies of storm structure indicate that it is not likely that two downdrafts would be separated by less than 3 mi.

From these data, it is concluded that a pilot flying in the rain areas under thunderstorms may expect downdrafts ranging up to 20 ft/sec or more, depending upon the altitude above the terrain at which a flight is made. With consideration of the speed and width of the downdrafts and the speed of modern military or commercial airplanes, it seems unlikely that a plane could be carried downward more than 1,500 to 2,000 ft. by the action of a downdraft alone, although light planes with relatively slow forward speeds may be carried farther downward. The downdraft probably reaches its maximum width at altitudes less than 2,000 ft. above the ground, but at this level its speed should be relatively low. Under these conditions, a plane flying in this region might be carried downward at a slow rate for a considerable period of time, making it possible for the pilot to institute some corrective action to reduce the effects of the draft. However, it is well to point out that a pilot attempting such corrective action may place the plane in a sufficiently nose-high attitude that a gust could cause it to stall. Gusts in the lowest few hundred feet under the cloud may, under certain conditions, be as strong as those at higher altitudes in the storm.

Hail.—Hail is regarded as one of the worst hazards of thunderstorm flying. In the flights through storms in Ohio, hail was encountered on 51 of the 812 traverses. A thorough analysis of the collected hail data was made, and it was found that hail usually occurs during the mature stage of cells having an updraft of more than average intensity. This is not surprising, since the formation of hail requires large quantities of liquid water and strong updrafts to delay the fall of the hail nucleus sufficiently long for it to acquire a thick coating of ice. Further, it was found that the maximum occurrence of hail in Ohio storms is at the 10,000- and 15,000-foot levels. No relationship between hail occurrence and the color of the cloud or a peculiar shape or intensity of the radar echo from the cloud could be found.

Because hail is such a great hazard, it might have been desirable for the Project to have conducted its operations closer to the maximum hail region in the United States. There can be little question that the frequency of hail in thunderstorms of the Kansas–Colorado region is higher than that found in the Ohio thunderstorms. This presents the interesting possibility that the draft speeds, and, as a consequence, the gustiness of storms of this region may be greater than those found in the Ohio storms.

On the basis of Project data, it might be concluded that the bigger the storm, the more likely is the pilot to encounter hail. If, however, he can avoid the active portions of the cells, the frequency of his encountering hail will be greatly reduced.

Icing.—There were too few instances of icing encountered in the Project flights to permit conclusions as to how or where to fly to avoid this hazard. Indications were that the lack of icing in the Project flights resulted from the fact that the speed of the planes did not allow them to remain in the cell core, where high liquid water concentrations are found, long enough to pick up a heavy coating of ice. On July 22, 1946, a Project sailplane, spiraling upward in an updraft region of a cell, iced so heavily that the pilot lost the use of the elevator control surfaces. In this instance the sailplane had been in the cloud above the freezing level about 12 min.

Lightning.—The generation of strong electrical potential gradients is a characteristic phenomenon of the thunderstorm. When the gradient exceeds a certain critical value, dependent upon the air density, number and size of water drops, etc., a crash discharge occurs. This discharge is known as lightning. An airplane flying through a thunderstorm may be struck by such a discharge. Another more frequent electrical phenomenon observed from airplanes is the brush, or corona, discharge. Frequently the airplane itself picks up a charge as a result of solid precipitation forms striking it. This induced charge on the airplane may become great enough to cause discharges from points of charge concentration such as the propellers, nacelle tips, wing tips, nose, and tail. On other occasions the induced charge on the plane acts to strengthen the effect of the electric field in the cloud, and a resulting crash discharge may use the airplane as a part of the conducting path.

Since considerable damage can result when an airplane is struck by lightning, it is only natural that there have been many laboratory and flight investigations for the purpose of more accurately defining the hazard and developing remedial measures. Two such investigations have been conducted—by the National Advisory Committee for Aeronautics, Subcommittee on Lightning Hazards to Aircraft [**29**], and the Army/Navy Precipitation Static Project [**2**]. Laboratory experiment has indicated that potential gradients of the order of magnitude of 1,000,000 volts per meter are required to produce a crash discharge. On the other hand, under certain conditions, brush discharges reaching crash proportions may occur when the potential gradient reaches a few hundred volts per meter. Either of these two discharges may be called "strikes" when an airplane is involved.

It was the desire of the Thunderstorm Project to tie in the measured electric field with the structural picture of the thunderstorm. For this purpose, electric field meters were installed in the P–61's for the Ohio flights. Unfortunately very few usable data were obtained, primarily because of malfunction of the meters. There was evidence, however, that the presence of the airplane itself is important in bringing about lightning discharges. A total of 21 strikes were reported during the two seasons of flying. Many of them were the only lightning seen on a traverse, which might indicate the importance of the airplane in bringing about the discharge.

As would be expected from the results of previous investigations, most of the lightning strikes reported by the Project pilots occurred at the 15,000-foot level. Strikes were comparatively rare at the lowest flight altitudes. The data also indicate that electric fields measured at a distance sufficiently far from the cloud to allow the pilot to take evasive action cannot give forewarning of impending strikes. Project data, however did not lend themselves to an analysis which would uphold the results of other studies which have indicated that the number of strikes encountered is a function of the airspeed of the plane. Nor were they adequate to check the often-repeated statement that the stage of development of a thunderstorm cell can be determined from the direction of the lightning strokes observed. It does appear that lightning is not found in a cell until the top of the cell reaches a height where the temperature is less than —20°C. (p. 89). Prior to that time it may contain drafts and turbulence of major concern to a pilot; it therefore appears that he should not rely on lightning to give warnings of thunderstorm conditions.

Roll cloud.—The roll cloud, a horizontal vortex of air and cloud particles near the base of a thunderstorm, has been of great interest to aviation because of its visible motions and turbulence. Project data indicated, however, that it does not occur with every thunderstorm. In two years of observations there were five reports of this phenomenon. Four were from observers stationed in the surface network for the purpose of making and recording visual observations. On one afternoon the roll cloud was reported by two of them stationed about 10 mi. apart. Two of the four reported roll clouds were associated with storms along a pronounced squall line. The fifth report was from a pilot flying the 5,000-foot level over Ohio.

The cause of the roll cloud probably is to be found in the shear between the updraft and the downdraft. It probably does not differ materially from other vortices which form in this shear layer at higher levels. Since a minimum of heavy turbulence was found at the lowest levels of Project flights, indications are that the roll cloud is not as severe a flight hazard as has sometimes been thought. This leads to the conclusion that the roll cloud is held in awe only because it is strikingly visible, and that it is only a foretaste of what is to be found inside the cloud.

Interrelation of precipitation and turbulence.—As was pointed out in previous reports of the Project [**8**], it has been found that the greatest turbulence in the thunderstorm is found to be associated with the highest water concentrations. This relationship was found to hold at all levels within the storm. The association obviously results from the fact that the gusts are largely induced by the drafts, and it is in the updraft that large quantities of water vapor are converted into liquid water, which, when it falls to the ground as rain causes a vigorous downdraft to develop. These associations further show the interrelationship between the cells and the weather elements found within them.

Radar and thunderstorm flying.—Radar is, without question, one of the best instrument aids to thunderstorm flying currently available. Analysis of Project data indicated that the maximum turbulence and drafts are coincidental in space with regions of high water content, and consequently are within the area delineated by the radar echo. It was found that most of the turbulence in the storms flown was confined to the area delineated by the radar echo presented on the 'scope of the control radar on the ground. In many instances there were light parts of the echoes, indicative of the presence of lesser amounts of liquid water. Since such areas were frequently at the boundaries of the cells, it was concluded that they indicated a region of minimum turbulence. Until more detailed measurements of this nature are available, it seems wise to advise the pilot to fly the areas indicated by weak spots on the radar echo to avoid the most severe turbulence. Radar is particularly useful also

for planning flights at higher altitudes, where it is known that there is considerably greater distance between convective centers (p. 98) than at low altitudes. In daylight these open areas might be visible, but they are not visible in darkness or in the presence of enshrouding cloud layers. In such cases, indications from the radar equipment should enable the pilot to select a flight course which will completely avoid turbulent areas.

The use of radar is not limited to the selection of areas of minimum turbulence, however. From a radar 'scope, cloud positions, size, and orientations can be determined. If it then becomes necessary to fly through a thunderstorm, the length of time that the plane will be in the storm can be determined. In the case of squall lines, it is possible to pick a route that will take the plane through the line in the least time and will result in its encountering the least turbulence. Project data indicated that even in intense squall lines it is seldom that the cells are so close to one another that a pilot could not find a flight path through it without having to detour excessively from his original flight plan. If his plane is equipped with a radar set having a reasonably long range and plan-position indicators, the pilot may observe the structure of the squall line while still many miles away and take action to plan his penetration or circumnavigation with a minimum loss of time.

CHAPTER X. THE THUNDERSTORM AS IT AFFECTS GROUND OPERATIONS

The most important thunderstorm phenomenon likely to affect airplanes at the time of take-off or landing (considered as ground maneuvers) is the gusty surface wind associated with the outflowing of the cold air from the downdraft. Such surface-wind fluctuations may reach an intensity comparable to the gustiness within the thundercloud itself, yet there is almost no published material on the nature of these fluctuations and their effect on airplane operations. The importance of considering these surface-wind fluctuations was pointed out in earlier reports of the Project [**56**], where considerable attention was devoted to the nature of the sharp wind change accompanying the passage of the discontinuity zone at a station.

From the Project's continuous records of surface wind speed and direction, computations were made of the peak wind speeds which occurred with the passage of the discontinuity zone, and of the effective first-gust velocity—which was defined as the difference between the previously prevailing wind and the velocity component of the first gust along the previously prevailing wind direction. The value of the concept of the effective first-gust velocity lies in the fact that it is also the airspeed change that an airplane would be subjected to if it were just taking off or landing as the first gust passed. Values of the peak gust speed and the effective first-gust velocity occurring with the passage of the discontinuity zone are shown in figures 119 and 120.

Further analysis showed, however, that in many respects the data contained in these figures were not adequate to describe the wind fluctuations likely to be encountered by airplanes taking off and landing, primarily because the Project wind measurements were all made within 20 ft. of the ground, whereas data obtained by other investigations showed that maximum wind fluctuations occur considerably above this height. Measurements of the winds in the lower 350 ft. of the atmosphere have been obtained from a tower operated by the Daniel Guggenheim Airship Institute at Akron, Ohio. Although the number of measurements made from the tower during thunderstorm conditions was limited, it has been possible to combine these data with those from the Thunder-

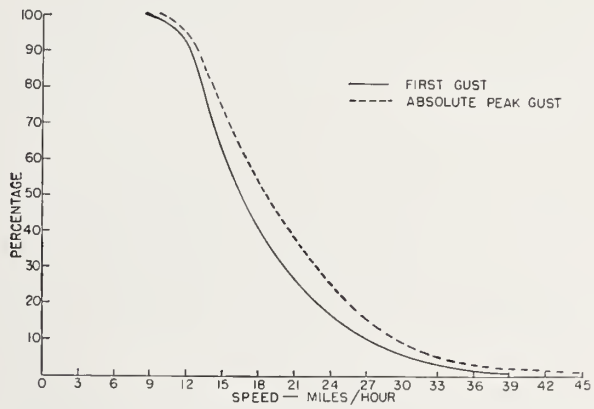

FIGURE 119.—A graph showing the cumulative percentage distribution of first gust and absolute-peak gust speeds greater than the indicated amount. The absolute-peak gust is the highest wind speed measured during the period following the first gust.

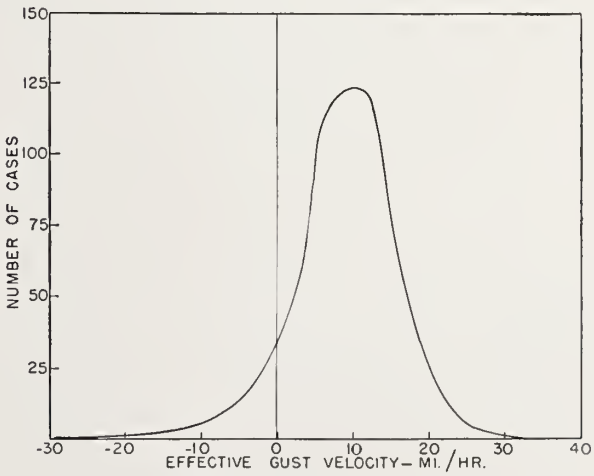

FIGURE 120.—A graph showing the frequency distribution of the effective first-gust velocity. The negative velocities would result in a decrease of airspeed; positive velocities would result in a gain of airspeed.

storm Project to arrive at the more complete picture of the wind conditions under a thunderstorm[75].

Turbulence in the winds near the earth's surface.—The region of minimum turbulence found at the lowest levels of the thundercloud probably extends down below the cloud base to a level a few hundred feet above the surface. In the lowest few hundred feet of the air, however, there is an increase in the turbulence, brought about by the effect of terrain roughness on the winds near the surface. The height to which this effect extends depends upon the speed of the winds and the nature of the terrain. Over comparatively smooth terrain, such as that of the surface network in Florida and Ohio, this low-level turbulence appears to reach a maximum in the lowest 100 ft. This can be seen from figure 121, prepared from the tower data, which shows the wind speeds and general gustiness associated with the passage of a fairly intense discontinuity zone. Immediately evident from this figure are the marked fluctuations in the winds at the 40-foot level. The magnitude of these fluctuations decreases at successively higher altitudes. If an airplane like the P–61 encountered the maximum gust shown in figure 121, it would experience an airspeed increase or decrease of 30 mi/hr, and, if it is assumed that the gust was isotropic, and had a horizontal extent approximating the span of the plane, the resulting acceleration would be equivalent to an effective gust velocity of approximately 20 ft/sec.

[75] Dr. P. O. Huss, University of Akron, kindly supplied the Project with data from this 350-ft. tower.

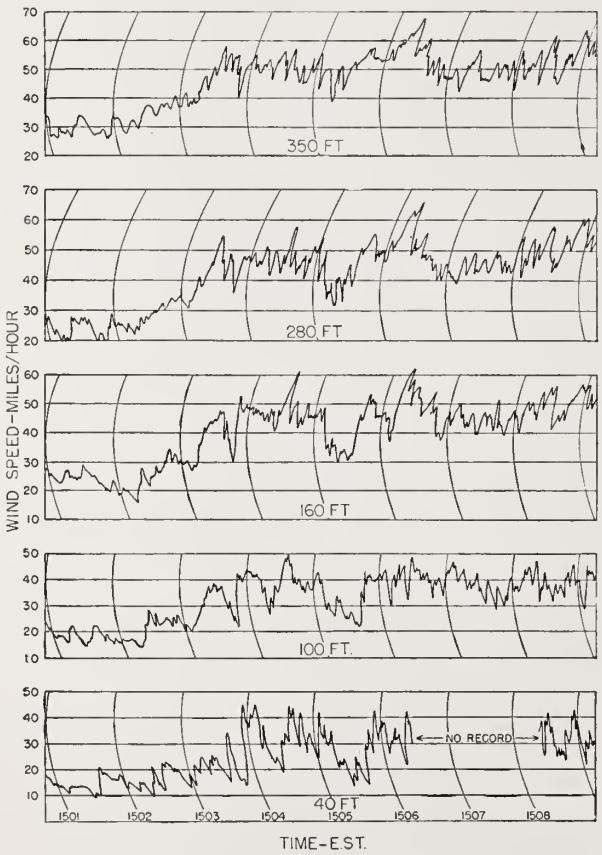

FIGURE 121.—A reproduction of section of records of instantaneous horizontal-wind speeds measured simultaneously at the levels (above the ground) indicated. During the period shown, a discontinuity zone associated with a thunderstorm passed the observation tower. (Based on data loaned by the University of Akron.)

Finding gusts of this magnitude near the surface follows the experience of pilots who have found that in thunderstorm conditions the turbulence in the lowest few hundred feet can be quite severe. The reason for gusts at such low levels is that the earth's surface forms a rigid boundary which serves to cause local accelerations in the surface wind and strengthening of the gusts which result from the vertical shear in the horizontal outflow. As a result of such strengthening, wind speeds (in gusts) exceeding 90 mi/hr are occasionally observed in thunderstorm conditions (without tornadoes). Although a means of direct comparison between the strength of surface gusts and the strength of gusts measured by the Project airplanes is not readily available, it seems reasonable to conclude that, under certain conditions, the speeds of the gusts near the surface may approximate those found within the thundercloud. Fortunately for the aviator, the conditions necessary for the formation of these extreme surface gusts are relatively infrequent. It appears that it is only near the discontinuity zone, which everywhere separates the cold outflow air from the environment air (see p. 55), that the surface winds are strong enough to cause gusts of a size to be of major concern in airplane operations. Probably not over one storm in 100 would have surface gusts of the strength shown in figure 121. Since they are induced partly by accelerations caused by terrain obstacles, it is expected that they would be found most frequently at locations where the outflow wind passes over obstacles like low hills, large groups of trees, and large buildings.

Project measurements showed that the maximum surface outflow winds occur on the downwind side of the thunderstorm at the time and place where the downdraft first reaches the surface. The data indicated that this occurs approximately 5 min. after the start of heavy rain from a particular cell. Therefore, great caution in landing and take-off is advisable when a new thunderstorm development is near the upwind side of an air terminal.

On the basis of Project data, it appears unlikely that strong gusts will occur after a discontinuity surface has traveled 4 or 5 mi. from the thunderstorm. However, it must be realized that a favourable location for new cell development is over the dome of

cold air flowing out from the rain area and, therefore, the downdraft from a new cell, several miles downwind from an older one, may cause a new area of severe low level turbulence. Since it is highly unlikely that such a downdraft could occur from a cell too weak to give a radar return, radar can be used as an aid in anticipating gusty surface winds.

In order to cope with the problem presented by the outflow from thunderstorms, it seems desirable that every tower operator be well-versed in the ways of the thunderstorm. With adequate preparation and continuous observation, the passage of the discontinuity surface can be anticipated. Because of movement and continual development of the storms, it cannot be expected that a weather station can give adequate warning of these winds unless, of course, provision is made to place the weather station in a commanding position for observation and to provide sufficient personnel and equipment to permit continuous observation while storms are in the vicinity.

To aid airplane pilots and base personnel in combating the hazards of these sudden fluctuations in the surface winds, the following items are enumerated. They are based upon the analysis completed by the Thunderstorm Project and covered elsewhere in this report.

1. The marked change in the surface wind accompanying thunderstorms occurs along the edge of the outward-flowing cold air which has come down as the downdraft in the rain area.
2. The downdraft, and consequently the gusty surface winds, first appears shortly after the start of heavy rain from a particular cell.
3. A ring of high gusty winds spreads outward from the cell, the speed of advance being greatest in the direction of the prevailing wind flow.
4. The maximum gust speeds associated with a given cell occur very close to the rain area from it and at the time when the downdraft first reaches the ground. Therefore, the more distant the storm, the less violent the surface gusts. A station near the center of a cell at the time when the downdraft reaches the surface may experience gusts of a magnitude comparable with the most severe found within the storm itself.
5. The wind will invariably blow outward from the rain area after the passage of the discontinuity surface.
6. The strength of the gustiness at any particular location decreases after the passage of the discontinuity surface. An airplane whose take-off is delayed approximately 5 min. after the passage of the first gust will not encounter exceedingly heavy turbulence in the surface air layers. It must be remembered, however, that this take-off, if made into the wind, will take the airplane toward the region of the thunderstorm downdraft.
7. The maximum turbulence in the surface winds occurs in the lowest few hundred feet.

Surface pressure changes and altimeter errors.—During a thunderstorm, rapid surface pressure variations can occur. The typical pressure sequence associated with a thunderstorm passage over a particular station is the falling of pressure ahead of the storm and under the updraft; a sharp pressure rise accompanying the rain; followed by a return to the previous pressure after the rain subsides. Occasionally after the storm, the pressure falls below normal and then rises to the normal. In a majority of cases this sequence of pressure changes occurs within a 10- to 15-minute interval.

By means of Project measurements, a study was made to determine whether these pressure changes are enough to prove hazardous in airplane operations. The results are shown in tables 47 and 48. Table 47 shows that in 22 percent of the cases if a pilot had landed during the rain (time of maximum pressure), using an altimeter setting given him only a few minutes earlier, his altimeter would have indicated that he was 60 ft. or more below his true altitude. Of

TABLE 47.—*Frequency distribution of altimeter readings lower than true altitude values due to error resulting from pressure rises (based on surface pressure measurements made beneath Ohio and Florida thunderstorms)*

Interval of altimeter error (ft.)	Number of cases	Percentage of cases
0–19	18	37
20–39	14	29
40–59	6	12
60–79	6	12
80–99	5	10
100 or more	0	0

TABLE 48.—*Frequency distribution of altimeter readings higher than true altitude values due to error resulting from pressure falls (based on surface pressure measurements made beneath Ohio and Florida thunderstorms)*

Interval of altimeter error (ft.)	Number of cases	Percentage of cases
0–19	25	51
20–39	11	23
40–59	5	10
60–79	3	6
80–99	3	6
100 or more	2	4

greater concern, however, are pressure-altitude readings which would be too high. If a pilot had used an altimeter setting given him during the period of maximum pressure and landed after the pressure had fallen, on 26 percent of the days he would have found his altimeter still reading 60 ft. or more above his true altitude after he was on the ground. On two days his altimeter would have read more than 140 ft. too high (table 48).

Since these data, based on two years of measurements, were considered insufficient to provide a good statistical picture of the pressure changes which may occur during thunderstorms, barograms were obtained for a period of 10 yr., 1938 through 1947 inclusive, from each of 10 cities in widely scattered parts of the country. From these barograms the larger pressure variations due to thunderstorms were tabulated, using the following criteria for selection of cases to be considered in the study: (1) The pressure change must have taken place at a rate equal to or exceeding 0.03 in/30 min; and (2) the total magnitude of the pressure change must have equalled or exceeded 0.03 in. With these limitations, the number of thunderstorm days that could be considered ranged from 25 percent, at Los Angeles, to 75 percent, at Kansas City, Mo. (fig. 122).

Although it was desirable to distinguish between the sharp rise which is frequently associated with the heavy thunderstorm rain (pressure nose), and the more gradual rise which extends over a longer time interval (pressure dome), in this study no such distinction could be made.

The magnitude of the pressure changes and the resulting altimeter errors which occurred at these 10 cities within the selected period were tabulated and are summarized (fig. 123). It is evident that of the 1,989 cases of pressure rise included, 5 percent were greater than 0.10 in., while 43 percent were greater than 0.05 in. Of the 1,156 cases of pressure falls, 10 percent were greater than 0.10 in., while 45 percent were greater than 0.05 in. It can be seen that the altimeter would read 100 ft. above the true altitude in 8 percent

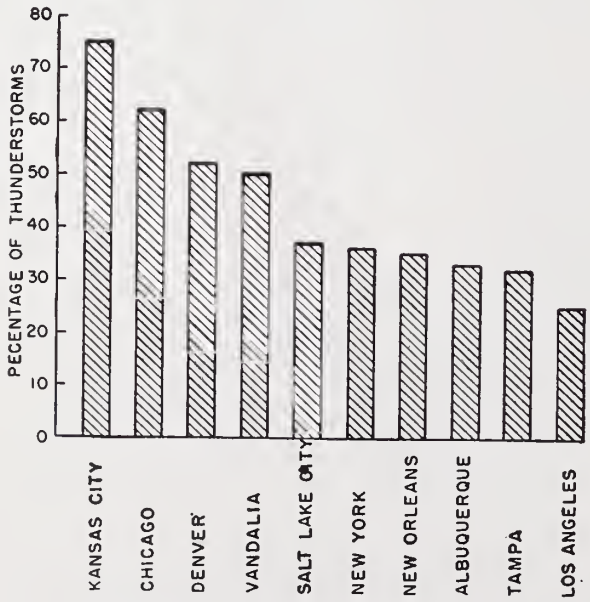

FIGURE 122.—A diagram showing for 10 locations the percentages of thunderstorms that produced marked pressure changes.

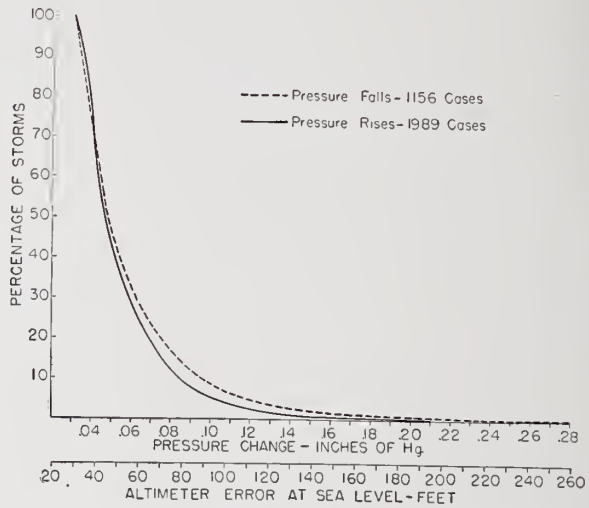

FIGURE 123.—A chart showing the cumulative percentage distribution of pressure changes and resulting altimeter errors produced by thunderstorms. Curves based on 3,145 cases of pressure change occurring at 10 cities during a 10-year period.

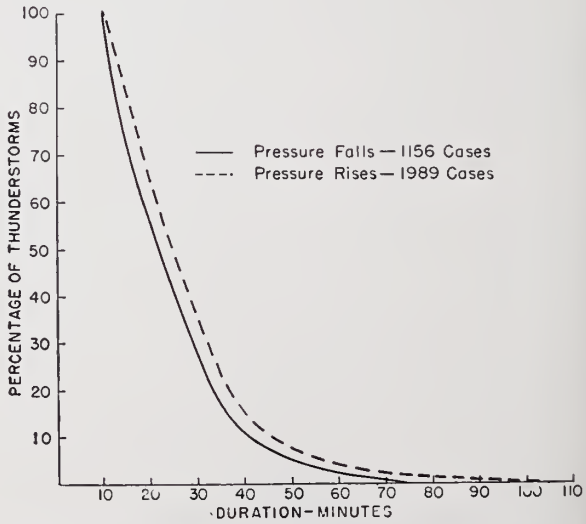

FIGURE 124.—A chart showing the cumulative percentage distribution of the length of time the pressure was rising or falling in periods of thunderstorm conditions. Curves based on 3,145 cases of pressure change occurring at 10 cities during a 10-year period.

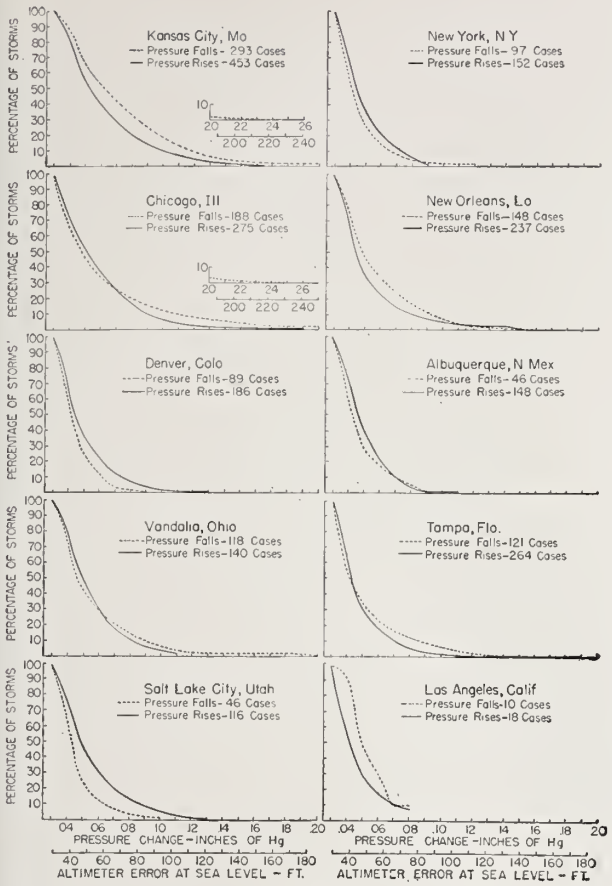

FIGURE 125.—Charts showing the cumulative percentage distributions of pressure changes and resulting altimeter errors produced by thunderstorms. The data for each city is based upon a 10-year period.

of the cases and 100 ft. below the true altitude in 5 percent of the cases. It is evident from figure 124 that 80 percent of the pressure rises and 72 percent of the pressure falls took place in less than 30 min.

The corresponding data for the individual cities are shown in figure 125. In this figure the solid line denotes the percentage frequency of the number of cases in which the altimeter would read *below* the true altitude of the airplane. It is interesting to note that the percentages of pronounced pressure changes are much larger for the storms at Kansas City and Chicago than for the more tropical cities such as Tampa, or for arid cities like Albuquerque, Salt Lake City, and Los Angeles.

Caution is advised in the interpretation of these charts inasmuch as there is the tendency to exaggerate the percentage frequency of the hazardous pressure changes in thunderstorms. It is to be emphasized that these charts are based on the more violent pressure changes whereas relatively insignificant pressure changes were omitted from the study. A possible source of error in this study must be noted, since pressure traces for the actual times at which thunderstorms occurred were not used. Instead, marked pressure rises were used to indicate the times of the thunderstorms. Some of the pressure rises may not have been due to the thunderstorms occurring on the days in question but may have been due to some other disturbance. However, it is the opinion of the analysts that the greater majority of the pressure fluctuations considered were actually due to thunderstorms.

PART THREE. EXAMPLES

INTRODUCTION

In order to present some of the material from which the conclusions given in the foregoing chapters have been derived, several complete sets of thunderstorm observations made during Project operations are included in the following pages. The data selected for this presentation include: (1) the analyzed results of observations made during the occurrence of five thunderstorms, and (2) three sets of reproductions of radar-'scope photographs which demonstrate the characteristics of squall lines. The sets of analyzed data from two of the thunderstorms (July 9, 1946; August 14, 1947) provide examples of information obtained from two sources, namely, the stations of the surface network and the airplanes which probed the storms. With these complete data it is possible to illustrate the features of thunderstorm structure and circulation and the variations in the meteorological elements measureable at the surface beneath the storm. Data obtained only from airplane penetrations of two more storms (August 6, 1947; August 21, 1947) are illustrative of special features of these particular storms. Still other special features are apparent in the analyzed surface data of a single additional storm (August 13, 1947). The squall-line examples comprise photographs taken of the 200-mile-range radar-'scope presentations for the following dates: July 14, August 14, and September 5, 1947.

The instruments used to obtain the measurements presented in this section are fully described in the appendix, and the techniques used to prepare the data for analysis were outlined in the several sections of the preceding chapters.

Method of presentation.—In order to provide the reader with a ready reference to the general synoptic situation with which each of these storms was associated, a surface synoptic chart, a schematic picture of the actual radar echoes presented on the PPI-radar 'scope, and a chart showing both radiosonde and upper-wind data from the nearest regularly reporting stations are included in all of these sample sets of data. The measurements made by the Thunderstorm Project are presented in the form of: (1) surface network charts for 10-minute intervals during the time the storms were over the surface network, (2) horizontal cross sections of the thunderstorm, on which are plotted measurements made by the Project airplanes if such were available, and (3) a time series of radar 'scope photographs showing the growth and development of thunderstorms as depicted by radar. In addition, for each of the examples, there is a brief text summarizing the synoptic situation and the important features of the storm. Individual descriptions of the situations presented on the sets of charts for each successive time interval are also included.

Surface charts.—In the examples involving surface data, a chart interval of 10 min. was used for the pressure, temperature, and the relative humidity data; however, in keeping with the practice used throughout the analysis of Project data, rainfall accumulations are given for the 5-minute interval ending at the time shown on the rainfall chart. On this chart, the dashed isohyet labeled "L" denotes the limit of detectable rain but does not necessarily represent the actual boundary of the area of rainfall. Relative humidity and temperature values presented are the instantaneous readings of the instruments at the time of the chart, while the wind speed and direction shown are average values for the 5-minute interval preceding the time of the chart. On the surface charts the wind is plotted in vector form with wind speed also indicated in mi/hr. The pressure values plotted represent the changes in pressure from the given reference time, with the normal diurnal pressure changes removed.

Airplane charts.—The airplane data measured within the storms are also grouped into 10-minute intervals and are plotted on a chart showing the radar echo for the midpoint of the interval. Each chart shows the paths of all airplanes that passed through the storm during that particular 10-minute interval, regardless of the altitude at which the plane was flying. In order that the paths of the airplanes might be shown in the proper relation to the storm, they have been displaced from their true position with respect to the earth's surface and plotted so that the midpoint of each traverse is in its correct position with respect to the radar echo shown. Because of this, the end-

positions for successive traverses do not appear to be consistent in space and time.

Along each plotted airplane path the drafts measured during the traverse are indicated. It will be noticed that on some occasions airplanes recrossed an area where a draft had previously been encountered, apparently without re-encountering it. It should not be presumed that the draft had ceased to exist by the time of the recrossing, but rather it must be considered that computing it from the airspeed-altitude records for the later traverse may have been impossible because of indications of excessive control movement or changes in power setting made by the pilot and/or the attitude of the airplane (ch. II, sec. 1).

As was pointed out in the discussion of thunderstorm structure and circulation, one of the characteristic features of a cell is the turbulence occurring therein. Consequently a region of no turbulence, or of a minimum of turbulence occurs at the boundary of each cell. Usually, the turbulence ceases entirely for a period of at least 10 sec. (approximately ½ mi.), when an airplane passes through the boundary between cells. These breaks in the turbulence, obtained from the accelerometer records, are also shown on the airplane charts.

On another set of charts for each time interval, the temperature anomalies computed from the thermistor indications are plotted for each airplane traverse if they were available. Only points of inflection, maxima, and minima of the temperature curve are shown. Thus, a straight-line interpolation between successive points gives an adequate picture of the temperature field. Before examining the temperature charts, it is suggested that the reader refer to section 3 of chapter I to review the method of determining the temperature anomalies and the nature of the corrections that must be applied to temperatures measured from a moving airplane. In examining the temperature data presented in this part of the report, it will be found that in many instances they are in apparent disagreement with the over-all picture of the temperature field discussed in earlier chapters. It is quite possible that many of the discrepancies between the data shown for any one of these single storms and the conclusions presented regarding the march of temperature within a cell are the result of imperfections in both the system of temperature measurement and in the corrections applied.

Squall-line photographs.—For examples of squall lines, a series of reproductions of the echoes on the long-range radar 'scopes are presented. These photographs show the location of the radar at Jamestown, Ohio, as a white spot at the center of the 'scope. The radiating lines are azimuth indicators, and the concentric circles represent range from the radar in intervals of 50 mi.

THUNDERSTORM OF JULY 9, 1946
[1240 E.S.T. to 1520 E.S.T.]

On this day, Florida was under a col between the Atlantic high-pressure area and another warm high over the Gulf of Mexico; it was also between a well-developed cyclone centered over North Dakota and a low-pressure area southeast of Cuba (fig. 126). The 700-millibar chart indicated the presence of a warm high over the area. Radiosonde observations from Tampa, Fla., and Miami, Fla., are shown in figures 127 and 128.

The airplane, surface, and radar measurements for this storm were as complete as for any which were flown during the Florida operations. A discussion of the storm was presented in an earlier Thunderstorm Project report [**17**], but further analysis of this case and especially of the surface data, warranted its inclusion in this series of examples. The numerical designation which was assigned to each cell in the previous report has been retained here.

The Project radar-'scope photographs taken on this day indicate that there was considerable thunderstorm activity, but in general the storms were fairly well isolated. A series of these photographs is presented in figures 129 and 130. The first echo associated with this storm appeared between 1200 and 1215 E.S.T. north of the western portion of the network. In the course of about two hours, the storm developed into one of the most vigorous which occurred during the period of observations. The first cell to pass over the surface network was designated as cell I, and it appeared on the radar 'scope at 1223 E.S.T. Visual observations from the surface indicated that this cell produced rain as early as 1230 E.S.T. It did not produce rain over the network, however, until 1244 E.S.T. The general movement of the entire storm system was approximately southeastward.

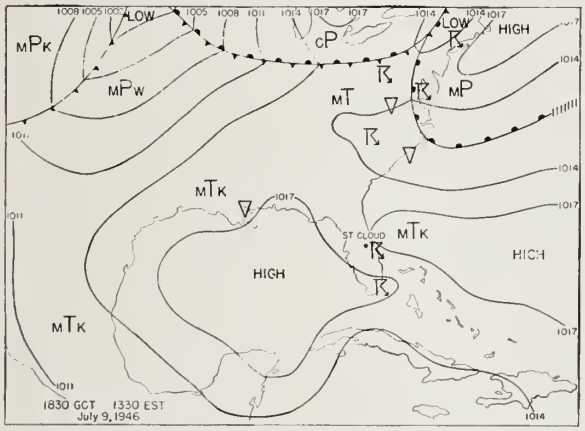

FIGURE 126.—A surface synoptic chart for 1330 E.S.T., July 9, 1946.

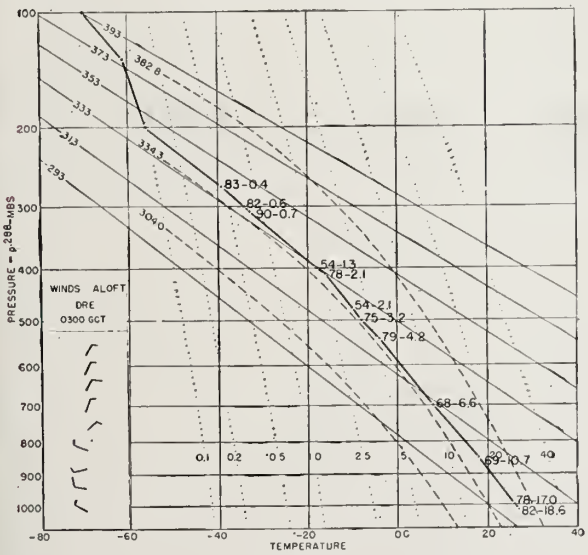

FIGURE 127.—Upper air sounding for 0300 G.C.T., July 9, 1946, from Tampa, Fla.

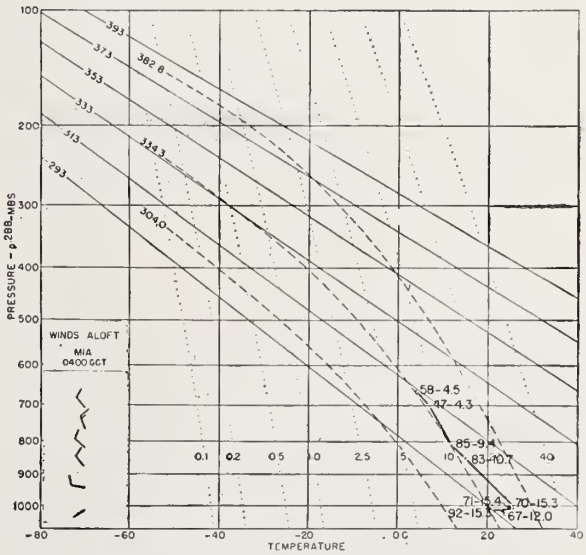

FIGURE 128.—Upper air sounding for 0300 G.C.T., July 9, 1946, from Miami, Fla.

841051—50——11

1240 E.S.T.
(*fig. 131*)

In addition to the group of cells located northwest of the network, there were a number of cells due west. It is apparent that the outflow from these latter cells produced the westerly winds recorded at station 3 (fig. 131). However, effects of the inflow associated with this storm and the one in the northwest are apparent from the wind directions shown southwest of East Lake Tohopekaliga.

At this time station 1 was already affected by the cold air from the western storms, but the stations which were not under the influence of the cooling from these storms recorded temperatures ranging from 89° through 93°F. The variations were probably due to local effects such as differences in the amount of cloudiness, instrument error, station exposure, and on-shore winds from the lake. As the radar showed, cell I had just reached the surface network, but no rain was yet recorded. The slight drops in surface pressure, typical of the area surrounding developing thunderstorms, were prevalent over most of the surface network.

1250 E.S.T.
(*fig. 132*)

By this time heavy rain associated with cell I was recorded at station 7. Confluence of the outflowing cold air from cell I and from the western storms resulted in an area of relatively strong convergence in the northwestern part of the network. The temperatures had begun to drop markedly in the area covered by the outflowing air and relative humidities rose substantially. Under the cold air, the pressure rose slightly; however, there was also an increase in surface pressure slightly ahead of the surface of cold-air discontinuity. Pressure continued to fall in the eastern half of the network. As pointed out in another part of this report (ch. III, sec. 4) these pressure falls may have been due to the divergence aloft brought about by a reversal in the vertical circulation with the establishment of a strong downdraft.

1300 E.S.T.
(*fig. 133*)

Cell I is the only cell of the storm flown that is evident on the network at 1300 E.S.T. As a result of the confluence of the outflow produced by the downdraft from cell I with that from the storm west of the network, a region of strong convergence has developed in the vicinity of stations 1, 2, 8, and 9. It is in this general area that the radar echo from cell IV appears at a later time. Elsewhere over the network there was little change in temperature or humidity, inasmuch as the air in the surface layers was not yet affected by the storm. The pressure rose directly under the cold outflow air but pressure falls were occurring over the central area of the network where active convection was taking place.

1310 E.S.T.
(*figs. 134 and 135*)

Cell I was traversed by the airplanes at 11,000 and 16,000 ft. Turbulence and moderate rain were observed at both levels and light rime icing was reported at the 11,000-foot level. Although no drafts could be evaluated from the flight records, this cell is believed to have been in the mature stage of development, primarily because the surface precipitation was so intense. As a result of heavy rain and downdrafts, there were marked temperature falls and an increase of relative humidity in the northwestern portion of the network.

Cell II was not penetrated during this period. It had first been visible on the radar at 1248 E.S.T. and since its echo was still growing rapidly, it was considered to be in the cumulus or building stage of development.

Cell III was not penetrated by the airplanes until about 1415 E.S.T., but it was believed to be in the cumulus stage of development at this time.

Cell IV was the only cell of the storm which developed and remained over the surface network. It was detectable as an independent radar echo southeast of cell I at 1259 E.S.T. It is an excellent example of a so-called "first-gust" echo showing evidence of forced development both at the surface and aloft. The 16,000-foot airplane encountered an updraft and moderate rain in the western side of the cell between 1306 and 1307 E.S.T. The surface rainfall recorded at station 14 was attributed to this cell. It is important to note that there is little evidence on the surface chart to indicate that the rain recorded at stations 11 and 14 was from different cells, although this is indicated from the airplane measurements and from the time history of the radar echoes of this storm. This apparent inconsistency illustrates that there are occasions on which the nature of the measurements do not allow a unique solution to the problem of cell structure in thunderstorms.

Cell VII appeared on the radar 'scope at 1309 E.S.T. within the area of weak echo from stratus deck associated with a rapidly dissipating cell to the east. Gustiness and an updraft were recorded from the flight at 11,000 ft., indicating that the cell was in the cumulus stage of development.

Three other cells are indicated in figure 134: East of cell VII is the dissipating cell, which first appeared on the radar 'scope at 1218 E.S.T., and within which the airplane flying at 16,000 ft. recorded light gustiness and moderate rain but no drafts; two relatively short-lived cells are present on the northwestern and eastern sides of the storm in which gusti-

ness, but no drafts, were found. The latter cells remained on the radar 'scope for only 30 min.

1320 E.S.T.
(*figs. 136 and 137*)

Cell I was traversed by the airplanes at 6,000 and 16,000 ft. during the interval from 1315 to 1325 E.S.T. Gustiness, light rain, and light hail were reported at 16,000 ft., while moderate rain, but no measurable gustiness, was encountered at 6,000 ft. No drafts could be computed from the records, but a loss of altitude was recorded at the 6,000-foot level. This fact, together with the almost complete lack of turbulence in the cell and the nature of the surface rainfall from it, leads to the conclusion that the cell was in the dissipating stage. The surface temperatures under this cell continued to fall and relative humidities were near saturation. An area of very intense divergence (17.5 hr^{-1}) developed; a characteristic outflow pattern may be seen in figure 137. Surface pressures under the cell continued to rise, as is usual in the area of heavy rain and intense divergence.

Cell II was penetrated by the 6,000-foot airplane; from the records, updrafts encountered at the northern and southern extremities of the cell were computed. Moderate rain and gustiness were reported. Since the presence of precipitation at this level is usually accompanied by downdraft, this cell was apparently in the late building or possibly very early mature stage.

Cell III was found to contain an updraft at the 16,000-foot level, but the spreading and weakening of its radar echo during the next few minutes indicated that a well-developed downdraft must have existed also. Therefore, the cell was in the mature stage.

Cell IV was considered to be in the mature stage of development and it reached peak intensity during this period. It was traversed at the 6,000-foot level by an airplane which encountered a downdraft in the northwestern portion and an updraft in the southwestern portion. The cell boundary was well delineated by gust breaks (areas of minimum turbulence). The pilot reported moderate rain within this cell, and at the surface the rainfall was very intense (station 14 recorded 0.54 in. for 5 min.). As would be expected, there was divergence associated with this intense rainfall. Substantial pressure rises occurred, and a separate center of minimum temperature was established. It is interesting to note that the cold outflow, primarily from this cell, had by this time spread over one-half of the network. As a result of this strong outflow, a marked temperature gradient existed over the network; there was a difference of 22° F. between the northwestern and southeastern portions. Of special interest are two centers of minimum temperature (at station 11 and at station 17), which provide additional evidence that there were independent outflows from cells IV and I.

Cell VII was marked by gust breaks, moderate rain, and a weak updraft at the 6,000-foot level. Although the presence of this updraft was definitely established, its magnitude could not be determined from flight records. Since rain was reported at this low level, it is likely that the cell was already in the early mature stage at this time. However, the radar echo grew rapidly within the next few minutes.

The three other cells present during the previous period were still found on the radar 'scope. The cell on the eastern side of the storm was strong enough to produce gustiness at the 16,000-foot flight level, but no drafts or precipitation were reported by the plane flying this level.

1330 E.S.T.
(*figs. 138 and 139*)

Several major changes in the radar echoes were apparent during the interval from 1320 to 1330 E.S.T.; large areas of weak echo spread rapidly to the southwest of cells I and III, presumably due to the presence of the strong northeasterly winds above 21,000 ft.; a new development was evident to the south of cell IV; the identity of the cumulus development to the northwest was lost; and, finally, at the close of the period, the storm itself divided into two sections with the break occurring between cells I and VII.

Cell I was traversed by airplanes flying at 6,000 and 16,000 ft. Gustiness was reported as present throughout the cell at the 16,000-foot level, but none was found at 6,000 ft. No drafts or precipitation were reported at either level, a condition typical of cells in the dissipating stage. The radar indicated a large, weak echo, probably from stratiform clouds, extending southwest from this cell.

The surface rainfall decreased in intensity under cell I but still could be considered as heavy. There was still pronounced outflow with very intense divergence. Temperatures remained approximately the same, since the maximum cooling had been attained earlier, but the surface pressure continued to rise.

Cell II was still in the building stage, and updrafts continued throughout the cell. A break in the gustiness found by the plane at the 6,000-foot level indicated the separation between cells II and VII.

Cell III was not penetrated by the planes during this period. The weak appearance of its radar echo on the western and southern edges indicated that it was in the late mature stage of development.

Cell IV was still in the mature stage of development during this period. As is shown in figure 138, a downdraft of considerable extent was measured at the 6,000-foot level, whereas in the eastern portion of the cell updrafts were recorded by the airplanes

flying at 16,000 and 21,000 ft. The only precipitation reported was light snow at 16,000 ft. in the northern portion of the cell. Gust breaks at 6,000 and 16,000 ft. defined the cell's southern and northwestern limits.

The surface rainfall from this cell continued to be very heavy, with station 17 reporting 0.34 in/5 min. The divergence area, united with that of cell I, was quite pronounced. Similarly, the area of minimum temperature was merged with that of cell I, and the relative humidities were high throughout. It is interesting to note the separate center of high pressure which had formed underneath cell IV. The pressure continued relatively low, however, over the extreme eastern portion of the network. Some of the low-pressure values were probably associated with convective activity in that area which resulted in the development of a new storm, the echo from which first appeared on the radar 'scope at 1340 E.S.T.

Cell VII was traversed by all three airplanes. At 21,000 ft. a strong downdraft was measured in the northeastern portion of the cell. Directly south of this area updrafts were encountered at 6,000 and 21,000 ft. A third updraft was encountered on the western edge at 16,000 ft. Heavy snow, at 21,000 ft., and heavy rain, at 6,000 ft., were reported in the area of up- and downdrafts in the northeast, and moderate hail was encountered at the 16,000-foot level. The cell, which was in the mature stage, was well-defined by gust breaks.

Cell VIII was first detected on the radar 'scope at 1322 E.S.T., as an outgrowth of the echo from cell IV. An updraft was recorded 6 min. later by the plane flying at 6,000 ft., and the cell echo showed a rapid growth. There was as yet no surface precipitation or cold-air outflow from this cell. The pressure under it was low but had risen since the time of the previous chart. This cell was considered to be in the building stage.

The gustiness found at the 16,000-foot level of flight continued to indicate an area of cell activity to the northwest of cell VII, but the radar echo suggested that this cell had merged with cell II. The two cells which had been present at the eastern edge of the storm no longer produced radar echoes.

1340 E.S.T.

(*figs. 140 and 141*)

Cell I was traversed by airplanes at the 6,000- and 16,000-foot levels, although the gust- and draft-recording instruments for the lower airplane were not turned on. Gustiness was reported at 16,000 ft., but no drafts or hydrometeors were reported; heavy rain was encountered at 6,000 ft. Surface rain persisted but decreased in intensity, and the pressures lowered. Nevertheless, there was still substantial divergence underneath this cell and the temperatures remained at their minimum values. In view of the surface weather conditions, and the fact that the radar echo intensity rapidly weakened, cell I was considered to be in the dissipating stage.

Cell II was still in the mature stage of development, and at the 6,000-foot level of flight both updrafts and downdrafts were measured. No drafts were measured at either the 16,000- or the 21,000-foot levels in the western part of the cell. Heavy rain was reported on the first traverse at 6,000 ft., while moderate snow was reported at 21,000 ft.

Cell III was penetrated by airplanes at two levels during this period, but gust and draft data are available only for the 21,000-foot level. A strong downdraft was recorded at this level in the northern portion of the cell, which, from the appearance of the radar echo, was weakening rapidly. For these reasons, the cell was considered to be in the dissipating stage.

Cell IV was traversed only by the plane flying the 16,000-foot level, and a single downdraft was recorded. Breaks in the gustiness delineated its southern and northern limits. In spite of the relatively heavy precipitation which was associated with the cell, at the surface, no precipitation was reported by the flight crew. The downdraft area extended across most of the cell, although an updraft area probably still existed (as shown in fig. 140). Cell IV was therefore considered to be still in the mature stage of development. There were still a few slight falls in temperature, and the relative humidities remained high under the cell. Very pronounced divergence was associated with the cell at this time. However, pressures dropped, and the closed center of pressure on the previous map had disappeared. The manner in which the radar echo grew from 1330 to 1340 E.S.T. indicated the possibility of further cell development on the southeast edge of cell IV. Since no airplane data were available for this area, an analysis of the activity could not be made.

Cell VII had changed very little in the interval from 1330 to 1340 E.S.T. The downdraft area, as measured at the 6,000-foot level, was still concentrated in the northeast sector, while updrafts were found elsewhere in the cell at 16,000 and 21,000 ft. Through the eastern edge of the cell the pilot flying at 6,000 ft. reported heavy rain; on the western side, moderate snow was encountered at 21,000 ft.; in the central portion, the pilot flying at 16,000 ft. reported light rime icing and moderate rain mixed occasionally with moderate hail. This cell was in mature stage of development at this time.

Cell VIII continued to grow southeastward during the period. A single plane traverse made through this building cell at 16,000 ft. indicated an updraft, but

precipitation was not reported. It was possible to distinguish this cell from cell IV to the north by the existence of a break in the gustiness. Except for the drop in surface pressure recorded at station 20, there appeared to be no surface effects attributable to this cell.

The new development to the north of cell II was first visible on the radar 'scope at 1334 E.S.T. and persisted until about 1354 E.S.T. Several traverses cross this area, and gustiness was recorded but no drafts were encountered. This was presumed to be an isolated cumulus development, stimulated by the outflow at the surface from cell II. Attention is also called to two new echoes which developed over the extreme eastern portion of the network at about this time. It appears that these echoes were also of the type that develop after the passage of a first-gust line and may be considered as examples of first-gust echoes. A distinctive area of low temperature developed as a result of the cold-air outflow from these echoes, and a divergence center was established. At 1340 E.S.T. no precipitation was reported over the surface network from this storm.

1350 E.S.T.
(*fig. 142*)

By 1350 E.S.T. a marked decrease in the intensity of the outflow occurred in the western part of the network under cells I and IV. Further evidence of the weakening of these cells was evident from the rainfall map, which showed a substantially diminished rate of rainfall. Nevertheless, there was a marked spreading of the rain area.

The storm over the eastern part of the network continued to increase in intensity, with rain of 0.06 in/5 min recorded at station 38. As a result of the presence of this cell, a drop in temperature in the vicinity of Lake Lizzie was observed. In spite of the let-up in the winds and rain over the western part of the network, there was an increase in surface pressure; as a matter of fact, almost every station on the network showed a pressure rise. The general pattern of higher pressure underneath the western cell and lower pressure to the east remained unchanged.

1400 E.S.T.
(*fig. 143*)

The echo associated with the western storm diminished in size, and rainfall intensities decreased even more. However, the eastern storm grew in size, and heavy rain — 0.15 in/5 min — was recorded at station 38. The rain area associated with this storm also spread out. A new radar echo located over the southern portion of Alligator Lake appeared between the eastern and western cells, but rainfall from this cell was not observed. The temperature pattern in the western section showed little change, although the minimum temperature under the eastern storm dropped 4° F. since the time of the previous map. Relative humidities were near saturation in areas over which rain occurred but were considerably lower in other regions.

The wind charts show that outflow was present from both the eastern and western storms. Due to the effect of the opposing outflows from these storms, a center of relatively strong convergence was established in the vicinity of stations 35 and 48.

Although earlier the pressures had been high in the western portion and low in the eastern portion of the network, due to the dissipation of the western storm and the formation of a downdraft from the storm in the east, the pressures tended to become equalized over the network. An area of slight minimum pressure occurred between Alligator Lake and East Tohopekaliga Lake, where there was no rainfall and the surface temperatures were still high. Nevertheless, this area was not completely unaffected by the storms on both sides, since the pressure was significantly higher than it had been at the reference time.

1410 E.S.T.
(*fig. 144*)

Although the echo of the western storm had all but disappeared, many areas of lingering rainfall were evident on the surface chart. In the east the rainfall had decreased in intensity and a new center of relatively light rainfall appeared in connection with the small echo over Alligator Lake. There was little change in temperature other than a little cooling in the southeastern part of the network, and a little warming in the northeast. There was still evidence of outflow and weak divergence in connection with the western and eastern storms. The area of pronounced convergence, believed to be due to confluence of the outflow from these two storms, was still evident and had increased in areal extent.

Pressure falls occurred over most of the surface network but were greatest over the western portion, resulting in the establishment of an east-west pressure gradient. The highest pressures on the map were under the eastern storm.

1420 E.S.T.
(*fig. 145*)

By 1420 E.S.T. the rain over the network had stopped except for comparatively light precipitation over the extreme eastern portion. The wind field remained very weak over the entire network, and evidence of outflow from the western storm had by this time all but disappeared; outflow associated with the eastern storm was still evident, however. Pressures had continued to fall over most of the network, but the mag-

nitudes of the decreases were about equal in the eastern and western portions.

1520 E.S.T.
(*fig. 146*)

One hour after the passage of these storms, only a few, small, isolated radar echoes (without precipitation) were found over the network. Temperatures had risen over most of the network, except in the extreme east where there had been slight drops. The relative humidity, as might be expected, had decreased as the air was heated by solar radiation. There were areas of light divergence and convergence, as shown in figure 146, but it was difficult to attribute these to convection cells, inasmuch as the winds were light and variable.

Most of the pressures were within about 0.01 in. of the reference pressure of 1230 E.S.T. Nevertheless, there was a maximum difference of 0.02 in. between station 1, in the extreme west, and station 43, in the extreme east.

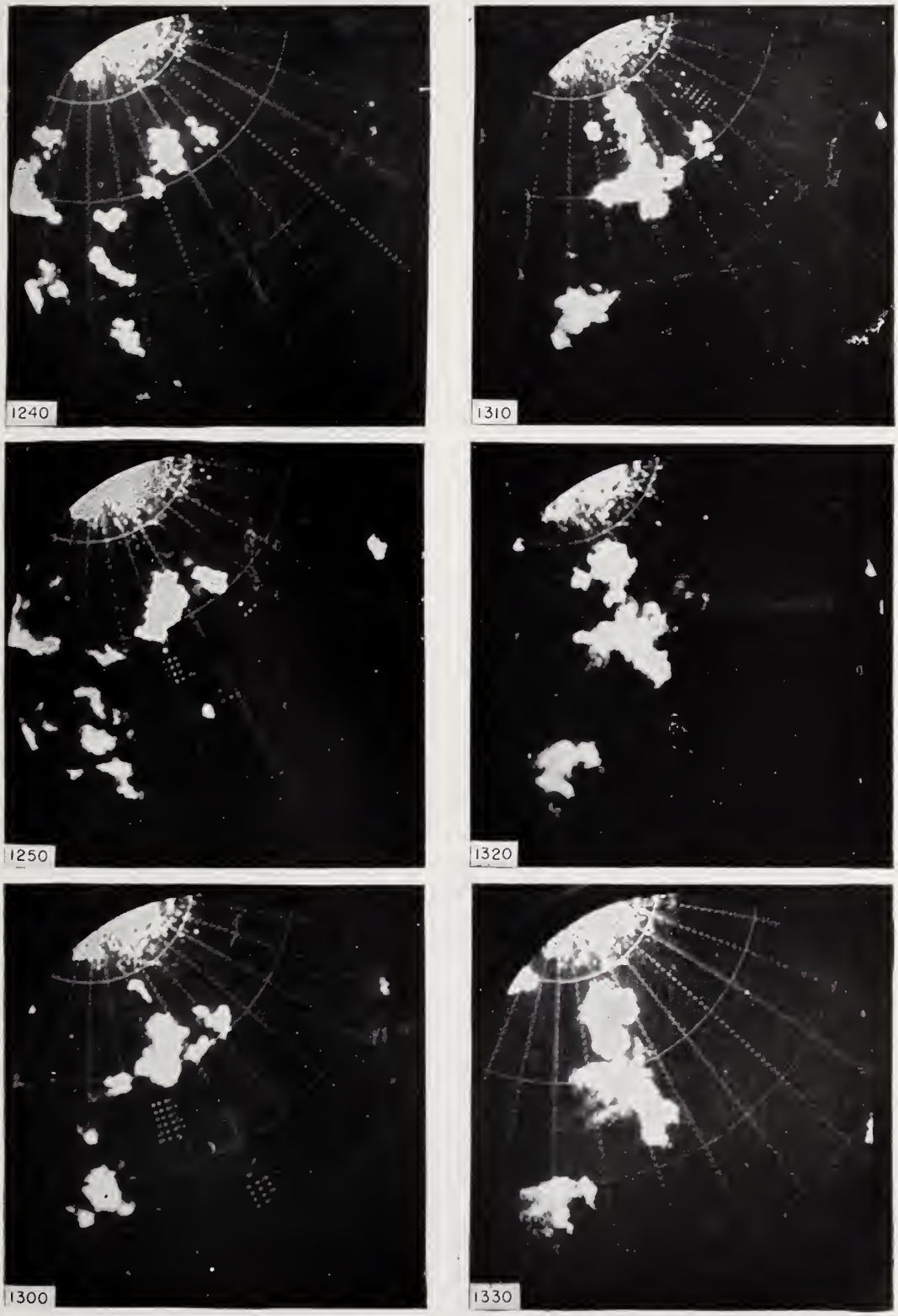

FIGURE 129.—Control-radar PPI 'scope photographs. 1240–1330 E.S.T., July 9, 1946. Off-center presentation; range circles for every 10 min.; surface network approximately in the center of the photograph.

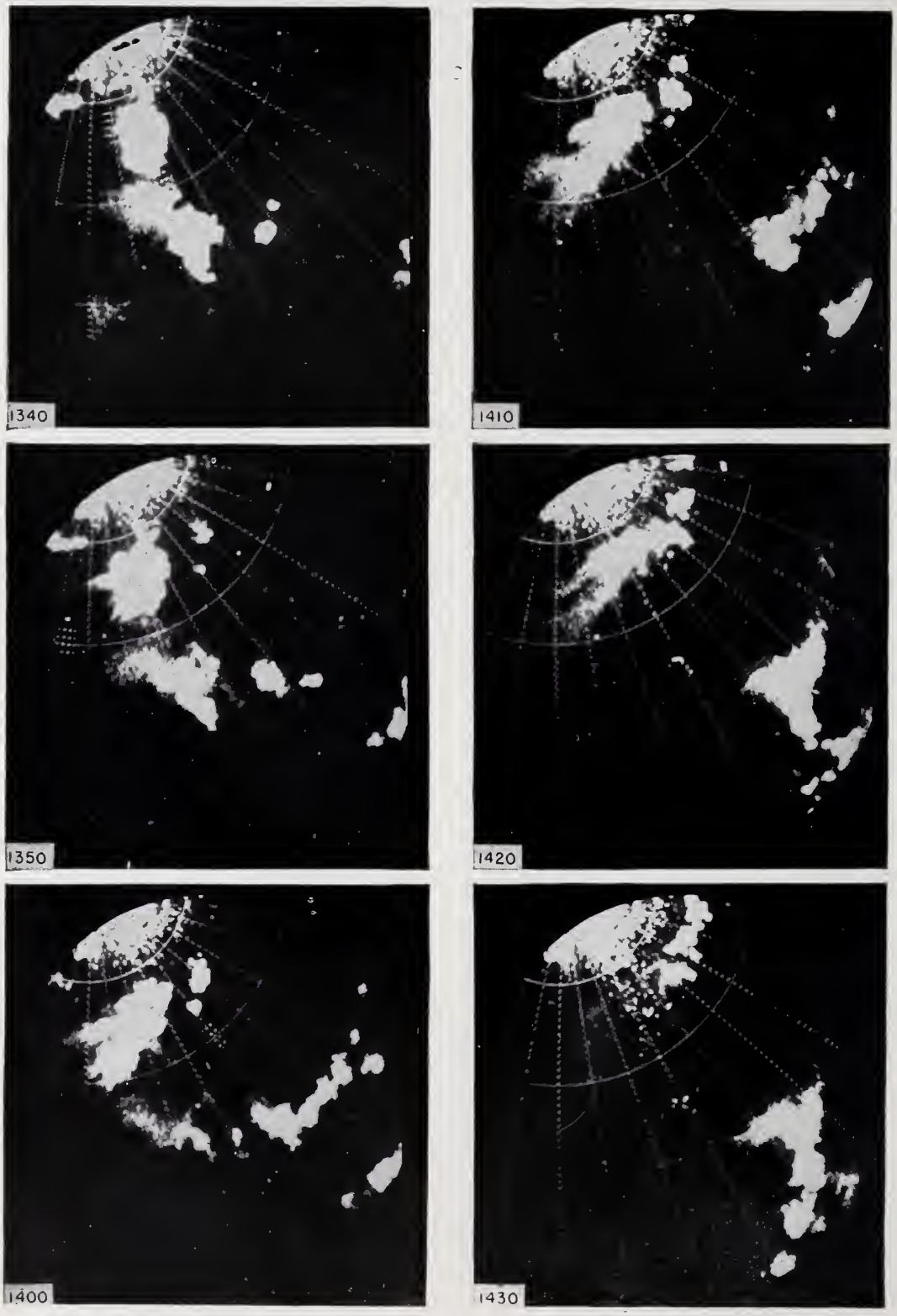

FIGURE 130.—Control-radar PPI 'scope photographs, 1340–1430 E.S.T., July 9, 1946. Off-center presentation; range circles for every 10 min.; surface network approximately in the center of the photograph.

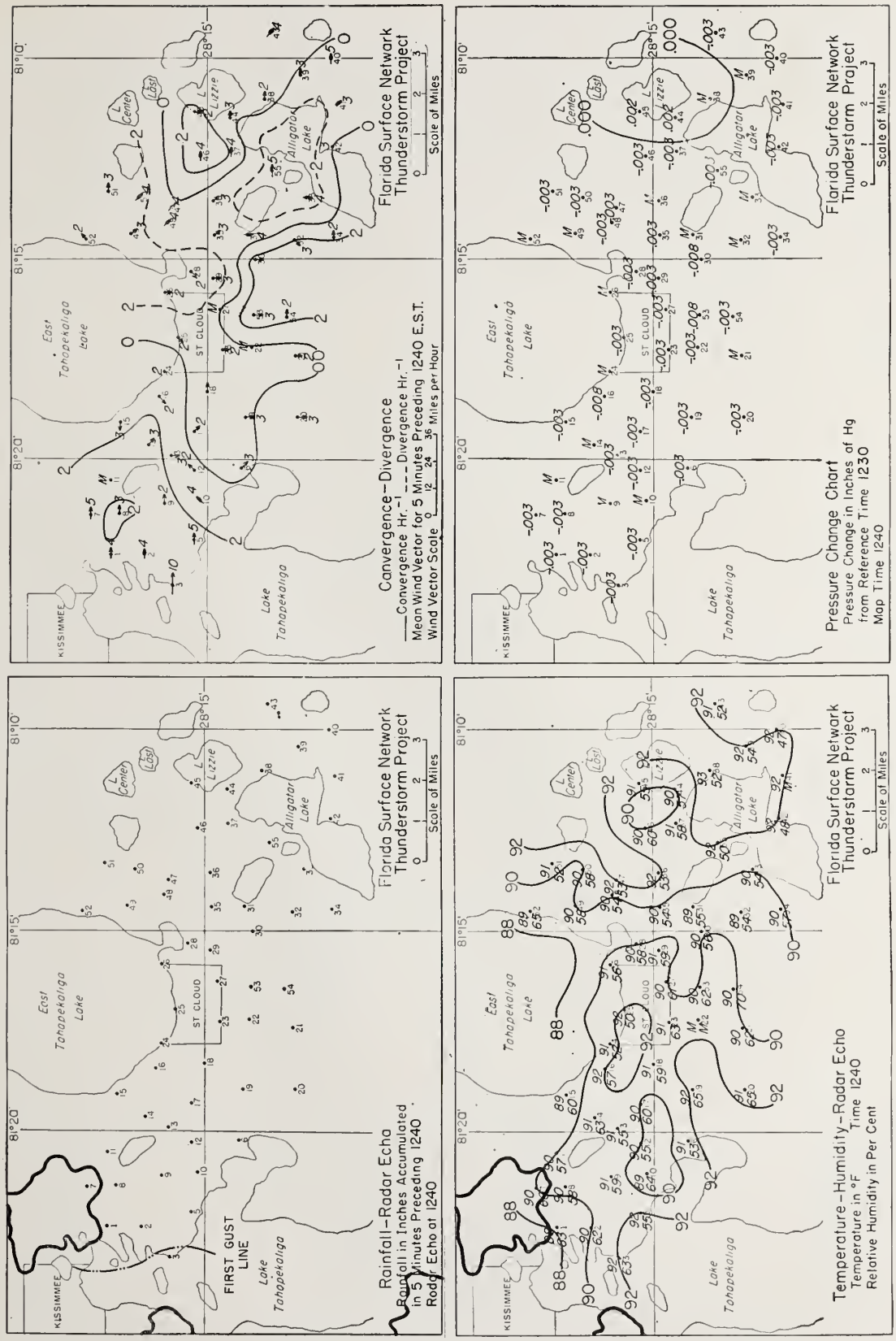

FIGURE 131.—Florida surface network, 1240 E.S.T., July 9, 1946.

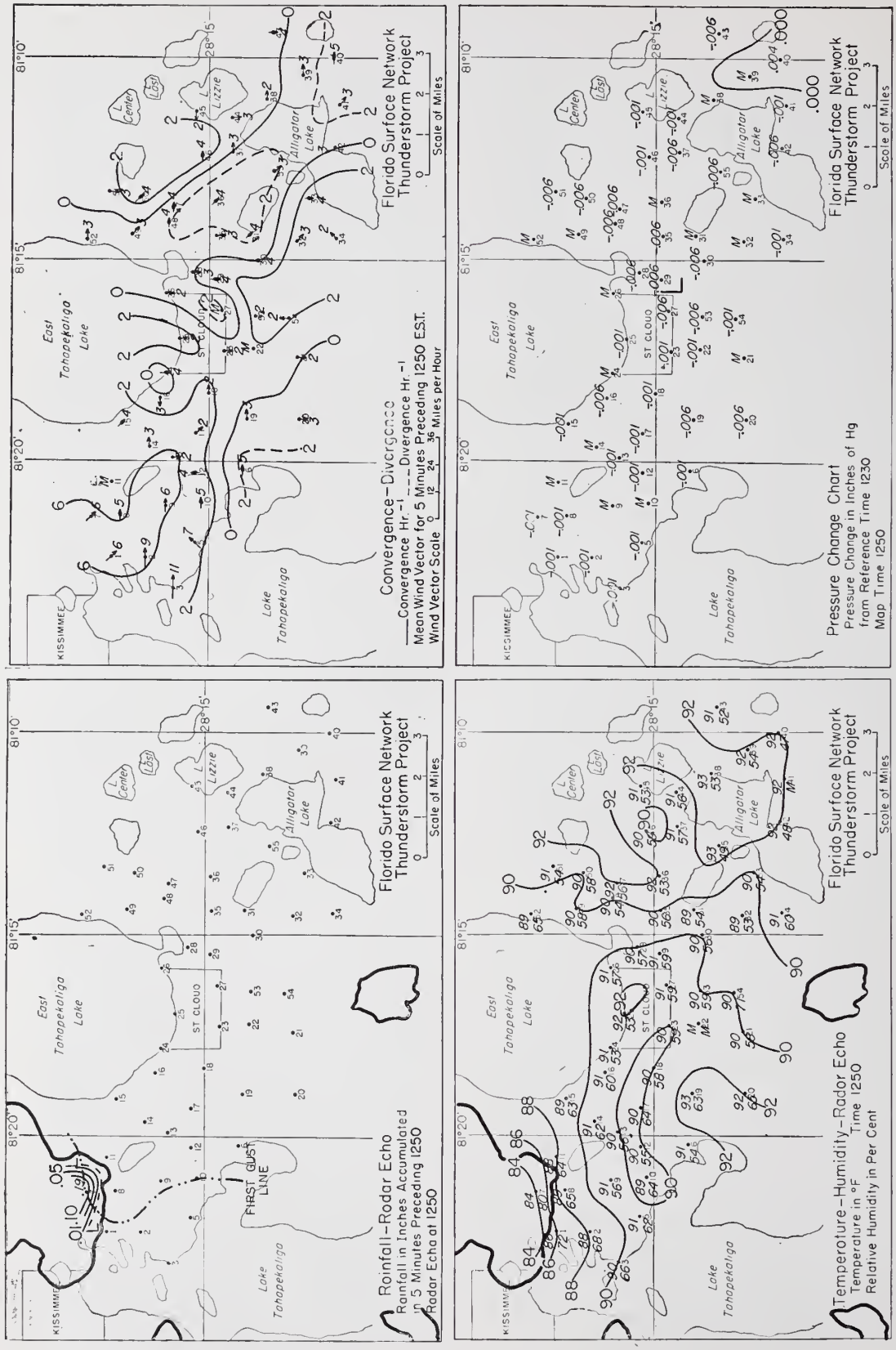

FIGURE 132.—Florida surface network, 1250 E.S.T., July 9, 1946.

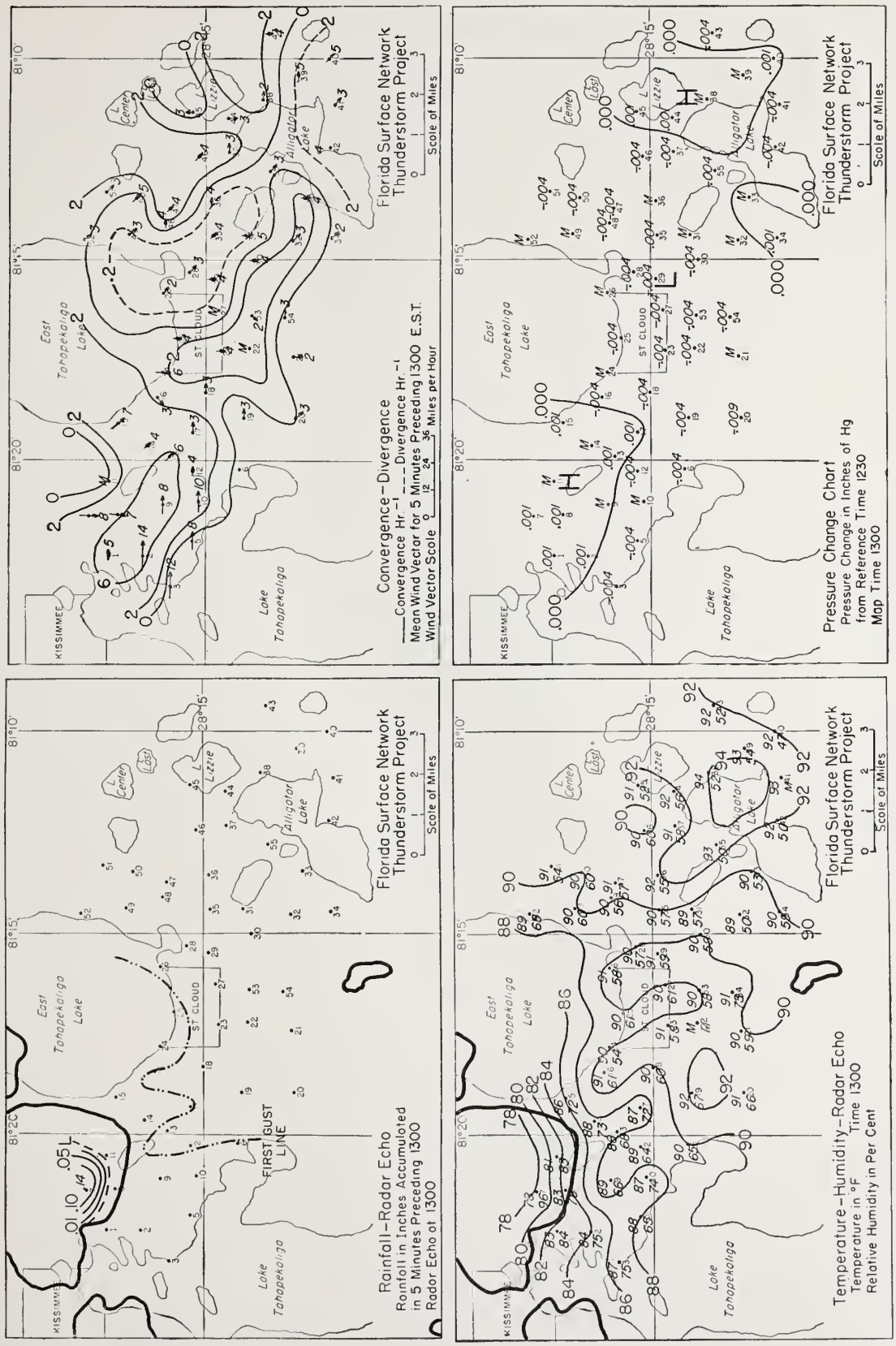

FIGURE 133.—Florida surface network, 1300 E.S.T., July 9, 1947.

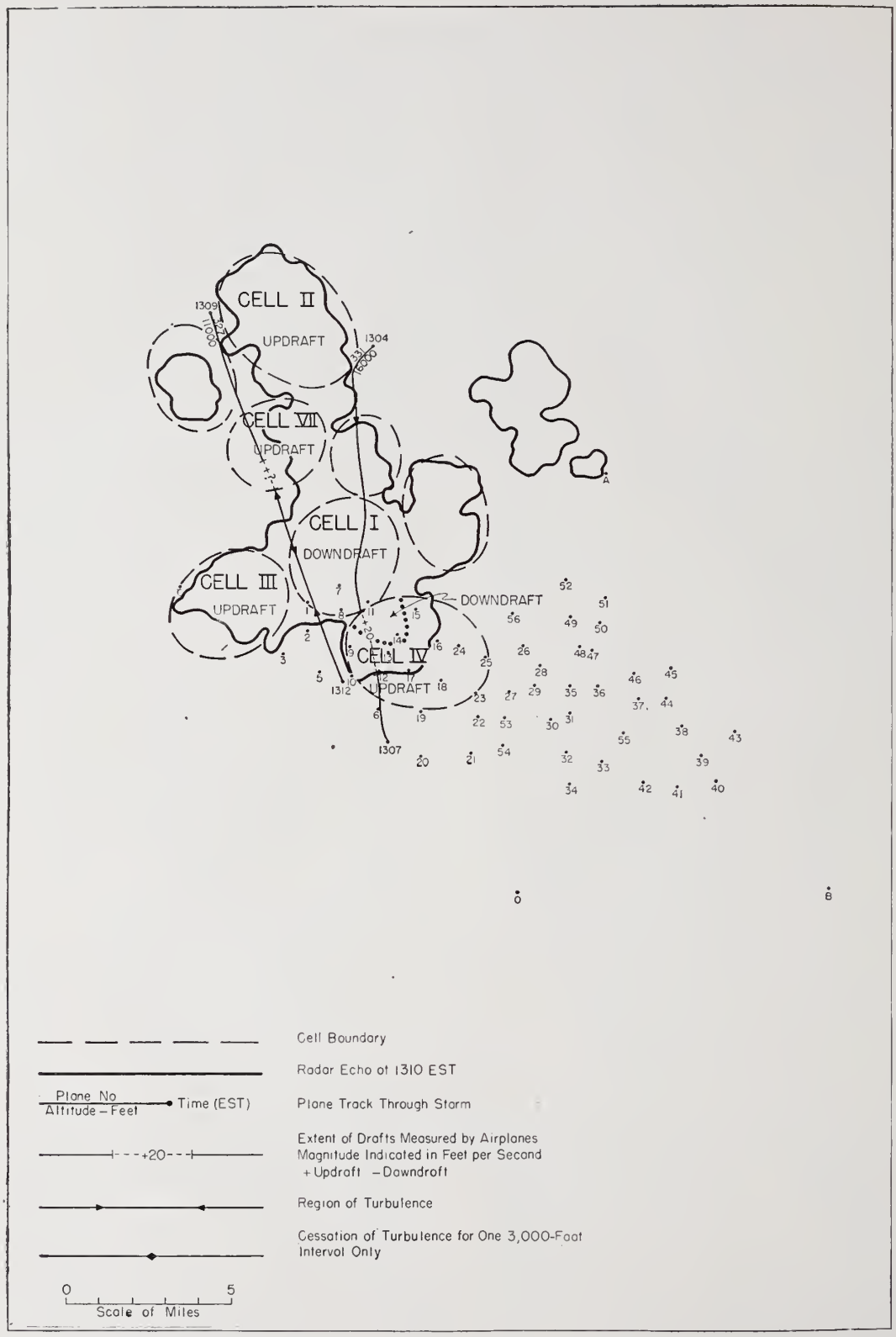

FIGURE 134.—PPI radar echo at 1310 E.S.T., and airplane paths from 1305 to 1315 E.S.T., July 9, 1946.

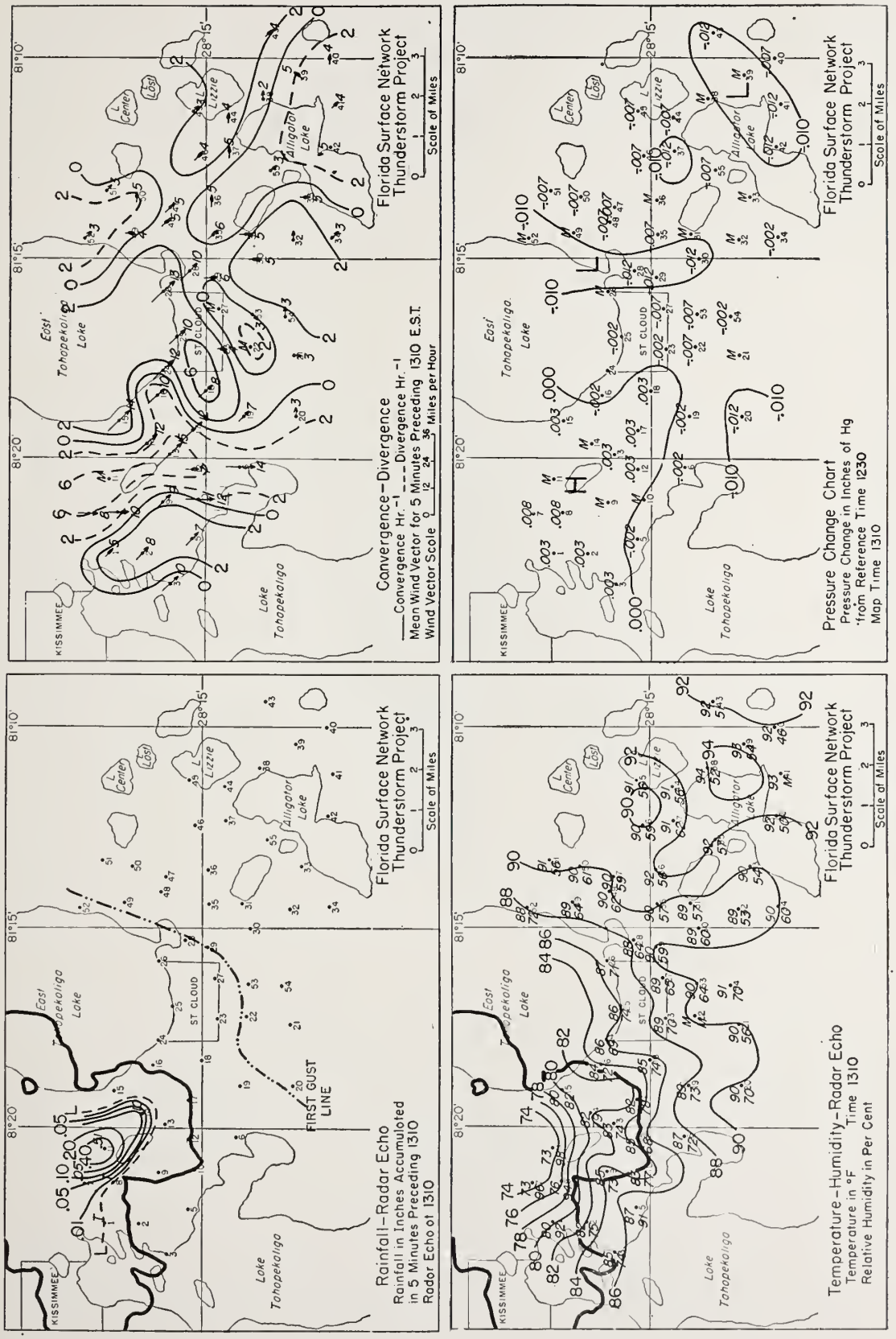

FIGURE 135.—Florida surface network, 1310 E.S.T., July 9, 1946.

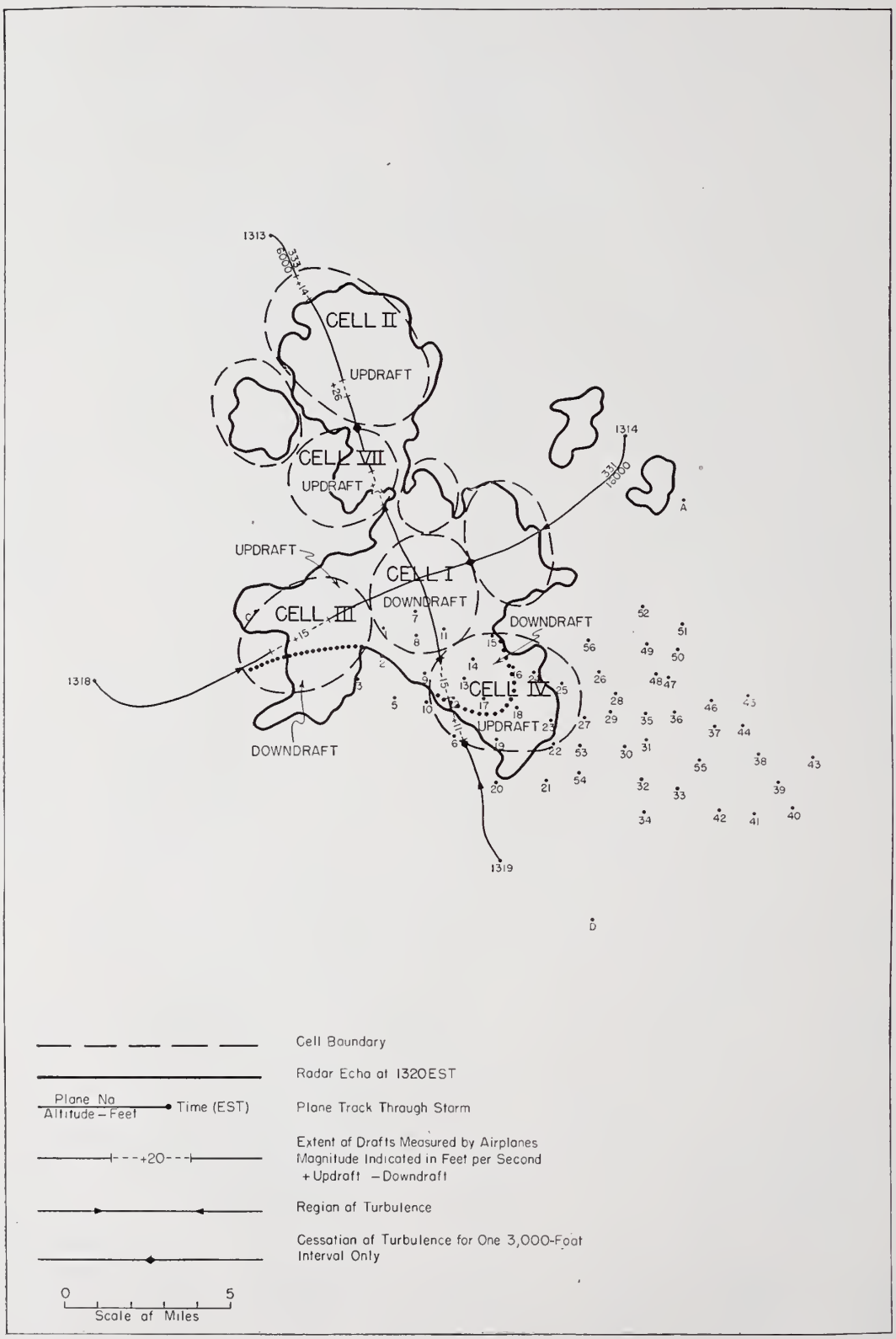

FIGURE 136.—PPI radar echo at 1320 E.S.T., and airplane paths from 1315 to 1325 E.S.T., July 9, 1946.

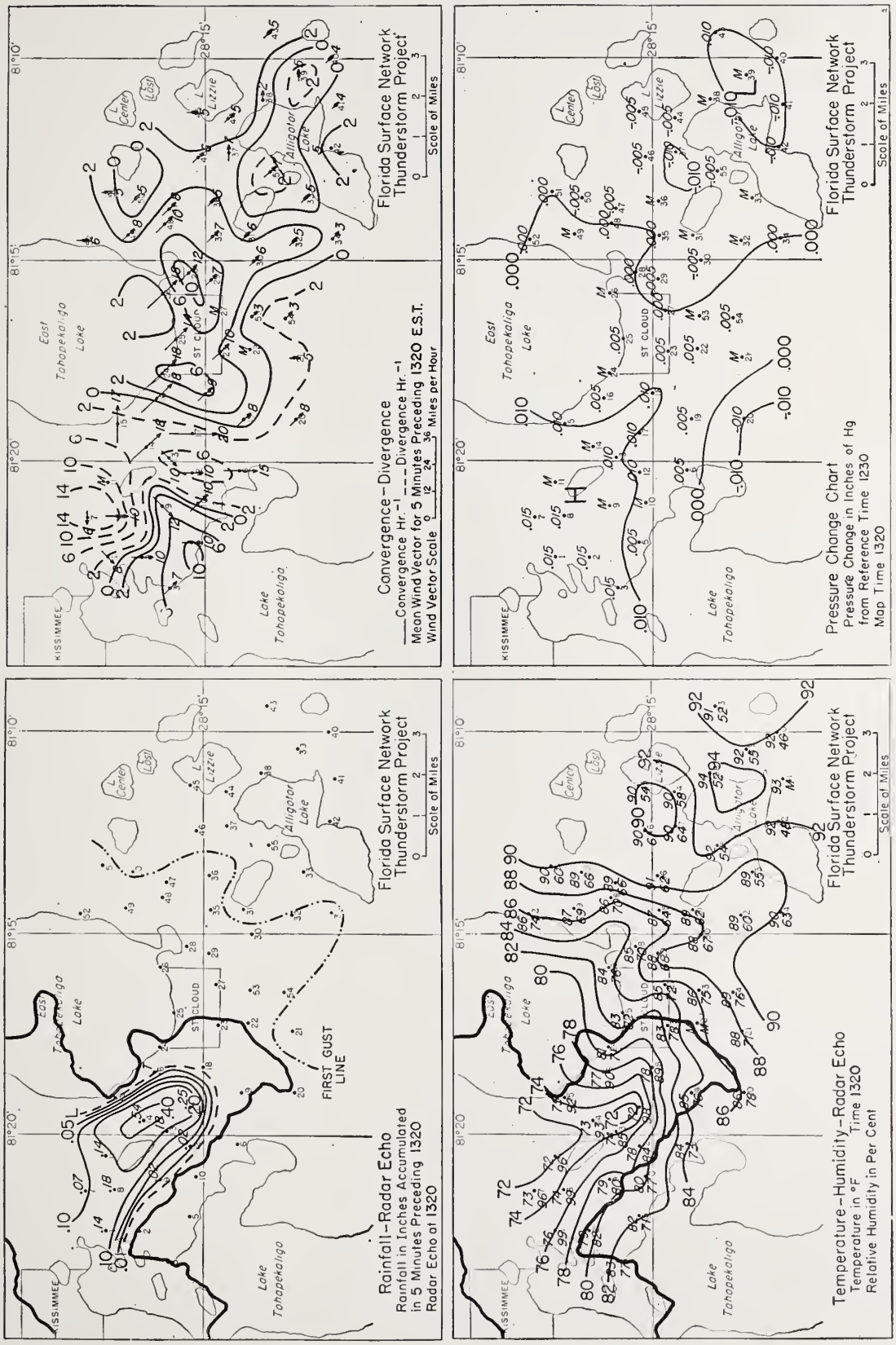

FIGURE 137.—Florida surface network, 1320 E.S.T., July 9, 1946.

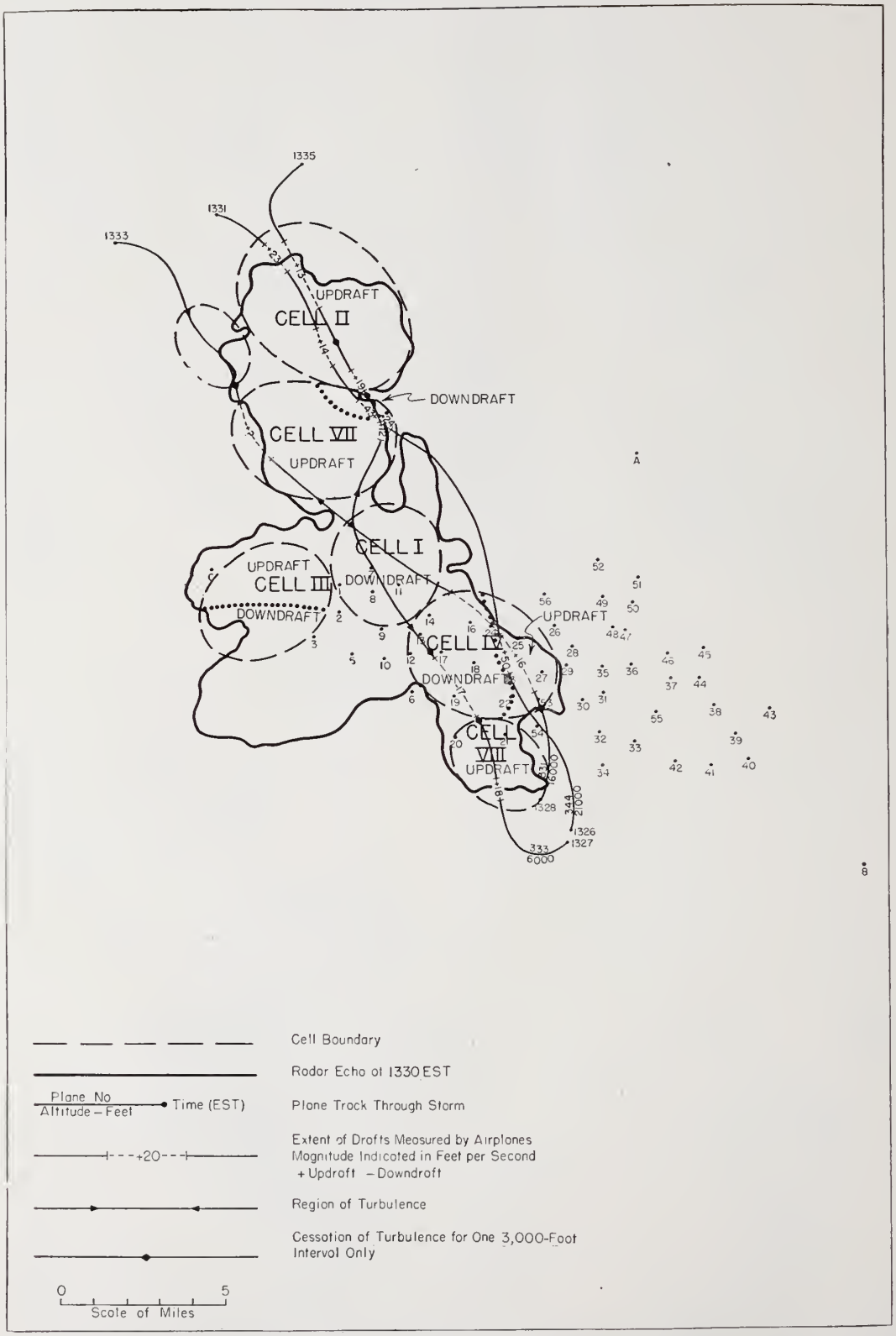

FIGURE 138.—PPI radar echo at 1330 E.S.T., and airplane paths from 1325 to 1335 E.S.T., July 9, 1946.

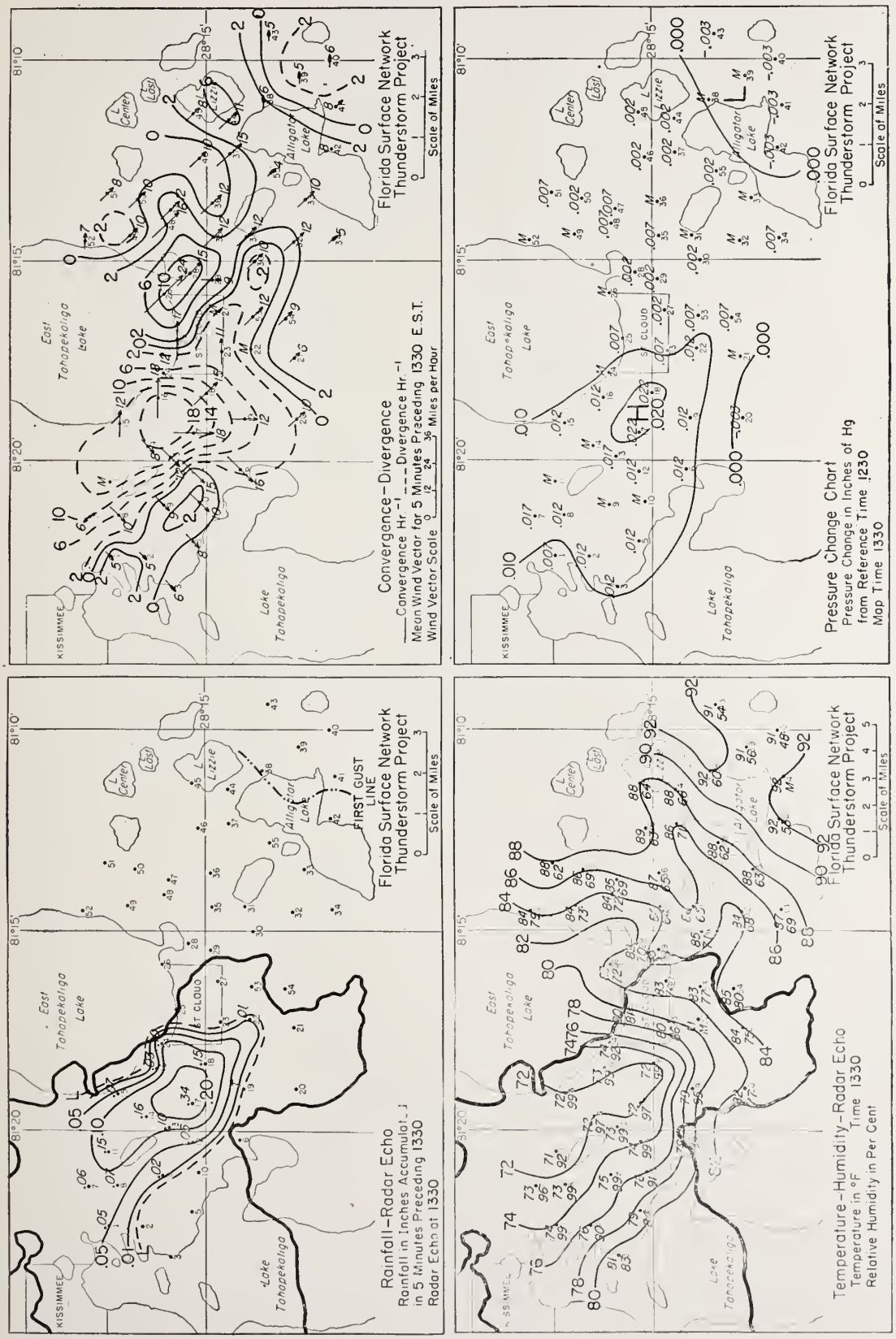

FIGURE 139.—Florida surface network, 1330 E.S.T., July 9, 1946.

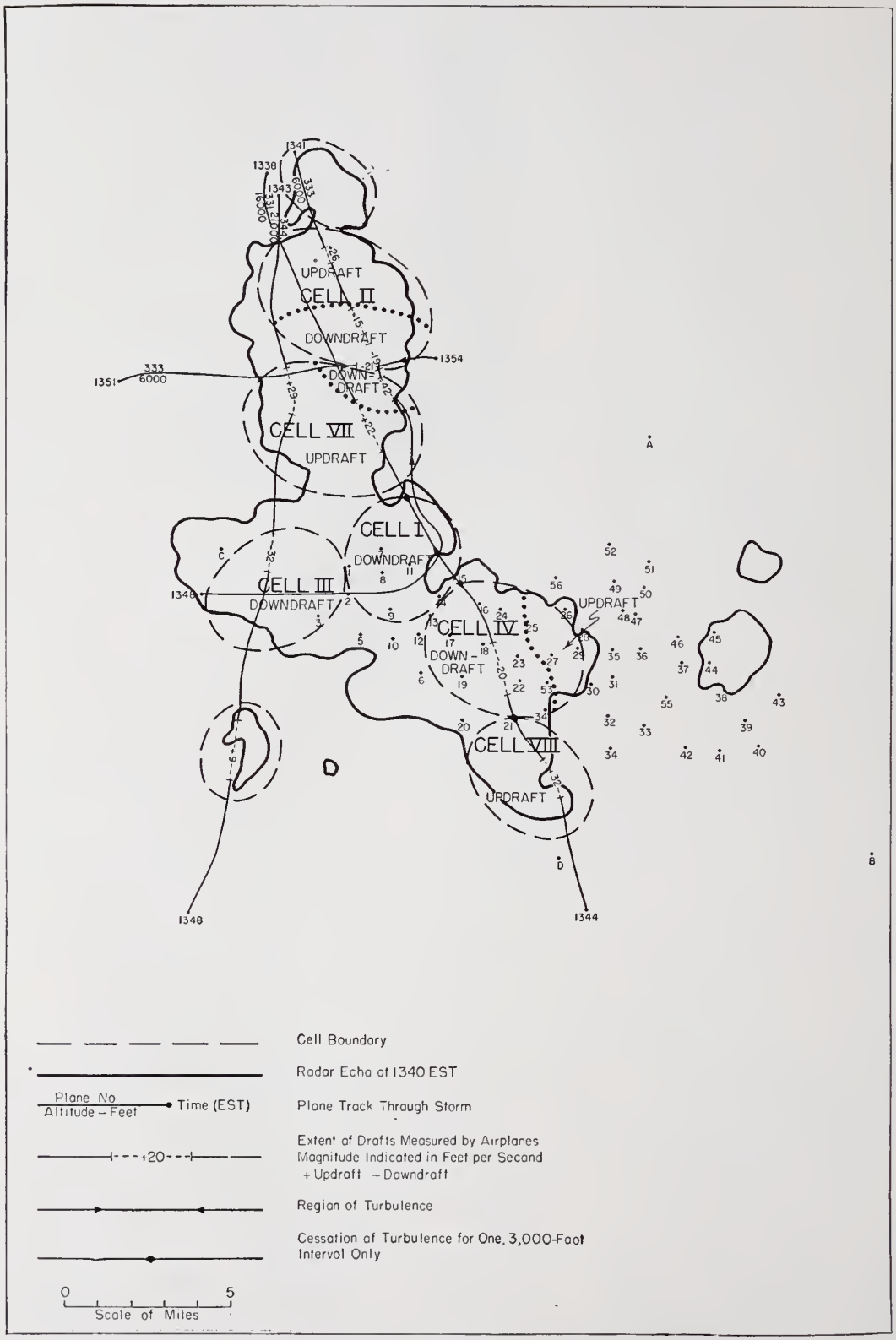

FIGURE 140.—PPI radar echo at 1340 E.S.T., and airplane paths from 1335 to 1345 E.S.T., July 9, 1946.

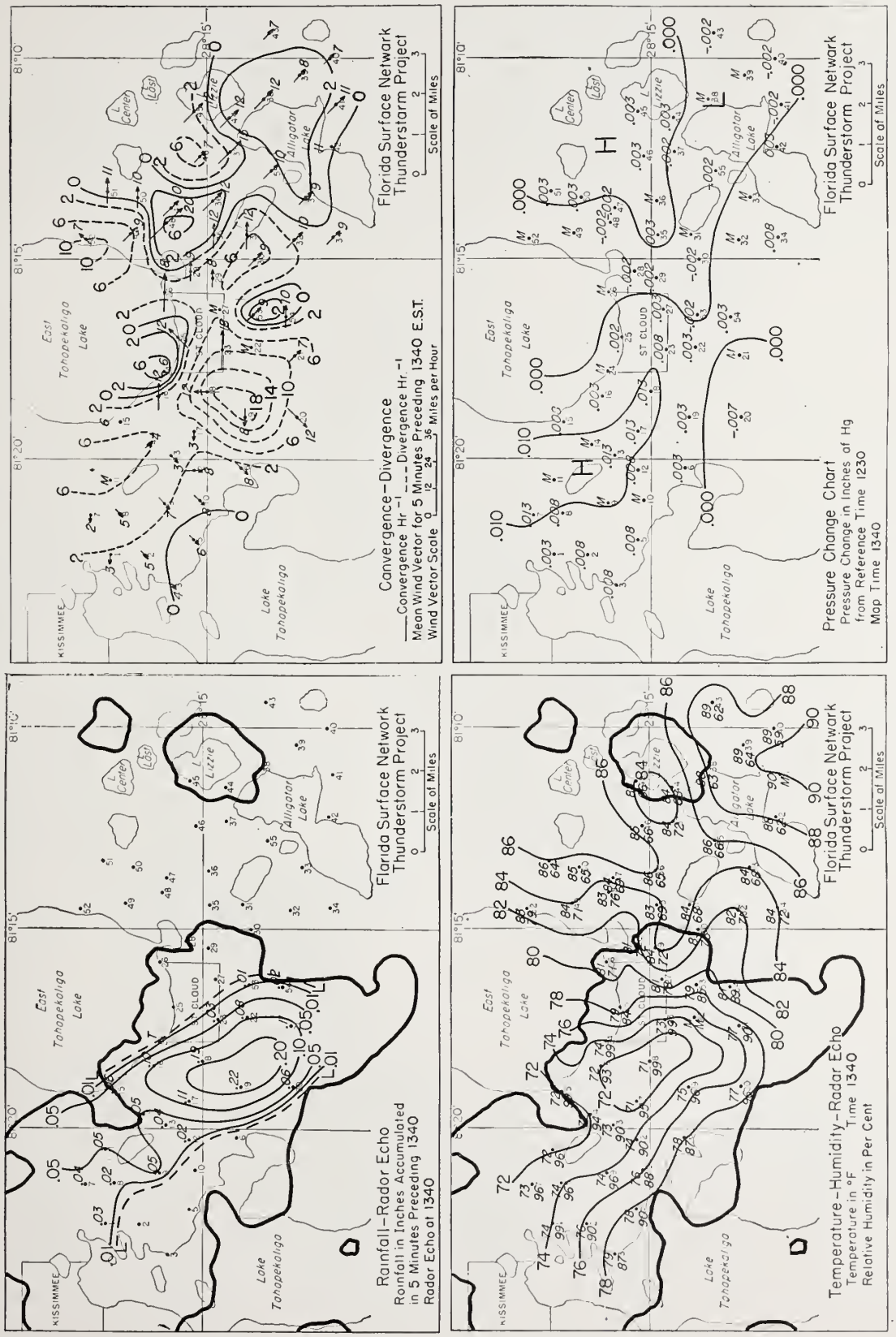

FIGURE 141.—Florida surface network, 1340 E.S.T., July 9, 1946.

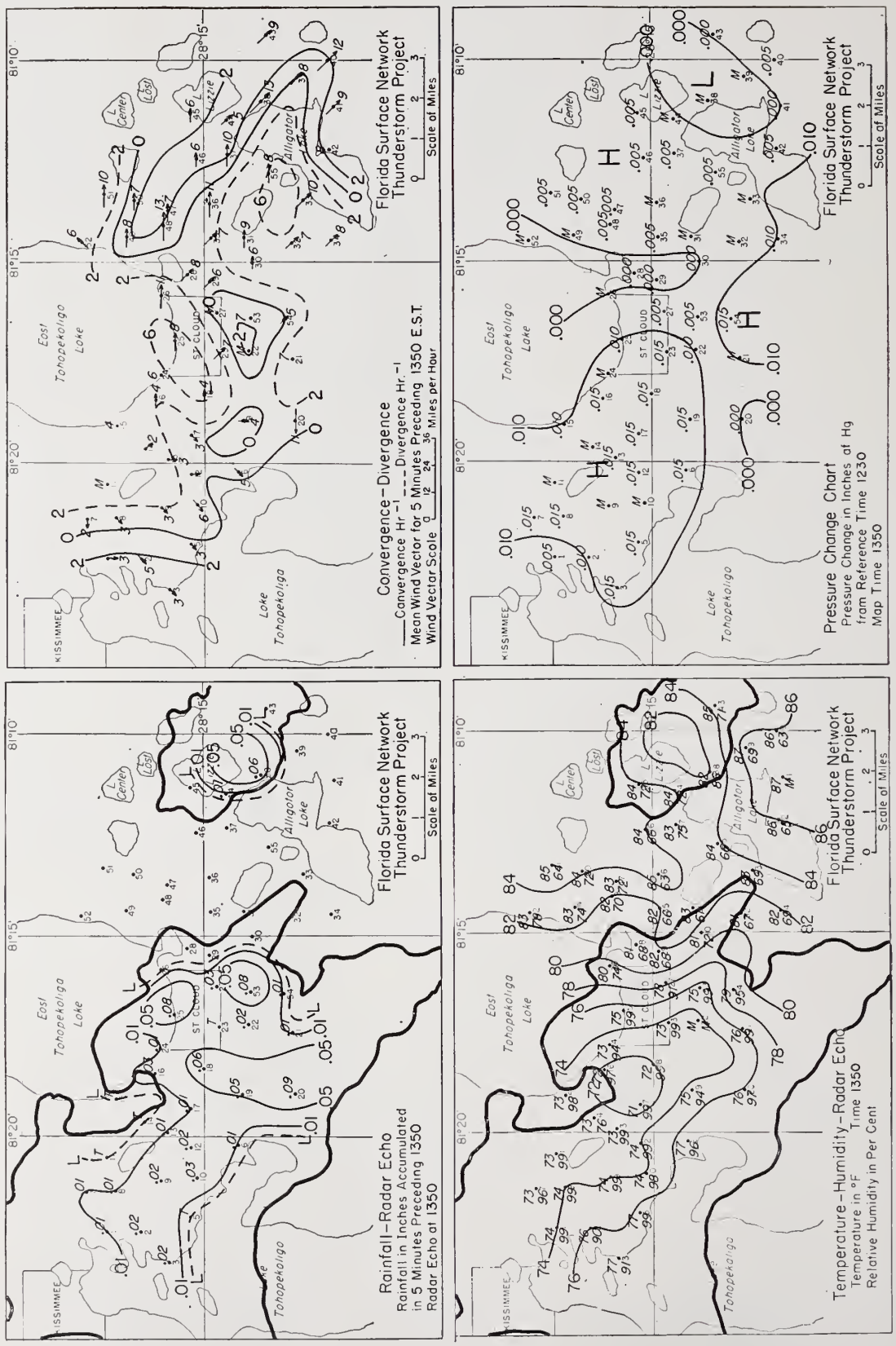

FIGURE 142.—Florida surface network, 1350 E.S.T., July 9, 1946.

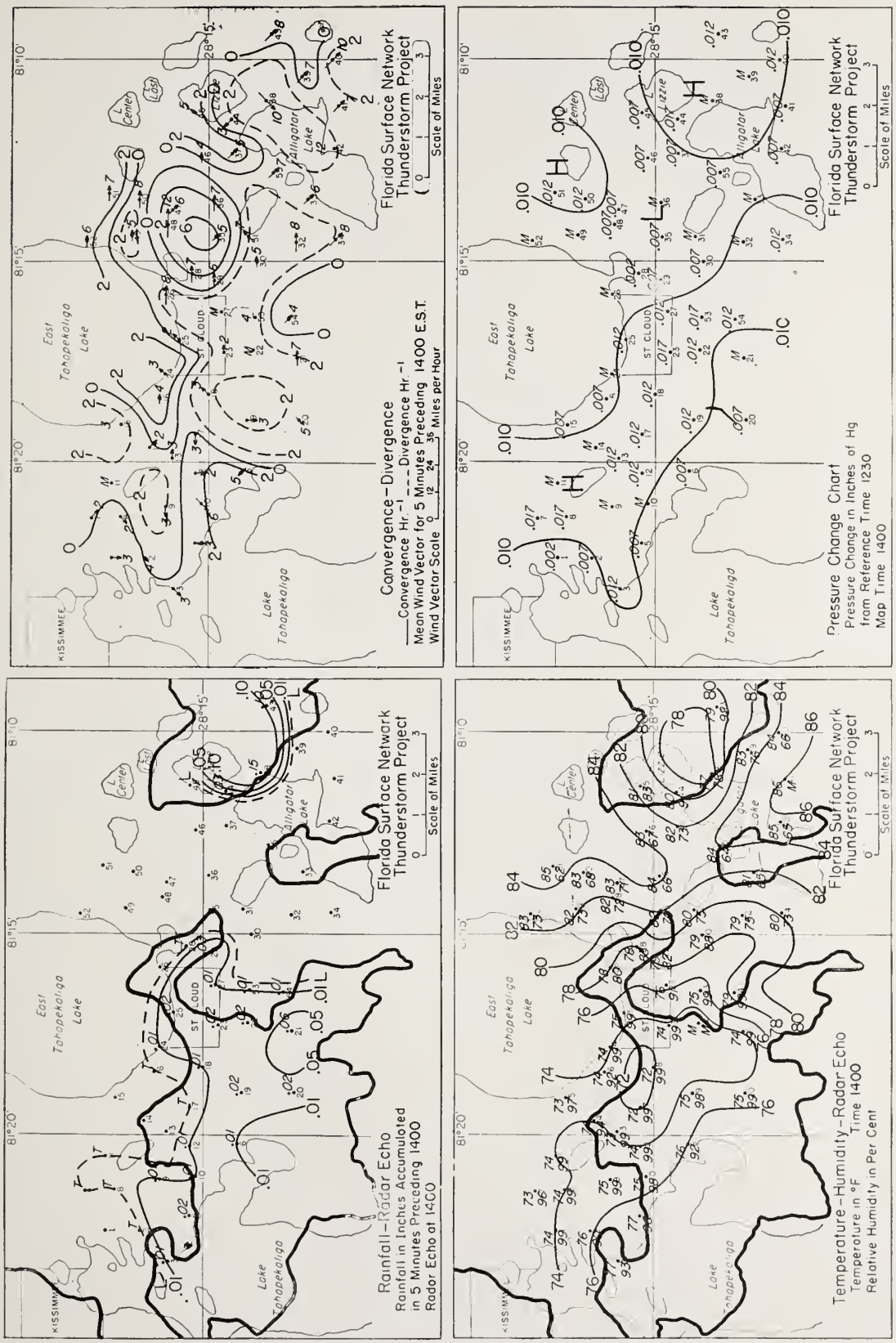

FIGURE 143.—Florida surface network, 1400 E.S.T., July 9, 1946.

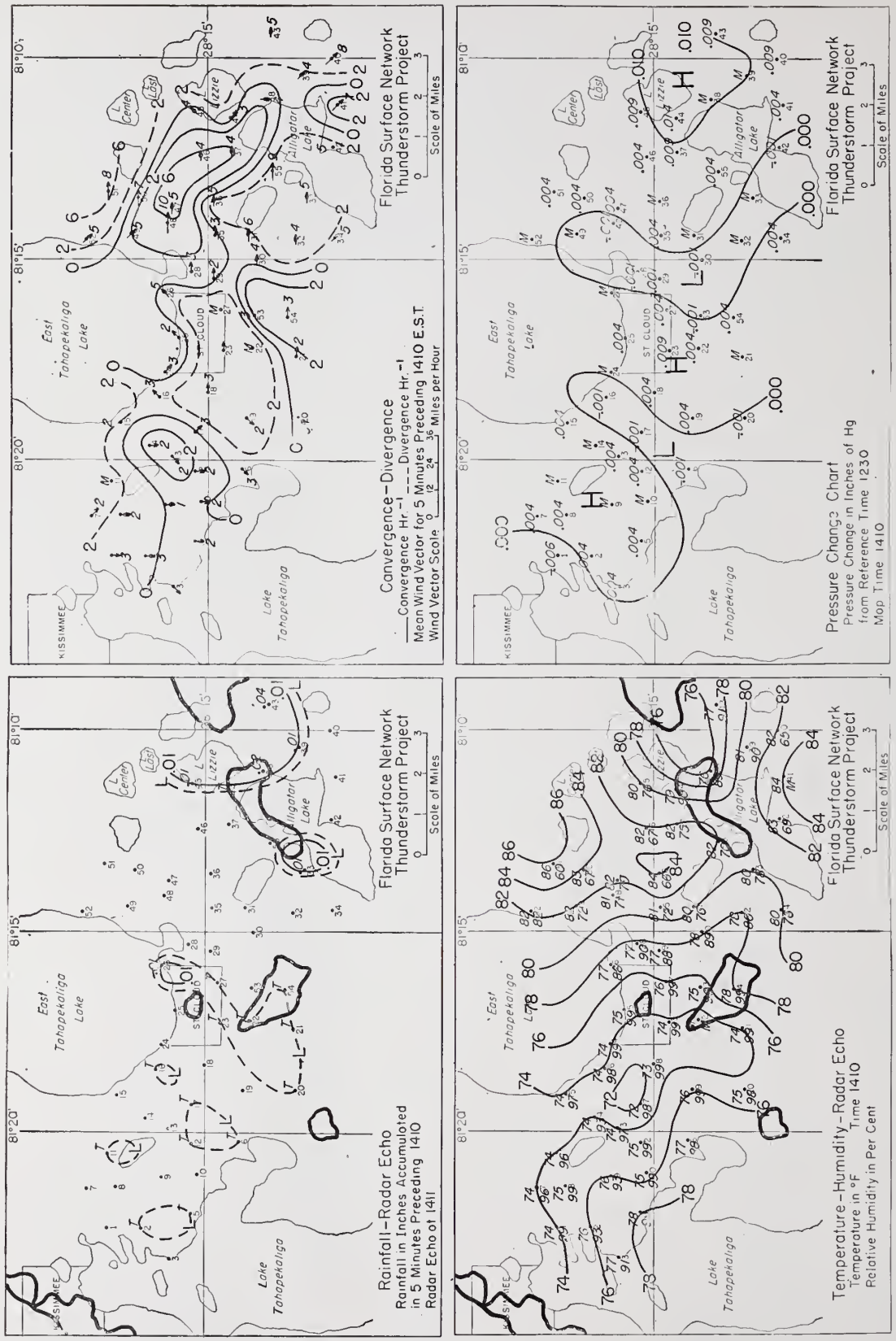

FIGURE 144.—Florida surface network, 1410 E.S.T., July 9, 1946.

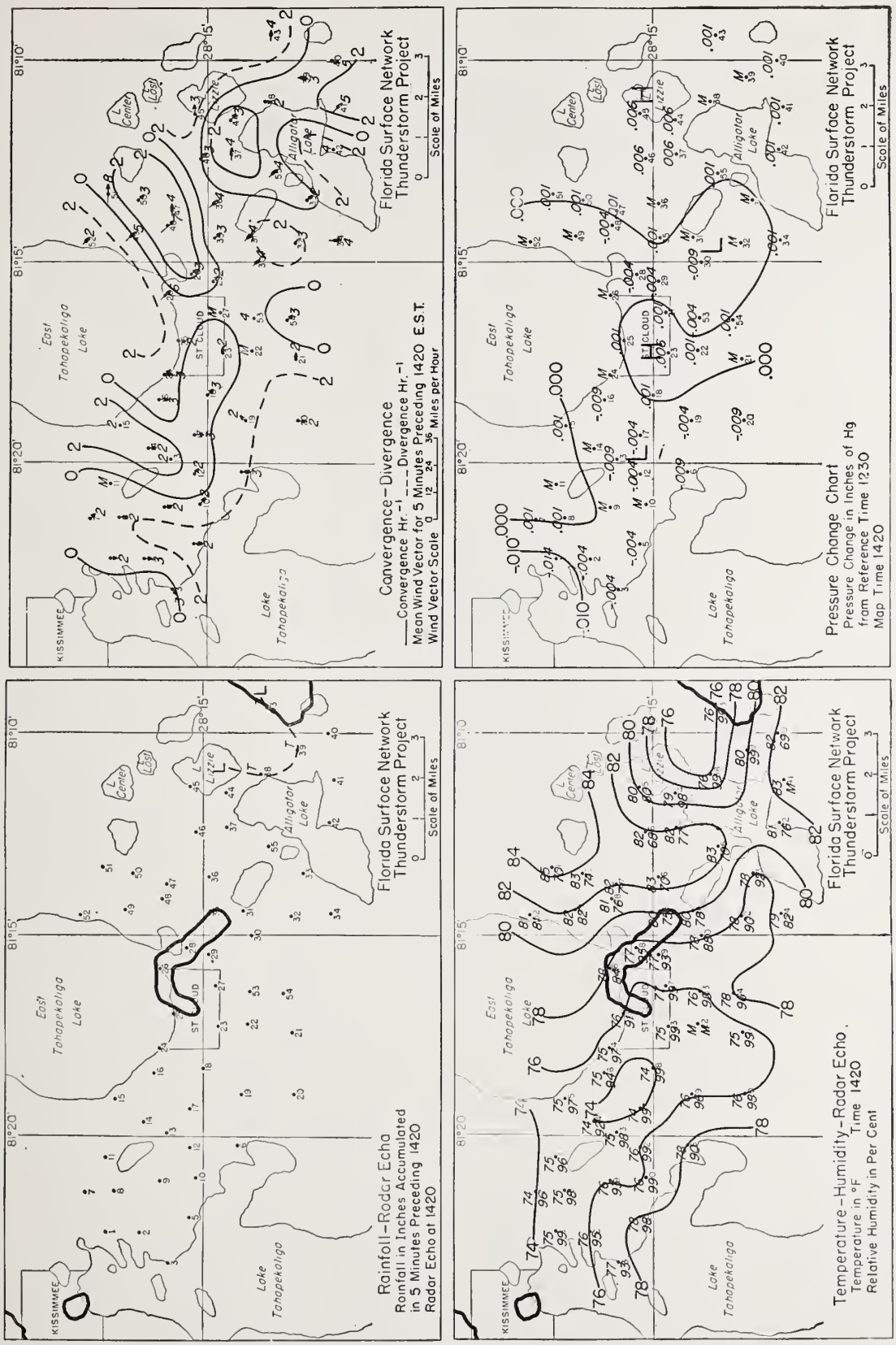

FIGURE 145.—Florida surface network, 1420 E.S.T., July 9, 1946.

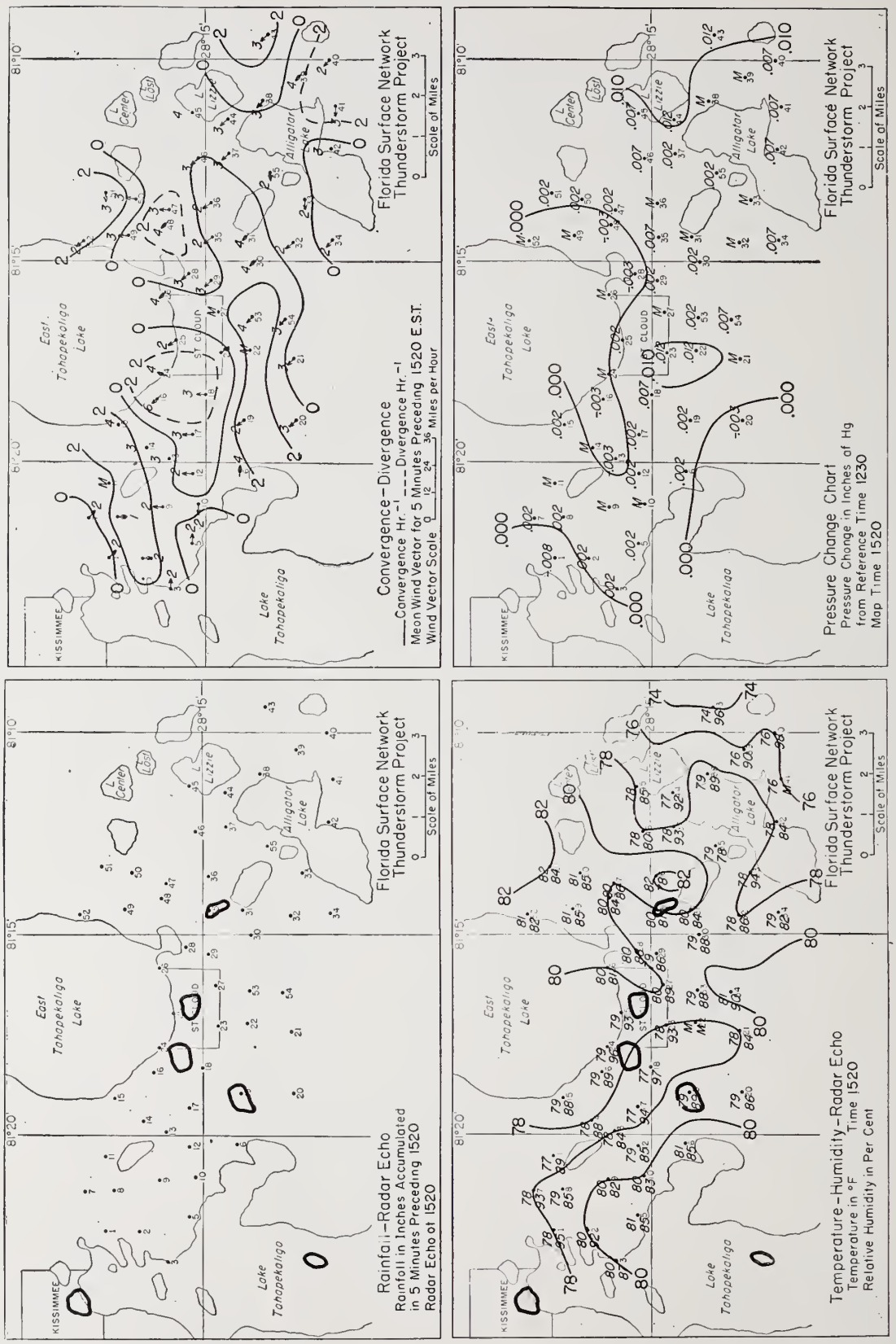

FIGURE 146.—Florida surface network, 1520 E.S.T., July 9, 1946.

THUNDERSTORM OF AUGUST 6, 1947
[1520 E.S.T. to 1550 E.S.T.]

The data obtained on the flights of August 6, 1947, are unusual among those gathered by the Project, since measurements were made by airplanes penetrating the cloud prior to detection of a PPI radar echo from the storm. The storm to be studied was selected by the pilots while in flight. This one was chosen because it appeared to be developing rapidly from a swelling cumulus cloud and was expected to attain full thunderstorm proportions. The choice was excellent, for it developed from a single cell to a storm containing four cells, and measurements were made during the major portion of its period of growth.

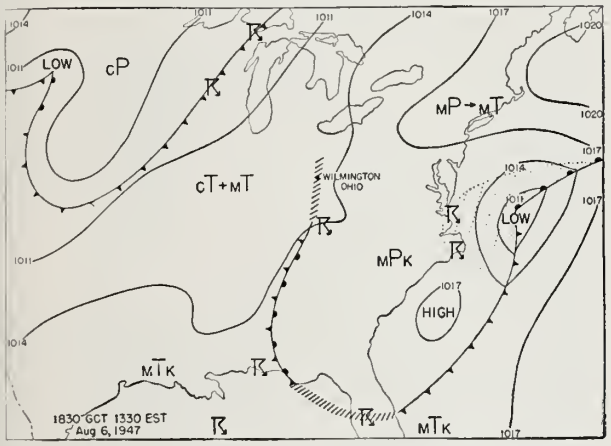

Figure 147.—A surface synoptic chart for 1330 E.S.T., August 6, 1947.

The synoptic map for 1330 E.S.T. on August 6, 1947 (fig. 147), shows as its major feature, in the area of the Project's operations, a dissipating stationary front extending through Wilmington, Ohio. Figures 148 and 149 show the 0300 G.C.T. soundings for Huntington, W. Va. and Joliet, Ill., respectively, for the day of the storm. Figure 150 is a schematic picture of a 200-mile-range PPI radar 'scope, with the actual radar echoes from convective storms present at 1545 E.S.T. shown in black. It is interesting to note the concentration of echoes along the line corresponding to the position of the surface front shown on the synoptic chart. The echo from the storm flown is so marked.

The traverses through this storm began at approximately 1514 E.S.T. and continued until 1553 E.S.T. During this period the echo from the storm moved southward (189°) at approximately 14 mi/hr. All of the airplane observations made were east of the surface network, which at this time was under the influence of a larger storm located to the northwest of the one studied. The spatial relationship of the storms in

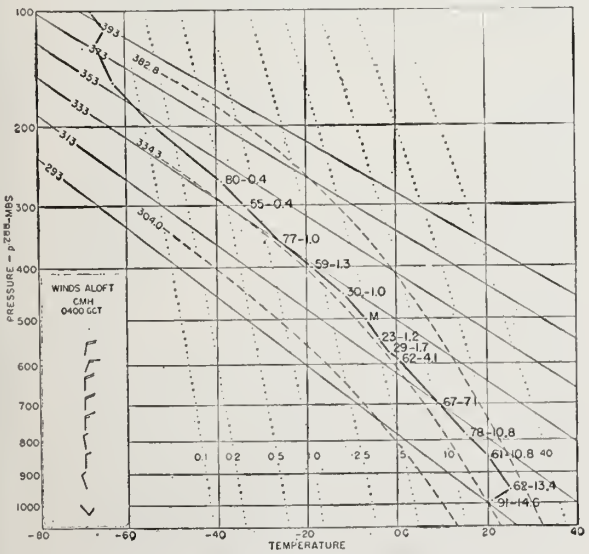

Figure 148.—Upper air sounding for 0300 G.C.T. from Huntington, W. Va., and the winds-aloft observation from Columbus, Ohio for 0400 G.C.T., August 6, 1947. These stations were east of the surface front.

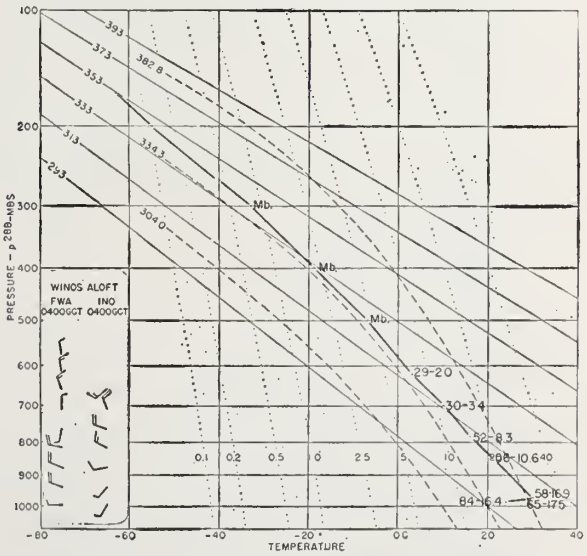

Figure 149.—Upper air sounding for 0300 G.C.T. from Joliet, Ill., and the winds-aloft observations from Fort Wayne and Indianapolis, Ind. These stations were west of the surface front.

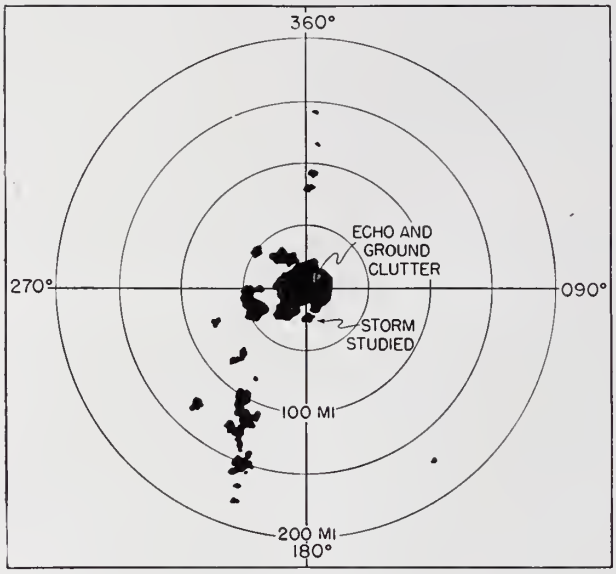

FIGURE 150.—A schematic drawing of the 200-mile-range PPI 'scope showing the actual radar echoes at 1545 E.S.T., August 6, 1947.

the area is shown on the radar 'scope photographs in figure 151. The first photograph shows, just right of center, the echo from cell I soon after its appearance on the 'scope. The next two photographs, taken at 1530 and 1535 E.S.T., respectively, present not only cell I, but also cells II and IV, which developed to the northwest and northeast of the original one. The photographs made at 1540 and 1545 E.S.T. show that cell I had dissipated and that cell III had developed to the north of cells II and IV, while the final picture depicts the growth of these three remaining cells and the development of cell V to the north of cell IV by 1550 E.S.T. In this series of photographs, the approach of the storm from the northwest should be noted. This storm had been in existence for a considerable length of time, and the cold air from downdrafts associated with it had spread over the surface network from the west by 1515 E.S.T.

1520 E.S.T.
(*fig. 152*)

Cell I was penetrated by airplanes prior to the appearance of the radar echo. For three of the six traverses through the cell at this time, it was possible to evaluate updrafts. No downdrafts were found. The reports of the presence of liquid water within the cloud characterized it as light, very light, or dew-like rain. The rain extended to the 20,000-foot level, and no snow was encountered. Cell I was in the cumulus stage of development during this period.

1530 E.S.T.
(*fig. 153*)

The traverses made at each altitude have been shown in separate sections of figure 153, since they were made one above another. As is shown, only the radar echo from cell I was apparent at 1530 E.S.T. This echo had first appeared at approximately 1525 E.S.T.

Cell I was intersected by airplanes flying at 10,000 and 20,000 ft., and at both of these levels updrafts and downdrafts were encountered. The earliest measurement of the downdraft was made simultaneously with the initial detection of the radar echo — an unusual condition. At 10,000 ft., fine, very light rain was again reported, while at 20,000 ft., light, fine, moist snow was encountered. This cell was in the mature stage of development during this time.

Cell II was first intersected during this period. At all three levels of flight updrafts were experienced, but a radar echo from this cell was not yet detectable. However, the existence of the updrafts and the localization of the turbulent areas encountered clearly indicate the area of convective activity associated with this cell. Light, dew-like rain at 6,000 ft., light and moderate rain at 10,000 ft., and light snow and rain at 20,000 ft. were reported. This cell, characterized by the updraft and relatively small amount of liquid water, was in the cumulus stage of development.

1540 E.S.T.
(*fig. 154*)

As is shown in figure 154, the PPI radar photographs showed considerable change in the radar echo from this storm had taken place during the interval between 1530 and 1540 E.S.T. The echo from cell I had virtually disappeared, and cell II had become predominate.

Cell I was not penetrated at this time, but because of the rapid disappearance of the radar echo, it must be assumed that the cell had entered its dissipating stage very early in this interval and was characterized by downdraft.

Cell II was traversed by airplanes at all three levels, but no drafts could be evaluated from the records. Photographs made by an observer at the surface (station 39) showed rain from the western portion of the cell at 1540 E.S.T., but none was recorded by the gages of the observational network. It is probable that this cell contained both an updraft and a downdraft during this period, but, because of the lack of definite information, these are not indicated in the figure 154. At 10,000 ft., light rain was again encountered, and light snow was found at 20,000 ft.

Cell III became evident from an updraft, measured at both the 6,000 and 20,000-foot flight levels, although the radar echo from it had not yet been detected. Light, dew-like rain was reported from the plane flown at 6,000 ft., and at 10,000 ft. very light rain was encountered, except in the region of the up-

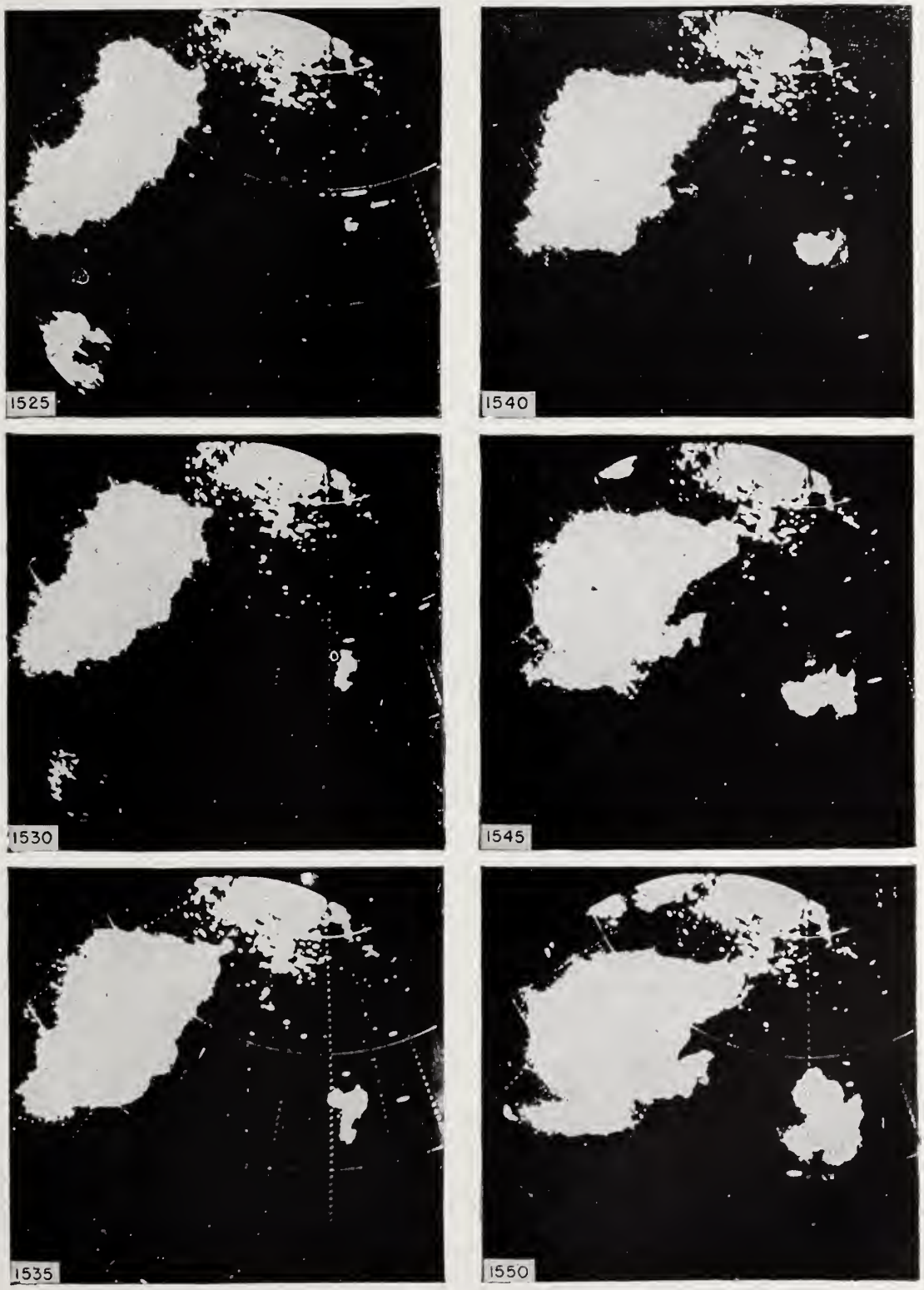

FIGURE 151.—Control-radar PPI 'scope photographs, 1525–1550 E.S.T., August 6, 1947.

draft, where heavy rain was found. This cell was in the cumulus stage of development.

The turbulence indicated to the east of cell II was attributed to cells IV and V, discussed in the following paragraphs.

1550 E.S.T.
(*fig. 155*)

Cell IV and Cell V were penetrated during the last period of observation of this storm. Cell I by this time had completely dissipated. Cells II and III were in the mature stage and, in all probability, contained both updrafts and downdrafts at this time, although information to support this supposition was lacking. No rain was recorded by the surface network, and the winds at stations that would have been affected by outflow from these cells continued to blow from the west; the outflow from the storm to the northwest of the network was predominant.

Cell IV was penetrated by airplanes at 10,000- and 20,000-foot levels, but no drafts could be evaluated from the records. At 20,000 ft. moderate to heavy rain was encountered, while at 10,000 ft. very heavy rain was reported. It is probable that this cell had entered or was just about to enter the mature stage of development.

Cell V was in the cumulus stage of development but had not yet extended to 20.000 ft., for the airplane at that level did not enter cloud or encounter turbulence until it reached cell IV. At 10,000 ft., however, an updraft was encountered and light rain was reported.

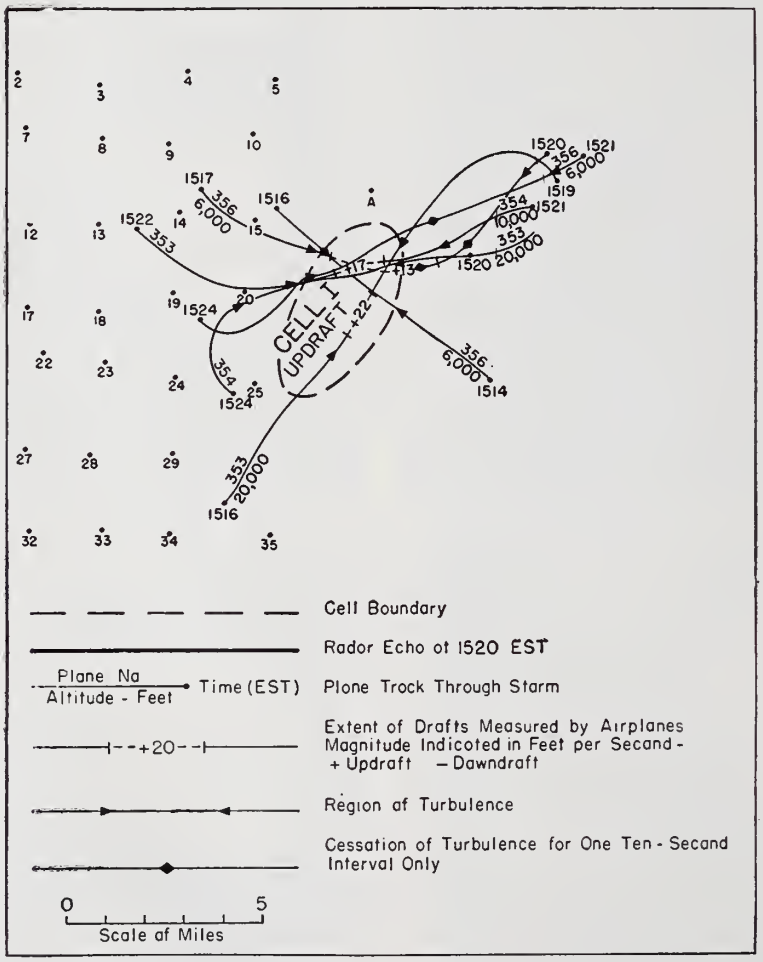

FIGURE 152.—PPI radar echo at 1520 E.S.T., and airplane paths from 1515 to 1525 E.S.T., August 6, 1947.

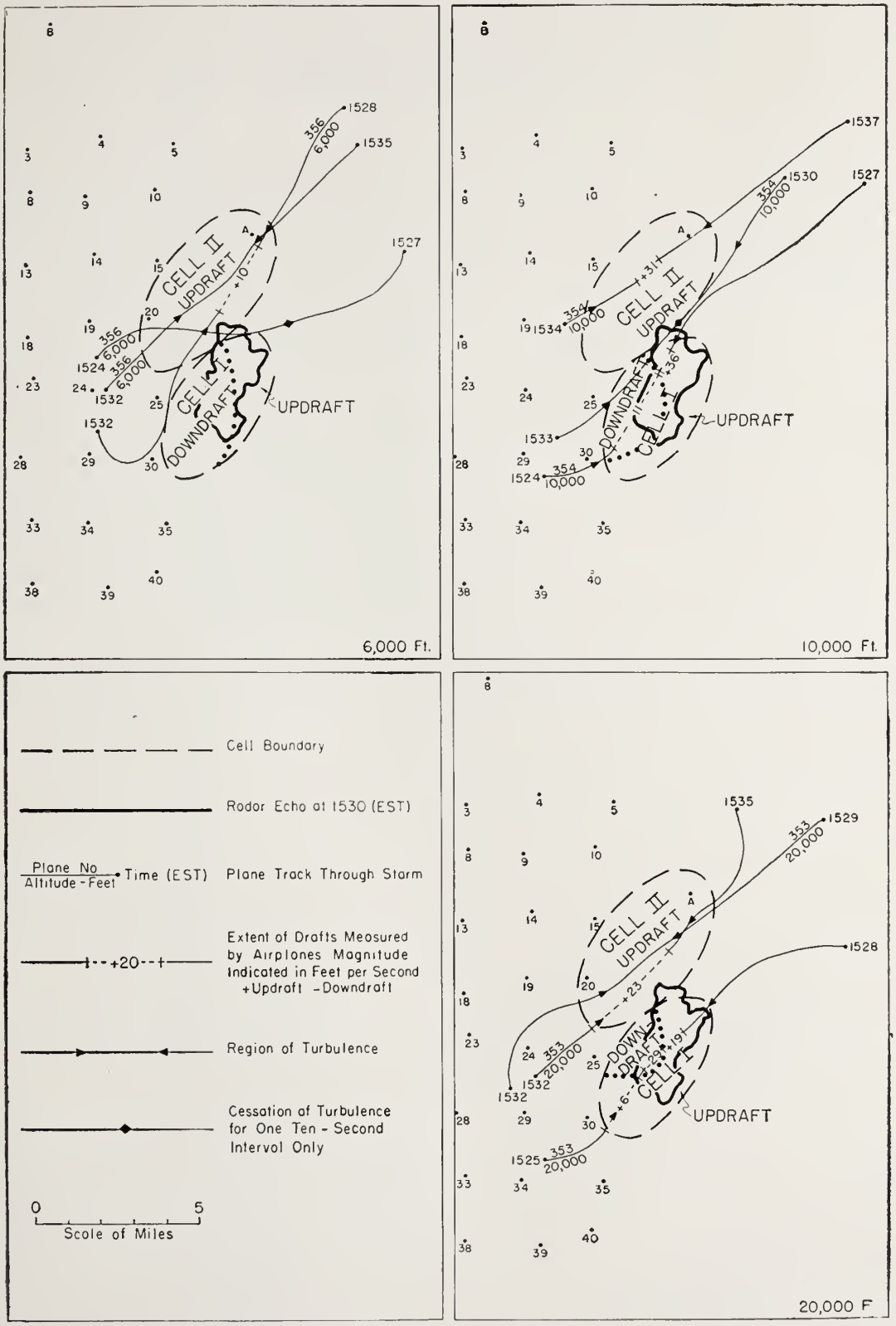

FIGURE 153.—PPI radar echo at 1530 E.S.T., and airplane paths from 1525 to 1535 E.S.T., August 6, 1947.

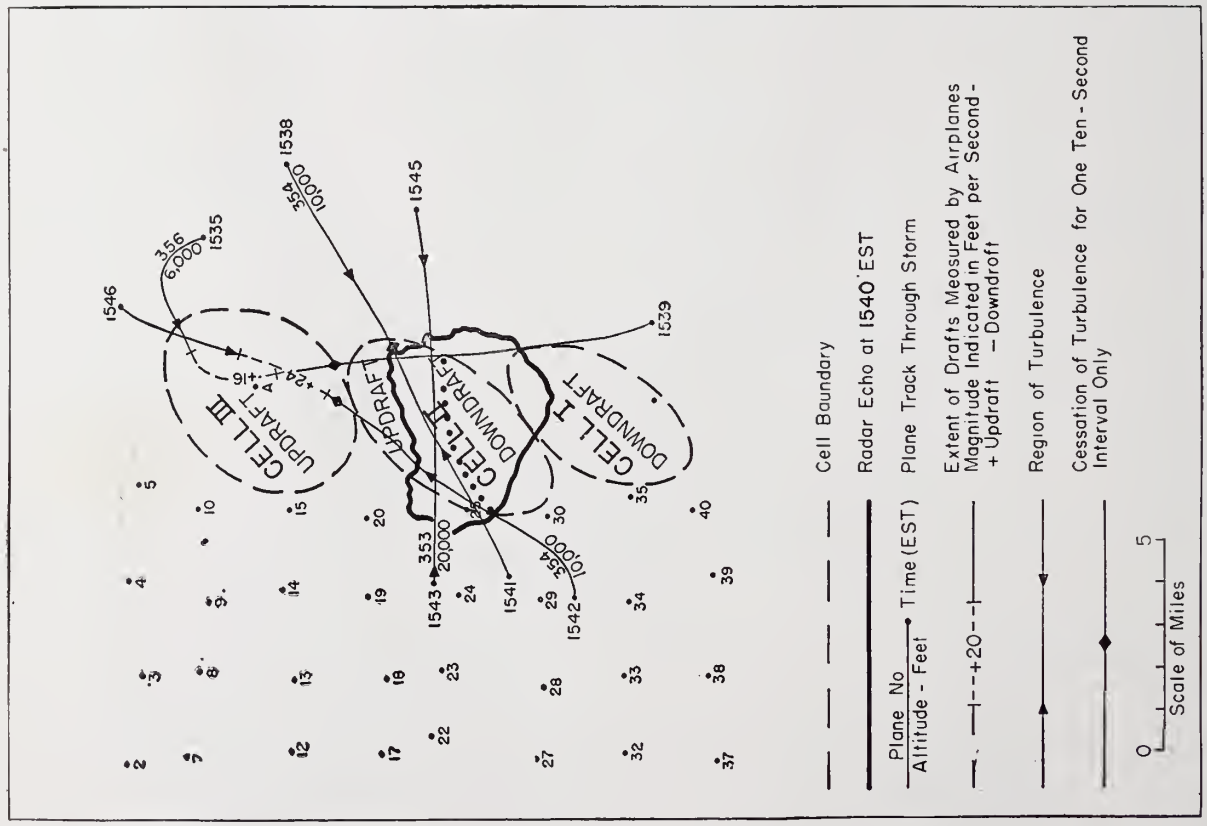

FIGURE 154.—PPI radar echo at 1540 E.S.T., and airplane paths from 1535 to 1545 E.S.T., August 6, 1947.

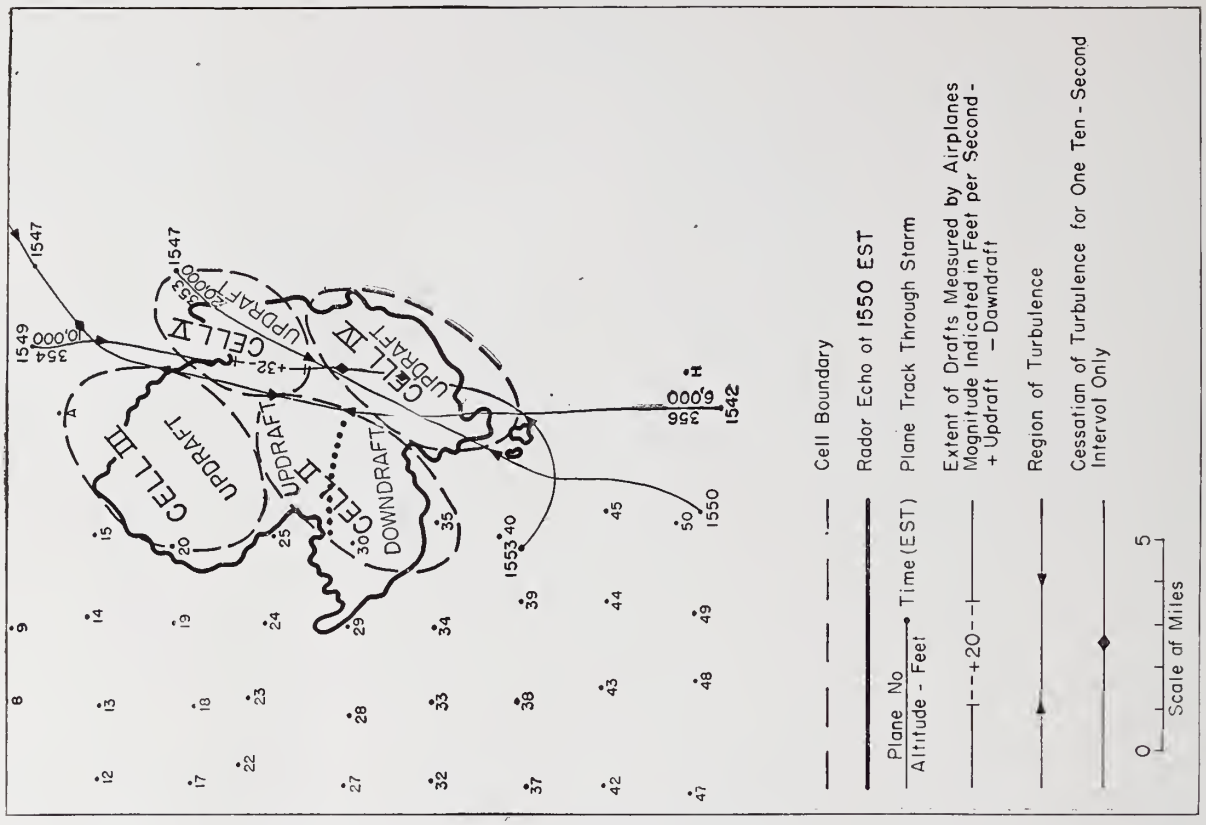

FIGURE 155.—PPI radar echo at 1550 E.S.T., and airplane paths from 1545 to 1555 E.S.T., August 6, 1947.

THUNDERSTORM OF AUGUST 13, 1947
[1510 E.S.T. to 1650 E.S.T.]

This storm is included in the examples because it was a relatively isolated one and several of the cells associated with it went through their life cycles over one end of the surface network. These features allow a study of the cold outflow, with the associated variations in the surface weather elements, as it traverses the entire length of the surface network.

On this day Ohio was under the influence of a southwesterly current which was associated with the warm high-pressure area over the southeastern United States and was transporting maritime tropical air from the Gulf of Mexico to most of the central and eastern part of the country. To the northwest, over the Minnesota-Manitoba border, an active low-pressure area with a well-developed frontal system was present (fig. 156). The low-pressure center and the northern portion of the associated cold front were moving eastward at a rate of 20 to 25 mi/hr. Figure 157 shows the upper-air sounding for the day of the storm.

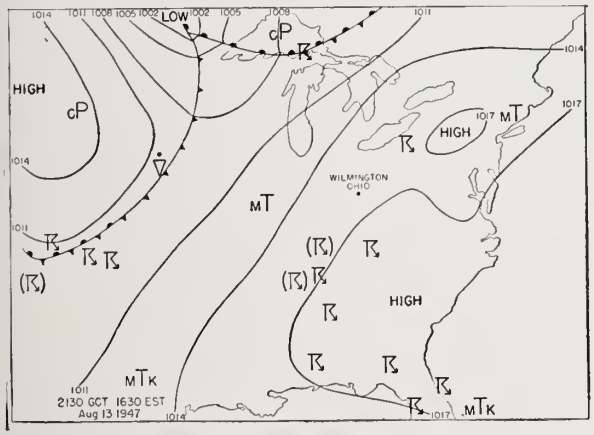

Figure 156.—Surface synoptic chart for 1630 E.S.T., August 13, 1947.

During the afternoon, scattered showers and thunderstorms occurred along both the warm and cold fronts and over scattered areas in the tropical air east of the cold front. The photographs from the high-power radar showed that widely scattered thunderstorm activity continued throughout the afternoon within 200 mi. of Jamestown, Ohio (see fig. 158). The radar-echo history of the storm studied is shown in figures 159 and 160.

1510 E.S.T.
(*fig. 161*)

From figure 161 it may be seen that at 1510 E.S.T. there were several local areas of maximum tempera-

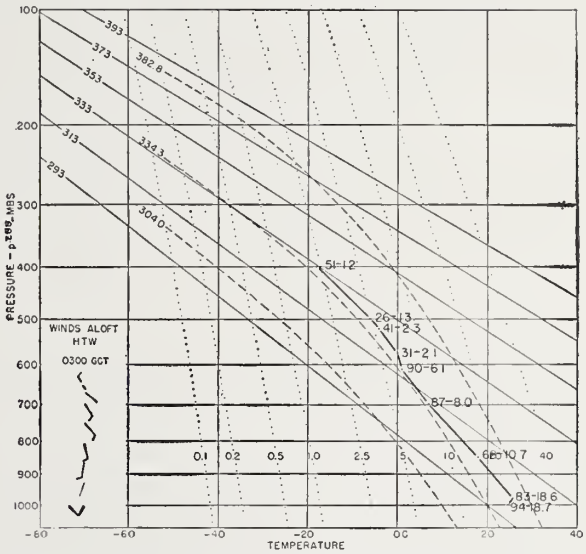

Figure 157.—Upper air sounding and winds aloft observation for 0300 G.C.T., August 13, 1947 from Huntington, W. Va.

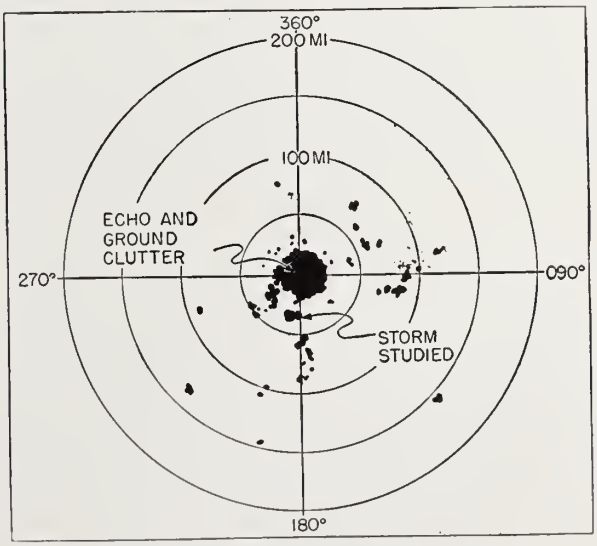

Figure 158.—A schematic drawing of the 200-mile-range PPI 'scope showing the actual radar echoes at 1600 E.S.T., August 13, 1947.

ture — due perhaps to differences in cloudiness, station exposure, and instrument errors. Earlier, a storm over the network had caused temperature falls at the northwestern stations (1 and 2). Toward the south, however, temperatures were substantially higher, with a value of 90° F. having been recorded at station H. Relative humidities in the area which had been affected by the previous storm were high, but they were in the sixties and seventies throughout the remainder of the network. In the southern part of the network, beneath the region of cell development, the pressures were low, but there were also other low-pressure areas of equal magnitude in the eastern part of the network. Winds over the network were easterly, in general, but there was also a southerly component directed toward the area of echo development. This resulted in weak convergence. In the northern portion there was a northward turning of the winds. Although the radar showed that a thunderstorm was located about 4 mi. south of the network at this time, its effects were not evident over the surface network.

1520 E.S.T.
(*fig. 162*)

One of the principal radar echoes associated with this storm had appeared on the radar 'scope at 1515 E.S.T., but no rain was yet recorded at the surface. Slight temperature falls occurred in the region under the echo, probably due to radiational cooling resulting from the presence of clouds, since the outflow which comes from a cold downdraft had not yet begun. The winds continued to be light, and their inward turning toward the region of echo development was more pronounced, particularly in the vicinity of station 46. The outflow from the storm south of the network had by this time caused large changes in the wind direction observed at station 53. Pressures were still low under the region of convective activity, but they had risen in the period from 1510 E.S.T. to this time.

1530 E.S.T.
(*fig. 163*)

The first rainfall recorded from this storm appeared at station 46 at 1526 E.S.T., and rain was measured at station 47 at 1528 E.S.T. Since the rain had been falling for such a short time by 1530 E.S.T., the temperature effects associated with cold-air outflow were not yet apparent. The winds continued light, and the inflow toward the area of storm development increased slightly. Pressure falls were apparent in much of the area beneath the cell and in surrounding regions. A sharp pressure rise — probably associated with the pressure nose which occurs when a downdraft reaches the ground — was recorded at station 46.

1540 E.S.T.
(*fig. 164*)

By 1540 E.S.T., the rainfall from the western echo of the storm was intense (0.22 in/5 min at station 46), and the downdraft was well established, resulting in pressure increases over most of the southern portion of the network. Relatively strong divergence (over 6 hr^{-1}) developed near station 46 as a result of outflow, and convergence developed along the leading edge of the first-gust line. The band of divergence in the central part of the network was created by the inward turning of the winds toward the storm. As a result of the cold downdraft, the temperature at station 46 fell 9° F. during the interval from 1530 to 1540 E.S.T., thus establishing a very strong thermal gradient. A new echo formed just east of the existing one, and later charts showed heavy rain and other intense weather conditions to be associated with it.

1550 E.S.T.
(*fig. 165*)

Under the western echo, the rainfall diminished and the pressure fell slightly. However, continuing vigorous outflow and further temperature falls indicated that the downdraft continued. Under the eastern echo, heavy rainfall and marked pressure rises were recorded at this time. In addition, the elongation of the 78° isotherm and the increase in wind speed observed at station 48 show that this cell also had a strong downdraft. Relative humidities rose, as is usual in the area of cold-air outflow. It is to be noted that the strong outflow was counteracting the inflow component of the winds from the north, which had been observed in an earlier period, and the result was an area of relative calm ahead of the outflowing cold air. The convergence ahead of the first-gust line and the divergence behind it were apparent.

1600 E.S.T.
(*fig. 166*)

The continuing temperature falls and the divergence of the surface winds under the storm indicated that the cold downdraft continued. Around the periphery of the outflowing cold air, convergence was evident. The rainfall from the eastern echo increased markedly, but the rain associated with the western one had either diminished greatly or had moved off the surface network. The increased size of the western echo suggested that a new cell had developed in the vicinity of station E. This supposition was supported by observations at that station of increased winds and pressure. Except for a band of low pressure which persisted over the eastern border of the network, pressures continued to rise.

1610 E.S.T.
(*fig. 167*)

By 1610 E.S.T. the rate of rainfall under the western echo was comparatively light, and the rain from the eastern one had decreased substantially. Both had well-defined areas of minimum temperature, and the radial outflow of the cold air was well illustrated by the configuration of the isotherms on the temperature chart. Divergence under the storm area and convergence ahead of the first-gust line persisted. As the cold air continued to spread outward over the network, the pressure continued to rise. Pressure rises also occurred, however, on the northern and eastern edges of the network in areas not yet reached by the cold-air flow at the surface. If these pressure effects, outside the area of outflowing cold air, were due to the thunderstorm and not to large-scale synoptic effects, it appears that the circulation associated with this storm extended over large distances, and that convergence or divergence aloft took place 10 or 15 mi. away from the center of thunderstorm activity.

1620 E.S.T.
(*fig. 168*)

Rainfall continued under both echoes at 1620 E.S.T., but it was comparatively light for thunderstorm rainfall. The cold-air pool reached its minimum temperature at this time, but temperature falls were still occurring to the north with the passage of the discontinuity surface. The radial outflow from the storm, with its resulting divergence, continued. Pressure falls were recorded south of the storm area, and very slight rises occurred in the northern part of the network.

1630 E.S.T.
(*fig. 169*)

The isohyetal pattern for 1630 E.S.T. and the manner in which the radar echo dissipated indicated that the eastern echo of the storm may have been composed of several cells. Moreover, it appears that the rainfall recorded at stations 39 and 40 might have been the result of new cell development. Appreciable divergence still persisted over the area covered by the eastern echo; a value of 5 hr^{-1} was computed for the area bounded by stations 32, 33, 37, and 38. The convergence associated with the first gust was evident in the northern portion of the network. Slight pressure rises associated with the arrival of the cold-air discontinuity were recorded. Pressures continued to fall in the south, even though the areas of minimum temperature were still located there.

1640 E.S.T.
(*fig. 170*)

By 1640 E.S.T., little remained of the radar echo associated with this storm, although, as is frequently the case, lingering rainfall persisted at some stations. The temperature field remained essentially unchanged from that which had existed 10 min. previously, and the wind field showed weak divergence over most of the network. It is to be noted that the wind speeds in the center of the network were very light or calm, while they were stronger along the northern and southern boundaries. Such a wind pattern may result from the flattening of the cold-air dome or from the downward gliding of air along an equipotential surface inside the cold-air dome. Such a wind field is frequently found under cells in the dissipating stage.

1650 E.S.T.
(*fig. 171*)

There was no rainfall recorded over the surface network during the period from 1645 to 1650 E.S.T. (period for which the 1650 E.S.T. rainfall map was prepared), and all radar echoes had dissipated or moved from over the network. The temperatures began to warm up slightly in the areas where rainfall had been heavy, but there was still slight cooling in the continuing outflow in the northern part of the network. The divergence continued to decrease and the general appearance of the wind and pressure fields was similar to that which had existed at the time of the previous chart.

1750 E.S.T.
(*fig. 172*)

At 1750 E.S.T., no rain or radar echo were present over the surface network. It is noteworthy that the isotherms showed the same general configuration (with the area of minimum temperature still maintaining its identity over the southern part of the network), as had existed at 1650 E.S.T. However, there had been slight warming in the southern areas and slight cooling to the north. The winds were extremely light over the entire network, and only very weak convergence and divergence areas were present, to which no significance can be attached. In the hour from 1650 to 1750 E.S.T., the pressure dropped slightly over the entire network and assumed about the same values as had been present 2½ hr. earlier.

841051—50——13

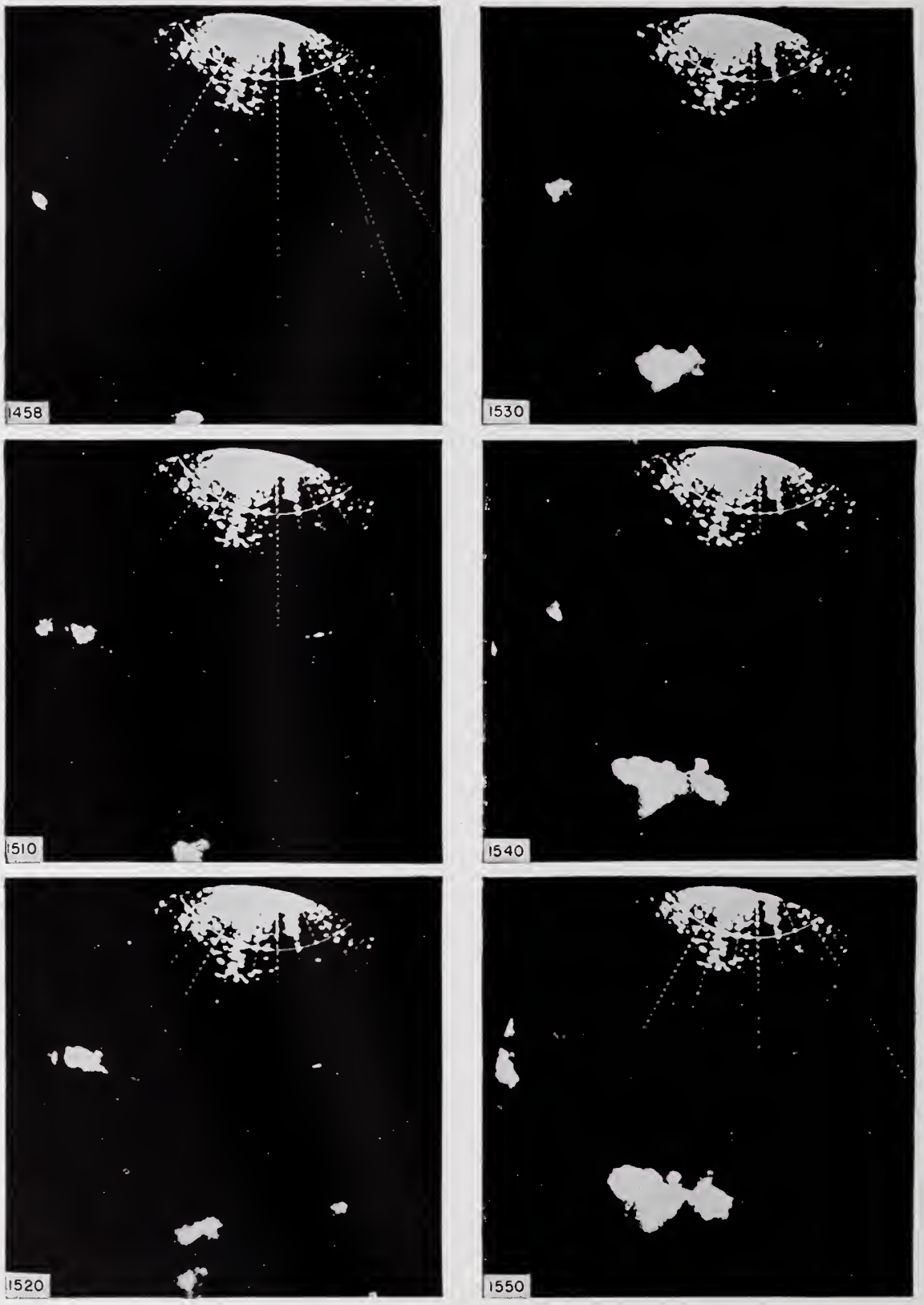

FIGURE 159.—Control-radar PPI 'scope photographs, 1458–1550 E.S.T., August 13, 1947.

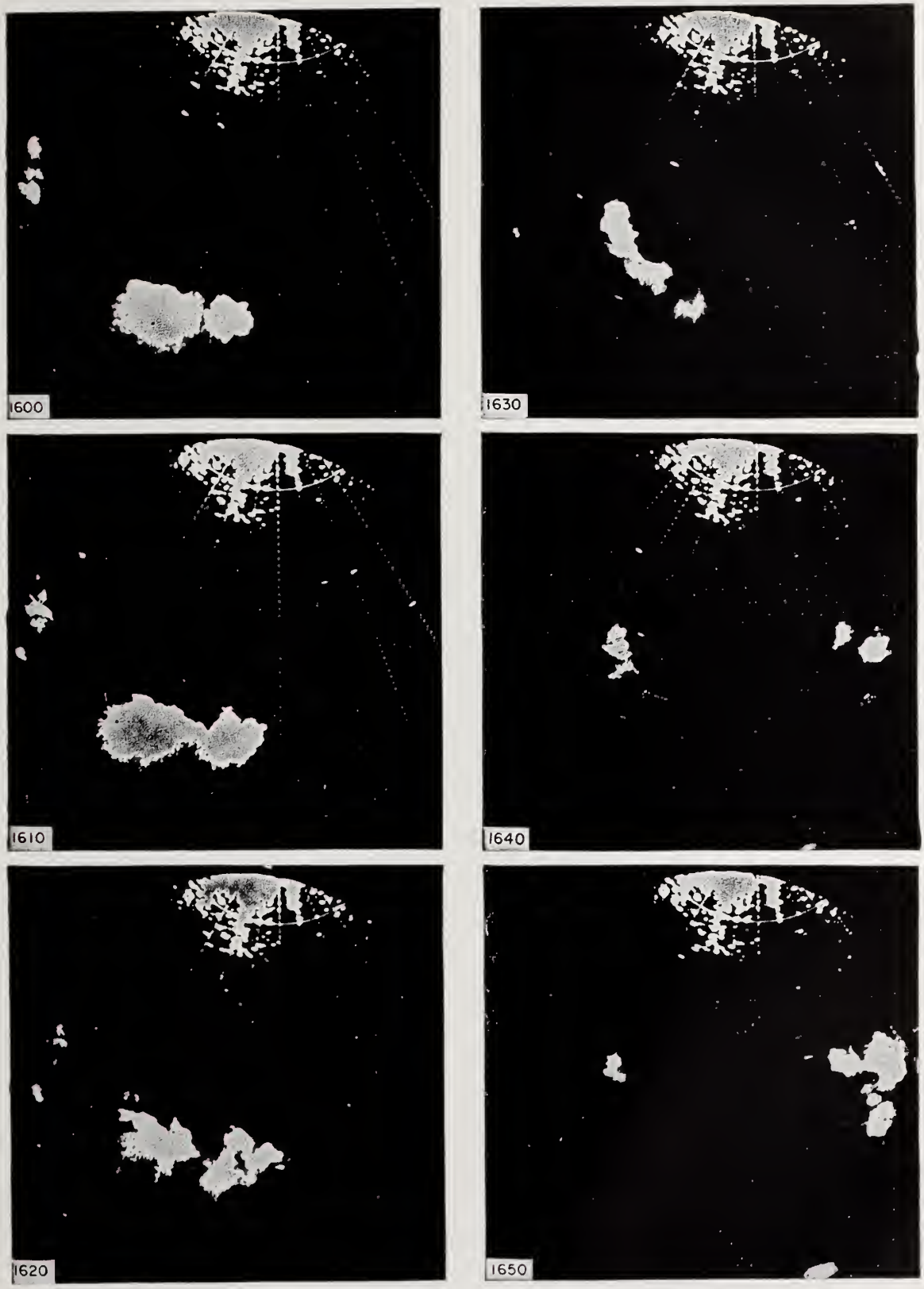

FIGURE 160.—Control-radar PPI 'scope photographs, 1600–1650 E.S.T., August 13, 1947.

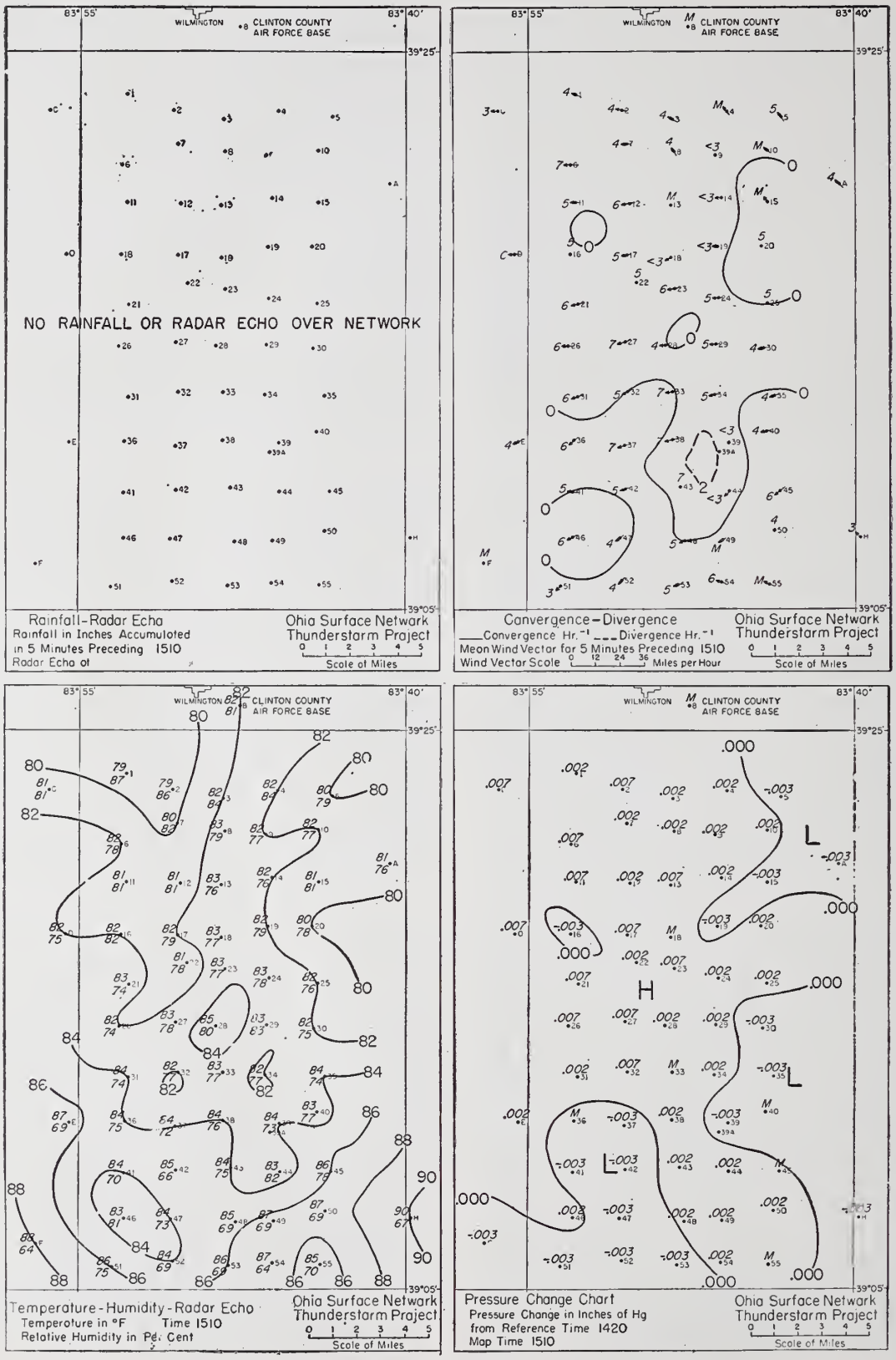

FIGURE 161.—Ohio surface network, 1510 E.S.T., August 13, 1947.

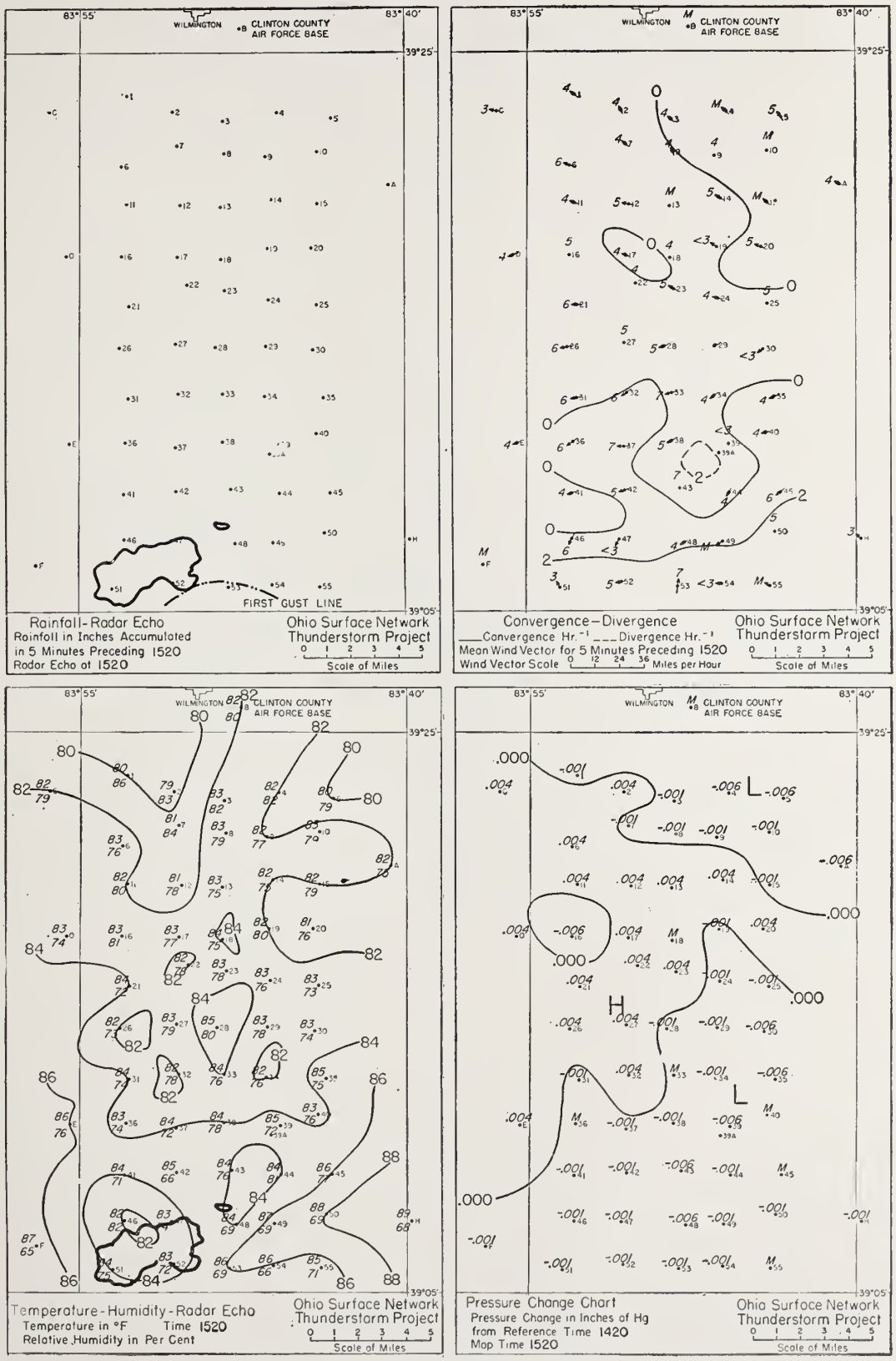

FIGURE 162.—Ohio surface network, 1520 E.S.T., August 13, 1947.

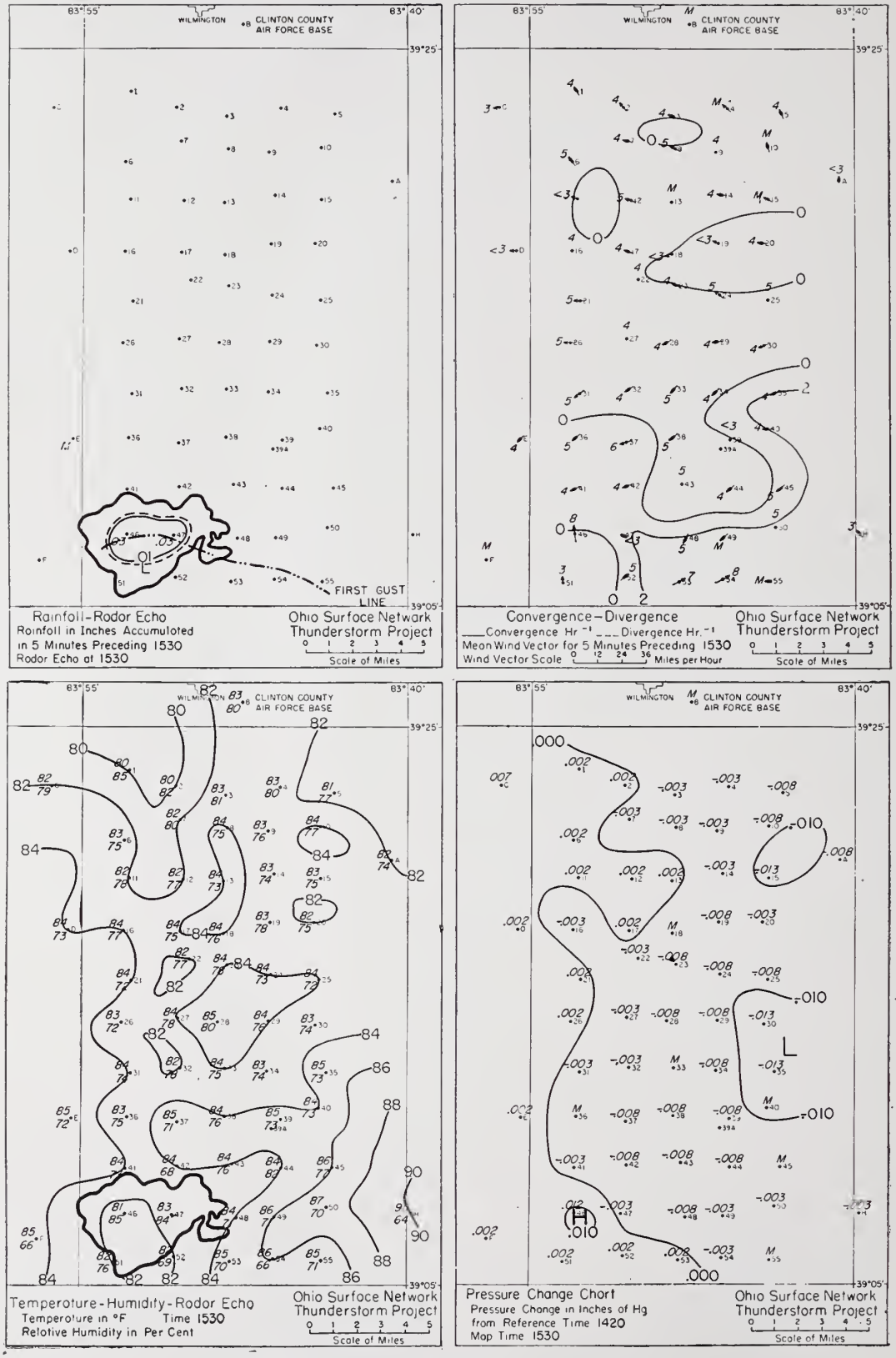

FIGURE 163.—Ohio surface network, 1530 E.S.T., August 13, 1947.

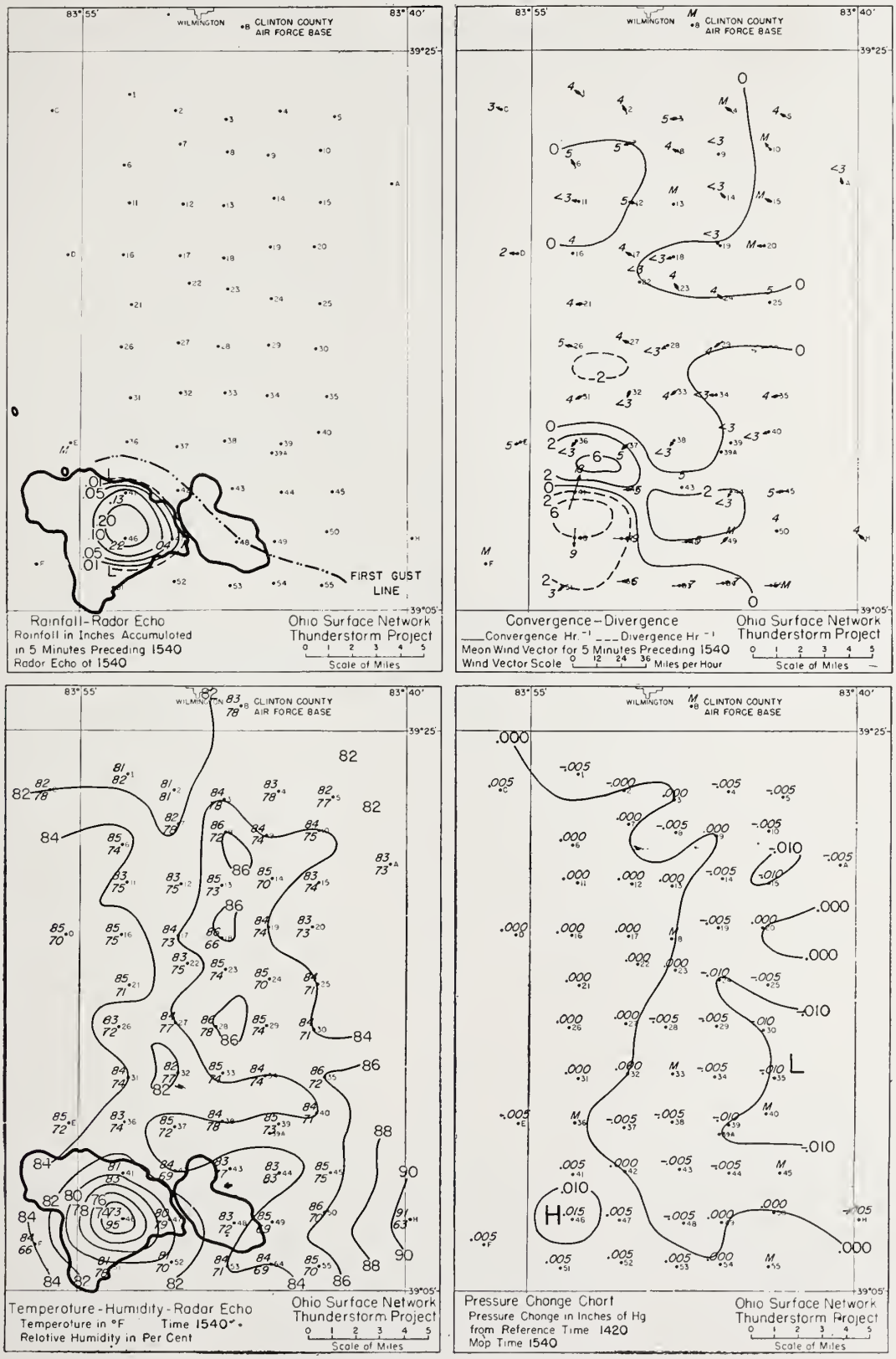

FIGURE 164.—Ohio surface network, 1540 E.S.T., August 13, 1947.

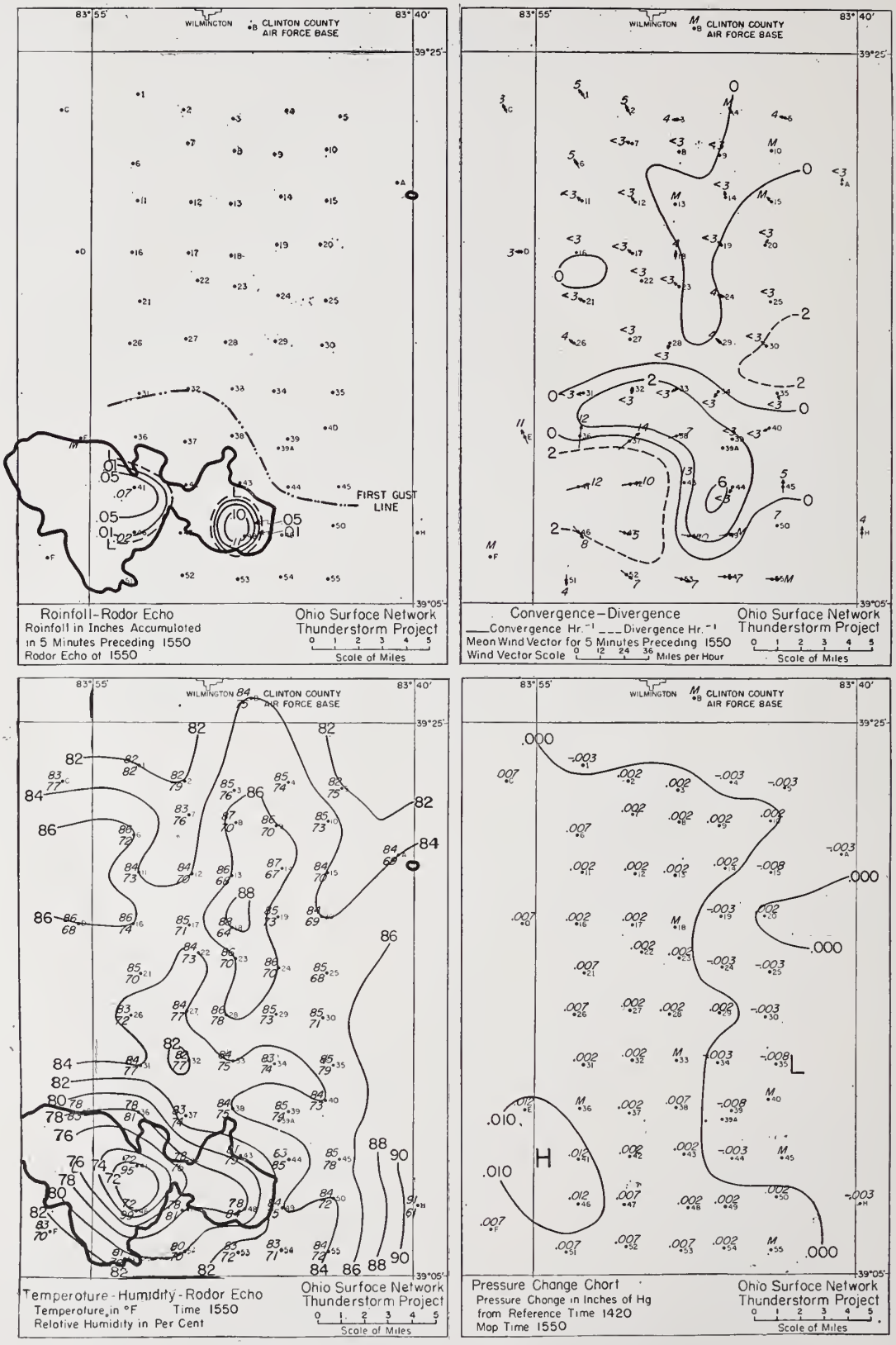

FIGURE 165.—Ohio surface network, 1550 E.S.T., August 13, 1947.

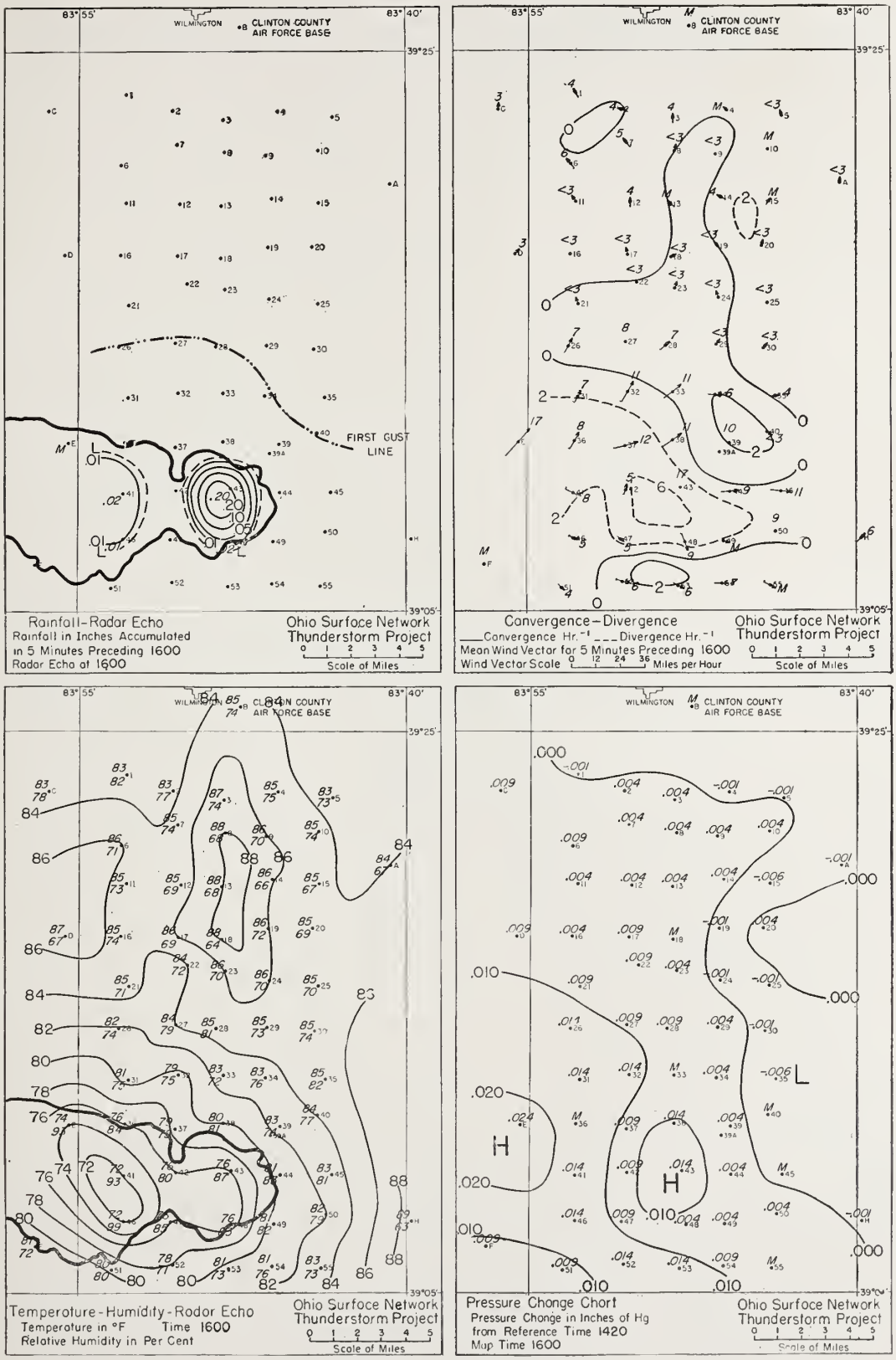

FIGURE 166.—Ohio surface network, 1600 E.S.T., August 13, 1947.

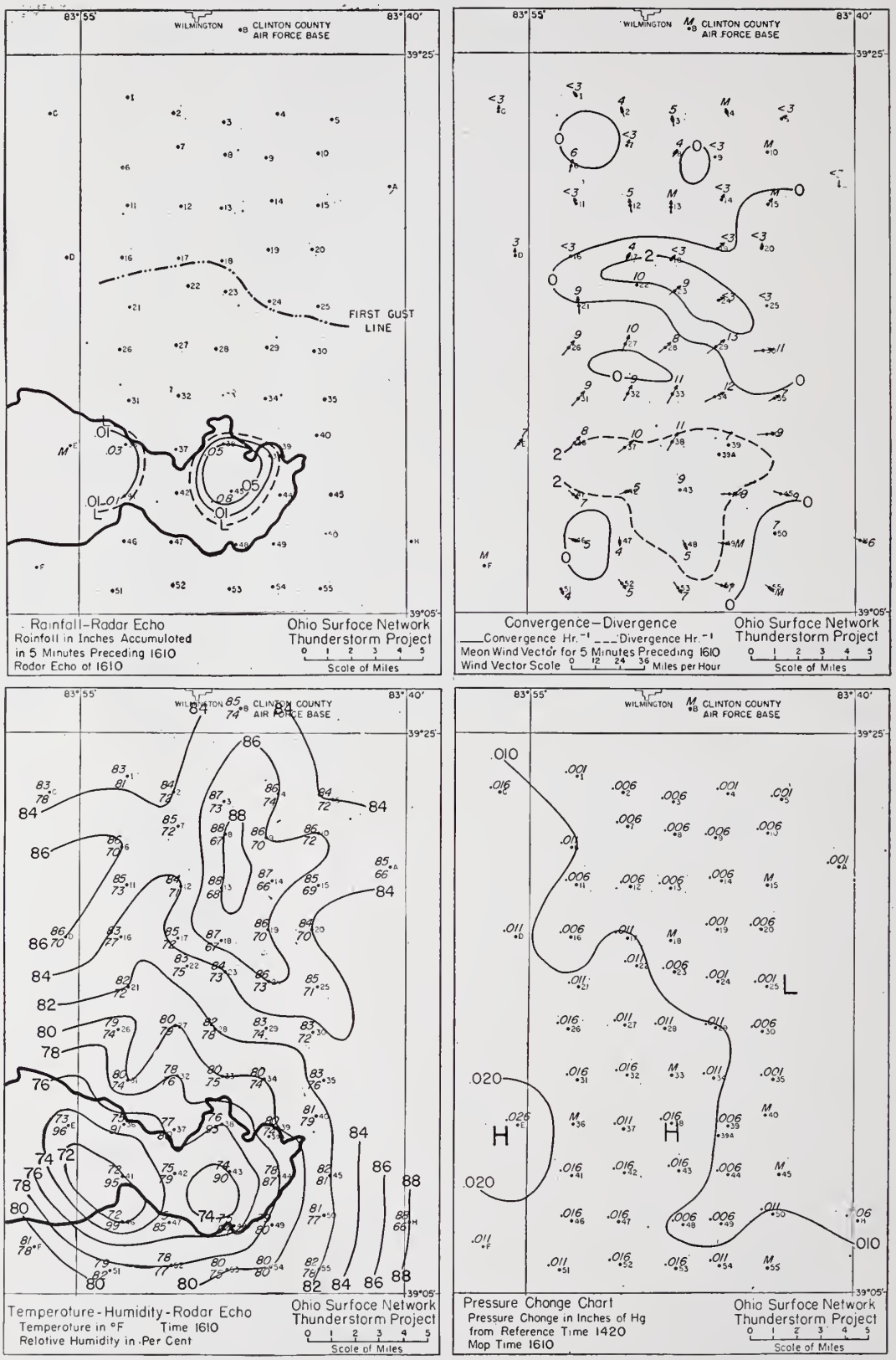

FIGURE 167.—Ohio surface network, 1610 E.S.T., August 13, 1947.

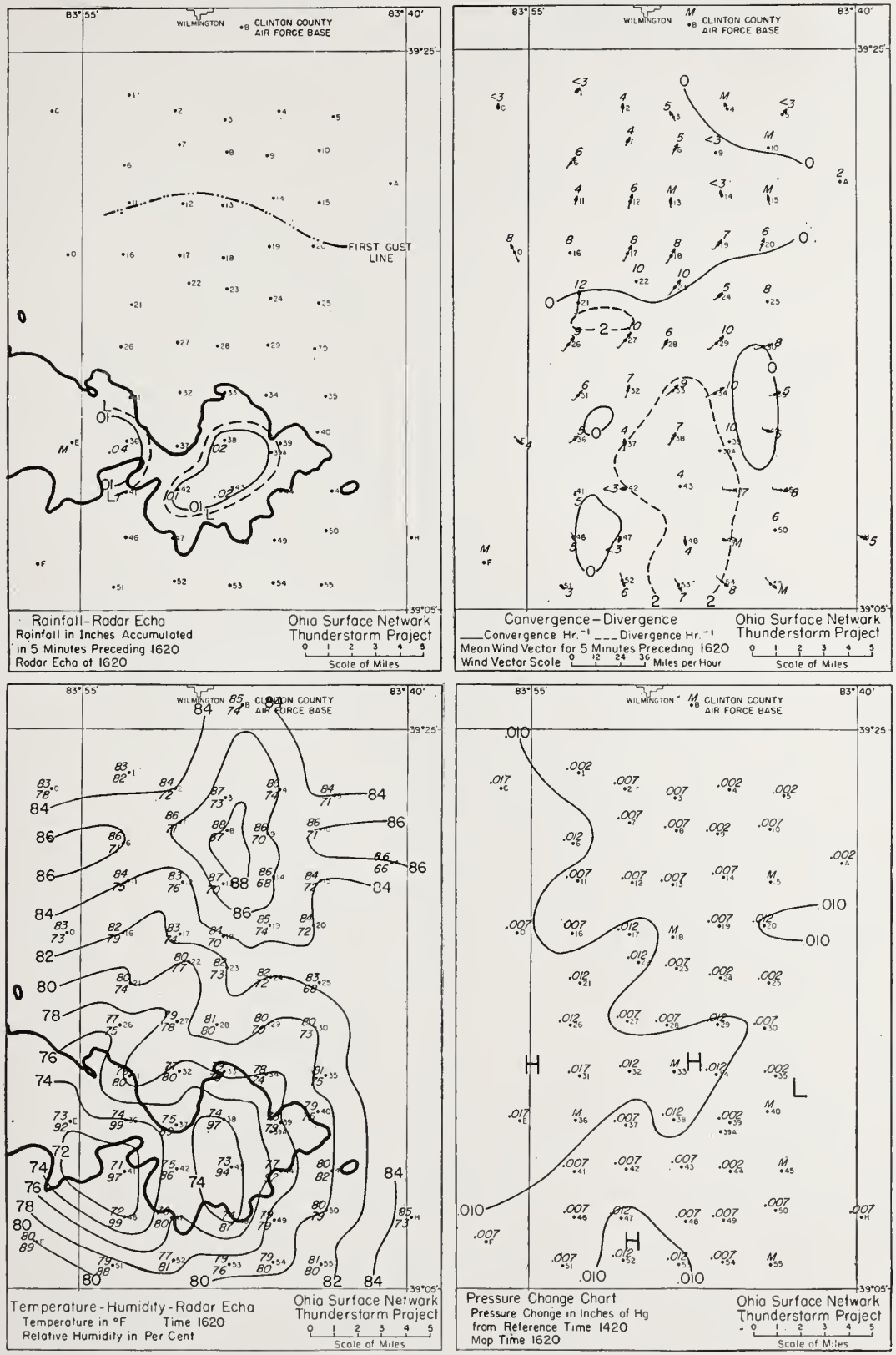

FIGURE 168.—Ohio surface network, 1620 E.S.T., August 13, 1947.

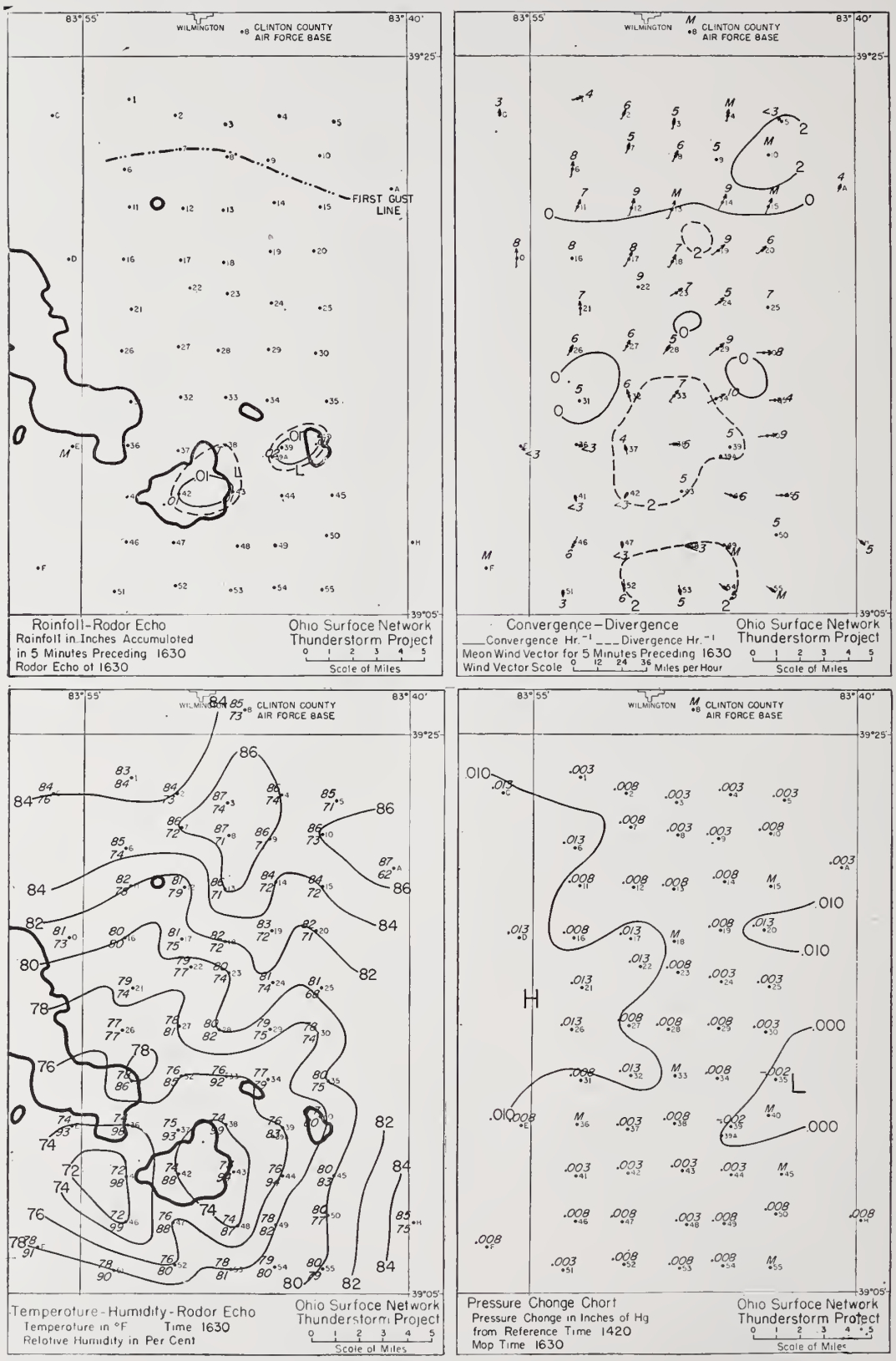

FIGURE 169.—Ohio surface network, 1630 E.S.T., August 13, 1947.

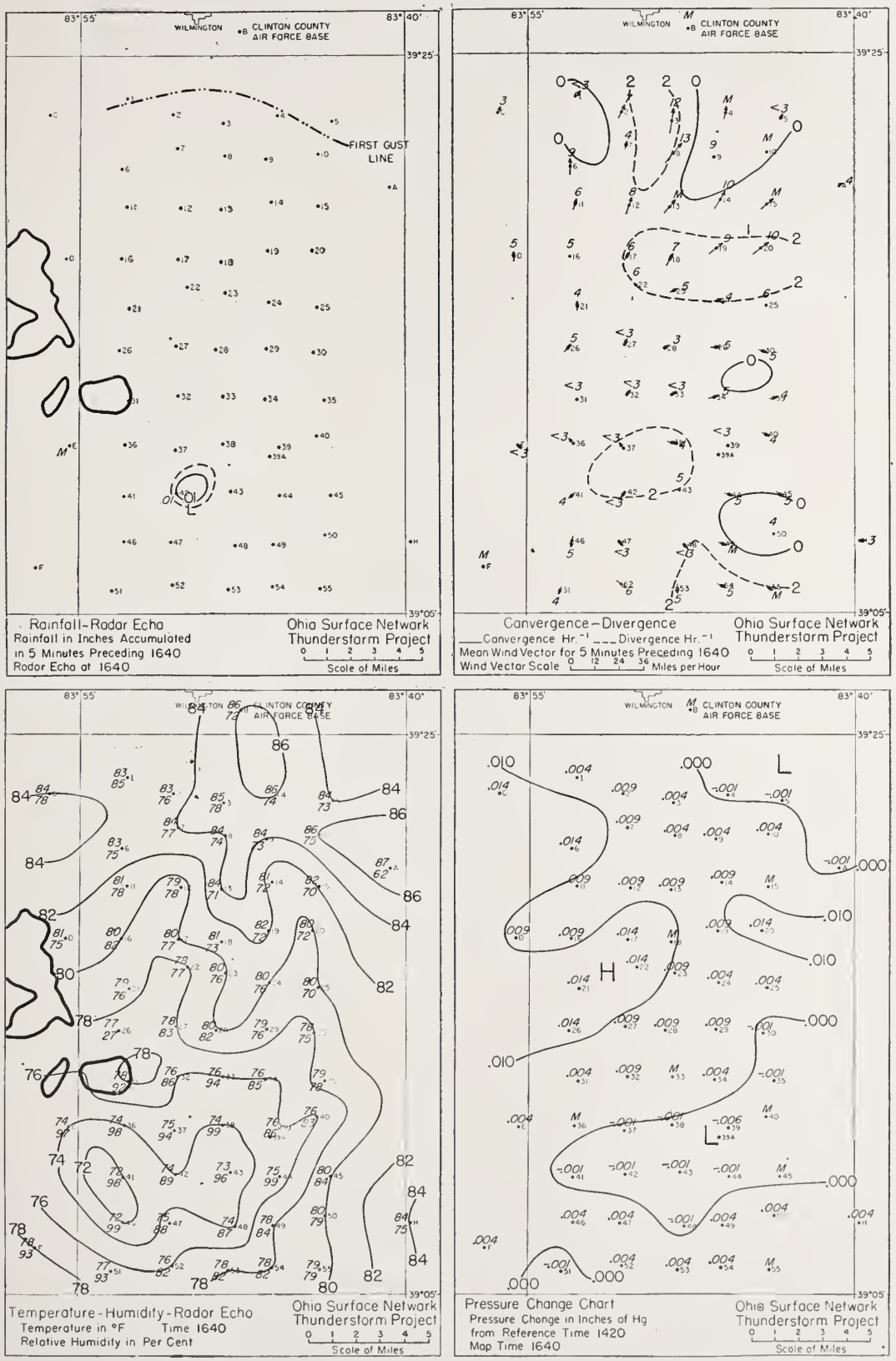

FIGURE 170.—Ohio surface network, 1640 E.S.T., August 13, 1947.

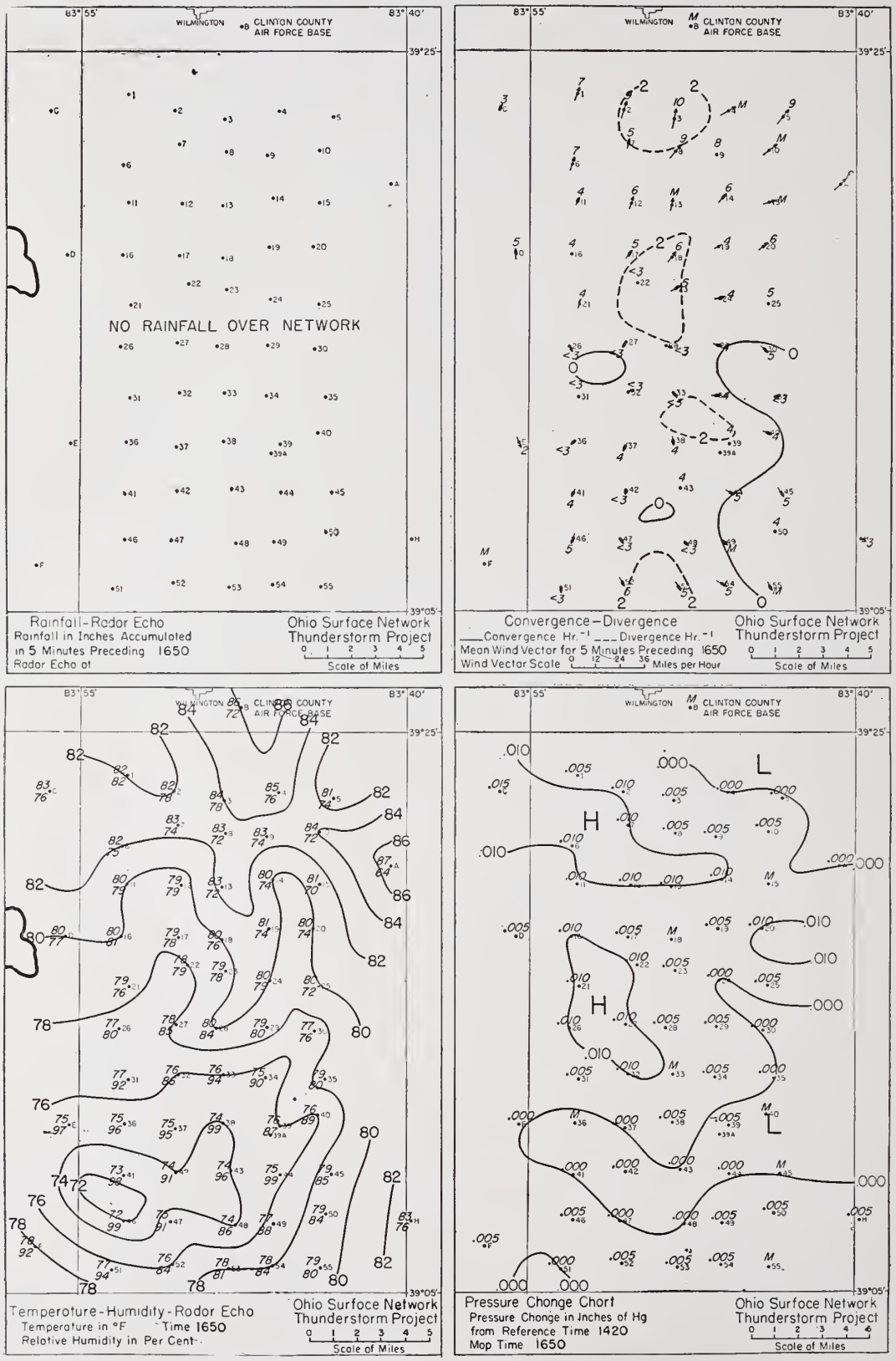

FIGURE 171.—Ohio surface network, 1650 E.S.T., August 13, 1947.

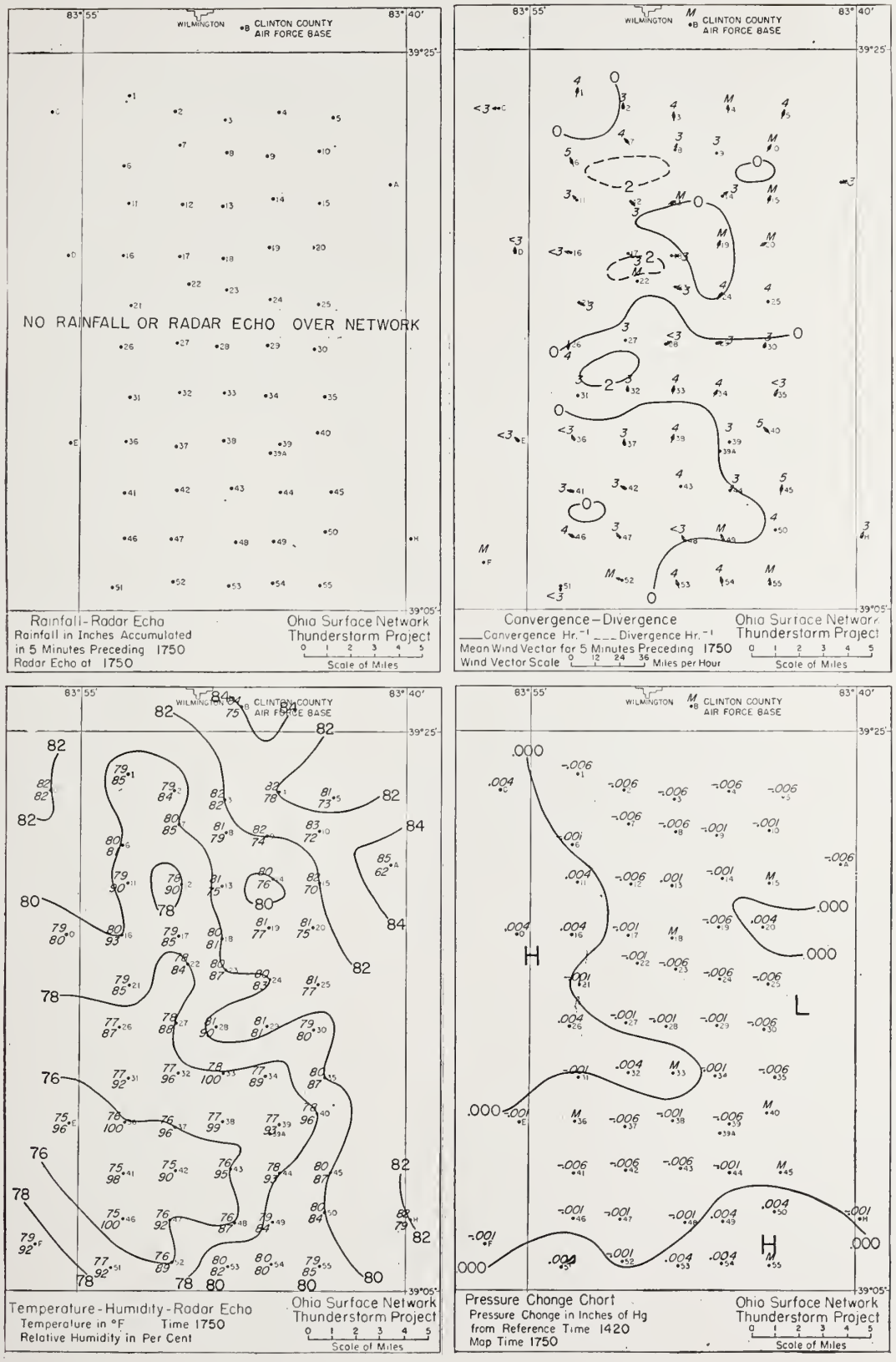

FIGURE 172.—Ohio surface network, 1750 E.S.T., August 13, 1947.

THUNDERSTORM OF AUGUST 14, 1947
[1340 E.S.T. to 1630 E.S.T.]

During the afternoon of August 14, 1947, the surface network and the area in the vicinity of Wilmington, Ohio, were directly under the influence of an excellent example of a pre-cold-frontal squall zone (see ch. VIII). At 1330 E.S.T., the cold front was 200 mi. to the northwest of the network, oriented northeast to southwest and moving southeastward at 18 mi/hr, while the zone of convective activity lay between about 100 and 300 mi. to the southeast of the front (fig. 173). The thunderstorm under consideration was imbedded nearly in the center of the zone and its outlines are indicated on the tracing of the 200-mile-range on-center PPI 'scope (fig. 174).

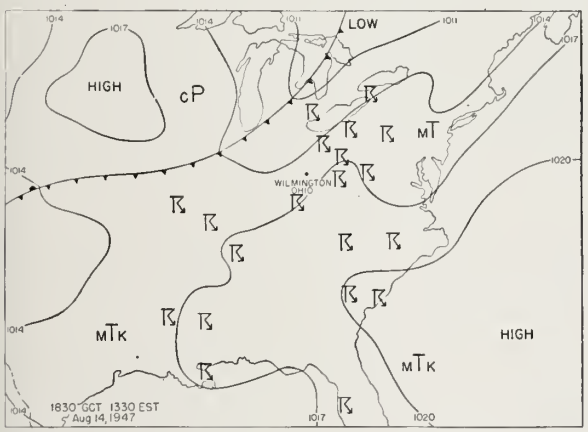

FIGURE 173.—A surface synoptic chart for 1330 E.S.T., August 14, 1947.

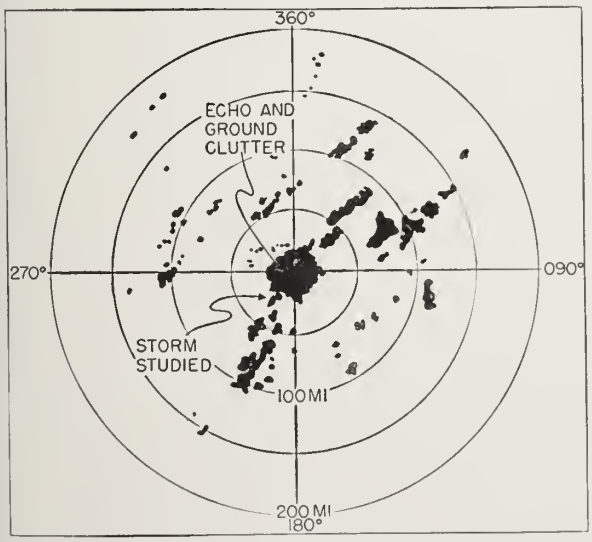

FIGURE 174.—Schematic drawing of the 200-mile-range PPI 'scope showing the actual radar echoes at 1345 E.S.T., August 14, 1947.

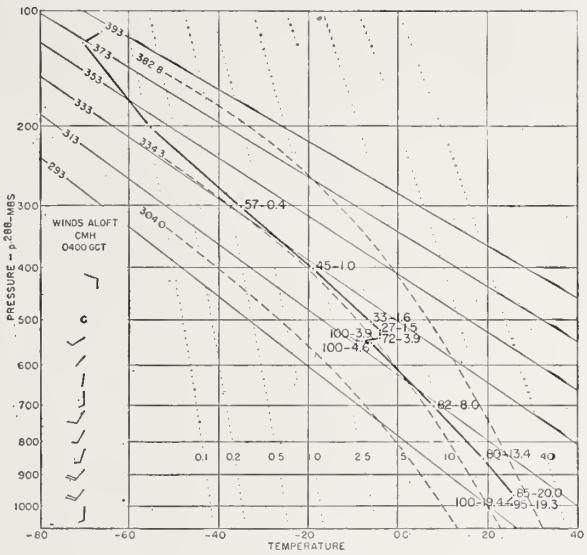

FIGURE 175.—Upper air sounding for 0300 G.C.T. from Huntington, W. Va., and the winds-aloft observations from Columbus, Ohio, for 0400 G.C.T., August 14, 1947.

Surface circulation was generally from the southwest, but over the immediate storm area winds backed from westerly, at 1330 E.S.T., to southwesterly at 1530 E.S.T. At 700 mb., the circulation to the north of the storm area was also from the southwest and contained a weak pressure trough which terminated in a flat gradient to the south. Wind observations made over the network prior to and during operations showed a shear zone from 20,000 to 25,000 ft. in which winds shifted from westerly to northerly. Other upper-air data are shown in the sounding chart of figure 175.

Since it was in a squall zone, the storm studied was not isolated and, especially in later stages, did not maintain its identity but appeared only as a group of cells within a large area of convective activity.

The first portion of the storm flown by the aircraft appeared on the PPI 'scope at 1338 E.S.T., 9 mi. to the west of the surface network. The storm moved east-southeastward at a mean rate of 8 mi/hr, with its major development occurring directly over the network between 1400 and 1500 E.S.T. Plane traverses

841051—50——14

were made between 1353 and 1505 E.S.T. at the 6,000-, 10,000-, 15,000-, and 20,000-foot levels. Altogether, more information was obtained during this storm than during any other of the 1947 season.

Figures 176 and 177 are photographs of the PPI 'scope depicting development of the storm from 1330 through 1520 E.S.T. Five cells were delineated by means of the airplane data for the entire time and area flown, while the presence of several others in the immediate vicinity was suggested by the radar photographs and surface records.

1340 E.S.T.
(*fig. 178*)

The radar echoes which appeared in the northeastern portion of the surface network at this time represent cells of an earlier storm which was in the dissipating stage of development. This is indicated by the rainfall charts, which show that the precipitation from thunderstorms was decreasing in intensity, and covered a relatively small area. The area of pronounced cooling associated with the rain area suggests that the storm had been a vigorous one, a fact that is confirmed by the recorded weather data for times prior to 1340 E.S.T. Although the temperature gradients over the remainder of the network were relatively flat, the temperatures varied from 84° to 92° F. Such variations are due, in part, to exposure, the amount of cloudiness which prevails, and to instrument error.

In the areas directly affected by the cold outflow, the relative humidities were high—in the eighties and nineties. Over the rest of the network they ranged from 60 to 80 percent, which is typical of Ohio conditions on a summer afternoon when maritime tropical air prevails.

The divergence field was relatively weak. It is interesting to note, however, that the winds in the northern part of the network indicate that some outflow from the earlier storm was still in progress. The almost calm conditions denoted by the winds at stations 4 and 5 near the center of the cold-air pool, and the higher wind speeds in the northwest, are characteristic of a storm in its dissipating stages.

The 1340 E.S.T. chart shows that pressure falls had occurred in the northern part of the network where marked convection took place, while small rises occurred in the south.

1350 E.S.T.
(*fig. 179*)

By this time all of the echoes over the network, except the one between stations 7 and 8—which is designated on later figures showing data measured from airplanes as cell III—had decreased in size. It is difficult to say whether the rain observed at station 3 was associated with this latter cell or represents "lingering" precipitation from the storm to the east. The outflow from the northeastern cell had been effective in slightly reducing the temperature in the west. There was also a fall in temperature at station D, probably caused by the cells designated as I and II in a later figure. No significant relative humidity or wind changes had occurred since the time of the previous chart. The pressure had continued to fall slightly in the north but had risen in the central and southern portions of the network. Note, however, that a few stations in the extreme northwest showed rises in pressure.

1400 E.S.T.
(*figs. 180 through 182*)

Cell I had been detected by the radar at 1338 E.S.T., and by 1400 E.S.T., it was in the mature stage of development, as shown by the extension of the RHI radar echo below the zero-elevation line, which is an indication that rainfall is occurring at the surface [**18**]. The RHI echo attained its maximum vertical height of 44,000 ft. during this period. An updraft, turbulence, and heavy precipitation were encountered at 15,000 ft. in the only traverse made through this cell in this time interval. Within the cell, the computed air temperatures at 15,000 ft. (fig. 182) show only slight variations from the computed mean clear-air temperatures, except at one point in the region of the updraft where the temperature was 3.6° C. warmer than the cloud environment.

Cell II first appeared on the PPI radar 'scope at the same time as cell I; by 1404 E.S.T., station D began to record very light rainfall, indicating that this cell, too, had entered the mature stage of development. The surface chart for 1400 E.S.T. shows cooling in the northwestern portion of the network, particularly at station C, probably due to the outflow from cells I and III. As indicated by the change in the winds at stations 16 and 21, an inflow component ahead of cell II had developed. This turning of the wind toward a developing storm is frequently observed; an associated band of divergence develops ahead of the turning, as is shown by this wind chart (fig. 181). Only very small pressure changes had occurred since the time of the preceding pressure chart.

Cell III, located over the surface network, was also in the mature stage of development. Updrafts were recorded at 15,000 and 20,000 ft., and at 10,000 ft. the pilot reported a downdraft which could not be evaluated from the records. Temperature data, from the 15,000- and 20,000-foot levels (fig. 182), show that the computed temperatures within the cell in the updraft area were slightly higher than the mean clear-air temperature, the maximum anomaly being 2.2° C. Outside the cell, the temperatures at the

20,000-foot level were slightly below the determined clear-air mean for that level. At 15,000 ft. the only anomaly of significant magnitude was 2.9° C., found in the updraft area. Beneath the area traversed by the plane at 10,000 ft., rain was recorded by the surface stations. In spite of the rain under this cell, there was as yet very little cooling and little change in the relative humidity. This may have resulted, in part, from the presence of a previous storm in this area. The winds indicated that the downdraft was not too well established; this is borne out by the pressure chart which shows only a general pressure increase in the area under this cell.

As indicated by the decreased size of the PPI echo, the cells due east of cell III had continued to dissipate. One traverse through these cells was made by the airplane at 15,000 ft. Although the outflow is still evident on the charts, no drafts were encountered during the traverse, but light turbulence and light snow were encountered. Little further change in surface temperature had taken place. Slight pressure falls had occurred under this storm area, as might be expected, with the outward spreading of the cold air associated with these dissipating cells.

1410 E.S.T.

(*figs. 183 through 185*)

Cell I at this time was in the dissipating stage of development. The RHI echo still indicates the existence of surface rain, but the echo had definitely become weaker in the levels below 10,000 ft. The PPI echo was somewhat smaller, as is shown in figure 184. No drafts were measured in this cell, and turbulence was encountered at only the 15,000- and 20,000-foot levels of flight. Light precipitation was reported at all levels, with snow at 15,000 ft. and above, and rain below. At 15,000 ft., a break in the clouds was reported by the pilots of the airplane which passed from cell I into cell II. At 6,000 ft., the computed temperatures were found to be lower than the mean clear-air temperature, as is shown in figure 183. At 15,000 ft. the temperature anomalies were quite small with the greatest anomaly being positive. (The smooth character of the trace of the temperature indicator made during this traverse suggests that the thermistor element may have been coated with ice; consequently, the computed temperatures cannot be considered as reliable.) The records from the traverse made from 1406 to 1410 E.S.T. at the 20,000-foot level were also subject to question. Icing was reported by the radar and weather observers, and it is possible that the relatively high temperatures indicated were a result of the release of the latent heat of fusion as ice formed on the thermistor element and/or (for reduction purposes), the use of incorrect airspeed readings resulting from momentary blocking of the pitot tube by ice. The second traverse shown in the figure for the airplane assigned to the 20,000-foot level was made at somewhat higher altitude, and, accordingly, the temperatures for that traverse were reduced to 21,000 ft. rather than to 20,000 ft. There was no evidence of icing during this penetration, and, as is shown, the computed temperatures indicated that the air within the cell was colder than the mean temperature of the clear air.

Cell II moved in over the western border of the surface network. At 1410 E.S.T. rain had not yet begun at stations 11 and 16, but it was recorded at both before 1415 E.S.T. A trace of rain, however, was measured at station D. From the position of the radar echo and the strength of the cold-air outflow, as indicated by the winds at stations 6 and 11, it is evident that appreciable rain was reaching the ground in areas west of the network. The fact that winds at stations D and 16 had southerly components shows that the downdraft was still concentrated in the northern portion of this cell. The airplane measurements confirm this: A plane flying at 6,000 ft. encountered a downdraft, although 3 min. earlier, above the same area, the airplane at 20,000 ft. passed through an updraft[76].

Heavy rain associated with the downdraft was encountered at 6,000 ft. The airplane at 10,000 ft. also encountered heavy rain, and at 20,000 ft. heavy snow was observed. The updraft measured at 10,000 ft. in the southern portion of this cell indicates that it was still in the mature stage of development. The temperature measurements made in cell II at the 15,000- and 20,000-foot levels during this period are subject to the same criticisms discussed in connection with cell I. At 6,000 ft., however, where the measurements may be considered as reliable, small, predominantly negative anomalies were found. Beneath this cell, in the cold air of the downdraft, the temperatures at the surface dropped only 1 centigrade degree in the 10 min. prior to the time of the map shown in figure 185. Accompanying this drop in temperature there was an increase of a few percent in the relative humidity. As is characteristic in areas over which the cold air outflow passes, the pressure rose in the vicinity of this cell.

Cell III was still in the mature stage of development at this time. Airplanes made traverses at the 6,000- and 10,000-foot levels, but no drafts could be evaluated from the records obtained. However, the divergence in the surface winds beneath the echo from this cell showed that the downdraft was still present. It is interesting to note that the outflow from this

[76] While this might seem untenable when first considered, reference to figure 18 will show that this situation should actually be expected. The sloping boundary between the up- and downdrafts contributes to the maintenance of the downdraft by permitting the precipitation to fall out of the updraft into the downdraft area.

cell is much greater to the west than to the east. This may be explained by the fact that the air to the west was warm and more unstable than that to the east, and the outflow followed a path of least resistance. Light to moderate rain was reported by the crews of the airplanes at both the 6,000- and 10,000-foot levels. However, the center of maximum rainfall associated with this cell was slightly to the northeast of the path taken by the 10,000-foot airplane and south of that taken by the 6,000-foot airplane. Heavy rainfall, 0.14 in/5 min, was reported from this cell at station 3.

The small positive temperature anomalies found at the 6,000-foot level throughout the downdraft and in the updraft areas within this cell are not representative of conditions which would be expected. It is possible that there was only slight vertical motion in this portion of the cell and that the true temperatures consequently did not vary greatly from the environment temperature.

The 1410 E.S.T. surface charts show that little change in the temperatures and only slight rises in relative humidity had occurred under this cell. Pressure rises of .009 in. were recorded at stations 8 and 9 during the previous 10 min.; the other stations under the cell also showed rises.

Cell IV, which first appeared on the radar 'scope between 1400 and 1410 E.S.T., was penetrated by the airplane at the 20,000-foot level. Turbulence and light snow were encountered. Also, an updraft, in which temperatures were as much as 2° C. higher than the mean clear-air temperature, was found in the northwestern portion. Its fairly recent origin, the presence of a measured updraft, the lack of outflow winds at the surface, and the presence of surface pressure falls to the east of it all indicate that this cell was in the building or cumulus stage of development at this time.

It is interesting to note the area of turbulence experienced outside the area of radar echo by the airplane flying at 10,000 ft. on a 270° heading, after its passage through cell III. Note also the updraft between cells II and III, measured by the airplane flying at 6,000 ft. Both of these features were apparently associated with building cumuli which had not yet developed sufficiently to produce radar echoes.

1420 E.S.T.
(*figs. 186 through 188*)

Considerable growth and coalescence of the PPI radar echoes took place in the 10-minute interval preceding 1420 E.S.T. Since only one airplane penetrated the storm during this interval, the indicated changes in the cells were determined, by analysis, on the basis of continuity and using the measured surface data. Figure 188 shows the computed temperatures for the 6,000-foot level. During the period of this traverse, temperature anomalies were negative and, even in the areas of updraft in cells II, III, and V—where most of the data were obtained—these anomalies had magnitudes that appear significant. It is possible that at this low level the downdrafts in cells II and III covered more area than has been indicated in figures 186 and 188. Similar reasoning cannot be used to explain the low temperatures in cell V, for this was a newly developed cell and there was no evidence of downdraft.

Cell I bordered the surface network to the west, and rain from it was recorded at station D. The airplane flying at 6,000 ft. passed through the southernmost portion of this cell and encountered light turbulence and light rain but no drafts which could be evaluated from the records. Cell I was considered to be in the dissipating stage of development. Although station D was probably under the influence of the outflow from cell II, the northern component of the recorded surface wind suggests that there was still outflow from cell I. The temperature at station D had fallen 4° C. since the time of the previous map, and the relative humidity had risen substantially due to the effect of the outflow. The pressure continued to rise under the influence of this cold air.

Cell II continued in the mature stage of development during this period, with heavy rainfall and marked temperature falls being recorded at stations near its center at 1420 E.S.T. These features indicate that the downdraft was well established by this time. Note that the characteristically radial outflow indicated by the winds at stations 6, 11, and 16 suggests that the center of the downdraft that reached the surface was southwest of station 11 and north-northwest of station 16. The airplane which passed through this cell encountered the draft slightly to the south and east of the location of the cell center indicated by the surface data. The breaks in the turbulence between cells I and II, as well as between cells II and III, were marked, and the pilot of the airplane reported that he momentarily broke into the clear between the latter two cells. At the surface, there was an area which showed marked temperature drops associated with the downdraft from this cell. The heavy rainfall caused the relative humidity to rise to near-saturation values, and, as is usually the case at this point in a cell's development, the pressure rose sharply throughout the area underneath the cell.

Cell III was still producing heavy rain beneath its northern portion, although the center of the maximum rainfall moved southward. The 6,000-foot airplane encountered turbulence and light rain during this period, but it was not possible to evaluate either up- or downdrafts from the records obtained. Because the rainfall remained in the northern section of the cell, it is presumed that an updraft persisted in the

southern section and that the cell was still in its mature stage of development. The cold downdraft associated with the cell produced marked temperature drops, and a closed center of low temperature formed, as is indicated in figure 187. The drop in humidity at station 3 was associated with the relative humidity dip.

Cell IV had increased considerably in size since 1410 E.S.T. Unfortunately, no airplane data for this cell are available. The surface stations still did not show effects of its proximity; however, by 1425 E.S.T. rain had begun at stations 21 and 26, and surface winds indicated outflow. For these reasons, a downdraft area is indicated beneath the northwestern portion of the cell.

Cell V appeared on the radar 'scope between 1410 and 1420 E.S.T. It formed where the airplane flying at 10,000 ft. had encountered turbulence outside the radar echo on the previous traverse. While passing through this cell, the pilot of the 6,000-foot airplane reported light rain and light turbulence; however, no rain was as yet detected on the surface network, indicating that the cell was still in the building stage. Because of the proximity of cells II and III, the effects of cell V on the surface observations were obscured, although a decrease in surface pressure occurred at station 1. This pressure fall is very interesting, especially because it occurred in an area over which the cold air from cells II and III had already spread.

1430 E.S.T.
(*figs. 189 through 191*)

Cell I, nearing the end of the life cycle, still produced light rain at station D. However, after 1433 E.S.T. rain from this cell was not detectable at this station, which, as surface winds indicated, was located beneath the western edge of the cell. The two airplanes which flew through the cell during this interval encountered no measurable drafts, but turbulence was found at the 20,000-foot level. On the other hand, the pressure at station D rose appreciably, which, with the recorded temperature fall, was indicative of increased depth of the cold-air dome under this dissipating cell. At 15,000 ft. small negative anomalies were found in this cell, but at one point near the center of the cell, at the 20,000-foot level, the temperature within the cell reached a value 1.1° C. warmer than the mean clear air at that level.

Cell II was still in the mature stage of development, and the airplanes flying at 15,000 ft. and 20,000 ft. both passed through an area of strong updraft in its southern portion. As is shown in figure 190, positive temperature anomalies reaching a maximum of 4°C. were found in the updraft area at 20,000 ft. At 15,000 ft., however, small anomalies were found, and for the most part these indicated that the temperature within the cell was slightly colder than that of the clear air, although the airplane flying at this level traveled in an updraft throughout the cell. In the northern section of the cell, the crew of the 6,000-foot airplane reported light rain, which increased to heavy rain as the plane reached the eastern side of the cell. This was accompanied by light to moderate turbulence. At the same time, the surface stations recorded heavy rain—0.20 in/5 min—with falling temperatures and increasing humidities in the area where the winds indicate outflow from the downdraft. A marked rise in surface pressure also had occurred. At station 17 this pressure rise since the time of the previous chart amounted to nearly .02 in. A further sharp pressure increase, associated with a pressure nose, occurred at this station at 1433 E.S.T.

Cell III was well into the dissipating stage of development by 1430 E.S.T. Rain was still recorded at the surface under it, and the one airplane that intersected it reported light rain and light turbulence. There was little change in the surface temperature or relative humidity under this cell; however, the pressure rise was almost as great as that which occurred under cell II which was still in the mature stage. Additional measurements of the circulation and temperature fields would be needed to adequately explain such pressure changes.

Cell IV was not penetrated by the airplanes, but the rainfall, the divergence of the surface winds, and the center of low temperature present at the surface all indicate that the downdraft was still confined to its western portion. This suggests that an updraft was present in its eastern portion and that this cell was still in the mature stage of development. The marked rises in surface pressure at stations 21, 26, 31, and other stations in the vicinity were associated with the heavy rain and pronounced outflow.

Cell V was in the mature stage of development at 1430 E.S.T. The airplane flying at 10,000 ft. encountered heavy rain accompanied by light, soft hail throughout the cell. Surface stations 2 and 3 reported heavy rain, 0.22 in/5 min and 0.20 in/5 min, respectively. A downdraft in the eastern part of the cell was reported by the pilot, but this could not be confirmed from the airspeed and altitude records. Nevertheless, the divergence center shown on the surface charts was one of the most intense recorded for the entire storm and substantiates the pilot's report. A surface pressure rise had occurred in the area beneath the cell; the maximum rise associated with the pressure nose occurred at station 2. Lesser rises which occurred at stations under the cell between 1420 and 1430 E.S.T., ranged in magnitude from 0.01 to 0.03 in. It is interesting to note that the area of

maximum rainfall associated with this cell coincided with the area of maximum pressure rise, although the coldest air, as indicated on the surface charts, was displaced slightly to the east. The areas of temperature minima may have been due to the previous cells which have passed over this area.

1440 E.S.T.

(*figs. 192 through 194*)

Cell I was no longer detectable by 1430 E.S.T. from the data recorded in the airplanes. However, a trace of "lingering" rain was recorded at station D of the surface network.

Cell II continued in the mature stage of development with both an updraft and a downdraft indicated by the airplane records. Throughout the cell at 6,000 ft., the temperature was found to be colder than the mean clear-air temperature, suggesting that the downdraft extended over the entire area traversed. The airplane flying at 21,000 ft. measured slight positive temperature anomalies in the area of the updraft, while in the downdraft the temperature decreased steadily as the airplane progressed through the cell. The heaviest rain, 0.26 in/5 min, still fell under the northern portion of the cell. The wind field beneath both this cell and cell IV were typical of wind fields beneath two vigorous cells in the later part of their mature stage. It is evident from the 1430 E.S.T. chart that cell II and cell IV behaved as a couplet, producing a well-developed outflow area. The rainfall and the pressure, however, showed two distinct closed centers. The pressure rise observed under cell II (station 17) was the largest observed in the entire storm. It is noteworthy that this pressure maximum and that associated with cell IV were each distinguishable.

Cell III is still identifiable from the rain recorded at the surface and the extremely light turbulence and moderate to heavy snow recorded by the airplane at 15,000 ft. The computed in-cloud temperatures at this level were lower than the mean computed clear-air temperature but not appreciably different from the temperatures encountered immediately prior to the plane's entry into the cell. The surface winds beneath this cell were influenced primarily by the outflow from cell II. As a result, convergence, instead of the characteristic divergence, was observed beneath this dissipating cell.

Cell IV was not penetrated by the airplanes during this period. The fact that the rain fell only from the northern portion of the cell is evidence that an updraft was probably still present in the southern portion and that the cell was, therefore, in the mature stage. The surface temperature continued to fall and the humidity continued to rise, due to the effects of the rainfall and the cold downdraft. The pressure continued high underneath this cell, with the center of maximum pressure near station 27. It is to be noted, however, that marked pressure rises occurred to the east of station 26 between 1430 and 1440 E.S.T., due to the movement of the entire system in an eastward direction.

Cell V was considered to be in the dissipating stage of development and to contain only downdrafts. Although two aircraft traverses were made through it, the airspeed and altitude records did not permit draft computations. Both airplanes encountered precipitation—moderate rain at 10,000 ft. and snow at 15,000 ft.—accompanied by moderate turbulence at both levels. At 15,000 ft., negative temperature anomalies were found. Very heavy rain, 0.30 in/5 min, was recorded at station 3, directly underneath this cell. As is usually the case with such heavy rain, there was very marked divergence, 15.2 hr^{-1}, indicating that the cold downdraft was well established. Attention is called to the area of intense convergence in the region of stations 7, 8, 12, and 13. Such intense convergence is frequently found when each of two vigorous outflows opposes the other.

Northwest and west of cell V there was a considerable amount of radar-echo area that has not been divided into cells, as shown in figure 192. This echo was produced by stratiform cloud layers associated with the storm and by cumuli congesti which surrounded the main cloud. Due north of cell V a new cell developed, but the airplane at 10,000 ft. made the only traverse through it. This cell was not over the main surface network, and the echo from it was partially within the area on the 'scope covered by ground clutter. Because of the lack of precise information, no attempt has been made to analyze this cell. There was also additional radar development to the southeast of cells II and V, which was not identifiable as a cell at this time. Some of the echo in this area was produced by stratiform shelves, but most of it was probably associated with developing cumuli.

A new group of cells which had been developing south of the network made its first appearance on the charts at this time. This storm developed into one of the most intense recorded throughout the entire season. The surface winds showed appreciable convergence associated with its development. It is also pointed out that while the pressures rose markedly in the northern part of the network, the pressures in the southern part remained low and, in some cases even fell, in response to the influence of new convective development.

1450 E.S.T.

(*figs. 195 through 197*)

This was the last period during which the airplanes gathered data for this storm.

Cell II, the only one for which airplane data were obtained during this late interval, had entered the dissipating stage. Slight downdrafts were recorded at the 6,000- and 10,000-foot levels, but none were evident from the records made by the airplane flying at 15,000 ft. The computed temperature for the 6,000-foot level was lower than the mean clear-air temperature. At 15,000 ft., the temperature differed only slightly from the environment temperature, as would be expected at this level in a dissipating cell. At the surface, very heavy rain (0.34 in/5 min at station 18) from this cell was recorded, and the divergence of the surface winds was intense. The radial outflow associated with this cell is illustrated in figure 197. The surface temperature at stations 12, 17, and 22 continued to fall, reaching a low of 70° F. The maximum high pressure evident at station 17 on the 1440 E.S.T. chart had decreased in magnitude, indicating that some readjustment took place.

Cell IV was in the dissipating stage as determined on the basis of a continuity analysis and surface data. Rainfall spread beneath the entire area of the cell, but its intensity was less than at the time of the previous chart. This indicates that the cell was in the dissipating stage of development. The outflow field associated with cell IV was still merged with that of cell II. There was also a slight decrease in surface pressure under the cell.

Cell V was also in the dissipating stage at 1450 E.S.T. As evidence of this, the rainfall and pressure decreased in intensity. The intensity of the outflow also decreased and began to merge with that of cell II directly to the south. However, the divergence under cell II was still intense. Southeast of cells II and IV, the airplane passed through developing cumuli in which some updrafts were encountered. Although rain fell under this region, there were insufficient data available for cell analysis.

The cell in the south end of the network continued to develop, and heavy rain was recorded at stations 53 and 54. It is very interesting to note that an area of marked convergence was located just north of the rain area. This convergence was associated with the fast-moving outflow air which came in contact with the relatively slow-moving air it was displacing. From the appearance of the winds at stations 53 and 54, it seems very likely that divergence associated with strong outflow was present south of the station network. The very sharp drop in temperature associated with the rainfall and the marked pressure rise at station 54 were associated with a very active cell near the southern edge of the map. In the extreme northern part of the network, new development was also indicated by rain and falling temperature at station B.

1500 E.S.T.
(*fig. 198*)

By this time there was a marked reduction in the intensity of the rainfall from the cells of the northern portion of the network, and the individual cells II, IV, and V were no longer distinguishable from the rainfall data. However, the rain in the cell-II area was the most intense. The cell in the southern portion of the network had increased in intensity, and one of the most intense rates of rainfall recorded during any storm — 0.58 in/5 min — was recorded from 1455 to 1500 E.S.T. at station 49. The storm in the extreme north was apparently still vigorous, but since only station B furnished data concerning it, an analysis was not attempted.

The temperature field still showed one area of minimum temperature in the general vicinity of station 22. Although the greater portion of the rain area associated with the storm had moved eastward, this area of minimum temperature persisted. At station 49, which recorded very heavy rainfall for this period, the temperature dropped rapidly to 68° F. — a drop of 13° F. from 1449 to 1456 E.S.T. An area of minimum temperature was also present with the cell near station B.

The relative humidities were generally higher over the network than during the preceding interval, except in the extreme south, where it appears that the downdraft was not completely saturated; a condition perhaps due to one of the processes mentioned in chapter III, section 5.

The divergence in the wind field continued to show the presence of radial outflow from the large dome of cold air in the middle of the network and from the downdraft area of the cell to the south. In the latter area the intensity of the divergence continued to increase; in a later period it was one of the areas which showed the most intense divergence found in the Thunderstorm Project data.

Since winds, rainfall, and temperature drops were also great under this storm in the south, it is not surprising that very marked pressure rises had also occurred. Station 49 showed a pressure nose at about this time. The high pressure associated with the storm in the northern half of the network had been decreasing as compensations and adjustments took place.

1510 E.S.T.
(*fig. 199*)

The radar echo over the central portion of the network had decreased and the associated rainfall area had diminished in size.

Some of the stations in the north-central area reported rainfall amounts as high as 0.02 in/5 min without the presence of a radar echo directly above;

such "lingering" rainfall may persist for as long as 20 min., but its intensity is usually quite light. This is a phenomenon which is frequently found at the trailing edge of the radar echo.

Over the southern part of the network, the radar echo still grew in size; rainfall covered an increasingly larger area and remained very heavy. The rain area in the southern part of the network appeared to have moved northward; however, this should not be taken as evidence that the cell from which the initial rain fell had moved northward, since surface wind and temperature records offer evidence that new cells had developed to the north of the original one.

There appeared to be little change in the temperature configuration since 1500 E.S.T., except in the south, where cold downdraft air had poured into the southern part of the network so that the temperatures were slightly lower in that region. Relative humidities had continued to rise under the influence of the cold air and the precipitation.

Divergence continued to decrease over the central part of the network. It is interesting to point out that in this region where a cold dome was present there were relatively light winds near its center but much higher winds around the periphery. As shown in chapter III, this phenomenon may be explained by the downward-gliding motion of the air within the cold dome, which may result both from the addition of new cold air from higher levels and from the flattening of the dome. At this stage, the pressure usually falls as it did here. This would be expected since the colder air, in spreading out over a larger area, is reduced in vertical thickness.

In the southern part of the network, the divergence was at the maximum intensity, attaining a value of 22 hr^{-1}. It must be remembered that this computation was based on the 5-minute average winds and that divergence values based on 1-minute winds would be considerably higher. Very strong gusts were recorded with this intense outflow, a maximum gust of 40 mi/hr having been recorded at station 40 at 1508 E.S.T.

Striking changes in the surface pressure also occurred in this region. The presence of the pressure maximum over station 39 at this time was evident from a pressure nose recorded there. Pronounced pressure falls had taken place in the extreme southwestern portion of the network — as much as .017 in. at station 46, and .007 in. at station 51.

1520 E.S.T.
(fig. 200)

By 1520 E.S.T. the radar echos had all but disappeared and light, lingering rainfall was observed at a number of stations. The storm in the southern portion of the network had continued to propagate northeastward, and station 40 showed the maximum rainfall on the network. In the central part of the network the characteristically persisting area of minimum temperatures remained in the vicinity of station 22. A similar low-temperature area persisted in the southern portion; in spite of heavy rain recorded at stations 39 and 40, the minimum temperatures remained in the vicinity of station 49. Relative humidities continued to rise over most of the network. The winds at station 40 were still relatively strong, but over the remainder of the network winds were light.

Pressures over the north and central portions of the network had continued to fall, as the effect of the cold air dome and the downward-gliding motion diminished but were still higher in the southern part of the network. Unfortunately, the barograph at station 40 was inoperative. It is not unlikely that a pressure maximum, associated with the heavy rainfall, was present there.

1530 E.S.T.
(fig. 201)

Except for heavy rain in the southeastern portion of the network, precipitation was comparatively light by this time. Although there was some indication of warming at a few isolated stations, the temperature pattern in general remained the same as on the previous charts, with the areas of minimum still near the points where the rain had been heaviest. The wind field was light and in some cases calm conditions prevailed. It is interesting to note that at the exterior stations of the network there was evidence that the general outflow was still present. The pressure continued to drop in the northern and central portions but remained relatively high to the south.

1630 E.S.T.
(fig. 202)

At 1630 E.S.T., 1 hr. after the time of the previous chart, there was no precipitation recorded by the station network; nevertheless, the centers of minimum temperatures persisted in the areas where maximum rainfall had occurred during the storm. The temperatures ranged from 71° to 78° F., and the air was near saturation over a large portion of the network, especially where the heavy precipitation had occurred. A marked change in the pressure field took place in the hour following 1530 E.S.T. Rises of several hundredths of an inch occurred in the southern portion of the network, while pressures in the north remained unchanged. This, of course, resulted in a stronger pressure gradient than had been present before the

storm. It is interesting to note that the winds were rather uniform, stronger than before the storm, and blew across the gradient. It is pointed out, however, that part of the differences in pressures existing in the northern and southern portions of the network may be explained by the fact that the reference pressure, taken at 1330 E.S.T., was chosen for a time when there was cold air present over the northern portion of the network. Therefore, the pressure gradient was actually smaller than it appears from the chart.

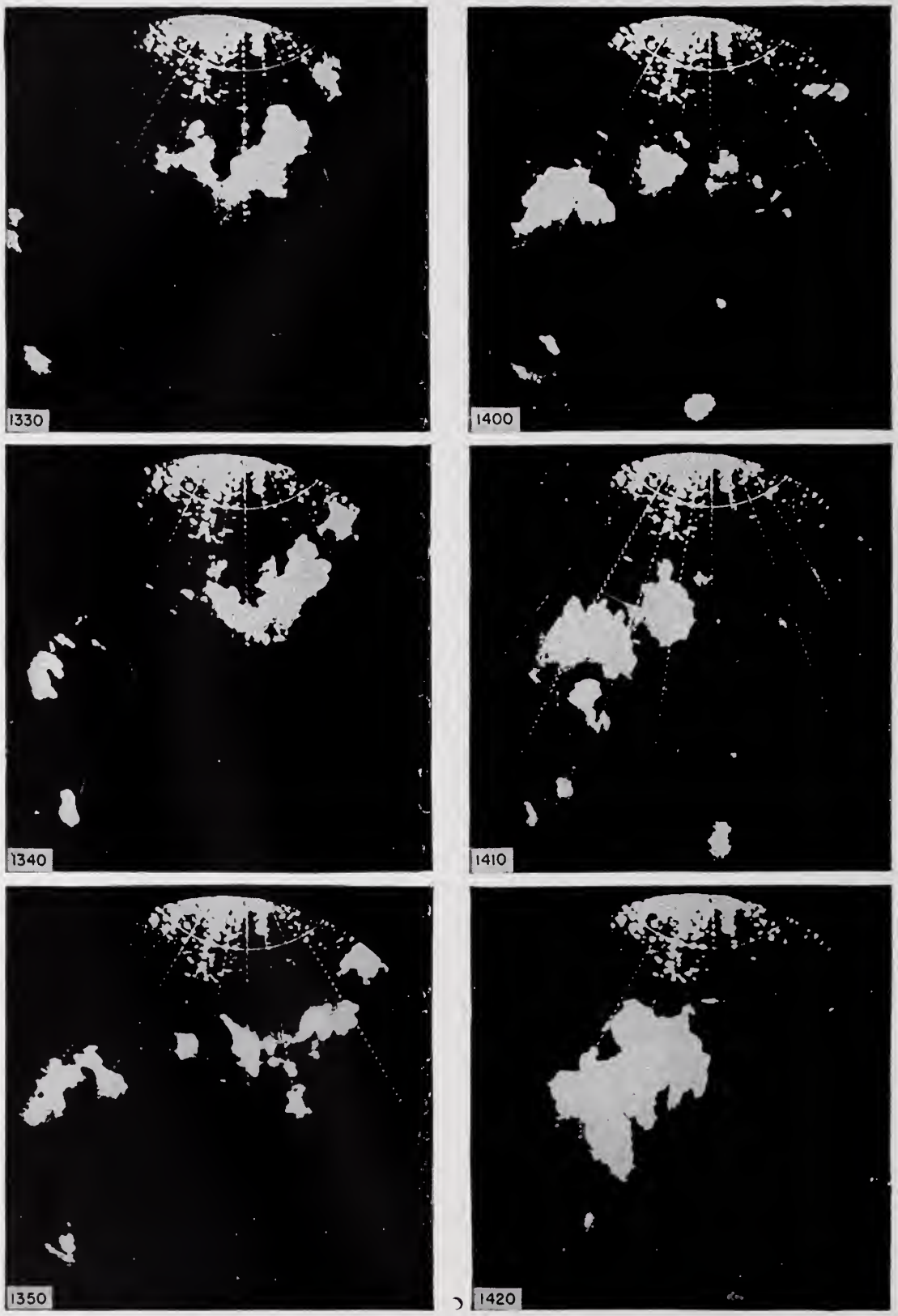

FIGURE 176.—Control-radar PPI 'scope photographs, 1330-1420 E.S.T., August 14, 1947.

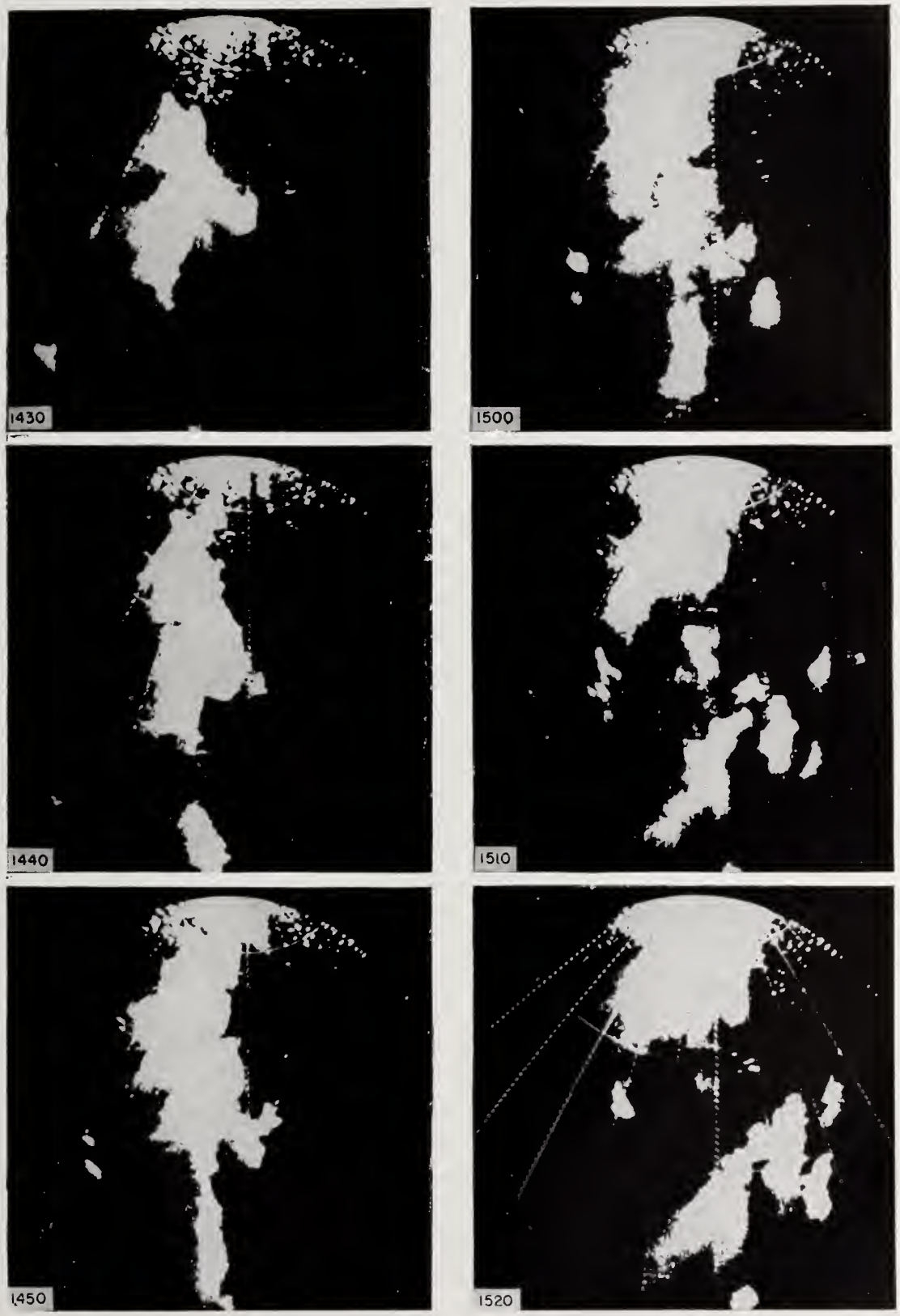

FIGURE 177—Control-radar PPI 'scope photographs, 1430–1520 E.S.T., August 14, 1947.

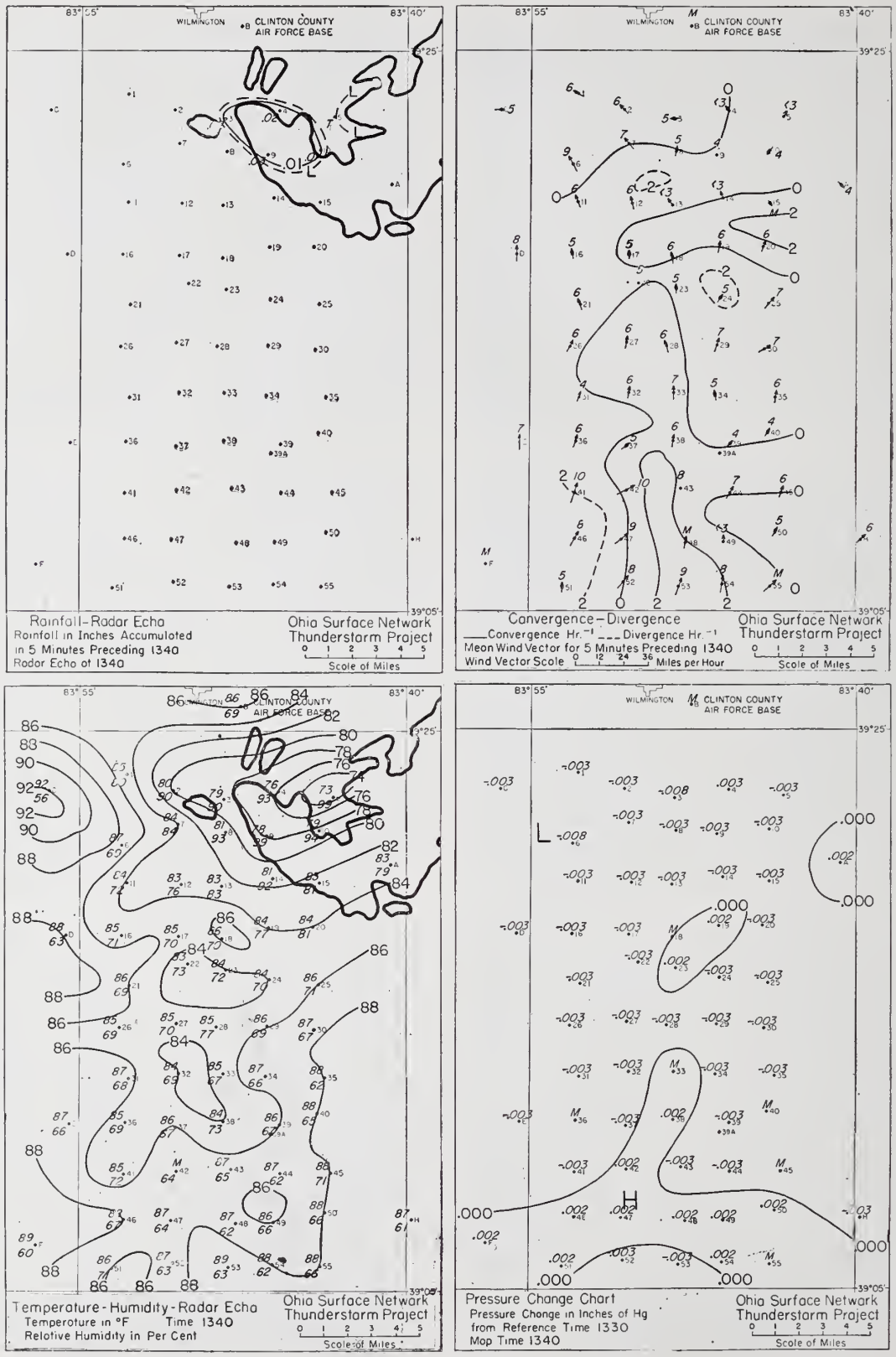

FIGURE 178.—Ohio surface network, 1340 E.S.T., August 14, 1947.

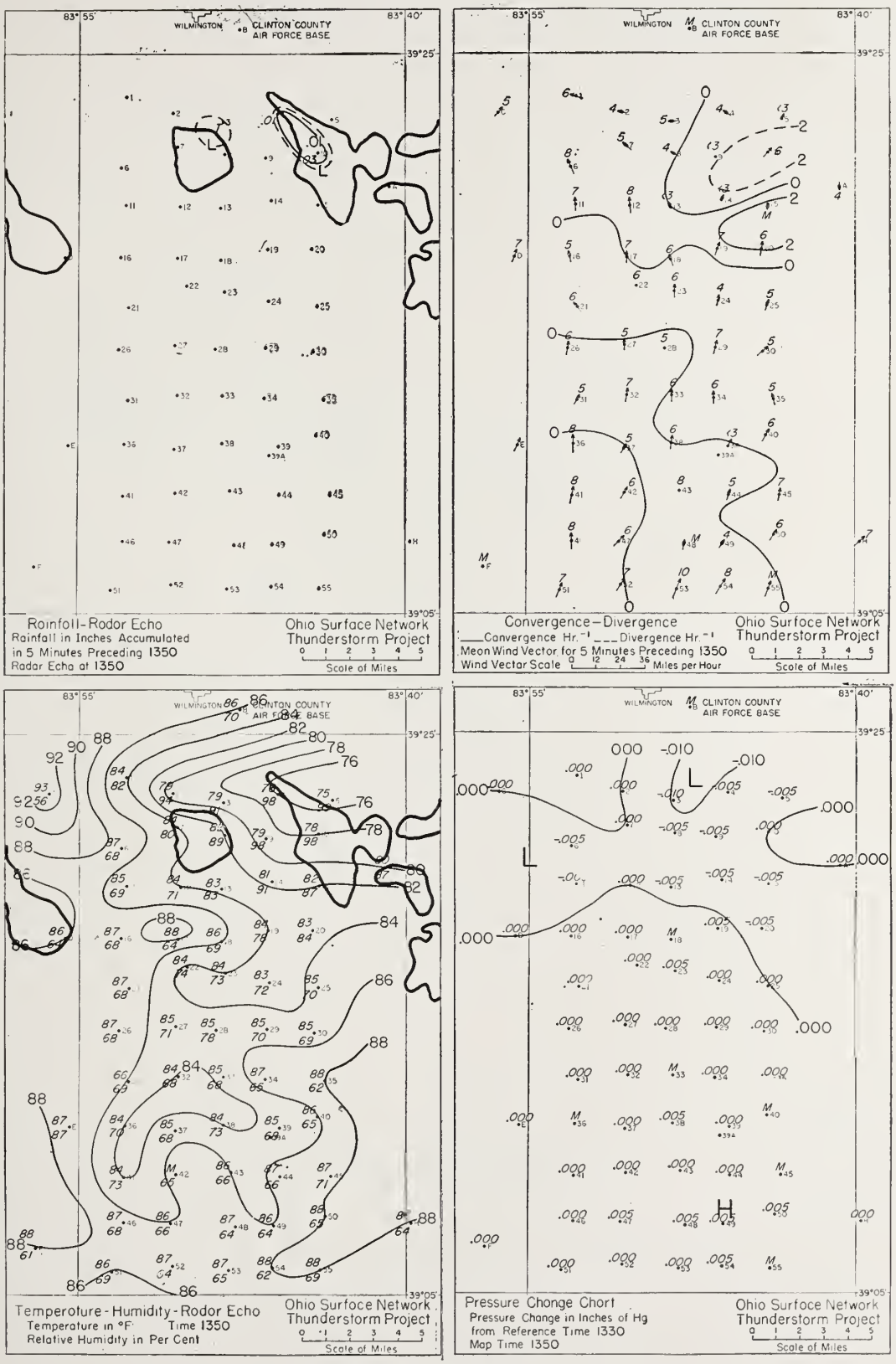

FIGURE 179.—Ohio surface network, 1350 E.S.T., August 14, 1947.

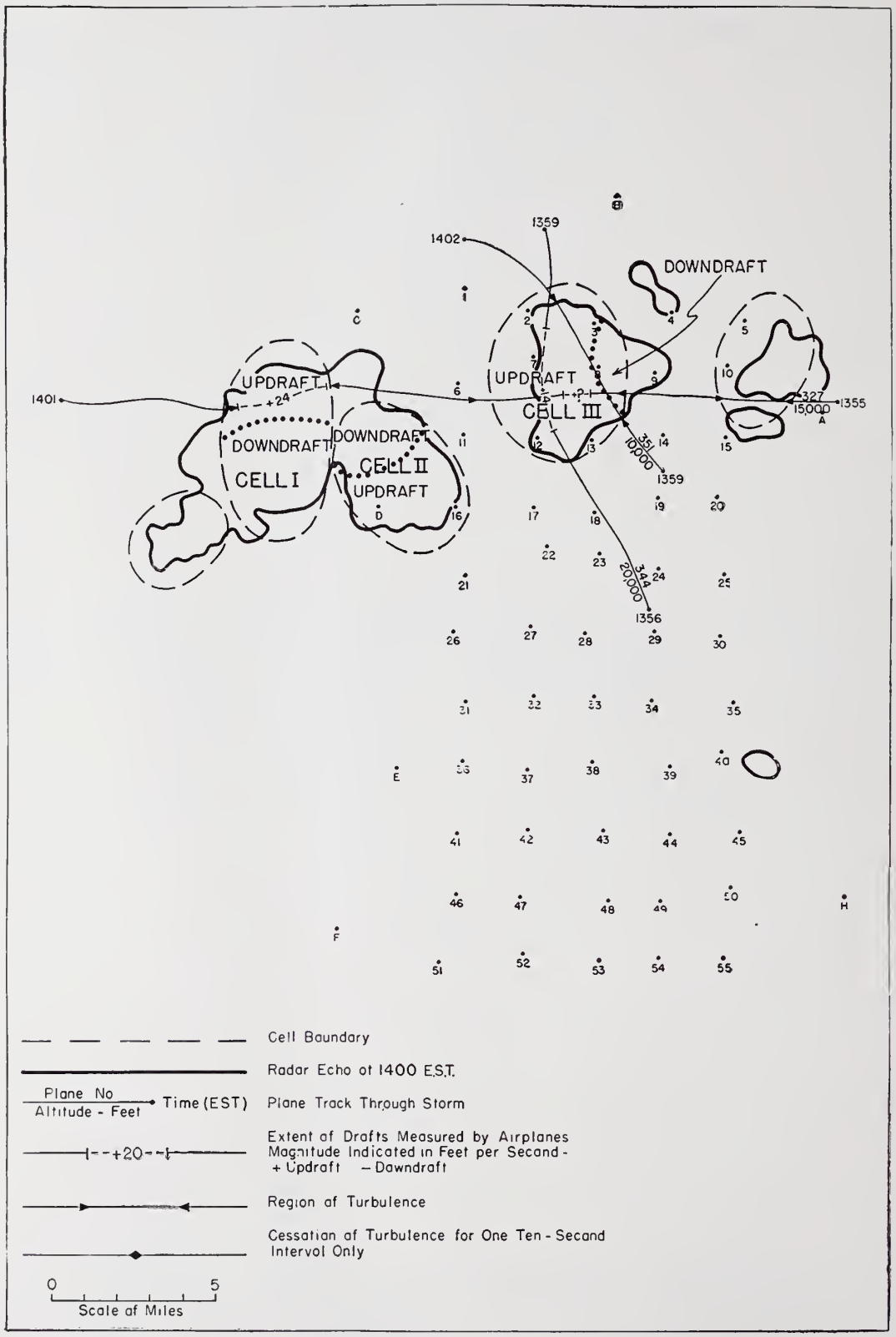

FIGURE 180.—PPI radar echo at 1400 E.S.T., and airplane paths from 1355 to 1405 E.S.T., August 14, 1947.

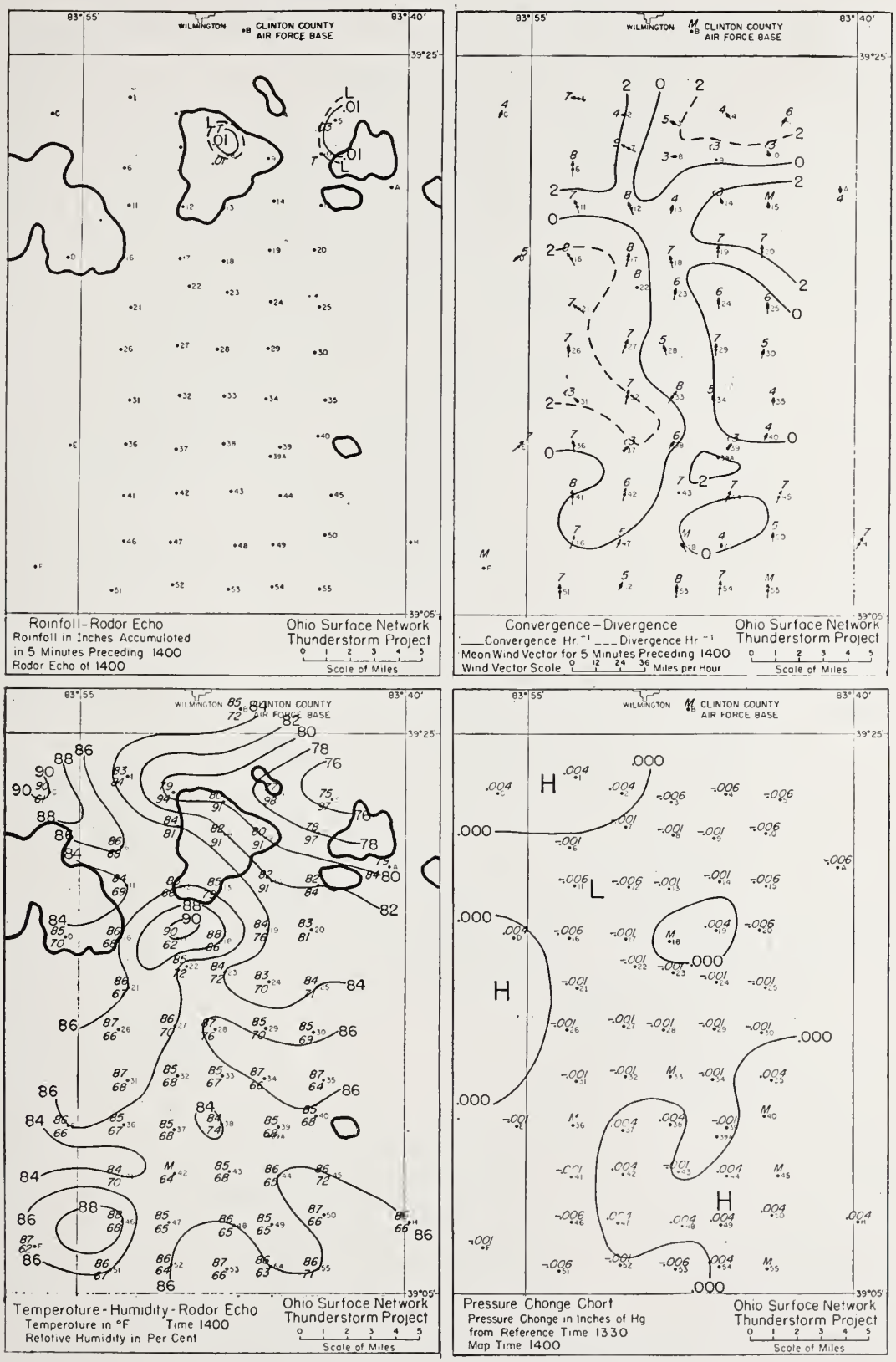

FIGURE 181.—Ohio surface network, 1400 E.S.T., August 14, 1947.

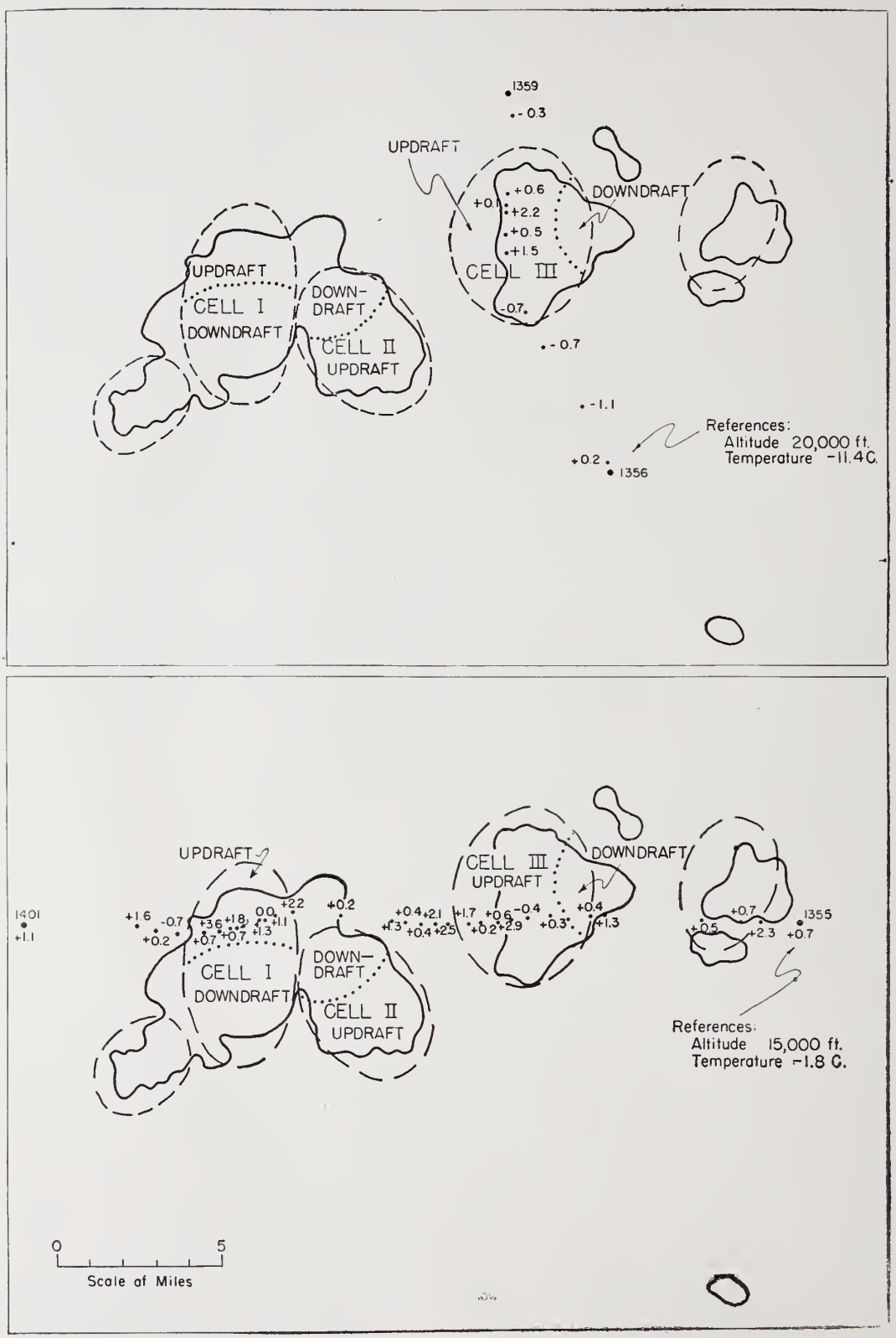

FIGURE 182.—Air temperature measurements, 1355–1405 E.S.T., August 14, 1947.

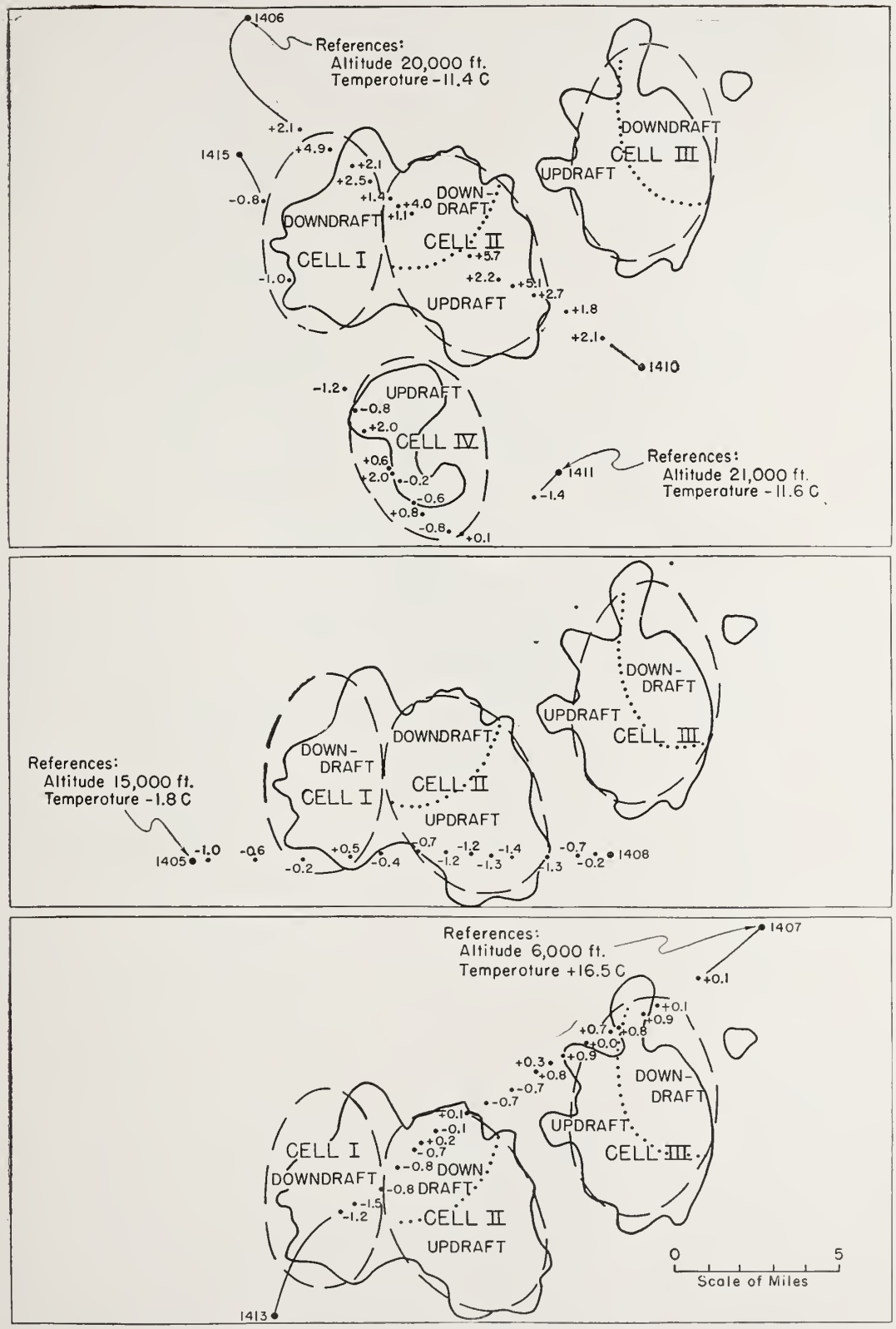

FIGURE 183.—Air temperature measurements, 1405–1415 E.S.T., August 14, 1947.

341071—50——15

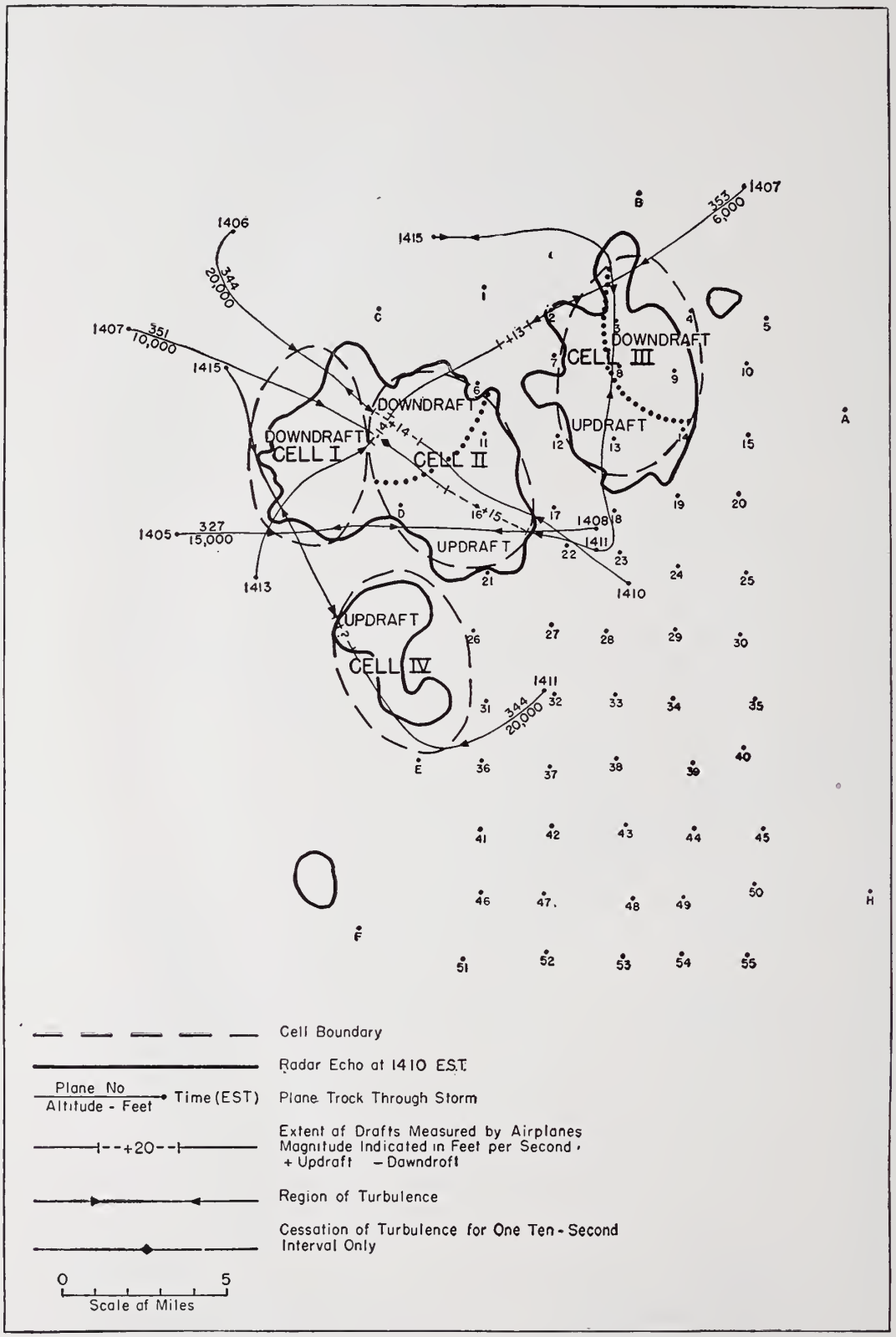

FIGURE 184.—PPI radar echo at 1410 E.S.T. and airplane paths from 1405 to 1415 E.S.T., August 14, 1947.

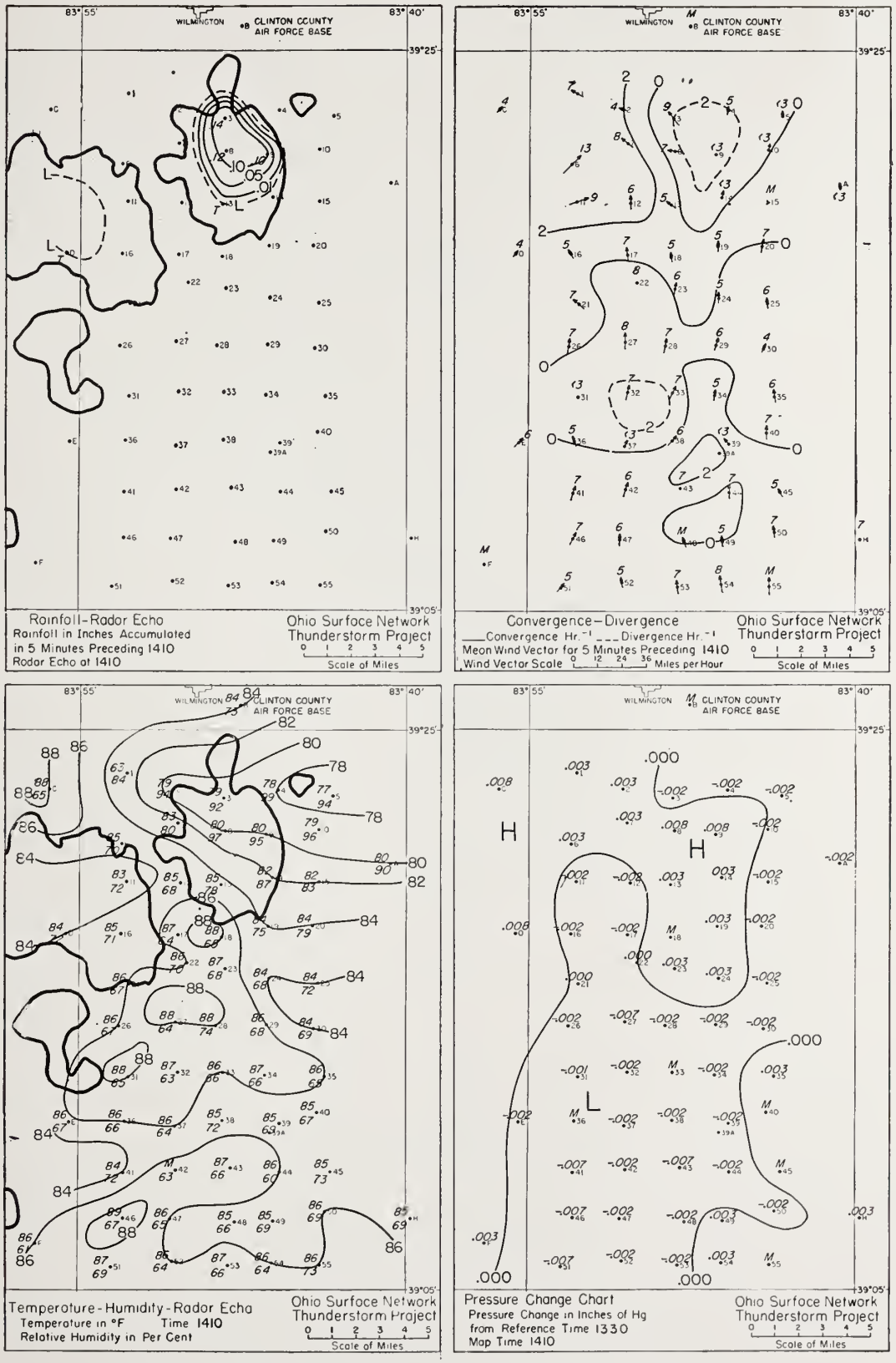

FIGURE 185.—Ohio surface network, 1410 E.S.T., August 14, 1947.

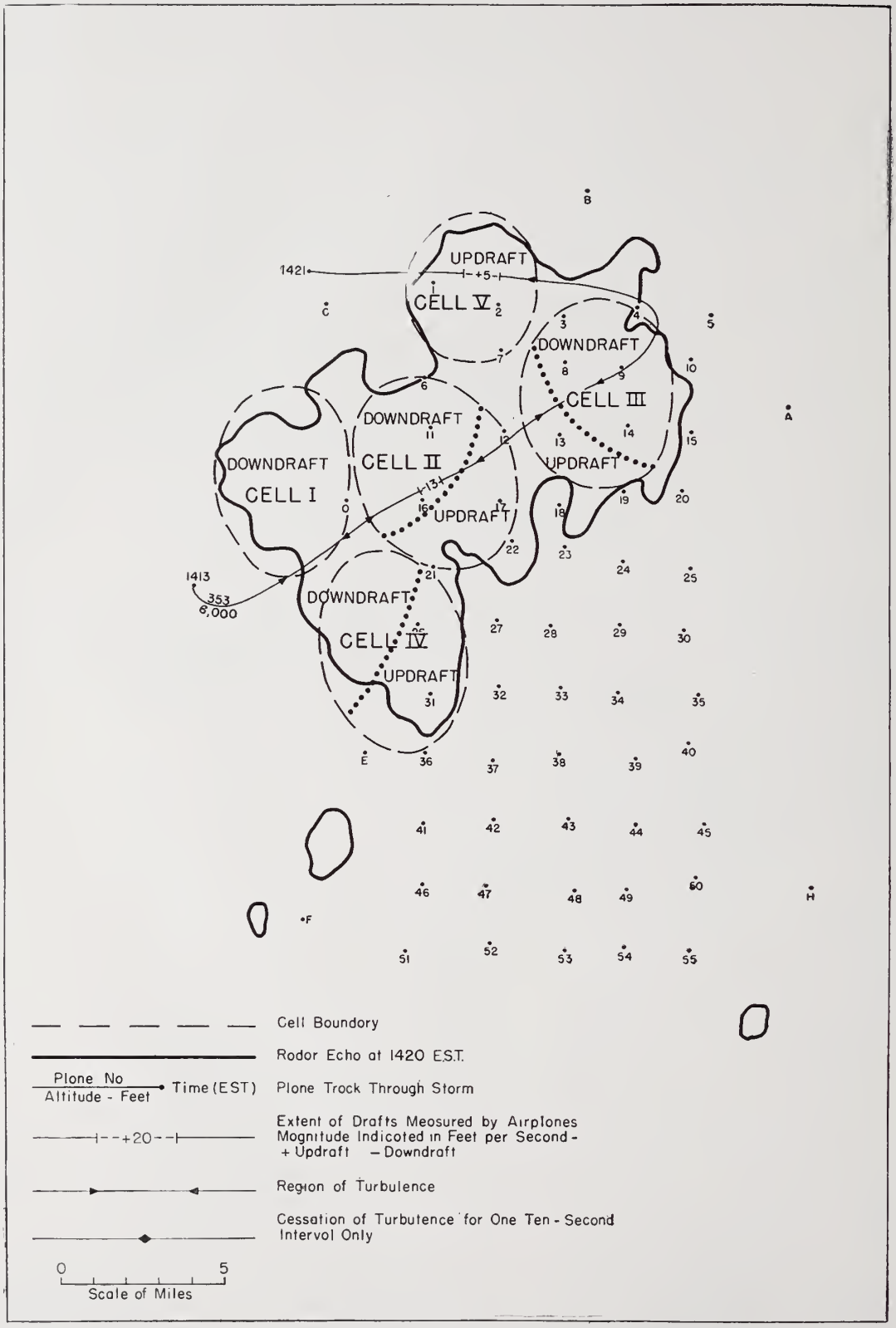

FIGURE 186.—PPI radar echo at 1420 E.S.T., and airplane paths from 1415 to 1425 E.S.T., August 14, 1947.

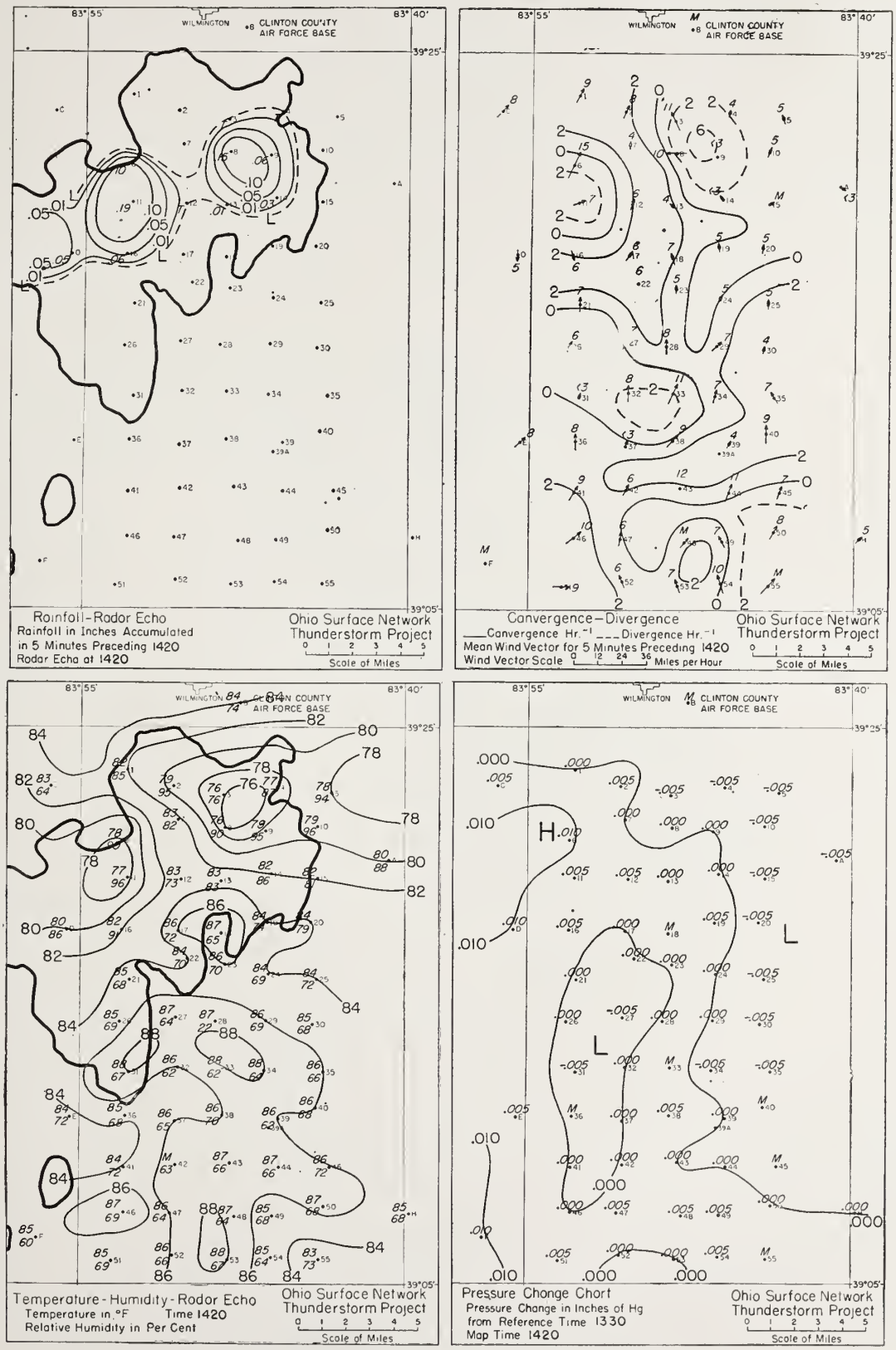

FIGURE 187.—Ohio surface network, 1420 E.S.T., August 14, 1947.

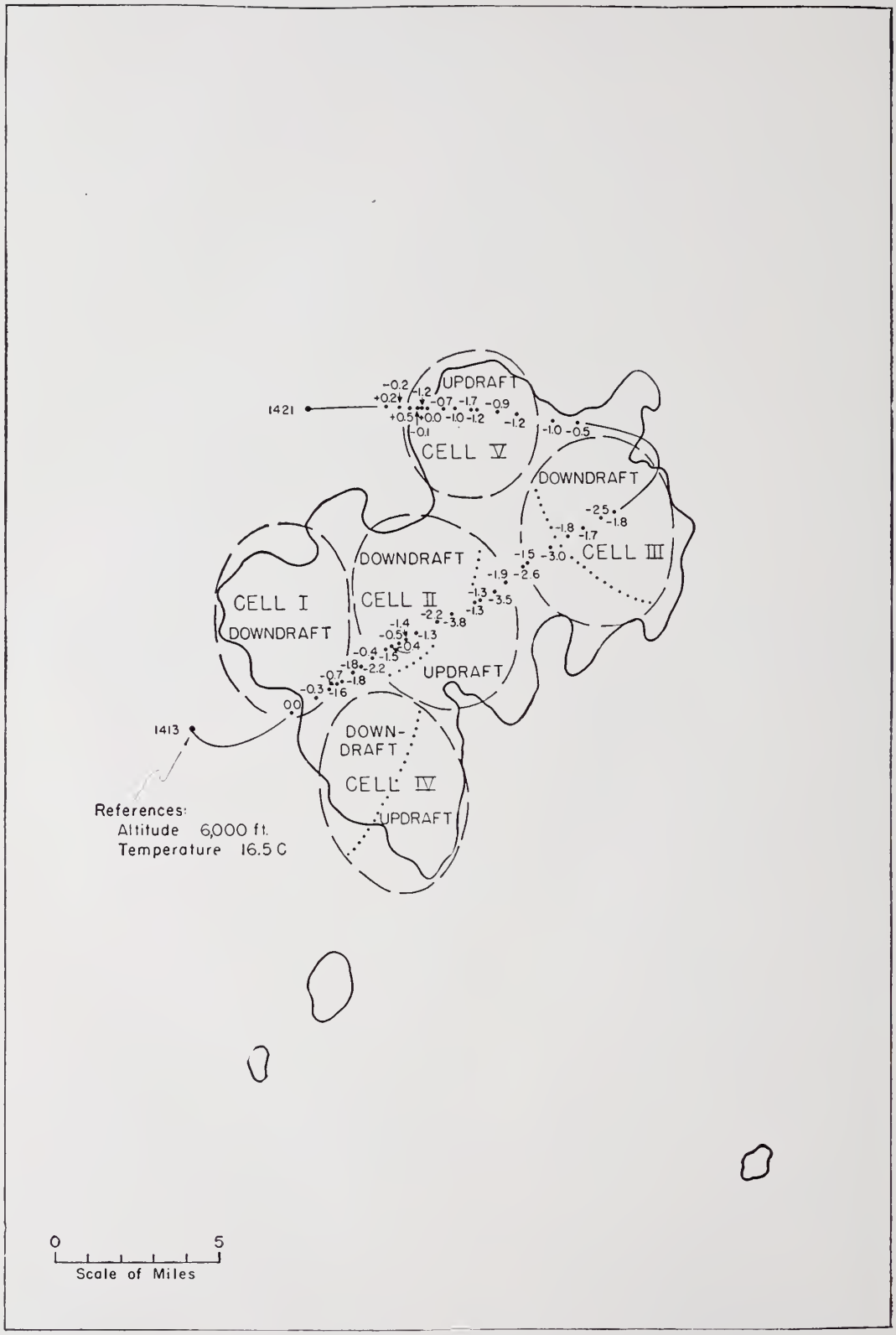

FIGURE 188.—Air temperature measurements, 1415–1425 E.S.T., August 14, 1947.

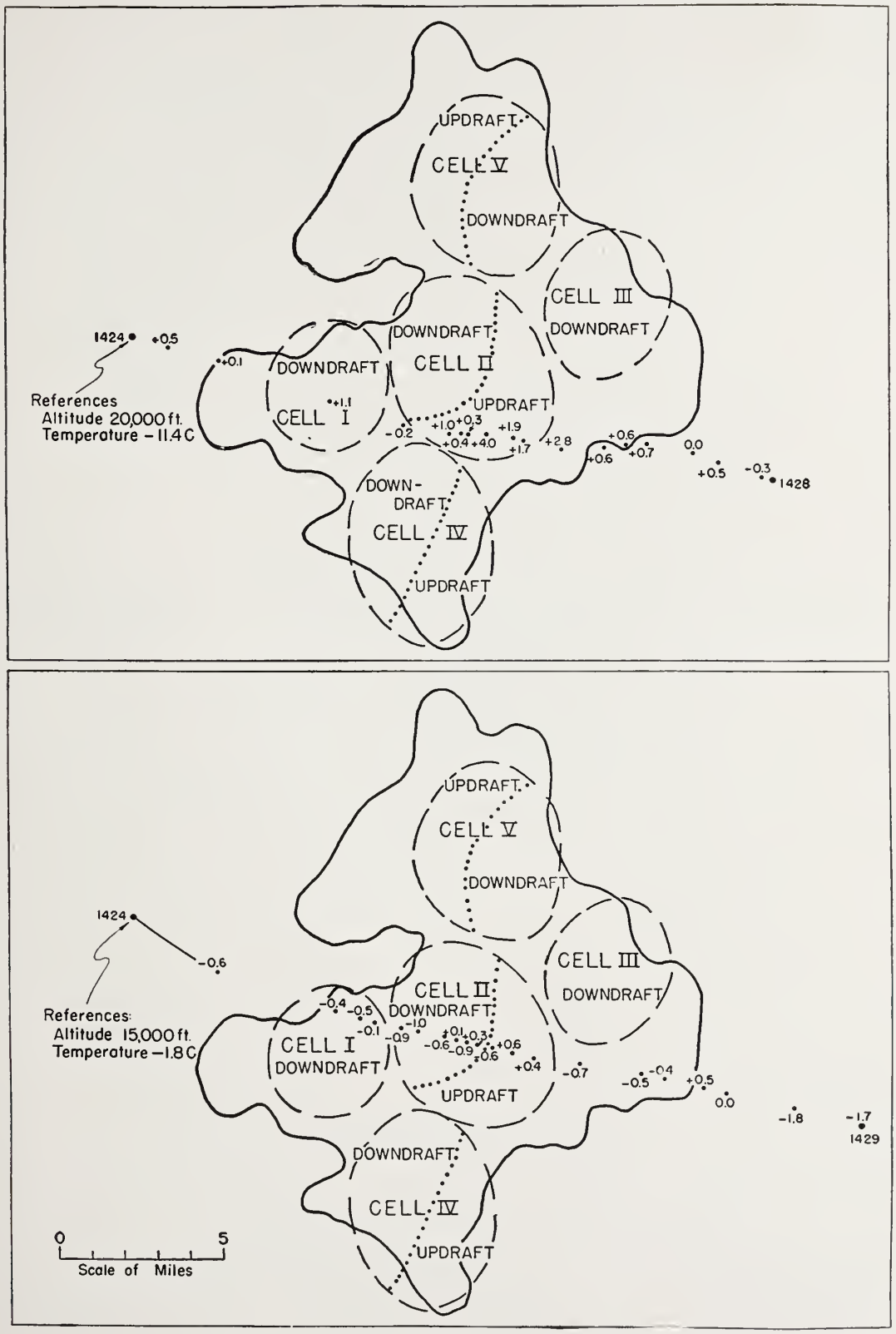

FIGURE 189.—Air temperature measurements, 1425–1435 E.S.T., August 14, 1947.

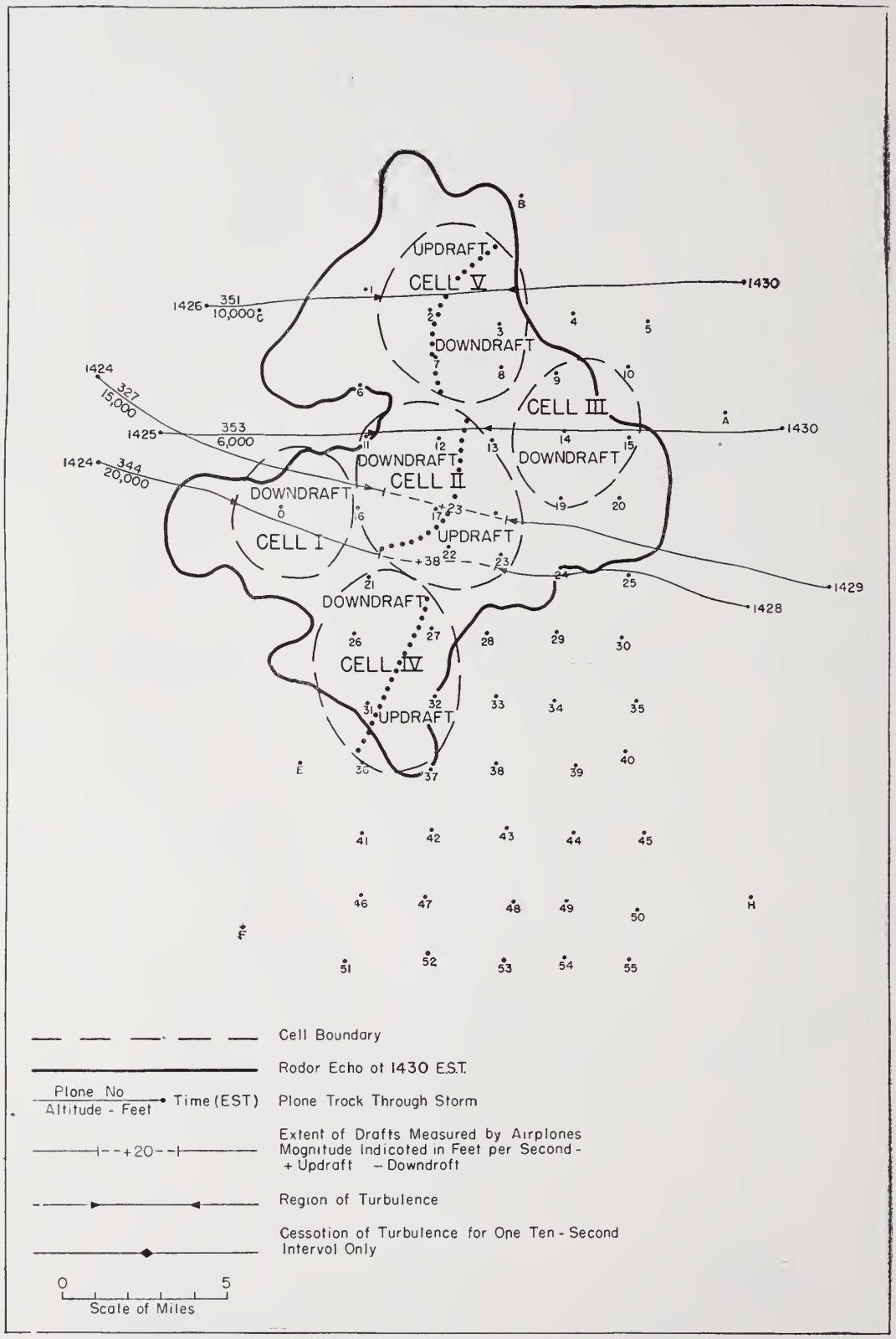

FIGURE 190.—PPI radar echo at 1430 E.S.T. and airplane paths from 1425 to 1435 E.S.T., August 14, 1947.

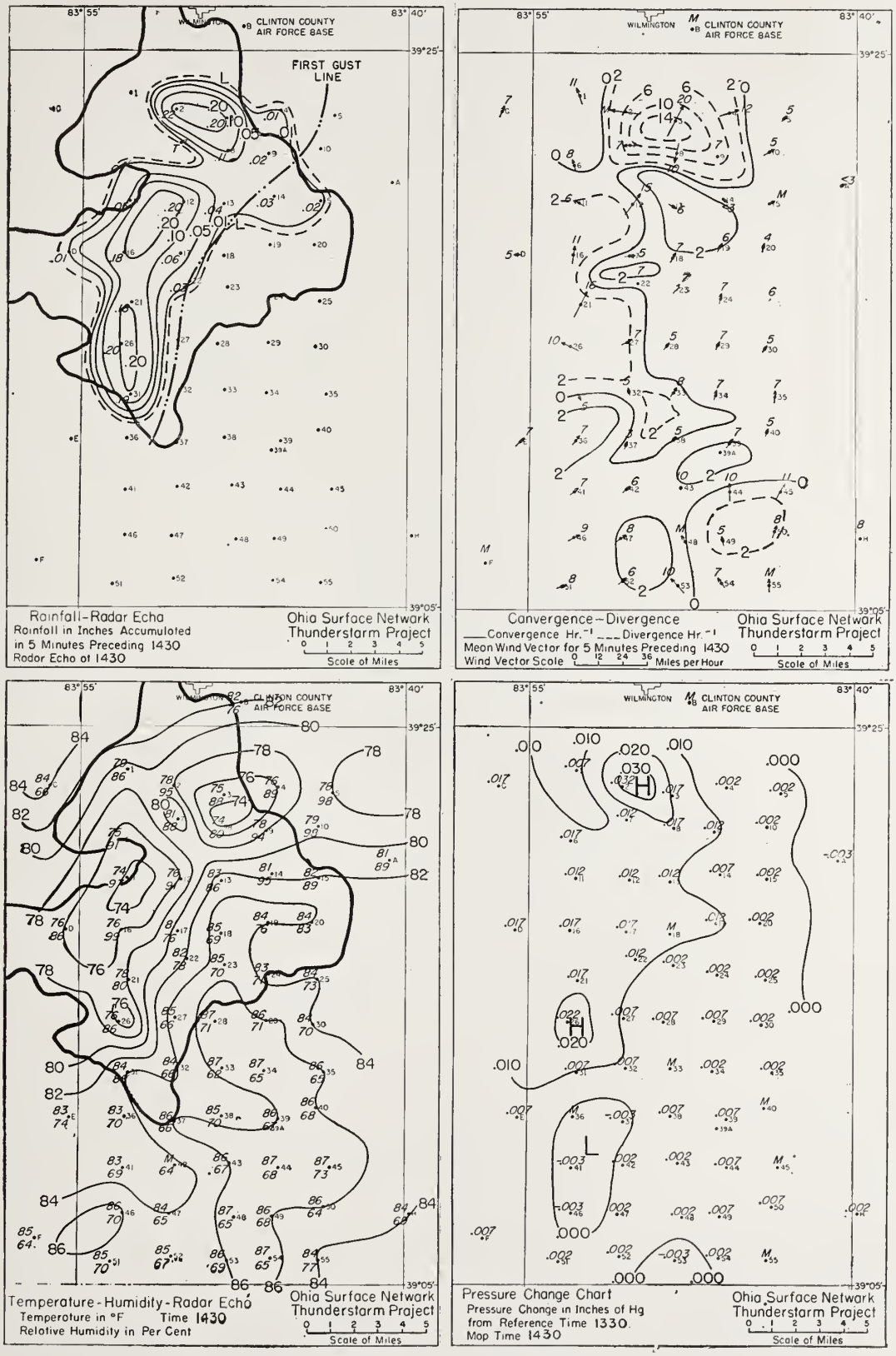

FIGURE 191.—Ohio surface network, 1430 E.S.T., August 14, 1947.

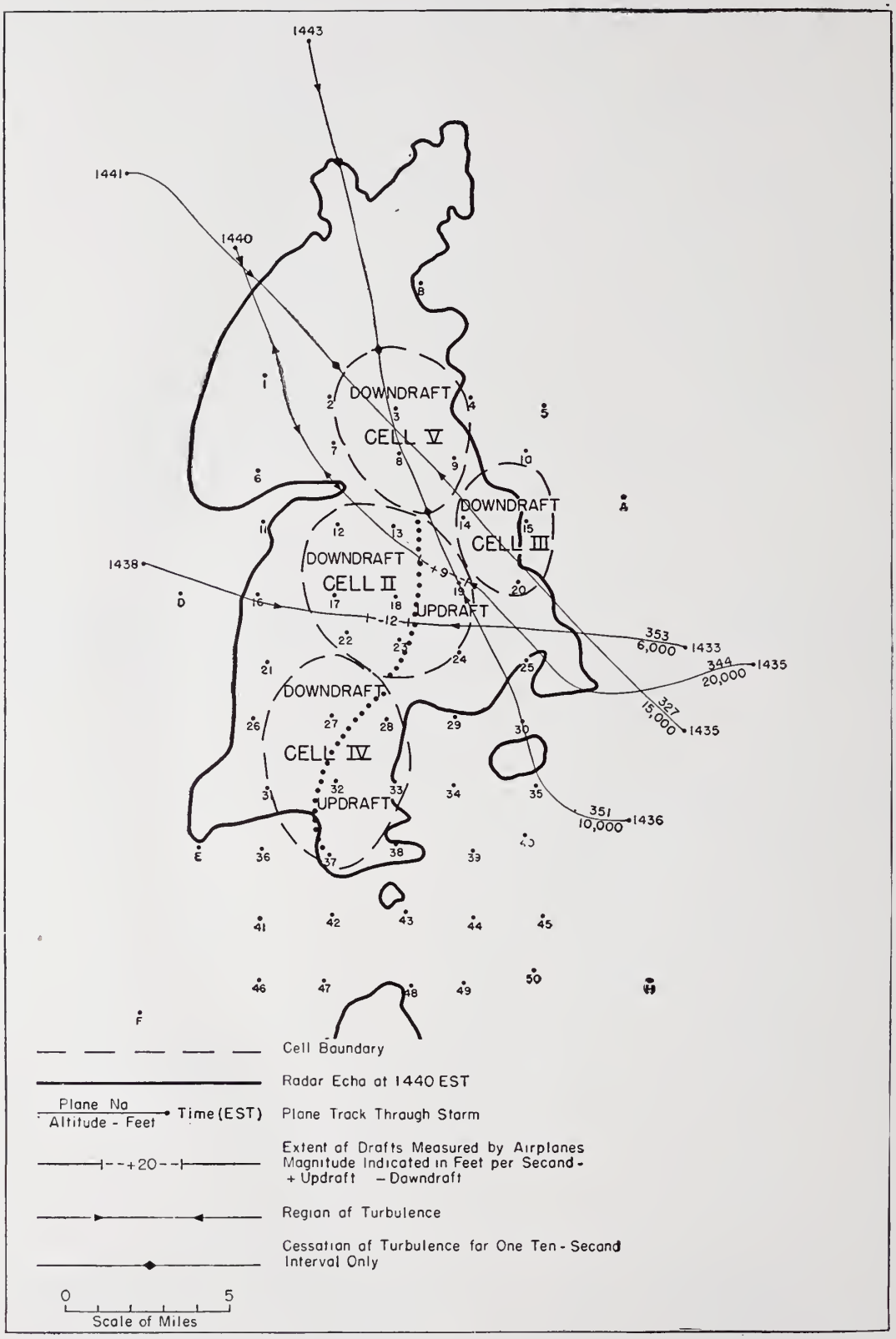

FIGURE 192.—PPI radar echo at 1440 E.S.T., and airplane paths from 1435 to 1445 E.S.T., August 14, 1947.

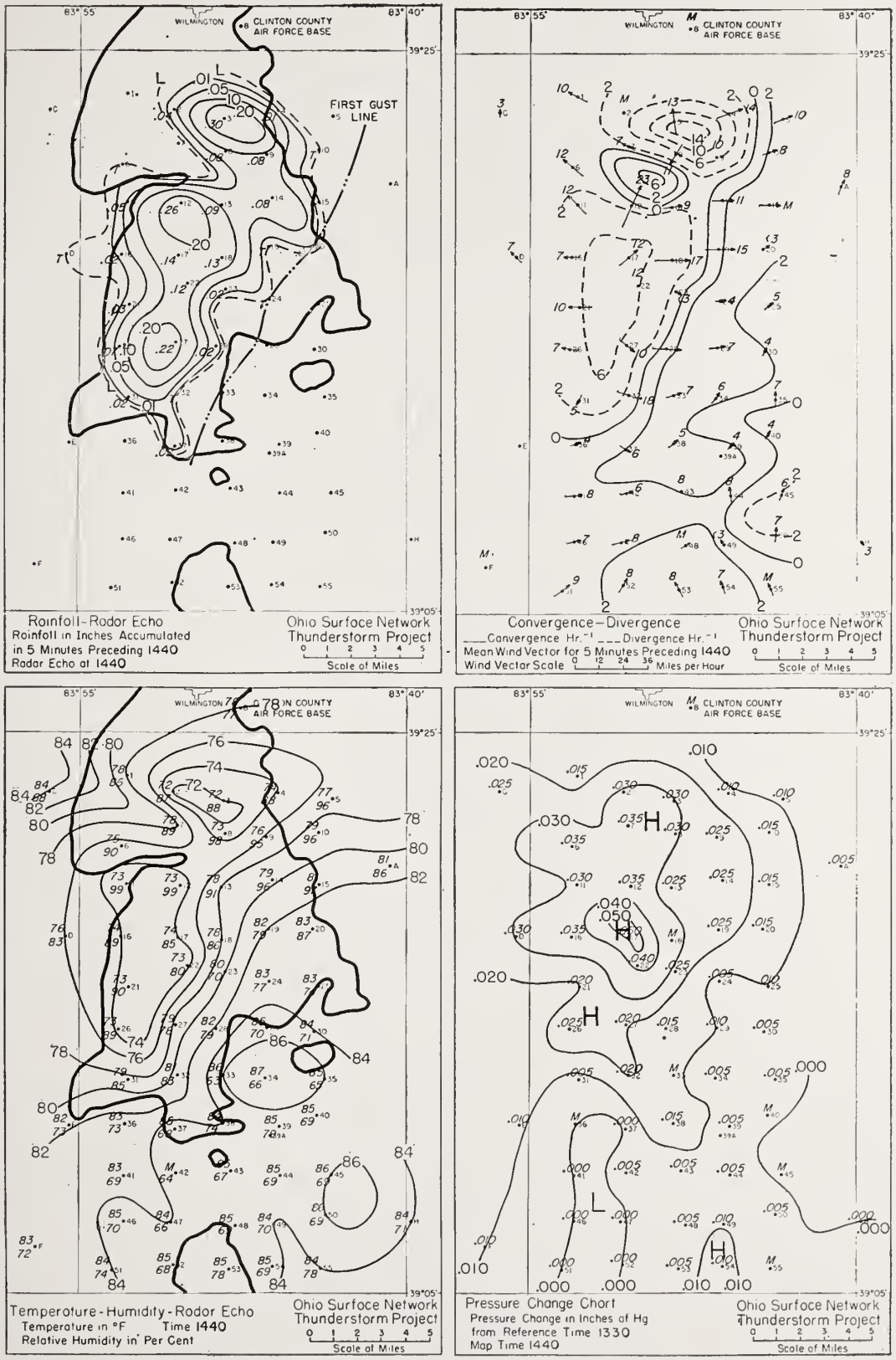

FIGURE 193.—Ohio surface network, 1440 E.S.T., August 14, 1947.

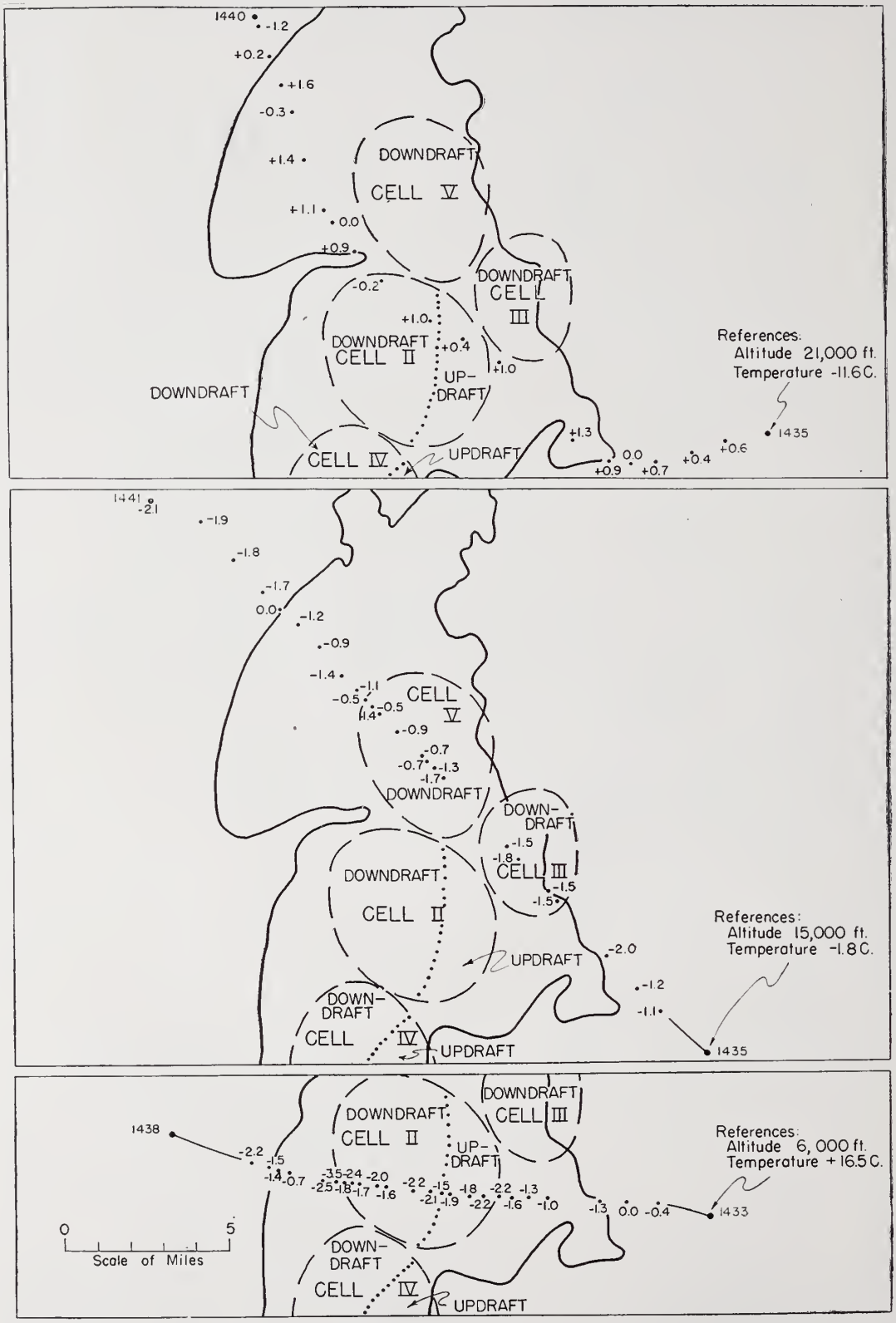

FIGURE 194.—Air temperature measurements, 1435–1445 E.S.T., August 14, 1947.

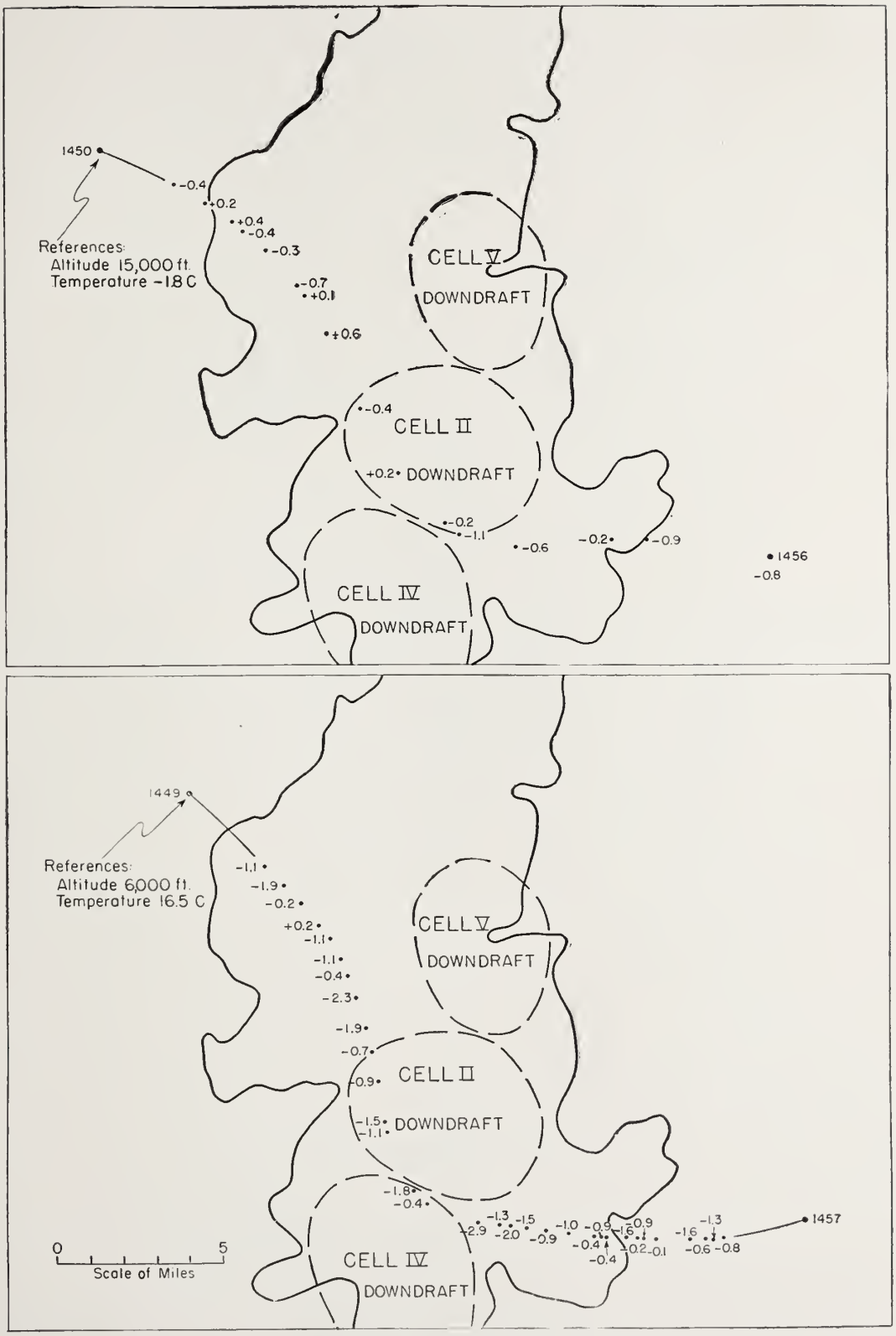

FIGURE 195.—Air temperature measurements, 1445–1455 E.S.T., August 14, 1947.

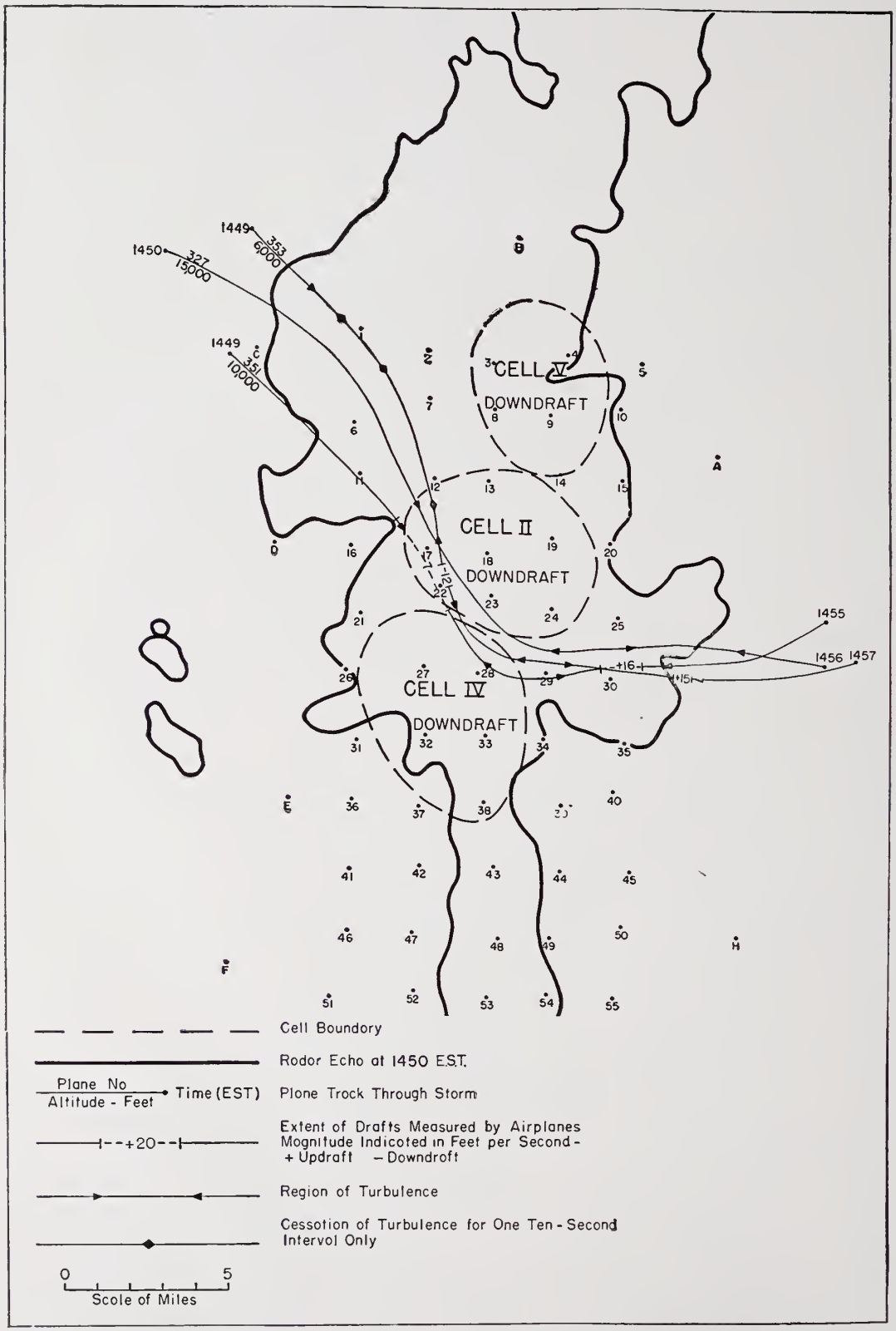

FIGURE 196.—PPI radar echo at 1450 E.S.T., and airplane paths from 1445–1455 E.S.T., August 14, 1947.

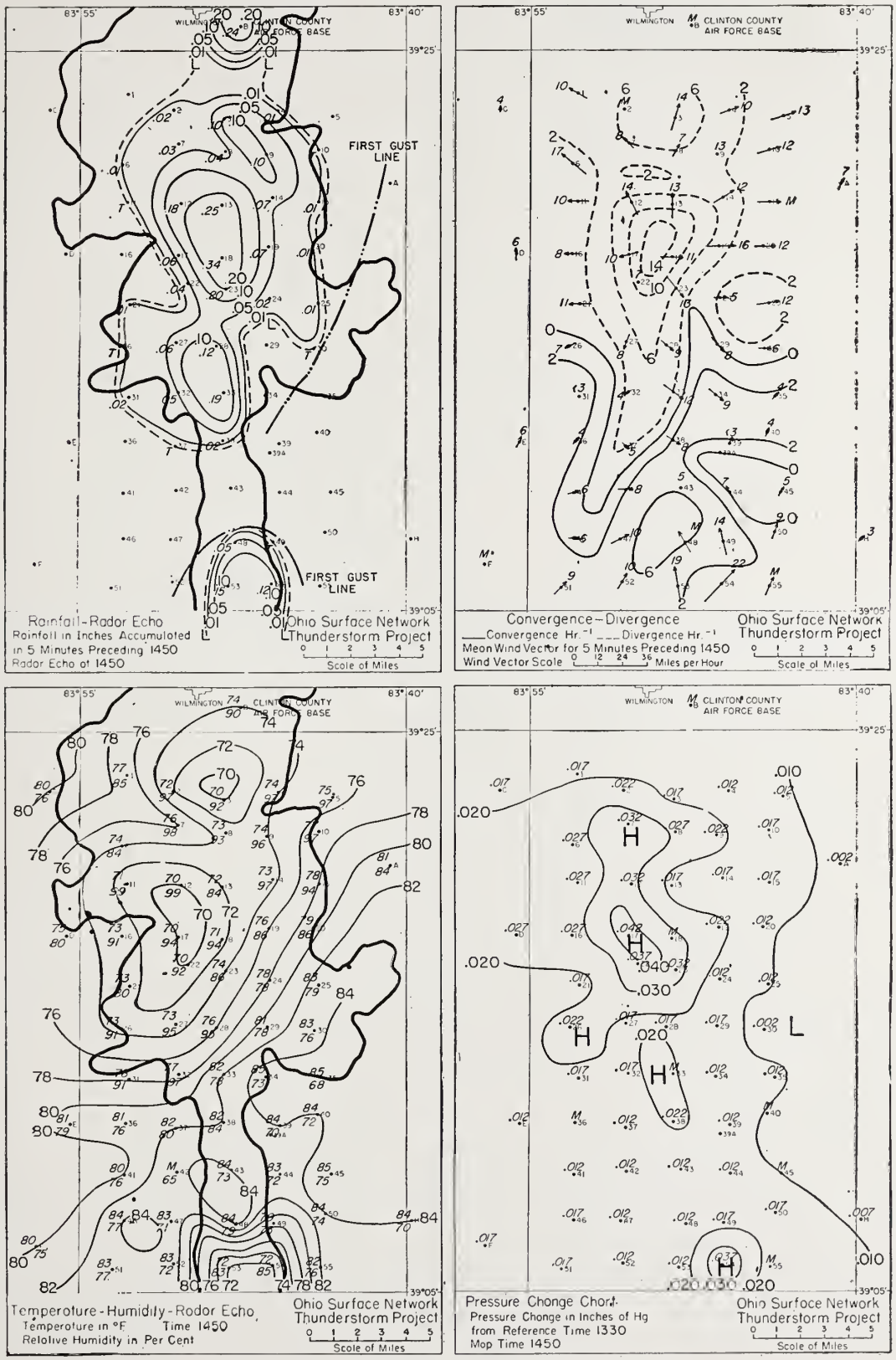

FIGURE 197.—Ohio surface network, 1450 E.S.T., August 14, 1947.

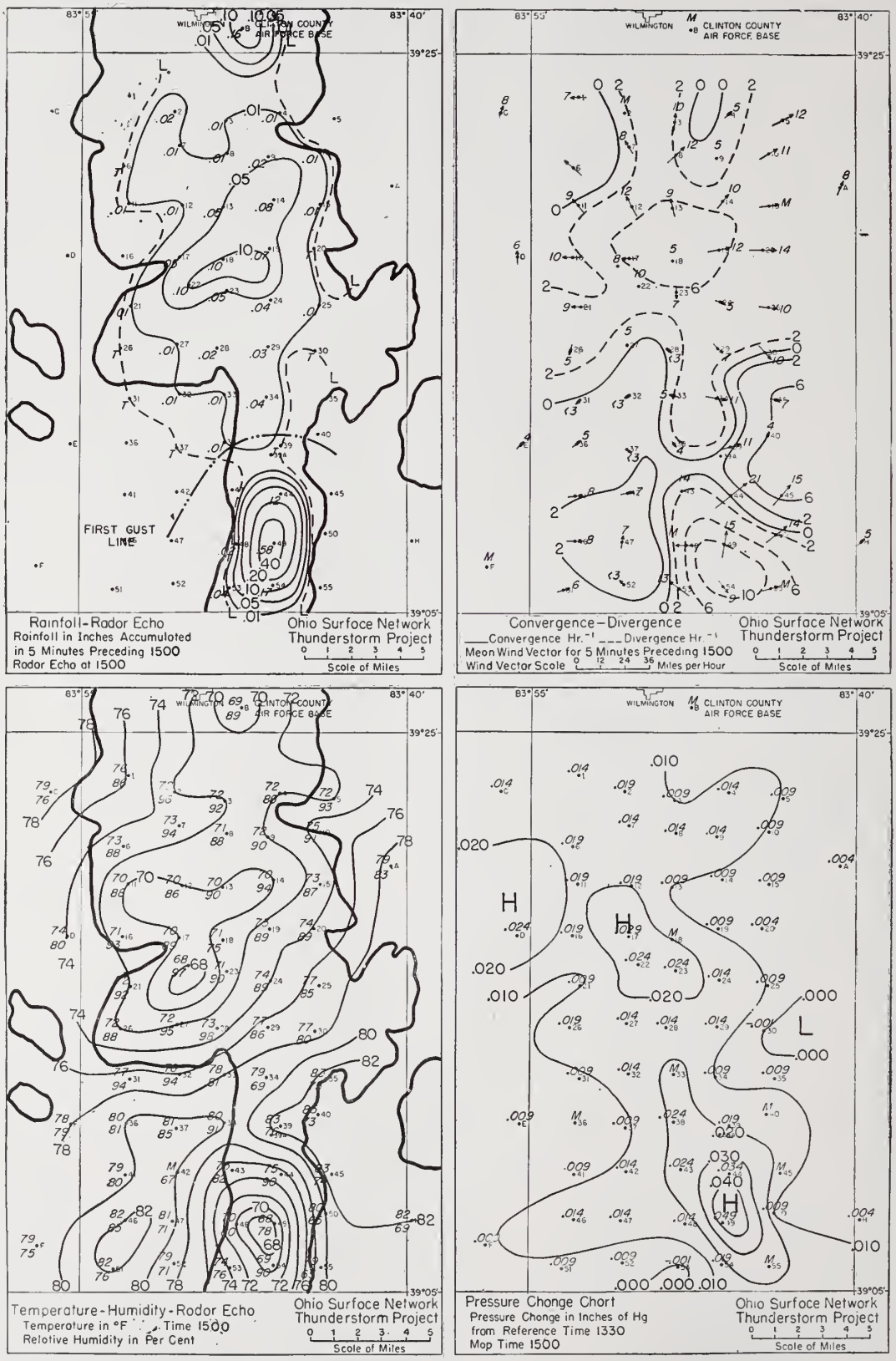

FIGURE 198.—Ohio surface network, 1500 E.S.T., August 14, 1947.

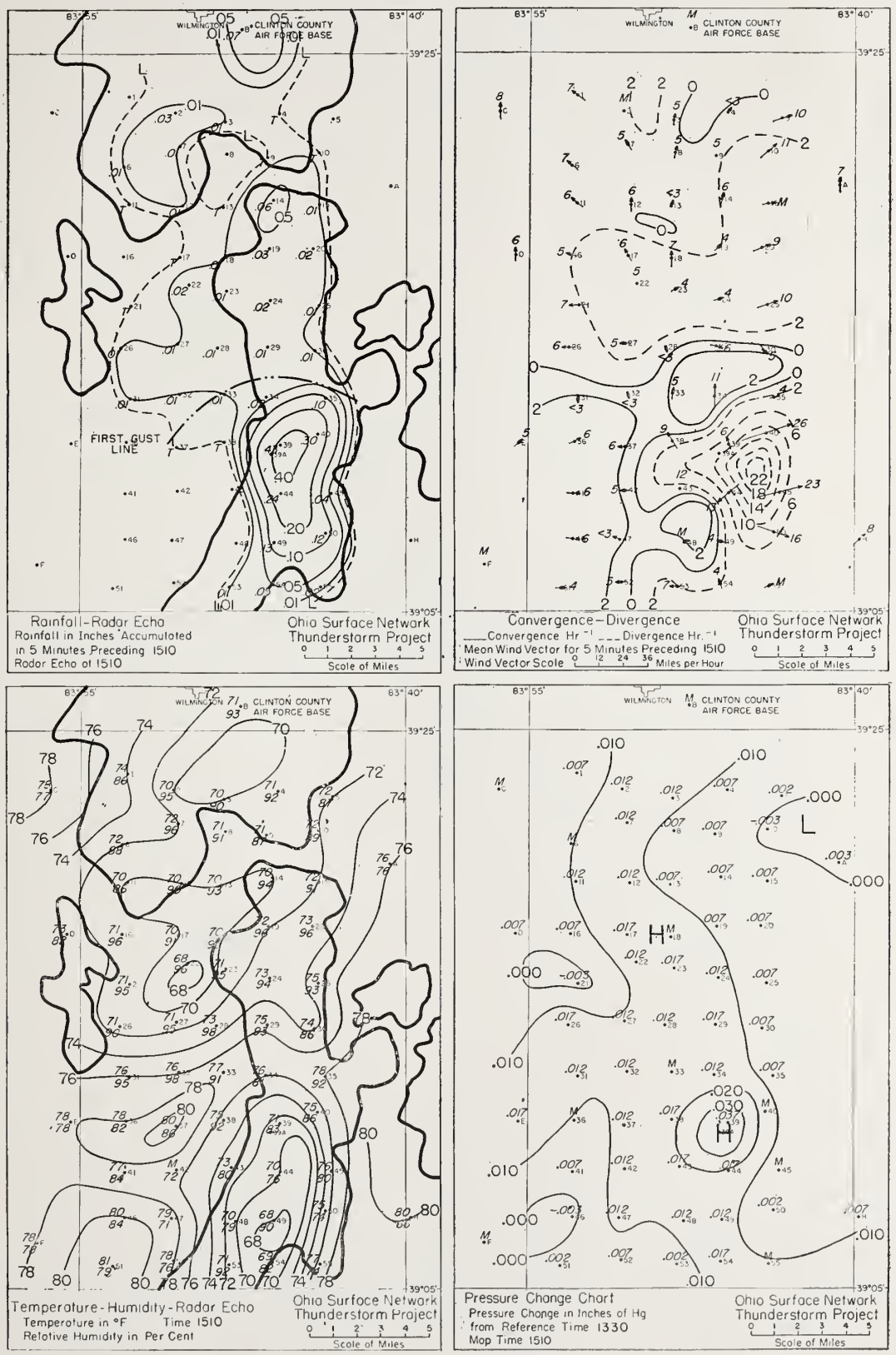

FIGURE 199.—Ohio surface network, 1510 E.S.T., August 14, 1947.

841051—50——16

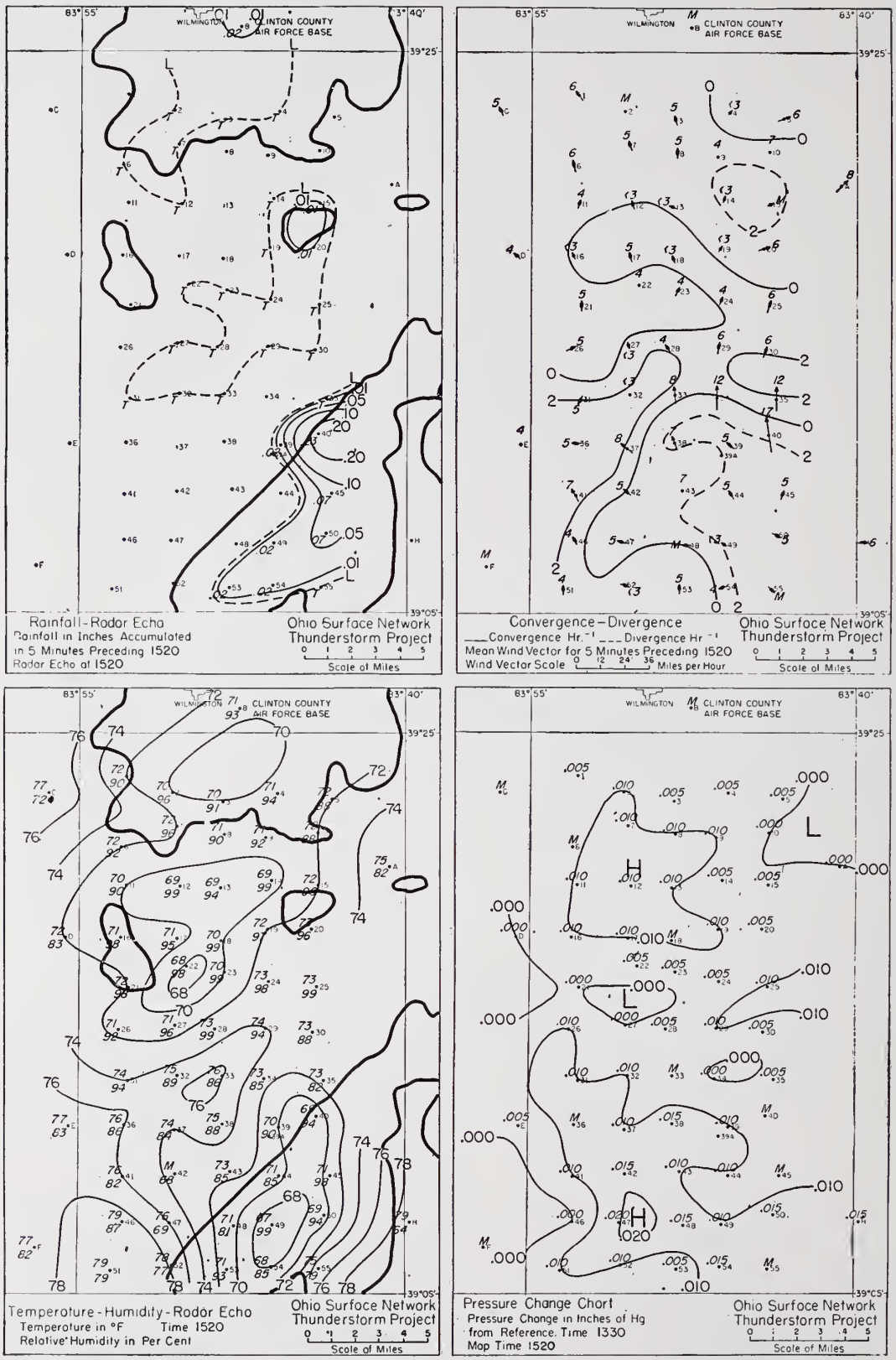

FIGURE 200.—Ohio surface network, 1520 E.S.T., August 14, 1947.

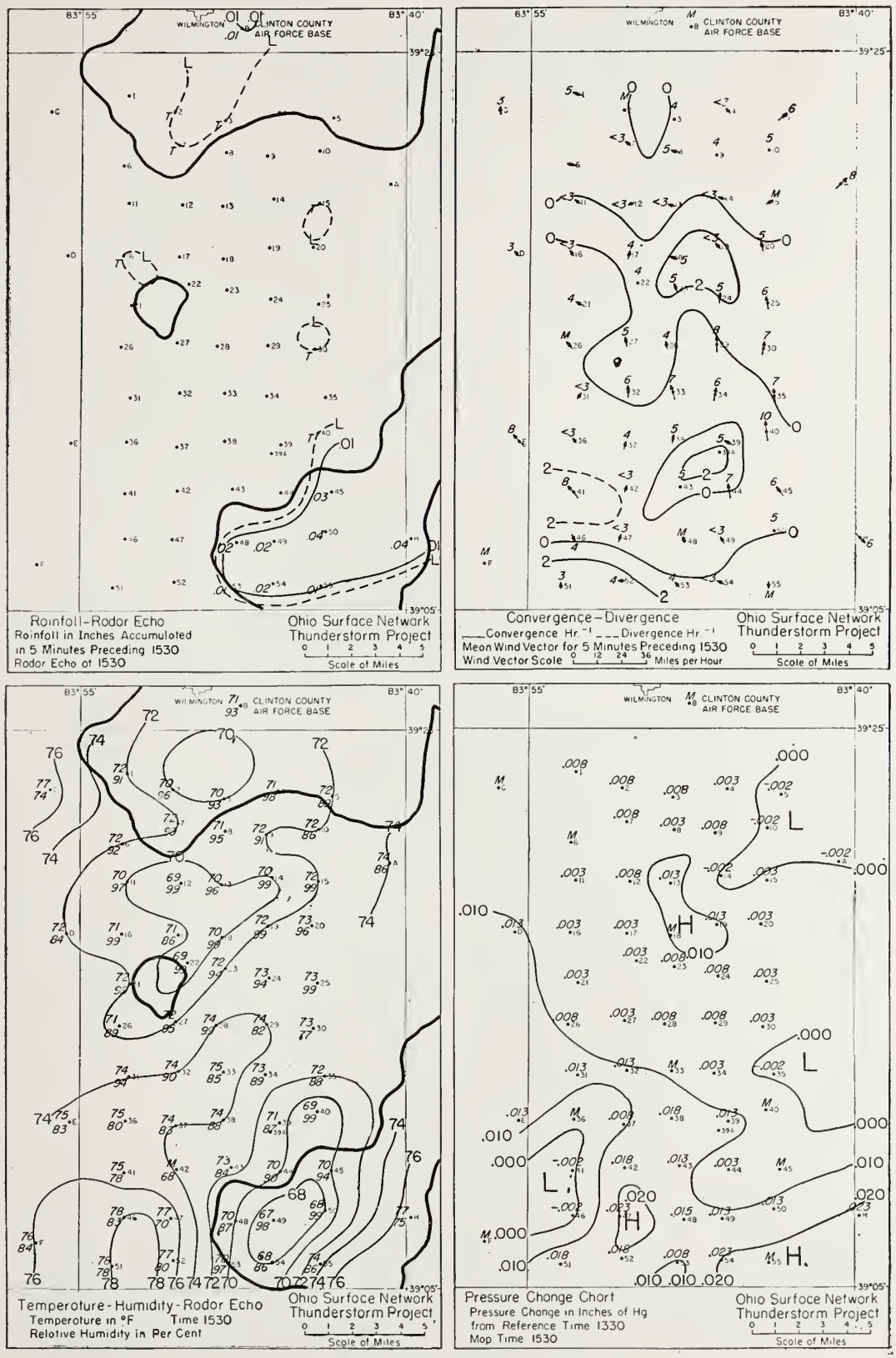

FIGURE 201.—Ohio surface network, 1530 E.S.T., August 14, 1947.

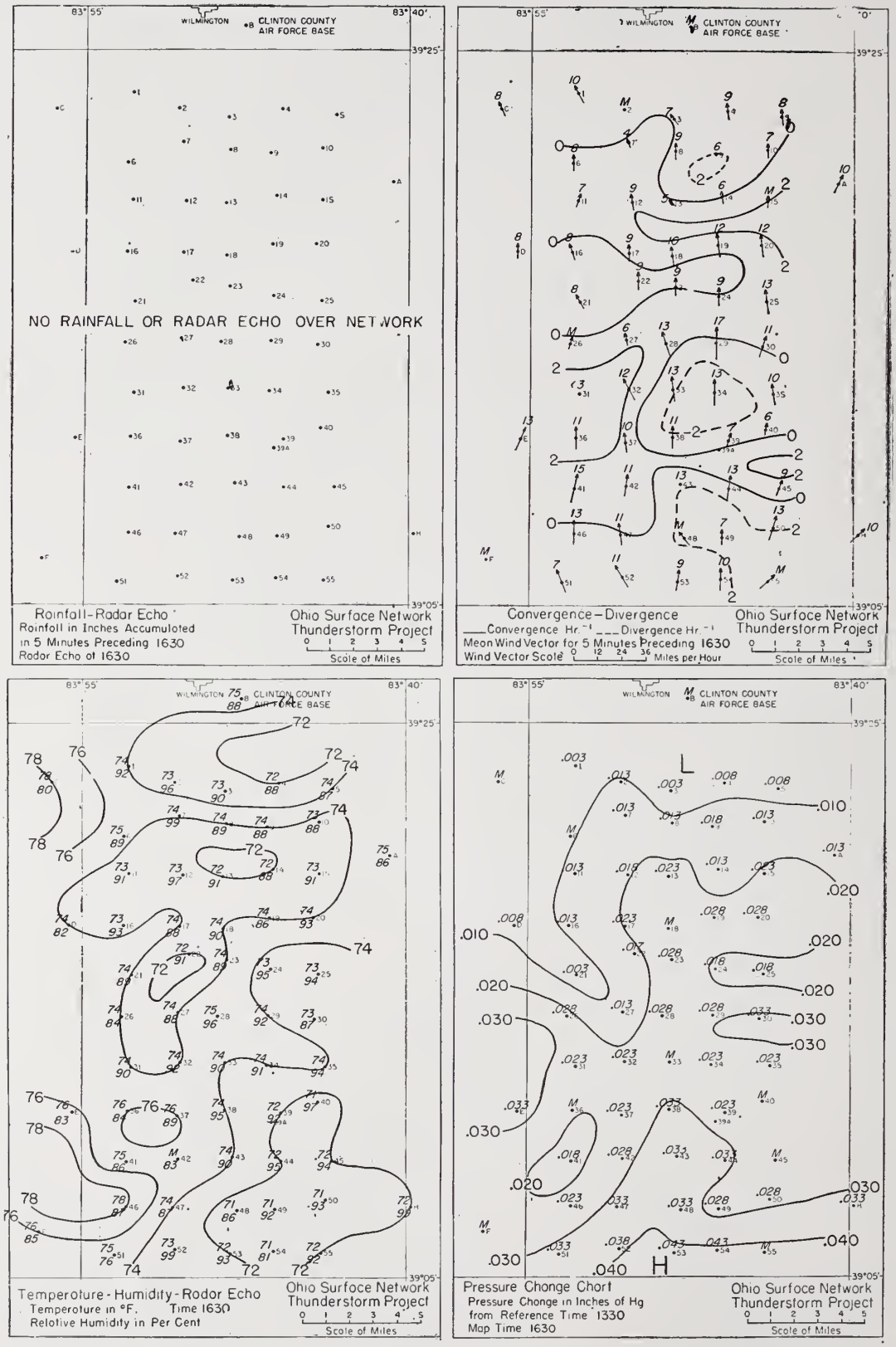

FIGURE 202.—Ohio surface network, 1630 E.S.T., August 14, 1947.

THUNDERSTORM OF AUGUST 17, 1947
[1430 E.S.T. to 1540 E.S.T.]

This thunderstorm is included among the examples because its cells appeared to have a circulation somewhat different from that found in cells undergoing normal life cycles. Although, seemingly, ample data are available, it has not been possible to divide the history of these cells into periods corresponding to the three stages of development.

As shown in figure 203, the storm was one of a group of air-mass thunderstorms that occurred in maritime tropical air flowing around a high-pressure area centered over the Carolinas. The principal features of the synoptic situation are shown in figure 204, the surface map for 1330 E.S.T. The 0300 G.C.T. radiosonde observation from Huntington, W. Va., is plotted in figure 205, with the winds-aloft observations from Evansville, Ind., as well as from Huntington, W. Va. Records from radiosondes released from stations of the Project network at 1350 and 1505 E.S.T. showed the air at about those times to be considerably drier in the upper levels than was indicated by the Huntington sounding; the relative humidities recorded by the former instruments were less than 50 percent above 18,000 ft.

Figures 206 and 207 show the radar-echo history of the storm studied. Before flights through it were made, the storm, which was moving eastward at about 8 mi/hr, had passed to the east of the surface network, so data from surface stations were not available for the analysis.

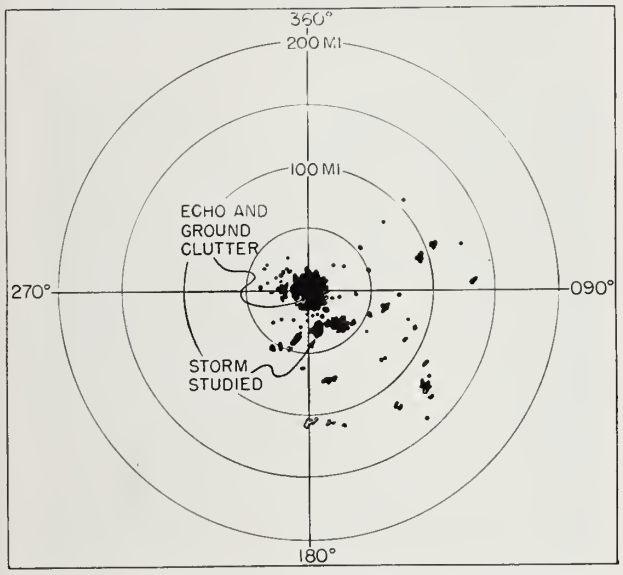

FIGURE 203.—A schematic drawing of the 200-mile-range PPI 'scope showing the actual radar echoes at 1445 E.S.T., August 17, 1947.

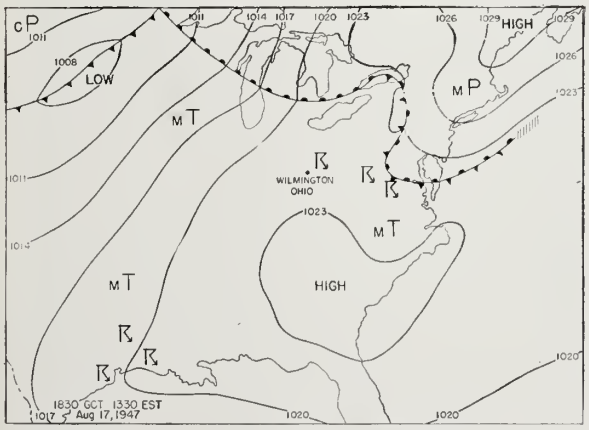

FIGURE 204.—A surface synoptic chart for 1330 E.S.T., August 17, 1947.

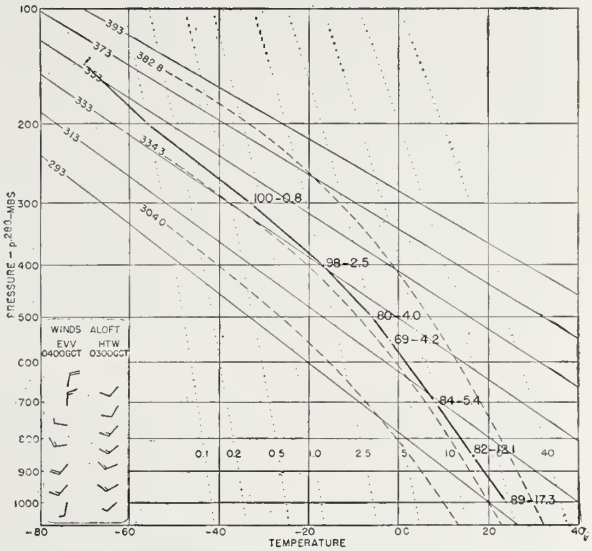

FIGURE 205.—Upper-air sounding and winds-aloft observation for 0300 G.C.T. from Huntington, W. Va., and the winds-aloft observation from Evansville, Ind. for 0400 G.C.T., August 17, 1947.

1430 E.S.T.
(*fig. 210*)

The first composite cross section for the storm shows penetrations by airplanes at three levels; the airplane at 15,000 ft. made two traverses through the

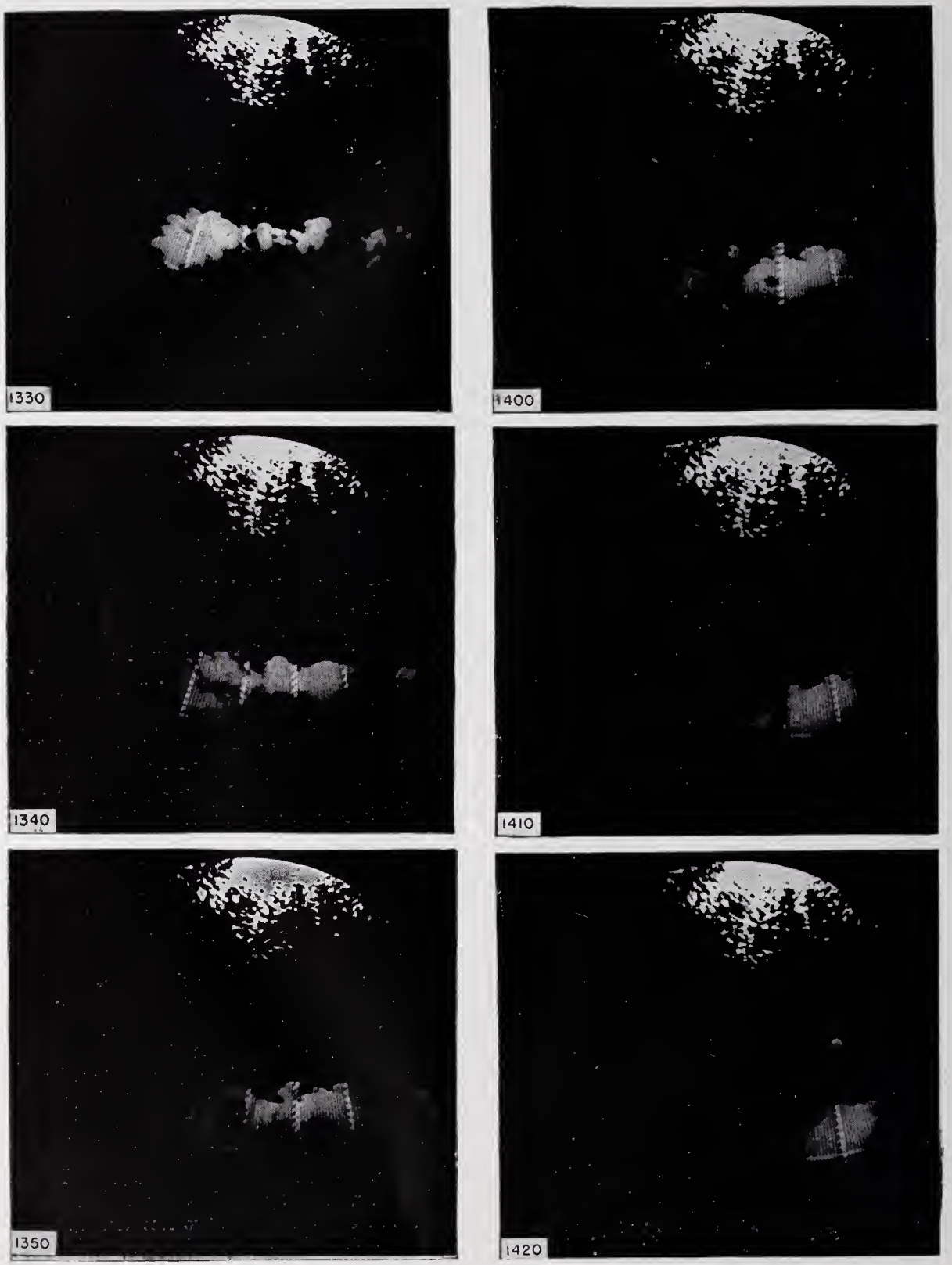

FIGURE 206.—Control-radar PPI 'scope photographs, 1330–1420 E.S.T., August 17, 1947.

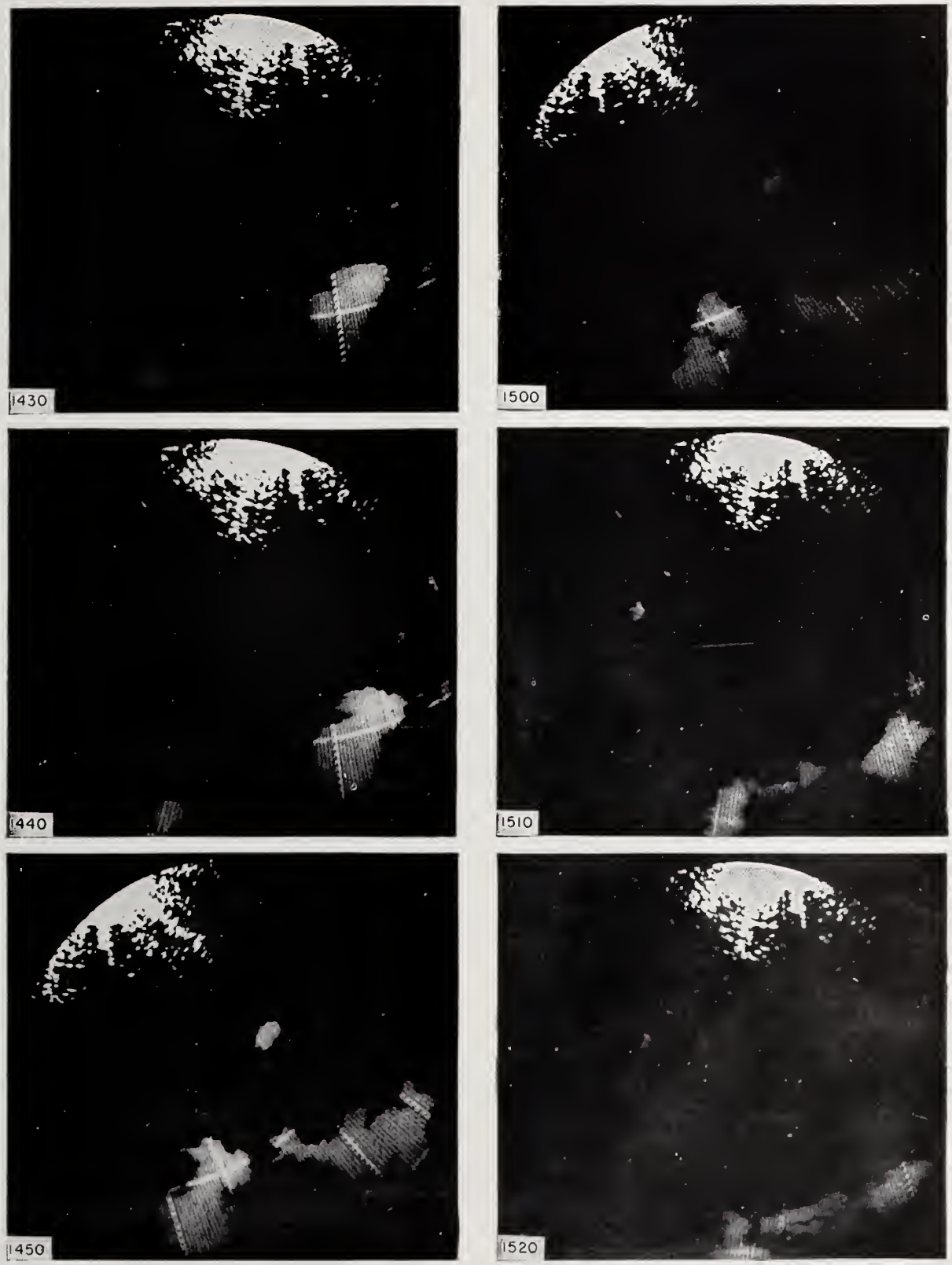

FIGURE 207.—Control-radar PPI 'scope photographs, 1430–1520 E.S.T., August 17, 1947.

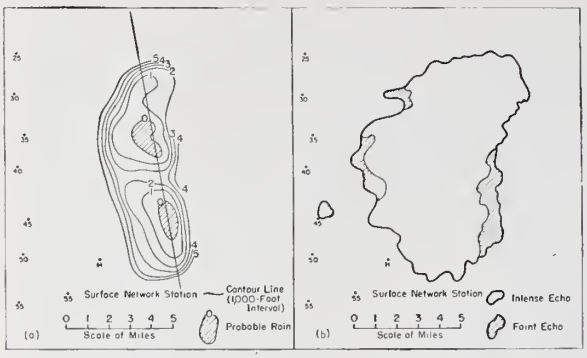

FIGURE 208.—(a) Drawing showing contours of the height above the surface of the base of the RHI radar cloud. Contours drawn only for areas where the echo base was below 5,000 ft. Hatched areas show regions where rain was falling. The straight line represents the azimuth along which the radar was directed when the photograph (fig. 209) was made (1430 E.S.T., August 17, 1947). (b) PPI radar echo at the time for which the base contours in (a) were drawn.

storm. Almost as soon as the storm moved east of the surface network, at approximately 1330 E.S.T. the RHI radar showed echo extending down to the zero-elevation indicator, which is evidence of rain falling to the surface [**18**]. The precipitation continued and was still falling at the time the first flights were made. Figure 208 shows the contour lines (height above the surface) of the base of the RHI echo for 1430 E.S.T. The two hatched areas represent those regions where the RHI echo extended below the zero-elevation line. The photograph of the RHI radar 'scope shown in figure 209 is along an azimuth of 168° at 1430 E.S.T. and shows the cellular nature of the echo as well as the areas where rain was falling. Analysis of the radar echoes indicate that two regions of activity, i. e., two cells, comprised this storm.

Cell I was readily delineated by means of the gust and draft records from the airplanes. Figure 210 shows the areas of gustiness coincident with this cell, as well as the grouping of the large-scale vertical motions in that area. Both updrafts and downdrafts were measured, as is indicated, and in addition, the records of the airplanes flown at 10,000 and 20,000 ft. showed losses of altitude in the region marked as downdraft on the cross section.

The presence of both an updraft and a downdraft in this cell demonstrates that it was in the mature stage of development at this time. However, as is pointed out above, rain had been falling from it since 1330 E.S.T. This is an exceptionally long period for the mature stage of a cell to continue.

A study of the RHI radar echoes from this cell indicated that a maximum echo height of 50,000 ft. was reached by 1418 E.S.T., over an hour after it was first detected on the RHI. By 1435 E.S.T. the echo top had lowered to 20,000 ft. This rapid decrease in cell height during a period when updrafts were present might be attributed to a shift in the winds aloft causing an increased shear with height, accompanied by increased evaporation if the new advection aloft were bringing in drier air. It was pointed out that the radiosondes released from network stations at 1350 E.S.T. passed through air with relative humidities below 50 percent above 18,000 ft. It was not known when the air at these upper levels changed from the moist air reported by the 0300 G.C.T. Huntington soundings to the dry air reported by the Project soundings, but it is possible that the advection did not begin until after the thunderstorm under consideration had developed.

Evidence of the presence of shear was shown by the RHI echoes during the early period of this storm, since a shelf of echo extended southward from cell I at levels above 20,000 ft. The shear was also evident in the winds-aloft observations made from the Project stations. These observations showed winds with a northerly component which increased in speed with height above 14,000 ft.

Cell II developed beneath the shelf that extended southward from cell I at the upper levels. The PPI radar echo associated with cell I showed a protuberance to the south as early as 1410 E.S.T., but this was identified on the RHI 'scope as a shelf from cell I. It was not until 1425 E.S.T. that a separate echo which could be attributed to new-cell development was distinguishable. By 1435 E.S.T. the top of this echo,

FIGURE 209.—A photograph of the RHI radar 'scope directed along the 168° azimuth at 1430 E.S.T., August 17, 1947.

which was cell II of the storm, extended to 29,000 ft. As shown in figure 208, the RHI echo from this cell extended below the zero-elevation indicator at 1430 E.S.T., so it is assumed that rain was reaching the surface at that time.

Cell II was penetrated by airplanes at three levels during the time interval covered by figure 208. No drafts were indicated by the airplane records, but breaks in the turbulence occurred at the cell boundaries. Since rain was falling from this cell, there was probably a downdraft in the lower levels. All three airplanes passed through the cell west of the area of surface rain, and the two planes flown at the lower levels intersected only the extreme western edge of the cell. Therefore, it is not unexpected that the downdraft was not encountered. At 20,000 ft. only light turbulence was reported, but light snow and rime icing were observed. To the west, the airplane flying at 15,000 ft. passed through an area of light snow; at 10,000 ft. an updraft, followed by moderate rain, was reported. Since this updraft could not be verified from the flight records, it was not indicated on the cross section.

Thus far, cell II appeared to be following the usual life cycle, except that it entered the mature stage rather soon after the detection of the initial radar echo.

To the northeast of cell I, the airplane at 10,000 ft. passed through a developing cell and encountered an updraft. The size and subsequent growth of the echo from this convective area suggest that a cell was in the building stage of development at 1430 E.S.T. However, data from this region are lacking, so analysis of the cell was not attempted.

1440 E.S.T.
(*fig. 211*)

Cell I was traversed once by the airplane flown at 15,000 ft. and twice by the airplane flying at 20,000 ft. during the period from 1435 to 1445 E.S.T. The lower airplane passed through a downdraft and an updraft on its penetration of the cell. Light snow was observed in the downdraft area and light rain was reported elsewhere. At 20,000 ft. only turbulence was reported. The cell remained in the mature stage during this period.

Cell II was penetrated twice by the airplanes at 10,000, 20,000, and 25,000 ft. and once by the airplane at 15,000 ft. As shown in figure 211, updrafts were found in the northwestern and southeastern sections of the cell and downdrafts were encountered in the central and southern portions. At 10,000 ft., on the first traverse light rain was observed throughout the cell, except in the area of the updraft where heavy rain was encountered. During the second pass through this cell, light rain was reported until, just before the plane left the cloud, a small area of heavy rain was encountered. Light or moderate snow was found at the 15,000-foot level and above on all traverses. In the weak downdraft measured at the 15,000-foot level, hail was observed by the flight crew. The RHI echoes showed that precipitation reached the surface intermittently in the region beneath the downdraft.

The arrangement of the up- and downdraft areas in the cell during this period was unusual. It suggested that downward motion had started in the central area of the cell, but such a condition has not been found in any of the other cells analyzed. Normally, the downdraft is initiated near the cell's edge.

1450 E.S.T.
(*fig. 212*)

Cell I had become smaller in area since the previous group of traverses were made. However, the cell was still in the mature stage. At the 10,000-foot level updrafts were encountered, but no drafts could be computed from the records of the five traverses at the other levels. It was the opinion of the flight crews that the cell was dissipating at this time, and indeed, the RHI echo only extended to 16,000 ft. and its base no longer indicated the presence of surface rainfall.

Light to moderate rain was reported on the two traverses at 10,000 ft., and light rain and snow mixed were encountered at 15,000 ft. Above the latter level, light to moderate snow was found on the three penetrations.

At 20,000 ft., the flight crew reported a break in the clouds between cells I and II.

Cell II was traversed seven times by airplanes at four levels. Updrafts were measured at all levels except 20,000 ft. At 25,000 ft., a downdraft was recorded in the central portion of the cell. The precipitation reported was similar to that observed in cell I — light to moderate rain at the lowest level, light rain and snow mixed at 15,000 ft., and light to moderate snow at the two levels above. In the updrafts measured at the 10,000- and 15,000-foot levels, very heavy rain was observed.

During this period, the downdraft area again seemed to be surrounded by an area of updraft. It was possible to measure the downdraft only at the highest level of flight.

1500 E.S.T.
(*fig. 213*)

Cell I, during the period from 1455 E.S.T. to 1505 E.S.T., underwent a considerable change. The RHI echo top extended to just above 15,000 ft. at 1500 E.S.T. but dissipated rapidly, and by 1507 E.S.T. was only detectable as a faint return between 4,000 and 11,000

ft. As shown on the radar 'scope photographs in figure 207, the PPI echo dissipated quickly after 1500 E.S.T. and was last visible about 1510 E.S.T.

The flight crew of the airplane at 25,000 ft. reported that they were already in clouds when about 3 mi. north of the edge of the PPI echo. This was apparently a stratiform deck of clouds not thick enough to produce a radar return. No turbulence was encountered by this airplane until it reached the center of this dissipating cell. The airplane at 20,000 ft. was in clear air while passing through the area occupied by cell I and did not enter cloud after it left cell II. Below this level in cell I, however, the flight crews reported very light rain in the cell. It is probable that gentle subsiding motion was present in this cell, but it was not possible to measure it from any of the airplane records.

After a prolonged mature stage, cell I rapidly dissipated, with actual disappearance of the cloud in the middle levels. There was no evidence of the downdraft's extending into the western portion of the cell, so it seems probable that the cessation of activity was due to the slowing down of the updraft because its source of energy was exhausted, rather than because the accumulated water within the updraft caused a drag greater than the force of the updraft.

Cell II was traversed by airplanes at all four levels. Only at the 10,000-foot level was it impossible to detect an updraft. No downdrafts were found, although the RHI radar echoes indicated that rain was falling from the southwestern portion of the cell during the period from 1455 to 1500 E.S.T. Heavy snow and rime icing were found in the strong updraft encountered by the airplane flown at 25,000 ft. Moderate rain and snow mixed were observed at 20,000 ft., while moderate rain at 15,000 ft., and only light rain at 10,000 ft. were reported.

The last traverse through this cell was completed at approximately 1506 E.S.T. Thereafter, only radar data were available for study. The PPI echo showed that the cell had begun to weaken in intensity as early as 1455 E.S.T. However, it was still detectable at 1540 E.S.T. when it moved out of the range of the radar. The RHI echo dissipated rapidly after 1509 E.S.T. and was last visible as a faint echo detectable only between 10,000 and 15,000 ft.

It is possible that the later history of cell II was similar to that of cell I, i.e., the vertical motion continued to be predominately upward until the energy source was exhausted and the cloud mass then dissipated through evaporation without any formation of persistent downdrafts.

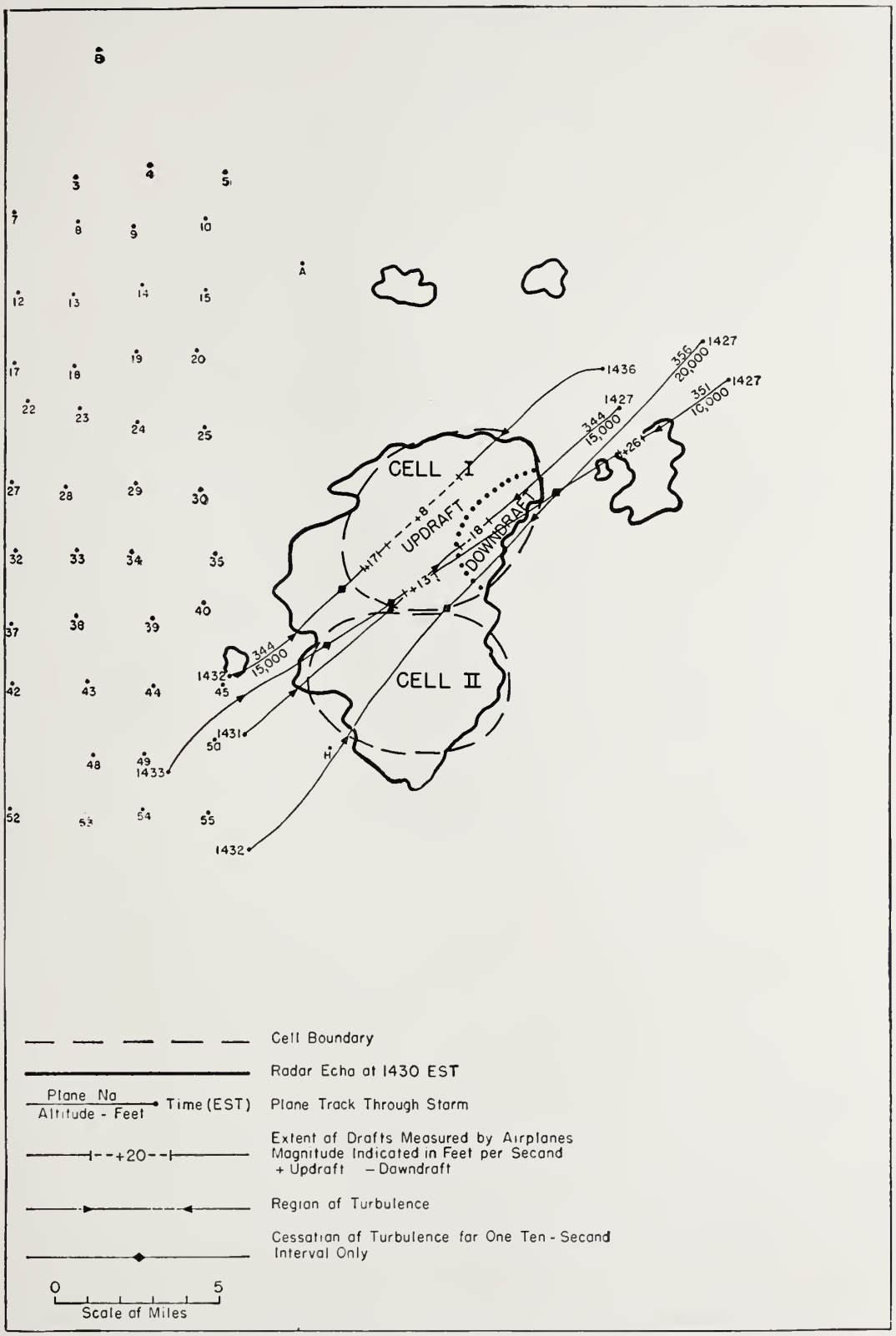

FIGURE 210.—PPI radar echo at 1430 E.S.T., and airplane paths from 1425 to 1435 E.S.T., August 17, 1947.

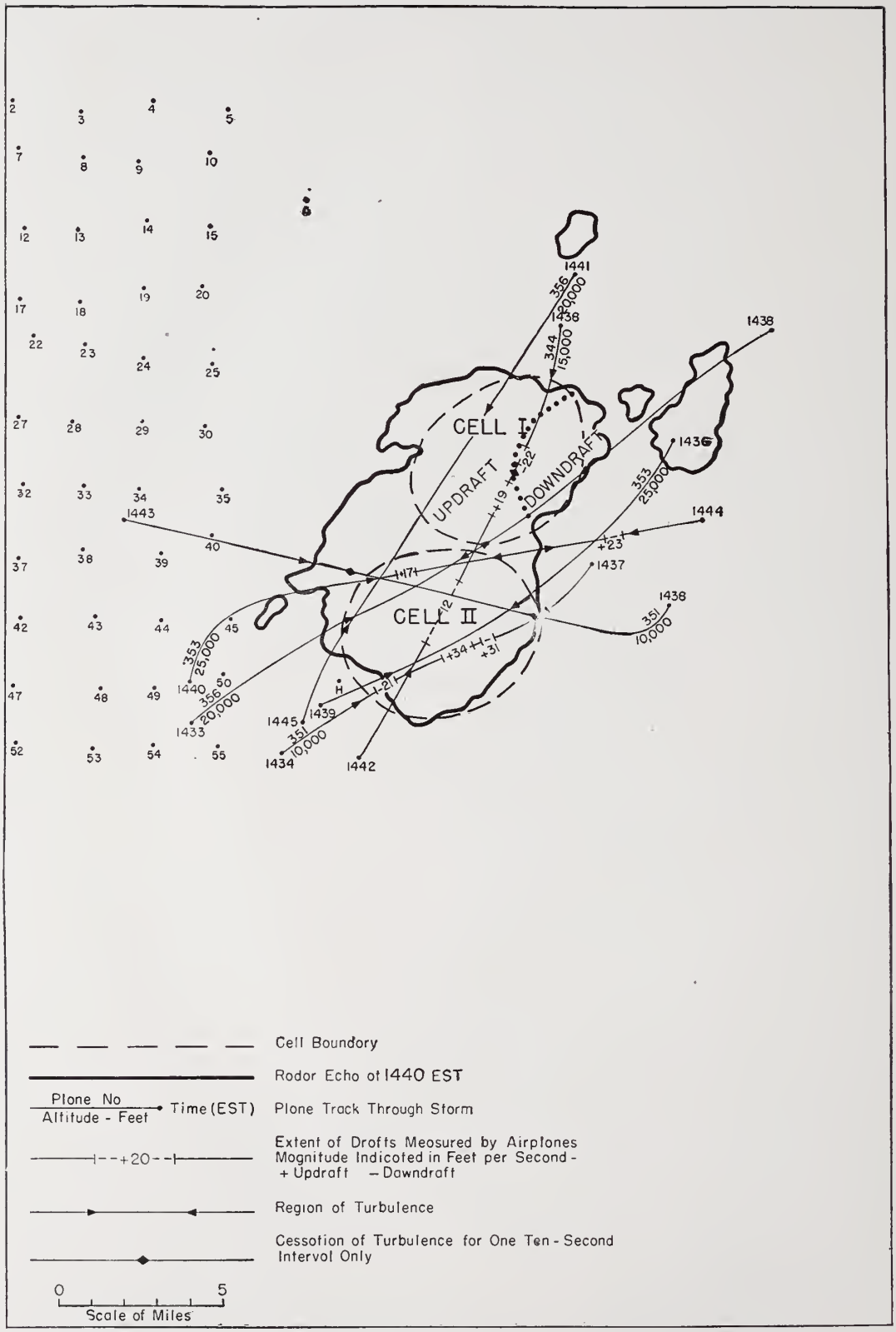

FIGURE 211.—PPI radar echo at 1440 E.S.T., and airplane paths from 1435 to 1445 E.S.T., August 17, 1947.

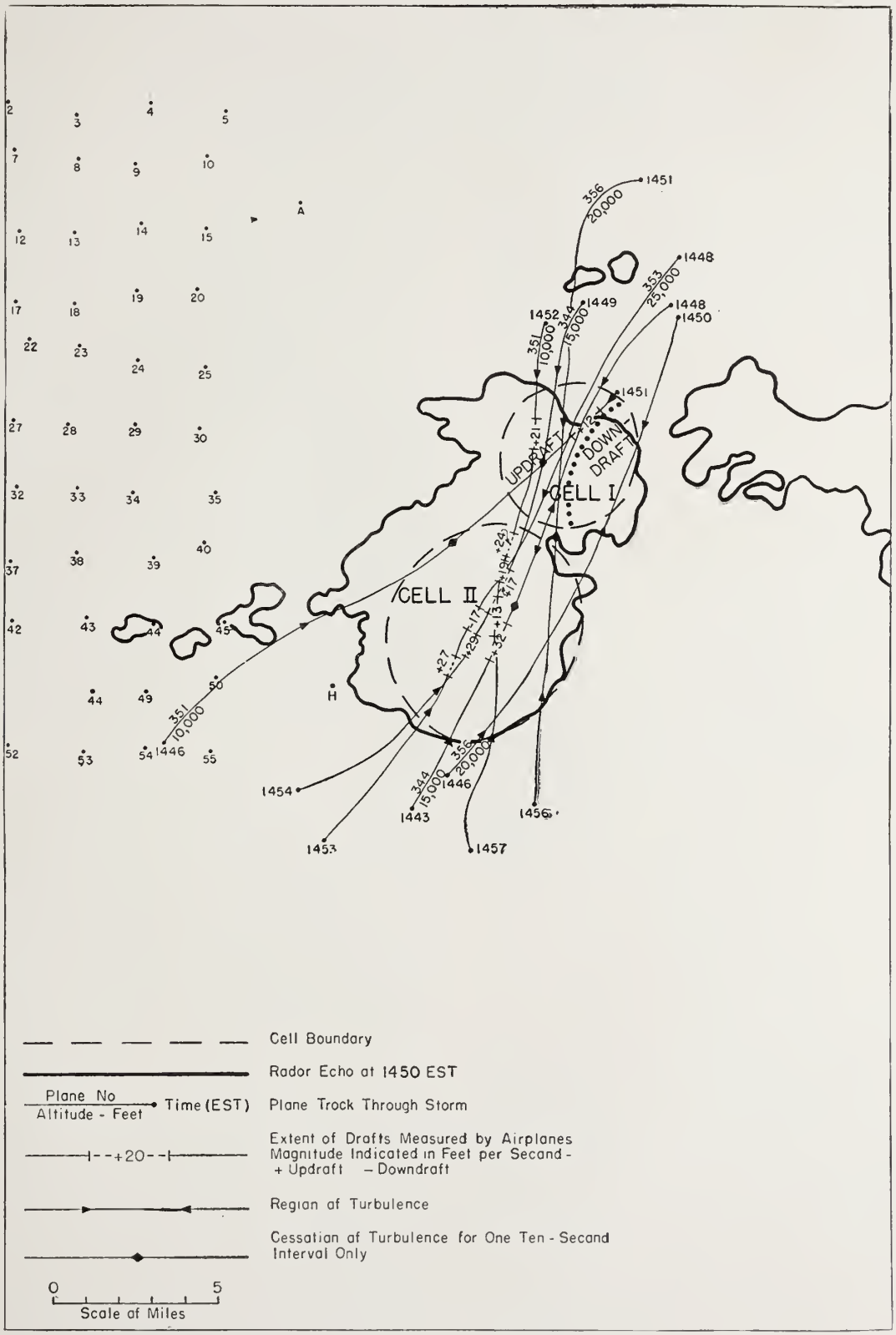

FIGURE 212.—PPI radar echo at 1450 E.S.T., and airplane paths from 1445 to 1455 E.S.T., August 17, 1947.

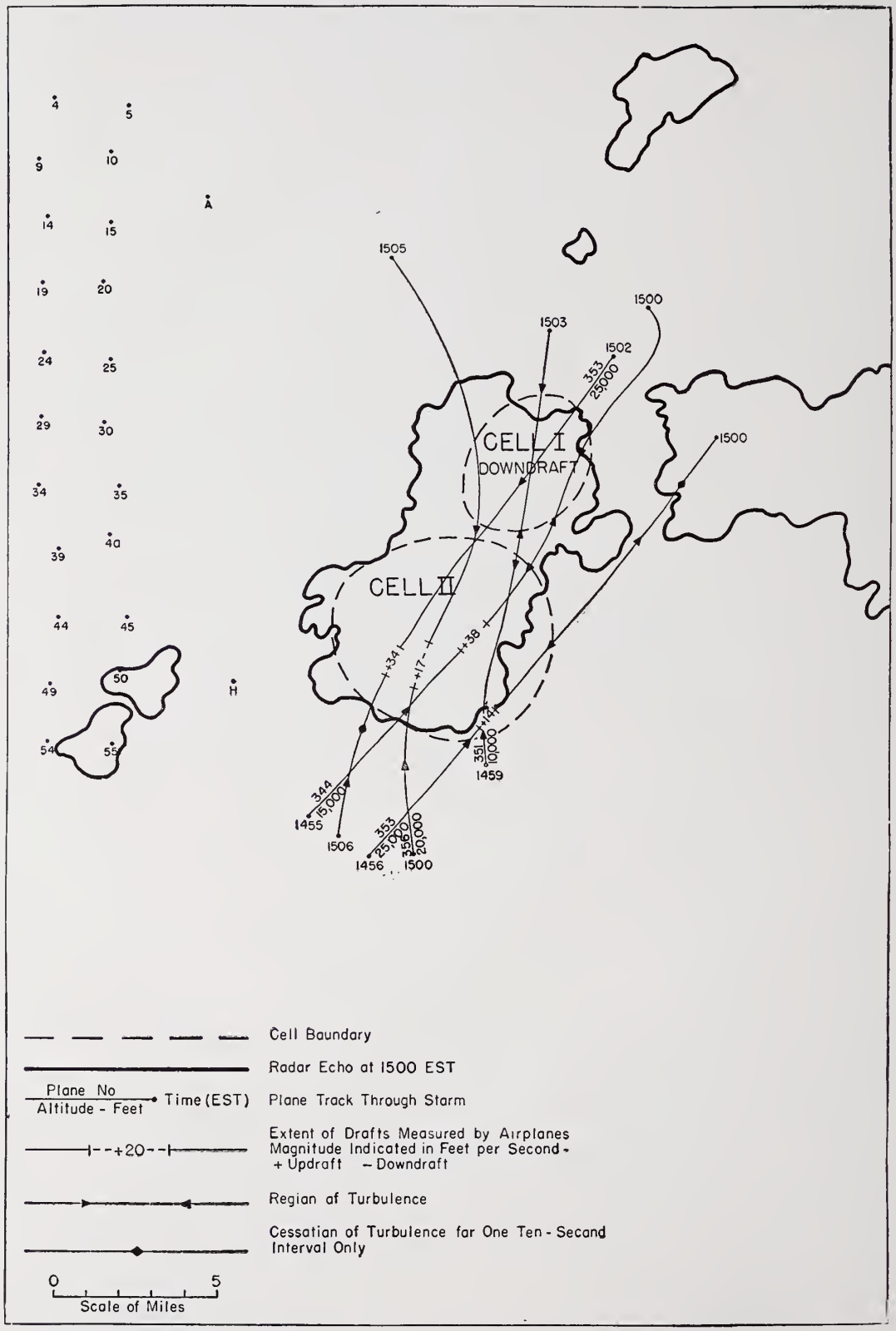

FIGURE 213.—PPI radar echo at 1500 E.S.T., and airplane paths from 1455 to 1505 E.S.T., August 17, 1947.

SQUALL-LINE EXAMPLES

Long-range radar is a valuable instrument for studying squall-line details inasmuch as it permits continuous observations of lines which cannot otherwise be observed. Its wide areal coverage permits presentation of details and variations of lines which extend over a considerable area, and these details are not obscured by surrounding low clouds.

During the Ohio operations of the Thunderstorm Project, motion picture records were made of the echoes presented on the long-range radar 'scope over long periods of time. From these records, three sets of photographs (representing pictures taken at 15-minute intervals) have been selected for the purpose of showing some commonly observed characteristics of squall lines. The series of photographs for each of the three examples presented here (July 14, 1947; August 14, 1947; and September 5, 1947) is accompanied by a synoptic map, which shows the weather situation at the time the squall lines were present, and a reproduction of the upper-air sounding chart for a nearby raob station (figs. 214 through 224).

JULY 14, 1947
(*1245 E.S.T. to 1530 E.S.T.*)

The surface synoptic map at 1330 E.S.T. (fig. 214) shows a low-pressure area centered over northern Michigan. A cold front, oriented north-northeast to south-southwest and moving toward the east at 16 mi/hr, extended out of the low. Preceding it was a large zone of thunderstorm activity. As would be expected from the appearance of the map, many of the stations in the midwest reported thunderstorms. This widespread convective activity occurring in advance of the cold front was also indicated on the long-range radar 'scope (figs. 216 and 217).

Very little convective activity was detected by the radar at 1245 E.S.T., but by the time of the next photograph a large number of echoes had appeared on the 'scope. These echoes were primarily concentrated in two regions. One region is southeast of the radar site (represented by the white spot in the center of the pictures), where several well-defined echoes appear arranged in an elongated area oriented roughly northeast-southwest. By 1400 E.S.T. these echoes appear well-defined and form a rather poorly defined squall line. The second region is northwest of the radar site, where a linear arrangement of echoes is suggested. By 1400 E.S.T. the echoes in this line had grown and joined into one solid line of echo almost 100 mi. long, while scattered echoes appeared at either end of the line.

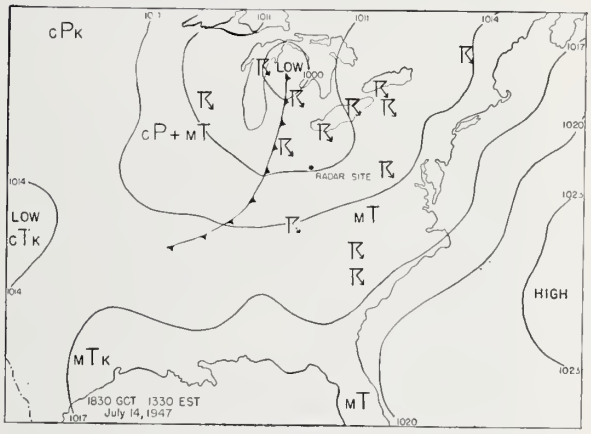

FIGURE 214.—Synoptic map for 1330 E.S.T., July 14, 1947.

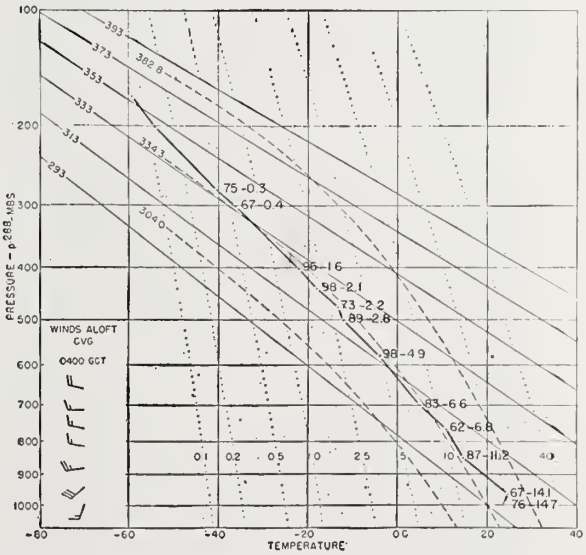

FIGURE 215.—Upper air sounding from Huntington, W. Va. for 0300 G.C.T., and winds-aloft observation from Covington, Ky. for 0400 G.C.T., July 14, 1947.

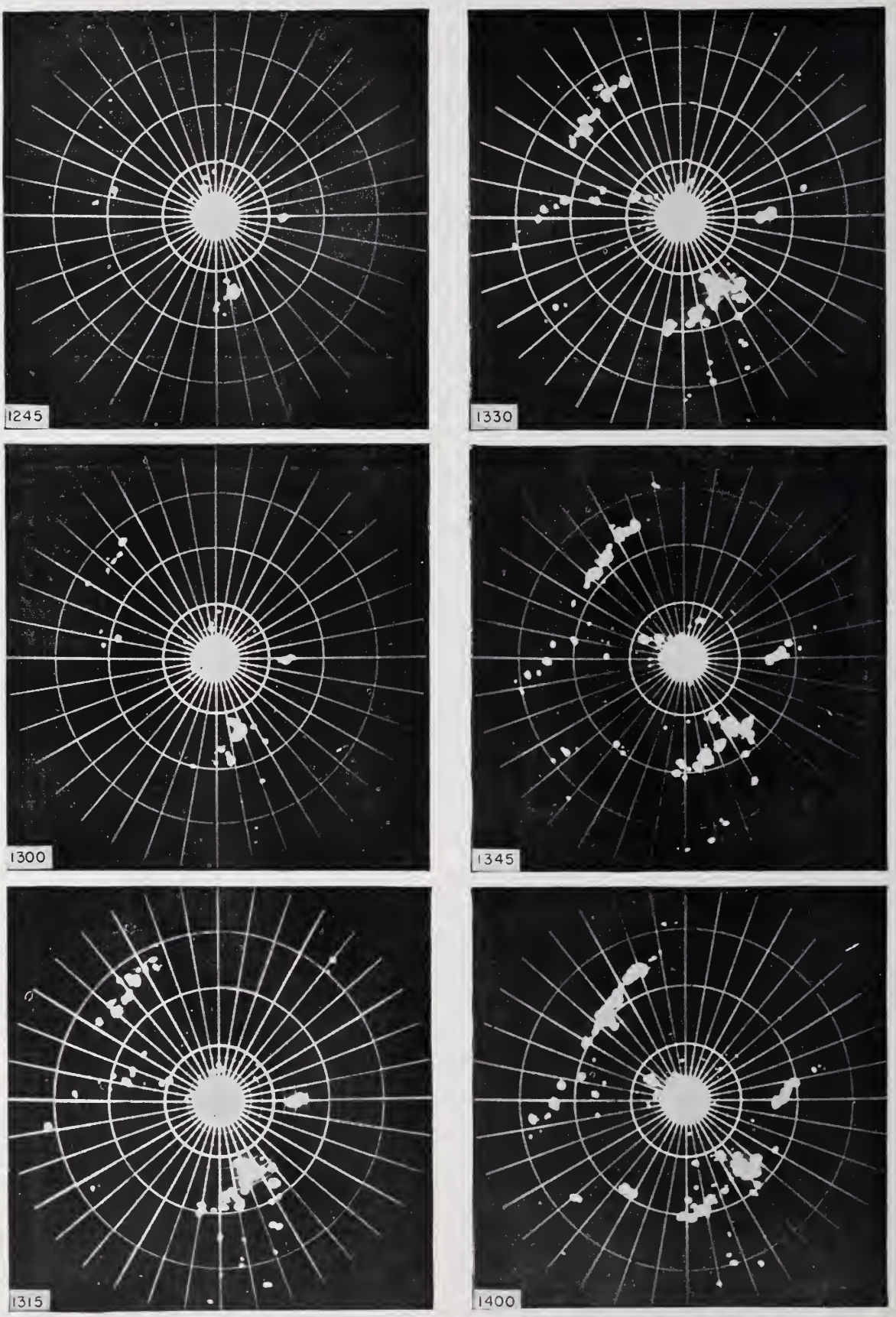

FIGURE 216.—Control-radar 200-mile-range PPI 'scope photographs, 1245–1400 E.S.T., July 14, 1947.

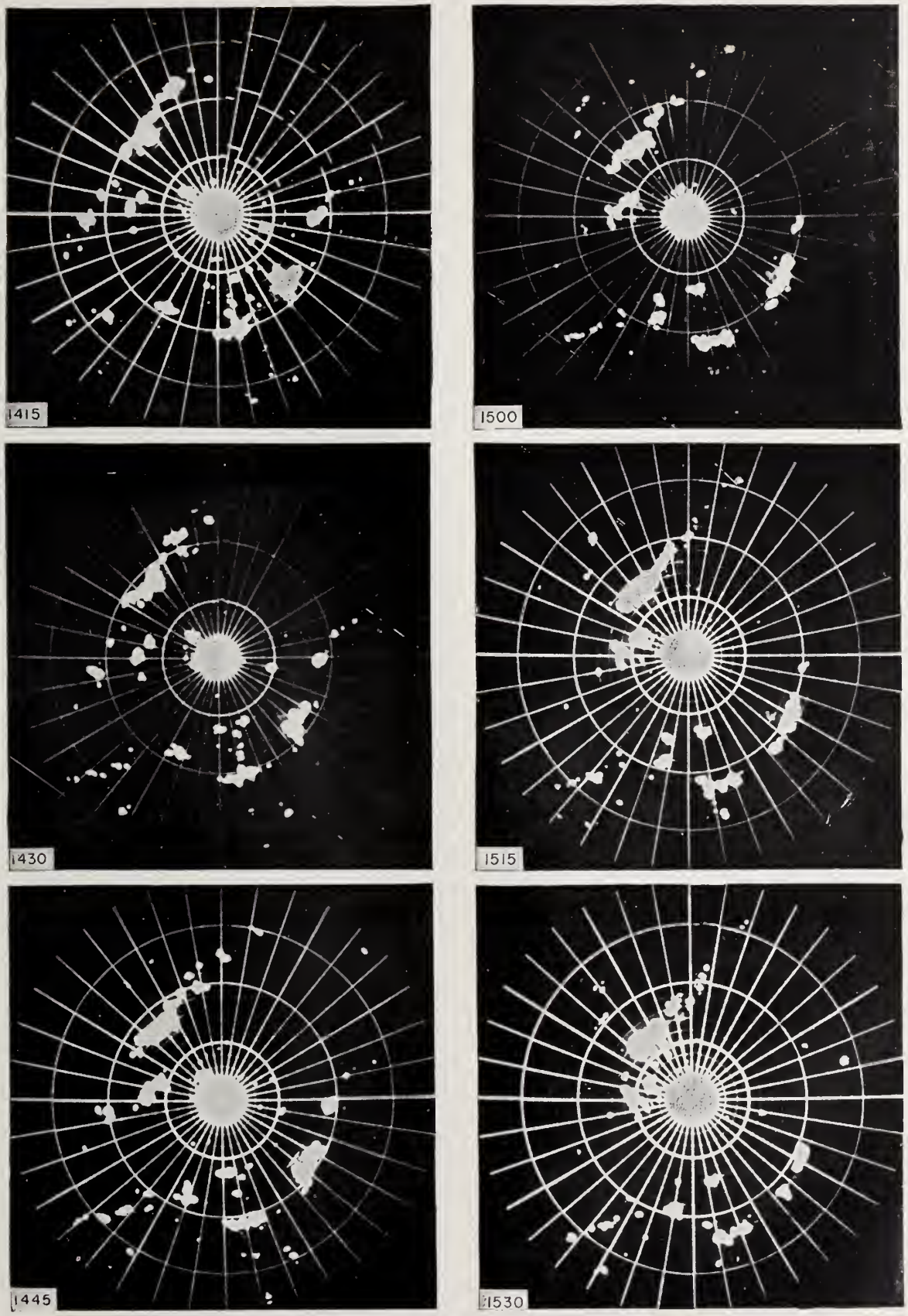

FIGURE 217.—Control-radar 200-mile-range PPI 'scope photographs, 1415–1530 E.S.T., July 14, 1947.

841051—50——17

The two squall lines were approximately parallel on the 'scope presentation. However, it is to be noted that they were oriented clockwise from the orientation of the front. The line to the northwest was 10° to 30° clockwise in orientation from the front; as a result, the squall line, at its northern extremity, was more than 100 mi. ahead of the front, while at its southern extremity it was almost on the front.

As may be seen from the photographs, the area between the squall lines was one of lesser convective activity, which is a typical condition for cases in which two parallel squall lines are spaced roughly about 50 to 200 mi. apart. This area may represent the region of "return settling" (see ch. I, sec. 1).

The entire zone of activity, comprised of both lines and the intervening area, is known as the squall-line zone (ch. VIII).

AUGUST 14, 1947
(*1102 E.S.T. to 1515 E.S.T.*)

On August 14, 1947, the weather in the vicinity of Wilmington, Ohio, was dominated by a pre-cold-frontal squall-line zone within which several lines of thunderstorms developed and dissipated[77]. The synoptic chart for 1330 E.S.T. (fig. 173) showed that a cold front, oriented northeast-southwest and moving southeastward at 18 mi/hr, was northwest of the radar site. At 1100 E.S.T., the cold front was located 220 mi. to the northwest and by 1515 E.S.T. the front had moved to within 145 mi. of the radar. The thunderstorms preceding this front were detected by the long-range radar. Figures 218 through 220 present photographs of the 200-mile 'scope taken at 15-minute intervals from 1102 E.S.T. to 1515 E.S.T. From them it can be seen that the thunderstorms formed in several lines which constantly changed in size and intensity.

At 1102 E.S.T. the echoes were so aligned that three relatively short, narrow lines could be identified. One was oriented from north to southwest of the radar site at a range of 50 to 100 mi.; another was northeast of the radar site at a range of 75 to 125 mi.; still another was east of the radar at a range of 100 to 200 mi. Between these lines were regions about 50 mi. in width which were almost completely devoid of echoes.

The definition of the two easterly lines became poorer after 1115 E.S.T. because new thunderstorms developed in the area between the lines and at the same time some of the original storms dissipated. It is to be realized that, at the greater ranges, the effects of the rain and range attenuation may also have caused some of the apparent dissipation of the lines. The westernmost line of echoes continued to develop rather slowly until about 1215 E.S.T., after which, rapid development of new echoes resulted in a well-defined line of intense echoes which reached a length of over 200 mi. by 1300 E.S.T. The extension of the line did not take place by a continual development of new thunderstorms at one end, but rather there appeared to be a simultaneous increase of the number and size of the radar clouds at many points along the line. By 1315 E.S.T. the development and grouping of thunderstorm echoes was such that they formed a separate line on either side of the intense line passing over the radar site. After 1400 E.S.T. there was considerable increase in the number of new thunderstorms, presumably as a result of the diurnal heating. The more or less random locations at which the new development occurred made delineation of individual lines difficult.

The orientation of the lines, as well as that of the zone into which most of the echoes fell, was roughly northeast-southwest, similar to that of the advancing cold front. The speed of movement of the lines was also generally the same as that of the cold front, i.e., towards the southeast.

An interesting feature of two of the squall lines was the tendency for the echoes to have a sinusoidal alignment. The group of echoes east of the radar site at 1102 E.S.T. can be seen to form a wave-shaped pattern with a wave length of about 130 mi. At 1245 E.S.T. the line of echoes closest to the radar site also exhibited a sinusoidal pattern. In this instance, the wave length was about 110 mi. The wave shape of this line was most evident at the time of first formation of the echoes making up the line; as the diurnal increase of convection became effective, the wave pattern was obscured.

[77] The synoptic map and upper-air sounding chart for August 14, 1947, are with the detailed analysis of the airplane and surface data for a storm observed on this day, which were presented in an earlier Example (figs. 173 and 175).

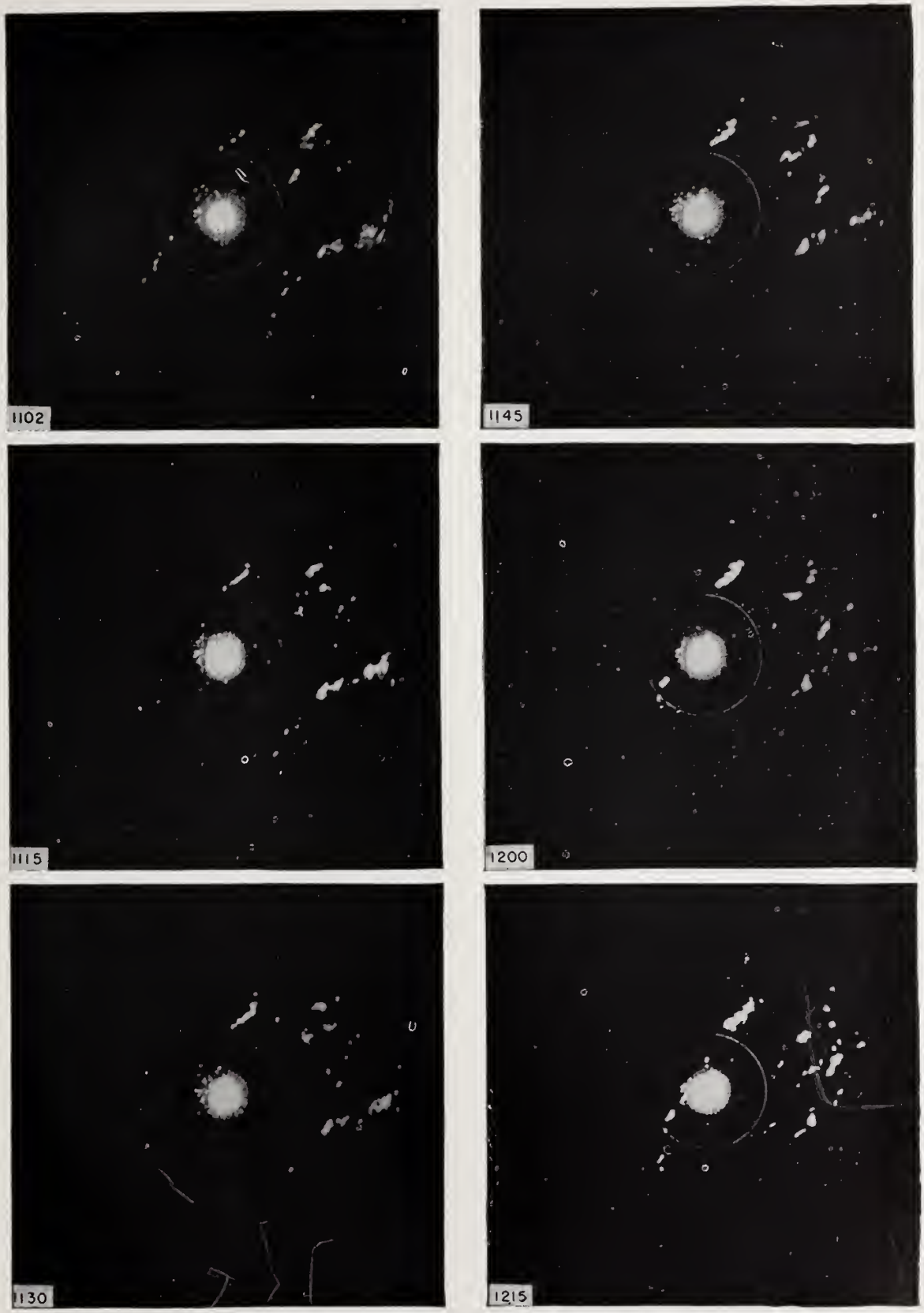

FIGURE 218.—Control-radar 200-mile-range PPI 'scope photographs, 1102-1215 E.S.T., August 14, 1947.

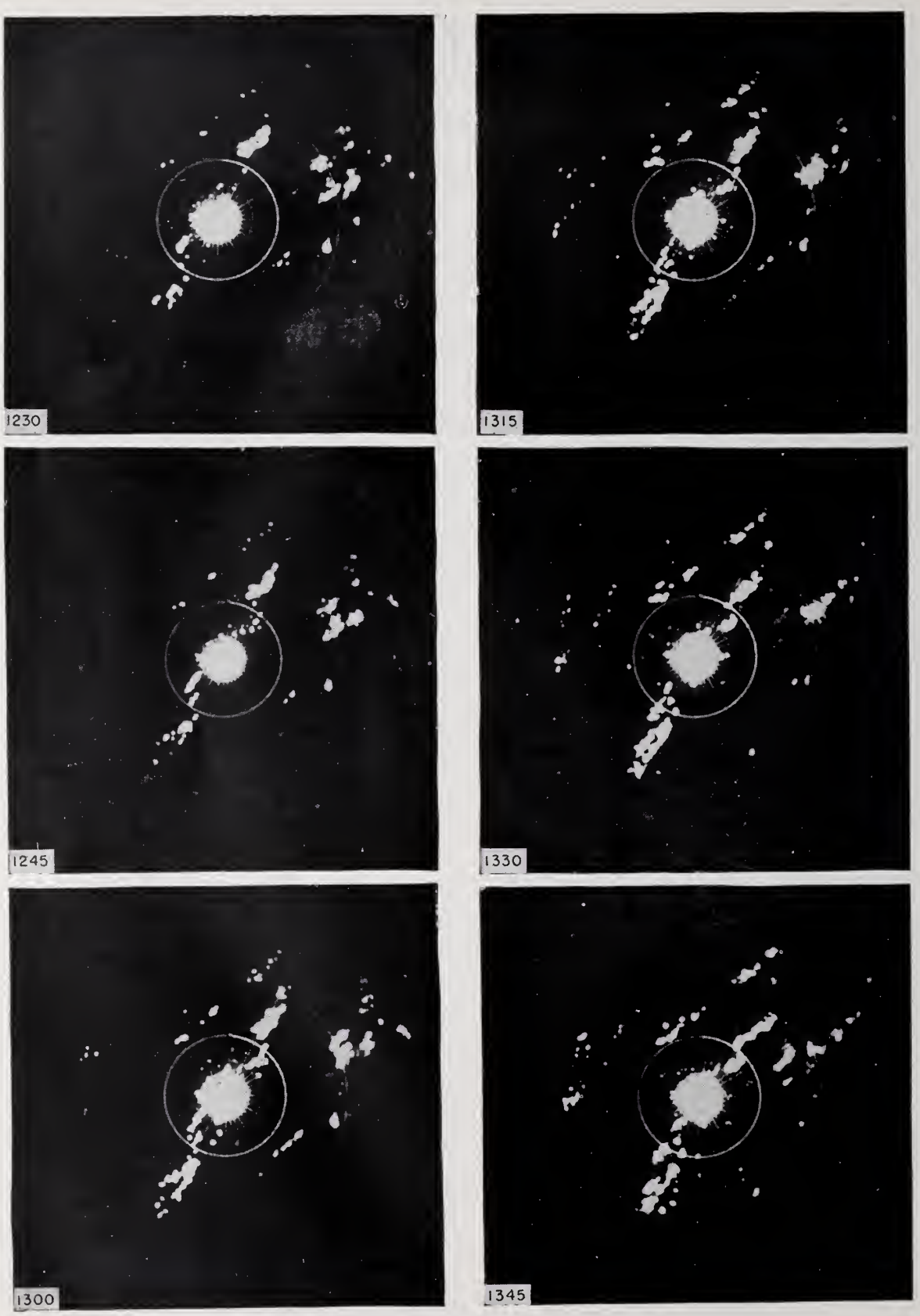

FIGURE 219.—Control-radar 200-mile-range PPI 'scope photographs, 1230–1345 E.S.T., August 14, 1947.

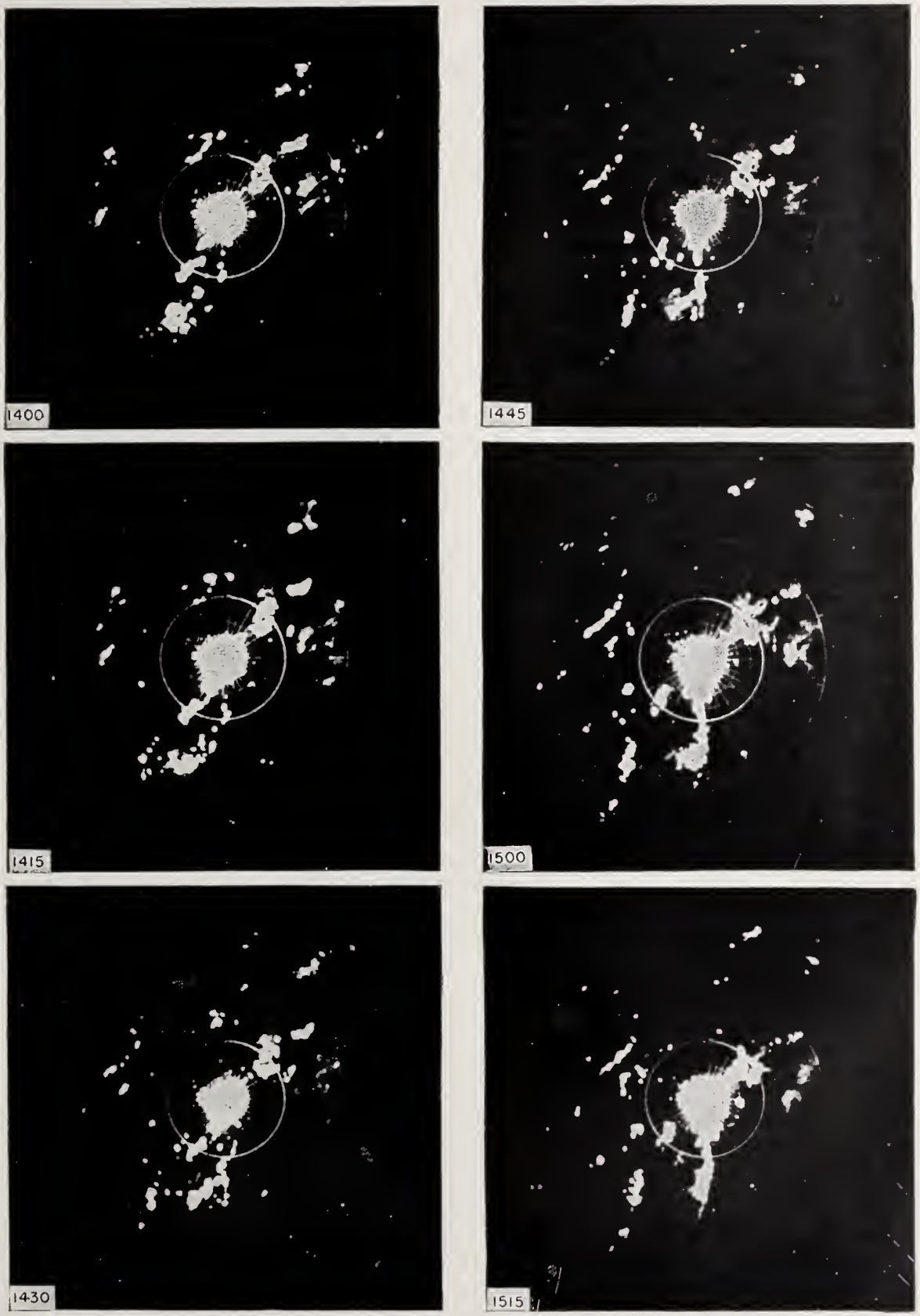

FIGURE 220.—Control-radar 200-mile-range PPI 'scope photographs, 1400–1515 E.S.T., August 14, 1947.

SEPTEMBER 5, 1947
(1200 E.S.T. to 1444 E.S.T.)

The surface synoptic chart at 1330 E.S.T. (fig. 221) on this date shows a closed low center located in northern Indiana. The warm-front part of the cyclone extended almost directly over the radar site, while the cold front, having a northeast-to-southwest orientation was located about 100 mi. to the west of the radar site. Over the period 1030 to 1330 E.S.T. the speed of the cold front was about 20 mi/hr toward the east.

The photographs of the 200-mile radar 'scope. given in figures 223 and 224, cover the period from 1200 to 1444 E.S.T. It can be seen that prior to 1230 E.S.T. there was a large echo to the southeast of the station with some small scattered echoes east of it. This echo appears to have been associated with precipitation from stratified-type clouds produced by lifting over the warm front. Some smaller convective echoes which started developing southwest of the station formed in a line about 90 mi. long by 1244 E.S.T. The sharpness of their outlines and the brightness of them indicate that they resulted from thunderstorms.

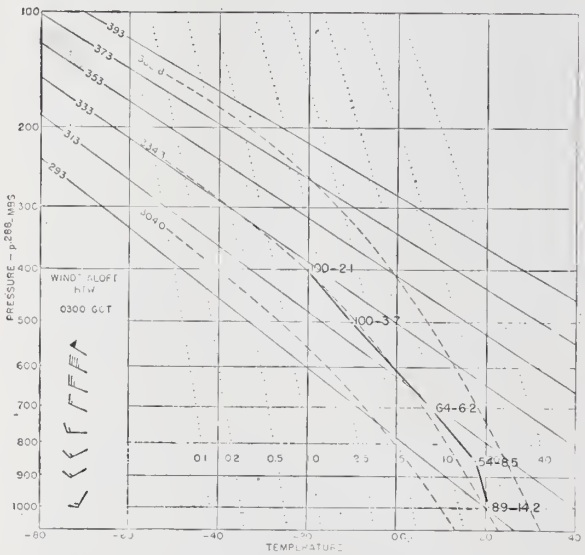

FIGURE 222.—Upper air sounding and winds-aloft observation from Huntington, W. Va. for 0300 G.C.T., September 5, 1947.

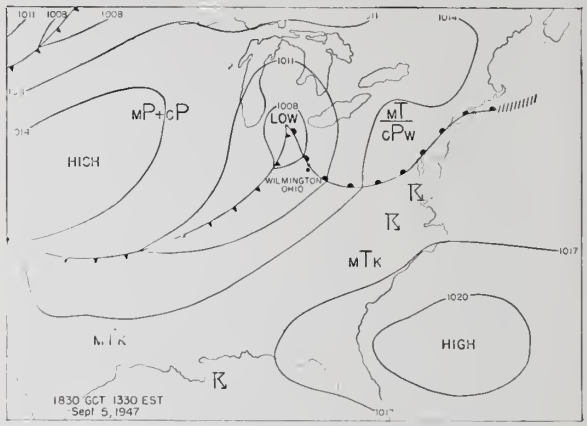

FIGURE 221.—Synoptic map for 1330 E.S.T., September 5, 1947.

This line of thunderstorms became stronger and more evident as the warm-front precipitation moved toward the east.

This line of thunderstorms was apparently associated with the cold front. The orientation was somewhat clockwise from that of the northern part of the front. The eastern extremity of the line of echoes extended over the warm-frontal surface and made a large angle with the surface front. In all probability. the thunderstorms forming this section of the line had relatively high bases. The development of a line of storms extending over the front and having such an orientation relative to it would lead to the belief that the explanation for its formation lies in a high-level dynamic process, probably connected in some way with the cold front.

By 1400 E.S.T. the length of the line had increased to about 150 mi. and the width was 20 to 25 mi. This is an excellent example of a continuous line of thunderstorms with no apparent breaks. After 1400 E.S.T., the movement and dissipation of individual thunderstorms of the squall line resulted in a distortion of its shape. Dissipation of the line continued until the termination of the radar operation at 1542 E.S.T. As the line dissipated, it was noted that the section north of the warm front dissipated first and most rapidly.

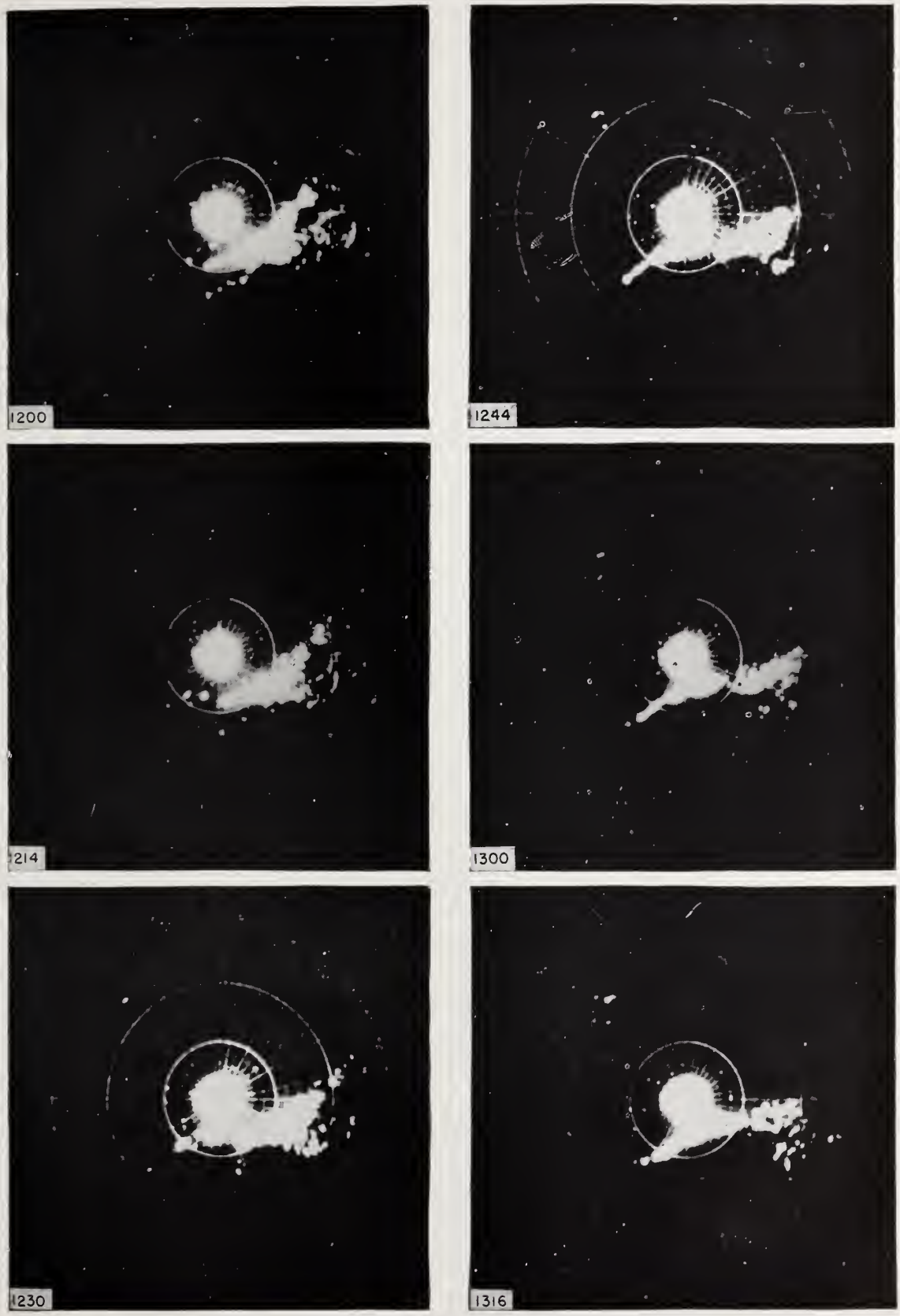

FIGURE 223.—Control-radar 200-mile-range PPI 'scope photographs, 1200–1316 E.S.T., September 5, 1947.

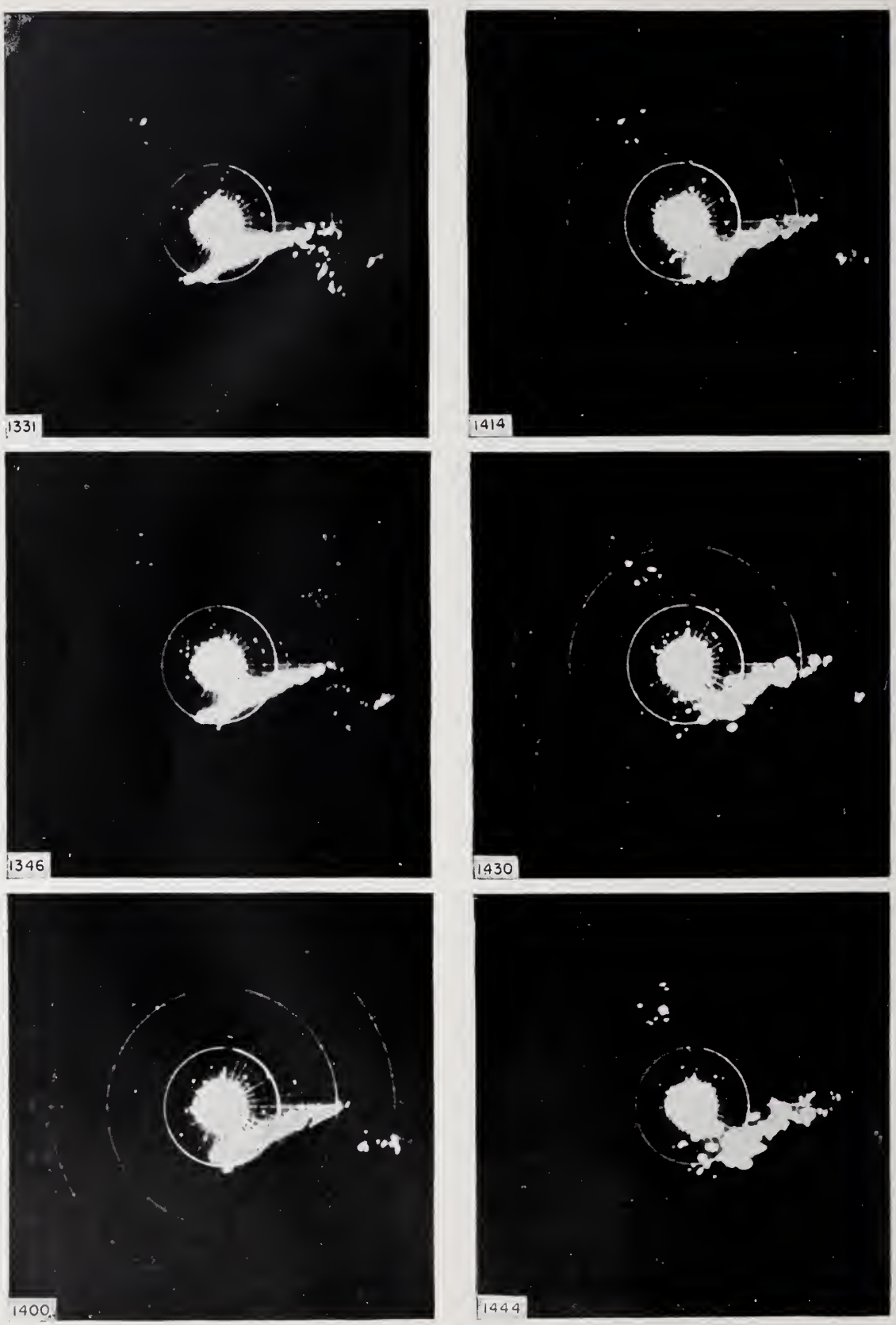

FIGURE 224.—Control-radar 200-mile-range PPI 'scope photographs, 1331-1444 E.S.T., September 5, 1947.

REFERENCES

1. American Instrument Co., *Instructions for TS-551 (XN-1) Electric Field Meter* (designed by Physics Special Research Division, Naval Research Laboratory, Washington, D. C.), A1019A, A Edition, Silver Spring, Md., October 1946.
2. Army-Navy Precipitation-Static Project, Report No. I: "The Precipitation-Static Interference Problem and Methods for its Investigation"; Report II: "Aircraft Instrumentation for Precipitation-Static Research"; and Report III: "Electrification of Aircraft Flying in Precipitation Areas," *Proceedings of the Institute of Radio Engineers*, vol. 34, April 1946.
3. Atlas, David, "Preliminary Report on New Techniques in Quantitative Radar Analysis of Rainstorms" (Pt. I); and "Some Experimental Results of Quantitative Radar Analysis of Rainstorms" (Pt. II). Air Materiel Command Memorandum Report AWNW 7–4 (restricted), Wright Field, Dayton, Ohio, October 1947 and May 1948. (Distribution is restricted to military use only.)
4. Austin, J. M., "A Note on Cumulus Growth in a Nonsaturated Environment," *Journal of Meteorology*, vol. 5, No. 3, June 1948, pp. 103–107.
5. Barrett, E. W., and Riehl, H., "Experimental Verification of Entrainment of Air into Cumulus," *Journal of Meteorology*, vol. 5, No. 6, December 1948, pp. 304–307.
6. Bellamy, J. C., "Objective Calculations of Divergence, Vertical Velocity and Vorticity," *Bulletin of the American Meteorological Society*, vol. 30, No. 2, February 1949, pp. 45–49.
7. Bénard, Henri, "Les Tourbillons Cellulaires dans une Nappe Liquide Transportant de la Chaleur par Convection en Régime Permanent," *Annales de Chimie et de Physique*, Paris, 7 Série, Tome XXIII, 1901, pp. 62–144.
8. Braham, R. R., Jr., and Pope, Capt. F. W., "Further Studies of Thunderstorm Conditions Affecting Flight Operations: Turbulence," *Air Weather Service Technical Report 105–39*, Washington, D. C., March 1949.
9. Brancato, G. N., *The Meteorological Behavior and Characteristics of Thunderstorms*, U. S. Weather Bureau Hydrometeorological Section, Washington, D. C., 1942.
10. Brooks, C. F., "The Local, or Heat, Thunderstorm," *Monthly Weather Review*, vol. 50, No. 6, June 1922, pp. 281–287.
11. Brooks, Herbert R., "A Summary of Some Radar Thunderstorm Observations," *Bulletin of the American Meteorological Society*, vol. 27, No. 10, December 1946, pp. 557–563.
12. Brunk, Ivan W., "Pressure Pulsations of April 11, 1944," *Journal of Meteorology*, vol. 6, No. 3, June 1949, pp. 171-178.
13. Brunt, D., "Natural and Artificial Clouds," *Quarterly Journal of the Royal Meteorological Society*, vol. 63, No. 271, July 1937, pp. 277-288.
14. Buell, C. E., "The Determination of Vertical Velocities in Thunderstorms," *Bulletin of the American Meteorological Society*, vol. 24, No. 3, March 1943, pp. 94–95.
15. Byers, H. R., "Atmospheric Turbulence and the Wind Structure near the Surface of the Earth," ch. XXIV, in *General Meteorology*, McGraw-Hill Book Co., Inc., New York, 1944.
16. Byers, H. R., "Nonfrontal Thunderstorms," *Miscellaneous Report No. 3*, University of Chicago Press, Chicago, Ill., June 1942.
17. Byers, H. R., and Braham, R. R., "Thunderstorm Structure and Circulation," *Journal of Meteorology*, vol. 5, No. 3, June 1948, pp. 71–86.
18. Byers, H. R., and collaborators, "The Use of Radar in Determining the Amount of Rain Falling over a Small Area," *Transactions of the American Geophysical Union*, vol. 29, No. 2, April 1948, pp. 187–196.
19. Byers, H. R., and Hull, E. C., "Inflow Patterns of Thunderstorms as Shown by Winds Aloft," *Bulletin* of the American Meteorological Society, vol. 30, No. 3, March 1949, pp. 90-96.

20. Byers, H. R., Moses, H., and Harney, P. J., "Measurement of Rain Temperature," *Journal of Meteorology*, vol. 6, No. 1, February 1949, pp. 51–55.

21. Byers, H. R., and Rodebush, H. R., "Causes of Thunderstorms of the Florida Peninsula," *Journal of Meteorology*, vol. 5, No. 6, December 1948, pp. 275–280.

22. Chandra, Krishna, "Instability of Fluids Heated from Below," *Proceedings of the Royal Society of London*, Series A, vol. 164, No. A 917, January 1938, pp. 231–242.

23. Cunningham, R. M., and Miller, R. W., "Five Weather Radar Flights: Measurements and Analysis," *Technical Report No. 7, Weather Radar Research*, Department of Meteorology, Massachusetts Institute of Technology, December 1948, p. 12.

24. Elster, J., and Geitel, H., "Bemerkungen über den electrischen Vorgang in den Gewitterwolken," (IX), *Annalen der Physik und Chemie*, Folge 3, Band 25, 1885, S. 116–120; and "Über die Electricitätsentwickelung bei der Regenbildung," (X) *Annalen der Physik und Chemie*, Folge 3, Band 25, 1885, S. 121–131.

25. Graham, A., "Shear Patterns in an Unstable Layer of Air," *Philosophical Transactions of the Royal Society*, Series A, vol. 232, 1934, pp. 285–296.

26. Gunn, R., "The Electric Charge on Precipitation at Various Altitudes and Its Relation to Thunderstorms," *The Physical Review*, vol. 71, No. 3, February 1, 1947, pp. 181–186.

27. Gunn, R., "Electric Field Intensity Inside Natural Clouds," *Journal of Applied Physics*, vol. 19, No. 5, May 1948, p. 481.

28. Harrison, H. T., and Orendorff, W. K., "Pre-Coldfrontal Squall Lines," United Air Lines Meteorology Department *Circular No. 16*, March 1, 1941.

29. Harrison, L. P., "Lightning Discharges to Aircraft and Associated Meteorological Conditions," National Advisory Committee for Aeronautics *Technical Note No. 1001*, Washington, D. C., May 1946.

30. Holford, J. F., and Morris, D. E., "An Interim Report on High Altitude Gust Investigation," *Report No. AERO 2235*, Royal Aircraft Establishment, 1947.

31. Humphreys, W. J., *Physics of the Air*, 3d edition, McGraw-Hill Book Co., Inc., New York, 1940, pp. 357–359.

32. Koschmieder, Harald, "Über Boën," *Meteorologische Zeitschrift*, Band 61, Heft 7, July 1944, S. 244–247.

33. Langille, R. C., Gunn, K.L.S., and Palmer, W. M., *Quantitative Analysis of Vertical Structure in Precipitation*, Department of National Defense, Defense Research Board, Canada, 1948.

34. Lenard, P. "Zur Wasserfalltheorie der Gewitter," *Annalen der Physik*, Folge 4, Band 65, 1921, S. 629–639.

35. Levine, J., "The Effect of Vertical Accelerations on Pressure during Thunderstorms," *Bulletin of the American Meteorological Society*, vol. 23, No. 2, February 1942, pp. 52–61.

36. Mal, Sobhag, "Forms of Stratified Clouds," *Beitrage zur Physik der freien Atmosphäre*, Band 17, Heft 1, Leipzig, 1931, S. 40.

37. Mal, Sobhag, and Rao, Y. P., "Effect of Vertical Acceleration on Pressure during Thunderstorms," *Quarterly Journal of the Royal Meteorological Society*, vol. 71, Nos. 309–310, July–October 1945, pp. 419–421.

38. Malkus, J. S., "Effects of Wind Shear on Some Aspects of Convection," *Transactions of the American Geophysical Union*, vol. 30, No. 1, February 1949, pp. 19–25.

39. Normand, Sir Charles, "Energy in the Atmosphere," *Quarterly Journal of the Royal Meteorological Society*, vol. 72, Nos. 312–313, April–July 1946, pp. 145–149.

40. Phillips, A. C., and Walker, G. T., "The Forms of Stratified Clouds," *Quarterly Journal of the Royal Meteorological Society*, vol. 58, No. 243, January 1932, p. 23.

41. Press, H., "A Statistical Analysis of Gust-Velocity Measurements as Affected by Pilots and Airplanes," National Advisory Committee for Aeronautics *Technical Note No. 1645*, Washington, D. C., June 1948.

42. Press, H., and Binckley, E. T., "A Preliminary Evaluation of the Use of Ground Radar for the Avoidance of Turbulent Clouds," National Advisory Committee for Aeronautics *Technical Note No. 1684*, Washington, D. C., September 1948.

43. Reynolds, S. E., and Workman, E. J., "I: Thunderstorm Observations," *Progress Report No. 4*, Research and Development Division, New Mexico School of Mines, 1947.

44. Rhode, R. V., "Gust Loads on Airplanes," *Journal of the Society of Automotive Engineers*, vol. 40, No. 3, 1947, pp. 81–88.

45. Rhode, R. V., and Donely, P., "Frequency of Occurrence of Atmospheric Gusts and of Related Loads in Airplane Structures," National Advisory Committee for Aeronautics *Advance Restricted Report No. L4I21*, November 1944.

46. Riehl, H., "Subtropical Flow Patterns in Summer," University of Chicago *Miscellaneous Report No. 22*, The University of Chicago Press, Chicago, Ill., 1947.

47. Ryde, J. W., "The Attenuation and Radar Echoes Produced at Centimetre Wave-Lengths by Various Meteorological Phenomena," in *Meteorological Factors in Radio-Wave Propagation*, Physical Society, London, 1946, pp. 169–188.

48. Schaffer, W., "The Thunderstorm High," *Bulletin of the American Meteorological Society*, vol. 28, No. 8, October 1947, pp. 351–355.

49. Schmidt, F. H., "Some Speculations on the Resistance to the Motion of Cumuliform Clouds," *Mededelingen en Verhandelingen*, Series B, Deel 1, No. 8, 1947 (published by Koninklijk Nederlands Meterologisch Institut, DeBilt, Netherland, No. 125).

50. Simpson, G. C., "On the Electricity of Rain and its Origin in Thunderstorms," *Philosophical Transactions of the Royal Society*, Series A, vol. 209, 1909, pp. 379–413.

51. Simpson, G. C., and Robinson, G. D., "The Distribution of Electricity in Thunderclouds, II," *Proceedings of the Royal Society of London*, vol. 177, No. A 970, February 1941, pp. 281–329.

52. Simpson, G. C., and Scrase, F. J., "Distribution of Electricity in Thunder Clouds," *Proceedings of the Royal Society of London*, Series A, vol. 161, No. A 906, August 1937, pp. 309–352.

53. Stommel, H., "A Summary of the Theory of Convective Cells," *Annals of the New York Academy of Sciences*, vol. 48, art. 8, September 1947, pp. 715–726.

54. Stommel, H., "Entraining of Air into a Cumulus Cloud," ***Journal of Meteorology***, vol. 4, No. 3, June 1947, pp. 91–94.

55. U. S. Weather Bureau, "Thunderstorm Rainfall," ***Hydrometeorological Report No. 5***, Waterways Experiment Station, Vicksburg, Miss., 1947.

56. U. S. Weather Bureau, "A Report on Thunderstorm Conditions Affecting Flight Operations," *Technical Paper No. 7*, Washington, D. C., April 1948.

57. Veryard, R. G., "Some Observations on the Thermal Structure of Cumuliform Clouds," *India Meteorological Department Scientific Notes*, vol. 6, No. 64, 1935, pp. 87–112.

58. von Ficker, H., "Über die Entstehung lokaler Warmegewitter," 1 Mitteilung, *Sitzungsberichte* der Preussischen Akademie der Wissenschaften, Physikalisch-Mathematische Klasse, Berlin, 1931, S. 28–39.

59. Weber, E. H., "Mikroskopische Beobachtungen sehr gesetzmässiger Bewegungen, welche die Bildung von niederschlägen harziger Körper aus Weingeist begleiten," *Annalen der Physik und Chemie*, Leipzig, Band 94, 1855, S. 452.

60. Wenzel, W., "Zur Frage der Temperatur in Cumulus-Wolken," *Meteorologische Zeitschrift*, Band 50, Heft 2, February 1933, S. 65.

61. Wexler, R., and Swingle, D. M., "Radar Storm Detection," *Bulletin of the American Meteorological Society*, vol. 28, No. 4, April 1947, pp. 159–167.

62. Williams, D. T., "A Surface Micro Study of Squall-Line Thunderstorms," *Monthly Weather Review*, vol. 76, No. 11, November 1948, pp. 239–246.

63. Workman, E. J., Holzer, R. E., and Pelsor, G. T., "The Electrical Structure of Thunderstorms," National Advisory Committee for Aeronautics *Technical Note No. 864*, Washington, D. C., 1942, p. 26.

APPENDIX

APPENDIX

1. Surface Instruments

A. FLORIDA, 1946

The surface network in Florida consisted of 55 recording stations, each equipped to measure wind speed and direction, temperature, pressure, relative humidity, and rainfall. All of the instruments recorded on open-scale charts capable of time resolutions of 1 min. The stations were attended once daily by Weather Bureau observers traveling in jeeps.

A photograph of a typical station showing the relative location of the equipment is presented in figure 225. The standard "Cotton-Region" instrument shelter was used for the hygrothermograph. A small air space separated the shelter from the wooden box or cupboard on which it was mounted. This box housed the microbarograph, the wind recorders, and a battery. The Fergusson-type weighing rain gage stood at a suitable distance nearby. In the following paragraphs a description is given of the instruments used for measuring each of the meteorological elements.

Wind instruments.—Most of the stations in the network were equipped with the well-known contacting cup and vane type of wind instrument mounted on an 18-foot pole. Every time one nautical mile of air passed the anemometer cups, a relay closed and a mark was made on the double-register record. Once each minute the wind direction was recorded to 8 points of the compass through contacts to the four printing arms, one for each cardinal direction. Wind directions between the cardinal directions were recorded by the simultaneous printing of two of the arms. Current for the double-register recorder drum was obtained from a 6-volt storage battery, which was replaced and recharged every 2 or 3 weeks to insure satisfactory operation of the equipment. The drum made one revolution in 6 hr.

It had been hoped to replace the mile-counting wind instruments by gust-recording equipment before the Florida season was over, but only 14 such installa-

FIGURE 225.—A photograph of a typical surface station showing the relative locations of the instruments.

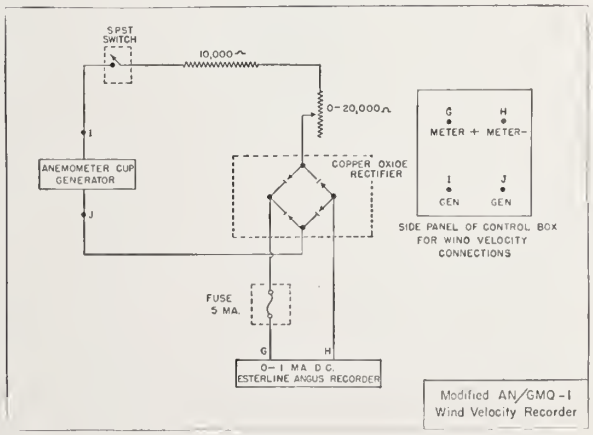

FIGURE 226.—A schematic diagram showing the circuit of the modified AN/GMQ-1 wind-velocity recording equipment used by the Project.

tions were completed due to their late delivery. These instruments were wartime Army Wind Equipment AN/GMQ–1, modified as recording instruments by Mr. Harry Moses of the Thunderstorm Project. In normal operation wind speed was measured by using a 3-cup anemometer which drove a small a.c. generator, whose output was rectified and measured by an indicating 0–1 milliampere meter. The following modifications were made to permit automatic recording and to improve the utility of the equipment for the measurement of wind speeds within the expected range (see fig. 226):

1. The indicating meter was replaced by a 0–1 milliampere Esterline-Angus Recorder.

2. The equipment was adjusted to record a range of from zero to 75 mi/hr by replacing the fixed, dropping resistor with a fixed 10,000-ohm resistor and a 20,000-ohm locking potentiometer.

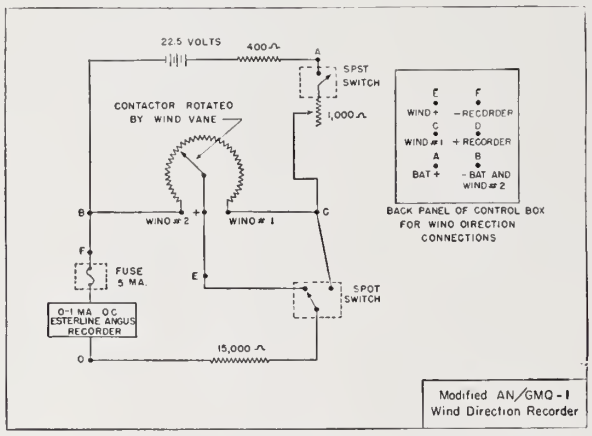

FIGURE 227.—A schematic diagram showing the circuit of the modified AN/GMQ–1 wind-direction recording equipment used by the Project.

Originally the AN/GMQ–1 equipment measured the wind direction by means of a self-synchronizing arrangement. Two movable contacts, actuated by the wind vane, moved on a continuously wound toroidal resistor tapped in three places 120° apart. The position of the wind vane was indicated by a repeater meter consisting of a stator and rotor which were encased in a copper cylinder to shield them from external magnetic effects. The stator consisted of three identical coils in a delta connection; the rotor was a small bar-type permanent magnet mounted on a shaft supported by jewel bearings.

In order to obtain a continuous record of wind direction, several modifications were necessary; the continuously wound resistor of the direction transmitter was broken at one point and one of the two moving contactors was removed so that a potentiometer arrangement resulted. Figure 227 presents a schematic diagram of the wind direction apparatus after the modifications were completed. A potential of 22.5 volts was placed across a series combination of the potentiometer, a fixed 400-ohm resistor, and a 1,000-ohm variable resistor. Since the wind vane was connected to the movable contactor, the potential difference from one end of the circular resistor to the contactor was a function of the positions of the wind vane. The potential difference was continuously measured and recorded by means of a 0–1 milliampere Esterline-Angus Recorder used as a voltmeter with a sensitivity of 1,000 ohms per volt. One weakness of this system was that whenever the contactor moved over the break in the resistor the indicated potential difference jumped from a maximum to zero. To minimize this effect, the break was placed in the position corresponding to the least frequent wind direction. In actual operation this was not found to be a serious weakness.

Temperature and relative humidity.—The measurements of these elements were made using the hygrothermograph, Type 594[78]. This instrument used a Bourdon tube filled with alcohol for measuring temperature and a hair hygrometer for measuring relative humidity. The instrument was fitted with 12-hour gears so that the drum made two revolutions in 24 hr. It was found that overlapping of the traces on one record sheet was not a serious problem, since normal diurnal variations of temperature and relative humidity resulted in sufficiently large differences during two succeeding 12-hour periods to keep the traces distinct. The calibration of the instruments was checked daily with the readings of a sling psychrometer.

Pressure.—Measurements of pressure were made with the microbarograph, Type 790, an instrument similar to the one used at many stations of the U. S. Weather Bureau. It has a double sylphon bellows as the pressure-sensitive element and uses a mechanical linkage system to magnify small displacements of the bellows. The microbarograph was the most unsatisfactory of the surface instruments, chiefly because of its lack of sensitivity. The instrument was fitted with 12-hour gears so that the drum made two revolutions in 24 hr. In general, the pressure changes during the day were such that it was usually not difficult to differentiate between the two traces on the chart. The calibration of the instrument was checked weekly with readings from an aneroid barometer.

Precipitation.—Measurements of rainfall were made using the Fergusson weighing-type rain gage, Type 775. The area of the standard 8-inch intake opening was enlarged 2½ times to increase the instrument's sensitivity. The operation of the rain gage is such that the recorder pen makes an upward and downward traverse across the chart as the water is accumulated

[78] The equipment was manufactured by the Friez Instrument Division of Bendix Aviation Corporation. Any modifications deemed necessary were performed by personnel of the Thunderstorm Project.

in the catch bucket. With the enlarged intake area, one complete traverse corresponded to an accumulation of 2.4 in. The instrument was modified to provide four revolutions of the drum in one 24-hour period. The nature of the traces during rain periods was such that there was very little difficulty in distinguishing all four. The minimum rainfall accumulation which could be resolved by the equipment was about 0.01 in.

Dew point.—The University of Chicago electronic dew-point indicator was used in conjunction with the Speedomax Recorder to obtain continuous records of dew-point temperature. Equipment was installed at station 26 during July 1946, but its use had to be discontinued because of the lack of maintenance personnel.

B. OHIO, 1947

The network of surface stations in Ohio consisted of 55 autographic weather stations distributed within a more or less rectangular area with 8 additional stations outside the rectangular area (fig. 11). These exterior stations were primarily sites for equipment used for obtaining upper-air data; however, all of them were also equipped for making meteorological measurements at the surface. As in Florida, all the data were recorded on open-scale charts which were changed daily by Weather Bureau observers. The observer's duties were the same as those performed in Florida, i.e., the inspection and adjustment of the equipment and the check of the calibration of all instruments and chronographs.

The instruments utilized for measuring and recording pressure, temperature, relative humidity, and precipitation were the same as those used in Florida. However, kerosene replaced the original dash-pot fluid in the microbarographs, resulting in improved operation. The wind observations at interior stations were made with the modified AN/GMQ-1 equipment which gave nearly instantaneous and continuous measurements. The exterior stations were equipped with the contact-type double-register equipment. The Esterline-Angus Recorders, employed in conjunction with the modified AN/GMQ-1 equipment, operated with a paper speed of 6 in/hr. This was a 50 percent reduction from that used in Florida but proved highly satisfactory and reduced the volume of records.

Several other instruments utilized during the Ohio observational season which were not available in Florida are described below. The more unfamiliar ones and those designed by Project personnel are discussed more fully than the standard meteorological equipment. References are given wherever possible to permit acquisition of additional details if desirable.

Rain temperature.—Data on rain temperature were obtained using an instrument designed by Mr. Harry Moses of the Thunderstorm Project. Rain was collected in a thin aluminum funnel (A), mounted on a wooden stand 3 ft. high (fig. 228). A small ceramic resistor (B), ½ in. long and 1/32 in. in diameter, was mounted on a wire frame at the apex of the funnel and was shielded from the sun by an aluminum cone (C). During moderate to heavy rain, water accumulated only up to the level of the overflow hole (D), which was about ⅛ in. above the temperature element. The hole (E) at the apex led to a capillary leak arrangement made from rubber tubing and an adjustable pinch clamp. The leakage outflow rate was set at approximately ⅓ cm^3/sec, in order to measure the temperature of the water surrounding the thermistor element within 10 sec. after it entered the funnel. A photograph of the instrument is presented in figure 229.

The ceramic resistor is made of the same material as the temperature elements of the radiosondes currently being used in this country. It has a large negative temperature coefficient, approximately 600 ohms per centigrade degree in the operating range, but the relationship is sufficiently non-linear to necessitate a careful calibration before use. Once calibrated, most resistors held their calibration to within 0.5° C. for weeks or even months.

Since the temperature element had to be continually immersed in water, it was necessary to completely insulate the resistor so that the parallel resistance

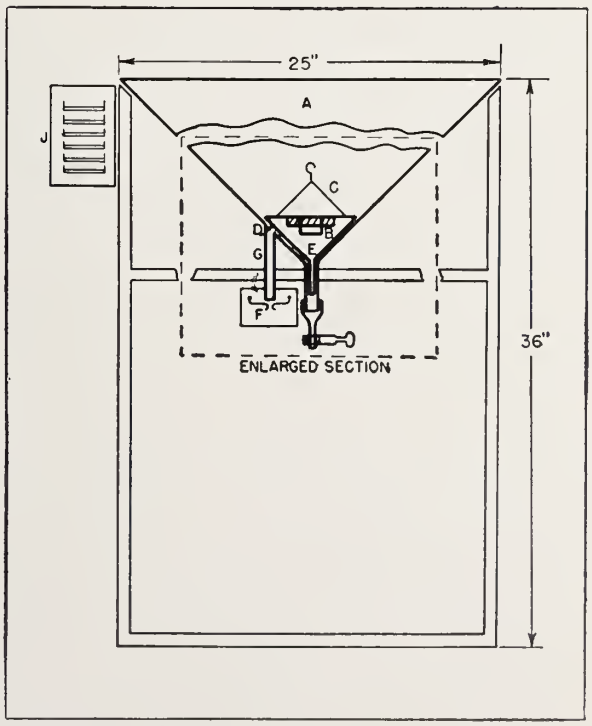

FIGURE 228.—A schematic diagram of the instrument used for measuring rain temperature. Details are given in the text.

FIGURE 229.—A photograph of the instrument for measuring rain temperature.

path through the water from one lead to the other, or to ground, was at least 1 to 2 megohms. After trying a number of substances, it was found that four or five applications of Glyptal No. 1201[79], followed by baking at 125° C. for 2 hr. after each coat, provided satisfactory insulation. Before the first painting it was necessary to carefully eliminate all sharp edges, since insulation breakdowns are more apt to occur at such points. Although the coats of Glyptal increased the lag of the ceramic resistor, the lag coefficient, or time-lag constant, was still less than 1 sec., a value more than sufficiently sensitive for the measurements which were made.

Measurements of the ambient air temperature were made essentially simultaneously with the measurements of rain temperature. A small thermoscreen (J in fig. 228), housing a second ceramic resistor, was mounted on the funnel stand. The element was always dry and consequently did not have to be insulated. At the time that measurements were being made, the wind speed was usually sufficiently high to provide the necessary ventilation.

The resistance, and consequently the temperature, of both thermal elements was measured by a vacuum tube ohmmeter and recorded by a 0–5 milliampere Esterline-Angus Recorder used in place of the usual indicating milliammeter. A motor-driven switch alternately introduced the rain and air resistors into the measuring circuit every 30 sec. The vacuum-tube ohmmeter was of the same type used for air temperature measurements by airplanes, with some minor modifications. The circuit diagram (fig. 230) shows that the basic element of the ohmmeter is a bridge circuit. It may be seen that changes in the resistance of the temperature resistors varies the grid bias of V_1 and consequently causes a change in the plate current of this tube. The resulting change in potential across the bridge, from points A to B, is recorded on the Esterline-Angus Recorder. In the operating range the relationship between the resistance of the temperature elements and the meter was approximately linear.

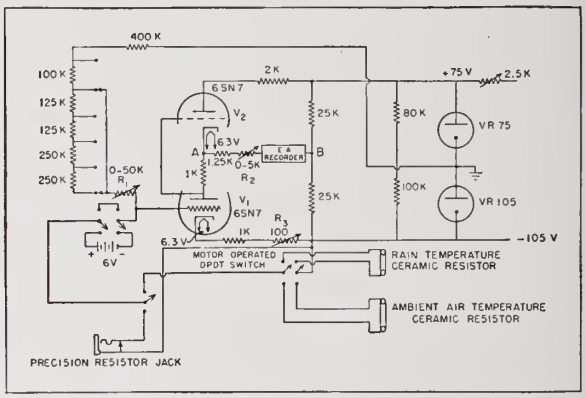

FIGURE 230.—The circuit diagram of the vacuum-tube ohmmeter used to measure the resistance of the rain- and the air-temperature measuring elements.

Valid rain temperature measurements are obtained only when the ceramic element is completely immersed in water; it is evident from figure 228 that this must occur whenever water flows through the overflow tube, since the element would then be ⅛ in. below the water level in the apex of the cone. On occasion, when the rate of rainfall is just equal to the capillary outflow rate, no water will pass through this tube even though the element is immersed. An auxiliary apparatus, designed by Mr. Patrick J. Harney, was used to indicate the immersion of the element by recording the passage of water through the overflow tube.

Further details of the equipment and the results of analysis of the data obtained by the installation located at station B are presented in a recent paper by Byers, Moses, and Harney [**20**].

Electric field.—The equipment employed for measuring the electric field intensity at the surface was designed by the General Electric Co. It consisted of a needle-point antenna and a device which could measure and record the current flowing through the antenna. When the exposed antenna was under the in-

[79] Glyptal No. 1201 is manufactured by General Electric Co.

fluence of an electric field, charges were attracted to the antenna tip. The motion of the charges caused a deflection on the recorder. When the electric field became sufficiently strong, a corona discharge occurred. This corona current, caused by the high-frequency discharges, produced a continuous deflection of the recorder pen, since the lag of the instrument was too great to permit recording of each individual current fluctuation. A calibration curve showing the relation of corona current to the electric field intensity was drawn for each antenna.

The number of bound charges at the tip of the antenna varied with the intensity of the electric field. In the event of a sudden field change, such as that caused by a lightning discharge, there occurred a simultaneous change in the quantity of charges bound to the antenna. The sudden flow of charges through the antenna registered on the recorder as a sharp deflection of the trace. Thus, it is possible to use the trace to detect the occurrence of lightning strokes from the sudden sharp deflections and to determine the strength of the electric field from the continuous deflection. Figure 231 presents a portion of a recorder trace which illustrates the more or less continuous deflection produced by corona current and the sharp deflections which indicate the occurrence of lightning discharges.

Two of the surface stations, 19 and 39, were equipped with electric field meters employing high-speed photoelectric recorders manufactured by the General Electric Co. A third point antenna, identical to the ones obtained from the General Electric Co., was constructed by personnel of the Thunderstorm Project and installed at station B; a Leeds & Northrup Speedomax Recorder was used with this equipment. At this station provision was made to connect two

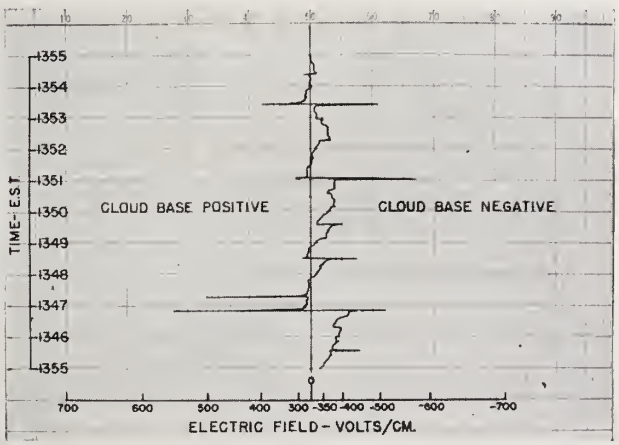

FIGURE 231.—Trace made by a surface electric-field meter using a needle-point collector and a Leeds & Northrup Speedomax recorder. High-amplitude, rapid fluctuations in the electric field such as shown at 1351 E.S.T., indicate lightning discharges.

additional point antennae in parallel with the needle-point for the purpose of increasing the equipment sensitivity.

A schematic diagram of the installation using the G. E. Recorder is given in figure 232 (a). It can be seen that its positive terminal was connected to the needle-point antenna and its negative terminal to ground. Thus, when there was a negatively charged cloud overhead, the recorder pen was deflected negatively. The chart drive of the G. E. Recorders could be operated at two speeds — 1 in/hr or 1 in/min. During periods of minor electrical activity the slow speed setting was used. When a thunderstorm was in the vicinity, the recorder was put on the high speed to permit the separation of the individual deflections.

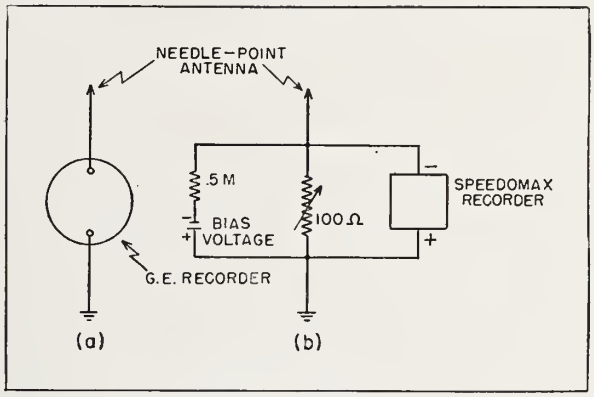

FIGURE 232.—A schematic diagram of the electric-field intensity recorder using (a) General Electric recording photoelectric microammeter and (b) Leeds & Northrup Speedomax recorder.

A schematic diagram of the installation using the Speedomax Recorder is given in figure 232 (b). It can be seen that the positive side of the Speedomax was connected to the ground and the negative terminal of the antenna. Thus, when there was a negatively-charged cloud overhead, the deflection pen was deflected positively from the center of the scale. A biasing voltage was applied to keep the pen at the center when there was no electric field. This recorder was operated at either of two speeds—1 in/hr, or ½ in/min.

Meteorological measurements at fixed levels above the surface.—Continuous measurements of the meteorological elements at levels several hundred feet above the earth's surface were obtained by means of three different techniques which had the similarity of employing some type of inflated balloon to carry and suspend the instruments at the chosen altitude. The most desired measurements were those to be made when a thunderstorm was approaching and moving over the station. However, at these times winds at the levels where suspended instruments were located were very strong, and the balloon behavior was such that

the measurements were difficult and often impossible to evaluate. The equipment employed with the three methods used are discussed in the following paragraphs:

(a) The first instrument employed was a 72-megacycle radiosonde, AN/AMQ–1, suspended from a combination of Kytoons[80] and radiosonde balloons. A nylon cord attached to the balloon was used to moor the equipment to the ground and to control its altitude. The radiosonde signals were radioed to the ground and received on an S-36 Hallicrafter Receiver and recorded on a Leeds & Northrup Speedomax Recorder. In place of the usual baroswitch, a battery-operated motor-driven switch selected the temperature and relative humidity signals. Altitude was measured by means of an azimuth and elevation angle-recording apparatus, described below.

The chief difficulty with this method was that a reasonable combination of Kytoons was unable to hold the heavy instrument aloft without frequent nose-diving or bursting in high winds. Another disadvantage was that the period of operation was limited by the life of the battery and that of the lithium chloride humidity strip. The calibration of the latter drifted to the extent that the data became unusable after about an hour in fair weather and much sooner in rainy conditions.

(b) Since the major difficulty with this equipment as described in the previous paragraphs, was insufficient lift, an attempt was made to eliminate a substantial portion of the weight by sending aloft only the temperature and the humidity elements mounted in a radiation shield similar to the type used by the Navy Radio and Sound Laboratory wired-sonde. A light three-wire cable made of fine plastic-covered aluminum wires moored the Kytoon and instrument to the ground and at the same time connected the temperature and humidity elements to a 72-megacycle radiosonde located in an instrument shelter. The humidity and temperature signals were transmitted to the radiosonde ground equipment.

This method had the advantage of using batteries located on the ground, so that operations for long periods of time were feasible. However, it was found that the gustiness associated with thunderstorms in the layer from the surface to 1,000 ft. was sufficiently great to cause even one Kytoon to become unstable and to nosedive frequently. There was still insufficient lift to allow the Kytoon to fly at an angle of more than about 20 deg. with the horizontal during thunderstorms. Also, the conventional radiosonde lithium chloride strip, with its inherent calibration shifts, was used for the humidity measurements.

[80] The Kytoon, manufactured by Dewey and Almy Co., Cambridge, Mass., is essentially a miniature barrage balloon.

(c) The third and final technique used, was designed to eliminate the difficulties encountered in the previous methods. Temperature and humidity measuring elements were sent aloft in a specially designed radiation shield and the rest of the measuring equipment remained on the ground. An Army 3,000-cubic-foot barrage balloon, type M–1, moored by a .072 inch music-steel wire was used to support the measuring elements. Five strands of the No. W–130 wire formed a cable which ran alongside the steel wire to connect the measuring elements to the recording equipment.

Temperature was measured by the conventional radiosonde temperature element, connected to a battery-operated vacuum-tube ohmmeter with a 0–1 milliampere Esterline-Angus Recorder. Relative humidity was measured by means of a hair hygrometer of the type used in radiosondes built by the Washington Institute of Technology. The elongation and contraction of the hairs caused a contactor of a potentiometer to move. With such an arrangement, the potential difference between the movable contactor and one end of the resistor became a measure of the relative humidity and was recorded by an Esterline-Angus Recorder functioning as a voltmeter. All equipment was designed for continuous operation. Although the hair hygrometer has a greater lag than the lithium chloride strip, it is not subject to polarization or the same degree of calibration shift and is suitable for long-period, continuous operation.

Since measurements were to be made during thunderstorms, when visual observations of the balloon were impractical, it was necessary to develop a system which would provide data from which the altitude of the airborne instrument could be determined. The technique employed in all cases utilized two modified ML–203–B wind-direction transmitters. One was mounted with its axis of rotation normally vertical, and the other, with its axis of rotation horizontal, was attached to the rotating portion of the former. A 12-inch steel rod was attached to the rotor of the horizontally-mounted direction transmitter. To this steel rod was attached the wire leading to the balloon. The horizontally-mounted direction transmitter measured the elevation angle of the airborne instrument and the other measured the azimuth angle. The electronic circuit of the azimuth meter was the same as that used for recording wind direction, but the elevation-angle meter was slightly modified so that 90° instead of 360° of rotation, corresponded to approximately the full scale of the Esterline-Angus chart. Because of the catenary effect of the wire leading to the balloons, used with the equipment described in paragraphs (a) and (b), the accuracy of the elevation angle thus determined was questionable with low angles. However, the experience with the barrage bal-

loon indicated that the wire normally made an angle of about 75 or 80 deg. with the horizontal so that the catenary effect was negligible.

The fixed-level observations were made at station 39 with the first instrument on June 24, 1947. The method described in section (b) was introduced on July 7, 1947. Measurements on a 24-hour day basis using techniques as described in paragraph (c) were begun on September 4, 1947, and were continued until September 9, 1947, on which day a severe thunderstorm caused the barrage balloon to burst. Data for 15 periods of observation, including 4 thunderstorms, were obtained.

Duration of sunshine.—Records of the duration of sunshine during the day were obtained by means of the Marvin sunshine recorder. This instrument is essentially a differential air thermometer with a clear and a black bulb, mounted in such a position that the sun can shine about equally on both. The instrument is electrically connected to a pen which makes a mark on a chronograph whenever the radiation falls on the two bulbs and heats the black one more than the clear one. This recorder has several disadvantages, the chief one being that it is difficult to calibrate and adjust because of its sensitivity to diffuse radiation. Two sunshine recorders were installed — one at station 19, the other at station 39.

Hydrological measurements.—In cooperation with the Ohio Resources Board and Department of the Interior, three well gages and one river gage were installed to record variations in the water table and river level. The river gage was located on the East Fork of the Little Miami River near the center of the surface network (see fig. 11). The analysis of the data obtained is being carried on by the Ohio Resources Board.

2. Upper-air Equipment

A. FLORIDA, 1946

Meteorological measurements at the upper levels of the atmosphere were made using both the Radio Set SCR–658 and the Radio Set SCR–581[81]. The former supplied data on the vertical distribution of pressure, temperature, relative humidity, and wind velocity; the latter supplied only wind velocity measurements.

Rawinsonde equipment, Radio Set SCR–658.—This type of equipment (fig. 233) is being used currently by meteorological services for obtaining upper-air measurements. It combines the features of the standard radiosonde system for securing data on pressure, temperature, and relative humidity, with those of a radio-direction-finder for obtaining the azimuth and elevation angles of the airborne transmitter. The radiosonde transmitter is tracked manually through the antenna system by an operator who reads and records the elevation and azimuth angles every minute. Radiosonde intelligence is detected by the receiver of the SCR–658 and is recorded by the AN/FMQ–1 Cycloray Recorder. From the meteorological data, the altitude of the transmitter can be computed. This, in turn, can be used in conjunction with the angular measurements for determining its spatial position. The horizontal wind velocity may then be easily calculated using standard techniques.

The AN/AMT–2 radiosonde transmitter was used throughout Florida operations. Since the observational procedures required that six Radio Sets SCR–658 be operated simultaneously in a relatively small area (6 by 17 mi.), it was impossible to have each transmitter tuned to the design frequency of 397 mc. Experiments were conducted to determine the necessary frequency spread which would permit tracking of a particular transmitter in the vicinity of several others. Satisfactory results were obtained when using the following frequencies: 388, 391, 394, 397, 401, and 404 megacycles.

Early in the 1946 season a PE–75 generator supplied power for the operation of the SCR–658 equipment. This 2.5 kilowatt generator proved too small for the power load, and its frequency was not sufficiently stable for satisfactory recording by the AN/FMQ–1 Cycloray. By the middle of May 1946, PE–107 generators having an output of 5.0 kw. and a

FIGURE 233.—A photograph of the Radio Set SCR-658.

[81] The locations of the sites of the equipment are shown in the Introduction, fig. 6, p. 10.

more stable frequency were installed; this resulted in improved operation.

Full-scale operation of the rawinsonde network began May 29, 1946, and continued through September 20, 1946. Simultaneous balloon releases were made by all stations whenever it was deemed advisable by a controller located at the radar site at Orlo Vista. Communications between stations and controller were effected by using the Radio Set AN/TRC–1 (about 85 mc.). All stations scheduled for a release were allowed about 30 min. to prepare airborne and ground equipment. In addition to the rawinsonde ascents scheduled by the controller, a routine radiosonde run (72 mc.) was made at 0800 E.S.T. on each day. A summary of the number of balloon releases made and the altitudes attained in the ascents is presented on page 13.

Rawin equipment, Radio Set SCR–584 (Fig. 234). —This equipment is a microwave radar set which has automatic tracking and relatively high angular and range resolution, and thus may be used for the measurement of wind velocities up to high altitudes. An eight-corner reflector (ML–307) attached to the released balloon served as the target which the radar set tracked automatically. The Radio Sets SCR–584 used on the Project were modified to increase their maximum range and thus enhance their utility as wind-measuring devices. Power for the operation of the equipment was supplied by M–7 generators. The accuracy of the wind measurements obtained by using the SCR–584 is generally given as 2° in direction and 2 mi/hr in speed.

FIGURE 234.—A photograph of a Radio Set SCR–584 installation, showing the van housing the radar equipment and supporting the antenna. At the extreme left is the M–7 generator; on the right is the canvas balloon-inflation shelter. In the foreground the instrument shelter, rain gauge, and anemometer mast are shown.

Regular operation of the SCR–584 network, which included four installations was started on June 6, 1946. Simultaneous balloon releases made in conjunction with the SCR–658 stations were scheduled by the controller located at Orlo Vista. The number of balloon ascents made during the season and the altitudes attained are tabulated on page 13.

In addition to use for rawin observations, the SCR–584 was used for the following purposes:

a. To assist the controller in the scheduling of balloon releases, through indications of the locations of rain showers and thunderstorms on a 7-inch PPI 'scope.
b. To obtain permanent records of the distribution of radar clouds, through photography of the PPI 'scope.

B. OHIO, 1947

During the 1947 observational program the Radio Sets SCR–658 and SCR–584 were again utilized for taking upper-air measurements[82]. No significant changes in the technical characteristics were made prior to their installation in the new network. However, the procedures for the collection of the data were altered somewhat. The simultaneous release by all stations, which was used in 1946, was supplemented by releases in which only one or more stations participated. The specific stations which were to make an ascent at a particular time were designated by a controller located at the radar site or at one of the stations near the center of the surface network. Communication was maintained between the controller and stations by using the Radio Set AN/TRC–1.

The releases made were of four general classes:

(a) The "thunderstorm ascent," in which several or all stations participated, depending upon the advice of the controller who usually observed the thunderstorms on the PPI 'scope of the control radar set.
(b) The "cumulus or cumulonimbus ascent," in which several or all stations participated. The releases were scheduled by a controller located near the center of the network. The aim of this type of release was to have at least one balloon enter a building convective cloud, while the others remained outside it. The controller observed the clouds visually and received reports by radio from the weather observers who made visual observations at other upper-air stations. Also, when observations of the radar 'scopes were taken, upon request, they were relayed to him.
(c) The "stable-air ascent," in which releases were made at intervals of 2 hr. by all rawinsonde stations. The releases started at 0600 E.S.T., and continued until 1800 E.S.T., during several days when the atmospheric conditions were stable throughout the day. The objective of this type of release was the collection of data to permit the study

[82] The locations of the sites of the equipment are shown in the Introduction, fig. 11, p. 12.

of the sampling errors of the radiosonde and the horizontal variation of meteorological elements under stable conditions.

(d) The "stable-unstable-stable ascent," in which releases were made at approximately 2-hour intervals from 0600 to 1800 E.S.T. on days having an absence of convection in the early hours, the formation of cumuliform clouds in the afternoon, and the dissipation of the clouds near the end of the study period.

Systematic measurements by the balloon-borne instruments extended from May 13, 1947, until September 27, 1947. The numbers of releases of each type which were made, as well as information on the heights attained, are given on page 13.

Rawinsonde equipment, Radio Set SCR–658.—Although this set was the same type as that utilized in Florida, some of the equipment used in conjunction with it was changed. Also, the SCR–658 was used for tracking and receiving radio intelligence from instruments other than the radiosonde.

For the first part of the operational season the Army type radiosonde AN/AMT–2 was used with the SCR–658; however, beginning June 11, a more satisfactory type of balloon-borne instrument, procured by the Weather Bureau from the Bendix Instrument Division, and known as the 730,000-series rawinsonde, was employed. This instrument has the advantage that it uses a dry-cell battery and is easier to prepare for release. It also transmits a steadier and stronger signal than the AN/AMT–2.

The operation of the SCR–658 was facilitated by the use of a shelter S–1/FM (14 sides) at each station. The building was designed for housing the SCR–658 radio-direction-finding equipment and the AN/FMQ–1 Cycloray Recorder, which had been housed in separate places during the 1946 field program. With this arrangement, the necessity of telephonic communications between the operators of the two units of the rawinsonde station was eliminated and more accurate timing was possible. A photograph of an SCR–658 station, showing the 14-sided shelter and balloon inflation tent, is given in figure 235.

In addition to the radiosonde, several other balloon-borne instruments were tracked with the SCR–658. One of these was the W-sonde, an instrument designed and constructed by the Instrument Laboratory, Department of Meteorology, University of Chicago[83]. Its primary purpose is the measurement of the vertical velocities in the atmosphere. A measurement of the vertical speed of the air is obtained by means of a rotating propellor carried with the balloon, and subtraction of the rate of ascent of the instrument as calculated from measurements of rate of change of pressure. Eleven W-sonde runs were made with varying degrees of success.

FIGURE 235.—A photograph of a Radio Set SCR–658 installation showing the 14-sided shelter which housed the equipment. Also shown are the balloon-inflation shelter, instrument shelters, and the Jamesway Hut used for storage of supplies. The antenna in the right foreground was used with the Radio Set AN/TRC–1.

Another instrument released over the observational network with the assistance of Thunderstorm Project personnel and facilities, was one capable of measuring the electrostatic field strength. A conventional 730,000-series rawinsonde was modified so that field strength, temperature, and reference signals were transmitted to the receiver. The instrument was developed by Dr. S. Chapman, formerly of Stanford University.

Rawin equipment, Radio Set SCR–584.—The sets used during 1947 were the same ones as were used the previous year. The muddy ground which resulted from excessive spring rainfall made the movement of the 10-ton vans a difficult task, delaying the installation at stations F and G. The sets at these stations were not put into operation until late in June.

[83] "Report to the U.S. Weather Bureau on Research Performed by The University of Chicago, Department of Meteorology, in connection with the Thunderstorm Project," (Memorandum of Understanding No. Cwb–7624) Chicago, Ill., August 20, 1947.

3. Radar Equipment

A. FLORIDA, 1946

Radar equipment was used extensively by the Thunderstorm Project for obtaining meteorological data, for the guidance of airplanes engaged in observational missions, and for the control of balloon releases. The electronic equipment may be divided into two categories: (1) that which was located on the ground, and (2) that which was carried by the airplanes. Among the former were a long-range control radar set, a high-power height-finder, the AN/APN–19 (Rosebud) beacon receiver, and an IFF (identification, friend or foe) receiver. The airplanes were equipped with the Radio Set SCR–720, the AN/APN–19 transponder, and an IFF transponder. The maintenance and operation of the radar sets were carried on by personnel of the U. S. Air Force and the U. S. Weather Bureau. In the following paragraphs a discussion is given of some technical characteristics and the operation of the equipment[84].

Ground radar.—The long-range, high-power control radar in Florida operated on the 10-cm. band; it had a beam 1.5 deg. wide to half-power points in the horizontal plane, and extending from near the surface to altitudes exceeding the highest flight level. Six 12-inch plan-position indicators capable of adjustment for off-center presentation were available for use by the operations controller or for photographic purposes. Using a mixing circuit and a switching system he could obtain, on any of the 'scopes, any of the following combinations: (1) radar video[85], (2) IFF signals, (3) a combination of radar video and IFF signals, and (4) beacon signals alone. It was impossible to present a combination of the beacon signals and radar video using the available switching arrangement.

Data on the vertical growth and extent of thunderstorms were obtained by means of a high-power height-finder operating on the 10-cm. band. The equipment had a beam 1.3° wide in the vertical plane and 4.7° wide in the horizontal plane, both measured between half-power points. The antenna scanned vertically while at the same time it could be manually rotated in azimuth. Echoes were presented on a 12-inch range-height indicator (RHI 'scope) having a maximum possible range exceeding 100 mi. and a maximum altitude indication of 40,000 ft. Difficulties in siting the equipment and operating it without interference with the control radar set delayed the completion of the installation of the height-finder. Satisfactory operation commenced on about July 11, 1946, and continued until the termination of the 1946 observational season.

Equipment for location and identification.—Whenever an airplane was located within an intense rainstorm, its radar echo presented on the radar 'scope blended with that of the precipitation into a large, bright area, and it became impossible to isolate the echo from the airplane. It became necessary therefore to equip the airplane with instruments which would transmit signals at a frequency slightly displaced from the control radar frequency. The returned signals were detected by a receiver at the ground whose output was channeled to the indicators of the control radar. Two systems for identification and location of airplanes were available during the Florida operations. The one which was employed almost exclusively was an IFF system; the second made use of the Radio Set AN/APN–19, the Rosebud beacon. The Rosebud has an airborne receiver with two input channels; one is tuned by a cavity in the antenna circuit, and the other is untuned. The output of the receiver triggers a transmitter which is modulated by a coding device having seven different combinations for making possible the positive identification of the airplane echo on a PPI 'scope. The following difficulties prohibited the operational utilization of the Rosebud: (1.) The equipment in the plane was not properly shielded at the time of installation. This permitted the airborne radar, Radio Set SCR–720, to trigger the Rosebud transmitter. (2.) The location of the transmitting antenna was such that its radiation was often blocked by the airplane itself in the event of a turn, steep climb, or dive. This resulted in a fading or a complete disappearance of the beacon signals.

These difficulties were partly overcome during the 1947 observational season.

Airborne radar.—Each P–61 was equipped with the Radio Set SCR–720, which operates on the 10-cm. band and a peak power of 100 kw. and uses "B" and "C"[86] 'scopes for the presentation of the radar echoes. The antenna (fig. 236) was mounted in the nose of each airplane, and it rotated azimuthally at 100 r. p. m. while scanning vertically. One of the major disadvantages of this set is that it employs a "B"

[84] The technical specifications of some of the electronic equipment used in Florida and Ohio are still classified as restricted or confidential and may not be published at this time.

[85] The term "video" as used here applies to the video signals from energy returned by reflection or scattering of the transmitted radio waves.

[86] The "B" 'scope displays range vertically against azimuth horizontally; the "C" 'scope displays elevation vertically against azimuth horizontally.

'scope for the presentation of the radar echoes. The scale coordinates produce a marked distortion of the echoes especially those at the close ranges.

FIGURE 236.—A photograph of the antenna of the Radio Set SCR-720, located in the nose of a P-61C airplane.

B. OHIO, 1947

During the field operations in Ohio, radar equipment was utilized for the same general purposes as during the observational period in 1946. The sets were different in some respects but were of the same basic type and performed the same functions.

Ground radar.—Two 10-cm. radar sets were used for the control of balloon releases and airplane flights during 1947. From May 13, 1947, through July 11, 1947, a short-range control radar set located at Clinton County Air Force Base was utilized. This radar set had the serious disadvantage of having a maximum range of 40 mi. The approaching thunderstorms could not be seen until they moved within this distance, at which time they were very close to the surface and upper-air observing stations. This often made the scheduling of balloon releases and airplane flights a difficult task. The area of airplane operation was further limited by the fact that at the closer ranges the beam coverage was not sufficient to detect all of the airplanes taking part in the missions. Also, a study of such large-scale phenomena as squall lines by use of the data from the short-range control radar was necesarily incomplete, because dimensions of the line of thunderstorms often exceeded the 'scope diameter by a significant amount.

On July 12, 1947, the installation of the long-range, high-power, 10-cm. control radar set at a site near Jamestown, Ohio, was completed, and operation controllers moved to this location. This equipment had a vertically polarized beam which was very wide in the vertical plane but 1° in width in the horizontal plane. The radar set was equipped with eight 12-inch PPI 'scopes capable of being operated to give an off-center presentation. One of the 'scopes was adjusted to have a 200-mile radius, and had a time-lapse camera mounted on it. The radar data thus obtained have been used for the study of large-scale thunderstorm conditions (see ch. VII).

Height-finding radar.—During the 1947 season, the Radio Set AN/TPS-10 (Lil Abner), shown in figure 237, was utilized for obtaining vertical cross sections through radar thunderstorms. Two pieces of equip-

FIGURE 237.—A photograph of the Radio Set AN/TPS-10 (height-finding radar).

ment of this type were employed during the season; one was located at Clinton County Air Force Base, the other at the Jamestown site of the control radar set. Both had essentially the same operating characteristics. The sweep circuits were modified to permit the display on the range-height indicator to extend above 60,000 ft. The Radio Set AN/TPS-10 operated on the 3-cm. band and had a pulse length of 1 microsecond at a peak power of about 65 kw. Its antenna assembly consisted of an orange-peel paraboloid, which produced a beam 2.0° wide in the horizontal plane and 0.7° wide in vertical plane, both angles being measured to half-power points. The radar echoes were presented on a range-height indicator (RHI 'scope) having a maximum range of about 60 mi.

Identification and positioning equipment. — Throughout the observational season of 1947 the Radio Set AN/APN–19 (Rosebud) beacon was used for the location and identification of airplanes during the observational missions. The reception of the signal at the ground was improved by installing two transmitting antennae on each airplane, one on the upper side of the fuselage, the other on the lower part of the fuselage. This reduced the fading or disappearance of the beacon signals which ordinarily occurred during sharp banks or dives of the airplane when only one antenna was used.

Airborne radar.—During the early months of operation in 1947, the Radio Set SCR–720 was again used on the P–61 airplanes. However, the triggering of the AN/APN–19 beacon transmitter by the SCR–720, which was a factor preventing the use of the former during the 1946 observational program, could not be eliminated. It was decided, therefore, to discontinue the operation of the SCR–720 during further thunderstorm missions. No airborne radar data were collected after August 16, 1947.

4. Airplane Instruments

A. FLORIDA, 1946

Most of the data which were utilized for the study of the structure and circulation of the thunderstorms were collected by airplanes which made traverses through convective clouds. Each of the airplanes was equipped with instruments for measuring certain meteorological parameters, as well as for making a record of its own reaction to changes of the horizontal and vertical velocities of the air in which it was flying. By studying these reactions it was possible to compute the draft and gust velocities in the atmosphere.

Most of the instruments from which records were obtained are standard aircraft instruments; however, some special equipment was designed by Project personnel or procured from one of the cooperating agencies. In the following paragraphs, only those instruments which are not in common use are treated in detail.

Standard blind-flying instruments.—All the standard instruments on the pilot's panel in the 1946 season were photographically recorded by a camera mounted in the cockpit so as to "shoot" over the pilot's left shoulder. The following equipment was photographed:

a. Airspeed indicator
b. Sensitive pressure altimeter
c. Rate of climb indicator
d. Universal attitude gyro (electric)
e. Artificial horizon (suction)
f. Ball bank indicator
g. Directional gyro
h. Panel clock

In addition, the SCR–718 radio altimeter was installed in each airplane for obtaining its height above the ground. The comparatively level terrain in the vicinity of Orlando made the use of this instrument a very satisfactory means of measuring airplane altitude.

Instruments for measuring gusts and drafts[87].—For obtaining data from which to compute draft and gust velocities, the N. A. C. A. installed and maintained equipment for measuring and recording the time variation of air speed, altitude, and vertical acceleration of the airplane. The instruments were all tilting-mirror mechanical optical instruments recording on plenachrome film $2\frac{7}{16}$ in. wide. The following paragraphs give a brief description of the various instruments, including range, accuracy, and other pertinent characteristics:

a. Airspeed-altitude recorder.—The airspeed-recording part of the airspeed-altitude recorder consists of a corrugated-diaphragm capsule mounted in a pressure-tight case with the total-pressure tube connected to the capsule, and the static-pressure orifice to the case. The deflection of the diaphragm is proportional to the pressure difference, and through a connecting linkage, the diaphragm deflection causes a mirror to rotate, thereby resulting in a film deflection proportional to the pressure difference. Actually, three mirrors were used to give a total of 6 in. deflection for a

[87] The information contained in this section was prepared by the engineers of the National Advisory Committee for Aeronautics, Langley Field, for inclusion in this report.

range of 0 to 360 mi./hr. The hysteresis, aging, reading, and other errors inherent in the instrument were within $\pm 1/4$ percent of full deflection. The temperature error was approximately $+2$ percent per 100°F. decrease in temperature.

The altitude-recording part of the recorder is of similar construction, with the corrugated-diaphragm capsule being evacuated and the static pressure being applied to the pressure-tight case. In this instance, the diaphragm deflection, and therefore the film deflection, is proportional to the absolute pressure. A total of five mirrors was used to give a film deflection of approximately 10 in. for a range of 0 to 35,000 ft. The hysteresis, aging, and other inherent errors were within $\pm 1/4$ percent and included temperature effects, since the units were temperature-compensated. The time constants of the pressure system were less than 0.003 sec. over the altitude range encountered.

The airspeed-altitude recorder was mounted on suitable shock mounts in the nose section of the airplane, as shown in figure 238. In order to accommodate a separate pitot-static tube for the N. A. C. A. airspeed-altitude recorder, the existing pitot-tube installation of P–61C airplanes was modified as shown in figure 239. The pitot-static tubes used in the installation were standard high-speed heated tubes manufactured by the Aeronautical Instrument Corp. and the Kollsman Instrument Co. (Type 651). The installation-error corrections were determined for one airplane very accurately by standard calibrating techniques, and the error in other installations was determined by comparison with this installation in side-by-side flights.

b. Accelerometer.—The N. A. C. A. accelerometer consists of a brass cantilever vane which moves in an enclosed chamber so that the vane motions are air-damped. A lens fastened to the vane adjacent to the free end deflects the image of a fine lamp filament on the recording film so that displacements of the image on the film correspond to the acceleration forces acting on the vane. The instruments had a range of $+4\,g$ to $-1\,g$ for approximately 2 in. of film deflection.

The hysteresis, aging, reading, and other inherent errors of the accelerometer were within $1/2$ percent of full deflection. The temperature-error corrections were $+2$ percent for 100° F. decrease in temperature. The combined effects of all other accelerations did not exceed an error 1 percent of the reading. The instruments had a natural frequency of 13 cycles per second and were 0.7 critically damped at sea level and about 0.55 critically damped at 20,000 ft. This variation in damping would mean that the recorded values should be within 1 percent of the reading up to 4 cycles per second at sea level, and within 5 percent of the reading up to 4 cycles per second at 20,000 ft.

FIGURE 238.—A photograph showing the N.A.C.A. flight recorders mounted in the nose section of a P–61C airplane. This nose section was removed from the airplane and the photograph was taken looking down through an inspection opening.

FIGURE 239.—A photograph of the modified pitot-static tube installation on a P–61C airplane. The upper tube assembly is the one connected to the N.A.C.A. airspeed-altitude recorder.

The accelerometer was rigidly mounted on a ¾-inch plywood board along with the inverter, distribution box, timer, and mechanical-optical control-position recorder, as shown in figure 240. The accelerometer and the board were so installed in the airplane that the accelerometer was approximately at the center of gravity and so oriented as to record normal accelerations of the center of gravity of the airplane. The instruments were grouped on the board to facilitate transferring the instruments to other airplanes whenever necessary.

c. Mechanical-optical control-position recorder.—The mechanical-optical control-position recorder is shown in figure 240. The three elements of the control-position recorder were connected directly to the elevator, rudder, and aileron control cables by means of instrument cord covered with nylon-braid Fiberglas. Movement of the cord causes a mirror to rotate and results in a film deflection proportional to the control movement. The control-position recorders were set up so that 6 in. of control movement resulted in approximately 2 in. of film deflection. The overall accuracy of this instrument is within ±½ percent of full deflection. It can faithfully follow full-scale movements of a frequency up to 10 cycles per second, which is adequate for the maximum rate of control movement.

d. Timer.—The timer consists of a motor driving a chronometric escapement (similar to a regular clock) through suitable gearing and a friction clutch. A detent solenoid is used to keep the escapement's balance wheel poised for instant starting. For this Project, cams were fastened to and rotated with the escapement in such a way as to cause one set of contacts to put out extremely short, 1-second spaced timing pulses for synchronizing N. A. C. A. instruments. Another set of contacts put out pulses of ⅛-second duration at 1-second intervals for synchronizing instruments furnished by the other cooperating agencies. The accuracy of the timers was within ±½ percent including temperature, acceleration, and inherent errors.

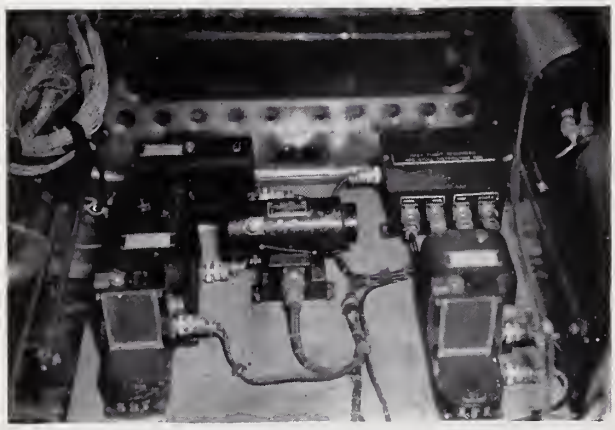

Figure 240.—A photograph showing the installation of the N.A.C.A. instruments in a P-61C airplane. The inverter is shown in the center, and clockwise from the upper right of the photograph are the power distribution box, control-position recorder, accelerometer, and timer. (This is a 1947 installation. The inverter was not used during 1946.)

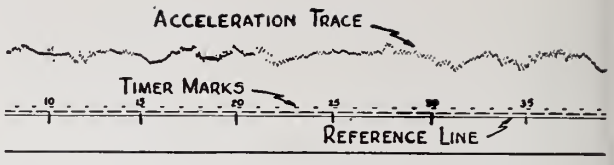

Figure 241.—A reproduction of a typical accelerometer record. This record was obtained on a flight in a Florida thunderstorm during 1946.

All the instruments were supplied with power from 12-volt batteries. Drums carrying 20 ft. of film and driven at ⅛ in/sec by a 12-volt (direct current) governed motor through a suitable gear train were used. The timing and synchronization of the instruments in each airplane were obtained by means of 12-volt (direct-current) pulse put out by the timer, which, in turn, caused a timing solenoid to function in each recording instrument. The timing solenoid caused a mirror to move when the pulses were received and thus caused a square wave to be recorded on the film. Figure 241 shows a typical record from this type of instrument.

Free-air temperature equipment[88].—Since existing instruments for measuring free-air temperatures using airplanes were unsatisfactory, an attempt was made to design one which could be used operationally. The equipment eventually mounted on the airplane consisted of a bullet-shaped housing (fig. 242), within which was a small sensitive resistor having a small time lag. The thermal resistor was connected through a suitable amplifier to a meter on the airplane panel and an Esterline-Angus Recorder in the rear of the airplane (fig. 243). It became evident, however, that the housing was unsatisfactory because of its large time lag, water and snow effects, and electrical leakage effects. The lack of time during the observational season prevented the development of another one for use during the observational missions. Prior to the start of the 1947 field operations, another housing was designed which gave much more satisfactory results. For the reasons cited above the temperature measurements made in Florida are of limited value.

[88] The free-air temperature equipment used during both seasons of operations was largely designed by Mr. Patrick J. Harney of the Thunderstorm Project, initially with the help of Lt. William O'Brien.

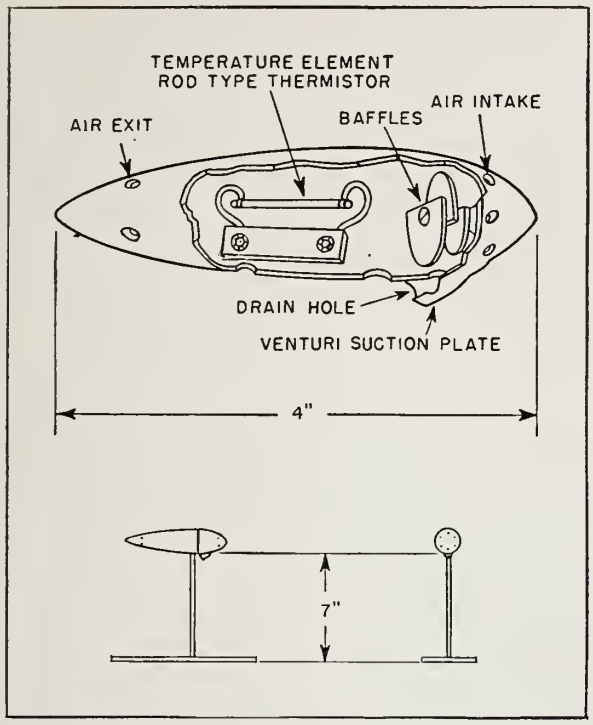

FIGURE 242.—A sketch of the 1946 thermistor housing, showing cut-away, front, and side views.

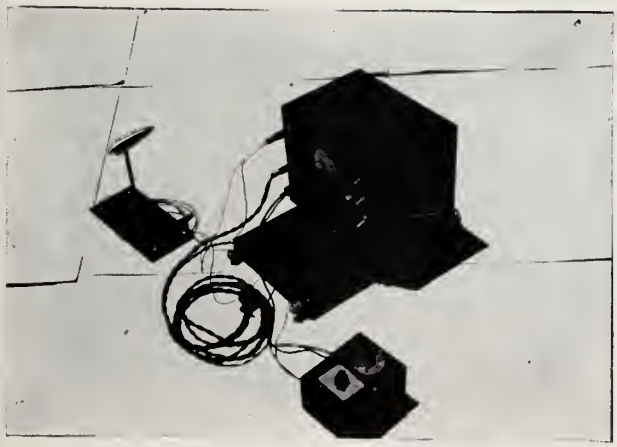

FIGURE 243.—A photograph of the component parts of the temperature-measuring equipment used during 1946. To the left is the bullet-shaped housing for the resistor, in the center is the vacuum-tube amplifier, and in the foreground is a control box used to adjust the measurement range of the instrument.

B. OHIO, 1947

The instrumentation of the P–61 airplanes during the observational period in Ohio was similar in most respects to that during the Florida field operations. Several changes were made to improve the accuracy of the measurements and the recording of the data. Also, a few additional instruments were installed to obtain other types of information. Figure 244 shows the location of the equipment on the P–61; the paragraphs which follow contain a description of the equipment on each of the airplanes.

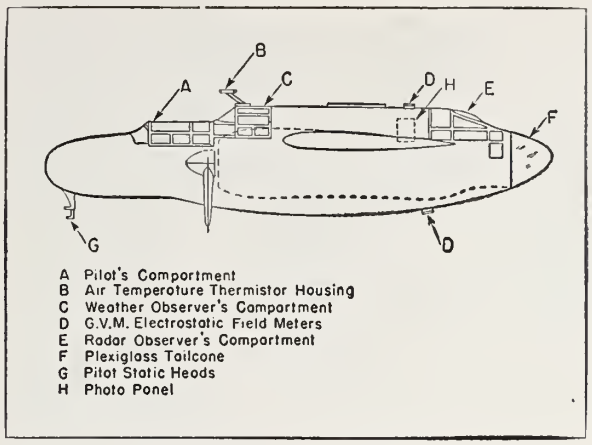

FIGURE 244.—A sketch of the fuselage of a P–61C airplane showing the location of the instrument used during 1947.

Photo-box.—The standard blind-flying instruments were again photographed to permit a study of the airplane behavior during the penetration through thunderstorms. However, the technique for the photography of the meters and other indicators was completely changed. Instead of photographing the instrument panel of the airplane, a specially constructed "photo-box" was used. The instrument indicators were mounted within and were photographed by a camera mounted outside the box, but having its lens assembly extending into it. The indicators of the panel instruments were all mounted on one face of the box (fig. 245), with a clock, and a counter, and a series of six lights, each one of which, when turned on, indicated the occurrence of a certain event. The six types of observations recorded using the lights were the following:

1. Lightning
2. Icing
3. Precipitation
4. Entry and exit from clouds
5. Drafts
6. Turbulence

The method of photo-recording using the photo-box gave much better results than the method used in Florida. One of the chief reasons was that the light intensity could be kept more nearly constant at a preselected level in the instrument photo-box than on the exposed airplane panel.

The radio set SCR–718 was again utilized for obtaining measurements of altitude above the terrain. Although in Florida the 'scope of this set was photographed separately, in Ohio it was photographed together with that of the SCR–720 by superimposing the images on the same plane by means of half-silvered mirrors.

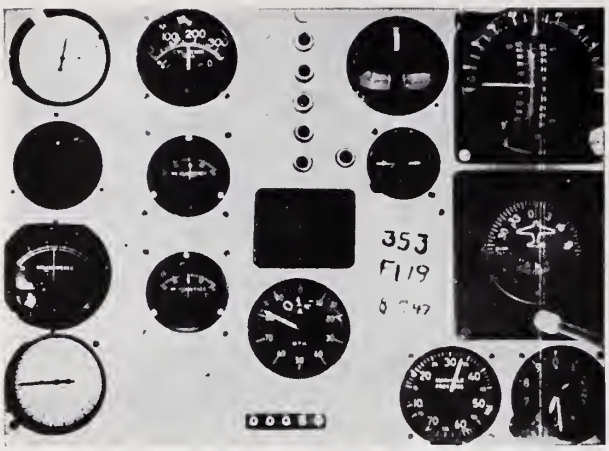

FIGURE 245.—A print of a frame of the 35-mm. film record of the special instrument panel installed in the P-61C airplanes.

Instruments for measuring gusts and drafts.—In 1947 the fundamental instrumentation by N. A. C. A. was similar to that used the previous year, but the power was obtained from the 27.5-volt (direct-current) ship's supply. This supply fed an Eicor 100-volt-ampere, 400-cycle, 3-phase, 115-volt inverter, which, in turn, fed this power to the various instruments through a distribution box. New synchronous motor-driven film drums were used that had a capacity of 50 ft. of $2\frac{7}{16}$-inch plenachrome film and were driven at a rate of $\frac{1}{8}$ in/sec. Timing and synchronization of the instruments in each airplane were obtained by means of extremely short-duration, 115-volt (alternating-current) pulses put out by the timer. These pulses flashed an argon lamp in the instrument bases. The flash resulted in a vertical line on the film because of the 0.006-inch slits which were used in the film drums. Figure 246 shows a typical record from this type of instrument.

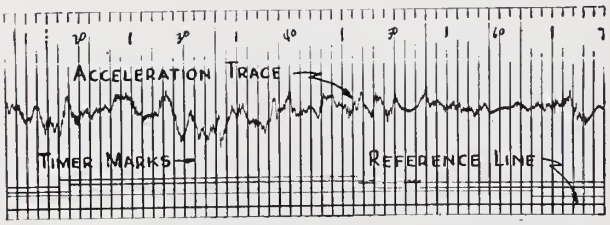

FIGURE 246.—A reproduction of a typical accelerometer record. This record was obtained on a flight through an Ohio thunderstorm during 1947.

Free-air temperature equipment.—The sensitive airplane thermometer used during 1947 was basically the same as the one used during 1946, with improvements which resulted from experience. The measuring element was a thermal resistor which was thoroughly insulated so as to prevent its short-circuiting by water. Another housing was designed to eliminate the difficulties encountered in Florida. It was fabricated at the University of Chicago and mounted on the airplane on short struts above the fuselage (fig. 247). The housing (fig. 248) was considerably larger than, and had a shape very much different from its predecessor. With the new housing, difficulties which resulted from water and snow effects, electrical leakage, and close dimensions were greatly reduced. The first difficulty, however, was still present to a large degree and contributed uncertainty to measurements made during certain parts of the traverses. The question as to whether the instrument measured the air temperature or the wet-bulb temperature often arises

FIGURE 247.—A photograph showing the 1947 thermistor housing mounted on a P-61C airplane.

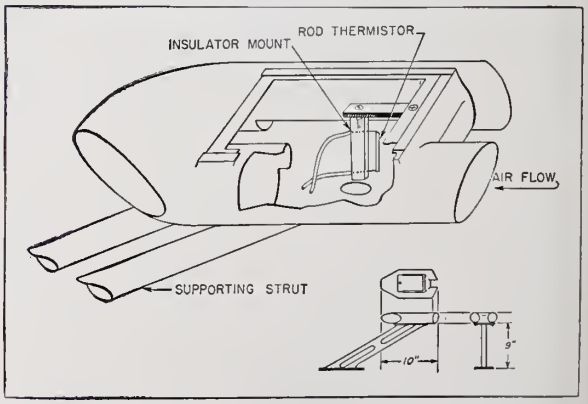

FIGURE 248.—A sketch showing cut-away and other views of the 1947 thermistor housing.

when the temperature measurements are being evaluated. It appears that considerably more work is required to design an airborne instrument for the accurate measurement of free-air temperature.

Although the technique of direct recording by a 0–1 milliampere Esterline-Angus Recorder was satisfactory, the recording was facilitated by photographing a remoted thermistor amplifier meter along with the standard flying instruments in the photo-box. Using this method, less power was required for simple remote meter operation from the thermistor. However, the potential usefulness of the ohmmeter—or amplifier, as it is often called—for the measurements dictated continuation of its use. The ohmmeter whose circuit diagram is shown in figure 249 was wired so that using a selector switch, an operator could select the range of temperature to be measured; thus, the measurements could be made more sensitive. The temperature ranges varied with altitude, of course, and were based on an average lapse rate.

The amplifier operated on either a 60- or 400-cycle, 115-volt alternating current. The 400-cycle power was provided by an inverter which also supplied the airborne radio and radar equipment. By careful wiring, the effects of the radar on the thermistor readings were reduced to a negligible value, except at the lowest temperatures. The amplifier, with its control switches and range selector, was placed in the middle compartment of the airplane where it could be read by the weather observer, and if necessary switched by

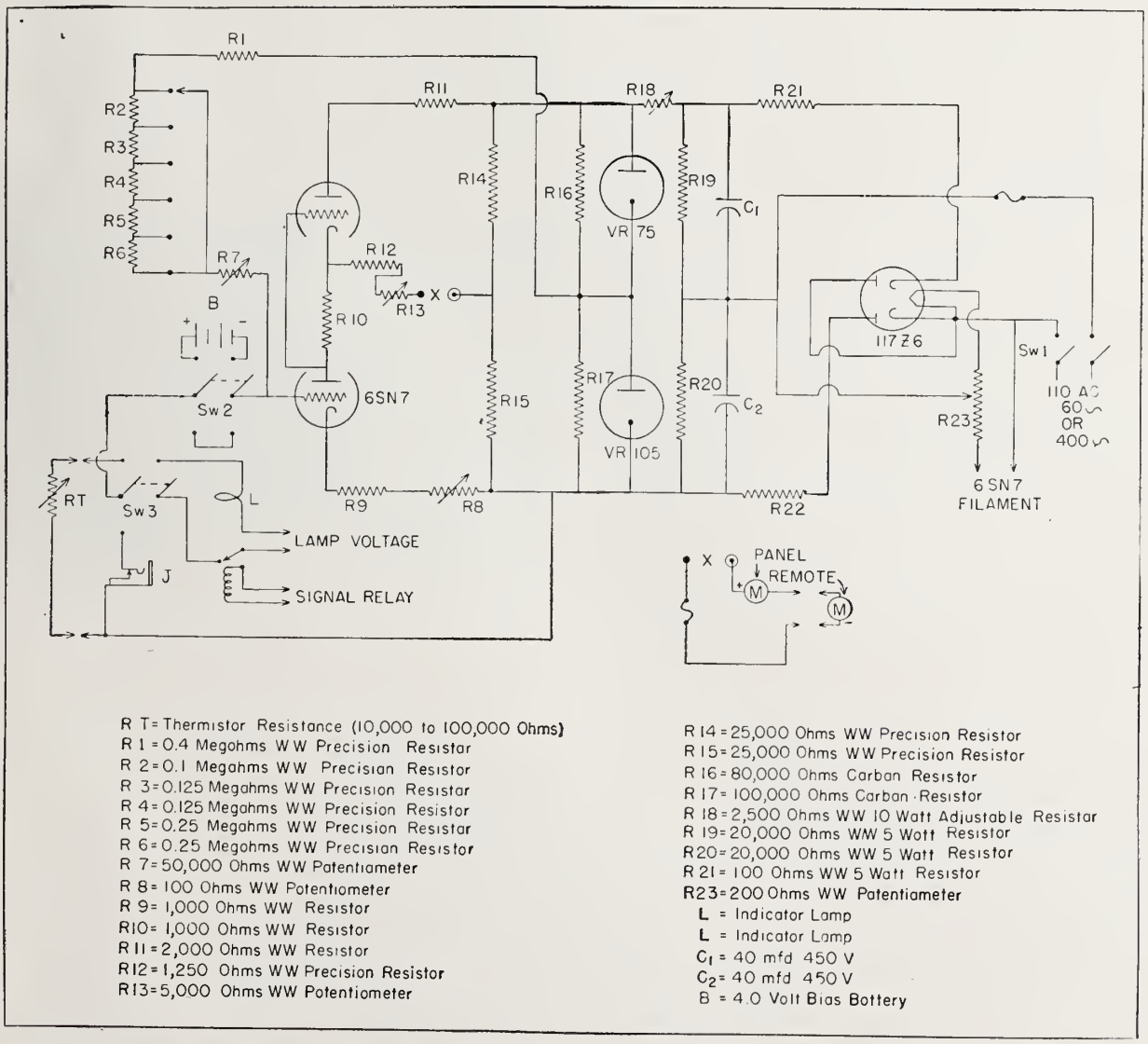

FIGURE 249.—A schematic diagram of the circuit of the vacuum-tube ohmmeter used with the thermistor on the airplane for measuring ambient air temperature.

the pilot. The housing of the thermistor could be seen by the weather observer who could thus determine its condition, i.e., wet, covered with ice, etc.

Before the temperature measurements made by this equipment could be utilized in the analysis of thunderstorm characteristics, it was necessary to apply several corrections to reduce the temperature of the thermistor element to that of the ambient air at a particular altitude. Corrections were necessary because (1) the air is dynamically heated as it strikes the fast-moving airplane, and (2) under saturated conditions, or when water or ice accumulates in the thermistor housing, there is evaporation and consequent cooling of the air which surrounds the thermistor element. Another correction which should be made for exactness, is one applied to account for the heating by frictional effects. However, in the airspeed range of the Project airplanes it is small and was neglected. Since it was desirable to study the horizontal distribution of temperature within and around the thunderstorm it was usually necessary to reduce the temperatures to a particular reference altitude. Such altitude reductions were made by using a moist-adiabatic lapse rate for values obtained inside the clouds and a dry-adiabatic lapse rate for those obtained in the clear air.

The dynamic or airspeed correction, as it is often called, will not be treated in detail here. It is considered sufficient to state that there is an increase of pressure as the air impinges on the airplane and has its relative velocity suddenly reduced. The pressure rise results in compression and heating, making temperature corrections necessary. All corrections for measurements recorded when the airplane was in clear air were made by using a dry-adiabatic compression rate. The measurements made within the cloud were corrected both dry-adiabatically and moist-adiabatically, and the values were compared[89].

By considering temperature changes with pressure changes to be moist-adiabatic, it is assumed that the air is maintained at saturation; thus, the evaporative cooling, mentioned as (2) above, is taken into account. Under conditions where only part of the element is covered with water which is evaporating, the temperature changes may be between the dry- and moist-adiabatic rates. In operation, however, the fractional area of the housing or element which was wet or iced, could not be determined, and consequently no attempt was made to approximate a rate different from either dry- or moist-adiabatic.

Electric field measurement equipment.—The Electric Field Meter TS–551 (XN–1) [1] designed by the Naval Research Laboratory and manufactured by the American Instrument Co., Silver Spring, Md., was used for measuring the component of the electric field perpendicular to the meter. It consists of three main units: The head, the motor, and the control box. The head (fig. 250) consists of a fixed stator and a grounded, motor-driven rotor. The rotor normally runs at 1,000 r. p. m. and alternately shields and exposes the stator to the electric field when one is present. This produces an alternating voltage across the parallel combination of resistance and capacitance (R_1 and C_1) shown in the circuit drawing in figure 251. The magnitude of the voltage is proportional to the strength of the electric field and undergoes a 180-degree phase shift when the direction of the field is reversed. The voltage is amplified and connected across a cam-operated switch and a meter in series. The cam, which is mounted on the rotor shaft, opens and closes the switch so that the meter circuit is completed only during alternate half-cycles of the signal. The switch thus acts as a linear, phase-sensitive rectifier whose direct-current output has a magnitude and sign which are controlled by the electric field intensity.

Each airplane had two electric field measurement

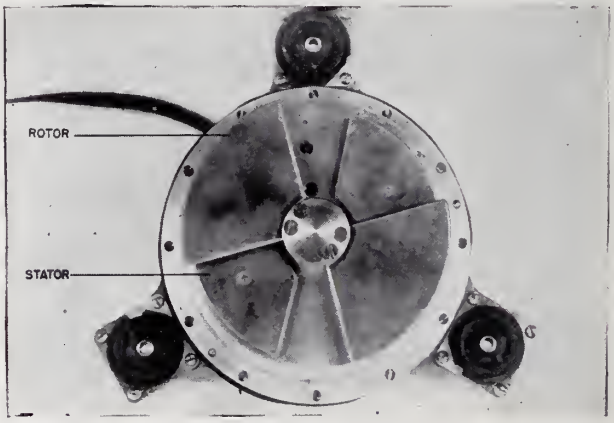

FIGURE 250.—A photograph of the electric-field meter head showing the two-vaned rotor and stator.

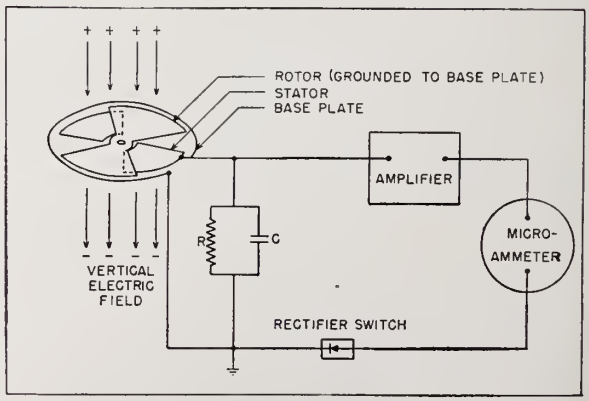

FIGURE 251.—A schematic drawing of the circuit of the electric field meter.

[89] See ch. I, sec. 3 for further details.

units; one on the top, the other on the bottom of the fuselage just aft of the wings (fig. 244). The meters for each one were located in the photo-box and were photographed with the other instruments. Considerable operational difficulty was experienced with these instruments, chiefly as a result of the entry of water into the heads and the subsequent corrosion and failure of the rotor bearing.

Equipment for voice recording and timing.—Some additional equipment used during 1947 is given below.

(a) A wire recorder, AN/ANQ-1A was installed in each airplane to record the in-flight comments of the pilot and crew. This equipment permitted a more accurate compilation of data concerning flight conditions and facilitated the task of timing the occurrence of specific reports of such phenomena as turbulence and precipitation.

(b) To enable the analysts to more accurately fix the time of the reported events, a ground radio transmitter, operating on the same VHF channel used by the Project airplanes during missions, was triggered every 5 min., and it transmitted a characteristic signal having a duration of about 5 sec. This signal could be heard by the airplane crew and by the ground controllers, and it was also fed to the wire recorders and to a light in the photo-box.

5. Photography

A. FLORIDA, 1946

During both observational seasons, the Thunderstorm Project made extensive use of photography for recording data on clouds, radar echoes, and the readings of the airplane instruments. The camera made possible simultaneous observations of several indicators, one of which was always a clock, and thus permitted the synchronization of the occurrence of certain events or a series of events. Also, time-lapse or motion pictures which were taken made possible projection of the film for study of the action at a reduced or increased speed.

Most of the cameras utilized during the Florida observational season and some information pertaining to each are presented in table 49. The film used in all cases was Army Class "L" or Ansco ultra-speed, with a speed rating of Weston 100.

Radar photography.—The 0-5 camera used for radar photography in Florida (see table 19) was mounted on a cone which served to eliminate stray light and to provide a rigid mount so as to maintain correct optical alignment of the camera with the radar 'scope. A clock and data card were housed in a separate section of the cone and were illuminated by two small 6- to 8-volt bulbs. Six volts across the filament of the lamps gave an illumination which was comparable to the light intensity produced by the luminous images on the radar 'scope.

The operation of the camera depended on the type of observational mission undertaken. When radar data were being collected for the control of balloon releases when an aircraft mission was not in progress, a photograph was taken at every tenth sweep, or approximately every 2½ min. Occasionally longer

TABLE 49.—*Listing of camera equipment utilized during the Florida and Ohio Project operations*

Type of photograph	Camera (Army type No.)	Lens aperture	Exposure time	Exposure rate	Manufacturer
	FLORIDA OPERATIONS				
PPI 'scope of control radar set	O-5	f:3.5	15 sec.	See text	St. George Co.
RHI 'scope of height-finder radar set	O-5	f:2.6	2 sec.	Variable	do.
Radio altimeter, SCR-718	B-2	f:3.5	1/24 sec.	2 per sec.	Eastman Kodak Co.
'Scopes of SCR-720	O-13 (modified GSAP)	f:5.6 to f:8	2 sec.	12 per min.	.....
Glider instrument panel	B-2	f:8	1/24 sec.	2 per sec.	Eastman Kodak Co.
Clouds (stills)	K-20	f:11	1/125 sec.	Variable	Folmer Graflex Corp.
Clouds (time-lapse)	B-2 (modified)	f:5.6	Unknown	6 per min.	Eastman Kodak Co.
	OHIO OPERATIONS				
PPI 'scope of control radar set	O-15	f:5.6	6 & 10 sec.	See text	Fairchild Camera & Instrument Corp.
RHI 'scope of height-finder radar set	O-15	f:5.6	1 sec.	do	do.
'Scopes of SCR-718 and SCR-720	O-5	f:2.5	3/10 sec.	100 per min.	St. George Co.
Airplane instrument panel	A-4A (modified)	f:11	1/10 sec.	4 per sec.	Bell & Howell Co.
Clouds (stills)	K-20	Unknown	Unknown	Variable	Folmer Graflex Corp.
Clouds (time-lapse)	A-4A (modified)	f:16	1/10 sec.	10 per min.	Bell & Howell Co.
Airplane instrument panel	GSAP (modified)	f:5.6 to f:8.	Unknown	5⅓ per sec.	Eastman Kodak Co.

841051—50——19

time intervals were used. During aircraft missions, a picture was taken for every sweep, or approximately every 15 sec.

Two PPI 'scopes from the control radar, labeled OV–1 and OV–2 were photographed. The 'scope OV–1 usually presented the low-beam video; however, when an airplane mission was being controlled, it presented the high-beam signals from the beacon or IFF equipment. 'Scope OV–2 presented the high-beam video at all times, with the IFF signals also included during airplane missions. During normal operations, both PPI 'scopes were adjusted so that the center of the electronic presentation was moved just off the edge of the 'scope on an azimuth of 330°. The range was adjusted so that the diameter of the 'scope represented 40 mi. from 5 to 45 mi. With this setting the surface network was located near the center of the 'scope. When the airplanes were investigating a storm in another area, the center of the presentation was moved off the center of the PPI 'scope along another azimuth to a position such that the storm being investigated appeared at the center of the 'scope.

The O–5 camera, employed to photograph the RHI 'scope of the height-finding radar (see table 49), also was mounted on a cone; however, the method of presenting the clock and data card was changed considerably from that used with the PPI 'scopes. In addition to the clock and data card, a self-synchronizing compass indicator showing the azimuth towards which the radar antenna was pointing was also photographed. The depth and space requirements of the azimuth indicator were too great to allow mounting in a section of the cone. As a consequence, the auxiliary units were installed in a tunnel at one side of the cone, and their images were brought into the field of view of the camera by means of a periscope, one mirror of which was half-silvered to permit both the 'scope and the data units to be in the field of view at the same time. The clock, data card, and azimuth indicator were illuminated by a 24-volt bulb operating with 20 volts.

The lens aperture of the camera was maintained at f:2.6 during most of the operations, and the shutter remained open for one complete vertical sweep of the antenna. The radar operator determined the azimuth which the radar antenna scanned as well as the interval between photographs. During the first half of the summer's operations, photographs were usually taken at every 2° of azimuth, while during the latter half, pictures were taken at every 4°, as the antenna was rotated azimuthally through the storm area being investigated. Occasionally a series of time-lapse photographs was taken at a fixed azimuth.

When there was a balloon mission on a day that the higher-power control radar was inoperative, the control of operations was handled at one of the SCR–584 stations. On such occasions, the PPI 'scope of an SCR–584 was photographed at half-hour intervals. For this purpose, an Army type C–3 Speed Graphic camera, mounted on a wooden cone, was used. Since a clock and data card were not photographed simultaneously with the radar 'scope, notes on each exposure were made. The comments were later written on the film itself.

The 'scopes of both airborne sets, the SCR–718 and SCR–720 (figs. 252 and 253) were fitted with cones on which were mounted the cameras listed in table 49.

Figure 252.—A photograph showing the camera mount for the SCR–718 radar.

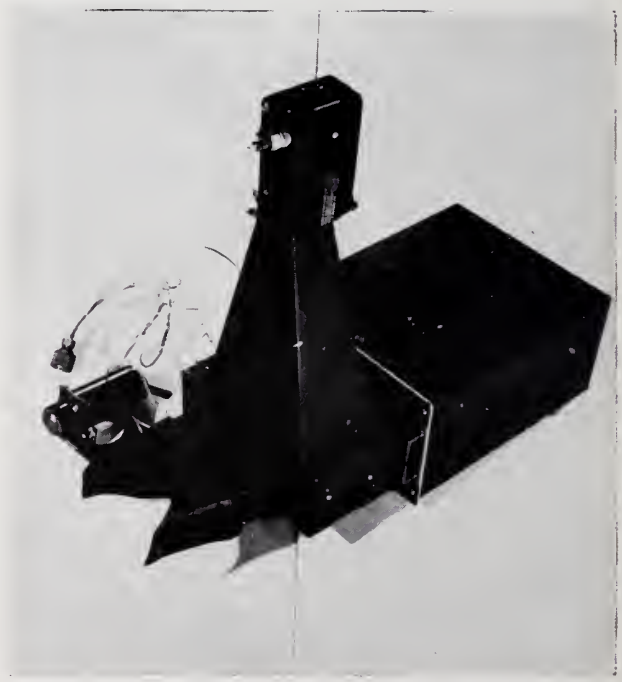

Figure 253.—A photograph showing the camera mount for the SCR–720 radar. Note that the radar 'scope is visible even though the camera is in position.

The cone supporting the camera used with the SCR–720 was turned at a right angle, and the "B" and "C" radar 'scopes were photographed through a half-silvered mirror. This arrangement served to make more space available to the radar operator and permitted him to view the 'scopes and make adjustments without disturbing or interrupting the operation of the camera. The use of the mirror resulted in the reversal of the top and bottom pictures. A clock and data card placed between the two 'scopes were illuminated with small lamps.

Photographs of airborne instruments.—The flight instruments section of the pilot's instrument panel of the P–61 was photographed using a 16-millimeter GSAP camera, modified to permit the speed of 5⅓ frames per second. This film was processed at the photographic laboratory of the N. A. C. A., and the original negatives were retained by them. Copies were furnished to the Thunderstorm Project. The instruments of the gliders, which made several flights in conjunction with the Thunderstorm Project, were photographed using two Army type A–4A cameras placed side by side just to the right of the pilot. Film for the first few days of operation was processed by the N. A. C. A.; film for the remainder of the summer's operations was processed by the Ansco Co. The original film was retained by the Soaring Society of America, but a copy was furnished to the Thunderstorm Project.

Cloud photography.—Cloud photographs were obtained from three sources. Army type K–20 cameras were supplied to each flight radar officer for the purpose of taking cloud pictures from the air. The airplane number, date, and altitude were inserted in the data slide of each camera. Notes were taken of the direction toward which the camera was pointing for each picture. Since the position of the airplane could be determined from the photographs of ground radar 'scopes, the position of the cloud with respect to the airplane could thus be calculated.

A K–20 type camera was also used at station A to take pictures of clouds over the network and of those being probed by airplanes, gliders, or balloons. Pictures were taken every half hour unless there was an aircraft or balloon mission, at which time the interval was 15 min. Station identifier, date, time, and camera heading were inserted in the data slide to be photographed simultaneously with the clouds.

The third source of cloud data was time-lapse photography, carried on from two towers by means of a modified Army type B–2 camera (see table 49). A clock was inserted in one corner of the field of view by a periscope and half-silvered mirror arrangement. Orange-colored plexiglass was used as a filter; the attenuation factor of the filter and half-silvered mirror are unknown. The shutter speed, which was changed when the camera was modified, is also unknown. During the modification, the camera was inverted; for this reason, all film must be projected backwards in order to appear correctly on the screen. One of these cameras was placed in operation August 15, 1946, on the control tower at Pinecastle AAF, directed toward an azimuth of 182°; the other one was placed in operation September 3, 1946, on a tower at Station B, directed toward an azimuth of 325°. Between July 12, 1946, and August 13, 1946, a GSAP camera, modified similarly with the B–2 was used on the tower at Pinecastle AAF.

841051—50——20

B. OHIO, 1947

During the 1947 observational season, photography was again used whenever practical for the recording of data. The modification and the installation of most of the photographic equipment and the film processing were accomplished by the Special Photo Section of the Air Materiel Command at Wright Field, Dayton, Ohio. Table 49 lists the cameras employed and some information pertaining to each.

Radar photography.—The Army type O–15 camera used to photograph the PPI 'scope of the control radar set was developed for installation on a 5-inch cathode-ray tube; however, with minor modifications it became a very satisfactory instrument for use on larger 'scopes. The camera was rigidly mounted on a cone which was painted black to reduce light reflections. A clock, counter, and data card with the necessary illuminating lamps were built into the camera. The photographic interval was determined by the frequency of activating electrical pulses and the position of the selector switch on the control box. The triggering voltage pulse was produced by the closing of a microswitch connected to the rotating deflection yoke on the cathode-ray tube. The switch was closed whenever the antenna was directed toward the north. Since the antenna of the short-range control radar set rotated at 10 r.p.m. and that of the long-range radar set rotated at 6 r.p.m., pulses at these frequencies were fed to the camera. The selector switch determined whether the camera would respond to every pulse, every other pulse, the first 3 out of every 12, or the first 5 out of every 60.

During an airplane mission, at every sweep of the antenna a photograph was obtained of an off-center 'scope having a diameter covering about 50 mi., with the echo from the storm being investigated located near its center. At the same time, another PPI 'scope showing only the beacon signals was adjusted so that the area displayed was the same as on the video 'scope, and it was also photographed at every sweep. When other types of operations were being carried on, one off-center 'scope displaying the sector enclosing

the surface network was photographed at the rate of 3 out of every 12 sweeps. One PPI 'scope of the long-range radar set, covering an area within a radius of 200 mi. of the radar, was also photographed at the rate of 3 out of every 12 sweeps.

The O–15 camera was also utilized to record the images on the range-height indicator of the Radio Set AN/TPS–10. At the Clinton County Air Force Base site, the azimuth toward which the antenna was pointing was recorded by mounting an azimuth self-synchronizing unit on the cone supporting the camera, and using two mirrors, one of which was half-silvered, to direct periscopically the image of the azimuth indicator to the same plane as that of the radar 'scope. This proved to be an unsatisfactory arrangement because the image of the azimuth dial masked the echoes, and because it was difficult to properly adjust the mirror so as to obtain a clear picture of the dial. The system for azimuth recording with the AN/TPS–10 located at the Jamestown site was considerably different and gave more satisfactory results. A small slot was cut out of the removable side of the data compartment of the camera, and a self-synchronous unit, with a cylindrical indicator having its periphery calibrated in degrees, was mounted so that the azimuth scale was photographed instead of the frame counter. Figure 254 is a photograph of the range-height indicator unit of the AN/TPS–10, with the camera and azimuth-indicator installations shown.

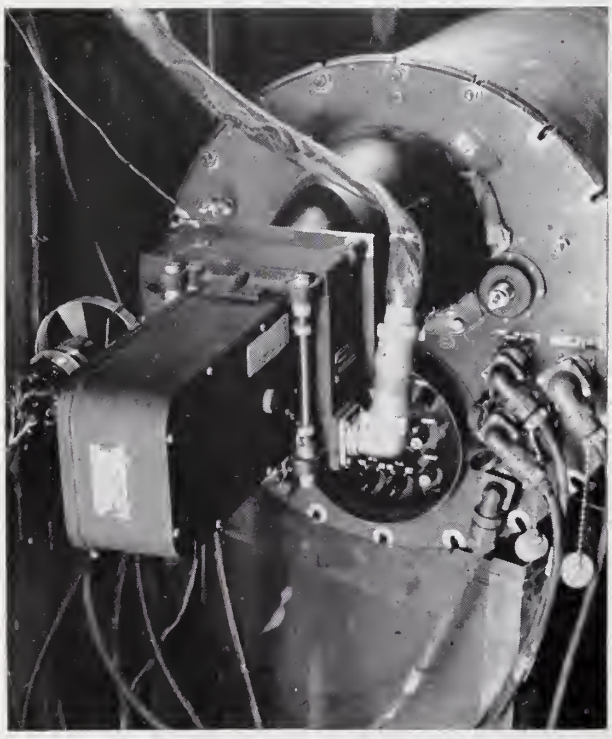

Figure 254.—A photograph of the range-height indicator unit of the AN/TPS–10 showing the mounting cone, the camera, and at the extreme left, the azimuth-indicator dial.

The exposure time was determined by the vertical scanning rate of the antenna and had a value of approximately 1 sec. A microswitch mounted on the antenna was briefly closed once for every complete oscillation of the reflector. The selector switch on the control box was usually adjusted so that the camera took a picture every other vertical sweep. This resulted in 'scope photographs at azimuth intervals of 3° to 4° as the antenna rotated azimuthally through a selected sector.

During the field operations in Ohio, the 'scopes of the Radio Sets SCR–718 and SCR–720 were photographed using the Army type O–5 camera. The images of the 'scopes of the two radio sets, along with a clock, counter, and data card were superimposed on the same plane using two half-silvered mirrors. The camera was activated by a microswitch mounted on the base of the antenna of the Radio Set SCR–720. A step circuit was incorporated to permit the camera to be triggered every fourth sweep of the antenna, which rotated at a rate of 100 r.p.m. The exposure time was determined by the shape of the cam which closed the microswitch.

Photographs of the airborne instruments.—The photo-box described in section 4 of the Appendix was photographed using the Army type A–4A camera. The speed of the camera was reduced to 1 frames per second before installation, by using reduction gears in the camera drive system. This modification proved suitable, but the increased torque developed caused structural failure of the camera when the film jammed. By employment of a 1,000-foot film magazine, the camera was capable of about 65 min. of continuous operation.

Cloud photography.—Time-lapse pictures were taken from 3 stations of the surface network—B, H, and F—using modified Army type A–4A cameras directed over the network. A clock and data card were mounted in front of the camera to permit their inclusion whenever a cloud picture was taken. The angle of coverage of the lens was increased by using a 1-inch, wide-angle lens. Although the exposure rate was usually 10 pictures per minute, an interval-meter which was part of the original installation made the selection of another rate possible.

As in Florida, the K–20 camera was used by observers at surface stations to make still photographs of clouds over the surface network, especially those being investigated by the balloons or airplanes.

INDEX

INDEX

Page

Accelerometer 44, 273
Air-mass thunderstorm 18, 96
  squall lines 122
Airplane, selection and instrumentation of 5
  instruments 270, 272, 281, 282
Airspeed-altitude recorder 44, 272
Andre, M. J. 71
Anvil top 97
Areas of operations of Thunderstorm Project 6, 9
  of thunderstorm development 115
Atlas, D. 52
Austin, J. M. 35
Autogeneous charge 81

Balloon-finding equipment:
  SCR–584 ..... 5, 268, 269
  SCR–658 ..... 5, 267, 269
Barograph (*See* Microbarograph)
Barrett, E. W. 36
Bellamy, J. C. 3, 32, 119
Bénard, H. 17
Bergeron, T. 50, 91
Binckley, E. T. 99
Bjerknes, J. 66
Bleeker, W. 71
Braham, R. R. ..... iii, 255
Brancato, G. N. 19, 110
Brooks, C. F. 24
Brooks, H. 108, 110
Brunk, I. W. 122
Brunt, D. 17
Bnell, C. E. 3, 69
Byers, H. R. 3, 6, 32, 119, 264

Caution zone 59
Cells 19
  adjacent, effect of 25
  cumulus stage of 20
  development of 77
  dissipating stage 25
  electric fields in 80
  growth, rate of 94
  hail within 138
  icing within 138
  lightning within 86, 138
  mature stage of 21
  precipitation from 21, 24, 25
  radar cross section of 97
  radar echo of 93
  stages of development of 19
  structure of 20, 24, 25

Page

  surface weather 50
  temperature within 20, 24, 25, 29
  turbulence within 20, 24, 25, 133
  wind shear of 27, 101, 104
Chandra, K. 17
Chapman, S. 269
Cloud, echo 90
  movement 78, 108, 127
  photography 281, 282
  shear 101
Cold air dome 54
Control position recorder 44, 274
Convection 17, 27, 36
Convergence, surface winds 20, 53, 67, 130
  aloft, around cloud 5, 31
  sea breeze causing thunderstorm development 119
  divergence of surface winds 24, 53, 129
Corona discharge 85, 138, 265
Cotton Region shelter 261
Countercurrent 31
Coverage of thunderstorms 100
Cunningham, R. M. 40

Data obtained 13, 151, 175, 181, 199, 235, 245, 279
Dew-point indicator 263
Discontinuity zone 55, 141
Divergence (*See* Convergence)
Diurnal variation of thunderstorms 7, 116
Donely, P. 3
Downdrafts below cloud base 42, 137
Drafts, airplane displacements by 137
  altitude distribution of 40, 42
  causes of 38, 39, 41
  computation of 40
  comparison with rate of change of radar echo 93
  cumulus stage 20
  dimensions of 40, 42
  dissipation stage 25
  electric fields in 81, 83
  entraining in 38
  instruments for measnring 4, 272, 276
  liquid water content of 32, 35, 40
  mature stage 24
  momentum transferred by 105
  rainfall within 62
  relative humidity of 77
  surface pressure changes 68, 69
  temperature within 29
Dynamic correction 28, 278

Effective gust velocity 44, 46
Effective temperature difference 37, 40

Page

Electric field, and drafts 81, 83
fair weather 80
meters 80, 265, 278
measurements 80, 264, 269
rainfall and 84
surface effects 85
turbulence and 85
Elster, J. 83
Entraining 19, 25, 31
cause of 33
computation of 35
cloud turrets with 94
distribution with height 32
Entrainment, new cell development with 77
region affected by 34
momentum transfer and 105
thermodynamics of 35
Examples of data obtained 151, 175, 181, 199, 235, 245, 279
Exogenous field 81

Ference, M. 3
First gust 55, 65, 68, 141
Fletcher, J. O. 3
Flight operations in thunderstorm conditions 133, 141
Frontal thunderstorms 96

Geitel, H. 83
Graham, A. 17
Growth of thunderstorms 77, 97
Gunn, K. L. S. 52
Gunn, R. 256
Gusts 39, 43
altitude distribution of 45, 136
association with drafts 43
cause of 43
description of 43
effect on airplanes 43
electric fields and 83
evaluation of 44
frequency of 45
gradient distance of 45
instruments for measuring 272, 276
measurements of 5, 44
sharp-edged 44
Gust load 136

Hail 48, 138
Hall, F. 3
Harney, P. J. 264, 274
Harrison, H. T. 126, 128, 130
Harrison, L. P. 3, 256
Heat source, high level 115, 117
Height of cloud, and lightning frequency 86
cross-sectional area and 98
height of radar echo and 90
rate of growth and 95
wind shear and 107
Height of level of first formation of radar echo 90
History of Thunderstorm Project 3
Holford, J. F. 256
Holzer, R. E. 19, 80
Holzman, B. G. 3
Hull, E. C. 32

Page

Humidity, dip 74
measurements 5, 262, 266
surface air 72
Humphreys, W. J 105, 112
Huss, P. O. 142
Hygrothermograph 5, 262

Icing 49, 138
Inflow, horizontal 5, 31
wind field, aloft 5, 31
wind field, surface 53, 67
Instruments, accelerometer 44, 273
airspeed-altitude recorder 44, 272
control position recorder 44, 274
dew point indicator 263
electric field meters 80, 265, 278
hygrothermograph 5, 262
Kytoon 266
microbarograph 5, 262
photo-box 275
point collector 85, 264
radiosonde 267, 269
rain gage 5, 262
rain temperature measuring 263
thermistor 28, 274, 276
thermometer 262
timer 44, 274
W-sonde 269

Jeffreys, H. 17

Koschmieder, H. 54
Kytoon 266

Lakes, effect of on development of thunderstorms 115
Langille, R. C. 52
Lenard, P. 83
Levine, J. 69
Lewis, G. W. 3
Lightning 80, 86, 138, 265

Mal, S. 17, 69
Malkus, J. S. 105, 106
Maynard, R. H. 3
Microbarograph 5, 262
Miller, R. W. 40
Momentum, vertical transfer of 53, 101, 105
Morris, D. E. 256
Moses, H. 262, 263, 264
Movement, of thunderstorms 108
of pre-cold-frontal squall lines 126

Nocturnal thunderstorms 10, 72
Normand, C. W. B. 32

Observational system, design of 4
Orendorf, W. K. 126, 128, 130
Outflow at top of cloud 33
Outflow wind field, surface 53, 66, 72, 75, 116, 141

Palmer, W. M. 52
Parcel method 31
Pelsor G. T. 19, 80
Phillips, A. C. 17
Photo-box 275
Pilot augmentation of gust loads 136

Page

Point collector 85, 264
Pope, F. W. iii
Pre-cold-frontal squall lines 124
Press, H. 46, 99
Pressure, surface air 66
dome 68
hump 69
jump 69
nose 69

Radar and thunderstorm flying 139
Radar cloud 90
compared with visual cloud 90, 100
coverage of 99
detection of 90
height of 41, 70, 96
level of first formation 90
shear 101, 104
turret 94
Radar equipment, airborne 270, 272
ground 270, 271
height finding 271
Radar photography 279, 281
Radar-rainfall relationships 51
Radar thunderstorm 90
Radiosonde 267, 269
Rain, and downdraft 137
and electric field 84
gage 5, 262
humidity dip and 75
surface 50
surface pressure 71
temperature 77, 263
within the thunderstorm 21, 24, 25, 47
Rao, Y. P. 69
Rayleigh, J. W. S. 17
Reichelderfer, F. W. 3
Relative humidity 72
dip 74
Return settling 18
Reynolds, S. E. 90, 92, 109
Rhode, R. V. 3
Rodebush, H. R. 6, 119
Roll cloud 139
Riehl, H. 36, 119
Ryde, J. W. 98

Schaffer, W. 69
Schmidt, F. W. 32, 40, 79, 93, 106
Scrase, F. J. 80
Sea-breeze, effect on thunderstorm development 119
Seasonal variation of thunderstorm activity 8
Shear of thunderstorm 101, 104, 107
Shearing stress 34
Simpson, G. C. 80, 83
Slice method 31
Snow within the thunderstorm 47
Squall line 18, 70, 96, 122, 245
airmass 122
element 127
pre-cold-frontal 124
zone 127
Stommel, H. 17, 32, 35
Sunshine recorder 267

Page

Surface, pressure 66, 71, 143
rainfall 24, 25, 50, 64, 71, 86
relative humidity 72
temperature 60, 64, 75

Temperature break 62
Temperature field, beneath a thunderstorm 60
within a thunderstorm 29
in thunderstorms 20, 24, 25
measurements 5, 27, 262, 266
measuring equipment 274, 276
of rain 77, 263
Tepper, M. 122
Thermistor 28, 274, 276
Thermometer 262
Thunderstorm, affecting flight operations 133
cell 19
circulation 17
development of 17, 77, 115, 117, 119
echo 90
electric fields in 80, 85
examples of 151, 175, 181, 199, 235
frequency in United States 7, 8
height of 96
hearth 115
high 69
horizontal extent of 97
percentage coverage of 99
movement of 108
rainfall 50
structure of 17
vertical growth of 92
turbulence in 39, 133
Thunderstorm project, cooperating agencies .....iii, 5
data obtained 13
design of observational system 4
history of 3
location of operations 4, 6
Timer 44, 274
Topography and thunderstorm development 115
Turbulence 39, 133
altitude distribution of 136
and electric fields 83
dissipating stage 25
intensity of 133
mature stage 24
and precipitation 139
variation with airspeed 135
winds near surface 142

Vertical, growth and extent of thunderstorms (*See* Growth)
transport of momentum (*See* Momentum)
Veryard, R. G. 30
Visual cloud and radar cloud 90, 100
Von Ficker, H. 115

W-sonde 269
Walker, G. T. 17
Weber, E. H. 17
Wenzel, W. 30
Wexler, H. 3
Williams, D. T. 129, 130
Winds aloft, cloud shear and 101, 104
cloud movement and 108
measurements (*See* Balloon-finding equipment)
surface 52
Workman, E. J. 19, 80, 81, 90, 92, 109

☆U. S. GOVERNMENT PRINTING OFFICE 1950—841051

Date Due

Due			
NOV 2 '59			
DEC 1 '56			
Jan 3 1956			
JAN 2 '65			
OCT 16 '65			
APR			
JAN			
Dec 11, 72 NOV 30 '72			
DEC 8 '72 DEC 8 '72			
JUN 1 '78 JAN 15 '74			
JUN - 3 MAY 18 '77			
DEC 14 '78 DEC 13 '78			
APR 07 1986 MAY 06 1986			

The thunderstorm; report. UGE
551.55 U585t

3 1262 01103 9202

551.55
U585t

ENGINEERING
SCIENCES
LIBRARY